NASA/CR–2010-216691

N+3 Small Commercial Efficient and Quiet Transportation for Year 2030-2035

Martin M. D'Angelo
GE Aviation, Lynn, Massachusetts

John Gallman and Vicki Johnson
Cessna Aircraft, Wichita, Kansas

Elena Garcia, Jimmy Tai, and Russell Young
Georgia Institute of Technology, Atlanta, Georgia

May 2010

NASA STI Program . . . in Profile

Since its founding, NASA has been dedicated to the advancement of aeronautics and space science. The NASA scientific and technical information (STI) program plays a key part in helping NASA maintain this important role.

The NASA STI program operates under the auspices of the Agency Chief Information Officer. It collects, organizes, provides for archiving, and disseminates NASA's STI. The NASA STI program provides access to the NASA Aeronautics and Space Database and its public interface, the NASA Technical Report Server, thus providing one of the largest collections of aeronautical and space science STI in the world. Results are published in both non-NASA channels and by NASA in the NASA STI Report Series, which includes the following report types:

- TECHNICAL PUBLICATION. Reports of completed research or a major significant phase of research that present the results of NASA programs and include extensive data or theoretical analysis. Includes compilations of significant scientific and technical data and information deemed to be of continuing reference value. NASA counterpart of peer-reviewed formal professional papers, but having less stringent limitations on manuscript length and extent of graphic presentations.

- TECHNICAL MEMORANDUM. Scientific and technical findings that are preliminary or of specialized interest, e.g., quick release reports, working papers, and bibliographies that contain minimal annotation. Does not contain extensive analysis.

- CONTRACTOR REPORT. Scientific and technical findings by NASA-sponsored contractors and grantees.

- CONFERENCE PUBLICATION. Collected papers from scientific and technical conferences, symposia, seminars, or other meetings sponsored or co-sponsored by NASA.

- SPECIAL PUBLICATION. Scientific, technical, or historical information from NASA programs, projects, and missions, often concerned with subjects having substantial public interest.

- TECHNICAL TRANSLATION. English-language translations of foreign scientific and technical material pertinent to NASA's mission.

Specialized services also include creating custom thesauri, building customized databases, and organizing and publishing research results.

For more information about the NASA STI program, see the following:

- Access the NASA STI program home page at *http://www.sti.nasa.gov*

- E-mail your question via the Internet to help@sti.nasa.gov

- Fax your question to the NASA STI Help Desk at 443-757-5803

- Phone the NASA STI Help Desk at 443-757-5802

- Write to:
  NASA STI Help Desk
  NASA Center for AeroSpace Information
  7115 Standard Drive
  Hanover, MD 21076-1320

NASA/CR–2010-216691

N+3 Small Commercial Efficient and Quiet Transportation for Year 2030-2035

Martin M. D'Angelo
GE Aviation, Lynn, Massachusetts

John Gallman and Vicki Johnson
Cessna Aircraft, Wichita, Kansas

Elena Garcia, Jimmy Tai, and Russell Young
Georgia Institute of Technology, Atlanta, Georgia

National Aeronautics and
Space Administration

Langley Research Center
Hampton, Virginia 23681-2199

Prepared under NASA contract
NNC08CA85C

May 2010

Acknowledgments

This work was funded by the Subsonic Fixed Wing (SFW) project, of the Fundamental Aeronautics Program, under NASA contract NNC08CA85C.

Available from:

NASA Center for AeroSpace Information
7115 Standard Drive
Hanover, MD 21076-1320
443-757-5802

Table of Contents

List of Tables

List of Figures

1.0 Introduction

GE, Cessna Aircraft, and the Georgia Institute of Technology have teamed to explore the potential of advanced, innovative aircraft and propulsion system technologies to enable direct, point-to-point regional air travel with minimal environmental impact. By employing smaller aircraft and under-utilized community airports, more air travel growth will be enabled than the future saturated hub and spoke network would otherwise allow. Door-to-door travel time can be reduced by half or more compared to hub and spoke air travel, with the additional benefits of reduced travel delays and stress. The reduced trip time and added convenience of this new regional travel mode will provide positive economic impact to the communities surrounding these small airports, and reduce congestion in the hub airports and ground transportation systems.

Our studies show that it is possible to develop a current technology airliner that meets noise and environmental regulations, and could capture a share of the current airline network market. Resistance to adding commercial service to small community airports can be high, however, and fear of increased community noise could limit the number of community airports willing to add significant additional traffic. Additionally, improvements in mission fuel burn and emissions are needed reduce the environmental impact of the significant additional air travel made possible by this new mode of transportation.

This report describes an innovative Advanced Air Vehicle and Propulsion Concept to enable significant point-to-point air travel in the Year 2030-2035 timeframe. Our selected Ultra Quiet and Efficient Airliner is targeted at ensuring small airport community acceptance of this new commercial traffic, while minimizing the environmental impact of the increased air travel enabled by this extremely convenient mode of transportation. The reduction in fuel burn and aircraft and propulsion system size will make this premium mode of transportation affordable to a much larger number or travelers than possible with current technology.

This study develops a future scenario that enables convenient point-to-point commercial air travel via a large network of community airports and a new class of small airliners. A network demand and capacity study identifies current and future air travel demands and the capacity of this new network to satisfy these demands. A current technology small commercial airliner is defined to meet the needs of the new network, as a baseline for evaluating the improvement brought about by advanced technologies. Impact of this new mode of travel on the infrastructure and surrounding communities of the small airports in this new N+3 network are also evaluated.

Year 2030-2035 small commercial airliner technologies are identified and a trade study conducted to evaluate and select those with the greatest potential for enhancing future air travel and the study metrics. The selected advanced air vehicle concept is assessed against the baseline aircraft, and an advanced, but conventional aircraft, and the study metrics. The key technologies of the selected advanced air vehicle are identified, their impact quantified, and risk assessments and roadmaps defined.

2.0 Study Goals and Metrics

This study is being conducted as part of NASA's N+3 research efforts for advanced subsonic commercial aviation for the Year 2030-2035. N+1 and N+2 research efforts have focused on technologies needed to meet aggressive goals for reduction of aircraft noise, fuel burn, emissions and field length in the 2015 to 2025 time frame. NASA has set even more aggressive goals for the 2030-2035 timeframe in their N+3 research, to dramatically reduce the environmental impact of future commercial air travel. Table 1 shows NASA's metrics and goals for these subsonic commercial research efforts.

Table 1. NASA Subsonic Commercial Research Metrics and Goals

CORNERS OF THE TRADE SPACE	N+1 (2015 EIS) Generation Conventional Tube and Wing (relative to B737/CFM56)	N+2 (2020 IOC) Generation Unconventional Hybrid Wing Body (relative to B777/GE90)	N+3 (2030-2035 EIS) Advanced Aircraft Concepts (relative to user defined reference)
Noise (cum. below Stage 4)	-32 dB	-42 dB	-71 dB or 55 LDN at average airport boundary
LTO NOx Emissions (below CAEP 6)	-60%	-75%	better than -75%
Performance: Fuel Burn	-33%	-40%	better than -70%
Performance: Field Length	-33%	-50%	exploit community airports

Because this study proposes a new mode of air travel and a new class of commercial airliner, the baselines and metrics for our N+3 study need further definition.

The key to enabling this new convenient mode of transportation is the need to open more than a thousand small community airports to commercial (or additional commercial) air travel. Therefore, the prime metrics must be acceptance by the local communities surrounding the airport and compatibility with the small airport infrastructure.

First, the aircraft must be able to meet the runway length and width requirements of a sufficient number of small airports to satisfy demand. The network demand and studies have determined that 95% of the US population lives within 20 miles of an airport with a 4000 ft or larger runway.

Next, the aircraft must be *allowed* to service these airports. Community noise is the key obstacle to community acceptance. As most small community airports currently have boundary noise levels in the low 60 to low 70 dB LDN range, it is not possible to meet NASA's 55 LDN goal as we are adding, not replacing traffic. So the goal here is to reduce the noise of the additional flights to a level that is virtually unnoticeable by the local community. Therefore, we chose to meet NASA's previous and current N+3 noise metric of 71 dB cumulative margin below Stage 4 requirements.

Ground emissions are also a factor in community acceptance. As we hope this new mode of transportation will actually enable increased air travel, it must also be environmentally responsible. We believe the N+3 goal of 75% reduction in LTO vs. CAEP 6 standards is a good metric. However, emissions regulations are a function of engine takeoff thrust, and are

unregulated for engines producing less than 6000 lbs of thrust. Additionally, the ICAO is still in early stages of determining how variable-pitch open-rotor and turboprop propulsion systems should be regulated. For idle emissions, the current standard on measuring emissions at 7% of takeoff thrust is inappropriate for open rotors and turboprops, as they can (and would) eliminate thrust entirely at ground idle by varying rotor pitch.

For this study, we chose to adhere to the goal of reducing emissions by 75% relative to the standard for 6000 lb thrust engines, no matter how small the engine is. Open rotor/turboprops propulsions were evaluated as if they were turbofans based on their net system thrust (propulsor + engine) at the takeoff, climb out, and approach test conditions. For idle, the shaft engine is set to produce 4% of takeoff power at 80% prop rotor speed. While this is an unrealistically harsh assessment of ground idle for a variable pitch propulsor engine, it is meant to represent the impact of some portion of the ground time spent taxiing. We also report on the LTO and Cruise NOx emissions of the Advanced 2030 Airliner Concepts vs. the current technology baseline aircraft.

NASA's goal of mission fuel burn improvement is extremely challenging for these small aircraft, as many fuel efficiency enhancing technologies cannot scale to this size. Additionally, regulation requirements also do not scale below a certain aircraft size. The selected Advanced Airliner concept comes within 1 percentage point of meeting the 70% fuel burn reduction metric. A conscious decision was made to choose those technologies most compatible with the small community airport infrastructure (fuels, maintainability) and an affordable ticket price.

Figure 1 summarizes the baselines and metrics used for evaluating the advanced concept in this study.

N+3 Small Commercial Subsonic Metrics and Baselines

Field Length

>Sufficient to utilize community airports and capture vast majority of population.

Noise: 55 LDN at Airport Boundary or 71 dB Cum Margin Below Stage 4

>Develop a notional Community airport. Establish Current Noise Level.
>Quantify N+3 Air Vehicle impact on noise w/ projected frequency of flights.
>Meet 71 EPNdB Cum Below Stage 4. Impact LDN at Airport Boundary << 1 dB.

-70% Fuel Burn

>Notional comparison of Baseline 2008 N+3 Aircraft/Network vs. Hub & Spoke
>Quantify improvement of Advanced Airliner vs. Baseline Airliner

-75% NOx LTO below CAEP/6 (g/kN FN)

>NOx unregulated below 6000 lb FN.
– Use 6000 lb FN Standard as Baseline.
>NOx unregulated for Turboprops/Open Rotor Systems.
– Treat Propulsion System Net Thrust as if Turbofan for Takeoff, Approach, and Climb
– Rational Substitute for Turbofan Idle. (4% Shaft Power, 80% Prop Speed)
>Baseline Air Vehicle & N+3 Network vs. Current Network (LTO NOx g/Pax/trip)
>Advanced Air Vehicle LTO and Cruise NOx vs. Baseline

Figure 1. Refinement of Study Baselines and Metrics

3.0 Future Scenario: Convenient N+3 Point-to-Point Air Travel

Future increases in population, GDP, and wealth are predicted to increase the demand for air travel beyond that of extrapolating the current rate of air traffic growth. This increase in growth will tax the capacity of major hubs, several of which are already approaching maximum capacity. Increases in the capacity of many major airports, and the supporting ground infrastructure, are anticipated to be extremely expensive and lag the increase in demand. The result will be increases in price pressure, travel time and inconvenience. Other potential negative impacts include increased pollution, noise, and ground traffic congestion in the major airport communities.

The current air transport network relies on relatively few airports, large aircraft, and major hub airports. Even passengers whose trip origins or destinations aren't near large cities are routed through major hubs and onto larger aircraft, often at a significant increase in travel length and time. Figure 2 shows a typical trip scenario for travel of a trip originating near a small or moderate size city to a large city some significant distance away. Typically, this involves driving to the small/moderate size city airport, a flight on a regional jet or turboprop to a large hub, a flight on a larger airliner to another large city, and ground transportation to the ultimate destination. This can add 50% or more travel path length vs. great circle distance from origin to destination. Figure 3 shows actual distance traveled vs. desired travel distance for 500 to 600 mi trips with today's hub-and-spoke system.

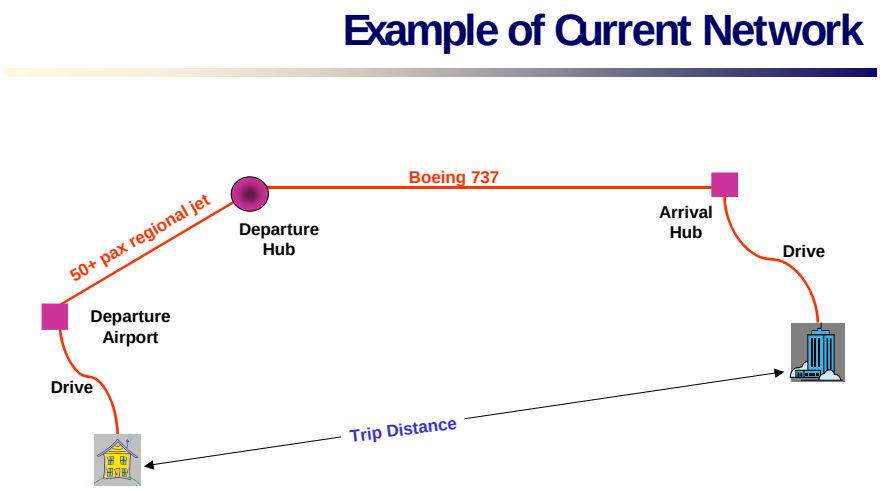

Figure 2. Current Air Transport System: Typical Trip with Hub-and-Spoke Network

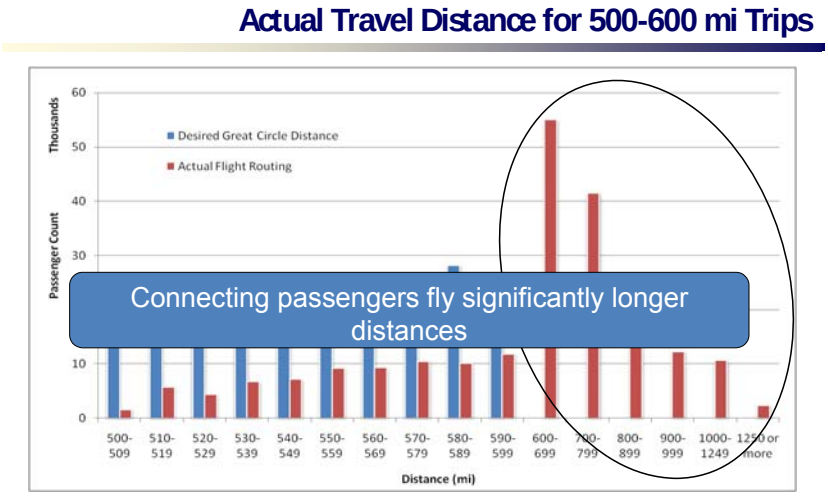

Figure 3. Current Hub & Spoke System: Actual Travel Distance for ~550 mile Trips

In order to look at these detour distances in more detail we made use of DB1B data, which represents a 10% sample of airline tickets from reporting carriers collected by the Bureau of Transportation Statistics. The data presented in the figure below includes origin, destination and other itinerary details of passengers transported and manipulation of the flight coupon data allows for identification of true O-D trips including any connections. Results from this analysis including only routings with one connection are presented in Figure 4. The x-axis in this figure displays the true OD distance in nmi. The y-axis represents the additional distance traveled due to hub routing. Finally, the size of the circles captures the number of trips that meet that OD distance and detour length. While there are a number of trips involving a zero detour distance, there are also a number of trips involving distances significantly larger than a direct trip. Typical detours range between 20 and 40% of true OD distance and a 200 nmi detour is frequent for trips between 200 and 800 nmi.

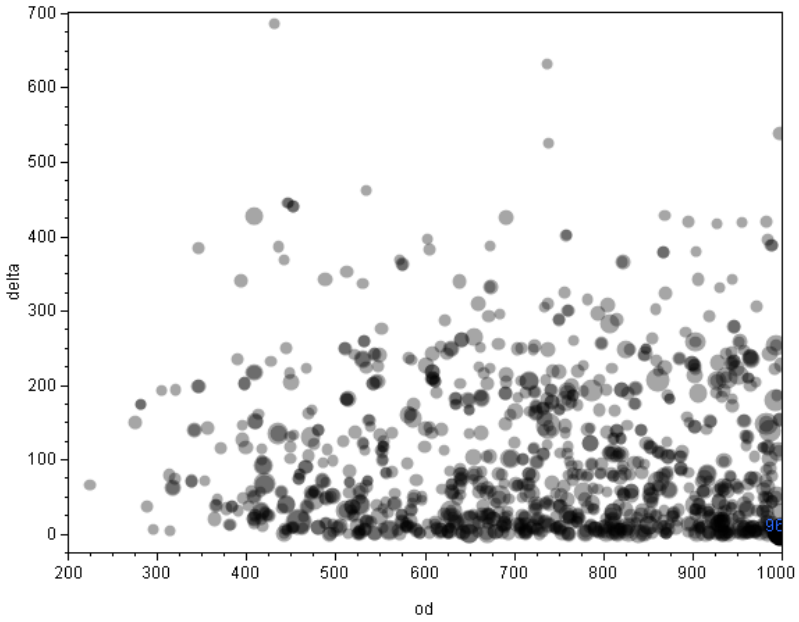

Figure 4. Detour Distance vs. True OD Distance (nmi)

Also considering DB1B data, the majority of trips today involving air travel are less than 850 nmi in length (See Figure 5). Additionally, the majority of desired city pairs today (the real origins and destinations of travel) have relatively low travel volume for these short-range trips. Figure 6 shows number of passengers per day between all city pairs in the 500 to 600 mile range. This shows that a very large number of city pairs have 20 passengers or less traveling between them each day, while many more have 100 passengers or less. If local community airports could be utilized, a large percentage of these trips could be serviced efficiently with direct flights using ~20 passenger aircraft, with one or more flights a day.

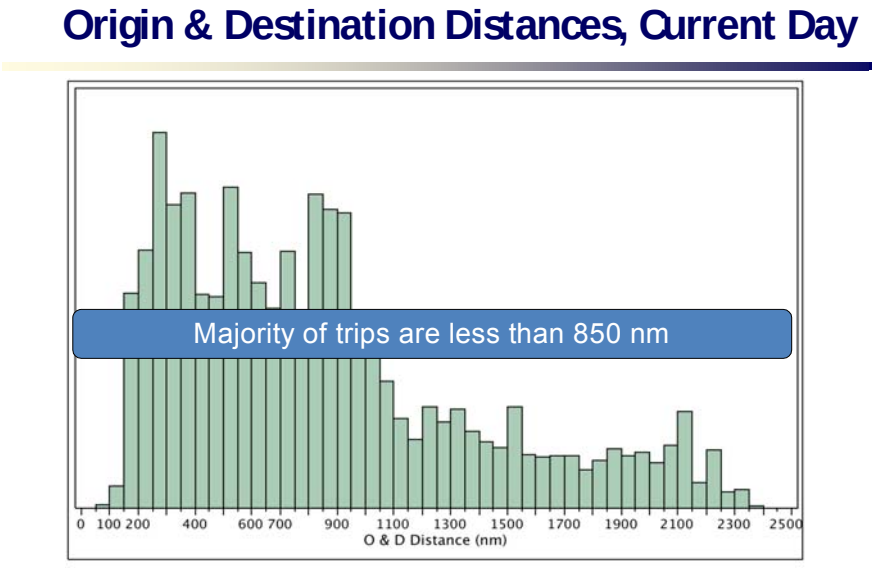

Figure 5. Current Day Travel Distances between Origin and Destination

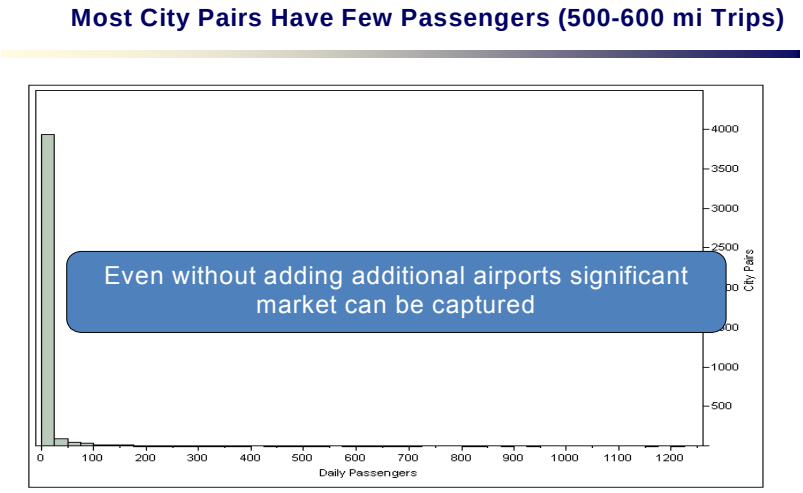

Figure 6. Current Daily Passenger Volume for 500-600 nmi City Pairs

Many of the anticipated issues with growing the air transport system to address 2035 demand could be alleviated with direct flights between desired city pairs, with a smaller aircraft (~20 passengers), if community airports could be utilized. Short range (<1000 miles), low volume (20 to 150 passengers/day) traffic that would normally have to be routed through a major hub could be serviced with direct flights (See Figure 7). Significant capacity of the major hubs would be freed up to absorb the increased demand for travel to or from large cities. Aircraft utilization rates for the low volume city pairs would be much higher with a 20 passenger aircraft than the larger (50+ passenger) regional jets that typically service these routes. Increased flexibility would be allowed with semi-scheduled operations to add another 20-passenger flight when demand is present. Ground transport distances would also be reduced, as the drives to the larger city airports would be replaced by shorter trips to the local community airport.

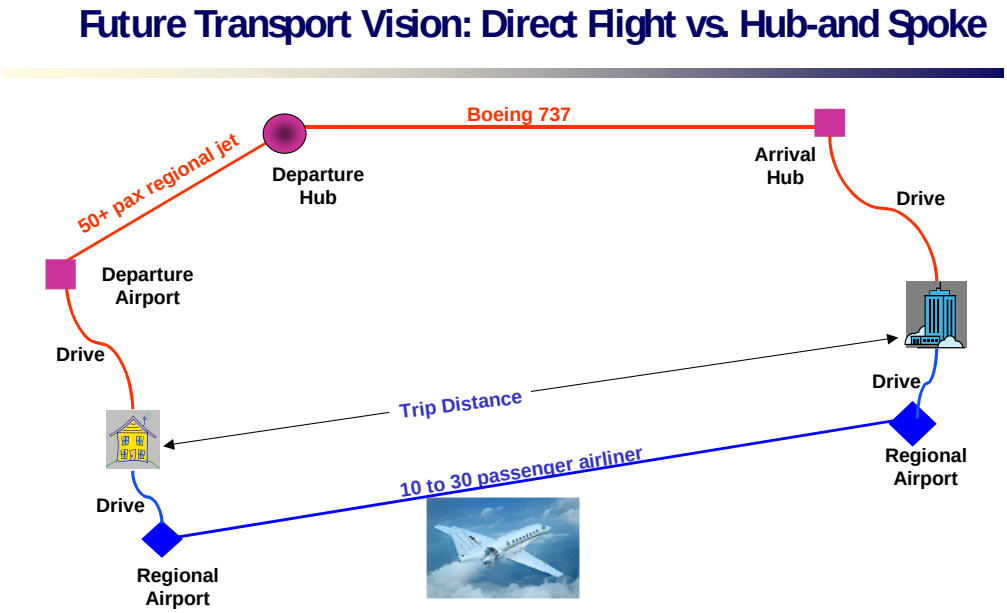

Figure 7. Future Direct Flight Scenario vs. Current Hub and Spoke System

3.1 Defining a Notional Trip

We can use the information gleaned from the data above to define a notional trip and consider the differences in convenience and travel time obtained using a small aircraft point-to-point network vs. the existing hub and spoke network. The assumptions used for this notional trip are summarized in Table 2.

Table 2. Notional Trip Assumptions

	Hub-and-Spoke		**N+3 Aircraft**
	Regional Jet	**737**	
Flight distance	150 nmi	550 nmi	400 nmi
Load Factor	70%	80%	87%
Wait times	No extra security time, 1hr layover		N/A
Drive Distance	25 mi		12 mi
Driving Fuel Consumption	20 mpg		
Driving Speed	30 mph		

Today's travelers are forced to travel circuitous routes in order to utilize the hub & spoke network. Meanwhile community airports that, thanks to federal investment, have the infrastructure to serve this demand more conveniently go largely underutilized. This project aims to investigate the feasibility of a smaller aircraft enabling a more direct and convenient point-to-point network. Table 3 shows that fuel burn and NOx emissions per passenger (current technology aircraft) are quite competitive with current Hub-n-Spoke numbers for the trip comparison shown in Table 2. This network has the potential to provide increased mobility, while a suitably designed aircraft would minimize negative impacts on local communities.

Table 3. Fuel and NOx for Small Airliner Trips vs. Hub-n-Spoke (Table 2)

Fuel/Passenger			LTO NOX		
N+3	Hub	Diff	N+3	Hub	Diff
123.1	119.4	**3.1%**	43	64.1	**-26%**
Door to Door Dist			**Door to Door Time**		
N+3	Hub	Diff	N+3	Hub	Diff
421	643	**-35%**	143	241	**-41%**

3.2 Enabling N+3 Service

As described above, a 20 passenger aircraft and point-to-point routes provides significant benefits in passenger convenience, travel distance, and trip fuel burn. A future transportation service with 20 passenger aircraft is anticipated to include (1) trips between the satellite airports of current hub communities (Figure 8), (2) trips between small communities and the satellite airport of a hub community (Figure 9, Figure 10), and (3) point-to-point trips between small communities (Figure 11). This enables future small airliners (20 – 60 passengers) to provide capacity augmentation between large hub communities, to connect small communities to hub airports for long distance (greater than 800 nm) trips, as well as to provide service between small communities without burdening the traffic volume at the hub airport. This transportation concept enables economic development in smaller communities where land and labor are affordable, links these communities with existing businesses in large communities, and provides a transportation service that offloads the traffic at hub airports without the infrastructure investment required for additional large hub airports. Infrastructure investment in trains or bus service that connects current hub airports to nearby suburban airports enables a direct connection between this new distributed network service and the traditional hub and spoke transportation system.

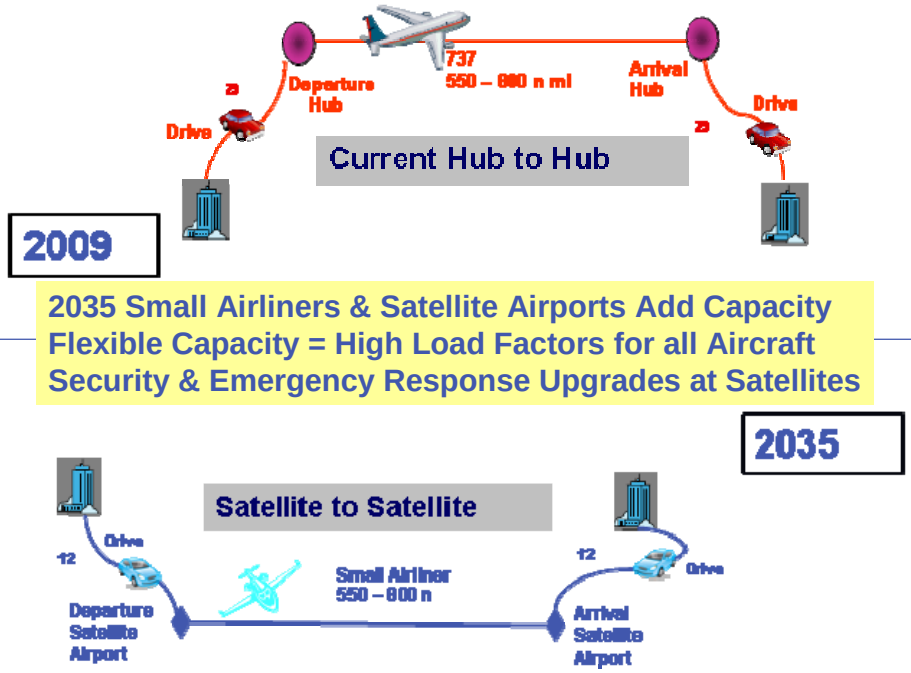

Figure 8. Hub-Satellite to Hub-Satellite Trips

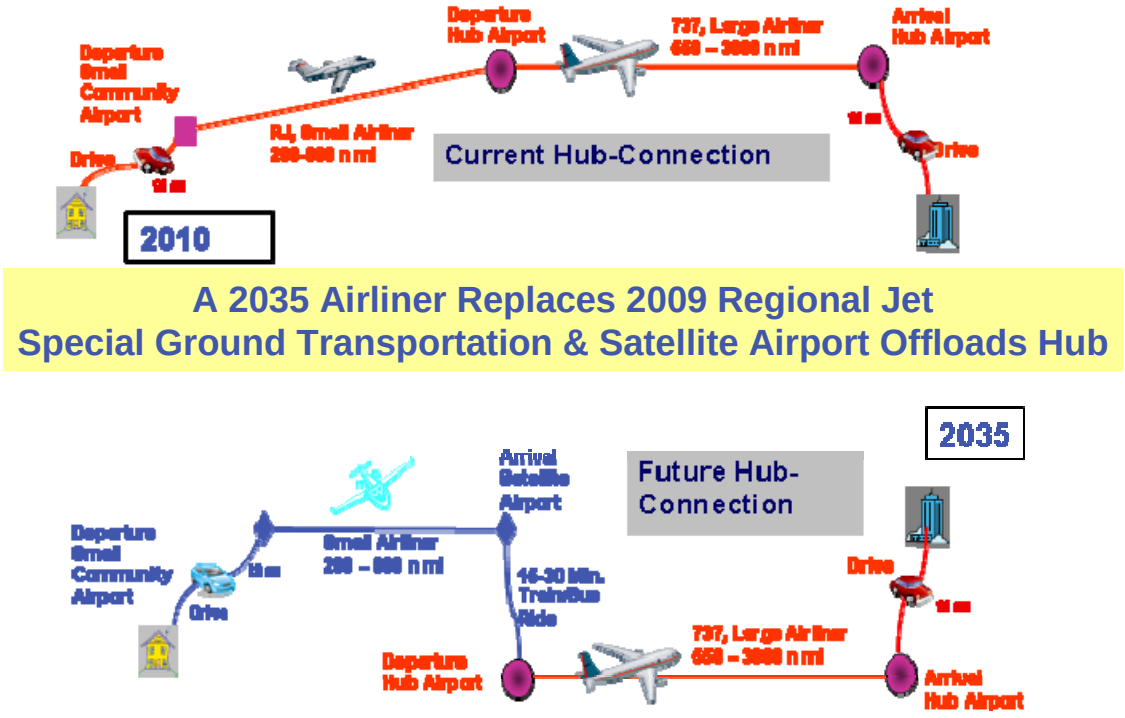

Figure 9. Small Community to Hub Airport Trip

Figure 10. Hub-Satellite to Small Community Trips

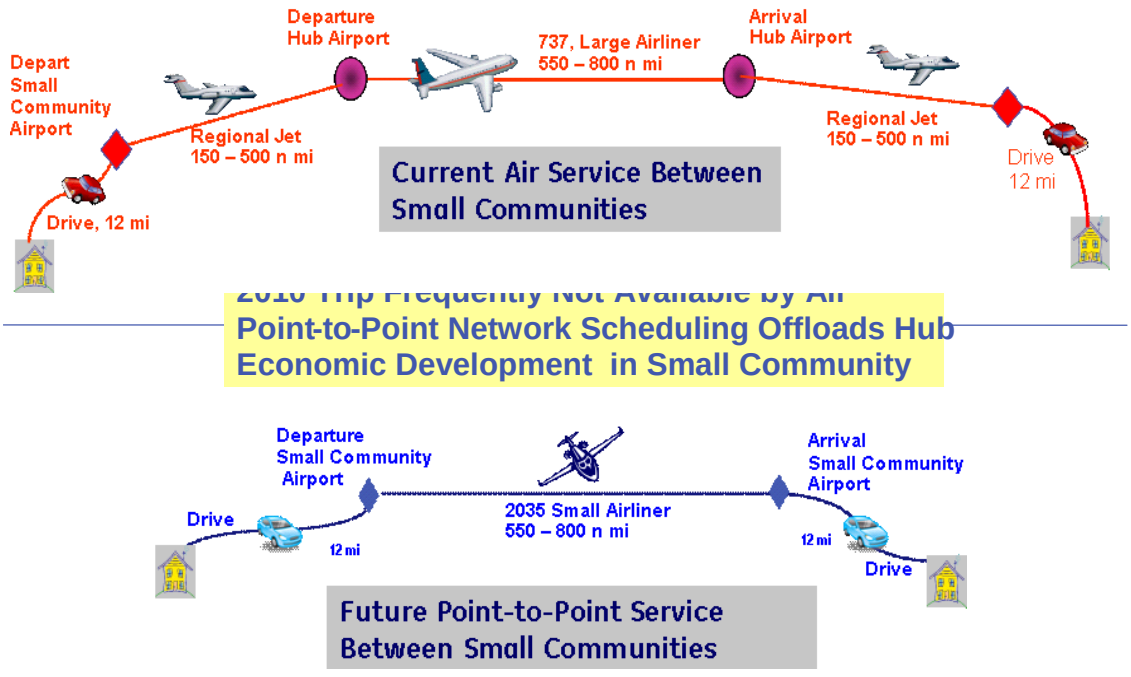

Figure 11. Small Community to Small Community Trips

The trip scenarios of Figure 8 through Figure 11 define multiple transportation system needs for small airliners in the 2035 time frame. Clearly, the movement of lots of people from one large community to another large community is better served with large aircraft (> 100 seats). However, there will be a need in 2035 to connect small communities with large ones and to provide more flexible capacity augmentation between large communities. One would expect current communities that are served by regional jets to grow in population such that larger aircraft would be needed. One would also expect small communities that don't have air-service today would demand air-service in 2035. Consequently an air transportation system of the future is expected to need efficient replacements for current technology turboprops and regional jets as well as the desire for point-to-point travel between small communities.

The mixture of trips defined in Figure 8 through Figure 11 also enables an operator of small airliners to establish a schedule and route network that is served by a broad base of customers. Figure 12 shows a potential schedule for one day of operation with a small airliner. This schedule enables the airline to access customers from both large and small population centers and construct route networks that could be offered almost every day. Computer scheduling tools and interaction with customers through the internet also enables daily schedule that serve only point-to-point trips between small communities. However, these communities would need to demonstrate sufficient daily demand for an airline to offer this service every day. Seasonal schedules during high demand periods and service offerings once a week or every other day are also alternatives for these distributed point-to-point networks. Fortunately, current airline scheduling systems and the scheduling software utilized by fractional business jet operators enables the optimization of these types of networks on a regular basis.

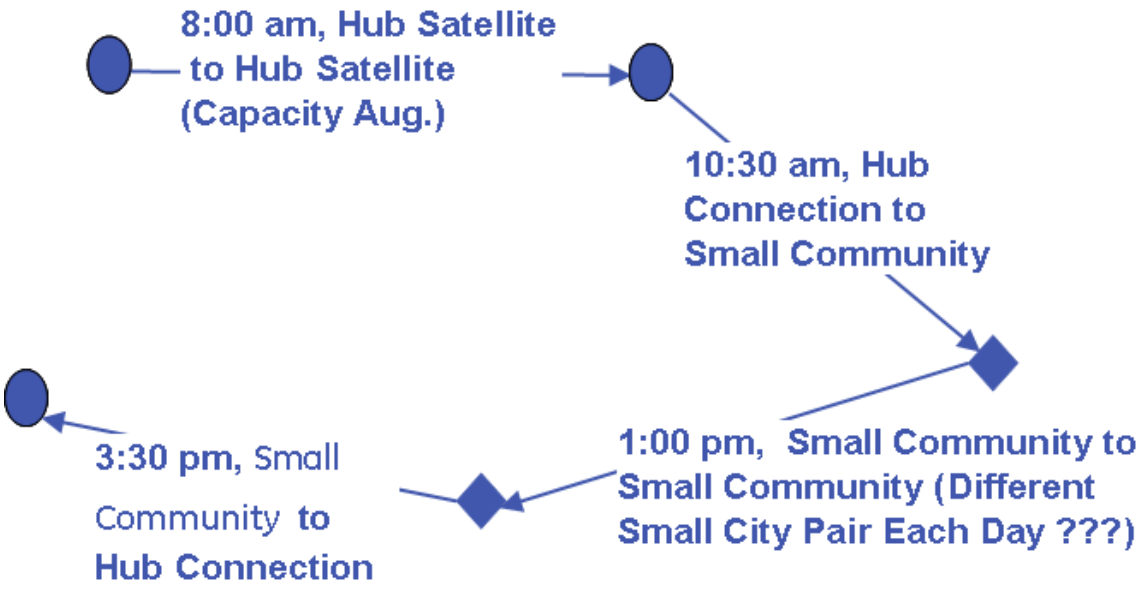

Figure 12. Notional Daily Schedule for Small Airliner

The variety of trip options presented here for small airliners also enables both an increase in overall air transportation network efficiency and an opportunity for the small airline to optimize the maintenance and support if its fleet. The transportation network efficiencies come from (1) the ability to deal with small increases in demand during peak periods, and (2) the reduction in total trip distance for many passengers. Providing capacity augmentation between hub communities with small airplanes enables both large and small aircraft to fly with large load factors. Route structures like the one presented in Figure 12, enable an operator of small airliners to bring the majority of its planes home to a maintenance facility in a large community every night. This enables the airline to streamline its maintenance services and reduce the required inventory of parts.

4.0 N+3 Network Demand and Capacity Study

Defining what the future aircraft and its network will look like requires due consideration of the market for this transportation approach. Defining how close to the demand we can bring the new service will ultimately dictate whether there is a future for such an endeavor. As such, demand modeling becomes a key element of this study.

4.1 Aviation Demand Modeling Methodology

A characterization scheme of air transportation called the "PACE" breakdown, illustrated in Figure 13, will be used to aide in discussion of air transportation demand models[1,2]. In this terminology, total enplanements E_i at airport i are divided into produced P_i, attracted A_i, and connecting enplanements C_i. It is important to note that total enplanements at a specified airport is not simply the sum of produced and attracted demand, but rather also a function of the air transportation network in the form of connection enplanements.

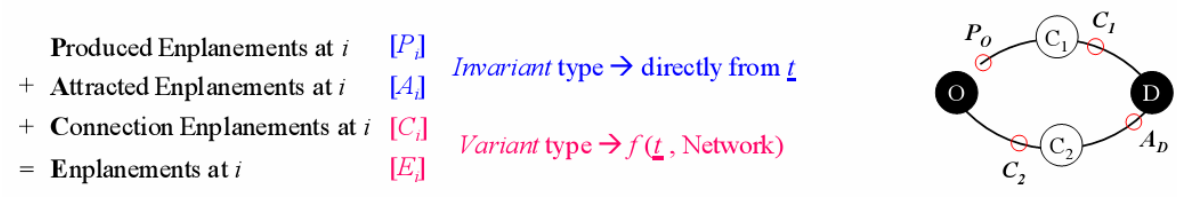

Figure 13. PACE Breakdown

The desire of a demand model in this study is to capture enplanements from origin to final destination, known as true Origin-Destination (O-D) demand, without confounding from the current network. This approach allows alternative network structures to be considered.

4.1.1 Gravity Law Based Approach

For the OEP 35 airports, a remarkably linear growth trend of attracted and produced enplanements was found between 1993 and 2005, with only total volume increasing (see Figure 14).[1,2] The ratio of attracted to produced enplanements (A_i/P_i), notably, is significantly greater for Las Vegas McCarran International Airport (LAS) and Orlando International Airport (MCO), which service areas with large tourism industries. Since the growth and declination of a region is usually gradual it can be theorized that A_i/P_i for an airport can be modeled with appropriate socioeconomic data of the surrounding area.

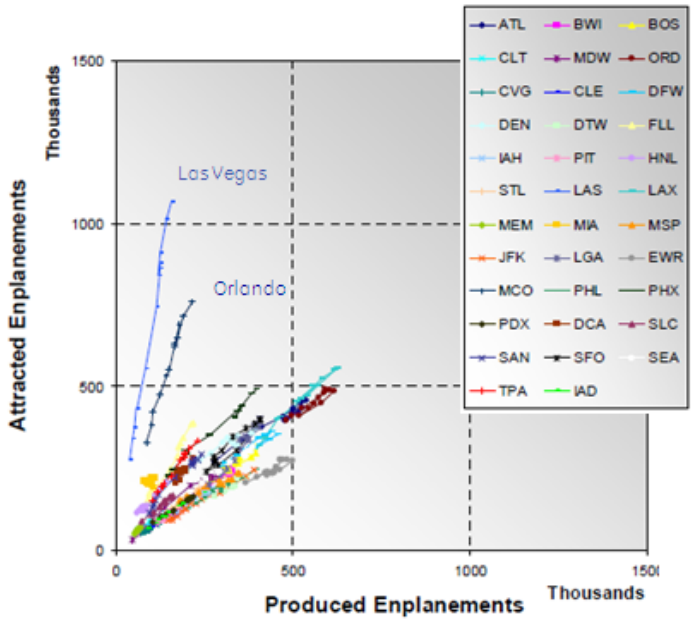

Figure 14. Growth of OEP 35 Airports from 1993 to 2005

A gravity law based approach, dubbed a push-pull model[2], has been used to calculate true O-D demand for the OEP 35 airports. The model theorizes that an airport pulls demand based on its distance from surrounding counties, the population of the counties, and the median income of the counties as illustrated in Figure 15. Overall produced demand at an airport is simply an aggregate of p_{ij} from surrounding counties, while p_{ij} is a simple function of the county's population, median income, and great circle distance from the airport. To model attracted enplanements of an airport, median income is replaced by the county's total revenue in several entertainment industry categories. As shown in Figure 16, the gravity law based approach showed satisfactory fits for both produced and attracted demand for the OEP 35 airports, with the exception of a select few satellite airports and aviation stars. T he results for year 2030, however, are solely dependent on socioeconomic projections of each region. With constant growth projections, the model predicts extreme demand at many airports, as shown in Figure 17. After calibration for smaller airports, the model could be capable of predicting future demand for air transportation based on simple socioeconomic projections. The level of geographic granularity of the gravity model is the county as socioeconomic data is readily available.

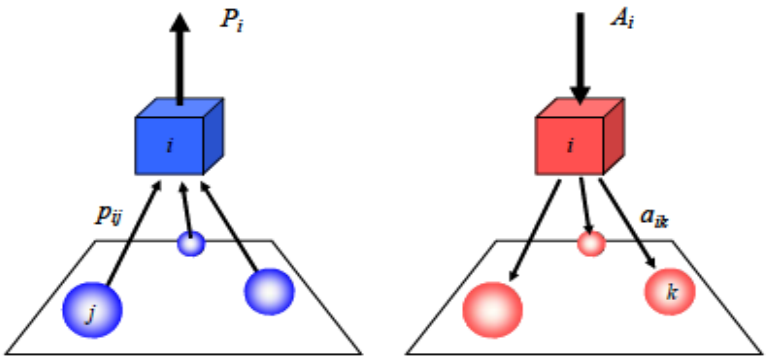

Figure 15. Concept of Gravity Law Based Approach

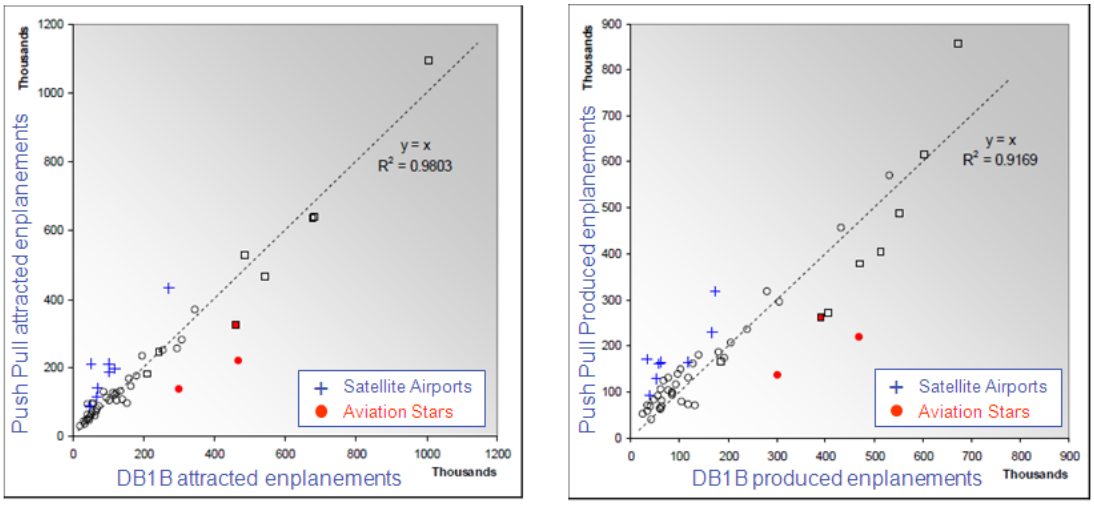

Figure 16. Model Results for OEP 35 Airports (Y1997)

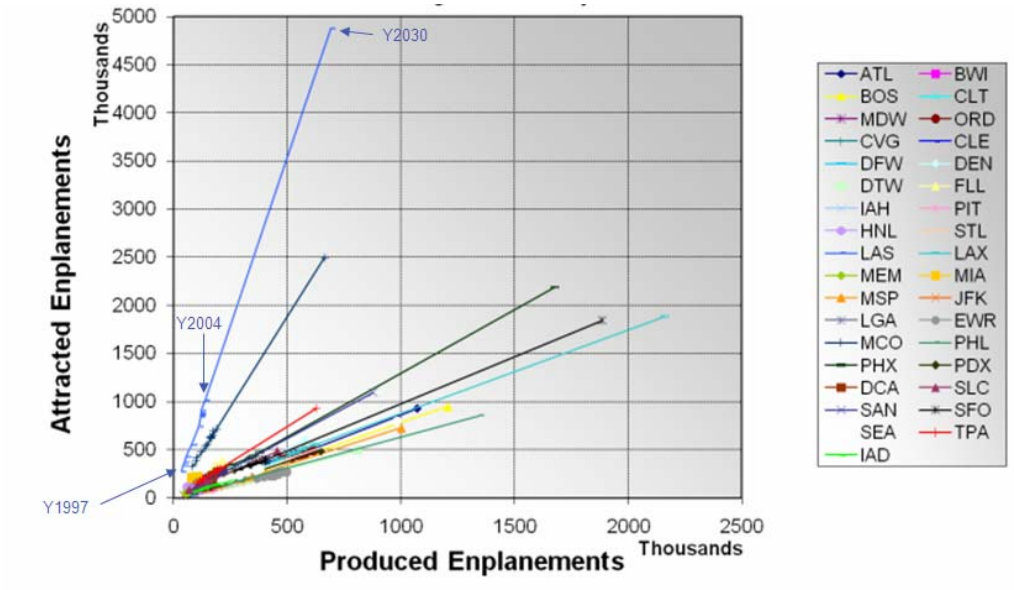

Figure 17. Projected Demand at OEP Airports

Since demand is simply a function of socioeconomic parameters, it is unclear whether the model could be adjusted to yield meaningful conclusions about the impact of vehicle and network design on consumer preference for the N+3. The model results for 2030 look quite outlandish, but this is because a constant growth rate was assumed. Furthermore, the regression used to calculate that growth rate was between the years 1997 and 2004 when airports experienced rapid growth. As the current recession has shown, there will likely be periods of small growth or even declining airport enplanements, which if they were taken into account this model may give more accurate results. Predicting these recessions and recoveries and accurate growth rates is beyond the scope of this study, but if it were performed this model would give more accurate results.

For this study, a fundamental factor that needs to be considered is how consumers will choose one mode of travel from another. Since the gravity law based approach does not include a modal choice selection algorithm, it cannot produce the desired results necessitating consideration of a different model.

4.1.2 Agent-Based Approach

While the gravity law based approach efficiently provides true O-D demand between major city pairs, it is unable to account for fundamental shifts in consumer behavior. A relationship between enplanements and socioeconomic metrics like median income, population and entertainment indices will certainly continue to exist, however, the calibration coefficients valid for 1997 are likely to change in three decades. In addition, the limited number of variables in the gravity law model makes sensitivity analysis difficult, as any variation in future scenarios must be mapped to population estimates, median income data, and entertainment indices. Thus, for a more in depth sensitivity study of air transportation demand in 2030, a model that can capture consumer behavior for a wide range of scenarios is preferable.

To this end, an agent-based approach, in which individual consumers are represented as agents with prescribed geographic, demographic, and socioeconomic properties, is promising.

One such a model is called ***Mi***, which was originally developed to study the effects of design requirements of personal air vehicles under the ground rules from NASA's SATS program (References 3 and 4) and has since been expanded to capture general aviation demand (see References 5 and 6 for details). The latest version of ***Mi*** applies spatial explicitness with a granularity of the Metropolitan Statistical Area (MSA) and assesses the interaction between commercial air transportation supply and demand (References 7 and 8). Agents are distributed into a virtual continental United States (CONUS) environment and assigned socioeconomic properties based on statistics of publicly available data. Each agent operates in a dynamic environment, selecting a list of desired trips, executing trips it can afford to take, and choosing a transportation mode based on a mobility budget space concept; specifically, the agent must never exceed a total travel time and cost, the values of which are specified based on the agent's socioeconomic properties. The agent-based model has been validated against the 1995 American Travel Survey (ATS) modal split (air and ground transportation) data (Reference 9).

The goal of this study is to obtain meaningful sensitivities of demand for the N+3 service to both design and external factors. As the only variables in the gravity law model are population, median income, and entertainment indices, sensitivities could likely only be obtained for external socioeconomic factors. The bottom-up agent-based model, on the other hand, simulates the consumer decision making process, accounting for the numerous factors that affect modal transportation choice. As such, sensitivities to controllable variables of a future air transportation system, such as ticket price, travel time, and flight range, along with sensitivities to external factors, like population and income growth rates, can be obtained. Further, since the transportation mode decision making process is a function of time and cost savings, incorporating a new N+3 mode would simply give agents another option. For these reasons, the agent-based model ***Mi*** was selected for use in this study.

4.1.3 Agent-Based Modeling of the National Transportation System

In order to determine the consumer preference for a future small aircraft operating in a point-to-point network, the hypothetical N+3 service must be evaluated against competing modes of travel. Therefore, the intermodal and multimodal relationships between traditional hub-and-spoke air transportation, automobile ground travel, and the N+3 service must be understood. For the purposes of this study, maritime, bus, and train travel were assumed to capture minimal modal share. It is quite evident that both the National Airspace System (NAS) and national highway system are individually complex systems with poorly understood macroscopic behavior. Thus, to evaluate the relative attractiveness of a new aviation service, it was hypothesized that a bottom-up, agent based approach should be utilized to capture emergent behavior of the multimodal transportation system. This approach aims to replicate the individual consumer decision making process of whether to travel, and if so, by which mode.

In ***Mi***, transportation consumers are represented as agents whose properties are sampled from geographic, demographic, socioeconomic distributions. Calibrated to the travel propensity of American families and enterprises as reported by the 1995 American Travel Survey, each agent generates a list of desired trips. A mobility budget space concept, in which an agent cannot exceed a prescribed total travel time or cost, determines whether the agent actually takes the trip. Finally, the agent selects the best mode of travel according to a multinomial logit model. Each agent can pick from three transportation modes: ground transportation by automobile, commercial air transportation, and the N+3 service provider. The ***Mi*** framework is shown in Figure 18. These travel options are described in further detail in later sections.

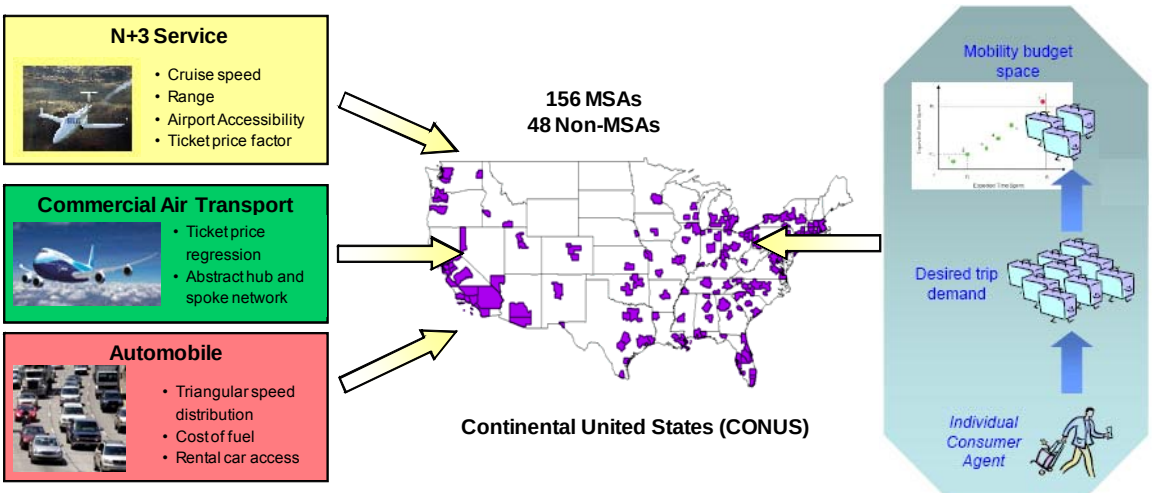

Figure 18. Agent-Based Model *Mi* Framework

4.1.3.1 Consumer Agents

For reasons related to calibration and computational resources, the MSA definitions in the 1995 American Travel Survey are chosen as the level of physical granularity[1]. The ATS MSA granularity was extended to include non-MSA locales, grouped at the state level. Therefore, this study has a CONUS scope constituted by a collection of 156 MSA locales and 48 non-MSA locales. These 204 locales are represented as coordinate-specific nodes in the model, where consumer agents are statistically populated into these locales using 2000 U.S. Census demographic data. Each consumer agent represents a single household and is unique in that it possesses a unique geographic location, income level, and travel budget. The origin coordinates of consumer agents populated in non-MSA locales are determined using an agent displacement method that assumes a probabilistic displacement in the shape of a circle centered at the population centroid, with a radius calculated based on land area.

Consumer agents are further categorized as either household agents or enterprise agents, which generate personal and business trips respectively. The number of households and business establishments throughout the 204 locales serves as the probability density function for determining the origin coordinates of household and enterprise agents respectively. According to the U.S. Census Bureau (1997) and Office of Advocacy (1999), there were a total of 93.3 million households and 6.18 million business establishments in the U.S. in 1990. Households, instead of individuals, are used as the consumer agent unit. This is justified as personal trips are often taken with family members, travel decisions are usually a collective decision of a household, and a reduced number of agents ease the computational burden of simulation. Personal trips are further divided into personal business and leisure trips, similar to the categorization of the 1995 ATS.

To replicate the true socio-economic picture of the population in a given locale and maintain individualism of the agents, a unique value for income is sampled from an income distribution model of the corresponding locale. This model is based on translating historical income

[1] In general, MSAs are defined and updated by the U.S. Office of Management and Budget as a core urban area with a population of 50,000 people or more and a typical MSA consists of the counties containing the core urban area as well as any adjacent counties that have a high degree of social and economic integration with the urban core.

distributions into continuous cumulative distributions. Income distributions are well-fitted to a piece-wise function of the Richards growth model for the lower income groups and a Pareto model for the higher income groups (Reference 5).

4.1.3.2 Transportation Modes

Three transportation options were offered to the traveler agents: Ground Transportation capturing the essence of driving in a personal car, Commercial Air Transportation representing the hub and spoke network, and the N+3 Service embodying the proposed new mode.

4.1.3.2.1 Ground Transportation

The 2001 National Household Travel Survey conducted by the U.S. Department of Transportation (DOT) and the Bureau of Transportation Statistics (BTS) reported that over 97 percent of all long distance trips less than 300 roundtrip miles are performed by personal vehicles (Reference 9). Since that time, longer security lines and takeoff delays have undoubtedly only decreased the modal share of air transportation in short range trips. Thus, in these short-range scenarios, where commercial air services cost more money and do not provide adequate time savings, agents immediately select the automobile modal choice.

Unlike the N+3 service and commercial air transportation, it is assumed that all agents have access to ground transportation, whether it be by personal or rental automobile. Several other assumptions were made prior to calculating ground transportation utility.

- Driving distance is assumed to be 1.25 times the great circle distance computed from the origin and destination coordinates.
- The automobile speed for each agent is probabilistically sampled from the triangular distribution Δ{50, 55, 60} mph.
- An overnight stay with incurred time and cost is added to trips via a piecewise probabilistic function with respect to travel times.
- The cost for automobile personal trips is primarily the cost of fuel, while business trips follow the Internal Revenue Service compensation rate.

4.1.3.2.2 Commercial Air Transportation

The conventional air transportation mode is implemented to emulate the effect of the traditional hub-and-spoke system, namely city pairs with large airports are afforded nonstop flights. Note that general aviation is not included as a travel option, as 1995 ATS data reveals its modal share was only about 0.7%. Further, General Aviation Manufacturers Association (GAMA) data[11] suggests that more than three quarters of general aviation trips are made by the aircraft owners. In order to capture the true air transportation options available to the consumer agent, air transportation is not offered to consumers that are extreme distances away from airports with current commercial service. A polynomial pricing function of airport to airport flight distance, regressed from historical air fare data, is used to generate air fares for commercial air routes.

Airport objects, constructed from a list of large, medium, and small hub airports provide geographic specificity to the network. As part of a doorstep-to-destination concept, the profile for air transportation trips was decomposed into the mission and secondary ground legs. The mission leg refers to the actual trip distance traversed from the origin airport to the destination airport. The block speed along the mission leg is probabilistically sampled from the triangular

distribution Δ{400, 425, 450} mph. The secondary ground leg is the trip distance traversed from the origin location to the origin airport and from the destination access point to the destination. The consumer agent is offered personal automobile, rental car, and taxi options for this secondary leg.

4.1.3.2.3 N+3 Service

The hypothetical N+3 service operates in a point-to-point network and utilizes a converted business jet; thus it is quite difficult to predict the consumer reaction to such a service, unlike ground automobile and commercial air transportation. It was decided that a preliminary study of consumer preference, such as this one, should focus on the basic time and economic characteristics of the N+3. Thus, the N+3 service was set up to be readily available within a specified distance of a network airport. According to the U.S. DOT, 78% of the U.S. population lives within 20 miles of an airport with commercial service, and 98% is within 20 miles of any National Plan of Integrated Airport Systems (NPIAS) airport[12]. Note that, for remote locations with low levels of demand, some of these airports may not be able to profitably sustain an N+3 service. Additionally, previous studies show that a significant minority of these airports have runways under 4000 ft long or 75 ft wide, preliminary target goals for takeoff length of a small N+3 jet aircraft. Therefore, the airport accessibility distance was varied as part of the sensitivity study.

The ticket price is considered an independent variable, and is referenced to a commercial air ticket in terms of a price multiplier. In reality, ticket price is a function of, among other factors, vehicle design characteristics and especially vehicle capacity, as a larger vehicle can capture demand at a lower per passenger cost. For the purposes of this preliminary sensitivity study, the effect of vehicle capacity on ticket price is ignored. Thus, rather than captured demand, the simulation result should be interpreted as the consumer preference for an N+3 service if it was readily available within the airport accessibility distance.

4.1.3.3 Trip Distribution and Mode Selection

Figure 19 shows the behavioral rules that govern transportation consumer behavior. The 1995 ATS delineates distributions of trip party size, trip frequency, and trip purpose. A large list of desired trips is distributed to the consumer agents using a gravity based model and calibrated to 1995 ATS O-D matrices. However, it is clear that not all of these trips would be performed due to time and monetary constraints. To generate a list of actual trips taken from the desired trip list, a mobility budget space concept is utilized, in which an agent cannot exceed a total travel time or travel cost, the values of which are specified based on the agent's properties. This is illustrated in the bottom of Figure 19. The mobility budget space imparts rational behavior to the agents to replicate the decision making process when considering a trip. The set of desired trips for each agent are executed one at a time until a maximum allowable trip cost or time threshold is exceeded. The time and cost utilization of each executed trip is recorded, which reduces the remaining mobility budget of the agent. For this study, the mobility cost threshold for each agent is sampled from a triangular distribution centered at a mean value of four percent of the agent's household income, with a range between 3.2 and 4.8 percent. The time threshold is similarly sampled, with the center starting at a baseline value of 100 hours a year and progressively adjusting for each agent based on actual time spent during pre-simulation calibration.

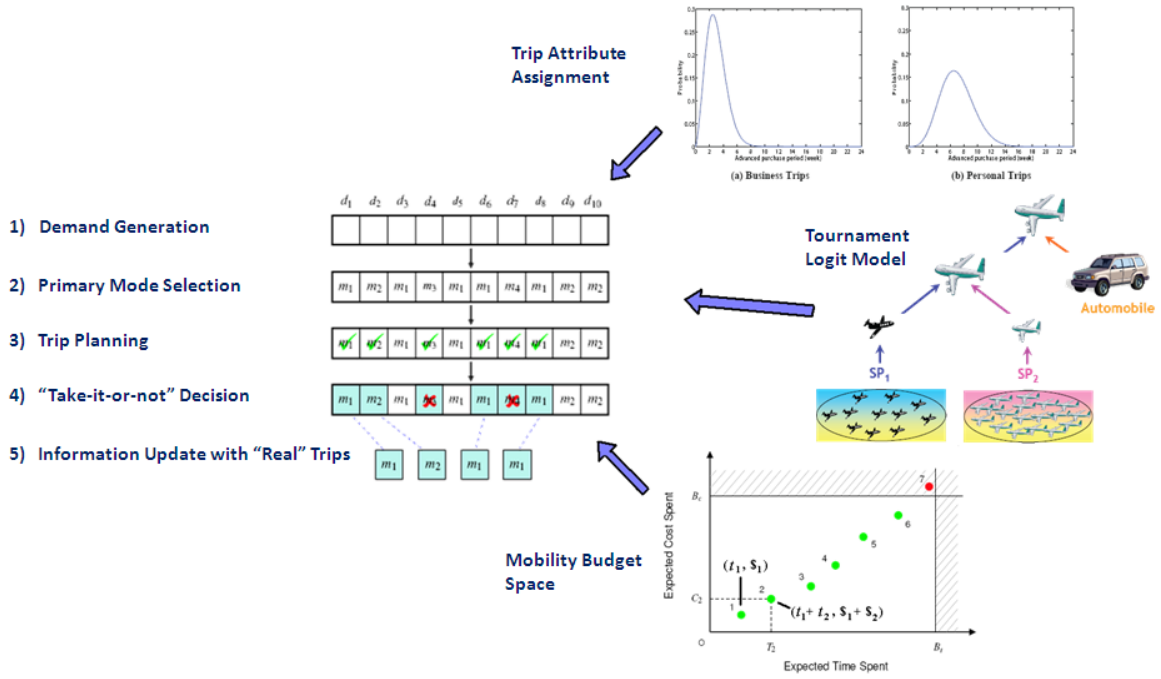

Figure 19. Transportation Consumer Behavioral Rules

The modal choice method that consumers use for executed trips is based on utility theory and a multinomial logit (MNL) model. The basic premise of utility theory is that a consumer logically chooses the mode of travel that offers the highest utility in terms of time and money savings. A utility function, which represents the attractiveness of each transportation mode to the traveler, is hard to directly quantify. However, a disutility function using the time and cost metrics as the mobility budget space is easier to assign. The disutility function of each mode is defined by Eq. (1) below.

$$D(t,c) = -V(t,c) = c + v_t * t \qquad (1)$$

where v_t = value of time, c = trip cost, and t = trip time

With the disutility function of each mode defined, the probability of selecting each transportation mode option is obtained using the tournament logit model[6]. The best offering of each service provider is chosen, and each is entered into a higher level competition. This nested model is therefore unbiased against the number of options offered by each service provider. At the higher level competition between modes, the probability of selecting a mode is given by Eq. (2) below. The calibration constant was determined to be 0.018 after calibration to 1995 ATS data.

$$P(mode_i) = \frac{e^{\alpha V(mode_i)}}{\sum_{j=1}^{n} e^{\alpha V(mode_j)}} \qquad (2)$$

where V = deterministic utility, n = number of modes, and α = calibration parameter

4.2 Consumer Preference Sensitivity Analysis

The goal of this study is to observe the main factors that affect the viability of a future small aircraft operating in a point-to-point network. To this end, the sensitivity study will be performed for the year 1995 and for the year 2030, utilizing practical predictions of population and income growth. Four independent variables were considered for the sensitivity study: vehicle cruise speed (V), vehicle range (R), airport accessibility distance (d), and a ticket price factor (X), referenced to average commercial airline ticket price. In the model, required travel distance to the airport is sampled from the triangular distribution $\Delta\{1, d, 20\}$ miles.

4.2.1 Simulation Parameters

For this preliminary study, each of the four independent variables is varied from its baseline value one at a time.

- X = [0, 1, 2, 3, 4, 5, 6, 7, 8], Baseline: X=3
- V = 344 * [80%, 100%, 120%, 140%] knots, Baseline: V=344 knots
- R = [400, 800, 1200] nmi, Baseline: R=800 nmi
- d = [5, 10, 15] miles, Baseline: d=10 miles

The target year for the N+3 service to begin operation is 2030, so the agent based model was updated with predictions of population and income for that year. The U.S. Census Bureau has projected a national population of 363,584,435 for the year 2030. The challenge, however, is to get county-level population forecasts. There are some proprietary sources that have county-level forecasts, but they are expensive and inhibit sharing of information and data. The highest granularity population forecasts publicly available are for each state and put out by the census bureau. Some states make their own county-level forecasts publicly available, but not all and there is no standard as to how the forecasting is done or the number of years that are forecasted. Therefore, for this application it was necessary to devise a way of forecasting county level populations that would add up to the state level forecasts. A simple solution would be to uniformly increase the population of each county in the state to match state forecasts. This method, however, is crude at best and ignores the shifting of population centers from rural to urban areas. In addition the final results after running Mi for the 2030 year based on this population forecast method would have little difference aside from volume if this method were used, making the effort of trying to uses appropriate values for the year 2030 unproductive. Another method would be to assume the same growth rate for each county from 1990 to 2000 applies all the way out to 2030. This method, however, when the population is summed for all the counties throughout the state gives a wildly different result than the Census Bureau's state forecasts. Instead, the approach taken was to use historical trends of each county's growth rate normalized by the state's population forecast to obtain county population forecasts that are consistent with both historical trends for each county as well as the overall trend for the state. This method is labeled as the hybrid method. Results of the different methods for a few select counties are shown in Table 4.

Table 4. Example of a County Population Forecast

State	County	Census 1990 Pop	Census 2000 Pop	Uniform State Growth Rate 2030 Forecast	Constant County Growth Rate 2030 Forecast	Hybrid Method 2030 Forecast
Georgia	Fulton	648,951	815,844	1,197,671	1,621,036	1,190,166
Ohio	Logan	42,310	46,005	46,805	59,141	47,446
Alabama	Autauga	29,592	37,412	41,005	75,600	45,629

The forecast method chosen for projecting personal income growth was to use national GDP per capita as a multiplication factor on personal income and apply that uniformly to the entire United States. While county level population forecasts were lacking, county-level personal income forecasts were non-existent. Most people are reluctant to project personal income growth even 1-2 years out. Due to this, a broader treatment of personal income growth was required. Since GDP is only forecast to 2019, however, an additional 11 years must be forecast. As the economy matures the year-on-year growth rate of GDP should become less volatile. This can be observed in Figure 20, which shows the year-on-year changes in real GDP per capita for the United States. A 1.5% year-on-year growth rate between 2019 and 2030 was assumed.

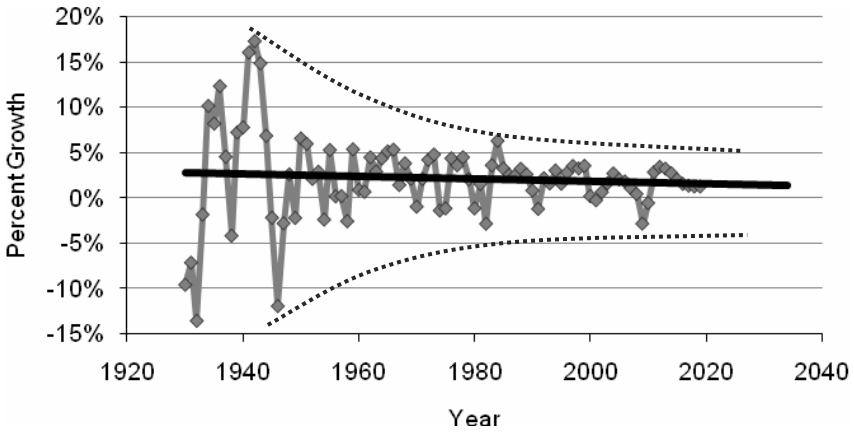

Figure 20. 2030 GDP Prediction -- YoY Changes in Real GDP Per Capita

4.2.2 Sensitivity of Modal Share to Ticket Price Factor

The agent-based simulation, stochastic by nature, was run with enough agents to obtain a stable response. Note that this study is limited in scope to sensitivity of market capture and total trips to design factors; thus it is not important for the actual cells within the O-D to be stable. A number of agents that corresponds to a half day sample of the national transportation system is sufficient for modal shares to reach equilibrium. Once the simulation is complete, the number of trips for each range segment can be added to calculate overall modal share of business air, business auto, personal air, personal auto, and the N+3 service. To simplify analysis for this study, business and personal trips are combined. Figure 21 shows the modal share distribution of trips between airline (ALN), automobile (AUTO), and N+3 modes for varying N+3 ticket price factor.

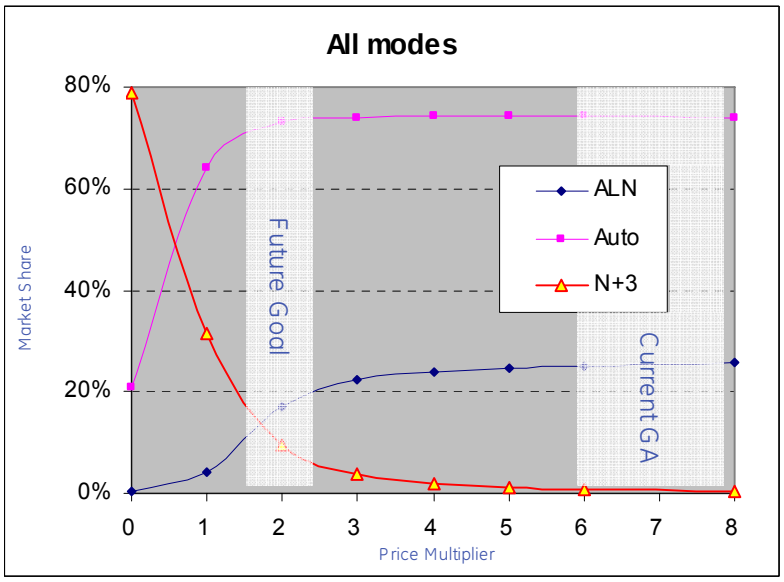

Figure 21. Modal Share Distribution

The first important characteristic of this result is the relative stability of all modal shares when the ticket price factor is greater than 3. At high ticket prices, an N+3 service would resemble general aviation and charter services of today, with less than 1% market share. Between a ticket price factor of 2 and 3, the N+3 service begins to capture market share of airlines. However, the market share of automobile travel does not significantly decrease until ticket price factor is near 2. In order for the N+3 to transform the national transportation system, it must cross this consumer perception threshold to capture market share from the automobile mode, especially since the N+3 would operate at ranges where automobiles are utilized more than airlines. Note that a ticket price factor of just under 2 also corresponds to the inflection point of the airline market share curve.

A closed form approximation of N+3 market share for varying ticket price factor is obtained from a piecewise approximation function, shown in Figure 22, with an exponential fit for price multipliers below 3 and a power fit for those above 3. Solving the elasticity equation with a constant *e* yields the power equation, as can be seen in Eq. (3). Therefore, elasticity of N+3 market share is constant at (-)2.7 for ticket price factors above 3.

$$e = \frac{\frac{dy}{y}}{\frac{dx}{x}} = \frac{dy}{dx}\frac{x}{y} \rightarrow y = c_1 x^e \qquad (3)$$

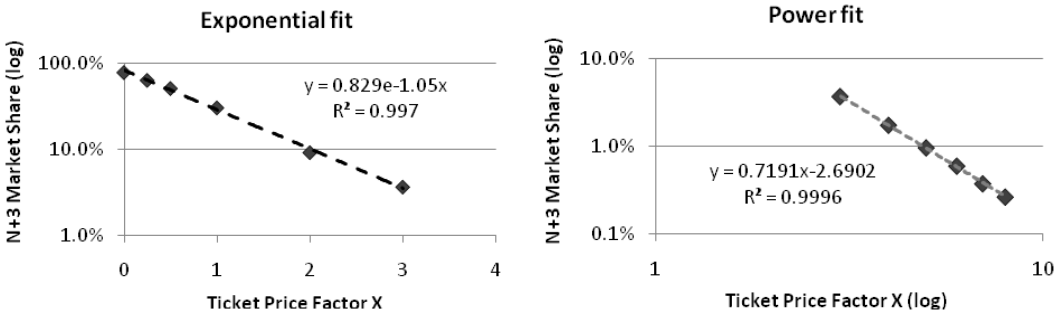

Figure 22. Piecewise Approximation Function

The price elasticity calculated for the airline service provider was (-) 0.7, while that of the N+3 service was (-)2.7. A price elasticity of (-)0.7 for a typical air service provider is consistent with a number of other studies as indicated by the histogram in Figure 23. This validates that the agent-based demand model is capable of producing realistic price elasticities for air travel. An elasticity of (-)2.7 for the N+3 service is on the high end of airline service elasticity, but this is to be expected given the higher price and convenience of a point-to-point service and a smaller accessibility distance.

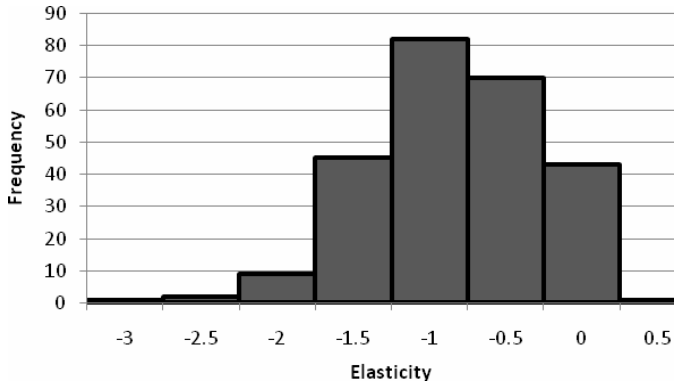

Figure 23. Elasticity Distribution for Air Travel from Past Studies[13]

4.2.3 Elasticity of Demand to Other Simulation Variables

Each of the other independent simulation variables were perturbed from their baseline values one at a time. Using the definition of arc elasticity, given in Eq. (4), a tornado chart of N+3 modal share elasticity to the independent variables is obtained.

$$e^{a} = \frac{\ln y_2 - \ln y_1}{\ln x_2 - \ln x_1} \qquad (4)$$

As seen in Figure 24, the ticket price multiplier is clearly the dominant factor that drives potential N+3 market capture. It is also important to note that N+3 modal share is penalized more for a 20% reduction in cruise speed than rewarded for a 20% increase. The airport accessibility distance and vehicle range appear to be secondary factors at this aggregate level of analysis.

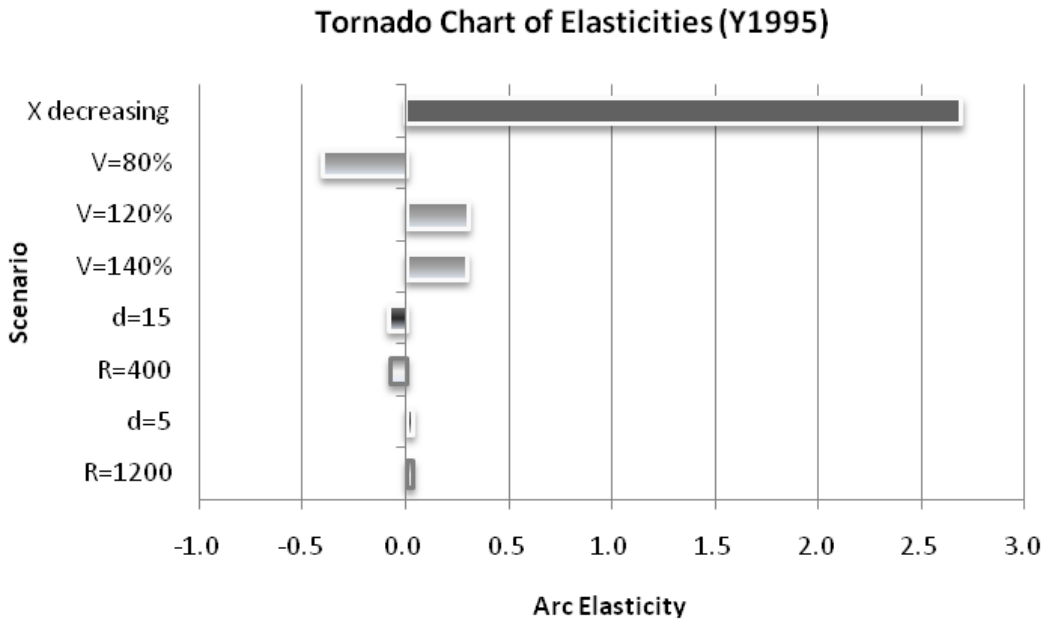

Figure 24. Elasticity of Demand to Simulation Parameters

4.2.4 Sensitivity of Modal Share to Cruise Speed

The distribution of trips across trip distances is useful to determine which market segment is most affected by perturbations in the design variables. The distribution of trips for two cruise speed scenarios, using 50 mile trip distance bins, is shown in Figure 25. For short range trips under 300 miles, cruise speed has negligible effect on trip demand, as airport accessibility, waiting times, and takeoff/landing activities constitute a larger time segment of the trip. A log plot helps to expose the relative impact of the velocity perturbations on N+3 trips. The two distributions do not begin to diverge until trips of over 1000 mile, which is approaching the maximum range envisioned for the N+3 vehicle.

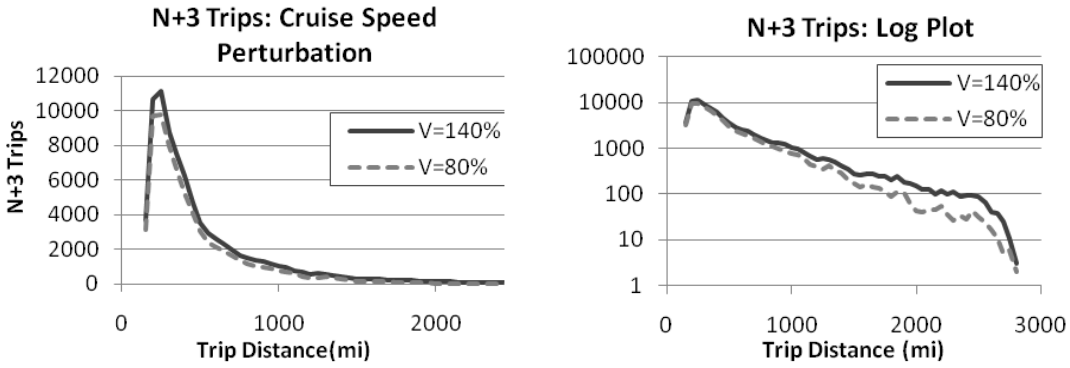

Figure 25. Sensitivity of Demand to Cruise Speed

4.2.5 Sensitivity of Modal Share to Range

For N+3 trips longer than the design range, an hour time penalty was assigned to account for refueling or transfer times. Thus, as seen in Figure 26, there are near identical distributions of trips below 400 miles for R = 400 and R = 1200 nm. For perturbations in range, only the market segment of trip distances between the perturbation points sees a significant difference in modal share. This difference is surprisingly small considering the sizeable time penalty assigned; however, it is likely that both negative consumer perception of a non-direct route and additional operating costs would render this network structure infeasible.

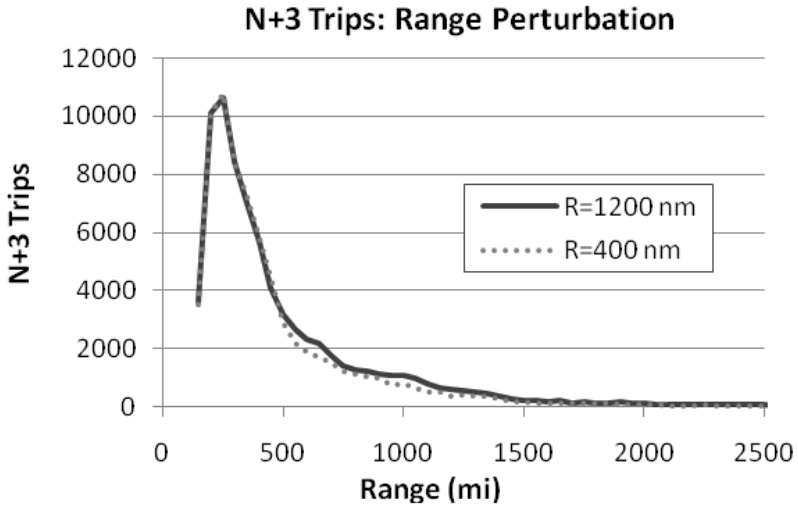

Figure 26. Sensitivity of Demand to Range

4.2.6 Simulation Results of Y2030 Scenario

For the simulation of travel modal choice in 2030 using income and population growth factors, the most important result is the growth of travel modes relative to each other. Figure 27 shows the volume of trips for each travel mode in 1995 and 2030. Regardless of ticket price factor, the N+3 mode is the biggest beneficiary of income and population growth, with a trip growth factor of 4. T he observed airline growth factor of 2X is consistent with predictions by the JPDO. It can be concluded that with economic expansion, consumers can better afford the more luxurious travel modes of airline and N+3. Price elasticity of demand for the N+3 service slightly decreases for the 2030 simulation settings, as seen in Figure 28. This observation is consistent with the basic economic theory that price elasticity of demand generally decreases with increased wealth. Otherwise, the elasticity of N+3 demand to the simulation parameters remains remarkably consistent from 1995 to 2030. Note that it was assumed that air and ground transportation in 2030 would closely resemble the status quo of 1995; delay times were not assumed to become more severe, even with the 2X increase in demand for commercial air transportation.

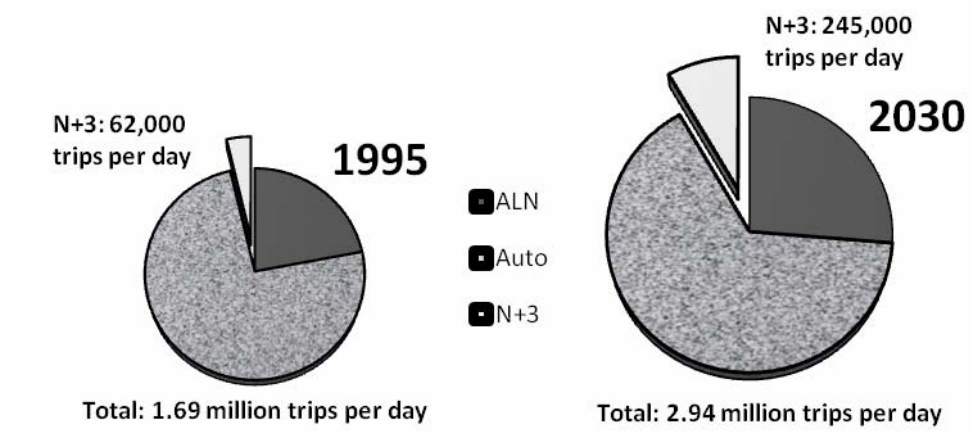

Figure 27. Growth of Transportation Modes from 1995 to 2030 (for X = 3)

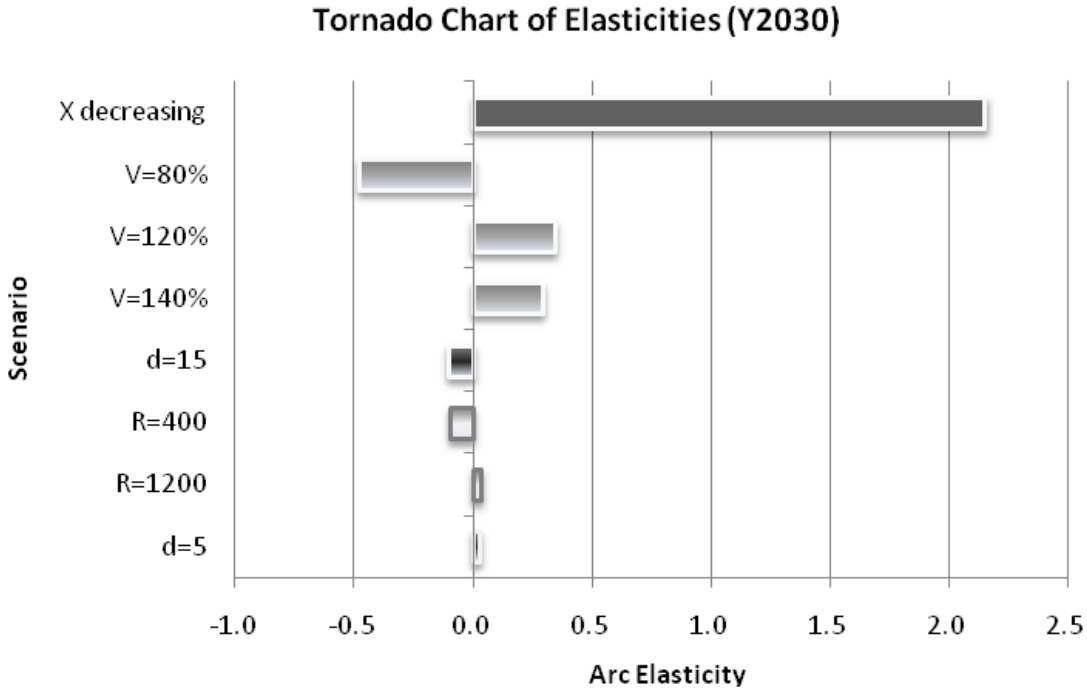

Figure 28. Elasticity of Demand to Simulation Parameters: 2030

4.2.7 Delay Sensitivity Study

A probabilistic treatment of delay was considered in order to observe the effect of delays of each mode. Two main parameters were adjusted to account for future scenarios:

- On-time reliability (perceived): Consumer's perception of how frequently a mode is on-time
- Delay distribution (perceived): Consumer's perception of the delay time they would likely experience

The results of the sensitivity study of each mode to delay are shown in Figure 30 and Figure 31. N+3 modal share increases from 11.6% to 14.4% when delays for ALN and Auto modes are increased from no delay to the 3X delay scenario.

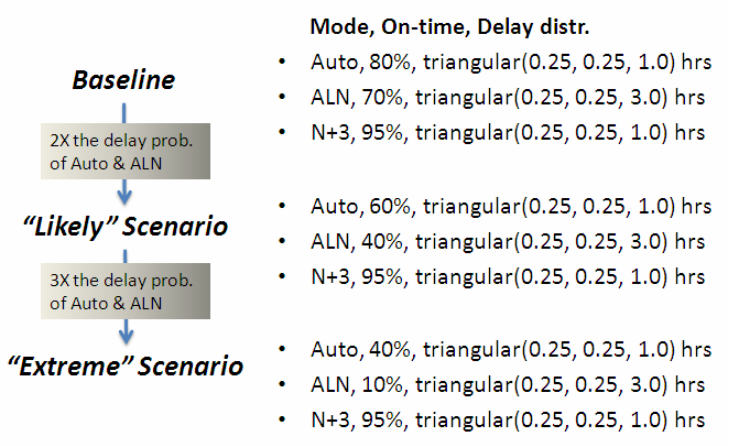

Figure 29. Delay Scenarios

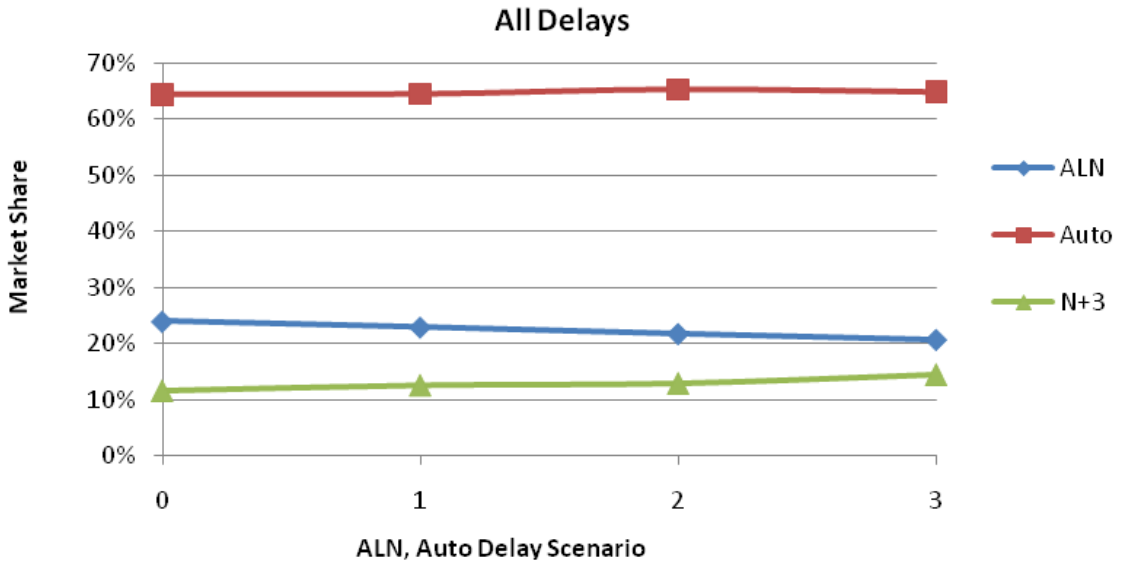

Figure 30. Modal Split (both ALN, Auto delayed)

Airline and auto delays were independently varied one at a time as shown in Figure 31. Increasing auto delays had a small effect on the modal split due to the perceived convenience of driving vs. other modes. Varying airline delays had a larger effect, with the market share lost by the airline being evenly redistributed between automobiles and the N+3 service.

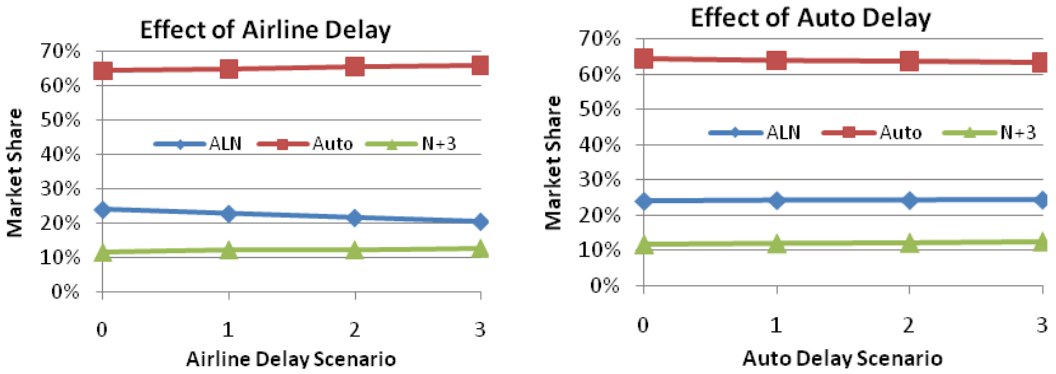

Figure 31. Modal Split (ALN, Auto delayed one at a time)

4.2.8 Conclusions of Consumer Sensitivity Study for N+3 Service

Using a bottom-up agent based approach, the demand for an N+3 service was calculated from a consumer preference standpoint, theorizing that transportation modes are evaluated by rational customers looking to maximize the utility constrained by travel time and cost budget. Consumer preference for the hypothetical N+3 service was quantitatively shown to be most sensitive to the economic metric of ticket price. Two analytic equations emerged that predict N+3 market share as a function of ticket price factor, revealing an elasticity of demand to ticket price consistent with expectations. Further, it was shown that cruise speed and range only have a significant effect on consumer demand for long distance trips, while the N+3 mode is primarily meant to capture commercial aviation and ground automobile market share for short and medium range trips. A significant advantage of the agent-based approach proved to be its ability to be extended to a 2030 timeframe with simple projections of population and income growth, enabling analysis of modal volume trends. While the sensitivity of market share to the design variables remained similar to the 1995 simulation, it was shown that growth of the N+3 mode of travel outpaced commercial air and ground transportation.

While this sensitivity study exposed the relative impact of main design parameters on modal preference, it did not answer the question of whether the N+3 service is viable. Two assumptions were made that prevent closed loop analysis of true captured market share. First, it was assumed that the N+3 service would be readily available within a small airport accessibility distance. In reality, however, the N+3 service can only offer point-to-point service to routes that have enough O-D demand to satisfy a threshold load factor for profitability. Second, ticket price of the N+3 service was treated as an independent variable. Without considering cost, a smaller aircraft could service more routes at a higher load factor, increasing market share of the N+3. But a small aircraft would undoubtedly result in a higher ticket price due to the economy of scale. To better understand the feasibility and the viability of an N+3 point-to-point service, a tradeoff analysis will be required between vehicle size, ticket price, eligible airports, and true O-D demand. The agent based model, as described in this study, is able to generate O-D matrices of true demand; however, the granularity level of these matrices remains at the MSA level, with state-level non-MSA locales. Therefore, the next level of analysis is the expansion of these O-D matrices to a higher level of granularity and selection of under-utilized airports that are compatible with the proposed aircraft. With basic assumptions about the structure and corresponding demand capture ability of an N+3 network, metrics such as load factor and aircraft utilization hours can be calculated, yielding a better understanding of the relationship between vehicle capacity, ticket price, and N+3 viability.

4.3 Capacity Study: N+3 Network

In this study, the tradeoffs between demand for a future point-to-point air transportation system and aircraft capacity are examined. The overall procedural description of the present study is summarized by the flowchart in Figure 32 where three phases are shown as analysis break points, each with an increased level of fidelity.

The study starts with tradeoff inputs such as aircraft capacity, speed, range, etc. Ticket price will be calculated as a function of vehicle capacity for the LEAF notional, single-engine converted business jet concept. This information will feed forward to the agent-based demand model that produces responses including consumer preference for the given aircraft; a simple algorithm will be used to derive true origin-destination (O-D) demand between 156 Metropolitan Statistical Areas (MSAs) and 48 non-MSA locales. The output of this Phase A is a simple analysis of passengers per day and operations per day for the notional point-to-point network.

However, this analysis assumes that that the point-to-point service is readily available to the agents. If demand for the point-to-point service within an MSA or non-MSA is sparsely distributed, an airline likely could not profitably serve these areas. Thus the concept of demand density is introduced to filter the raw demand numbers into a feasible estimate of captured demand. After this filtering process, the number of operations of the notional aircraft for varying passenger capacity gives a better indication of the attractiveness of different aircraft sizes to an airline. (Phase B)

In order to fully analyze the relationship between aircraft size and the notional point-to-point network, individual routes in the O-D matrix should be analyzed. However, the output of agent-based analysis contains non-MSA locales that are not spatially explicit; additionally, some MSAs are too geographically large to be considered a point source of demand. In order to convert the O-D matrix to a higher geographic granularity, a population clustering approach is introduced as part of Phase C of this study.

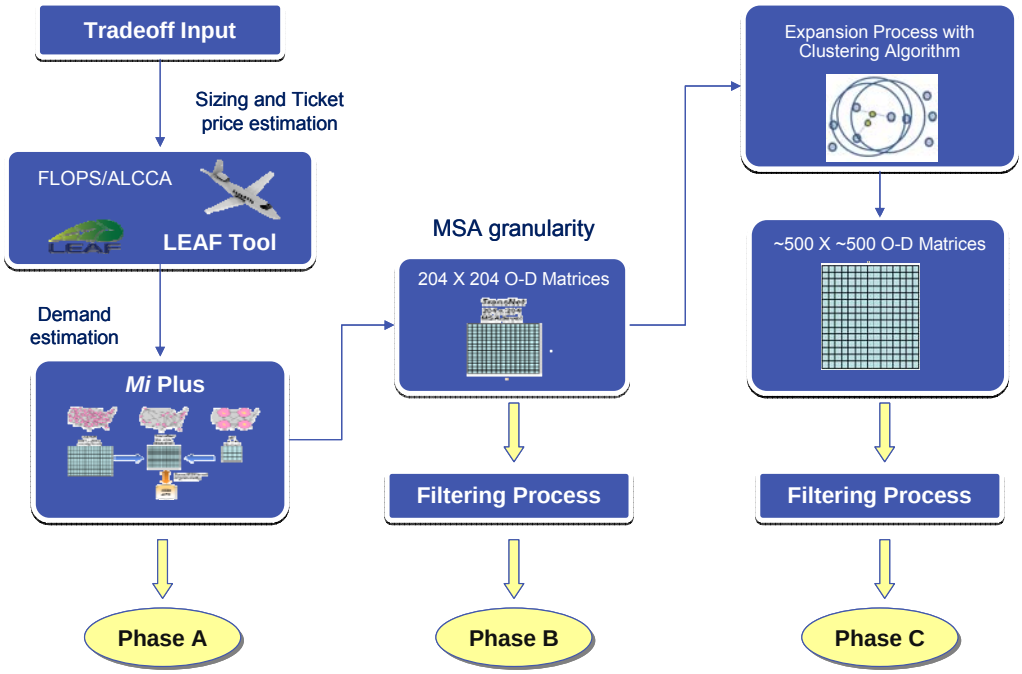

Figure 32. Overall Research Process

4.3.1 Model Ground Rules

4.3.1.1 Notional N+3 Aircraft

In order to proceed with the aircraft capacity study, a notional aircraft concept with known performance is needed. An advanced vehicle concept was selected via an interactive Reconfigurable Matrix of Alternatives. Figure 33 shows the product of this effort, a small aircraft with laminar flow wings, a V-tail for noise shielding, and a single fuselage-mounted high bypass ratio turbofan. This aircraft configuration was chosen to balance stringent NASA environmental and performance goals for the N+3 (2030-2035) time-frame. Such a concept relies on regulation changes to allow commercial operation of single engine (and single pilot) aircraft. Note that the analysis contained within this study is relevant in spite of configuration differences since the only output from the vehicle analysis to the demand and network modeling is the ticket price variation as a function of size. It is expected that this trend would be consistent for other configurations in this aircraft category and only the actual scale of the price would be sensitive to the aircraft performance.

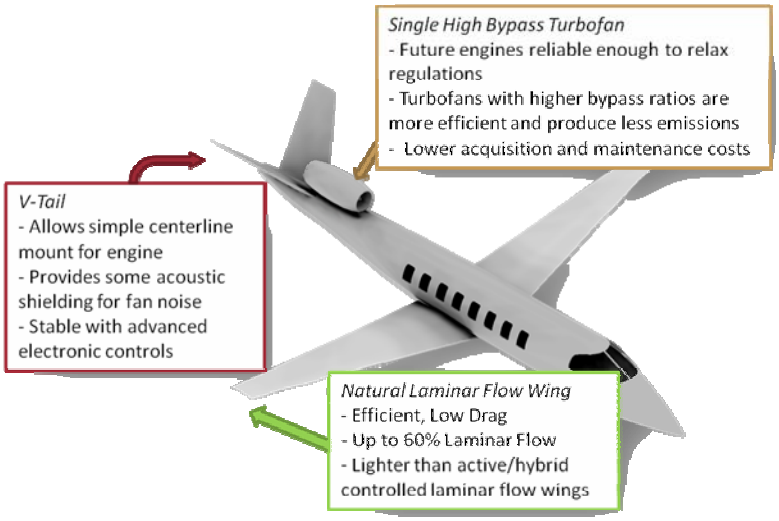

Figure 33. Advanced Aircraft Configuration

The Light Eco-friendly Aircraft Framework (LEAF), shown in Figure 34, was created to capture the performance of the notional concept (see Reference 14 for further details on LEAF). LEAF is an integrated, real-time tradeoff environment that, through the use of meta-models, allows for simultaneous analysis of mission requirements, design parameters, and technology packages. Outputs of the tool include preliminary economic and consumer preference analysis, vehicle performance, and technology ranking.

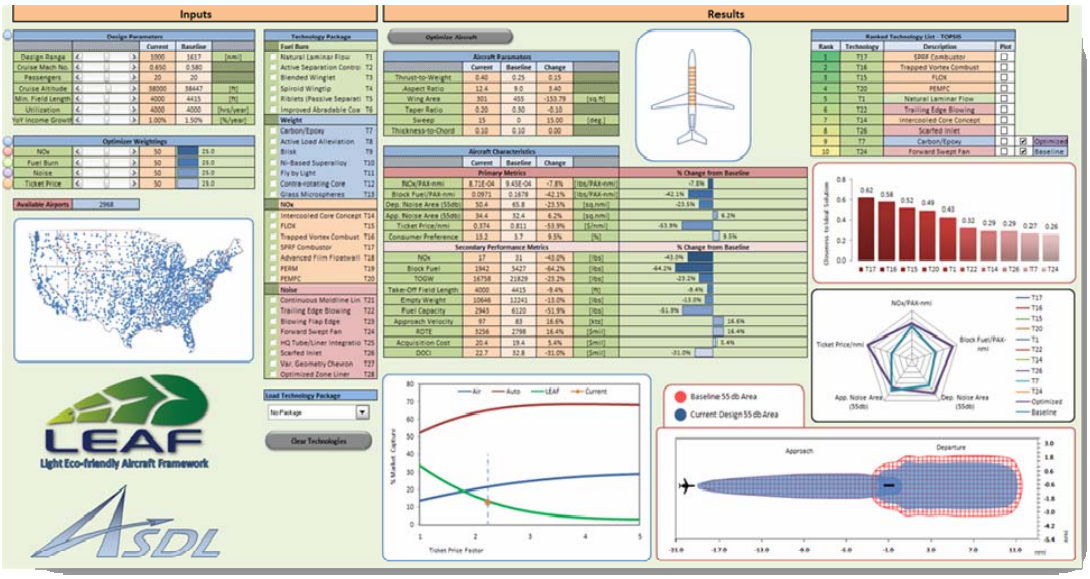

Figure 34. Light Eco-friendly Aircraft Framework (LEAF)

4.3.1.2 Ticket Price Variation

In reality, aircraft size can affect demand through secondary factors, such as airport compatibility, passenger comfort, and consumer perception of safety. However, when analyzing aircraft configurations of varying passenger capacity, it was assumed that ticket price is the primary factor that alters the demand structure for point-to-point air travel. The LEAF tool was used to calculate ticket price of the aircraft for varying aircraft size (10, 15, 20, 35, 30 PAX).

To isolate the effect of passenger size on ticket price, the user inputs were set to:

Design Range = 800 nmi	Field Length Constraint = 4000 ft
Cruise Speed = 344 kts	Utilization = 4000 hrs
Cruise Altitude = 41,000 ft	YOY Income Growth (1995-2030) = 1.5%

Ticket price is calculated by the Airline Life Cycle Cost Analysis (ALCCA) tool, which is integrated into the LEAF environment. The aircraft is re-optimized for each passenger size and the ticket price meta-model updates with a corresponding ticket price. The ticket price trend is converted to a ticket price factor to be used in ***Mi***, simply the ticket price normalized by that of a standard 150 PAX commercial transport. Figure 35 shows the result of the ticket price variation with passenger size of the notional aircraft.

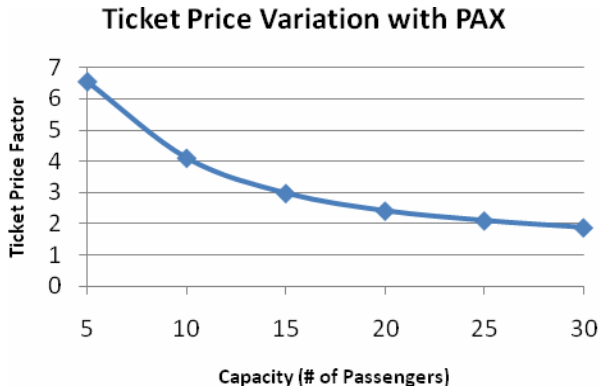

Figure 35. Ticket Price Variation with Aircraft Capacity

4.3.2 Phases A and B Results: Aggregated Results from Aggregated Approaches

In the agent-based formulation, there must be enough agents to produce a converging response. However, ***Mi*** is computationally taxing, so at the same time, the number of agents should be minimized. When only market share was the output of the agent-based approach, a small number of agents (around 100,000) was sufficient to obtain a stable response. When looking at the small raw demand numbers between origin and destination, however, many more agents are necessary. A sensitivity study of the total produced and attracted demand of each MSA and non-MSA for varying number of agents was performed. It was determined that 16 runs of ***Mi***, using about 50,000 agents for each case, produces a stable enough response for preliminary analysis of a point-to-point network. This corresponds to a sample of consumer travel of about 2 days. Figure 30 shows the run-by-run deviation of ***Mi***; after 16 runs (2 day sample), the average change in produced demand for an MSA is less than 5 passengers.

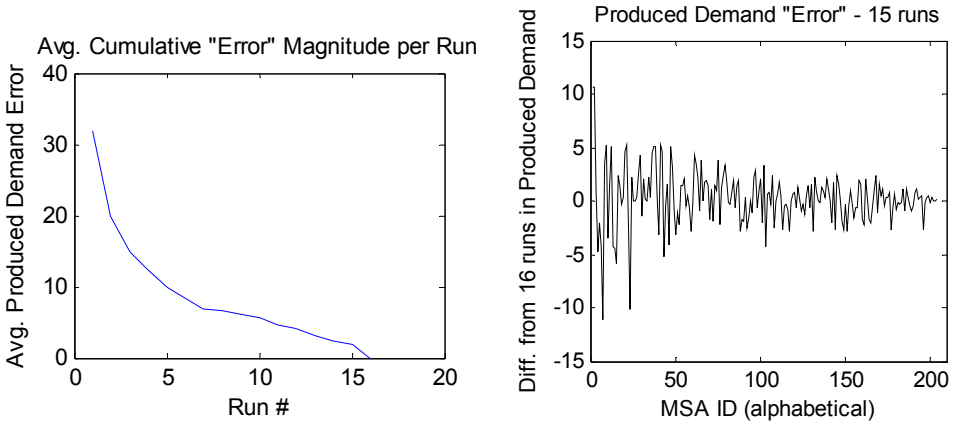

Figure 36. Change in Produced Demand from Run 15 to 16

4.3.2.1 Phase A Analysis

Phase A analysis of the origin-destination matrices is a simple calculation of total passengers per day for the point-to-point service. Assuming 100% load factor, a number of point-to-point operations, which represents a surrogate of ideal utilization hours, can be calculated. This initial analysis assumes that the point-to-point service is readily available to all prospective consumers and the decision to utilize the service depends on only the monetary and time expense of the service. In reality, the point-to-point service will not be feasible unless demand is concentrated within a reasonable distance of compatible airports.

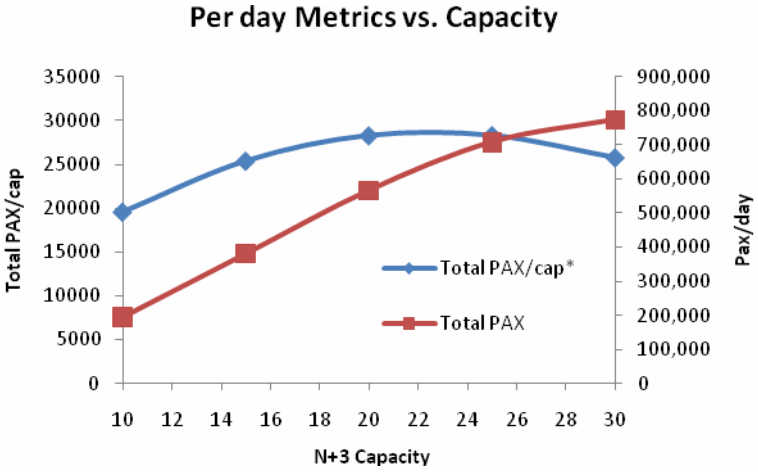

Figure 37. Phase A Result

4.3.2.2 Phase B Analysis

As part of Phase B analysis, a screening test is performed on the origin-destination matrices to translate raw demand into an estimate of captured demand. Using the county definitions of each of the 156 MSAs and 48 non-MSAs, data on the estimated area of each MSA is gathered. Demand density for an MSA or non-MSA is then defined as:

$$\rho_i = \frac{G_i}{\text{Area}_i}$$

Since the majority of trips will likely be round-trip, total demand, G_i, is the sum of produced and attracted demand: $G_i = P_i + A_i$

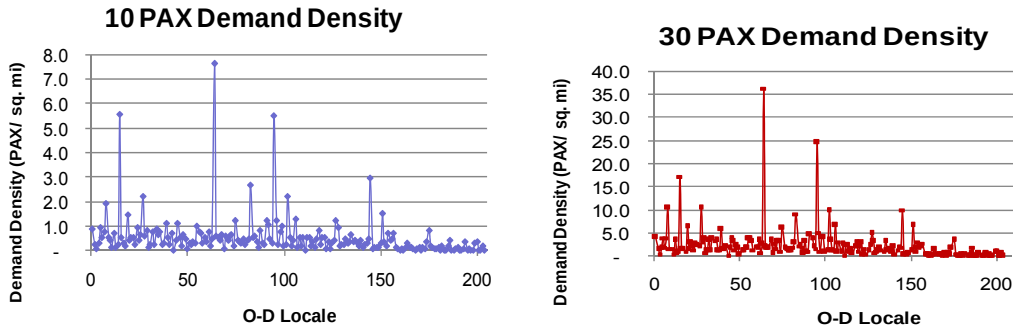

Figure 38. Demand Density of *Mi* Locales

A logistic distribution is used as a transfer function to translate demand density within an MSA to the capture percentage of raw demand. The initial result of this filtering process is shown in Figure 39.

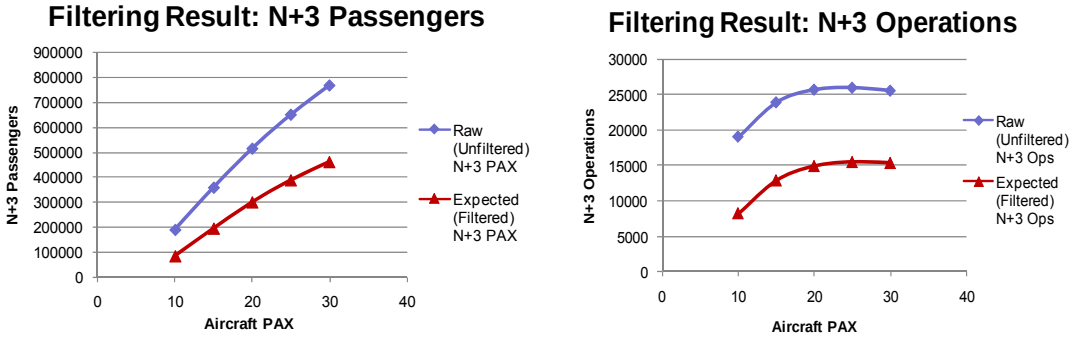

Figure 39. Demand Density Filtering Result

Both Phases A and B results suggest that an aircraft between 20 and 30 PAX maximizes the number of operations, and is thus more attractive to potential point-to-point airliners. This analysis assumed that raw demand could be aggregated into totals for each MSA and then filtered into a projected captured demand. However, if the produced demand within a given MSA is distributed in very small numbers between many different destination locales, then new filters for individual origin-destination pairs may be necessary to accurately project captured demand.

4.3.3 Phase C Study

The output of Phase C should be an origin-destination matrix where each of the indices represents an airport within the continental United States. Once this level of granularity is obtained, one can investigate the viability of each particular airport pair route and preliminary route networks can be defined. Taking the original 204 x 204 origin-destination matrix which represents 156 MSA areas and 48 non-MSA areas all the way to an airport-by-airport matrix requires many intermediary steps. The process flow of the intermediary steps is illustrated in Figure 40.

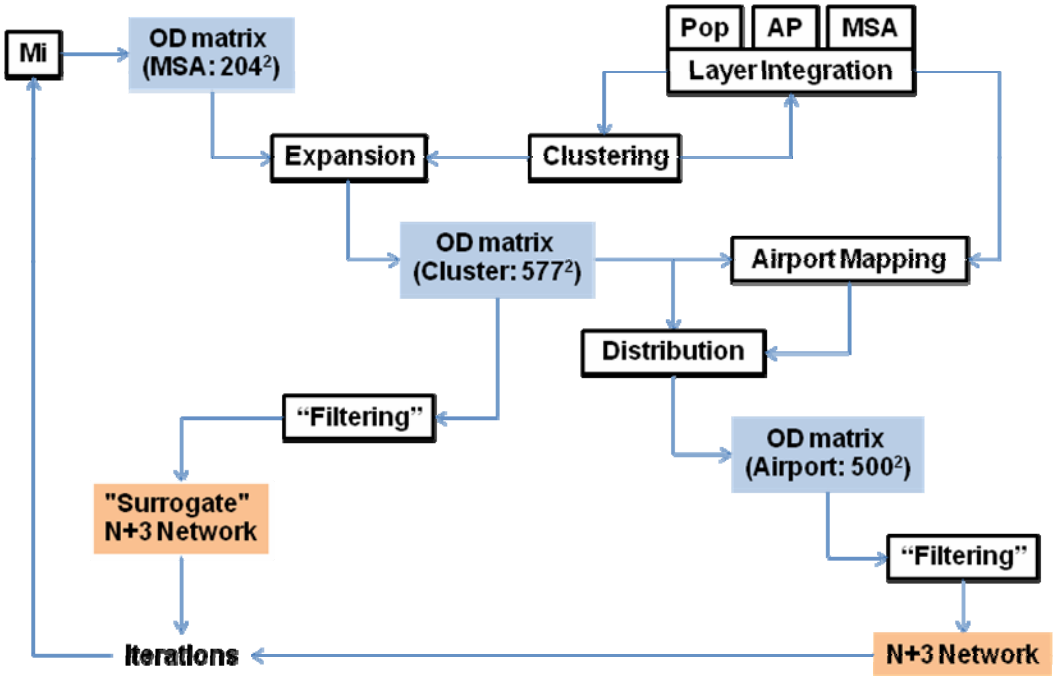

Figure 40. Phase C Work Flow

The main issue is that the airports in the United States are essentially points, while each of the OD pairs in the 204x204 matrix represents a large area. This issue is particularly glaring with the non-MSA areas which compose the entire area of a state that is not part of an MSA. To gain more specific geographic granularity, the population of the state (which of course the demand for air travel will be fundamentally linked to) must be used. For this purpose a clustering algorithm was developed to identify where the people in a state are geographically located. Once clusters have been formed, then the original MSAs and non-MSAs must be linked to those clusters. After this link is formed, then the demand from a particular OD pair in the original OD matrix must be expanded to the new cluster-level OD matrix. Finally, each cluster is linked to a particular airport to form the end result of an airport-by-airport OD matrix. Based on simple assumptions of minimum load factor, this matrix can be filtered to yield a network of viable routes. The final matrix for each passenger capacity can then be analyzed and compared to the Phase A and B results.

4.3.3.1 MSA Layer and Database Integration

In general, MSAs are defined and by the U.S. Office of Management and Budget as a core urban area with a population of 50,000 people or more and a typical MSA consists of the counties containing the core urban area, as well as any adjacent counties that have a high degree of social and economic integration with the urban core. The granularity of ***Mi*** is at a different MSA level since it uses the statistics in the 1995 American Travel Survey (ATS) database which defines its own MSA level. As mentioned earlier, a higher level of granularity is required to establish the viability of the N+3 service. To achieve the desired level of granularity, the counties described in the MSA definition were identified and their geographic as well as socioeconomic information was compiled into a master database that was used in later work. While working with the ATS MSA definitions, many errors and/or inconsistencies became evident. The correction to these problems was a new list of definitions, termed ATS+ MSA definition.

4.3.3.1.1 Different Granularity: New England Area

Oddly enough, the ATS MSA definition for New England area has town granularity as opposed to the usual county granularity as can be seen in Figure 41. This is problematic because one MSA could contain several towns on one side of a county, and its neighboring MSA could contain the other towns on the other side of the same county.

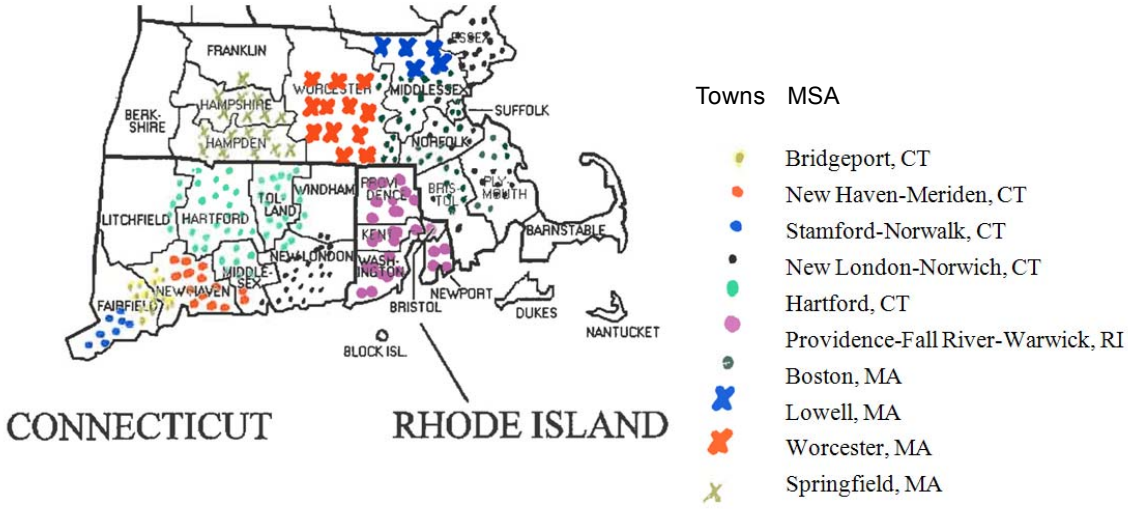

Figure 41. New England Area

To deal with the confusion, one of two actions was taken: either adjacent MSA's sharing a county was merged into one larger MSA, or all shared towns (and therefore, the entire county) were delegated to one MSA. The table below depicts what action was taken for each issue.

Table 5. Partial Counties

County	MSAs	# Towns	Action
Fairfield, CT	Bridgeport, CT PMSA	7	Merged into one MSA
	Stamford-Norwalk, CT PMSA	8	
New Haven, CT	New Haven-Meriden, CT PMSA	15	Merged into one MSA
	Bridgeport, CT PMSA	6	
Middlesex, CT	Hartford, CT MSA	8	All to Hartford MSA
	New Haven-Meriden, CT PMSA	2	
	New London-Norwich, CT MSA	1	
New London, CT	New London-Norwich, CT MSA	17	All to New London MSA
	Hartford, CT MSA	2	
Windham, CT	Hartford, CT MSA	3	All to Hartford MSA
	New London-Norwich, CT MSA	2	
Hampden, MA	Springfield, MA MSA	16	All to Springfield MSA
	Worcester, MA PMSA	1	
Middlesex, MA	Boston, MA PMSA	43	Merged into one MSA
	Lowell, MA PMSA	10	
Worcester, MA	Worcester, MA PMSA	33	All to Worcester MSA
	Boston, MA PMSA	11	

4.3.3.1.2 Inherent error in ATS MSA definitions

Specifically, the small populations in certain counties should have prevented them from being considered part of an MSA. After finding that a county was non-contributing, it was removed from its MSA definition. Nye County, NV is an example. Figure 42 shows satellite map of Nye County, NV. As is easily visible, this county contains no meaningful population centers that could possibly contribute to the demand of air travel. Therefore, the county was removed from its initial MSA definition.

Figure 42. Nye County, Nevada

4.3.3.1.3 "Trimming" non-contributors

In some cases, the MSA is too broad to capture differences in socioeconomic factors and transportation infrastructure between urban and rural areas. Figure 43 is an example of noncontributing counties in the St. Louis, MO-IL MSA. As can be seen, the four counties highlighted in purple have significantly less population than the other seven counties; therefore, they were removed from the ATS+ MSA definitions. Also, this practice is in line with access distance assumptions in the simulation model ***Mi***.

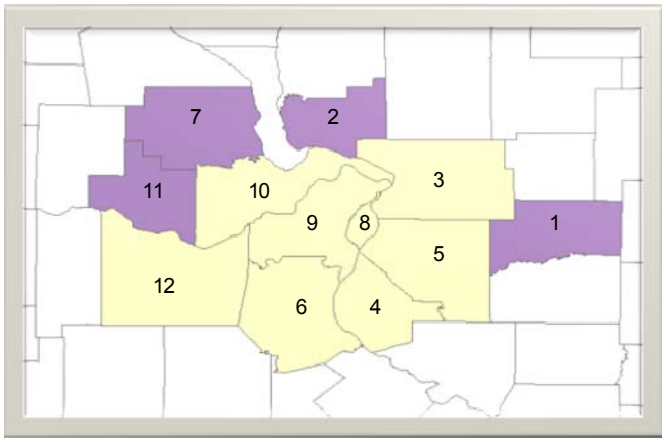

	County	Population
1.	Clinton	36K
2.	Jersey	22K
3.	Madison	259K
4.	Monroe	28K
5	St. Clair	256K
6.	Jefferson	198K
7.	Lincoln	39K
8.	St. Louis City	348K
9.	St. Louis	1M
10.	St. Charles	284K
11.	Warren	25K
12.	Franklin	94K

Figure 43. St. Louis Area

4.3.3.1.4 Creating a Cohesive Database

After taking care of the above issues in MSA definitions, the next task was to create a mapping table and to incorporate it within our own database. There are problems associated with this task mainly due to the inconsistency of the county level data sets. For example, contained in the ATS MSA definitions were two confusing entries: Miami-Dade County, FL and Broomfield County, CO. The county that is currently named Miami-Dade used to be just Dade County because its name was changed in 1997. This proved to be a problem since ATS MSA definitions come from 1995. The solution to this issue was to change its FIPS code as well to account for the change in alphabetical order, from 12025 (Dade) to 12086 (Miami-Dade). Broomfield County, CO was established in 2001 as it was separated from Boulder County on account of political differences. The same problem existed, as the ATS MSA definitions were from 1995, so Broomfield County received its own FIPS code.

A master table that contained all the information needed was created as seen in Table 6 which greatly expedited the subsequent processes, as everything necessary was in one place and easy to locate. This is only a section of the table: farther to the left are columns containing information on latitude, longitude, other years' populations and MSA definitions, and socioeconomic values.

Table 6. Master Table Example

FIPS	ST	ID	County Name	NoteCode	Comment	ATS MSA	ATS+ MSA	Area	Pop2000
1000	1	0	Alabama					50,644	4,447,355
1001	1	1	Autauga County			5240	5240	594	43,671
1003	1	3	Baldwin County			5160	5160	1,590	140,415
1005	1	5	Barbour County					885	29,038
1007	1	7	Bibb County					623	19,889
1009	1	9	Blount County			1000	1000	645	51,023

The geographical information software ArcGIS™ was obtained for the purpose of integration, visualization, and analysis of the various spatial datasets necessary for network formulation. The ArcGIS™ framework facilitated integration of a population cluster layer and airport layer within the county and MSA layers. This integration process proved to be valuable for cluster and airport queries based on spatial location with respect to political boundaries. The completed MSA layer is shown in Figure 6, overlaid on the county layer. This completed MSA layer together with the master table serve the basis for the next layers.

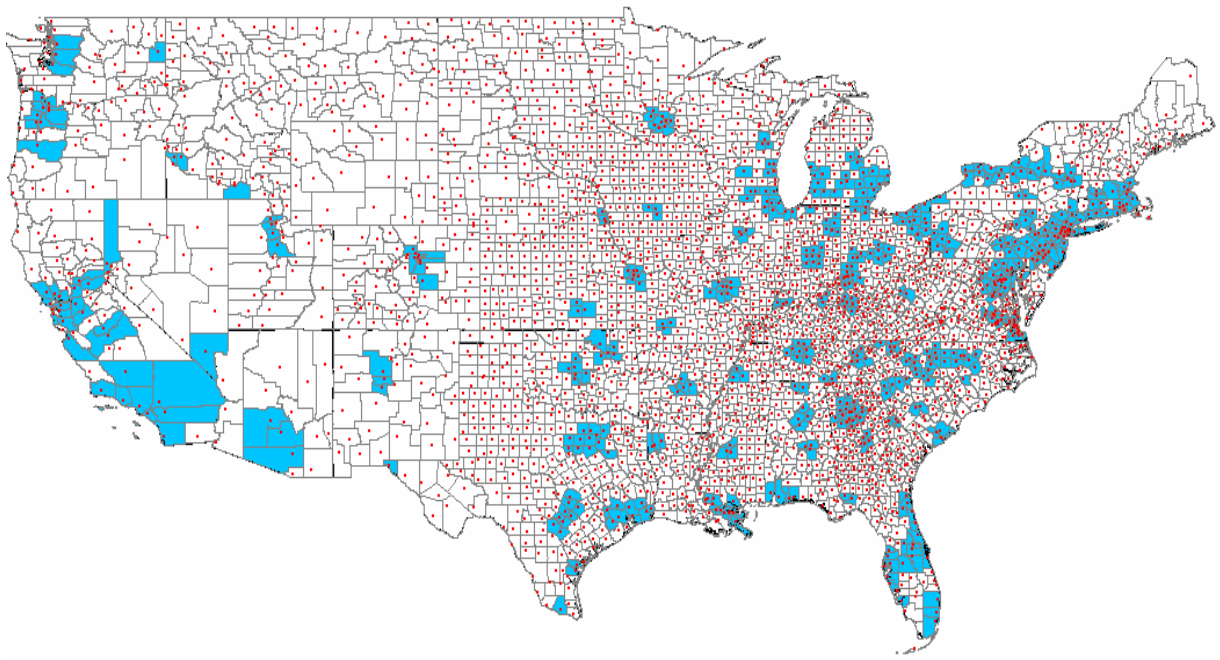

Figure 44. Final MSA Layer with Population Centroids of Counties in the CONUS

4.3.3.2 Population Clustering

Mi was validated against 1995 ATS data that has a granularity of the MSA. As a result, ***Mi*** accounts for remaining air travel demand outside of these MSAs with 48 non-geographic specific non-MSA locales, one for each state. For a conceptual point-to-point network for a small regional aircraft, however, identifying precisely where in those states the non-MSA demand originates and what airports could potentially be used becomes necessary. To examine demand between two communities, let alone two specific small airports, O-D matrices of higher granularity are needed. One approach to solving this problem would be to cluster the counties to identify where large population centers are outside of the MSAs. The non-MSA demand could then be distributed in a roulette-wheel fashion, with the area on the roulette wheel corresponding to the population of the cluster.

The problem then becomes selecting the best clustering algorithm for this specific problem. There are many different clustering algorithms such as k-means, hierarchical, quality threshold, fuzzy-c means etc. Hierarchical clustering has the advantage that the closest airports or counties will always be clustered, but it only considers distance as its clustering criterion, not population, and the memory required to store a matrix of the distance between all the different counties is prohibitive. K-means clustering has the advantage that pre-defined cluster seeds (starting points for the center of a cluster) are not necessary, but the selection of the next county to add to a cluster is arbitrary as long as it is within a defined radius. This can cause the clusters to become irregularly shaped. Quality threshold clustering avoids some of the problems of k-means clustering by considering every point as a possible seed. The drawback, however, is that it becomes much more computationally intensive and it still focuses solely on the distance between counties, not taking their population into account.

Fuzzy C-means (FCM) can use the population data to define initial seeds and then it assures that the counties closest to the seeds are clustered first to avoid irregularly shaped clusters. It also incorporates a filter to ensure that the population of the entire cluster meets a minimum threshold. The disadvantage of FCM clustering is the potential to have two clusters that are so close to one another that they should be just one, larger cluster. This arises from the way the initial seeds are distributed according to population data. This problem can be overcome with additions to the base FCM algorithm. Due to its main advantage of being able to consider both the distance between counties and their populations, FCM was the algorithm chosen for this problem.

The FCM algorithm was implemented in JAVA and minor modifications have been made to increase the percentage of the US population that will be captured. In particular these modifications make the selection of initial seed counties more robust. Typically in the FCM clustering algorithm the seed clusters would be identified solely based on whether the population of a particular county passes a threshold. If the standard FCM algorithm were used it was possible (and happened) that two close (<10-15 mi apart) counties would each be selected as a seed. This is undesirable because each of these counties would either be its own cluster, despite the fact that they were within the user-defined distance of each other, or one or both of the counties may not make it because their individual populations were less than the cluster population threshold. An example may be useful to illustrate this point. Consider two counties as depicted in the figure below:

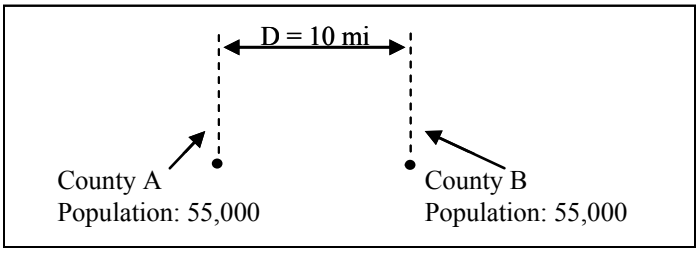

Figure 45. Clustering Modification Example Diagram

Suppose the user has selected the following four clustering parameters in this scenario:

1. Seed Threshold Population = 50,000
2. Maximum Distance between county and seed pair = 15 mi
3. Minimum Population to qualify as a cluster = 100,000
4. Minimum number of counties to qualify as a cluster = 1

For this set of user selected parameters applied to the example in Figure 45, one would expect that the two counties would be joined together into a single cluster. With the standard FCM clustering algorithm, however, the result would be that there are no clusters. Why? The answer is that each county is represented as its own seed because its population exceeds 50,000. With the standard algorithm two seeds cannot then be joined together. Since, each seed represents its own cluster, and the population of each cluster is only 55,000, neither meets criteria 3 where the cluster population must be at least 100,000 and therefore no clusters will be returned. The obvious fix to this situation is to allow seeds to be joined together, which has been implemented in the modified algorithm. The implication of this modification, however, is that the maximum distance between county and seed pair (Criteria 2), may in some cases be larger than the user-specified parameter. This was deemed acceptable for this particular application.

The major issue to resolve in this subtask (aside from algorithm development and implementation) is to determine the best mix of values for the 4 parameters listed above. The ideal goal is to capture as much of the continental US's population as possible, with the fewest clusters possible that maintain a relatively high granularity. The major trade-off contained in this goal is that larger clusters will capture more people, but at the cost of cluster granularity. To determine the best combinations of settings for the clustering, a design of experiments was created for the four clustering parameters. The results of the experiments can be visualized in terms of Pareto frontiers, one of which is shown in Figure 46. This particular graph was prepared using a maximum distance between county and seed pair of 25 miles. A Pareto frontier can be made for each distance value specified. Using this analysis it was identified that the points on the Pareto frontier typically have the following traits in common: the minimum number of counties to qualify as a cluster is 1, and the seed population and cluster population should have the same value.

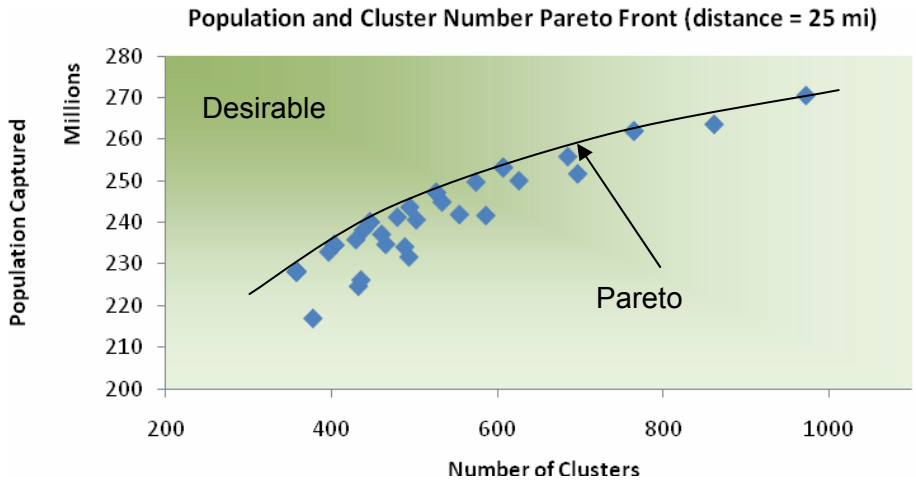

Figure 46. Cluster Pareto Front

Aside from the ideal goal of high granularity, minimum clusters, and maximum population, there are other constraints that also bound the problem. In this case MSA boundary lines represent a constraint, because ***Mi*** associates demand only to MSA and non-MSA areas. Some actual cluster trials demonstrating this effect can be seen in Figure 47.

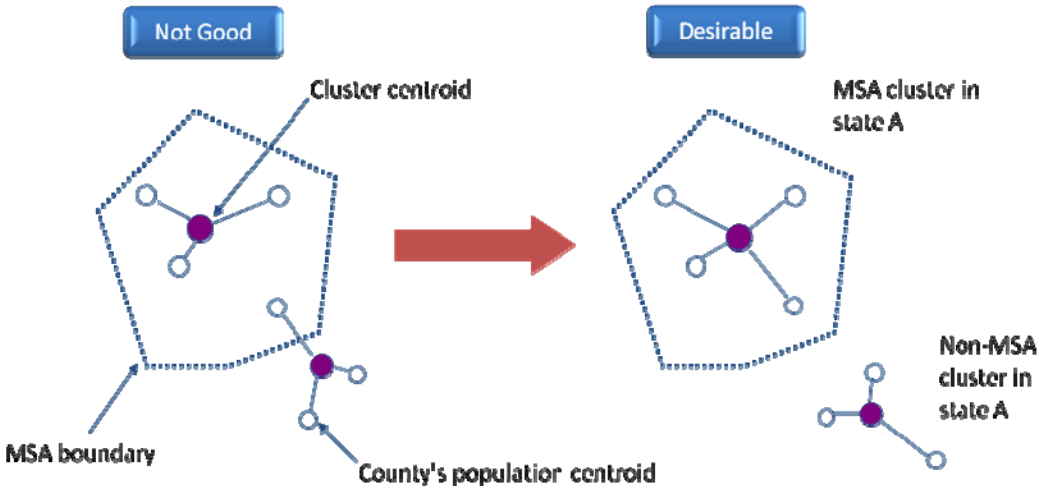

Figure 47. Clustering Issue with MSA Boundary

The irony is that the left figure is a superior solution in terms of smaller number of clusters as well as population percent captured but does not work with the ***Mi*** granularity imposed by the BTS. Note that this is a simple example because some MSAs have neighboring MSAs, or some MSAs belong to more than one state, adding more confusion. The following example shows a snapshot of two different parameter sets of clustering. In order to satisfy this constraint (BTS MSA def.), visual inspections and clustering iterations were performed.

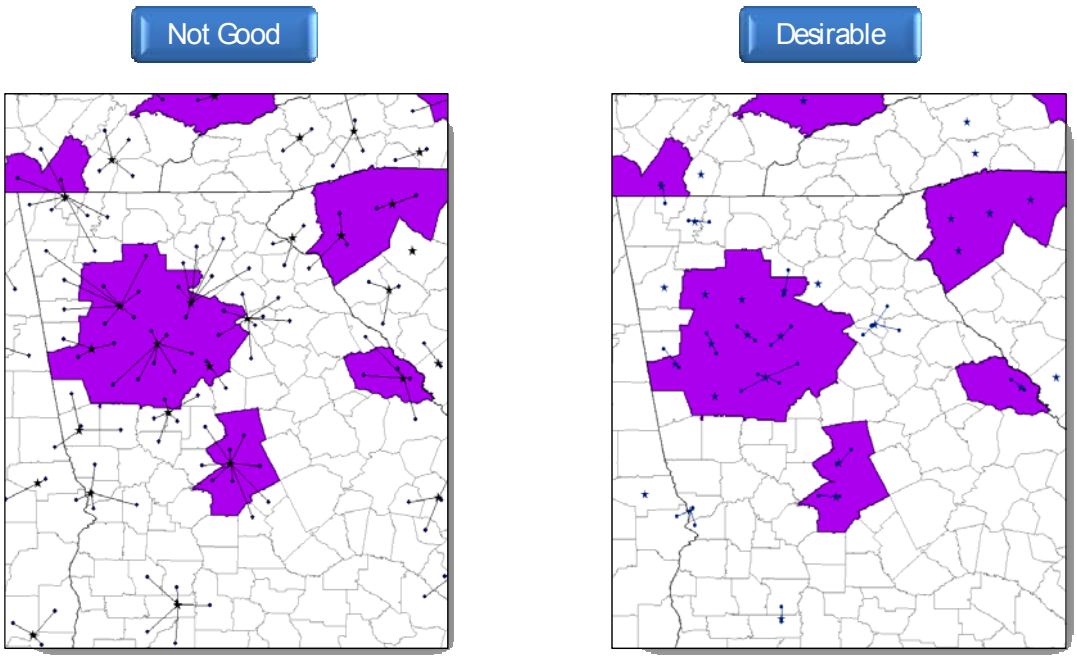

Figure 48. Comparison of Clustering Solutions near Atlanta Area

After utilizing the most robust set of selection parameters, the continental United States is represented as 565 clusters which capture 81.8 % of the population of the continental United States. The centroids of the clusters are shown in Figure 49.

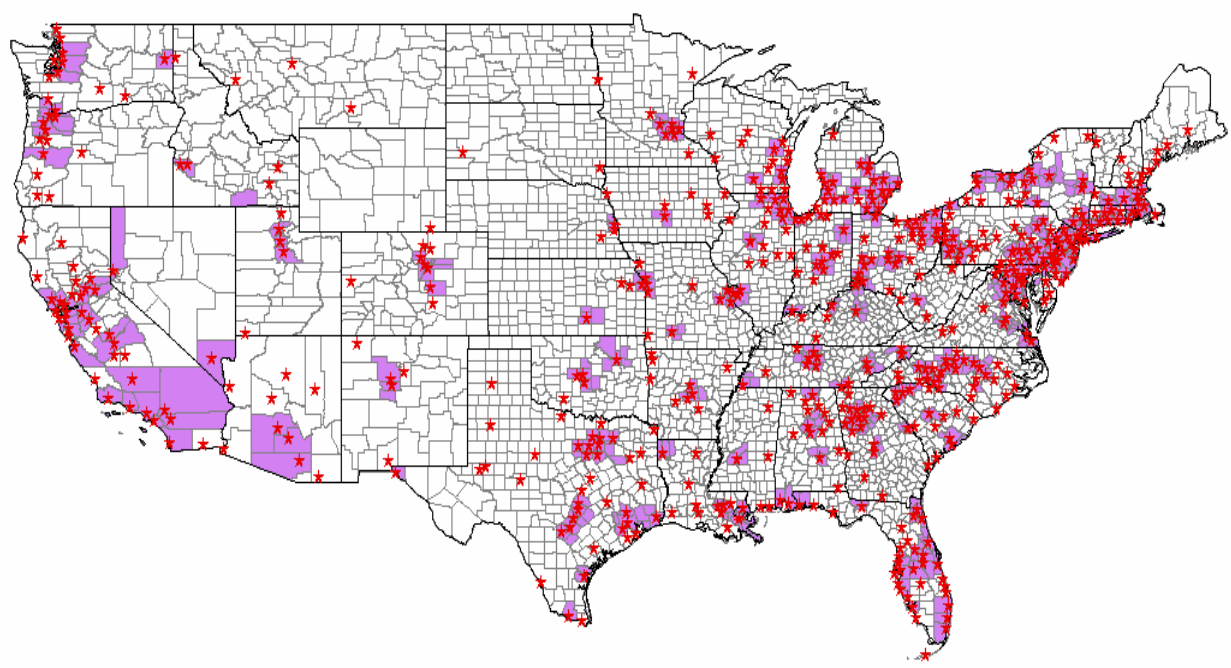

Figure 49. Final Cluster Selections

4.3.3.3 Candidate Airports Layer

According to the 2009-2013 NPIAS report, there are 19,815 airports in the United States. Many of these airports are closed to the public, and if those are taken away there are still 5,190 airports in the United States open to the public. Despite this staggering number of airports, 75% of US air passengers traveled through only 35 airports. Clearly there are many factors that conventional airlines use in selecting which airports to serve. The N+3 service provider must make similar selections as to which airports to serve. Before making those decisions, however, it is useful to identify which of the 5,190 airports are *capable of being served* by the N+3 aircraft.

The main problem in this subtask is to identify what criteria should be used to determine if an airport is *capable of being served.* For this there are some obvious requirements that the airport must meet, such as runway length, runway surface type, etc. More subtlety, part of the business case for the N+3 aircraft should be incorporated by eliminating large hub airports at which the small N+3 aircraft will not be competitive with the existing air carriers.

Using the given runway length from airport databases is not an adequate means to decide which airports to filter because airport elevation will have a significant effect. This is the reason why Denver International which is at a high elevation has some of the longest runways in the United States. To correct for the airport elevation effect, an 'effective' runway length measure was derived. The effective runway length measure was derived from the constraint analysis equation as applied to takeoff ground roll. This yields the following relationship between runway length and air density for two airports:

$$\frac{S_1}{S_2} = \left(\frac{\rho_2}{\rho_1}\right)^{\gamma}$$

The value for gamma depends on the type of engine the aircraft has. For a low bypass ratio turbofan gamma is 1.7, for a high bypass ratio turbofan gamma is 1.6, and for a turboprop gamma is 1.5. Since the aircraft in this study is similar to business jet which uses low bypass ratio turbofans, a gamma of 1.7 was used. The density was calculated using the International Standard Atmosphere (ISA) for the elevation of the airport. Therefore, an 'effective' runway length corresponds to an equivalent length and standard sea level conditions. For example, a 16,000 ft length runway at Denver international would have an equivalent or 'effective' runway length of about 12,000 ft at sea level.

Given the vision of a converted business jet for the N+3 concept, runway length and width were respectively restricted to greater than 4000 ft and 75 ft Figure 50 shows that this runway length and width represent the inflection point in the curve. Imposing this condition will result in a significant number of eliminated airports, but over a thousand airports are still eligible. Due to engine maintenance and operability concerns, runway surface type was restricted to various types of asphalt and concrete. Further, runways of condition 'fair' or 'poor' were eliminated; given a timeframe of 2030, further degradation of runway quality can be expected. Finally, large and medium hubs were eliminated, as these airports will still likely serve large aircraft in 2030. Military airports were also eliminated. The main filtering criteria used to obtain a list of eligible airports are shown in Table 7.

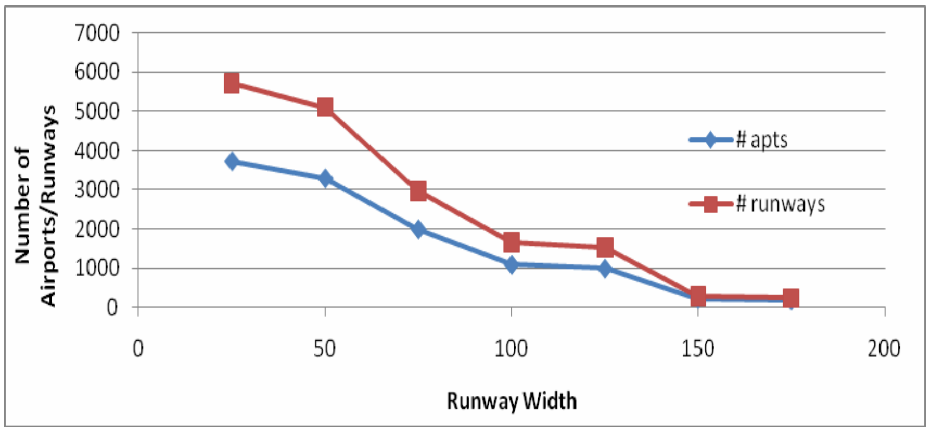

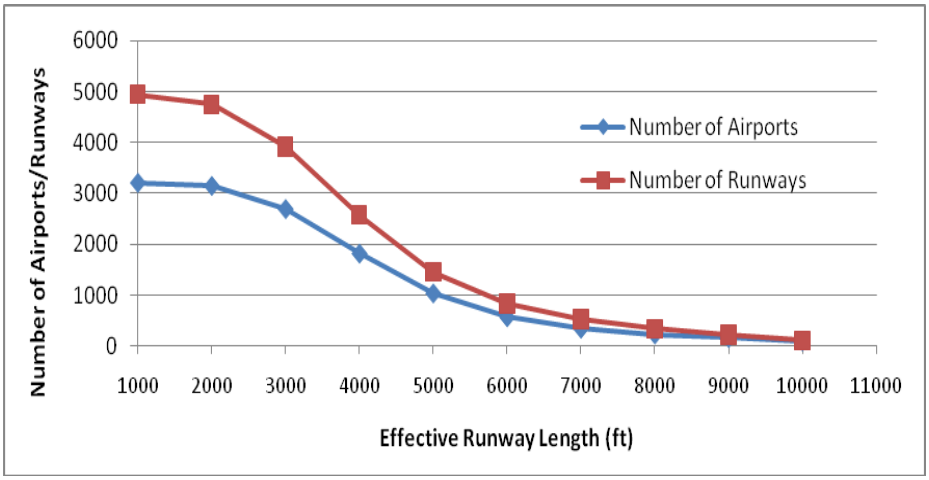

Figure 50. Runway and Width of U.S. Airports

Table 7. Airport Screening Criteria

Parameter	Condition
Runway Length	>= 4000 ft
Runway Width	>=75 ft
Surface Type	Concrete or Asphalt
Surface Condition	Excellent or Good
Hub Type	N/A, None, S
Airport Type	Commercial (no Military)

After using the screening criteria given, 1,356 airports remain, composing the candidate airports layer. The down-selection is shown in Figure 51 and still shows a good distribution over the CONUS.

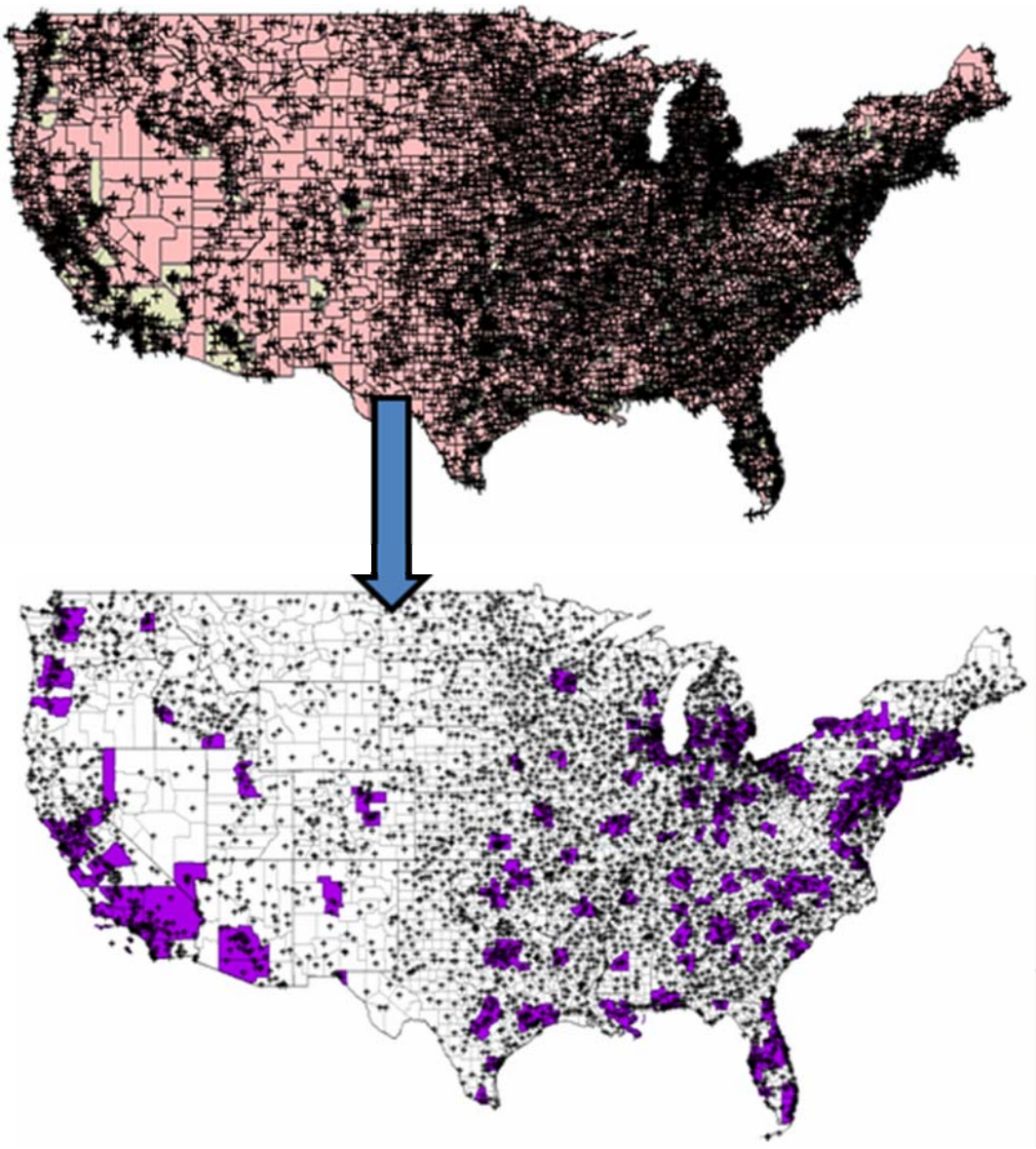

Figure 51. Down Selection to Candidate Airports

4.3.3.4 Expansion

Now that each of the three layers has been defined, the question is how does the original 204x204 OD matrix map to a 565x565 cluster level matrix? The first step in this process is to map each MSA area and non-MSA area to their respective cluster. This is a relatively simple process when using ArcGIS to simply associate all of the clusters inside an MSA area to that particular MSA or all of the clusters in a non-MSA state to that particular state's non-MSA. Despite this relatively simple process, some problems arose.

First, there was one non-MSA area, namely non-MSA Nevada, which did not contain any clusters. This can be seen in Figure 52. The reason this area did not contain any clusters is that the population is very sparse. There are two options for dealing with this, one is to eliminate non-MSA Nevada from the original OD matrix and the second would be to artificially make

clusters in non-MSA Nevada. Since the second option would be highly subjective, ad hoc, and not comply with the earlier definition of cluster parameters, the first option of eliminating non-MSA Nevada from the OD Matrix was chosen.

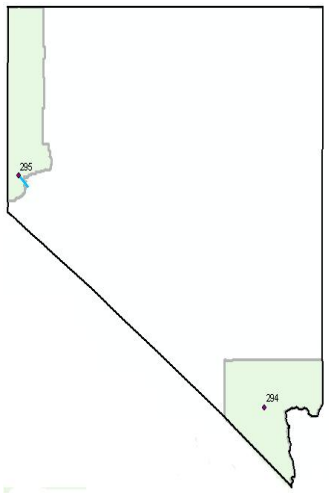

Figure 52. Clusters in Nevada

Second, there was one MSA area, Jefferson City, NJ (JCYNJ), where all of its population was being drawn into a cluster centroid located in a different MSA, Bergen County, NJ. This concept is shown in Figure 53. Here the solution was to add the origin (row) and destination (column) from JCYNJ to BERNJ. The resulting matrix of size 202x202 will be used in the expansion process.

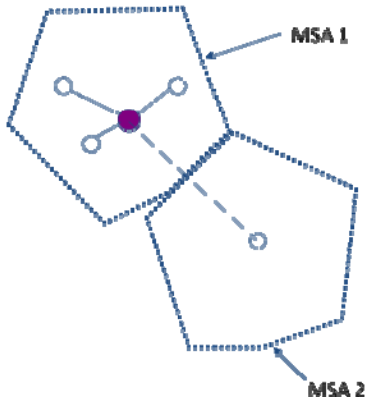

Figure 53. Population from One MSA Drawn Into a Different MSA

Third, it was observed that for non-MSA areas the typical situation would be to have a large geographic area (a whole state) associated with a non-MSA area, but then only a couple of clusters within that non-MSA area. It is highly unlikely that these few distinct clusters would capture the entire demand for the whole non-MSA area. Therefore, what was done was to add up the population within a 25 mi radius of the clusters and then divide that by the total population of the non-MSA area. This fraction represents what is capable of being captured with the given clusters. Therefore, the demand in non-MSA areas will be multiplied by this fraction to better reflect reality.

Once the cluster MSA and cluster non-MSA mappings are made, the next step is to expand the original OD matrix. This expansion process will take a single OD cell and expand it into a matrix of size n x m, where n = the number of origin clusters and m = number of destination clusters corresponding to the original OD pair. This process is shown graphically in Figure 54, where n = 2, m = 3.

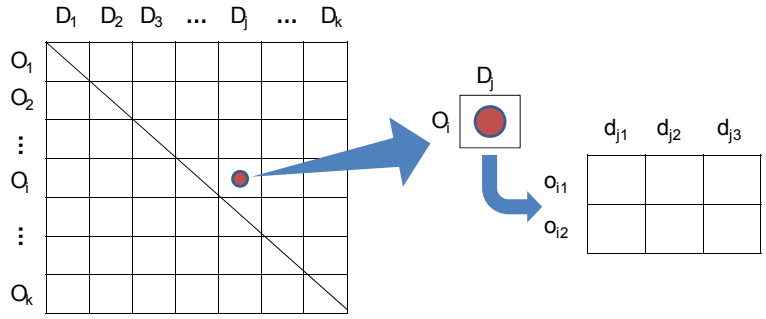

Figure 54. Expansion Representation

There is no clear way as to how the single OD number should be expanded into a matrix of numbers. An easy solution would be to just evenly divide the original OD number by the number of cells in the new matrix and assign that number to each cell. This, however, defies intuition as one would expect the demand in each of the new cells to be somehow related to the population of the origin and destination clusters. One could apply a formula that relates a combination of the origin and destination cluster populations to the total population of the new matrix, but this is a deterministic result and neglects the large amount of uncertainty in how the actual origin and destination demand will be distributed. To make the problem more stochastic in nature, a roulette wheel selection algorithm was used. In this approach there is a fitness function that relates each origin-destination pair with an area on a roulette wheel. Then, for each passenger in the original OD pair, the roulette wheel is spun and that passenger is assigned to whichever cluster OD pair the roulette wheel landed on. The fitness function must satisfy two conditions:

1. Each cell in the expanded matrix should have a unique fitness based on the cluster's origin and destination population
2. The sum of the fitness over all of the cells in the expanded matrix must equal 1

There are many different equations that can be made to satisfy these two conditions, but we chose to use one of the simplest, which is shown in the following equation.

$$Fitness_{ij} = \frac{PopC_i \cdot PopC_j}{\sum_{k \in O} PopC_k \cdot \sum_{l \in D} PopC_l}$$

4.3.3.5 Airport Mapping

As stated earlier, the result of the expansion process is a 565x565 cluster level OD matrix. The next step is to use a process similar to that used for the expansion algorithm to map the cluster level OD matrix to and airport level OD matrix. In the ideal situation there would be one airport associated with each particular cluster, and then all that would be involved in this step would be to change the names of the indices in the 565x565 OD matrix. In reality, there are

four different types of relationships that develop when trying to associate clusters with airports. These four relationships are:

1. 1:0 – For 1 cluster there are no candidate airports within 50 miles (cluster 4 in the figure below)
2. 1:1 – This is the ideal case, there is a unique airport for a particular cluster (clusters 5 and 6 in the figure below)
3. 1:N – Here there are N good candidate airports for every cluster (cluster 3 in the figure below)
4. N:1 – In this case N clusters are associated to 1 airport (clusters 1 and 2 in the figure below)

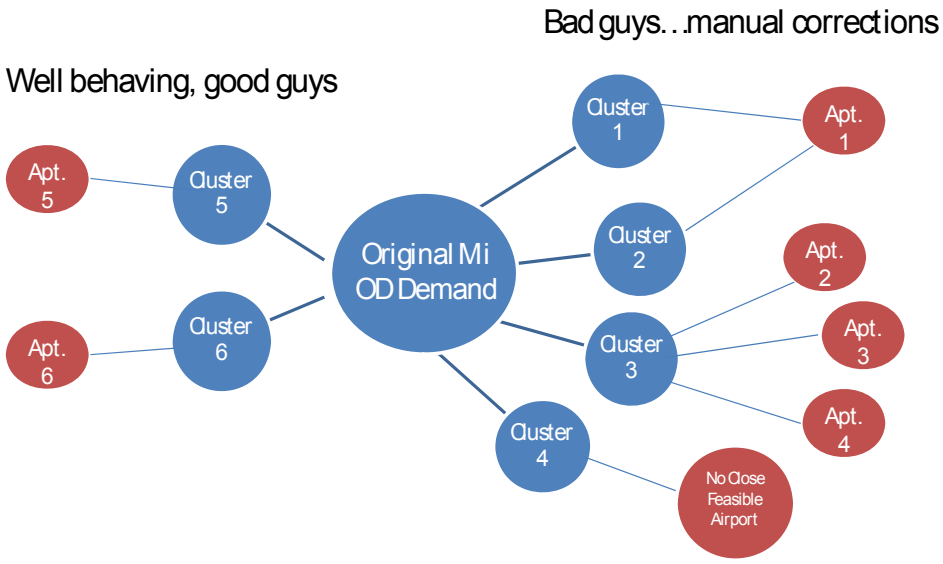

Figure 55. Airport Mapping Categories

Of all of these relationships, the ones that are most concerning are case 1 and 3. Case 1 is concerning because if there is not an eligible airport within 50 miles the demand to and from that cluster will be lost. Case 3 is concerning because it is splitting up the demand between airports that are in relatively close proximity. The first step in determining which clusters fall into each relationship was to simply assign the closest airport to the cluster centroid with that particular cluster as long as it is no further than 50 miles away. T his step will yield relationships 1,2, and 4. There were 2 clusters that fell into case 1: Jackson, MS and Port Huron, MI. Note that Canadian airports were not considered in this study. Since there is no eligible airport within a reasonable distance for either of these two clusters, these clusters cannot be served by the N+3 aircraft and so their OD demand will not be included in the airport-level matrix. Case 2 and case 4 are relatively straightforward.

Case 3 relationships will not be given through the first pass screening since it is highly unlikely two airports are *exactly* the same distance from a cluster centroid. Rather, case 3 airports were identified by visual inspection. Not all clusters that have multiple airports close by should qualify for case 3 relationships as the population and corresponding demand could not support service to that many airports. An example of this scenario is in Daytona Beach, FL. Daytona Beach has 3 airports within 15 mi of its cluster centroid: Daytona Beach International, Deland Muni, and New Smyrna Beach. Daytona Beach International currently operates around

10-20 commercial flights/day and the population of Daytona Beach is approximately 443,000. The reason for so many airports is because of the heavy general aviation demand in the area, rather than commercial flights. Clearly an N+3 service provider would choose only 1 of these airports to operate flights to and from rather than all three. Using this example as a guideline, clusters with a population less than 1 million were not allowed to have a 1:N relationship. Upon final down-selection, 10 clusters with 24 corresponding airports have a case 3 relationship. These clusters, their populations and corresponding airports are listed in Table 8.

Table 8. Clusters with a 1:N airport relationship

Cluster ID	Cluster Pop	MSA	AptID	Full name
18	3072149	Phoenix-Mesa, AZ	SDL	SCOTTSDALE
			DVT	PHOENIX DEER VALLEY
			GEU	GLENDALE MUNI
43	9519338	Los Angeles-Long Beach, CA	HHR	JACK NORTHROP FIELD/HAWTHORNE MUNI
			SMO	SANTA MONICA MUNI
			VNY	VAN NUYS
53	1545387	Riverside-San Bernardino, CA	HMT	HEMET-RYAN
			BNG	BANNING MUNI
54	1223499	Sacramento, CA	MHR	SACRAMENTO MATHER
			MCC	MC CLELLAN AIRFIELD
			SAC	SACRAMENTO EXECUTIVE
55	1709434	Riverside-San Bernardino, CA	L67	RIALTO MUNI /MIRO FLD/
			SBD	SAN BERNARDINO INTL
			REI	REDLANDS MUNI
56	2813833	San Diego, CA	SEE	GILLESPIE FIELD
			MYF	MONTGOMERY FIELD
111	2253362	Miami, FL	OPF	OPA LOCKA
			TMB	KENDALL-TAMIAMI EXECUTIVE
294	1375765	Las Vegas, NV	VGT	NORTH LAS VEGAS
			HND	HENDERSON EXECUTIVE
519	1446219	Forth Worth-Arlington, TX	FTW	FORT WORTH MEACHAM INTL
			FWS	FORT WORTH SPINKS
546	1737034	Seattle-Bellevue-Everett, WA	RNT	RENTON MUNI
			BFI	BOEING FIELD/KING COUNTY INTL

Implementing an algorithm that could simultaneously deal with each of the 4 relationships proved tricky, but was completed. In the end, the 565 clusters were associated with a total of 458 unique airports. Therefore, the final airport by airport OD matrix is of size 458x458.

4.3.3.6 Viability Filtering

The desired result of an airport-by-airport OD matrix was obtained in the last step, but this matrix contains a rather unwieldy 209,764 cells. Of course since the OD matrix was normalized, there are really only 104,882 unique cells, but this remains and unwieldy number and this is where the filtering process comes in. The vast majority of these cells will have either no demand or very little demand. The viable cells can be identified by checking if the daily number of passengers meets some minimum threshold. For instance, suppose the N+3 aircraft is assumed to have 20 passengers. To justify adding a profitable service route, one would expect the raw demand to be at least 125% of the aircraft's capacity. This is due to the fact that it would be highly unlikely for the N+3 aircraft to capture every single person at that location due to time concerns, pricing etc. The conventional air carriers use a similar rule and it is common practice to overbook seats for any given flight. This means that there must be at least 25

(20*1.25=25) daily passengers for a single flight per day for this particular example. Using this threshold criteria, all of the OD pairs that do not meet the threshold are reset to 0 and those meeting or exceeding the threshold are left. The number of viable routes will then vary based on the passenger capacity and viability percentage assumption.

An important factor to note is that this process does *not* consider if the airport is capable of handling the number of N+3 operations that would be required to support the raw demand. Assuming 12 hours of operation and 1 departure every 2 minutes (regardless of number of runways) an airport could theoretically support 360 operations per day. As a notional example consider the case of a 25 passenger N+3 aircraft. With this size aircraft and the theoretical operations limit, approximately 9000 passengers/day could be served. There may be a certain number of airports which exceed this limit, as is shown in Figure 56. In this case 17 of the 457 airports would be above the maximum capacity of the airport. The demand numbers that will be presented in this report will not be censored because of this capacity issue, but rather the reader should remember what is physically possible when considering the numbers presented.

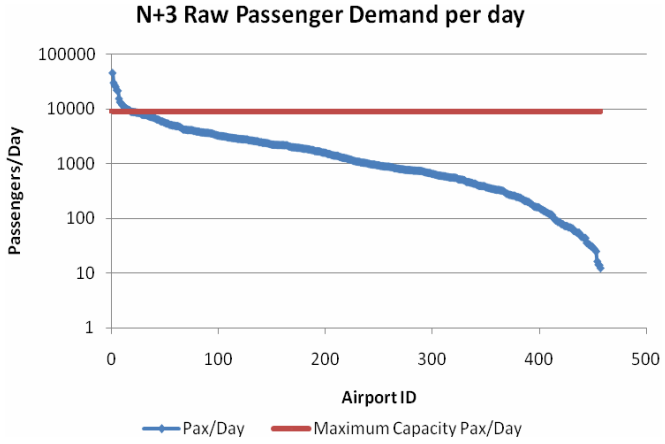

Figure 56. N+3 Raw Passenger Demand

4.3.3.7 Simulation Result

The result of this research is a viable p2p network for each aircraft capacity studied. The primary variables that need to be considered for each network are: the number of markets that can be served, the number of airports being used, the number of passengers being transported, and the number of operations required. One might expect that the number of markets that can be served would be greater with a small capacity aircraft since it requires fewer passengers on a particular route to create a profitable load factor. The reality from this exercise is that more markets can be served with a larger aircraft (on this particular scale) due to the fact that larger aircraft can offer lower ticket prices and hence attract more raw demand. This can be seen in Table 9. Weak filtering refers to a market viability criterion of a particular market having enough demand for a 60% load factor, while strong filtering refers to a 125% load factor. From a business perspective, 125% load factor is more realistic and hence the strong filtering will be used throughout the rest of the paper. As seen in the table the number of serviced airports is independent of aircraft capacity, but strongly correlated with the viability load factor.

Table 9. Effect of Viability Filtering

Aircraft passenger capacity		10	15	20	25	30
# of Markets (Pre-filtering)		49556	58732	64680	68810	72298
# of Viable Markets	Weak filtering (60% LF)	3497	4527	5019	5241	5238
	Strong filtering (125% LF)	1686	2257	2596	2675	2670
# of Serviced Airports	Weak filtering	393	415	417	414	412
	Strong filtering	325	345	350	347	346

A graphical depiction of the p2p network for the 10 and 30 passenger capacity aircraft for a single day's operations can be seen in Figure 57 and Figure 58. Immediately, the key markets for this type of an aircraft begin to emerge. The surprising result is that while the figure was generated assuming a p2p network would be utilized, from a top level it appears as though a hub-and-spoke model could meet the majority of the demand very well. This result arises just from the natural population distribution within the continental United States. Combine this natural emergence with efficiency gains by hub-and-spoke airlines and it becomes clear why the air transportation system of today is largely a hub-and-spoke system.

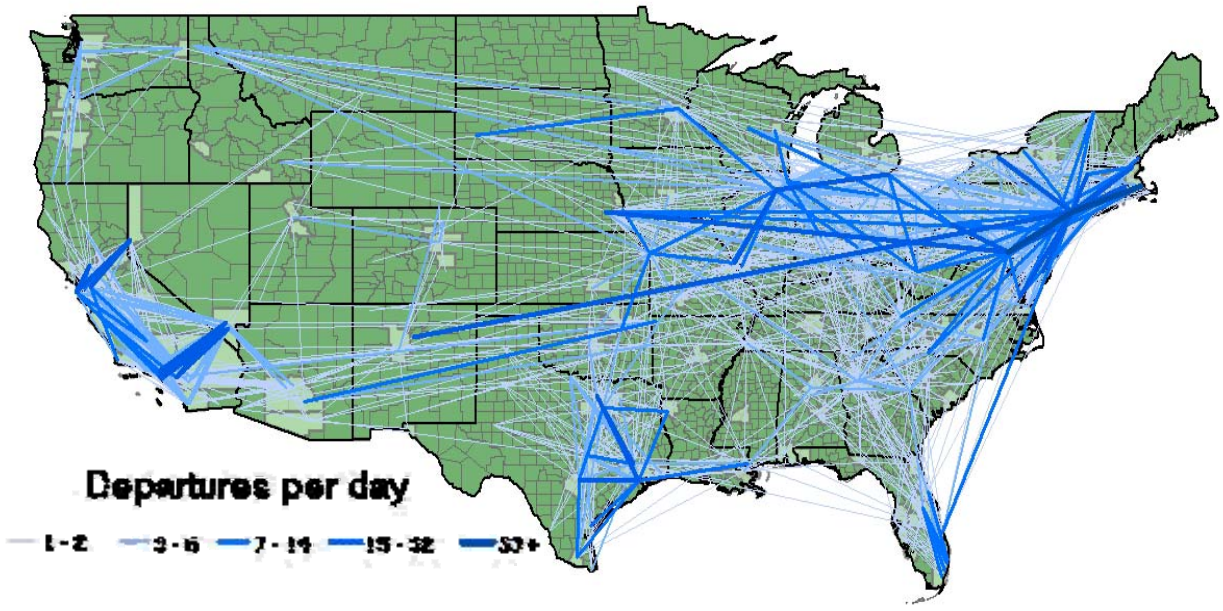

Figure 57. Ten (10) Passenger Capacity Network

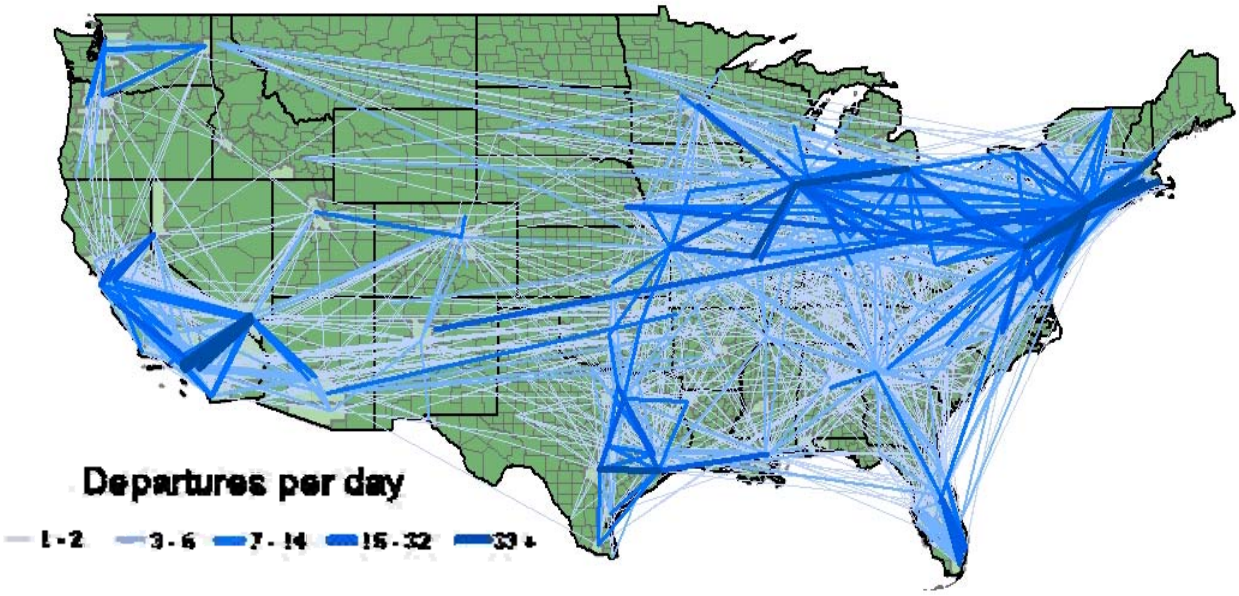

Figure 58. Thirty (30) Passenger Capacity Network

While Figure 57 and Figure 58 show the larger picture for what is happening with the networks across the entire United States, Figure 59 and Figure 60 show a zoom in on the California-Nevada market. Note that the scales have been changed and the smaller numbers of operations removed for clarity. Here it can be seen that what looked like one large market between Los Angeles and Las Vegas perhaps is actually several route pairs that utilize airports around the corresponding metropolitan regions.

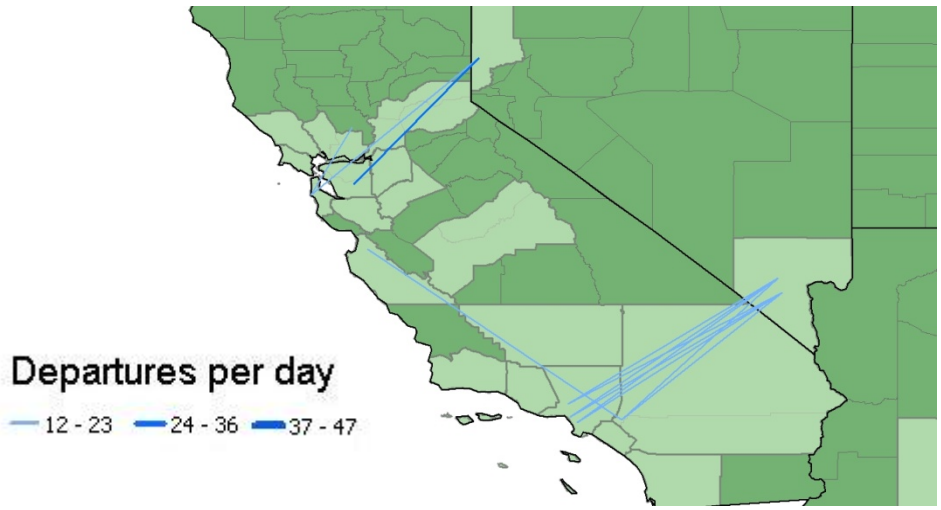

Figure 59. Zoom of California/Nevada Operations for 10 pax capacity

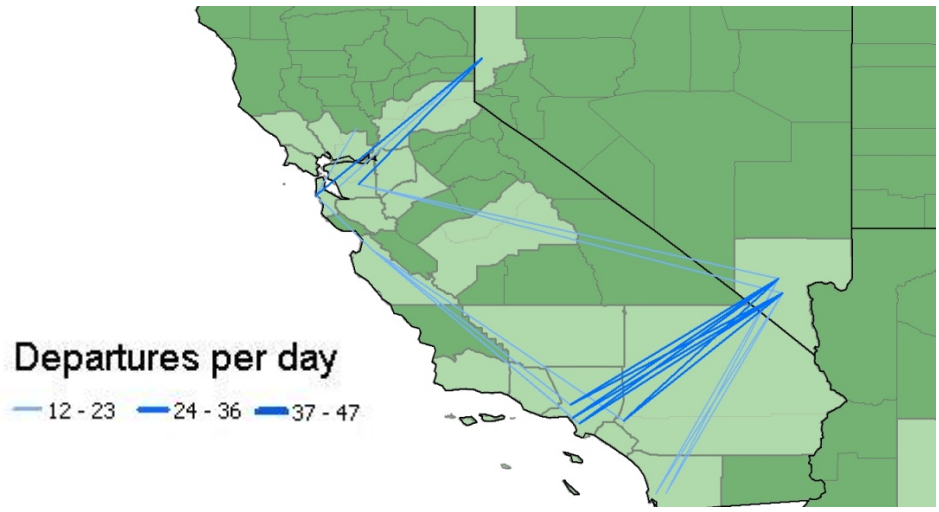

Figure 60. Zoom of California Nevada Operations for 30 pax capacity

Another way of visually analyzing and comparing the origin-destination matrices for each aircraft capacity is to organize the airports according their total number of passengers transported and then to use a three-dimensional bar graph to visualize the number of passengers being transported between each origin-destination pair. A comparison between 10 and 30 passenger capacities is shown in Figure 61. Due to size constraints, only the 100 airports with the most operations are shown. The x and y-axis correspond to airport indices, while the z-axis shows the passengers per day on that particular route.

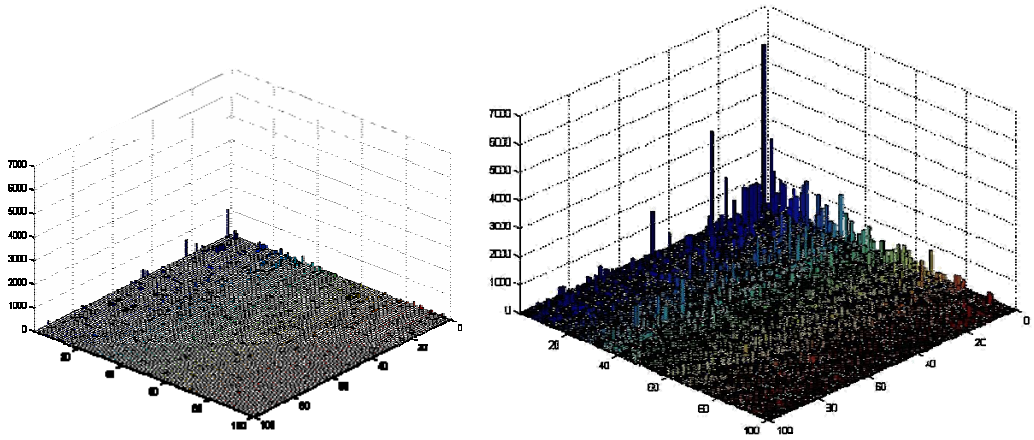

Figure 61. Number of Passengers on Top OD pairs for 10 pax (left) and 30 pax (right) aircraft

An analysis of the trip distance distribution weighted by the number of passengers for the 10 and 30 passenger aircraft is shown in Figure 62. The figures indicate that the majority of the trips fall in a 0-500 mile distance bracket for both aircraft capacities. This was the expected niche market for the small N+3 aircraft. Longer distance routes will be primarily served by the regular commercial airlines. It is interesting to see how similar the distributions are, but what is not shown in this graph is what was captured in the previous figure: the volume of trips is substantially higher for the 30 passenger case.

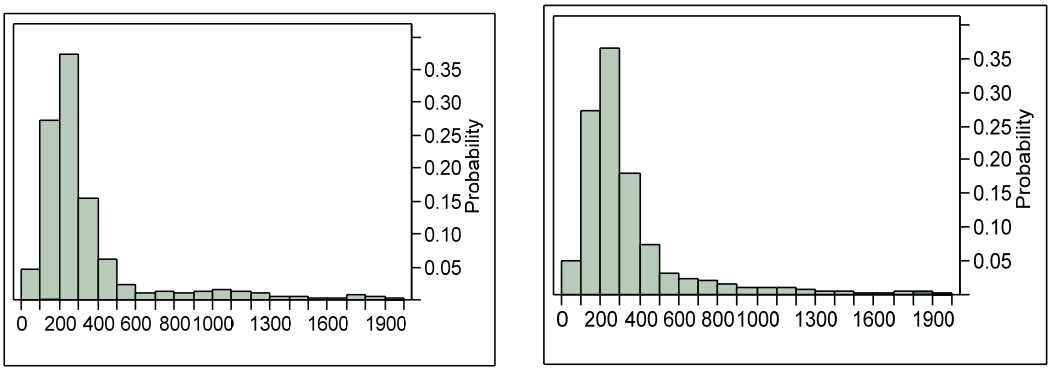

Figure 62. Trip Distribution Histogram (10 pax on left 30 pax on right)

The final airport-level filtered OD Matrix of size 458x458 is too large to present in this paper. The total number of viable round trip route pairs had a range between ~5000 and ~7000 airport pairs. If the total number of passengers and operations are summed for each N+3 capacity studied, summary information can be given. This summary information is shown graphically in Figure 63. The first conclusion that can be drawn is that overall the Phase C results look very similar in trend to the Phase A and Phase B, results which should be expected. The total number of passengers continues to trend upward with N+3 capacity due to the price factor, while the total number of viable departures levels off and begins decreasing from 20 passengers onward.

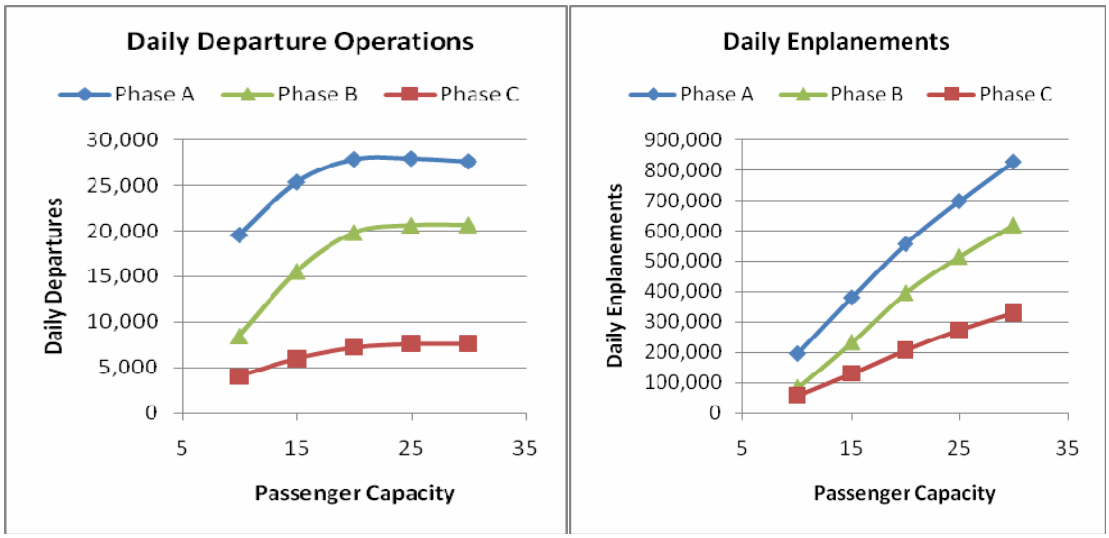

Figure 63. Phases Comparison

4.4 Summary of Aircraft Desirements for N+3 Service

Based on the demand study results we can identify some of the aircraft characteristics that would best serve the future N+3 network. The single most important factor in the viability of this future network will be the ticket price. Therefore, it is essential to design an aircraft that can be operated at minimum cost. This work well with the environmental goals of this project adding

another reason to desire the minimum fuel burn possible, since that is a key driver in operating costs. Aircraft acquisition and maintenance cost should also be minimizes as these also impact ticket price. In terms of range and speed the passenger preference was relatively insensitive, therefore, these should be subjected to the minimum fuel burn goal provided the range is sufficient to carry out the desired trip in one leg. Cruise Mach numbers of 0.55 or greater will be sufficient to great significant demand. Most flights are less than 850 nmi, according to DB1B data, so the N+3 aircraft does not need a longer design range. The other key element of a successful future network is maximizing accessibility to this new service. Therefore, the ability to operate in and out of airports with a 4,000ft runway will be a key requirement for the aircraft as well. Finally, the aircraft capacity sensitivity study indicated that an aircraft seating between 20 and 25 passengers would best meet the needs of the future network.

4.5 Noise Impact of N+3 Service

Considering the noise impacts of a new N+3 service is also a key element when considering the introduction of new flights at community airports. It should be noted that in order to avoid community sensitivities a notional airport was chosen and will not be disclosed. AEDT (Aviation Environmental Design Tool) from the FAA Office of Environment and Energy was used to calculate current and future noise levels at the notional airport with and without the N+3 service.

4.5.1 AEDT Noise Analysis

The Aviation Environmental Design Tool (AEDT) is the 'standard' tool used for fleet fuel burn and emissions analyses, and is replacing INM and MAGENTA as the standard for noise analyses and EDMS and SAGE as the standard for emissions analyses. It is designed to perform fuel burn, emissions, and noise estimates at any level ranging from a single airport to global operations. It is currently being developed, and functionality is continuously being added to meet the goals of its users and analysis requirements. Since AEDT will become the regulatory standard for aviation environmental analyses in the US; as such, using the AEDT for any desired aviation environmental analysis is be desirable, but there is a very specific framework which requires planning and preparation.

4.5.1.1 Data Requirements

There are two major parts to an aviation environmental analysis in AEDT: the aircraft involved, and the operations and procedures those aircraft fly. For the former, AEDT requires a specific characterization of each aircraft considered. This characterization is comprised mainly of Society of Automotive Engineers (SAE) Aerospace Information Report (AIR) 1845 and Base of Aircraft Data (BADA) definitions, with some additional information used to satisfy relational and other data requirements. This data is stored inside the AEDT Fleet database, which is a relational SQL database storing the aircraft modeling data and required related information.

If the capability is desired to analyze notional aircraft within AEDT, whether to compare to existing vehicles or to estimate impacts when added to a fleet, a translation of an aircraft definition to the AEDT characterization is paramount. This process requires transforming weight, aerodynamic, performance, and procedural information from all phases of flight into a set of coefficients used by the algorithms in AEDT. Depending on their use, the coefficients can have different meanings for piston-, turboprop-, and jet-powered aircraft. The consequence of these exacting data requirements is that a rigorous process must be developed to translate vehicle data to the AEDT format to support fleet level environmental analyses. Having such a process

in place greatly facilitates the integration of vehicles and concepts into aviation environmental studies.

The second portion of aviation environmental analyses is the scope and definition of operations and procedures aircraft fly. The intended scope of a study, which can range from flights at a single airport to all flights worldwide, affects the amount of data required when preparing a study. Information required for each unique flight considered in a study includes airframe, engine, departure and arrival airport, departure and arrival runway identifiers, great circle distance, cruise altitude, and departure and arrival date and time information, along with potential trajectory information, if available. With all this required information, the amount and detail of data for an analysis is directly tied to the number of flights to be considered in any analysis. Thus a great deal of planning and preparation is required to properly set up an environmental analysis, which should be adequately provided for at the outset.

AEDT is – by design – able to ingest data from a number of sources such as radar data and simulation data from a variety of simulation tools such as the Airspace Concepts Evaluation System (ACES). This data is normally split into flight records and trajectory records, which are cross-referenced to the flight level records. There are a number of automated tools, which may ease the work load for certain studies with large numbers of flights. To balance the effort required with the anticipated results, a study of proper scope should be identified to suit the needs of a project. For this noise studies a single notional airport was selected as described in later sections.

4.5.1.2 Noise Computations

In order to be able to calculate noise levels with AEDT the translation of the baseline operations said into the movements database format was required. The additional information required consisted of the great circle distance for each OD pair, which was obtained from an existing AEDT flight database were possible otherwise calculated based on the OD airport latitude and longitude coordinates from the AEDT airports database. The precise departure and arrival times which were also necessary were calculated by estimating trip duration based on the great circle distance and aircraft cruise speed. The precise aircraft engine type assignments were determined through lookups in the AEDT fleet database based on a given ICAO AC_TYPE.

It was decided that the metric of importance in this case was the day night level otherwise referred to as DNL. DNL represents a cumulative noise metrics that time averages be noise effect of individual flights and adjusts for human audible hearing. For this study the receptor grid at which the noise levels are calculated was a 16 x 16 nautical mile grid centered at the airport centroid. The noise engine was run using an adaptive noise grid using a grid refinement level of six for the 2006's scenario runs and a refinement level of eight for the 2027 scenario runs. It should be noted that a higher grid refinement may yield more precise contours which will affect the contour area.

Since exact runway end assignments for each operation were unknown, it was decided to assume that all flights were using runway 5--23. In reality if other runways are available takeoffs and arrivals will of course be spread among different runways if available. However, this is directly dependent on the airport configuration that was used during a particular day which in turn is again dependent on the exact weather conditions on that day. So it is a prudent assumption to make, if details about weather and airport configuration are unknown. The effects on the final DNL value is that the noise energy at any of the receivers not influenced by

both runways in a two runway configuration but only by one runway in a two runway configuration will effectively double by assigning all operations to a single runway. Since DNL is a logarithmic measure, this means there will be a variation of three dB. The DNL level also incorporates a nice time penalty of 10 dB for operations occurring between 10 PM and 7 AM. This represents a significant influence on the final noise levels because moving departure or arrival times just a few minutes across one of those boundary times will significantly change the overall contour and also the contour area. Therefore, for this study it was decided to simply place all of the operations into the daytime level and not alter their timing such that they would sometimes fall into the nighttime level penalty.

It should also be noted that due to certain limitations of the early developmental executable that was used for this analysis that departure and arrival single events had to be calculated separately and their respective DNL HAVE to be added together and recombined into the final DNL contour in post processing using the standard Doc 29 [15,16] methodology.

Methodology

1) From ECAC Doc 29: $$L_{eq,W} = 10 \cdot \log\left[\frac{t_2}{T_0} \cdot \sum_{i=1}^{N} g_i \cdot 10^{L_{E,i}/10}\right] + C$$

2) Our Implementation: $$Corr.DNL = \underbrace{10 \cdot \log\left[NoiseExp\right]}_{\text{AEDT 'Level'}} + 10 \cdot \log\left(\frac{1}{86400}\right)$$

(What's actually output by AEDT in our runs – the constant is post-processed)

AEDT split up Departure and Arrival noise calculations, so:

	Departure	Arrival
3)	$DEP\ DNL = 10 \cdot \log\left[NoiseExp_{DEP}\right] - C$	$ARR\ DNL = 10 \cdot \log\left[NoiseExp_{ARR}\right] + C$

4) $$NoiseExp_{Event} = 10^{\frac{Event\ DNL - C}{10}}$$

5) $$NoiseExp_{DEP} = 10^{\frac{DEP\ DNL - C}{10}} \qquad NoiseExp_{ARR} = 10^{\frac{ARR\ DNL - C}{10}}$$

6) $$NoiseExp_{TOTAL} = NoiseExp_{DEP} + NoiseExp_{ARR} = 10^{\frac{DEP\ DNL - C}{10}} + 10^{\frac{ARR\ DNL - C}{10}}$$

7) ➡ $$TOT\ DNL = 10 \cdot \log\left[NoiseExp_{TOT}\right] + C \qquad C = -49.365$$

4.5.2 Current Noise Levels at the Notional Airport

The notional airport was selected from among a list of airports that could be easily modeled by AEDT (Aviation Environmental Design Tool) from the FAA Office of Environment and Energy. The initial list was down selected with input from Cessna and data was gathered for the remaining airports in order to make the final selection. Suffice it to say that an airport with a 4000ft runway in good condition and access to basic services such as rental cars and baggage claim was chosen while airports currently offering commercial traffic were avoided.

A baseline set of operations at the notional airport was provided by Sensis and expanded to reflect current traffic levels at that location. The expansion was carried out while preserving the mix between arrivals and departures, and the equipment usage. It should be noted that 14 distinct aircraft were included in the original data set encompassing from small two seat aircraft

to regional jets. A similar schedule and origin-destination locations were also used, this encompassed 24 different origin or destination airports ranging from 40 to 1000 nmi away.

Although the notional airport chosen has two runways, there was insufficient information available to define all arrival and departure trajectories. Therefore, all traffic was assumed to arrive/depart out of a single runway using straight in/straight out trajectories. This will slightly overestimate noise along that runway while underestimating noise in other runway directions.

Baseline noise contours were calculated for this airport and are shown in Figure 64. Note that the noise at the airport boundary is already above the 55db stated goal with current day traffic levels.

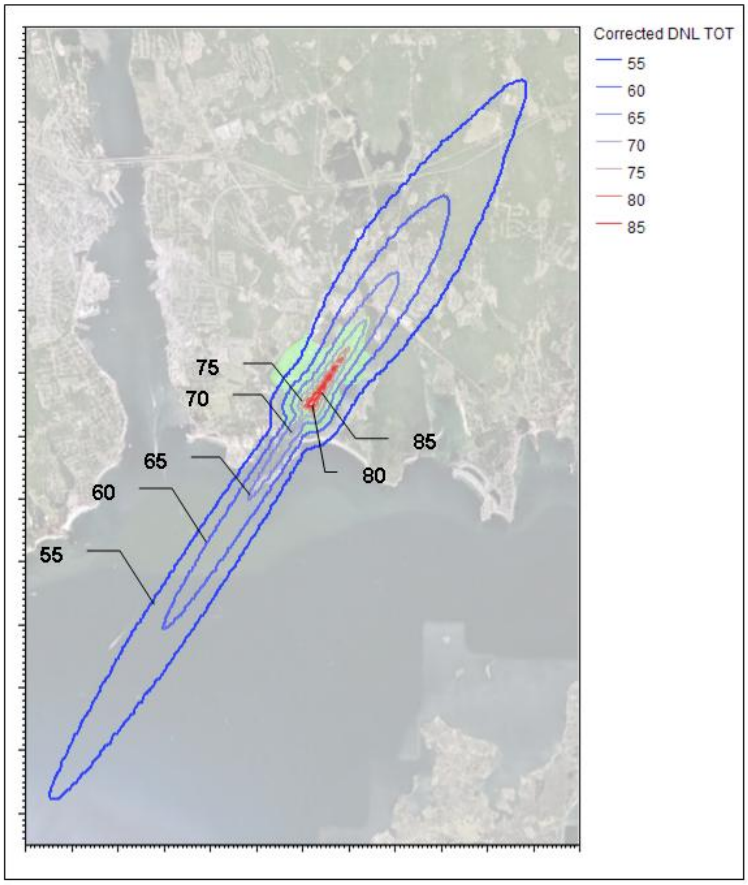

Figure 64. Baseline Noise Contours at Notional Airport

The demand estimates for N+3 travel in the current year, based on an aircraft size between 20 and 25 passengers, pointed to an average of 6 additional operations per US airport considered. Since, the forecasted travel demand for 2030 is expected to result in a four-fold increase in N+3 flights, sensitivity studies introducing between 6 and 36 operations of the baseline and advanced N+3 aircraft will be considered in later sections of this report.

4.6 Mobility and Fuel Burn Impacts of N+3 Service

Based on the assumptions outlined in the notional trip section, the N+3 aircraft network would provide a significant increase in mobility by reducing time and distance traveled even at today's technology level. Additionally, fuel burn and the resulting green house emissions were similar to the hub-and-spoke system in spite of carrying fewer passengers due to the reduction in distance traveled. Further, since only one landing/take-off cycle is required, LTO NOx emissions were also reduced. The results of this notional trip comparison are shown in Table 10.

Table 10. Current Day Hub-and-Spoke vs. N+3 Notional Trips

Fuel/Passenger			LTO NOX		
N+3	Hub	Diff	N+3	Hub	Diff
123.1	119.4	**3.1%**	43	64.1	**-26%**
Door to Door Dist			**Door to Door Time**		
N+3	Hub	Diff	N+3	Hub	Diff
421	643	**-35%**	143	241	**-41%**

As reported in the requirements definition section of this report, the demand is somewhat sensitive to block speed. The advanced aircraft, described in later sections of this report, is somewhat slower than the original baseline which could slightly decrease the demand. However, since the travel time reduction with respect to the hub and spoke network is still quite significant (see Table 11) it is unlikely that the demand would be significantly affected. Furthermore, the fuel burn decrease with respect to the baseline will significantly affect ticket price, increasing the demand for this mode of travel and easily offsetting and surpassing the negative impact of reduced speed.

Table 11. Current and Future N+3 Point-to-Point Trips Compared to Hub and Spoke

Baseline			Advanced		
Fuel/Passenger (lbs / pax)			Fuel/Passenger (lbs / pax)		
N+3	Hub	Diff	N+3	Hub	Diff
123.1	119.4	**3.1%**	45.4	119.4	**-62.0%**
Door to Door Time (min)			Door to Door Time (min)		
N+3	Hub	Diff	N+3	Hub	Diff
143	241	**-41%**	154	241	**-36%**

4.7 Other Impacts of N+3 Network

The N+3 concept is envisioned to operate as a point-to-point service using underutilized airports and much work has been done to identify these potential airports. So far, the critical criteria required of these airports were an effective runway length of 4,000 ft. and an acceptable surface condition. It is important to realize that the runway is only a small portion of an airport's infrastructure and many of the predicted N+3 airports could be currently unequipped to handle the expected future demand and therefore constrain the N+3 service. The first portion of this

study attempts to define the relationship between people, aircraft, and airport ground infrastructure as well as provide the means to obtain first-order estimations of required future ground infrastructure based on the ***Mi*** results.

Implementation of the N+3 concept will result in an influx of people traveling to, from, or through the serviced area and the latter portion of this study discusses the impact the N+3 service could have jobs and the local economy. The main focus is a discussion of the methods and models that are used to measure the economic impact that a proposed project could have on the local economy.

4.7.1 N+3 Ground Infrastructure

An airport's ground infrastructure consists of airside and landside facilities and is generally a function of the amount and type of passengers and aircraft utilizing the airport. The main components consist of automobile parking spaces, the passenger terminal building, and aircraft related systems such as aircraft gates and ramp area. Airport facilities can be classified first based on their functional role which is generally separated into three categories, originating-terminating stations, transfer stations, and through stations. The airports in the N+3 network most likely fall into the originating-terminating classification since it is intended to be a point-to-point service. Originating-terminating stations may have higher requirements for parking, ticketing, and baggage claim facilities since most of the passengers will be beginning or ending their trip at this airport[15].

Recent literature relating to airport planning or transportation engineering contains little information on quantifying the required ground infrastructure of an airport and is generally concerned with airports that have significantly higher volumes of passengers than most of the airports in the N+3 network. Further investigation revealed two FAA Advisory Circulars (AC) published in the 1980's with the specific purpose of obtaining first-order estimations of airport ground infrastructure. AC 150/5360-9, titled "Planning and Design of Airport Terminal Building Facilities at Nonhub Locations", is intended for airports with less than 250,000 annual enplanements while AC 150/5360-13, titled "Planning and Design Guidelines for Airport Terminal Facilities", provides guidelines up to 20 million annual enplanements.

The AC's mentioned above provide estimations for parking spaces, terminal building size and number of gates based on either annual or peak hour enplanements. The peak demand used to determine facility size is typically based on the peak hour on an average day of the peak month[16], but since the ***Mi*** results represent enplanements per day, it is assumed this is an average value and then multiplied by 365 to obtain annual enplanements. The AC's are then used to obtain an estimation of peak hour enplanements, as well as the number of aircraft gates, by use of the graph shown in Figure 65 [17].

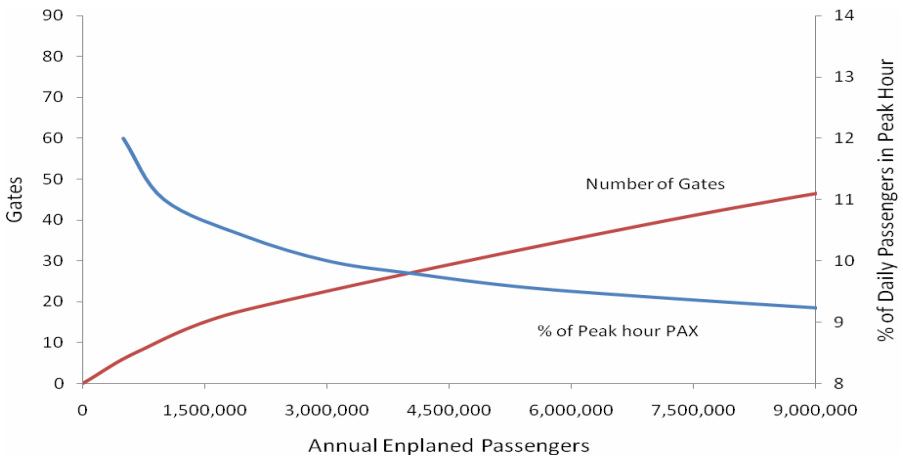

Figure 65. Estimated Number of Gates and Peak Hour Passengers

The two AC's are synthesized into one graph relating total terminal area per gate to annual enplanements by the process shown below in Figure 66 [18,19]. AC 150/5360-13 simply uses annual enplanements to find parking spaces and total terminal area per gate while AC 150/5360-9 requires conversion to peak hour enplanements and calculation of separate airport facilities, such as lobby area and baggage claim space, and then adding them together to obtain total terminal area per gate.

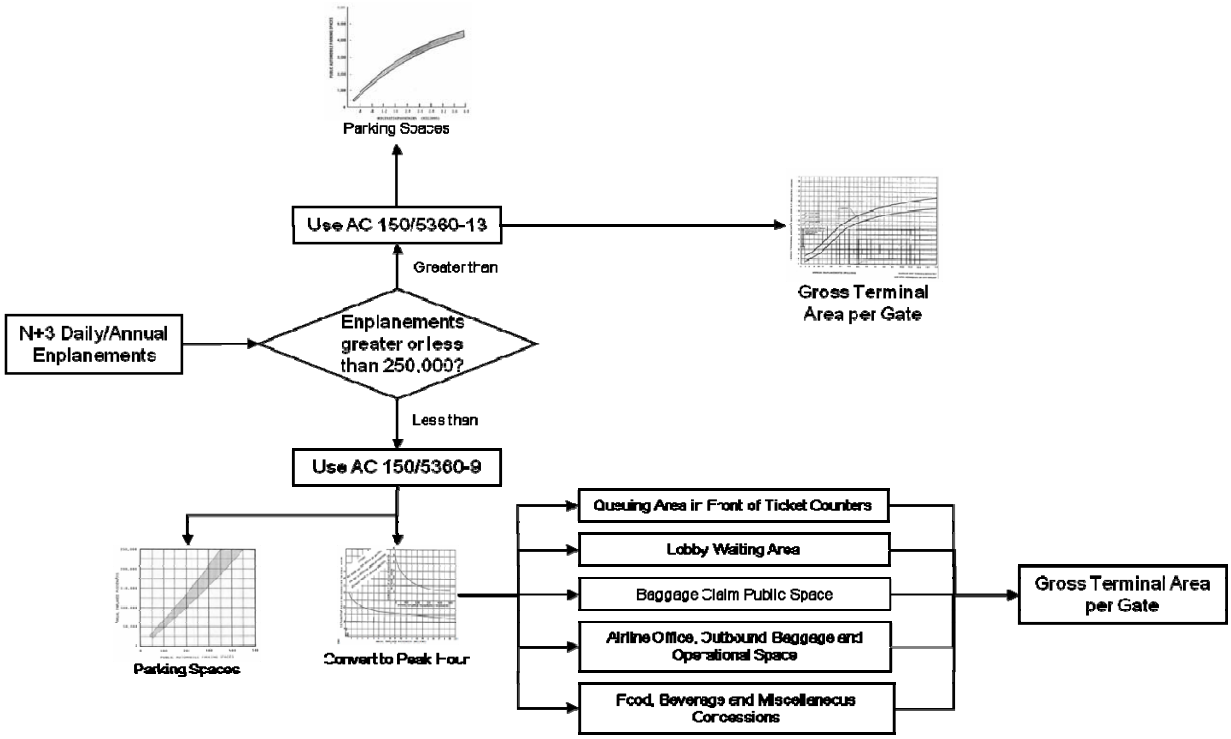

Figure 66. Decision Process to Synthesize AC 150/5360-9 and -13

The result of the process shown above is the graph in Figure 67, where total parking lot spaces are in blue and total terminal area per gate is in red. The extreme left portion of the graph (less than 250,000 annual enplanements), which represents approximately 66 percent of all the N+3 airports, is determined by use of AC 150/5360-9 and a larger view of this portion is shown in Figure 68.

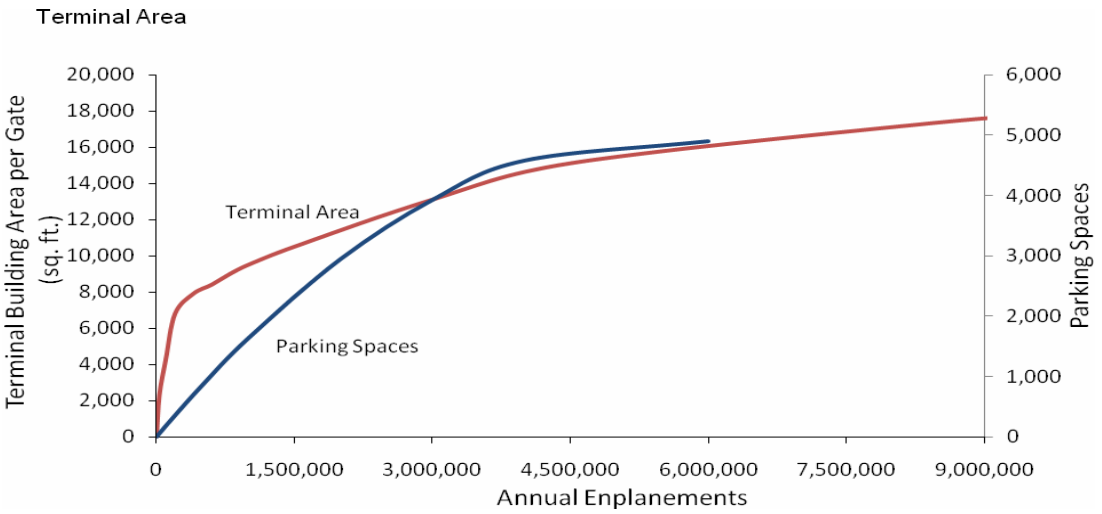

Figure 67. Total Terminal Area per Gate vs. Annual Enplanements

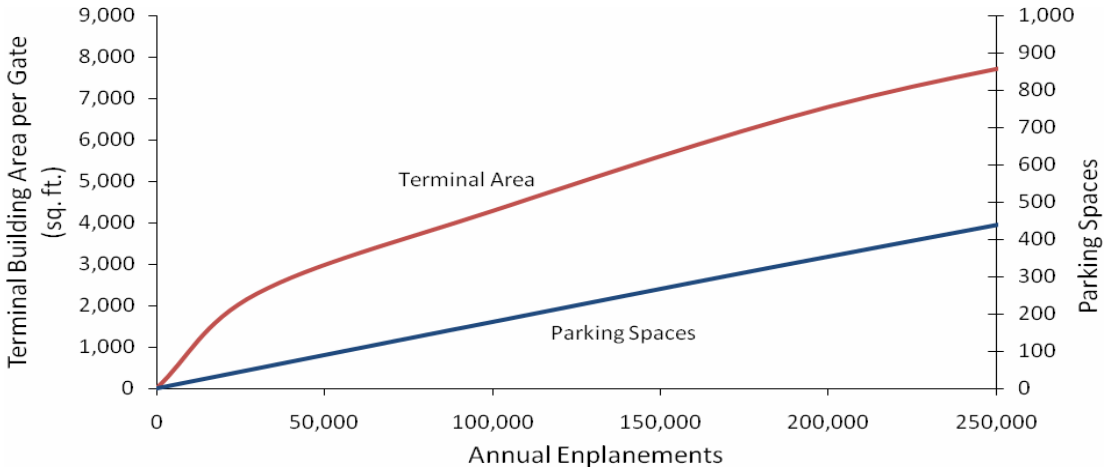

Figure 68. Total Terminal Area per Gate vs. Annual Enplanements

These figures can be used to obtain first-order estimates of the required future ground infrastructure of airports utilized in the N+3 network. As an example, the ***Mi*** results were used to select three airports based on their annual enplanement rank to show the wide range of estimated required infrastructure and the results are in Table 12. It is important to note that ground infrastructure, such as the number of aircraft gates and the size of the terminal building, is generally estimated based on peak hour operations and peak hour passenger flow, respectively. Peak hour activity will be heavily influenced by airline scheduling and therefore these estimations could widely vary from the actual facilities if further work was done to establish a preliminary N+3 schedule.

Table 12. Example Ground Infrastructure

Airport Code	Location	N+3 rank	N+3 Annual Enplanements	Parking Spaces	Number of Gates	Total Terminal Building Area (ft^2)
HHR	Hawthorne, CA	10	1,887,399	2,814	17	191,000
LZU	Lawrenceville, GA	101	419,021	726	5	40,500
CBF	Council Bluffs, IA	204	126,994	226	1	5,500

If the current airport infrastructure is known, the process and figures shown above could be used in reverse to estimate the current number of annual enplanements the facility is capable of handling. Most of the airports in the N+3 network are likely "pilot friendly" general aviation airports and their existing facilities are not designed to perform the functional requirements of a typical commercial passenger terminal such as ticketing, baggage handling, and security. The airports in the network, both general aviation and small commercial hubs, will need to be examined individually to determine the usefulness of their existing facilities and their limitations to growth.

Estimating ground infrastructure costs at this point is difficult since it will be a function of airline scheduling and each airport's existing facilities, both of which need further investigation. Examining various scales of airport terminal construction projects resulted in the cost of construction to average approximately $200 to $300 per square foot [20]. If this cost estimation is used and the process used to create Table 12 is applied to every viable airport in the N+3 network to obtain a total terminal building area for the whole system it results in a total terminal building construction cost of approximately $2 to $4 billion, which is approximately 0.5% of the $787 billion economic stimulus package passed in 2009. Not every airport in the system would need a new terminal building, but may need some sort of modification or expansion to handle the N+3 service. This cost estimation is associated with only the terminal building and does not include automobile parking, aircraft gates, or internal terminal systems such as a baggage handling system. Cost models for such infrastructure are currently unavailable, but could potentially be developed as the N+3 concept is further explored.

The methods and numbers previously described should be used as an order-of-magnitude estimation and more detailed analyses will need to be conducted as the N+3 concept is further developed. An architect or engineer performing these detailed analyses could use these figures to estimate the scope of the project in the early stages of the design process.

4.7.2 N+3 Airport Economic Impact

A complex relationship exists between an airport and the local economy since the two simultaneously support each other. Attempting to de-couple the interaction between the two and establish a "cause and effect" linear relationship will result in an inaccurate model of the real world. Generally, a region's economic activity can generate the need for some mode of transportation to ship and receive goods or facilitate face-to-face meetings between business representatives. But the relationship can go both ways, meaning that a cost-effective transportation system can in turn attract firms and generate economic activity. There is no doubt a link between airline service and economic development, but it is a challenging relationship to define and only a few studies appear to have made such an attempt.

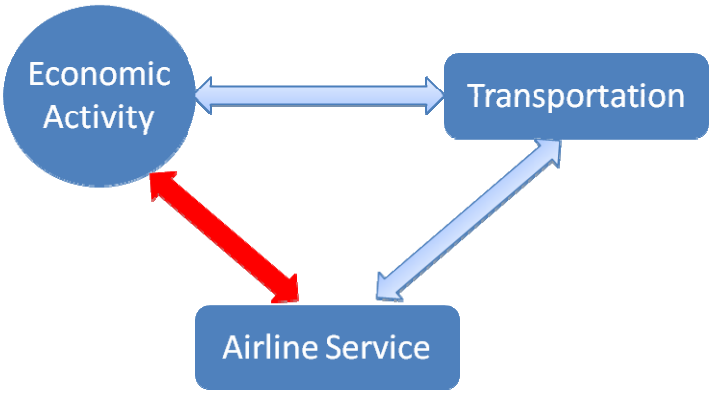

Figure 69. Economic Activity and Airline Service Relationship

Airport economic impact studies are commonly performed to estimate what an airport's services or activities contribute to the local economy. They can be used to demonstrate the significance of an airport to persuade decision makers to protect its existence or used as evidence in cost-benefit analyses for specific airport investment projects. Estimating the potential economic impact of the N+3 concept could provide justification for the significant investment that would be required to implement the system.

There are three methods that are commonly used today to perform economic impact analyses. They are the input-output method, collection of benefits method, and catalytic method. The collection of benefits method is a quantitative or qualitative measure of the benefits and costs associated with an airport such as time saved, costs avoided by using air transportation, stimulation of business, recreation, and community benefits. The catalytic method measures how the airport benefits the supply side of the economy, measuring the impacts on investment, trade, and overall productivity and is usually quantified in monetary terms. The input-output (I-O) method is commonly used to perform airport economic impact analyses and appears to have the most potential for estimating the impact of the N+3 concept.

The I-O method measures the impact of three separate areas defined as direct, indirect, and induced impacts. Direct impacts result from spending in the local area by airport employees and visitors and indirect impacts are related to off-airport entities and estimate the flow of dollars generated from the supply of materials, goods, or services that are attributable to the airport. Induced impacts, or multiplier effects, are a result of the dollars generated by direct and indirect impacts being spent throughout the local economy. The variables used to describe the total economic impact are usually output, payroll, and employment. Output related to the airport will typically include the value of goods or services sold, capital expenditures, and spending by visitors. Payroll is the wages paid to employees of the airport or employees who support or use the airport and employment is the jobs created or related to the airport[21].

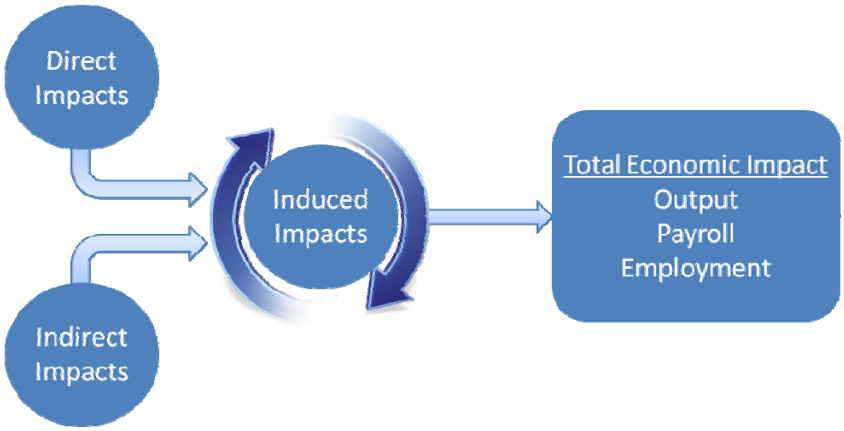

Figure 70. Input-Output Method

Applying the I-O methodology to perform economic impact analyses requires some sort of economic model such as the Regional Input-Output Modeling System (RIMS II). RIMS II was developed in the 1980's to be a cost-effective way for analyst to provide approximate order-of-magnitude changes in a regional economy due to a variety of projects such as shopping malls, sports stadiums, or airport construction and expansion. The RIMS II model estimates regional input-output multipliers, purchased from the Bureau of Economic Analysis (BEA), to estimate induced impacts based on a national I-O table, which takes into account the relationship of the nearly 500 industries contained in the database, one of which is commercial air transportation[21]. Ideally, this type of model would be applied to estimate the impact of the N+3 network. However, the data necessary to carry out such an in depth study is not currently available.

In an attempt to bypass a complex and time consuming method to obtain an order-of-magnitude estimation of the potential nationwide economic impact that the N+3 service could have, results of various airport impact analyses were compiled and compared against FAA enplanement data for that year. The goal was to establish a trend between economic activity and enplanements and to investigate whether a trend in one region is comparable to another. The figures below show the results of airport economic impact studies of commercial airports in the state of Texas compared against FAA enplanement data in 2005. As expected, there is a positive correlation between regional economic activity and enplanements.

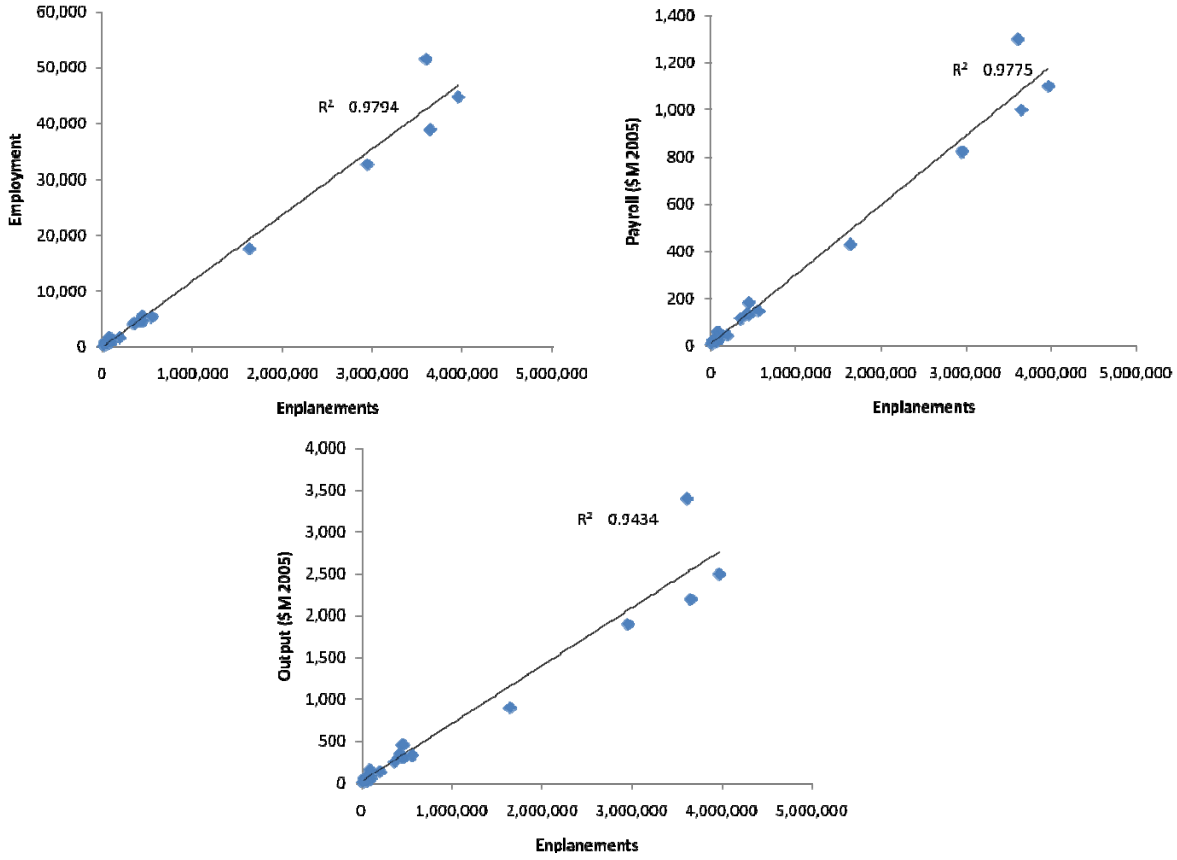

Figure 71. 2005 Texas Economic Activity vs. Enplanements [22]

The trends shown in Figure 71 were compared to a 2009 Iowa study to examine how one regional trend compared to another. Employment as a function of passenger enplanements for Iowa and Texas are shown in Figure 72 and the results show that a linear relationship still applies, but the slopes varies too widely for one regional relationship to be applied in another. This is not surprising since each region will have unique socioeconomic characteristics.

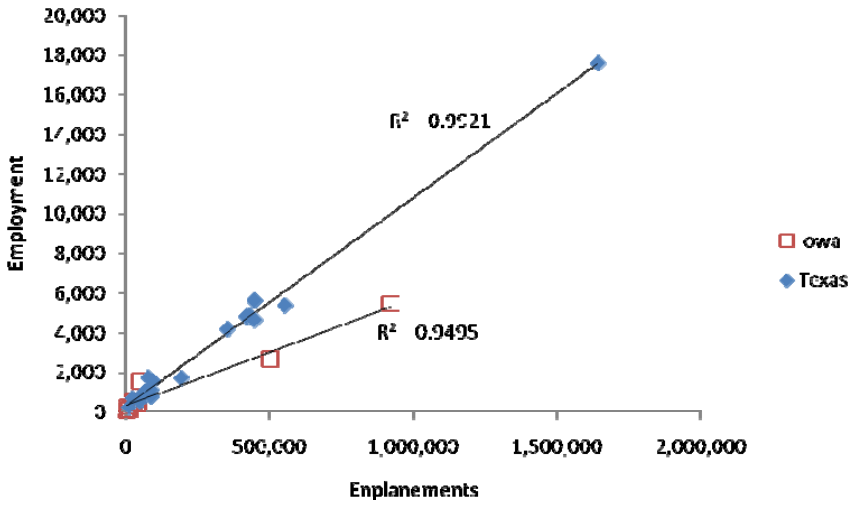

Figure 72. Comparison of Employment vs. Enplanements between Iowa and Texas[22,23]

These results agree with existing studies showing that there is a link between airport and economic activity. The results of some studies suggest that a 10% increase in enplanements will result in approximately a 1% increase in service related employment[24]. There is no question that airports play a significant role in their local economy. A 2008 FAA study estimated that the United States aviation industry resulted in 11 million jobs and accounted for 5.6% of the gross domestic product [25]. Qualitatively speaking, with the airports in the N+3 network already in place, establishing scheduled commercial air service will have positive effect on their surrounding economies. Quantifying that effect would require an extensive study beyond the scope of this Phase 1 study, but should provide additional incentive for acceptance of commercial service at local community airports.

5.0 Baseline 20 Passenger Airliner

The baseline airliner (B-20) is a current technology conceptual aircraft intended to provide point-to-point service to and from regional airports, and thereby avoid the added distance, time, and fuel consumption involved with an intermediate stop at a hub airport. This conceptual airliner is used for three purposes: (1) to compute mission sensitivities that will be used to develop an improved, year 2035 airliner, (2) to serve as a point of comparison to measure the improvement of the 2035 airliner compared to state-of-the-art, and (3) to provide a publicly-available configuration which can be used to calibrate the Cessna and NASA design and analysis tools (as used by the Georgia Institute of Technology).

With 20 passengers, two pilots, and one flight attendant, the B-20 is designed to meet 14 CFR Part 25 (transport category aircraft) certification requirements (Part 25 rules are the certification basis for all airliners with more than 19 seats). The network analysis suggests a design range at maximum payload of 800 nm at Mach=0.6 and a cruise altitude of 41,000 ft. Top-level specifications for the B-20 are shown in Table 13. Aft-mounted turbofan engines typical of 2009 technology provide low cruise noise and passenger acceptance.

Table 13. Top-Level Specifications for the B-20 Airliner

	B-20
Range with Max Payload (nm)	800
Cruise Mach No. (at 41,000 ft.)	0.60
Balanced Field Length (Sea Level, ISA, ft.)	4,000
Certified Ceiling Altitude (ft.)	41,000
Passenger Seating Capacity	20
Payload—20 passengers, with bags	
Crew—two pilots, one attendant	

5.1 B-20 Interior Layout and Design

Although a relatively small regional aircraft, the B-20 cabin is sized to provide comfort equivalent to a Boeing 737. In order to develop an interior layout for the B-20, Cessna used specifications from Reference 27, as appropriate for medium range jet airliners equipped for "normal" service (as opposed to "deluxe" or "economy" service). Interior layouts with two, three, and four seats abreast were considered. Three abreast seating was chosen as optimal for airliners in the twenty to forty seat capacities. Four abreast seating caused the fuselage fineness ratio to be too small for less than about 30 seats, and two abreast seating caused the fuselage fineness ratio to be too large for more than about 30 seats.

Three cabin cross-sections were drawn using a three abreast layout. A 100-inch outside diameter was chosen as best representing near-737 comfort. 95 and 105 inch outside diameter cabins were also considered. Figure 73 shows a 100 inch diameter and a top view of the cabin layout. A pull-down seat for a flight attendant mounted on the bulkhead just behind the pilot and

just to the left of the entry door (30 inches wide), an aft lavatory, and an aft pressurized checked baggage compartment with external access through a 24-inch wide baggage compartment door completes the definition of a cabin with passenger comfort and serviceability similar to a current day Boeing 737. Not shown in the cabin top view are the overhead baggage compartments. Two emergency exits (26 inches wide) located on either side of the aft cabin and a third exit (24 inches wide) across from the entry door provide safety features that are compliant with FAA Part 25 certification and Part 21 operational regulations.

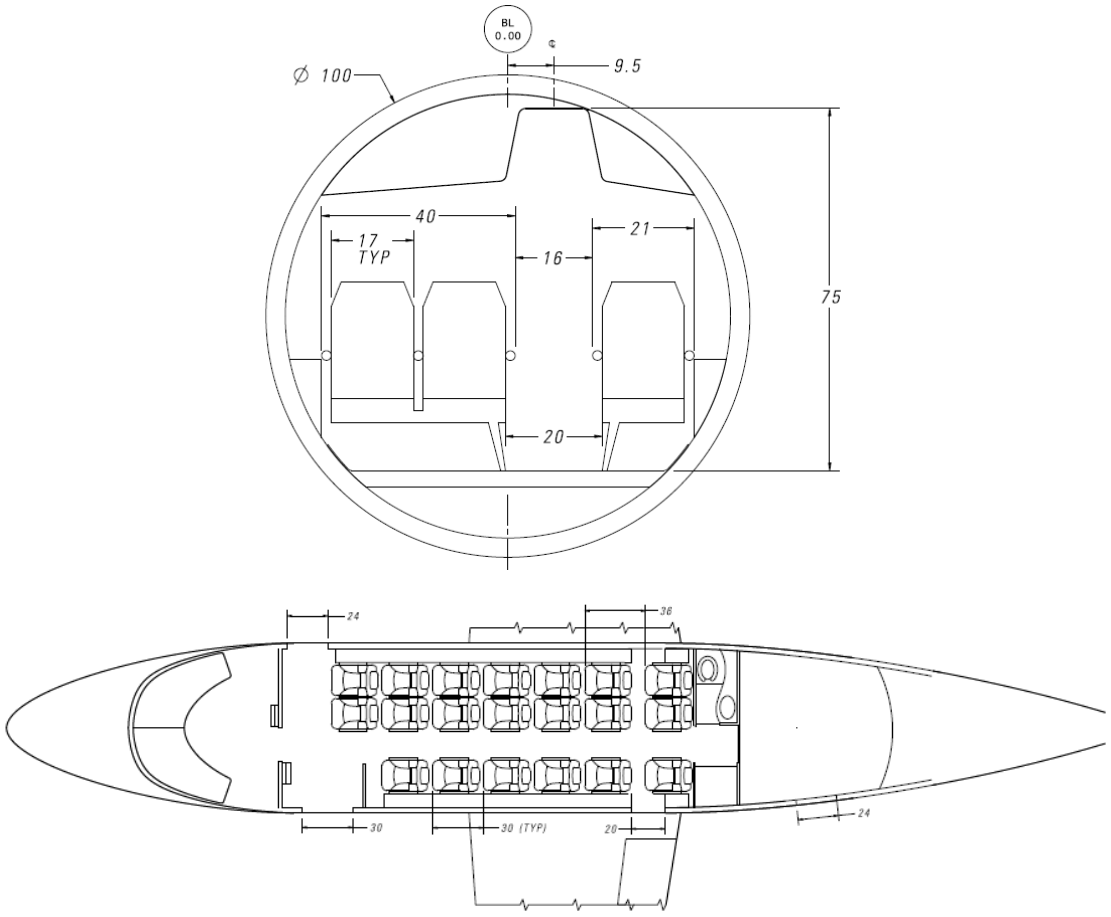

Figure 73. Cabin Layout for Baseline Airliner.

5.2 B-20 External Geometry

A three-view solid model of the B-20 airliner is shown in Figure 74. Geometric parameters aircraft are called out in Table 14. The wing is tapered and unswept. The wing span is 59.95 ft, and the wing thickness ratio is 0.138. The horizontal tail is swept and tapered with a lower aspect ratio. Horizontal tail area is 32% of wing area, and horizontal tail span is 28.61 ft. The vertical tail (at 21% of the wing area) is highly swept and tapered. The fuselage has a fineness ratio of 6.65. The nacelle fineness ratio is 2.6. Overall configuration length is 61.02 ft, and overall height is 19.72 ft.

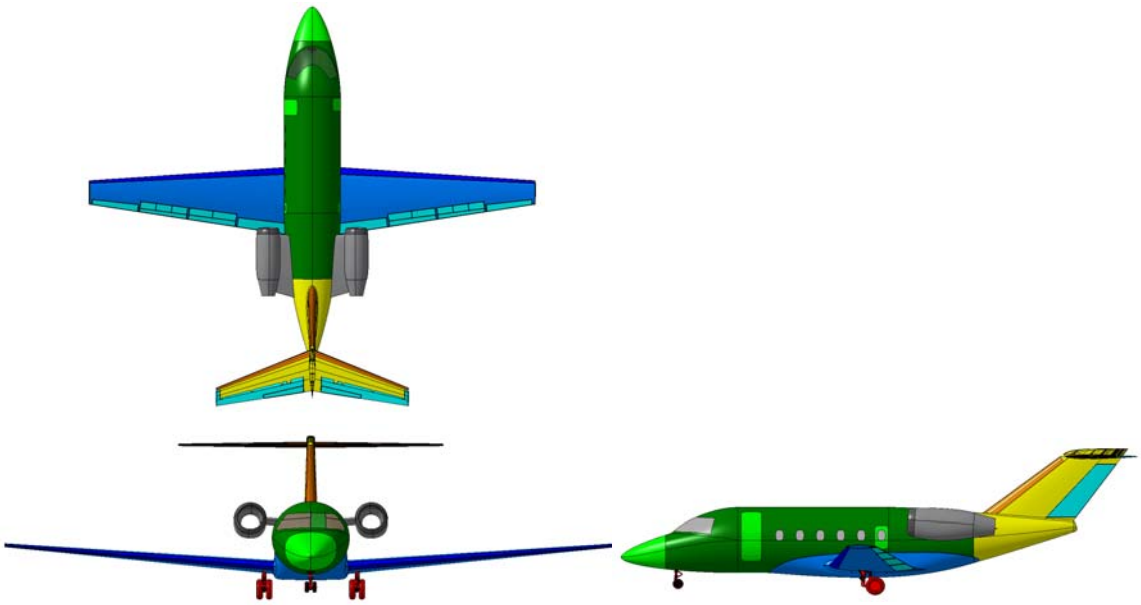

Figure 74. Three-View Picture of Baseline Airliner

Table 14. Baseline Airliner Geometry

	Wing	Horizontal Tail	Vertical Tail
Aspect Ratio	8.77	6.11	0.872
Taper Ratio	0.318	0.425	0.6
Sweep (c/4) (°)	0	20	49
Thickness-to-chord (%)	0.1375	0.0921	0.12
Reference Area (sq ft)	407.9	131	86.9
	Fuselage	**Nacelle**	
Length (ft)	55.42	9.43	
Diameter (ft)	8.33	3.55	

5.3 B-20 Systems Description

Preliminary estimates of B-20 weights suggest that the maximum takeoff gross weight is in the range of 20,000 to 25,000 pounds. The Cessna Citation Sovereign is a state-of-the-art business jet with a gross weight of 30,300 pounds, and a similar degree systems complexity as imagined for B-20. Because of these similarities, systems for the B-20 are patterned from the Citation Sovereign. The systems of the B-20 are briefly described in the following sections.

5.3.1 Landing Gear

The landing gear is a tricycle configuration, consisting of two dual-tire, trailing-link main landing gear assemblies, and a dual tire, chined nose landing gear assembly. Extension and retraction is powered hydraulically, with emergency extension by blow down (using nitrogen gas) and freefall. Hydraulic disc brakes are powered by main hydraulic system, with an electric backup pump.

5.3.2 Surface Controls

The surface controls are manual ailerons, elevator, and rudder. Ailerons are assisted with hydraulic roll spoilers. Power assist or boost will be used as necessary to satisfy pilot control force requirements. All axes have electric trim. The single-slotted Fowler flaps are electrically actuated.

5.3.3 Auxiliary Power Unit (APU)

The APU is a single turbine unit of the appropriate size. During ground operation, this unit provides compressed air for heating, cooling, and ventilating the cabin, and electrical power for lighting and avionics. The APU is the primary source of compressed air to start the main engines. The APU is not certified as “essential” (i.e., there is no requirement that the APU operate during flight), but it may be operated at lower flight altitudes, if desired.

5.3.4 Hydraulics

The hydraulics system is a single channel, 3,000 psi closed center system.

5.3.5 Electrical

One alternator (115 VAC) on each engine powers electric windshield anti-ice. All other electrical demands are met with one 28 VDC generator on each main engine along with one on the APU. The B-20 has a split-bus electrical architecture. Two nickel-cadmium batteries of the appropriate capacity are used to provide alternate power.

5.3.6 Avionics

The B-20 is similar in size to the Citation Sovereign which uses the Honeywell Epic system. It is assumed that the B-20 system will be similar in weight, if not in name, to the Epic system.

5.3.7 Environmental Control

A single air cycle system pressurizes, heats, and cools the cabin. There are separate flow paths and temperature controls for the cockpit and the cabin. In case of an air cycle machine failure, an emergency pressurization system bypasses engine bleed air around the air cycle system.

5.3.8 Ice Protection

The wing, horizontal stabilizer, and engine inlet leading edges are protected from ice using a bleed air powered system. The air data probes and windshield are protected electrically.

5.4 B-20 Weights Data

Component weights for the B-20 optimized to meet the mission requirements are shown in Table 15. Metal-bond aluminum structure and a combination of hydraulic, pneumatic, electric, and manual systems define the technologies for these components. This package of technologies is characteristic of regional airliners in 2009. An auxiliary power unit is also included. Tanks capable of holding 5, 197 lbs of fuel are located in the wing; there are no fuselage fuel tanks.

Table 15. Baseline Aircraft Weights

Component	Weight, lbs
Wing	2,202
Horizontal Tail	430
Vertical Tail	287
Fuselage	3,587
Landing Gear	793
Surface Controls	266
Nacelle and Air Induction	419
Propulsion Group	2,592
Hydraulics	184
Electrical	778
Avionics & Instruments	571
Furnishings and Equipment	1,522
Air Conditioning and Anti-Ice	585
Auxilliary Power	227
Unusable Fuel and Fluids	167
Empty Weight	**14,611**
Option Allowance	0
Crew	690
Basic Operating Weight	**15,301**
Mission Fuel	3,311
Reserve Fuel	1,311
Total Fuel	**4,622**
Full Fuel Payload	4,845
Ramp Weight	**24,768**
Taxi/Takeoff Fuel	205
Max TO Gross Weight	**24,973**

A breakdown of the interior weights, based on airliner weights from Torenbeek (Reference 27), is shown in Table 16. The weight of passenger refreshments (drinks and ice) and entertainment (magazines) is included in the interior weight.

Table 16. Furnishings and Equipment Weight Statement

Component	Weight, lbs
Flight Deck Interior	316.0
Passenger Seats	430.0
Lavatory	75.0
Carpet	34.8
Soft Goods, Closets	526.0
Cargo Restraints	13.0
Oxygen System	52.0
Fire Det. And Ext.	32.2
Escape Provisions	20.0
Drinks	16.0
Magazines	7.0

The payload and crew weight are shown in Table 17. Each passenger (at an average of 195 lbs) has 46 lbs of baggage (30 lbs checked and 16 pounds carry on), making a total allowance of 241 lbs per passenger. When combined with 25 lbs of air freight, the total payload weight is 4,845 lb. The crew, made up of two pilots and one flight attendant, has a total weight allowance (including baggage) of 690 pounds. As mentioned previously, the weight of passenger refreshments (drinks and ice) and entertainment (magazines) is included in the interior weight.

Table 17. Payload and Crew Weight Breakdown

Payload		
Passengers	195x20=	3900 lb.
Checked Bags	30x20=	600
Carry-on Bags	16x20=	320
Air Freight	25	25
Total Payload		4845 lb.
Crew Weight (including bags)		
Pilots	2x240=	480 lb.
Attendant	210	210
Total Crew		690 lb.
Included in Interior Weight		
Magazines		7 lb.
Drinks and Ice		16

Weight and other characteristics of the propulsion system group are provided in the upcoming section on Baseline Engine Description and Performance.

5.5 B-20 Aerodynamic Data

A drag polar for cruise drag (shown in Figure 75) was generated for the B-20 at Mach 0.6274 and 41,000 ft using Cessna's drag estimation tools. Compressibility drag is shown in Figure 76. Compressibility drag for the B-20 increases significantly above Mach 0.6 and exponentially above Mach 0.7. At Mach numbers above 0.6 and lift coefficients above 0.6, compressibility effects begin to dominate the cruise drag polar; hence Figure 75 is presented for Mach 0.6 up to a C_L of 0.6. Takeoff and landing drag polars were also generated using Cessna methods that have been validated with a combination of wind tunnel and flight test data for jets in the same size class as the B-20. The takeoff and landing polars are shown in Figure 77. Drag increments for climb and descent based on the cruise drag CD_0 were also developed. Those increments were -0.0013 for climb and -0.0025 for descent.

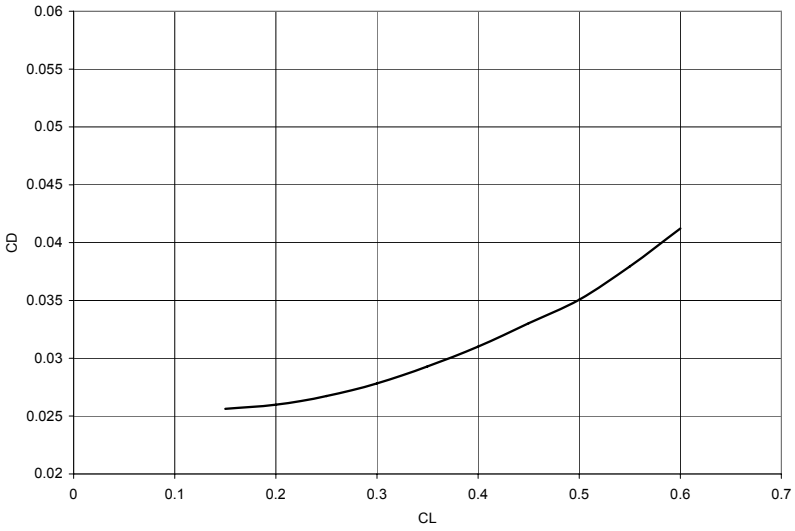

Figure 75. Cessna-Developed B-20 Cruise Drag Polar (M=0.6)

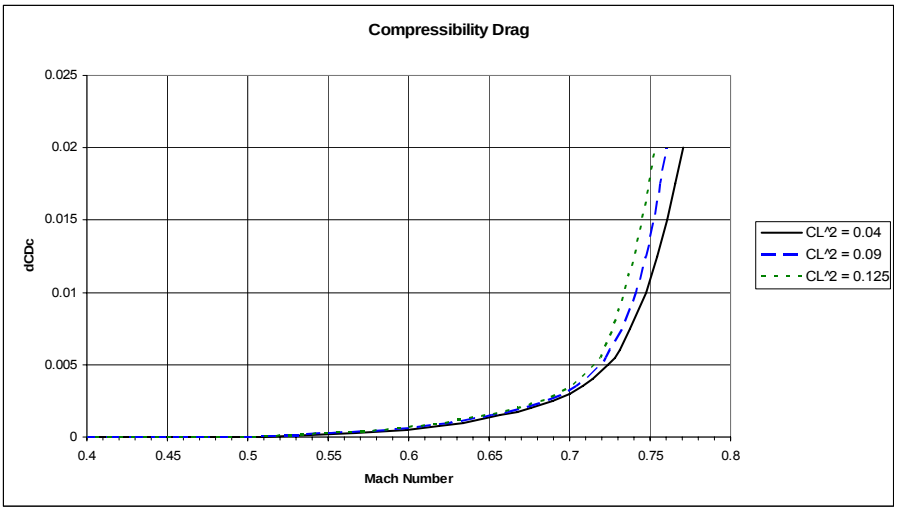

Figure 76. Compressibility Drag for the B-20

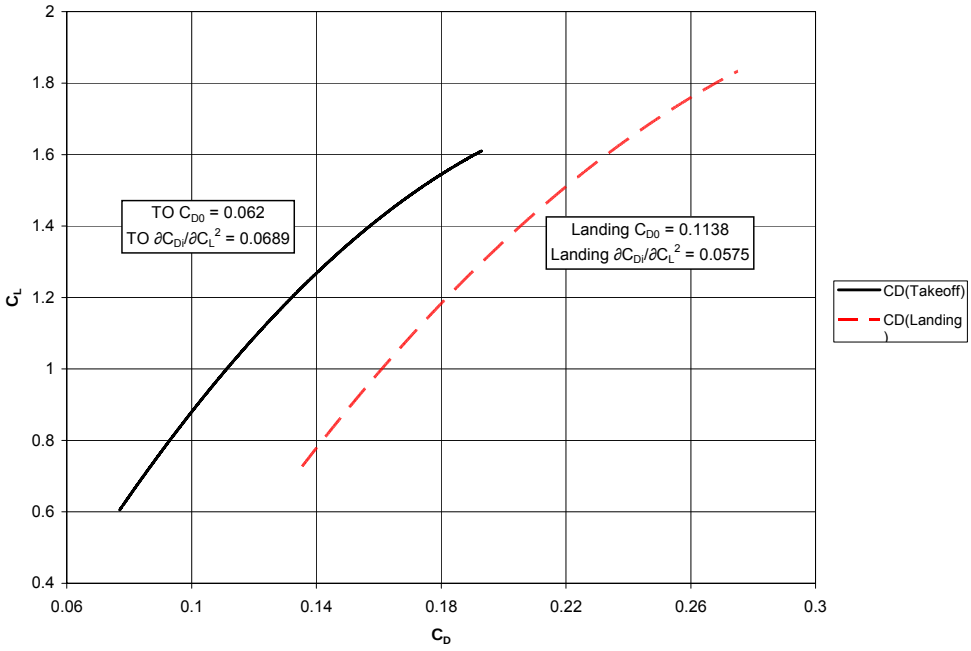

Figure 77. Cessna-Developed B-20 Takeoff and Landing Drag Polars

5.6 Baseline Engine Description & Performance

A scalable propulsion system, representative of 2008 fielded small commercial engines, was defined for the B-20 baseline airliner. A mixed-flow turbofan configuration was chosen for the current-day propulsion system, because it was felt to be more in line with the perception of comfort of today's passengers who are willing to pay a premium ticket price for more convenient air travel. The market of currently fielded commercial turbofan engines was surveyed to ensure the propulsion characteristics of the baseline engine would be representative of modern, fielded engines. SFC, weight, diameter, bypass ratio (BPR), overall pressure ratio (OPR), and other engine parameters were characterized as a function of thrust in the 2000 to 9000 lb range. Propulsion characteristics of the baseline engine were then reverse-engineered to be representative of the market. Scalable engine performance, weight, and installation data packages were developed and provided to Georgia Tech and Cessna for their aircraft simulations

The current day baseline engine is designed to meet the propulsion system requirements of the B20 baseline aircraft. The nominal thrust requirements, installation effects, and customer offtakes originally defined for the B20 airliner are shown in Table 18. Of special significance is the large customer offtakes requirement expected for the comfort and convenience of the passengers in our N+3 network. These offtakes consume ~10% of engine core power in the baseline aircraft's nominal thrust class. As advanced technology dramatically reduces both the aircraft and engine core size required to fulfill the mission, the customer offtakes will have an even greater negative impact on engine and aircraft performance.

Table 18. B20 Baseline Aircraft Propulsion Requirements

Nominal B20 Baseline Airliner Propulsion Requirements

Takeoff Thrust = 4400 lb, **Flat-rated to 80F**

- Installed, with Offtakes.
- 4600 lb FN, Uninstalled, w/o Offtakes
- **Scalable 3000 to 6000 lb FN**

Installation/Offtakes:	Normal Losses	Icing Losses
LP Bleed (lb/min)	---	11.5
Bleed (lb/min)	**24.1**	24.1
HP Bleed (lb/min)	---	47.1
Accessory horsepower	**34.0**	34.0
Inlet recovery	0.995	0.995

The nominal baseline engine is a moderate bypass (~3.8) mixed flow turbofan of configuration and characteristics typical of the market at this thrust class. Figure 78 shows the baseline engine configuration and overall characteristics. Table 19 shows its performance and cycle characteristics at key operating conditions. A mixed flow configuration was chosen to minimize both cabin and community noise using current technology. The mixed flow

configuration allows the baseline aircraft to meet Stage 4 requirements with 20 EPNdB cumulative margin. Combustor technology is of a modern rich quench lean (RQL) design, with LTO NOx emissions 25% below the CAEP 6 requirements for a 6000 lb FN turbofan.

Performance, weight and dimensions are consistent with the characteristics of currently fielded engines. Scalable models of engine characteristics (performance, weight, installation dimensions, etc.) were developed for the 3000 to 6000 lb thrust range. Figure 79 shows some of the characteristics of the current commercial turbofan marketplace, along with the nominal baseline engine concept, and scaling models. Additionally, a sensitivity study was conducted to assess the impact of engine bypass ratio on engine SFC, thrust, diameter, weight, and lapse rate to allow trades for cruise speed, altitude, etc. The results of this engine sensitivity study are shown in Figure 80.

Cessna and Georgia Tech used the baseline engine's scalable installation and performance data in their aircraft sizing and performance studies. The engine characteristic impacting noise were also defined and modeled at the aircraft level. The final installed thrust requirement was 4558 lb per engine installed, a 1.03 scale of the nominal baseline engine concept.

The baseline engine defined here is a good representation of current fielded commercial turbofans in this size class.

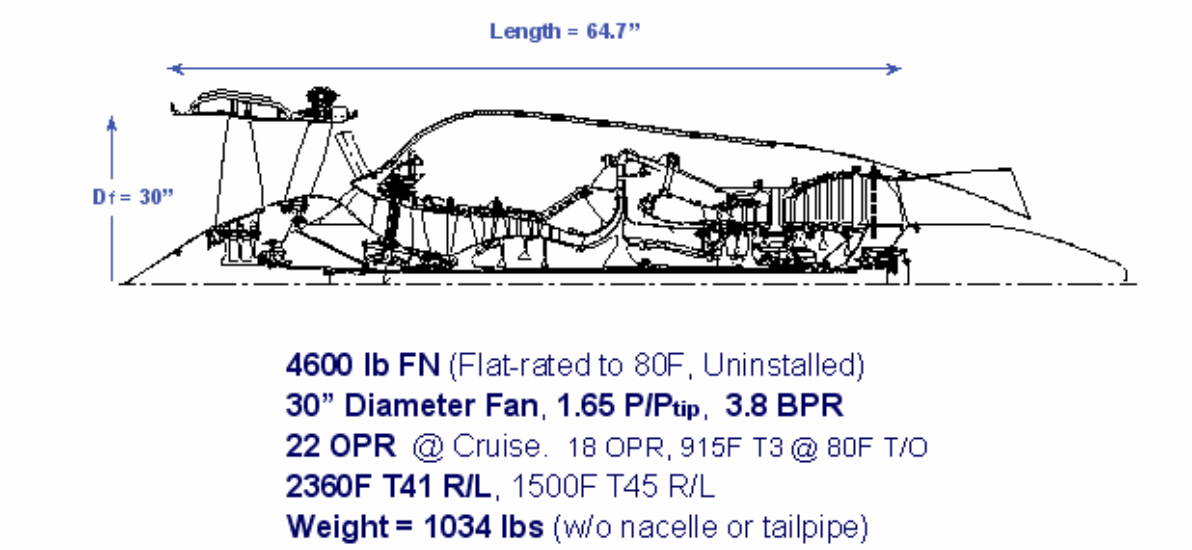

Figure 78. Nominal B20 Baseline Engine (Flat-rated to 4400 lb FN, Installed)

Table 19. Baseline Engine Performance and Cycle at Key Operating Conditions

	Cruise	*Max Climb*	*T/O*	*Uninstalled*
	41K/0.6/ISA	41K/0.6/ISA	SLS/80F	SLS/80F
FN (lb)	850	930	**4400**	**4600**
SFCq	.705	.707	.463	.453
WrFan (lb/s)	**179**	182	154	156
WrCore (lb/s)	**27.4**	27.9	24.5	24.6
BPR	3.7	3.5	3.8	**3.8**
FPR	**1.65**	1.7	1.47	1.49
OPR	**22**	23.5	17.3	17.7
T3F avg	705	730	903	**915**
T41F avg	**2020**	**2090**	**2200**	**2200**
T45F avg	1245	1295	1382	1383

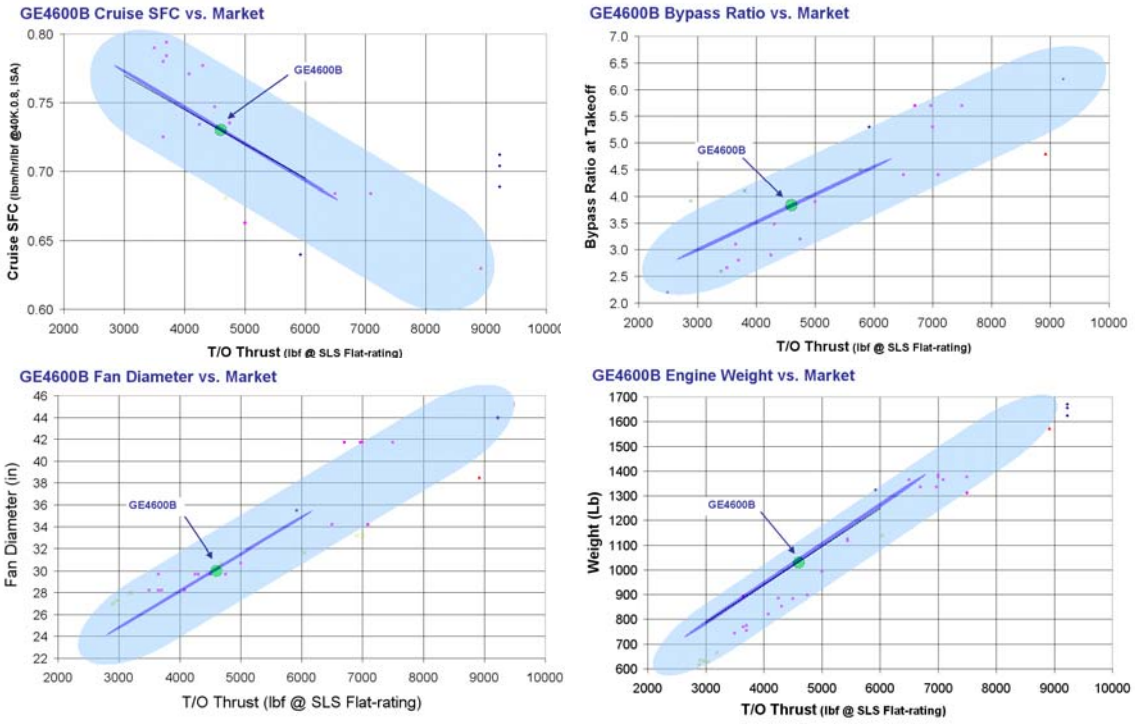

Figure 79. N+3 Baseline Propulsion System Characteristics & Scaling vs. Market

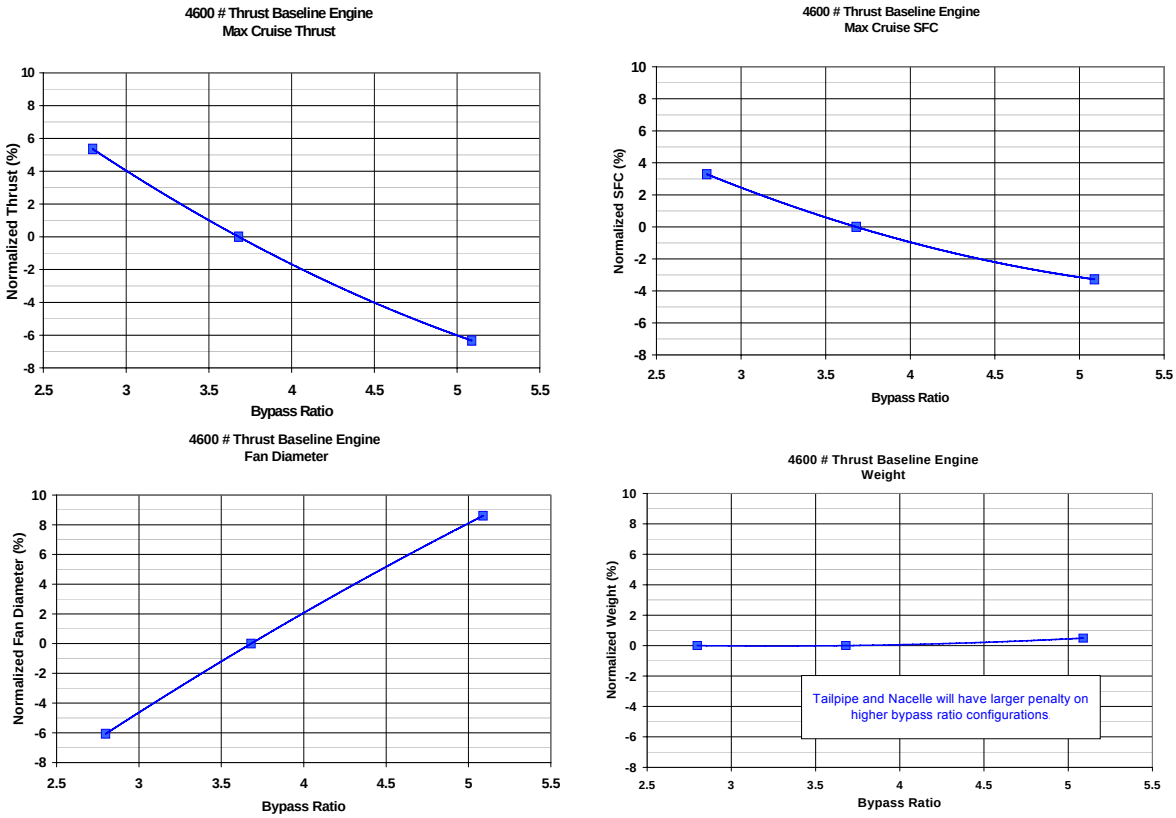

Figure 80. Baseline Engine Bypass Ratio Sensitivity Study

5.7 FLOPS Model Development and Calibration for the B-20

The Cessna/Georgia Tech team followed the same methodology for the B-20 that was used for the CJ-2+ to initially calibrate the computational tools (see Appendix A for details of the methodology used by the team to develop the calibrated CJ2+ FLOPS model). The Cessna-provided data for the B-20 was derived from the CATIA design model and judicious use of the Cessna weights equations and aerodynamic analysis with supplemental data and engineering judgment to account for any differences between the B-20 and typical Cessna aircraft. The Georgia Tech FLOPS model development used fixed Cessna component weights and drag polars to match the mission. Then FLOPS was run to tune the weight factors so that the mission still matched. Using the mission and the weight factors, FLOPS was then run with tuning factors so that FLOPS calculations would match the Cessna drag polars. At the end of this exercise, the FLOPS model is capable of nearly reproducing the Cessna model for the B-20 while still having the flexibility to optimize configurations with new technologies utilizing the internal FLOPS calculations. Comparison of the results between the FLOPS and MAPS optimizations for technology sensitivities provides confidence that the methods are accounting for the new technologies appropriately. The development of the B-20 FLOPS model will be described in the following sections.

5.7.1 FLOPS B-20 Modeling Methodology

Evaluation of the FLOPS software was performed in two phases. The first phase involved a FLOPS mission analysis with known or input values for weight. FLOPS allows the user to input component weights, drag polars, and engine performance data. This analysis enables direct comparison of fuel burn, range, climb, and descent performance with actual data from other design tools. The second phase involved an assessment of the analysis modules in FLOPS for each component of weight.

Data provided by Cessna describing their B-20 performance and weight data was used to develop the geometry and component weights input for FLOPS with a known mission definition. FLOPS was run with the B-20 range being fixed (IRW=1) and constant Mach number (IOC=2) at the set cruise ceiling.

5.7.2 B-20 Geometry

The B-20 layout and geometry was developed using Cessna standard tools. The baseline information was converted into geometric data for input into FLOPS as shown in Table 20. Each line in the table shows the FLOPS input parameter, a description of the parameter, a value, and the appropriate units. Not all FLOPS variables were used or are shown. Variables are not organized by the FLOPS namelist in which they appear.

Table 20. Aircraft Geometric Input for NASA FLOPS Aircraft Analysis Tool

FLOPS Parameter	Description	Value	Units
DIH	Wing dihedral	5.0	deg
FLAPR	Flap ratio	0.167448	
XL	Fuselage total length	55.42	ft
WF	Fuselage total width	8.333333	ft
DF	Fuselage Depth	8.333333	ft
XLP	Length of passenger compartment	22.75	ft
XMLG	Extended main landing gear oleo length	38.374054	in
XNLG	Extended nose landing gear oleo length	28.780541	in
MLDWT	Design landing weight calculation (0=default, WRATIO=1-0.00004*DESRNG)	0	
HHT	Decimal fraction of vertical tail span where horizontal tail is mounted (1.0=T-Tail)	1	
SHT	Horizontal tail area	131.03	ft^2
SWPHT	Horizontal tail ¼ chord sweep angle	20.	deg
ARHT	Aspect ratio of the horizontal tail	6.112	
TRHT	Taper ratio of the horizontal tail	0.425	
TCHT	Thickness to chord ratio of horizontal tail	0.092124	
NVERT	Number of vertical tails	1	
SVT	Vertical tail area	86.86	ft^2
SWPVT	Vertical tail ¼ chord sweep angle	49	deg
ARVT	Aspect ratio of the vertical tail	0.872	
TRVT	Taper ratio of the vertical tail	0.6	
TCVT	Thickness to chord ratio of the vertical tail	0.12	
NFIN	Number of fins	0	
TR	Wing taper ratio	0.318	
SWEEP	Wing ¼ chord sweep angle	0	deg
TCA	Wing thickness to chord ratio (weighted average)	0.137748	
AR	Wing aspect ratio	8.769	
WSR	Wing loading	61.23	lbs/ft2
XNAC	Average length of baseline engine nacelles	9.263	ft
DNAC	Average diameter of baseline engine nacelles	3.5	ft
NETAW	Number of input wing stations	3	
ETAW(1)	Wing station location 1 – fraction of semispan	0	
CHD(1)	Chord length at ETAW(1) – fraction of semispan	0.345714	
TOC(1)	Wing thickness to chord ratio at ETAW(1)	0.1448	
ETAW(2)	Wing station location 2 – fraction of semispan	0.41394	
CHD(2)	Chord length at ETAW(2) – fraction of semispan	0.248251	
TOC(2)	Wing thickness to chord ratio at ETAW(2)	0.1397	
ETAW(3)	Wing station location 3 – fraction of semispan	1.0	
CHD(3)	Chord length at ETAW(3) – fraction of semispan	0.110264	
TOC(3)	Wing thickness to chord ratio at ETAW(3)	0.12	
ETAE	Engine locations, fraction of semispan or distance from fuselage centerline	0.198019	Fraction

5.7.3 B-20 Weights and Engine

Predicted aircraft component weights, engine, and performance data from Cessna were used to evaluate the mission analysis provided by FLOPS. This approach isolated the mission analysis routine from the modules used to estimate weight and drag. Table 21 shows aircraft weights, payload weights, and the maximum operating Mach number for the B-20. Tables of engine performance data were generated and then input to FLOPS for this analysis comparison.

Table 21. B-20 Aircraft Data

FLOPS Parameter	Description	Value	Units
GW	Ramp weight	24973.	lbs
NPF	Number of first class passengers	0	
WPPASS	Weight per passenger	195.	lbs
BPP	Weight of baggage per passenger	46.	lbs
CARGOF	Cargo (other than passenger baggage) carried in fuselage	25.	lbs
WFLCRB	Total weight of flight crew and baggage	480.	lbs
WSTUAB	Total weight of flight attendants and baggage	210.	lbs
ULF	Ultimate load factor	4.22	
VMMO	Maximum operating Mach number	0.65	
FAERT	Decimal amount of aeroelastic tailoring used in design of wing (0=none)	0.	

Two GE4600B engines power the B-20. The engine is a 3.85:1 bypass, twin-spool design with 6 compression stages and 5 turbine stages; it produces 4,435 pounds of takeoff thrust at sea level, static conditions. A dimensioned sketch of the engine is shown in Figure 81. The rubber engine characteristics are shown in Table 22.

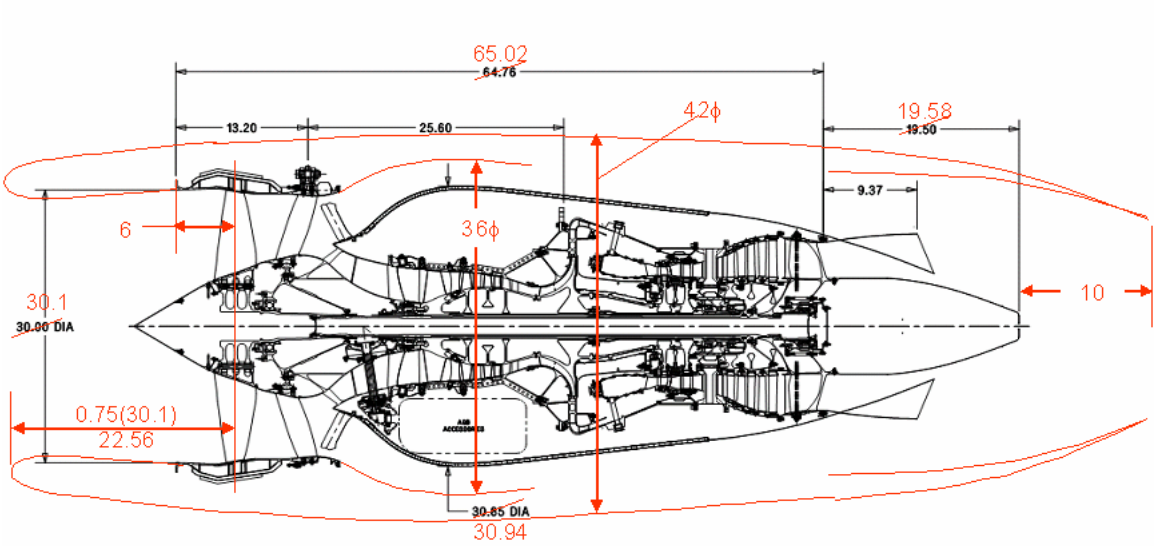

Figure 81. GE4600B engine scaled to 4,435 lb SLS

Table 22. B-20 "Rubber" Engine Characteristics

Engine Weight = 1,039 lb
Bypass Ratio = 3.85
Fan Diameter = 30.1 in
SFC Scalar = 0.999
Length Scalar = 1.004
Diameter Scalar = 1.003

A FLOPS-formatted GE4600B engine table consisting of thrust, fuel flow, and power setting for varying Mach numbers and altitudes was created for Mach numbers from 0 to 0.74 and altitudes of 0 to 45,000 ft. FLOPS was told to read the engine data from an external file by setting IGENEN = -1 and setting EIFILE equal to the file name. Other FLOPS input included setting IDLE=0 to specify that the lowest input power setting is assumed to be flight idle, MAXCR (maximum power setting at cruise) = 1. The FLOPS NPCODE variable defaults to 0 so that all power codes in the engine tables are used.

5.7.4 B-20 Evaluation Mission

The selected mission for the evaluation and calibration of FLOPS consists of a climb, cruise, descent, and reserve segment which are shown in Figure 82. The FLOPS mission inputs are shown in Table 23. The fuel flow was adjusted to match that of the flight manual data for the same weight and cruise altitude. The climb segment is composed of an accelerated a minimum fuel to climb to 35,000 ft at mach 0.6. The cruise segment is flown at a constant Mach number of 0.6 at 35,000 ft. The descent was done at the optimum lift-drag ratio to minimize fuel burn. The aircraft's mission design range was 800.3 nm.

The reserve segment is defined by National Business Aircraft Association (NBAA) 100 nm reserve mission. This mission consists of a 5 minute loiter at sea level, a climb to 5,000 ft, a hold for 5 minutes, a climb to 17,000 ft, a cruise at long range cruise setting, a descent to sea level for a total of 100 nm with enough additional fuel to loiter at 5,000 ft for 30 minutes. Rather than modeling this reserve mission fully, the missed approach time, distance to an alternate airport, and fixed fraction of reserve fuel (0.05) were used to model the reserve mission.

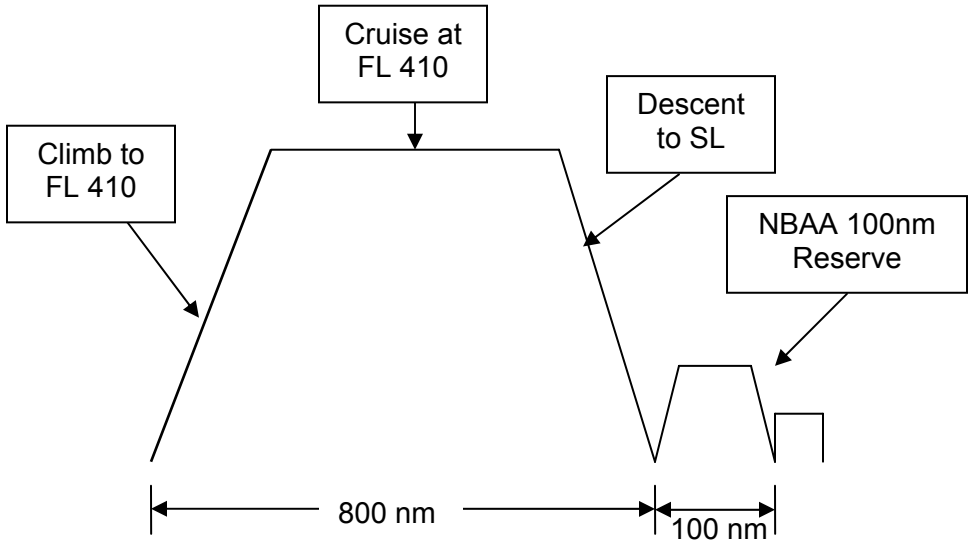

Figure 82. Representative Maximum Payload Mission for the B-20

Table 23. Aircraft Mission Parameters

FLOPS Mission Variables	Description	Value	Units
NPF	Typical Number of First Class passengers	0	
NPT	Number of Tourist (Coach) Passengers	20	
CH	Maximum Cruise Altitude	41,000	ft
CRMACH	Cruise Mach Number	0.6	M
CRALT	Cruise Altitude	41,000	ft
VMMO	Maximum operating Mach number	0.65	M
DESRNG	Design Range	800.3	nm
TAKOTM	Takeoff Time	1.	min
TAXOTM	Taxi Out Time	8.4	min
APPRTM	Approach Time	2.0	min
TAXITM	Taxi In Time	5.0	min
FWF	Climb Profile Optimization (-1=minimum fuel to climb)	-1	
CLDCD	Drag Coefficient Increment Applied to Climb	-0.001346739	
IOC	Cruise Option Switch (2=fixed Mach number at input maximum altitude or cruise ceiling	2	
RCIN	Instantaneous Rate of Climb for Ceiling Calculation	100.	ft/min
IVS	Descent Option Switch (Descent at Optimum Lift-to-Drag Ratio)	1	
DEMMIN	Minimum Descent Mach Number (default=0.3)	0.3779	M
DEAMIN	Minimum Altitude for Descent	0.	ft
DEDCD	Drag Coefficient Increment Applied to Descent	-0.002472414	
RDLIM	Limiting or Constant Rate of Descent	-3,000.	ft/min
IRS	Reserve fuel calculation switch (1=calculate reserve fuel for trip to alternate airport plus RESRFU and/or RESTRP	1	
ALTRAN	Range to alternate airport	100	nm
TIMMAP	Missed approach time	2.0	min
RESTRP	Reserve fuel as a fraction of total trip fuel weight	0.0	
RESRFU	Fixed reserve fuel	0.	lb

5.7.5 Mission Matching

Table 24 shows a comparison of the MAPS and FLOPS results by segment for distance, fuel burn, percent mission fuel, and time for the chosen mission. Although there are differences in individual segment distances up to 30%, the total mission distance is within 0.1 nm. Climb and descent fuel burns are greater for FLOPS than MAPS, but cruise fuel is slightly less in MAPS. The difference in mission total fuel is 114 lbs or 3.2%. Total mission time is 8.8 minutes longer in FLOPS than MAPS. Although cruise time is shorter in FLOPS, slightly more time is spent climbing and significantly more time is spent descending in FLOPS than in MAPS due to differences in climb profile procedures and the lack of a powered descent in FLOPS. These differences in mission profile will be covered in detail in the Observations and Recommendations at the end of this section.

Table 24. Comparison of MAPS and Georgia Tech FLOPS

	Distance (nm)		Fuel Burn (lbs)		Percent Mission Fuel		Time (min)	
Segment	**MAPS**	**FLOPS**	**MAPS**	**FLOPS**	**MAPS**	**FLOPS**	**MAPS**	**FLOPS**
Taxi-Takeoff	0	0	200	205	5.58	5.83	0	0
Climb	95.5	113.8	795	912	23.36	25.94	18.9	22.2
Cruise	621.5	568.4	2198	2060	64.61	58.59	108.4	99.1
Descent	83.2	118.1	209	339	6.14	9.64	14.5	29.3
Mission Total	800.3	800.3	3402	3516	100	100	141.8	150.6
Reserve	100	N/A	1584	1311	46.57	37.29	N/A	N/A
Total	N/A	N/A	4,986	4,827	N/A	N/A	N/A	N/A

5.7.6 Weights Calibration

To allow accurate evaluation and calibration of the FLOPS model, the component weights had to be calibrated. The weights were initially input as hard wired values during the mission performance calibration; this allowed the mission parameters to vary without the aircraft weight being affected, except for fuel weight. Once the mission was matched the component weights that were provided by Cessna were matched through the calculation in FLOPS by the use of component weight scaling factors. The scaling factors allow the component weight to be changed from a hard wired value such as 1000 lbs, to a scaling factor such as 0.9. The use of a scaling factor is important when altering the size, shape, or mission of a vehicle. The scaling factor allows the same total percent of the final weight to be kept constant, while finding the new actual component weight for a different vehicle size of similar configuration. Without the calibration of the weights with scaling factors the FLOPS component weights were not very accurate. The calibrated versus non calibrated data is shown below in Figure 83.

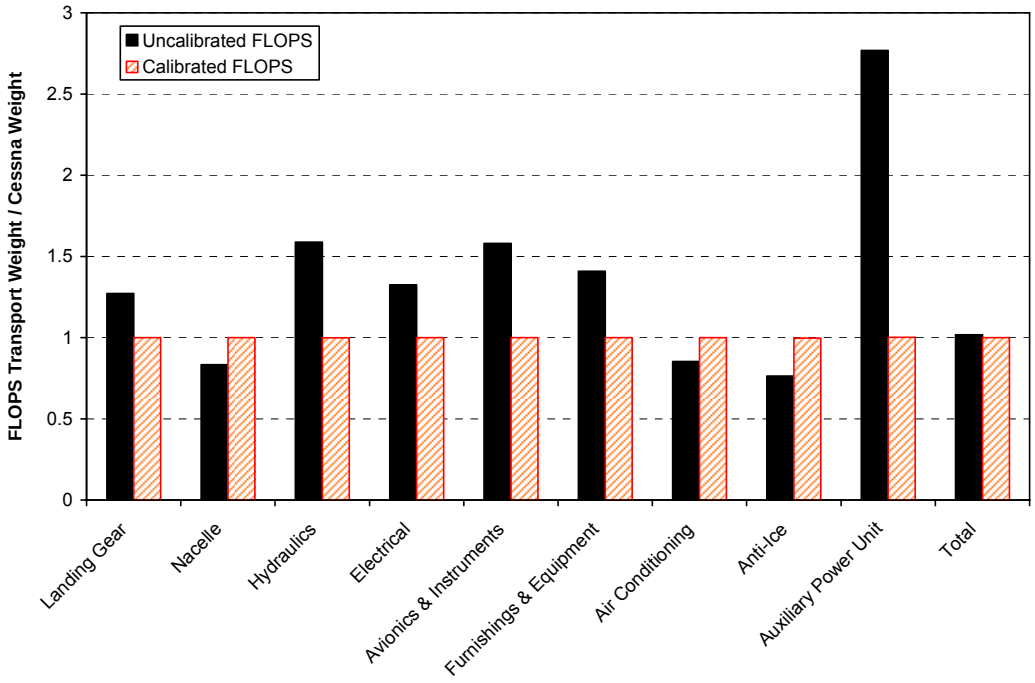

Figure 83. Comparison with the Non-Calibrated and Calibrated FLOPS Model using Transport Weight Equations

The final equations for weight calibration used in FLOPS were calculated using the transport weight equations. (In the CJ2+ calibration exercise, the general aviation category weights equations were slightly better. Comparing weights calculated by FLOPS using both the transport and GA weights equation to the Cessna-calculated weights showed that the transport weight equations did a better job estimating the B-20 weights.) The engine weight (WENG) does not scale like other weight factors for the components and was left fixed. The weights that were matched were provided by Cessna in a detail breakdown of the components. Based on the provided weights shown in Table 25, the scaling factors were found for the selected mission. The scaling factors necessary for FLOPS to calculate the provided weights are shown below in Table 26.

Table 25. B-20 Provided Component Weights

Operational Empty Weight	15301	lbs
Maximum Zero Fuel Weight	20146	lbs
Maximum Takeoff Gross Weight	24973	lbs
Maximum Fuel Weight	4827	lbs
Design Landing Weight	24173	lbs
Wing Group	2154	lbs
Vertical Tail Group	281	bs
Horizontal Tail Group	421	lbs
Fuselage Group	3508	lbs
Nacelle & Strut	410	lbs
Landing Gear	793	lbs
Surface Controls	260	lbs
Avionics	571	lbs
Instruments	0	lbs
Hydraulics/Pneumatics Group	184	lbs
Electrical Group	778	lbs
Environmental Controls System	585	lbs
Anti-Ice System	0	lbs
Furniture & Equipment	1522	lbs
Installed Engine Weight (per engine)	1072	lbs
Fuel System	127	lbs
Unused Fuel	167	lbs
Oil	0	lbs
Paint	158	lbs

Table 26. FLOPS Weights Calibration Factors

FLOPS Weights Calibration Factors	Transport
FRWI	1.002
FRHT	0.865
FRVT	0.86
FRFU	0.918
WFSYS	0.59
FRSC	0.92
FRLGN/M	0.797
FRNA	1.18
WHYD	0.59
WELEC	0.699
WAVONC	0.815
WFURN	0.718
WAC	1.435
WAI	0.0
WAPU	0.54

FLOPS can be calibrated with the use of the weight scaling factors to meet the individual component weights for this size of aircraft. All values are within one percent of the provided component weight from Cessna. However, the Cessna weight equations are of very different form compared to the weight equations used by FLOPS. Neither set of weight equations are completely appropriate for predicting weights when technology changes. Care must then be exercised when using these tuning factors; their values indicate which systems group weight equations require further scrutiny.

5.7.7 Drag Calibration

To allow for drag calibration Cessna developed and provided drag polars (cruise drag previously shown in Figure 75, compressibility drag polar shown in Figure 76, and takeoff and landing drag polar shown in Figure 77). As stated in the FLOPS Users Manual (Reference 28), the aerodynamics module uses a modified version of the EDET (Empirical Drag Estimation Technique) program (Reference 29) to provide drag polars for performance calculations. Modifications include smoothing of the drag polars, more accurate Reynolds number calculations, and the inclusion of the Sommer and Short T' method for skin friction calculations (Reference 30). Alternatively, drag polars may be input and then scaled with variations in wing area and engine (nacelle) size.

For the B-20 model, the Cessna-derived drag polar was input, the evaluation mission matched, and then FLOPS computed the drag polar by setting MYAERO = 0. FLOPS results will be compared to Cessna's results for lift-independent drag, lift-dependent drag, compressibility drag, climb and descent drag modifications, and takeoff and landing drag polars.

Lift-Independent Drag Comparison - FLOPS-predicted CD_0 varies from as little as 2% to as much as 70% (both greater than and less than) from Cessna-determined values for major components as shown in Figure 84. The total CD_0 calculated by FLOPS at M=0.6247 and 41,000 ft is 84% of FSDRAG total (CD0=0.0247). To calibrate CD_0 in FLOPS, set FCDO = 1.1861.

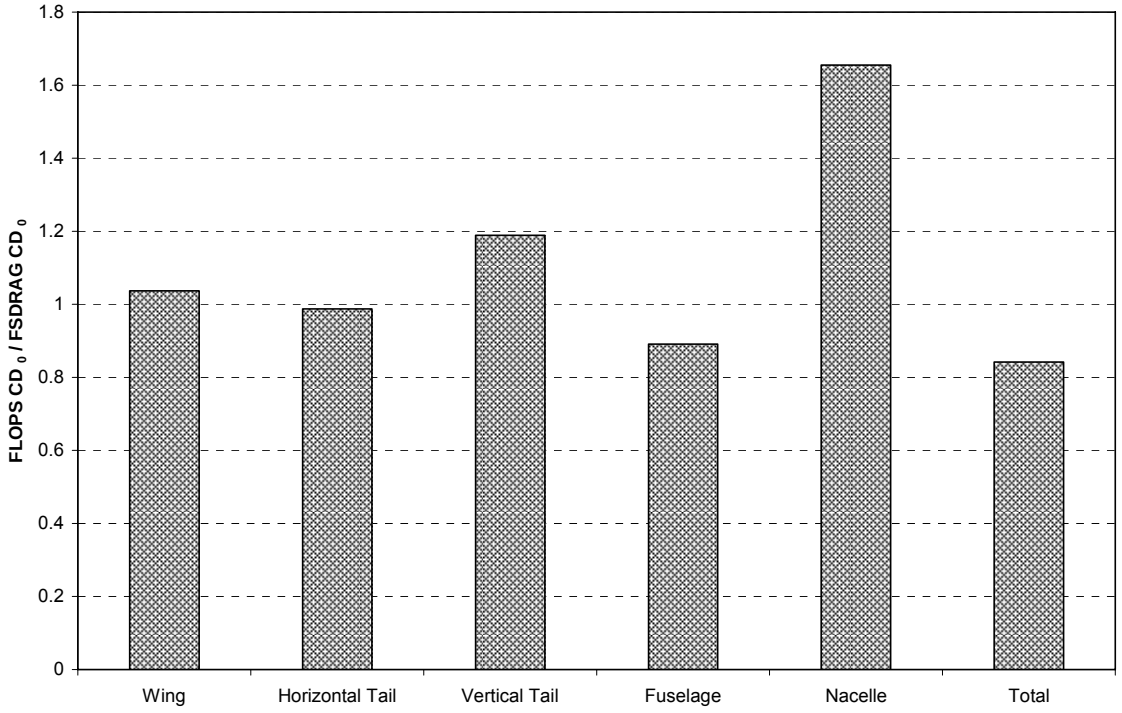

Figure 84. Lift-Independent Component Drag Comparison

To understand why the lift-independent drag prediction differences occur, some insight can be gained by examining the wetted area calculation comparisons between FSDRAG and FLOPS (see Table 27). The CATIA geometry is the reference standard. It is clear that FSDRAG and FLOPS have strengths and weaknesses in computing the wetted area. One obvious reason why the FLOPS value is somewhat less than FSDRAG is the absence of a modeled pylon. The pylons could be modeled in FLOPS as a canard or vertical tails to include the wetted area in the friction drag; modeling as fins would not change the drag calculations.

The largest difference in CD_0 is for the nacelle. Examining the elements in the drag calculation details shown in Table 28 provides insight into the differences. The discrepancy in nacelle CD_0 between FSDRAG and FLOPS can be traced primarily to the difference in form factor values: FSDRAG computes nacelle form factor as a linear function of nacelle fineness ratio, which gives a value of 1.132; this value is then multiplied with a fuselage/pylon interference factor of 1.3 to give 1.472. In comparison, FLOPS extrapolates fineness ratio from a lookup table, resulting in a value of 2.289.

Table 27. Wetted Area Calculation Comparisons

	CATIA	FSDRAG	FLOPS
Wing	821.35	826.278	820.44
Horizontal Tail	268.57	256.523	272.17
Vertical Tail	173.61	152.521	177.76
Fuselage	936.67+253.6 (1190.27)	1164.06	1047.20
Nacelle	172.52	182.35	181.56
Pylon	61.24	68.5	N/A

Table 28. Nacelle CD_0 Calculation Details

	FSDRAG	FLOPS
ℓ_{nac} (ft)	9.263	9.263
d_{nac} (ft)	3.5	3.5
S_{ref} (ft^2)	490	490
S_{wet} (ft^2)	$2.8123(\ell_{nac}+d_{nac})d_{nac}=182.35$	$2.8 d_{nac}\ell_{nac}=181.56$
c_f	0.00288	0.00282
Form factor, k	$1+0.35\frac{d_{nac}}{\ell_{nac}}=1.132$	2.289
Interference factor, IF	1.3	
CD_0	$kc_f\frac{S_{wet}}{S_{ref}}IF=0.00158$	$kc_f\frac{S_{wet}}{S_{ref}}=0.0024$

Lift-Dependent Drag - At a given C_L^2, FLOPS under predicts the induced (lift-dependent) drag in increasing amounts as C_L^2 increases as shown in Figure 85. The lift-dependent drag polars calculated by FLOPS can be tuned to match the Cessna polar by using either FCDI = 0.8339 in namelist $MISSIN or E = 0.821 in namelist $AERIN. Using FCDI gives slightly better results although FLOPS creator Arnie McCullers recommended using E.

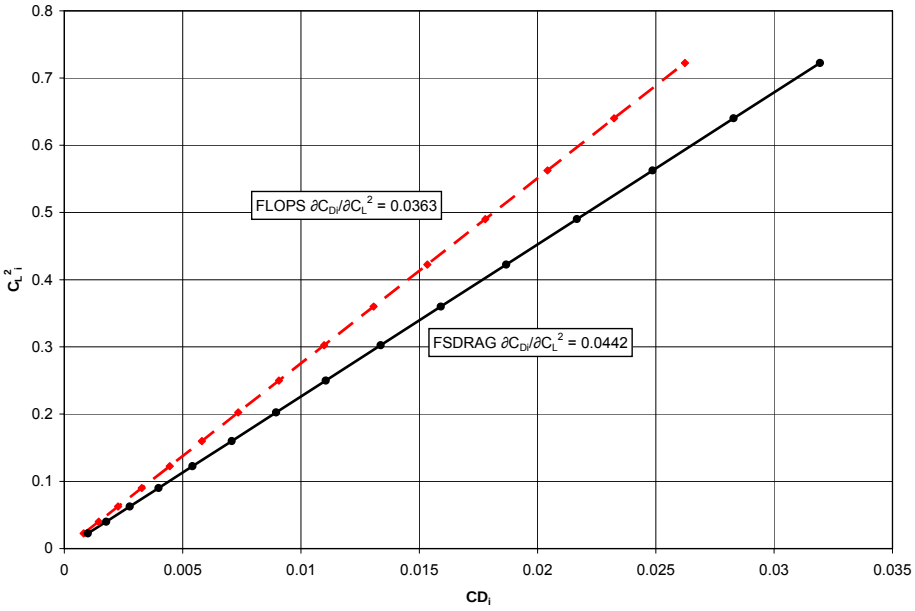

Figure 85. Lift-dependent drag comparison (CDi at M=0.6274 and 41,000 ft)

Compressibility Drag - The FLOPS-predicted compressibility drag CDC is just more than half of Cessna values at the design Mach number as shown in Figure 86. The FLOPS calculation could be improved by calibrating with FCDSUB. However, FCDSUB is not restricted to just compressibility drag; its effect is cumulative with FCDI and FCDO. Using FCDSUB would then require recalibrating FCDI and FCDO.

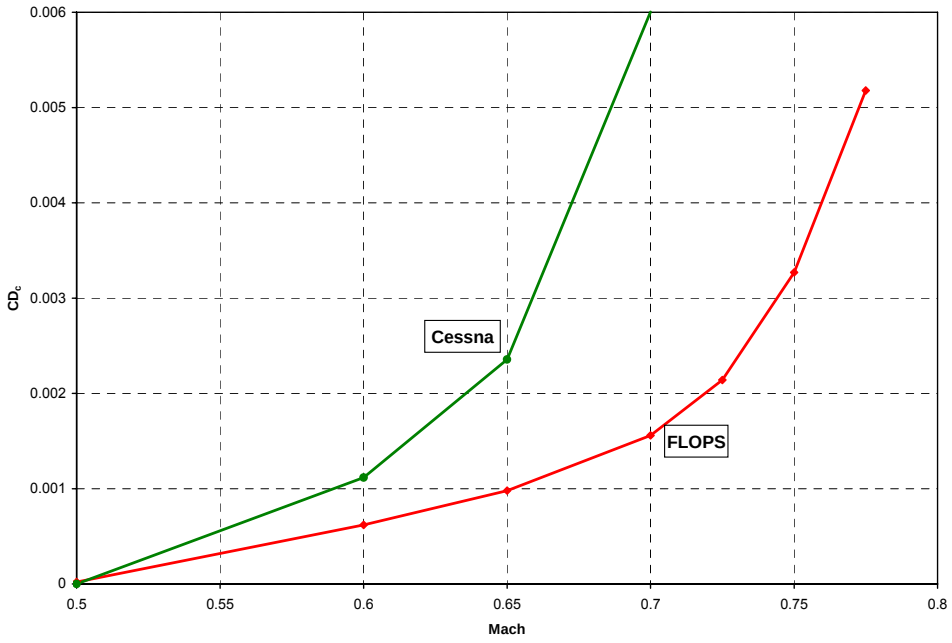

Figure 86. Compressibility Drag Comparison (CDC)

5.7.8 Observations and Recommendations of B-20 Calibration

A set of observations and recommendations were developed from the process of building a FLOPS model of the B-20 baseline airliner, comparing the FLOPS results with Cessna's results, and calibrating the FLOPS weights and drag polars with Cessna's. These include the importance of mission parameters (such as cruise at constant Mach and constant altitude versus cruise at constant power setting), reserve mission definition, and the validity of weight and drag calibrations as the team moves forward with using FLOPS to determine the effects of advanced technologies on the B-20 and its derivatives. These observations will be explored in the following subsections and will include recommendations for accommodating these issues in future work.

5.7.8.1 Mission Parameters

There are a multitude of options which must be specified to completely and accurately describe a mission. For example, climb can be optimized for minimum fuel to distance, minimum time to distance, or a combination of the two. MAPS and FLOPS both were capable of using minimum fuel to distance. Even so, there was variation in the altitude-distance profile.

Cruise can be flown at many conditions. FLOPS has ten different options. The original Cessna MAPS model used cruise at constant power with a step climb. This was the origin of the Mach 0.6274 (initial with average Mach = 0.6) at 41,000 ft/43,000 ft mission profile. FLOPS is not capable of this cruise profile. In order to match cruise profiles, both FLOPS and MAPS were instructed to use a constant Mach number, constant altitude cruise (IOC = 2 in FLOPS). The mission definition included Mach = 0.6 and altitude of 41,000 ft. Figure 87 shows how setting a fixed Mach number and altitude ensures that the fuel flows only vary as a function of the power setting. If the drag and weight models are correct, then the fuel burned calculation should match.

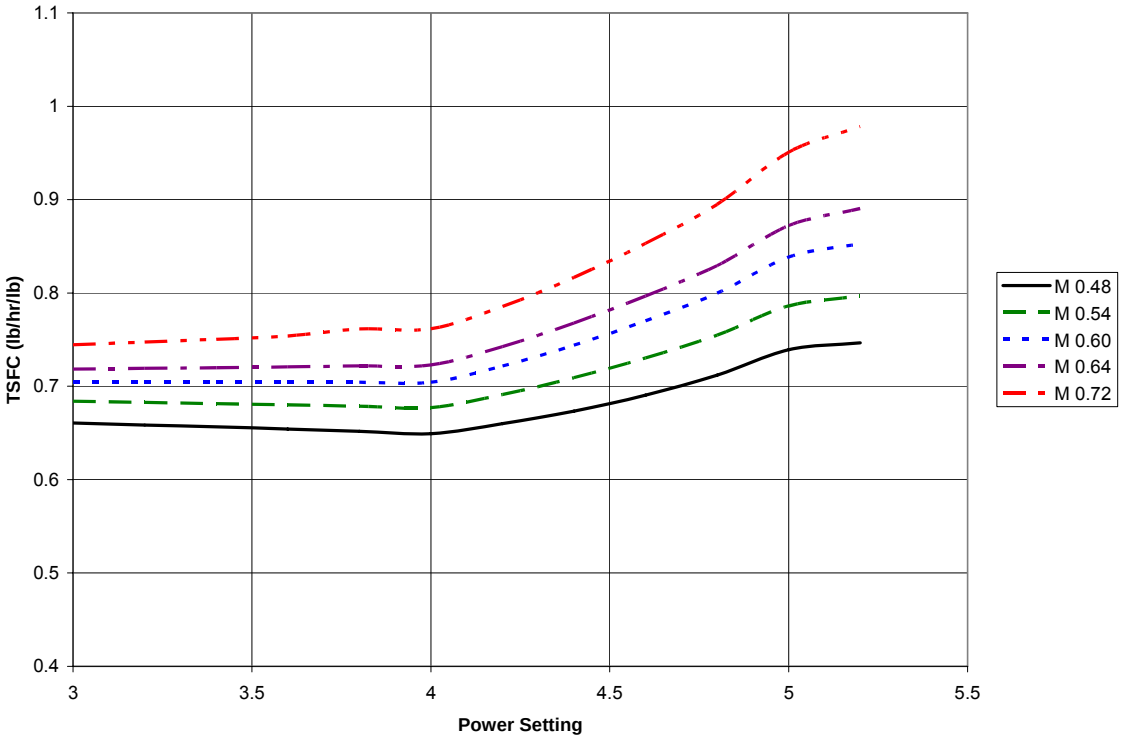

Figure 87. Fuel Flow as a Function of Power Setting at Multiple Cruise Mach Numbers

Climb and descent are problems that cannot be resolved. Figure 88 shows a comparison of the Mach number as a function of down range distance for MAPS and FLOPS. The climb profile from MAPS put into FLOPS stops at 38,000 ft and Mach 0.55. As advertised, FLOPS completes the climb with a minimum fuel profile to get to Mach 0.6 at 41,000 ft. FLOPS does everything possible to ensure that the end of cruise matches the start of climb. MAPS arrives at 41,000 ft at Mach 0.55 at the end of climb; start of cruise is at 41,000 ft and Mach 0.6. The acceleration is ignored – no fuel is burned during that segment.

MAPS files powered descents. Rate of descent is not allowed to exceed 3,000 ft. FLOPS has options of either descent at optimum lift-drag ratio or at constant lift coefficient, if descent is included at all (the third option). Even with adding a descent Mach number/altitude schedule to FLOPS, complete agreement was never obtained between MAPS and FLOPS on the descent portion of the mission. The descent Mach numbers in FLOPS and MAPS are shown on the right side of Figure 88. When descent starts in MAPS, the nose is pushed over and the Mach number immediately jumps to 0.69 with a descent rate of 3,000 fpm. In spite of telling FLOPS to fly that profile, the FLOPS descent Mach number does not exceed Mach 0.6 and the rate of descent is less than 3,000 fpm until about 21,000 ft. Fortunately, the descent contribution to the mission was small, making the difference less important.

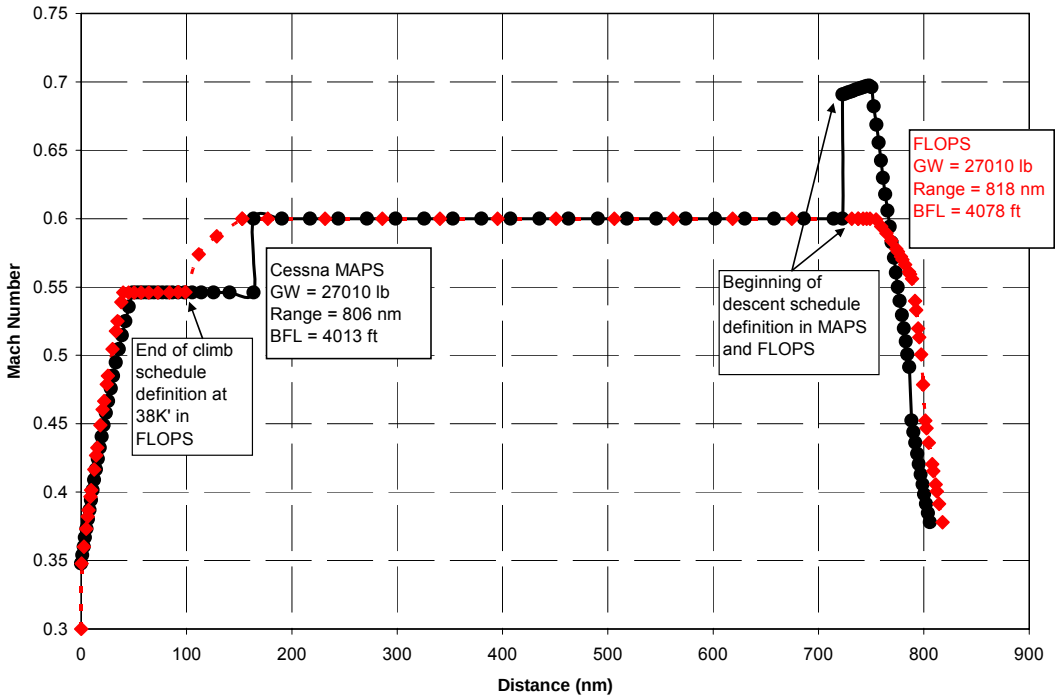

Figure 88. Mach Number Comparison Between MAPS and FLOPS

These same comments apply to the reserve mission. Fortunately, both MAPS and FLOPS do have the ability to fly the cruise leg of the reserve mission at fixed altitude, optimum Mach number for specific range and the hold leg at fixed altitude, optimum Mach number for endurance. These options match reality very well. The descent portion of the reserve leg occurs at whatever descent option/schedule was specified for the main mission.

5.7.8.2 Reserve Mission

The reserve mission originally defined included a 100 nm cruise leg. The required cruise leg for Part 25 aircraft is 200 nm. The difference in the B-20 baseline airliner is a change in weight (primarily) and size (somewhat). A review of reserve mission discussion indicated that pilots view the reserve fuel requirement as the bare minimum and typically include more reserve fuel (especially for longer range missions where conditions at the destination airport are questionable). What is important is that a reserve mission is defined, is used consistently, and is modeled the same in any tools being used.

The original attempt to match reserve fuel calculations was done by setting a reserve fuel factor in FLOPS to be a percentage of mission fuel. It was easy to make the match perfect. However, that percentage is only true for this one point. In order to accurately capture the effects of technologies, the reserve mission must be flown and the actual fuel burned calculated.

5.7.8.3 Weight and Drag Calibration

Cessna used the MAPS mission data and Cessna aerodynamic data to calibrate the FLOPS model weights and drag with great improvement in weights and moderate improvement in drag. In general, FLOPS has wide ranging options to use both data input (such as drag polars and climb and descent profiles) and calibration factors (such as for weights, induced drag, and lift independent drag) to match known aircraft.

The weight factors worked very well in matching FLOPS results with MAPS results. Of concern, however, was the ability of the basic equations to appropriately account for the impact of new technologies with or without calibration factors. The calibration factors add more uncertainty into the results from the weights module.

The calibration factors to match drag polars were not as robust and successful in allowing FLOPS to calculate results matching MAPS. The main issue was accounting for compressibility drag properly. Again, concern exists about the validity of the drag results when new technologies are considered.

5.7.9 Concluding Remarks - B20 Calibration

A FLOPS model of the B-20 passenger airliner was developed and compared the results from FLOPS with the results from Cessna's analysis tools. Mission matching was done by specifying the climb and descent profiles from MAPS in FLOPS. There were some problems with modeling the mission in FLOPS to match the mission specified in MAPS. Agreement of results between FLOPS and MAPS at an aircraft level was generally excellent with differences ranging from small to extreme occurring at the component level.

The calibration factors used to match FLOPS-calculated weights with Cessna weights worked well. Drag calibration attempts were not so successful, especially for compressibility drag. The weights and drags obtained when doing future technology sensitivity studies must be examined with critical engineering judgment to ensure that the comparisons and results are meaningful.

5.8 Baseline B-20 Airliner Performance

The performance characteristics of the baseline B-20 airliner are shown in Table 29. The mission profile is shown in Figure 89. The fuel available at the end of the mission as reserve fuel is 1,311 lbs and is more than sufficient to fly another 200 nm. The 4,000 ft Balanced Field Length allows the B-20 to operate out of most public use airports. The requirement for a balanced field length (BFL) of 4000 ft in sea level, standard atmosphere conditions sizes the wing of the baseline aircraft with single slotted flaps and a C_{Lmax} of 1.685. A current technology double-slotted fowler flap system (capable of C_{Lmax} of 2.45) is sufficient to reduce the BFL to 2,754 ft and enables wing sizing to be driven by the initial cruise altitude. The certificated noise levels are 20 EPNdB below the Stage 4 requirements, and the takeoff and landing NOx emissions have a 25% margin below the 6000 FN CAEF 6 standard.

Table 29. Baseline B-20 Airliner Performance

IFR Range (200 nm alternate)……	800 nm
Cruise Speed……	Mach = 0.60
Maximum Operating Altitude……	41,000 ft
Flight Crew ……	690 lbs
2 Pilots (240 lbs each)	
1 Flight Attendant (210 lbs)	
Payload ……..	4845 lbs
20 Passengers (195 pounds + 30 lbs checked baggage + 16 lbs carry on)	
Air Freight (25 lbs)	
Balanced Field Length, Part 25 ……	4,000 ft
Certificated Noise Levels	
Takeoff……	78.9 EPNdB
Sideline……	85.3 EPNdB
Landing……	86.9 EPNdB
Cumulative ……	251.1 EPNdB
Margin to Stage 4 ……..	**19.9 EPNdB**
Landing & Take off NOx Emissions	
Margin to 6000 FN CAEF 6 Standard …..	25%

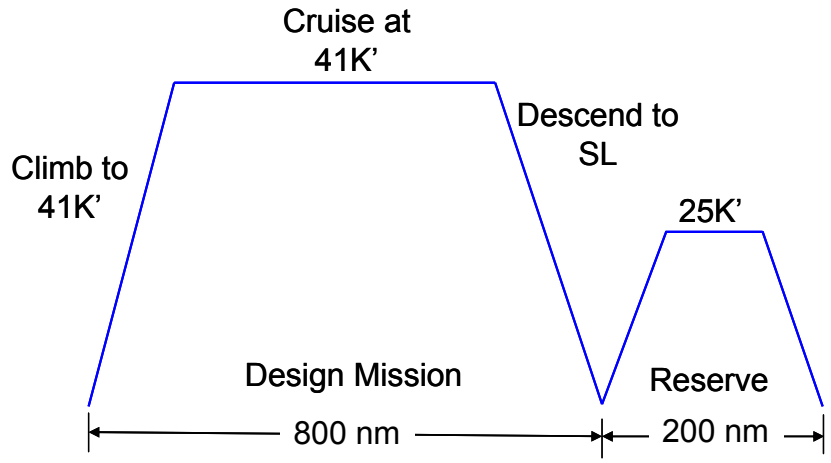

Figure 89. Maximum Full-Payload, Range Mission

Fuel usage for the mission is shown in Table 30. Total fuel is 4,827 lbs, with 3,516 lbs of the total being used for the mission (fuel fraction of 0.19). A final summary of the mission and configuration characteristics are shown in Table 31. The B-20 weighs 24,973 lbs. The wing area is 407.9 sq ft, giving a wing loading of 61.23 psf. Each engine has 4,553 lbs of SLS thrust, giving a thrust-to-weight ratio of 0.37.

Table 30. Mission Fuel

Mission Phase	FLOPS Fuel, lbs
Taxi/Takeoff	205
Climb	912
Cruise	2,060
Descent/Landing	339
Mission Fuel	**3,516**
Reserves	1,311
Total Fuel	**4,827**

Table 31. Baseline Airliner Performance Specifications

Wing Area, sq ft	407.9
Thrust per Engine, lb	4,558
Engine Size Factor	1.0276
Wing Loading, psf	61.23
Thrust-to-Weight ratio	0.37
Total Fuel	4,827
Fuel Fraction	0.19
Balance Field Length	4,000
Range, nm	800
Cruise Mach	0.60
Cruise Altitude, ft	41,000
MTOGW, lb	24,973

5.8.1 MAPS and FLOPS Comparisons

Optimization was used in both MAPS and FLOPS to determine the combination of MTOGW, thrust, and wing area in MAPS or MTOGW, thrust-to-weight ratio (T/W), and wing loading (W/S) in FLOPS which would meet the 800 nm range requirement, the balanced field length requirement, and all of the other performance constraints. Results from MAPS could quickly be put into FLOPS and performance verified. T/W and W/S are not inputs accepted by MAPS, making it more difficult to confirm FLOPS performance. In some cases, one code would produce a high thrust level and low wing loading while the other code would produce the opposite. When run individually, both would meet the requirements, indicating that the space around the optimum is relatively flat.

A comparison of the main features of the B-20 as predicted by FLOPS and MAPS is shown in Table 32. This is a case where the wing area is 6.0% smaller and the thrust 13.3% larger for the configuration optimized using MAPS. The difference in MTOGW is only 146 lbs or 0.58% - excellent agreement. The difference in maximum fuel is 159 lbs or 3.3%. The variation in fuel is

shown in greater detail in Table 33. MAPS under predicts climb and descent/landing fuel while over predicting cruise and reserve fuel. The MAPS mission fuel is 114 lbs or 3.2% less than the FLOPS mission fuel prediction. MAPS over predicts reserve fuel by 273 lbs or 20.8%. This difference can be attributed to allowing the reserve mission to size the B-20 in MAPS.

Table 32. Comparison of B-20 Characteristics

Parameter	FLOPS	MAPS
Wing Area, sq ft	407.9	383.4
Thrust per Engine, lb	4,558	5,165
Engine Size Factor	1.0276	1.1644
Wing Loading, psf	61.23	65.52
Thrust-to-Weight ratio	0.37	0.41
Total Fuel	4,827	4,986
Fuel Fraction	0.19	0.20
Balance Field Length	4,000	3,749
Range, nm	800	800
Cruise Mach	0.60	0.60
Cruise Altitude, ft	41,000	41,000
MTOGW, lb	24,973	25,119

Table 33. Comparison of Fuel Burned

Mission Phase	FLOPS Fuel, lbs	MAPS Fuel, lbs
Taxi/Takeoff	205	200
Climb	912	795
Cruise	2,060	2,198
Descent/Landing	339	209
Mission Fuel	**3,516**	**3,402**
Reserves	1,311	1,584
Total Fuel	**4,827**	**4,986**

Table 34 shows a comparison of the detailed weight statement from FLOPS and MAPS. While there are some differences in individual components, the total empty weight from MAPS is within 190 lbs or 1.3% of the empty weight in FLOPS. Mission fuel is within 2.7%, and total fuel within 7.3% due to differences in reserve fuel mission calculations and participation of climb during a reserve mission leg contributing to sizing the wing. In future studies, reserve fuel is fixed at 28% of mission fuel so that the configurations are sized by top of climb and maximum efficiency during the mission.

Table 34. Comparison of B-20 Weights from FLOPS and MAPS

Component	FLOPS Weight, lbs	MAPS Weight, lbs	% Difference in Weight
Wing	2,154	2,095	2.8
Horizontal Tail	421	405	4.0
Vertical Tail	281	268	4.9
Fuselage	3,508	3,512	-0.1
Landing Gear	793	797	-0.5
Surface Controls	260	251	3.6
Nacelle and Air Induction	410	451	-9.1
Propulsion Group	2,592	2,809	-7.7
Hydraulics	184	186	-1.1
Electrical	778	786	-1.0
Avionics & Instruments	571	574	-0.5
Furnishings and Equipment	1,522	1,524	-0.1
Air Conditioning and Anti-Ice	585	590	-0.8
Auxilliary Power	227	227	0.0
Unusable Fuel and Fluids	167	168	-0.6
Empty Weight	**14,453**	**14,643**	-1.3
Option Allowance	0	0	
Crew	690	690	0.0
Basic Operating Weight	**15,143**	**15,333**	-1.2
Mission Fuel	3,311	3,402	-2.7
Reserve Fuel	1,311	1,584	-17.2
Total Fuel	**4,622**	**4,986**	-7.3
Full Fuel Payload	4,845	4,845	0.0
Ramp Weight	**24,610**	**25,164**	-2.2
Taxi/Takeoff Fuel	205	200	2.5
Max TO Gross Weight	**24,815**	**24,964**	-0.6

5.9 Landing and Takeoff Noise

5.9.1 Certification Noise

Certification noise for the landing and takeoff of the baseline aircraft was modeled in NASA's Aircraft Noise Prediction Program. Because of the uncertainties involved with the prediction of some of the typically less dominant noise sources, the noise certification levels shown for the turbofan engines in this report were calculated using the jet, fan, and airframe sources only. Where possible, all "small engine" options were selected in ANOPP to maximize its applicability to an aircraft of this size. Performance data was used from the parametric cycle deck and WATE, and the aircraft trajectory was calculated by FLOPS, as discussed in the performance section. Table 35 shows the results at the three observer locations.

Table 35. Noise Certification Levels for the Baseline Aircraft

Baseline Aircraft Noise Levels		
Takeoff	78.89	EPNdB
Sideline	85.27	EPNdB
Approach	86.92	EPNdB
Cumulative	251.08	EPNdB
Cum Below Stage 4	19.92	EPNdB

5.9.2 B20 Noise Impact

In order to introduce the new service in 2035 at the notional airport the growth in operations at that airport was accounted for, in spite of the fact that it is expected to be quite small. Therefore, a new future baseline was created with this growth in mind and a sensitivity study was carried out for the introduction of up to 42 new N+3 flights.

The scenarios with the B-20 added were constructed such that flights from the original data set were chosen with similar takeoff gross weight and mission range to the B-20. Out of the original set of flights, five flights were identified and assigned to the B-20. These flights were then grown to six flights having three arrivals and three departures to account for future growth. The origin and destination schedule was assumed to be identical to the original flights. Again these flights were added in four stages where a delta of 1 represents six additional flights and a delta of four represents 24 additional flights.

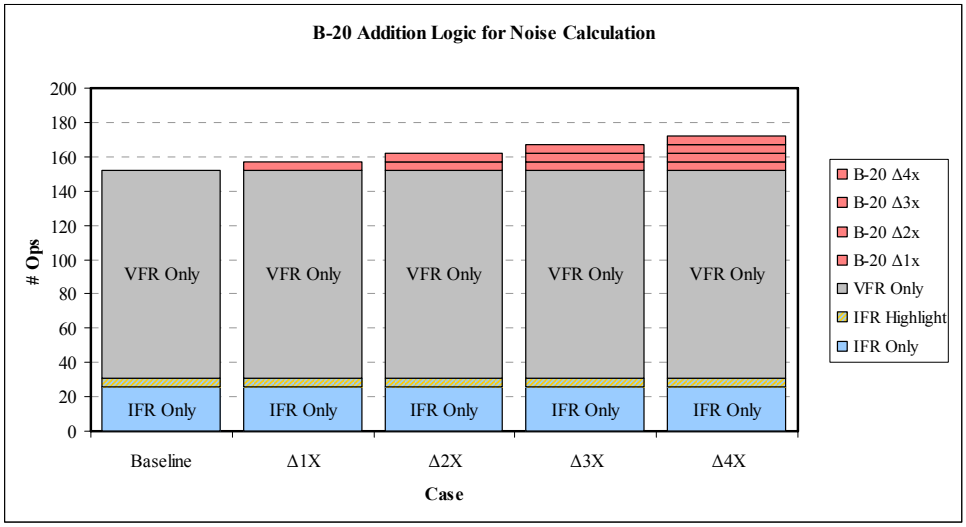

Figure 90. Addition Logic for B-20 Noise Scenarios

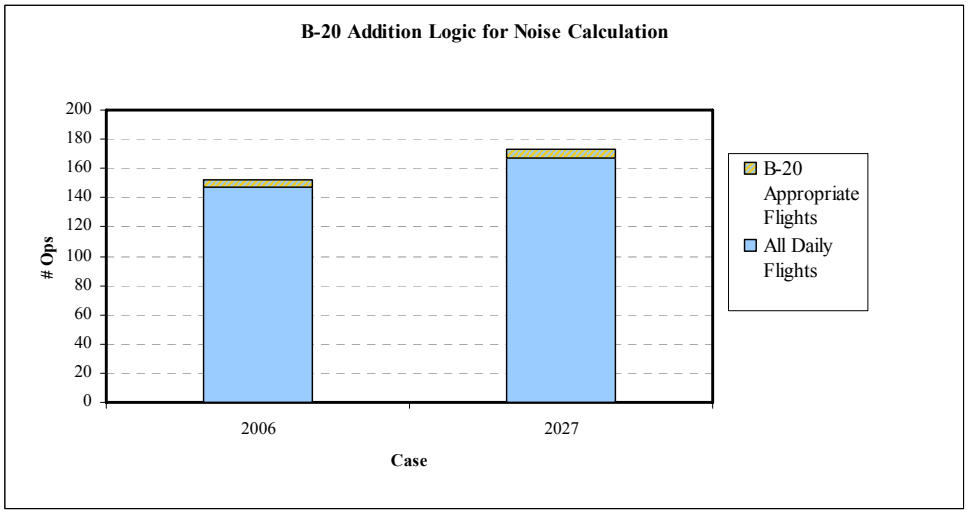

Figure 91. Comparison of B-20 Base Year and Future Year Scenarios

The introduction of the expected 24 B20 flights resulted in approximately a 0.5 nmi^2 growth in area encompassed by the 55db contour. As shown in Figure 92, the change in contours is small. It should be noted that this was in spite of the fact that the aircraft introduced for the N+3 service did not include any advanced technology.

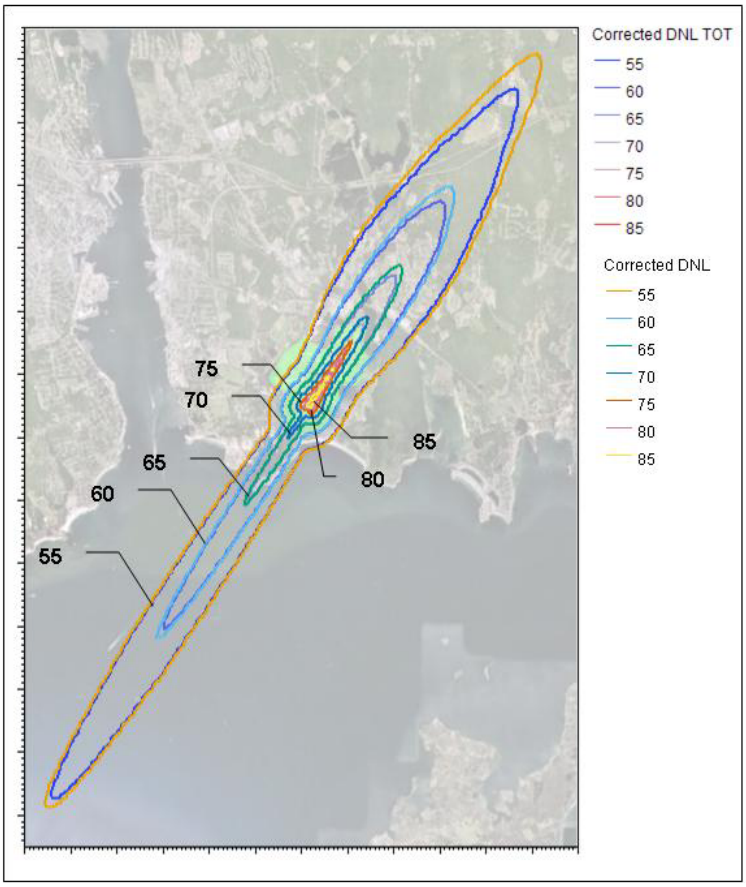

Figure 92. 2030 Noise Contours, With Traffic Growth and 24 B20 N+3 Flights

6.0 Advanced Air Vehicle Trades Studies and Analysis Report

As seen in the network studies, the N+3 network could satisfy significant demand, even with today's technology, with the benefits of dramatically reduced travel time and stress for the customer compared to the hub and spoke network. The baseline aircraft, with its modern, mixed flow turbofan engines meets the field length requirement for the N+3 network, and meets or exceeds anticipated Stage 4 noise and CAEP emissions regulations. Fuel burn and environmental impact are equivalent to the current hub and spoke network for most trips. Noise impact of the anticipated added traffic at today's demand would be relatively small.

The key to the realization of this extremely convenient mode of travel is the acceptance of commercial traffic at the community airports in the N+3 network. Many of these community airports are located in affluent suburbs where the people most likely to pay a premium ticket price live, but resistance to commercial air traffic (or added commercial air traffic) can be very high. Given that the predicted four-fold increase in future demand would result in increasing airport noise and ground emissions levels, driven largely by the N+3 traffic. Therefore meeting or exceeding ground noise and emissions regulations may not be adequate to satisfy the local community. The Advanced Air Vehicle must be quiet enough so that the added N+3 traffic must be nearly unnoticeable to the local community. Additionally, it must do so in an economical fashion, as ticket price is one of the main drivers of increasing demand.

6.1 Aircraft Configuration Trade Studies

6.1.1 Identifying Air-Vehicle Configurations to Meet N+3 Goals

Brainstorming sessions, simple Pugh matrix rankings, and an Interactive, Re-configurable Matrix of Alternatives (IRMA) workshop were employed to explore a variety of configuration and technology concepts to address the N+3 goals. These early assessments of configuration concepts were also intended to stimulate thought processes that might lead to synergistic relationships between technologies and air-vehicle configurations. The early discussions provided strategic direction for technology trade studies and for the selection of air-vehicle configurations concepts that may enable breakthrough performance in fuel burn, field length, noise reduction, and cost.

6.1.1.1 Configuration Candidates

Six aircraft configuration candidates are assessed in the context of NASA's goals for 2035 aircraft and in preparation for a team workshop that is focused on the identification, evaluation, and selection of technologies (TIES). Each of these configurations has been selected from a large set of configurations that were identified in brainstorming sessions and organized based on their potential to contribute to noise reduction, fuel burn, field length, and cost (see Appendix B). Cost was used as a key metric in this study instead of NASA's goal for the reduction of Nitrous Oxide (NOx) because NOx is driven primarily by an engine's combustion chamber and not likely to drive air-vehicle configuration decisions. Although cost isn't an explicit NASA N+3 goal, competitive direct operating cost will be a requirement for any future airliner.

6.1.1.1.1 Configuration 1, intended for low noise

Figure 93 depicts Configuration 1, which is intended to achieve low noise in a practical, cost effective configuration. From the perspective of an observer on the ground, a modestly forward-swept wing places the wing root far enough aft to block engine noise emerging from the inlets, while the horizontal and vertical tail surfaces block noise emerging from the nozzles. The vertical tail surfaces are canted slightly outboard to prevent engine noise from reflecting from the inboard surface of the vertical on the side of the plane opposite the observer. For further noise reduction, portions of the tail, wing, pylon, nacelle, and fuselage may receive acoustic treatment similar to that used in engine inlets. With the exception of the modifications to the wing and tail for acoustic purposes, Configuration 1 is a simple design, similar to most business jets.

Configuration 1 could also accommodate advanced engine concepts such as high bypass turbofans and open rotor designs. This would probably result in a trade of higher purchase price for lower fuel consumption. Double- or triple-slotted Fowler flaps could be integrated, resulting in a trade of higher purchase price for shorter runway length. In order for the weight of the aircraft to balance over the wing, aircraft with longer fuselages will require greater forward sweep in the wing, perhaps adding structural weight to prevent divergence of the wing.

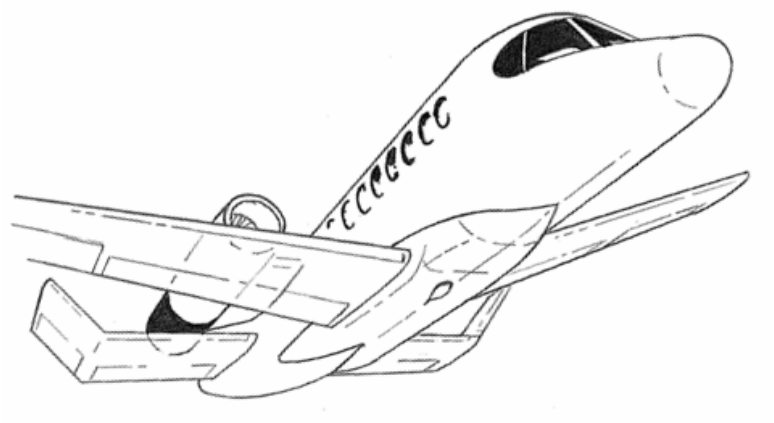

Figure 93. Concept Configuration 1.

6.1.1.1.2 Configuration 2, intended for low noise and cost

Configuration 2 is similar to configuration 1, except with a single engine, to reduce cost and fuel consumption. The engine might be integrated with a v-tail, similar to the Cirrus Vision, shown in Figure 94. The acoustic treatments and advanced engine and flap concepts mentioned for Configuration 1 could also apply to Configuration 2. A single, larger turbofan engine is probably lighter, less expensive, and more efficient than two or more smaller engines. Systems related to the engine are simplified as well, promoting a smaller, more efficient aircraft.

Figure 94. Concept Configuration 2, Cirrus Vision (V-Jet).

Single-engine aircraft are currently banned from FAR part 121 operations. It is thought that aircraft engines are not reliable enough to risk passenger service on a single-engine aircraft. However, engine reliability has been constantly increasing for 50 years, to the point that extended-range twin-engine operational performance standards (ETOPS) allows twin-engine aircraft to fly long, over water missions that previously required three or four engines. Engine reliability is expected to continue to increase through the 2030 timeframe. Furthermore, engine failures might be predicted and prevented through computer-driven trend monitoring. There is, of course, no guarantee that rules will be changed to approve single engine part 121 operations. Perhaps the best way to promote rule change, and the required improvement in engine reliability, is to demonstrate the benefit and reliability with operational twin engine aircraft.

6.1.1.1.3 Configuration 3, intended for low fuel burn and cost

Configuration 3, shown in Figure 95, is similar to Configuration 1, except without the acoustic treatment, and unusual wing and tail design. These changes will reduce aircraft cost and weight. Because weight is reduced, the engines can be reduced in size, and hence, fuel consumption. Engines might be further reduced in size due to slightly lower drag. Configuration 3 is also a relatively simple design, similar to many business jets. This configuration is a natural application of open rotor, high bypass, or turboprop engines, all of which have potential to reduce fuel burn. At a greater cost and weight, double- or triple-slotted Fowler flaps may be added. This aircraft might have increased cabin noise (with open rotor engines), and perhaps longer landing gear to prevent the open rotor or propeller tips from striking the ground during a nose high, wing low landing. The pylons, used to attach the engines to the fuselage, will be somewhat longer, heavier, and higher in drag.

Figure 95. Concept Configuration 3.

6.1.1.1.4 Configuration 4, intended for low runway length, fuel burn, and cost

Configuration 4 is similar to the Beechcraft King Air, shown in Figure 96 Engines could be highly efficient turboprops, or open rotor engines. Turboprop engines are expected to give superior takeoff acceleration, and shorten runway length requirement somewhat. To further reduce runway length, this configuration may be fitted with conventional high lift flap systems (single- double-, or triple-slotted Fowler flaps), or at higher cost and weight, externally blown flaps (EBF). This configuration (without EBF) is relatively simple and straight-forward, and has been successfully used on many designs in the past.

Figure 96. Concept Configuration 4, Beechcraft King Air 200.

EBF is generally thought of as working best with turbofan engines, so it may be found that some of the benefit is lost with the higher bypass ratio of open rotor or turboprop engines. Furthermore, there is some question of how effective EBF can be on a twin-engine aircraft, as discussed regarding Configuration 5.

6.1.1.1.5 Configuration 5, intended for low runway length requirement

Configuration 5 is similar to Configuration 4, except with a wing mounted high on the fuselage, allowing more effective propulsion system integration for the EBF. Configuration 5 is similar in concept to the Boeing C-17, shown in Figure 97. Turbofan engines (of any bypass ratio) may be used, as well as open rotor and turboprop engines.

Figure 97. Concept Configuration 5, Boeing C-17 Globemaster III.

The effectiveness of EBF depends, in part, on accelerating air by the engine, and then allowing that air to interact with the flap system. Since the wake from a turboprop engine is spread over a larger diameter, it might be expected to produce a less effective EBF than open rotor or turbofan engines. This should be studied carefully, since it represents a tradeoff of fuel efficiency (favoring higher bypass ratios) for high lift (favoring lower bypass ratios). Furthermore, since lift is derived from the power produced by the engines, it would be necessary to determine how to maintain lift when power is reduced for a landing, or if one engine is failed. With this thought in mind, it might be found that, for a twin engine design, EBF adds weight, cost, and complexity, without enhancing runway length beyond that of a more conventional flap system. A four engine design (such as the C-17) can more effectively deal with an inoperative engine, but probably is somewhat heavier, costlier, and less efficient during cruise.

6.1.1.1.6 Configuration 6, intended for low runway length and cost

Configuration 6 is a single-engine aircraft with a turboprop or open rotor engine similar to the PC-12 shown in Figure 98. Like Configuration 2, the single-engine design promotes a simpler, lighter, and less expensive airliner. Runway length requirement may be decreased with a turboprop engine, similar to Configuration 4. It is possible that runway length might be further reduced by the single-engine design, since all multi-engine planes are forced to certify takeoff distance based on initial climb out with one engine inoperative, but such a rule would be illogical on a single-engine aircraft.

Figure 98. Concept Configuration 6, Pilatus PC-12.

As with the other single-engine configuration, there is some question of the engine reliability required to use a single-engine plane for FAR part 121 operations. Since the engine in Configuration 6 is a distance in front of the windshield, in order for the weight of the plane to balance on the wing, the center of the passenger cabin would be somewhat aft of the wing. This suggests the potential for variations in center of gravity location with passenger loading. To compensate for these variations, the size of the tail may be increased, adding somewhat to weight and cost. Although passenger preference is not a criterion for the N+3 study, some passengers may unfairly think that Configuration 6 looks old and dangerous.

6.1.1.2 Pugh Matrix of Configurations

The previous section presents six candidate configurations, each with a unique set of qualifications for inclusion into the NASA N+3 study. In order to organize the benefits and drawbacks of the configurations, a simple Pugh matrix was included (Figure 99). In the figure, green indicates that the configuration helps meet a particular N+3 goal, red indicates that the configuration degrades the ability to reach the goal, and yellow indicates a more or less neutral affect.

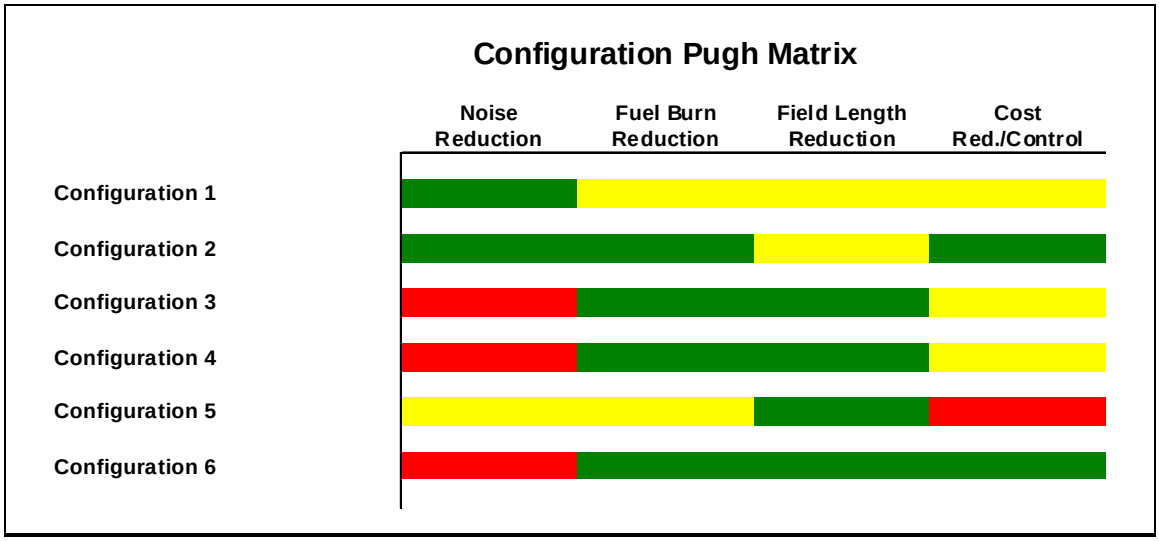

Figure 99. Pugh Matrix of Configuration Attributes.

For several reasons, Figure 99 offers only a qualitative, approximate description of configuration attributes. First, there are several ways of implementing most of the configurations. For example, the choice of an engine or a high-lift system may have an impact on the value of the configuration. Also, the figure does not indicate how much the configuration helps to reach a particular goal. The objective of this preliminary study is just to discuss the key NASA goals in the context of air-vehicle configurations and begin to develop insight that would help in the selection of an advanced configuration and an enabling set of technologies

The qualitative assessment of Figure 99 does suggest some general trends that need to be explored in more detail. First of all configuration 1 identifies the use of lifting surfaces to act as a shield for engine noise. This airframe shielding strategy is also identified as either neutral or negative relative to other configurations for fuel burn, field length, and cost. Configuration 3, 4, and 6 rank reasonably well with respect to fuel burn, field length, and cost, but are considered poor choices from the perspective of noise. A turbofan version of Configuration 4 is anticipated to eliminate the noise concern of this configuration without impacting the cost. Since field length does not appear to be a challenge for current technology aircraft in this size class (see B20 sizing results), Configuration 5 doesn't appear to be a viable candidate. Configuration 2 appears to rank the best, but suffers from the use of a single engine. Current regulations prohibit the use of single engine aircraft in airline operations with 20 passengers. It is interesting to note that two of the best configurations in Figure 99, Configurations 2 and 6, are single engine configurations.

Technologies or configuration modifications that benefit noise are clear needs for configurations 3, 4, and 6. It is also clear, that single engine operation could provide and advantage if it could become sufficiently reliable to allow regulatory change. Overall it appears as though a trade off between noise and fuel burn may become a strategic decision for the 2035 vehicle.

6.1.1.3 IRMA Workshop

The information presented above was used to populate a GT process and tool called IRMA. IRMA is an Interactive Reconfigurable Matrix of Alternatives, and was created to provide an "audit trail" to define reference systems upon which qualitative analysis could be performed in a structured, traceable, and systematic manner. IRMA builds upon the Morphological Analysis concept created by Fritz Zwicky. A Matrix of Alternatives is a way of completing defining all the relationships between design choices. In essence, it's a way of defining a certain design space. The first column lists all of the attributes of the given design space. In other words, these are all of the categories of choices that the designer has. For each row, all of possible decisions are listed. An example of this is shown in Figure 100.

		Metrics Selection		Alternatives (First)													
		Passenger Acceptance	Order of Selection	Alternative #1	Score	Select	Alternative #2	Score	Select	Alternative #3	Score	Select	Alternative #4	Score	Select	Alternative #5	Score	Select	Alternative #6	Score	Select
Vehicle Configuration	Wing-Body Blend	High	13	Fairing			Moderate Blend			Extreme Blend			-			-			-		
	Number of Wings	None	12	1			2			-			-			-			-		
	Wing Location	None	23	Low			Mid			High			-			-			-		
	High Lift System Type	Med	9	None			Tracked			Hinged			-			-			-		
	Wing Bracing	Low	20	None			Strut			Truss			-			-			-		
	Joined Wing	Low	14	None			Tip			Mid			Box			-			-		
	Morphing Wing	None	11	None			Variable Twist			Variable Camber			Trailing Edge Control			-			-		
	Wing-Tip Devices	None	22	None			Winglet			Raked			Morphing			-			-		
	Pitch Effecter	None	21	Conv. Horizontal			T-Tail			V-Tail			Canard			Wing TE			C-Wing		
	Yaw Effecter	None	24	Conv. Vertical			V-Tail			H-Tail			Winglet			Drag Rudder			-		
	Roll Effecter	None	25	Aileron / Spoiler			Wing Warping			-			-			-			-		
	Main Propulsor Location	None	19	Below Wing			Mid Wing			Over Wing			Aft Fuselage			Tip Mounted			Nose Mounted		
	Main Propulsor Type	High	3	Propeller			Counter-Rotating Open Rotor			Ducted Fan			-			-			-		
	Main Propulsors per Core	None	6	Discrete			Distributed			-			-			-			-		
	Energy Conversion	Low	2	Brayton			Const. Vol. Topping Cycle			Fuel Cell			Piston			Electric Motor			-		
	Propulsion Augmentation	Low	4	None			Batteries			Fuel Cell			Brayton			Solar Cell			Goldschmied Propulsor		
	Primary Fuel	Low	1	Liquid Hydrocarbon			Gaseous Hydrocarbon			Hydrogen (gas)			Hydrogen (liquid)			Batteries			-		
	Number of Main Propulsors*	Low	8	1			2			3			4			5+			-		
	Engine Integration	Low	7	Podded			Semi-Submerged			Submerged			-			-			-		
	Wing Sweep	Low	26	None			Forward			Aft			Compound			-			-		
	Gust Alleviation*	High	16	None			Yes			-			-			-			-		
	Trailing Edge Slots	Med	17	0			1			2			3			-			-		
	Leading Edge Device	Med	15	None			Slat			Krueger			Droop			-			-		
	Powered Lift	Med	5	Externally Blown			Internally Blown			Circulation Control			None			Upper Surface Blowing			-		
	Propulsor Drive (Remote)	Low	10	Direct Shaft			Variable Gearbox			Fixed Gearbox			Electric			-			-		
	Propulsor Airframe Shield	Med	18	None			Yes			-			-			-			-		
	Laminar Flow Control	-	27	None			Passive			Active			-			-			-		
	Longitudinal Stability	-	28	Stable			Neutral			Unstable			-			-			-		
	ALF Location	-	29	None			Fuselage			Wing			Nacelle			Tail			All		

Figure 100. IRMA Excel Spreadsheet

The IRMA was created to address shortcomings in the original Matrix of Alternatives formulation. For example, the Matrix of Alternatives formulation does not offer any guidance on how to down select a given configuration or set of configurations. IRMA incorporates decision making aids such as compatibility matrices that capture dependencies and incompatibilities of options within a single category and between categories. In other words, as the user makes a decision for one particular attribute, IRMA will not allow any subsequent decisions that are deemed incompatible. An example of this compatibility matrix is shown in Figure 101.

Compatibility numbering: 0: NOT compatible 1: Compatible 2: Enhances Do not fill in yellow cells			Fuselage								
			Wing-Body Blend			Number of Wings		Wing Location		
		The Chosen One	Fairing	Moderate Blend	Extreme Blend	1	2	Low	Mid	High
Wing-Body Blend	Fairing	0	1	0	0	1	1	1	1	1
	Moderate Blend	0	0	1	0	1	1	1	1	1
	Extreme Blend	0	0	0	1	1	0	0	2	0
Number of Wings	1	0	1	1	1	1	0	1	1	1
	2	0	1	1	0	0	1	1	1	1
Wing Location	Low	0	1	1	0	1	1	1	0	0
	Mid	0	1	1	2	1	1	0	1	0
	High	0	1	1	0	1	1	0	0	1
High Lift System Type	None	0	1	1	1	1	1	1	1	1
	Tracked	0	1	1	1	1	1	1	1	1
	Hinged	0	1	1	1	1	1	1	1	1

Figure 101. Compatibility Matrix Example for IRMA

These changes that IRMA incorporates add significantly to the effectiveness of the tool. These include enhanced understanding of the system and subsystems under consideration. Project systems and subsystems are clearly organized into a detailed taxonomy, and correlations and incompatibilities are tracked. IRMA allows a systematic process to obtain a sufficient set of reference systems. Decision makers are left with an organized information set. And finally, the IRMA enables a dynamic decision tool that is extendable and flexible, leading to a documented and repeatable process for decision making.

The team first decided on a list of metrics that would aid in configuration selection. This list started with the NASA goals, but also included metrics the team thought necessary and appropriate. The team next defined all of the attributes for the configuration selection. At this point, there was discussion as to how to distinguish between a configuration choice and a technology. It was decided by the team that a configuration choice differed from a technology in that a technology should be able to be applied to (virtually) any configuration. Thus, “wing location” would be a configuration choice, but “composite wing” would be a technology choice. The metrics and attributes that were considered are summarized in Table 36and Table 37.

Table 36. List of Metrics

55 DNL
Complexity
Cost/Ticket Price
Environmental Impact
Fuel Burn and/or Energy Consumed
LTO NOx Emissions
Passenger Acceptance
Safety
TOFL & Metroplex Compatibility

Table 37. Attributes for the Configuration Selection

Wing-Body Blend	Augmentation
Number of Wings	Primary Fuel
Wing Location	Number of Propulsors
High Lift System Type	Engine Integration
Wing Bracing	Wing Sweep
Joined Wing	Gust Alleviation
Morphing Wing	Trailing Edge Slots
Wing-Tip Devices	Leading Edge Device
Pitch Effecter	Powered Lift
Yaw Effecter	Propulsor Drive (Remote)
Roll Effecter	Propulsor Airframe Shield
Propulsor Location	Longitudinal Stability
Propulsor Type	Laminar Flow Control
Propulsors per Core	ALF Location
Energy Conversion	

Next, the team assigned weightings to each of the metrics as to how “important” they were to the overall research goals. Likewise, the team assigned a “low”, “medium”, or “high” value to each of the attributes to designate the importance of that particular decision to each metric. These rankings do not indicate the direction of the importance. For example, the number of wings decision was awarded a high relationship to the complexity metric. But this does not indicate whether or not additional or fewer wings contribute to more or less complexity. Rather, it simply establishes that the decision itself has a high impact on the complexity metric. A numerical scheme was used to quantitatively calculate the overall rankings.

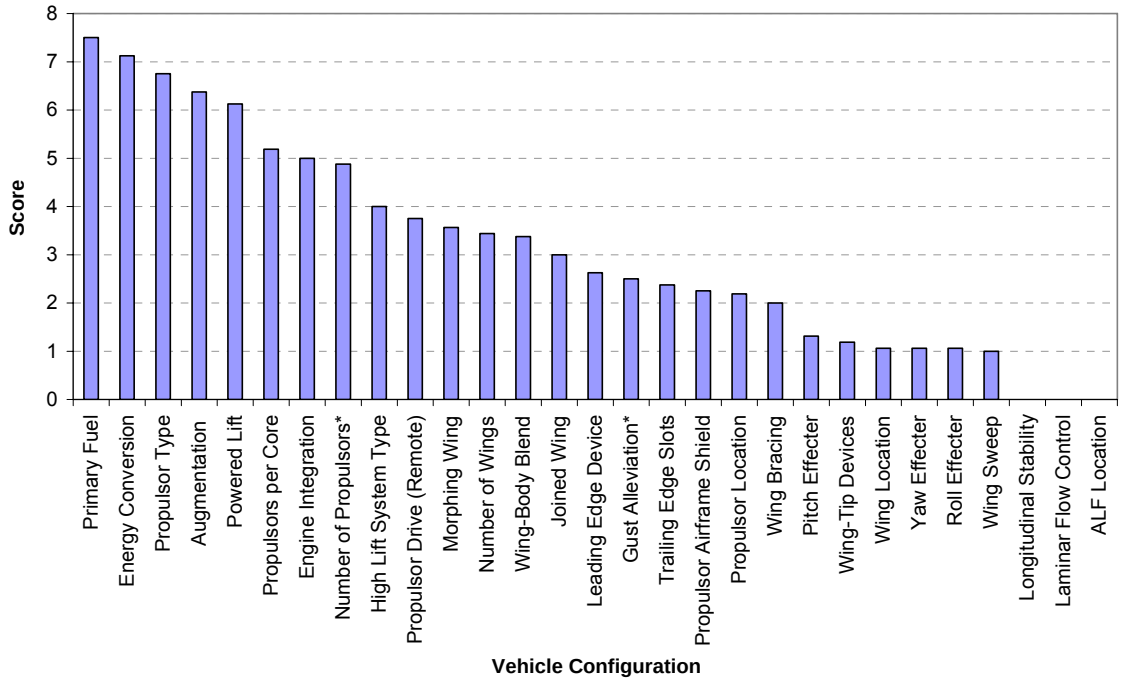

Figure 102. Attribute Rankings for IRMA

A drop down menu in IRMA can be toggled to each individual metric, showing the relationship ranking between the attribute choices and that particular metric. The Order of Selection column indicates which attributes are most important, given the weightings defined earlier. The team uses this information to make configuration decisions.

The Generated Concepts and the Initial Design Notes

Once the overall IRMA with all the pertinent attribute options were compiled, and the compatibility and ranking information was populated, the workshop participants broke out into several sub teams to identify potential configurations to study further. Each sub-team in the workshop used the IRMA as they saw fit. After making their decisions via the matrix, each team attempted to sketch out their configuration. Some teams chose to document their choices, while others did not. The resulting sketches from the workshop are shown, with the team's accompanying design notes (if any).

6.1.1.3.1 Blended Wing Body Low Noise Concept

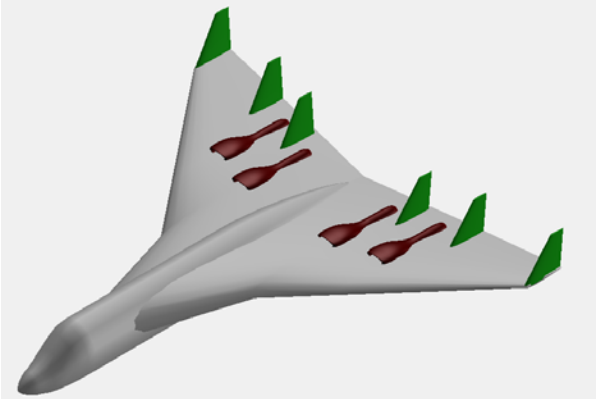

Figure 103. BWB Concept

This concept was thought to have a very low noise signature compared to the other concepts. It was also considered to be a concept which is hard to analyze considering the internal flow issues. Additionally the similar designs were unsuccessful in the past. It will be a high performance concept for the Takeoff Field Length considerations at the expense of fuel burn and therefore emissions. Cost concerns would be dominant.

6.1.1.3.2 Conventional Low Complexity Concept

This concept was generated with the complexity concerns in mind. The team is experienced with this particular type of aircraft and it will be cheaper compared to the other concepts. Since it is not revolutionary in any aspect, it is not thought to match N+3 goals. This version has a big wing without flaps but even a lower cost derivative can be created by having a low wing and conventional tail with a piston engine although currently there is no piston engine that can meet the necessary power and reliability requirements.

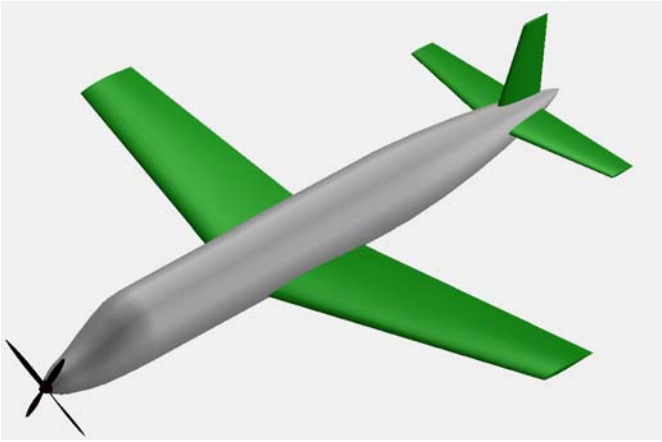

Figure 104. Conventional Low Complexity Concept

6.1.1.3.3 Low Fuel Burn Concept

The significant physical property of this concept is its high aspect ratio with open and electric driven rotors. To achieve higher Bypass Ratios, the number of propulsors was increased and the propeller diameter was minimized to minimize the blade tip speed. Concerns arise about the practical usage of the proposed electric motors by the planned timeframe of the N+3 scope. It is planned to have very low emissions featuring solar cells designed to augment in cruise and morphing wing with active gust alleviation. Its fuel cell driven electric motors may have issues with the night time operations capability.

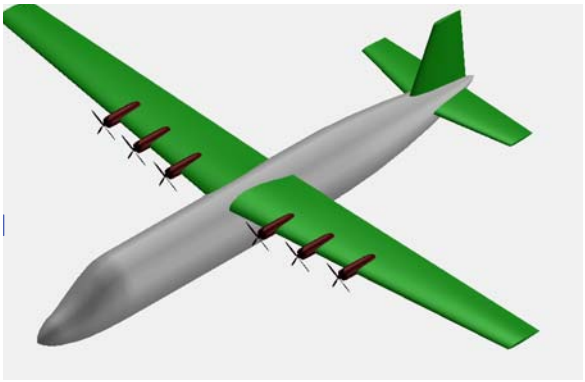

Figure 105. Low Fuel Burn Concept

6.1.1.4 Technologies for Future Air-Vehicles

The configurations discussed have been evaluated from the perspective of NASA's N+3 goals for 2035 airliners. All of these configurations could benefit from new technologies and new approaches to the integration of technologies into an air vehicle.

A key element of the research effort, therefore, is the identification and selection of candidate propulsion and airframe technologies to evaluate towards achieving NASA goals. The team started with a technology list generated by an in-house research group looking at enabling technologies that would achieve similar results to NASA's 2035 goals. This original list was augmented by a list generated by the IATA-TERESA workshop (TEchnology Roadmap for Environmentally Sustainable Aviation), held Sept 2008. Each technology was described, along with its most probably effect. In addition, its Technology Readiness Level (TRL) was assessed. Technologies were sorted into four categories (engine, airframe, air traffic management procedures, and fuel) in order to isolate those technologies of interest to this particular research study (in this case, engine and airframe technologies).

Team members from GE Aviation, GE Research Center, Cessna Aircraft and the Georgia Institute of Technology met for a two-day technology identification workshop in May, 2009. Additional subject matter experts augmented the GE and Cessna teams via teleconference. Various advanced propulsion and airframe technologies and configurations were identified and discussed in this meeting. The initial technology lists generated are included in Appendix B.

In general, technologies that reduce aircraft weight, reduce engine fuel burn, and reduce aircraft drag are the most promising. The following down selected list of technologies or vehicle

capabilities is recommended as a focus for the development of 2035 vehicles with breakthrough performance.

- Advanced propulsion systems (fuel burn)
- Laminar flow boundary layers (drag, fuel burn)
- Tailless and or reduced stability configurations (drag, fuel burn)
- Low wing loading for high altitude cruise (drag, fuel burn)
- Mission optimization through 4D trajectories (fuel burn)
- Active gust load alleviation (weight & ride control)
- Advanced composite airframe structures (weight)
- Multi-function structures (weight)
- More electric aircraft subsystems (weight, fuel burn, maintenance cost)
- Single engine airliner operation (weight, maintenance cost)
- Single pilot airliner operation (weight, direct operating cost)

6.1.1.5 Regulatory Review for Single Engine Concepts

Appendix C documents a review of current Federal Aviation Regulations for both the design and operations of small commuter airliners. The impact of certification altitude is also reviewed from the perspective of the systems or structures weight that is required for high altitude operation. Any weight that could be saved by operating at lower altitudes, with a single engine, or with a single pilot would have a clear benefit on aircraft fuel burn.

A relatively poor safety record for commuter aircraft led to a call for “one level of safety” for all airline operations in 1996. As a result, a number of rules were substantially rewritten or outright added. This extensive change is documented in the Federal Register, Vol. 60, No. 244, December 20, 1995, pages 65831-65940. Unfortunately, current regulations leave little room for the consideration of single-engine aircraft with single-pilot operations in airline service.

Although Appendix C identifies a small weight benefit in both systems and structures weight for cruise altitudes below 25,000 ft. These benefits are perceived as small relative to the savings in fuel burn associated with high altitude cruise.

It is recommended that 2035 vehicles considered in this report all have two engines, two pilots, and a flight attendant. It is also recommended that these airliners have the capability to fly over bad weather. However, it is recognized that the safety and reliability of modern technology be carefully monitored over time. The weight, fuel burn, and cost benefits of single engine operation remain appealing. Routine operations of unmanned air-vehicles in the national airspace system and continued development of automated systems and controls may enable an equivalent level of safety with one pilot and one engine.

6.1.1.6 Summary, Configurations and Goals

The NASA N+3 contract sets goals of dramatic reductions in noise, nitrogen oxide emission, fuel consumption, and runway requirement for airliners expected to enter service between 2030 and 2035. Six configurations have been used to understand general trends between configuration concepts and their ability to satisfy these aggressive goals. The configurations utilize a variety of unique features, some serving one goal best, other serving another goal best, thus providing a versatile palette from which to choose, regardless of which goals are to receive the most attention. A simple Pugh matrix is included to illustrate the relative strengths and

weaknesses of each configuration. A discussion of the IRMA process followed by the team and the resulting configurations are also included. Propellers, open rotors, and very high-bypass ratio turbofan propulsion systems are expected to offer significant fuel burn and field length benefits to any configuration.

Technology concept brainstorming identified several key approaches to performance improvement of any and all future concepts. For aerodynamic drag reduction, laminar flow, tailless configurations, and low wing loadings for high altitude cruise are identified for further study. Advanced composite structures, more electric subsystems, and the multi-function integration of subsystems and structures may all contribute to breakthrough reductions in weight. Single pilot operation of single pilot aircraft may provide meaningful reductions in fuel burn, but are considered too risky for 2035 aircraft given the current FAR regulations and the maturity of the automated systems.

It is recommended that explorations of new propulsion technologies, methods for aerodynamic drag reduction, and new materials that reduce weight be performed during the development and refinement of a 2035 vehicle. Quantitative benefits in drag, weight, and engine fuel burn for a current technology conventional configuration can be used to evaluate the relative importance of any proposed technology.

6.1.2 Aerodynamic Configurations & Technologies for Drag Reduction

Given NASA's aggressive goal of a 70% reduction in fuel burn relative to current technology aircraft all feasible technologies that may lead to reductions in compressibility drag, in induced drag, and in lift independent viscous drag need to be explored in detail. The 2035 vehicle configuration is driven by the need to provide a comfortable space for 20 passengers and to minimize the drag of the vehicle. Particular attention needs to be given to reducing the wetted area of the vehicle and to the development and maintenance of laminar flow.

6.1.2.1 Compressibility Drag & Mission Parameters

With mission distances less than 800 nm and cruise speeds less than or equal to a Mach number of 0.60 compressibility drag is not likely to be a major contributor to aircraft drag. In fact, modern airfoil design practices should enable the development of air-vehicles in this speed range with no compressibility drag. One would expect these vehicles to have wings with zero degrees of quarter chord sweep.

Another advantage of this approach to the elimination of compressibility drag is that it enables or simplifies aerodynamic design for natural laminar flow. Airfoil pressure distributions that are developed for low compressibility drag and high vehicle cruise speeds typically have adverse pressure gradients that trip a laminar boundary layer near the leading edge of the lifting surface. Furthermore, positive values of wing sweep lead to cross flow instabilities that force boundary layer transition from laminar to turbulent.

It is recommended that all of the 2035 air-vehicle trade studies include cruise speed as a design parameter, and that significant attention be given to the value of cruise speeds that remain at or below a Mach number of 0.60.

6.1.2.2 Laminar Flow

Since 50-70% of total aircraft drag for vehicles in this class (66% for the B-20 Turbofan) can be attributed to lift-independent viscous drag, it is reasonable to focus on the development and maintenance of laminar flow boundary layers. A thorough review of the state-of-the-art in laminar flow technologies is presented in Appendix F. This appendix suggests that laminar flow boundary layers reduce the skin friction coefficient by 75%. With an average of 60% laminar flow over the entire air-vehicle this would lead to about 50% reduction in lift-independent viscous drag.

Appendix F also identifies many of the challenges associated with the design and operation of air-vehicles for laminar flow. These challenges include

- a reduction in the maximum lift potential of a wing designed for natural laminar flow,
- the weight, power, and volume requirements for any active system that is required to maintain laminar flow,
- manufacturing tolerance for gaps and steps at joints in aircraft surface, and
- the difficulty of maintaining laminar flow in an operational environment that has bugs, rain, and ice.

These challenges suggest a vehicle design strategy based on the use of (1) low wing loadings rather than maximum lift to satisfy field length constraints, (2) aggressive design for natural laminar flow with limited use of active systems, (3) careful attention to the smoothness of the aircraft surface and the placement of doors, windows, and surface panel joints, and (4) the use of easy or self cleaning surface materials.

6.1.2.2.1 Natural Laminar Flow Design

Aggressive design for natural laminar flow leads to a fuselage fineness ratio trade study and a loft effort focused on developing favorable pressure gradients in the front half of the fuselage. Seating 20 passengers in 2-abreast, 3-abreast, and 4-abreast configurations leads to the fuselage fineness ratio trade study shown in Figure 106. These configurations start with a slightly oval cross section to accommodate the height constraint with 2-abreast seating, proceed through a nearly round 3-abreast seating configuration, and end with a slightly oval cross-section to accommodate the width of 4-abreast seating. All of these configurations were lofted with the following objectives and constraints

- Provide the appropriate volume for 20 passengers, their bags, and the necessary doors, isles, and emergency exits
- Maintain a constant distance from the center of the passenger cabin to the ¼ chord of the horizontal tail to approximate constant control authority in all configurations. This constraint establishes the length of the tail cone and the area of the horizontal tail.
- Minimize the total wetted area of the fuselage
- Maximize the extend of favorable pressure gradient and wetted area in the forward half of the fuselage

Figure 106 shows 8-9% reduction in fuselage wetted area associated with shorter and fatter fuselage shapes with a trend of diminishing returns by the time we reach the 4-abreast configuration. Both the lack of benefit in wetted area and the penalties associated with

supporting pressure loads in highly oval cross sections rule out 5 or 6-abreast seating arrangements.

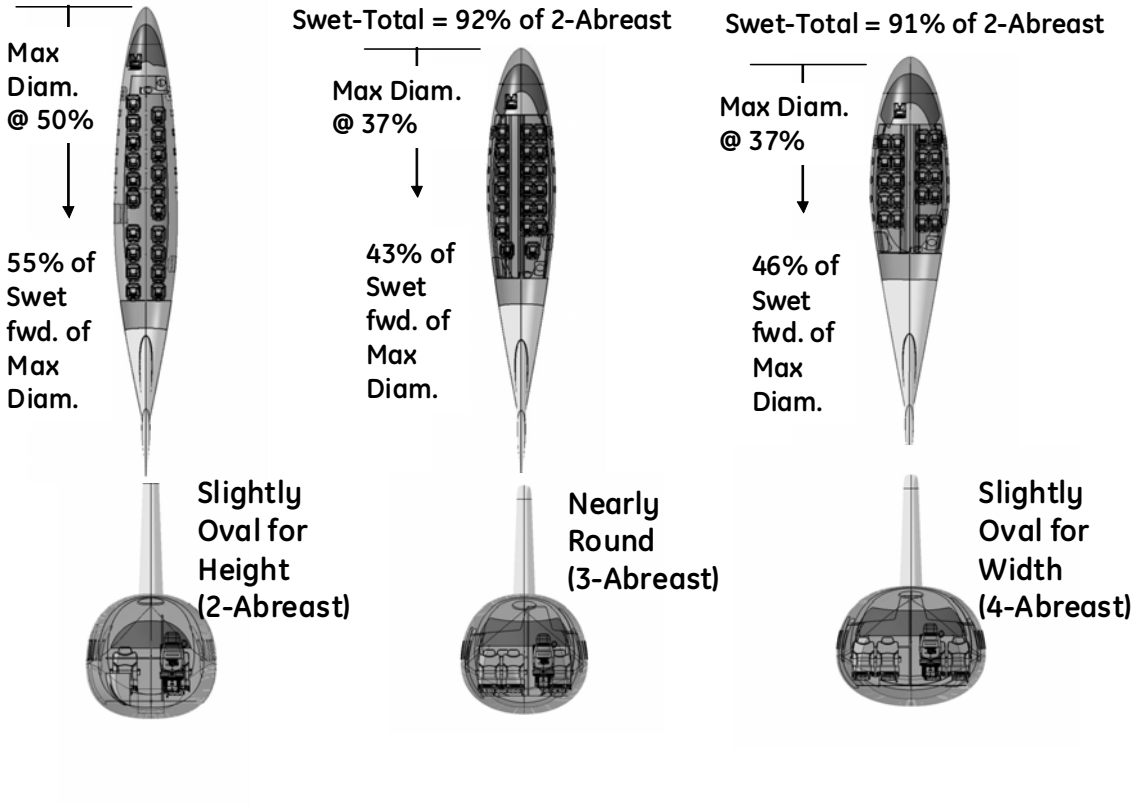

Figure 106. Fuselage Fineness Ratio Studies for Wetted Area and Laminar Flow

The 4-abreast configuration of Figure 106 saves 15% in wetted area relative to the baseline 20 passenger aircraft fuselage. Future aerodynamic optimization has the potential to reduce the wetted area an additional 2% and move the location of maximum fuselage width further aft. Even without this optimization, the 4-abreast configuration has 46% of the fuselage wetted area in a region of favorable pressure gradient and has 15% less total wetted area than the fuselage of the baseline aircraft (B20). This combination of wetted area benefits leads to the equivalent of 56% laminar flow on the baseline 20 passenger aircraft, in spite of the increase in form factor associated with the shorter, fineness ratio 5.4 fuselage (baseline fineness ratio = 6.7).

The risk of maintaining natural laminar flow past window, windshield, and door joints is addressed with (1) new approaches to structural assembly that minimize gaps and steps, (2) active breaking of the seals around emergency exits during use, and if necessary active suction in areas where joints are unavoidable (nose landing gear doors). Figure 169 show that the entry door of this advanced fuselage concept has been place aft of the region of potential laminar flow. Potential areas for natural laminar flow include the forward 46% of the fuselage, and the forward 60-80% of lifting surfaces. Appendix F reviews other work on natural laminar flow design for wings and airfoils. This task is not considered a risk for the 2035 vehicle.

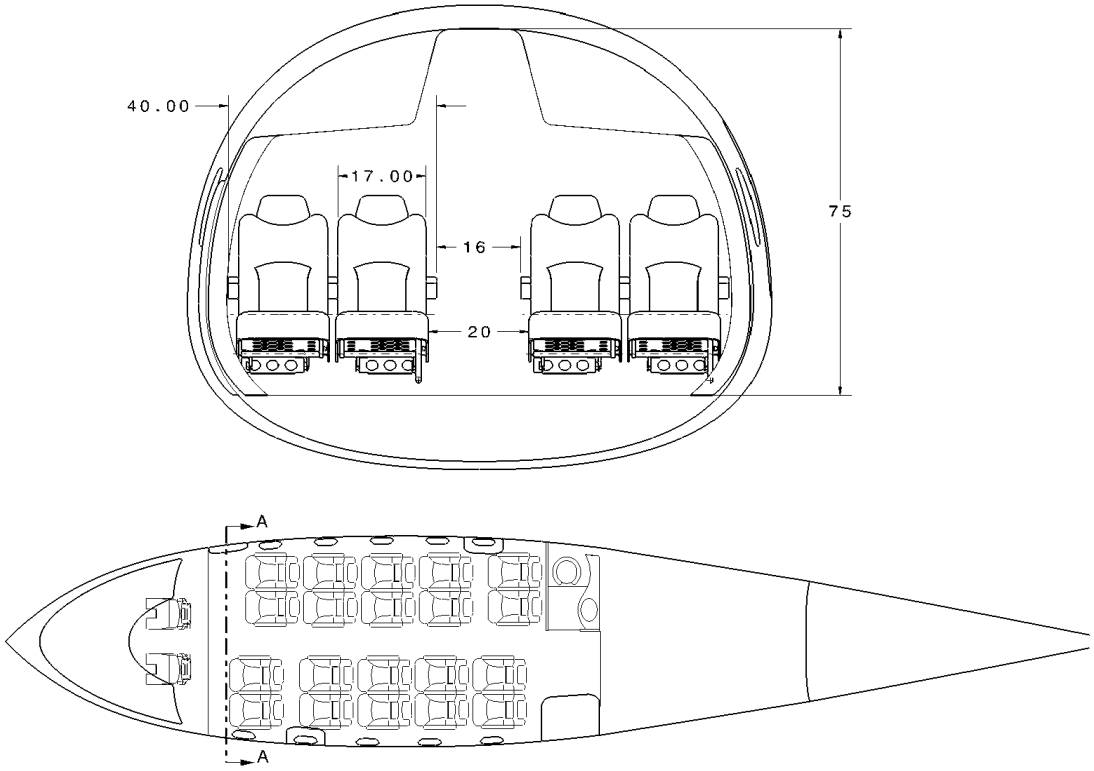

Figure 107. Top and Front View of 4-Abreast Cabin

Future work should be focused on the step and gap requirements necessary to avoid the use of suction in regions of favorable pressure gradient and in quantifying the weight and power consumption of any necessary active systems. Future work will also be required to sense the impact of laminar flow on the fuel burn and associated range of the aircraft. Rain or ice will cause some flights to lose some or all laminar flow for some portions of the flight.

6.1.2.2.2 Hybrid Laminar Flow Control

The unique shape of the fuselage ensures that a favorable pressure distribution could exist forward of the maximum fuselage width location and provide significant areas of natural laminar flow. However, disruption to the natural laminar flow is possible from doors, windows, and the windshield gaps and steps. Figure 108 shows the potential area for natural laminar flow on the fuselage. The white lines on Figure 108 indicate potential areas of active suction where steps or gaps could exist (around the windshield, windows, and door joints).

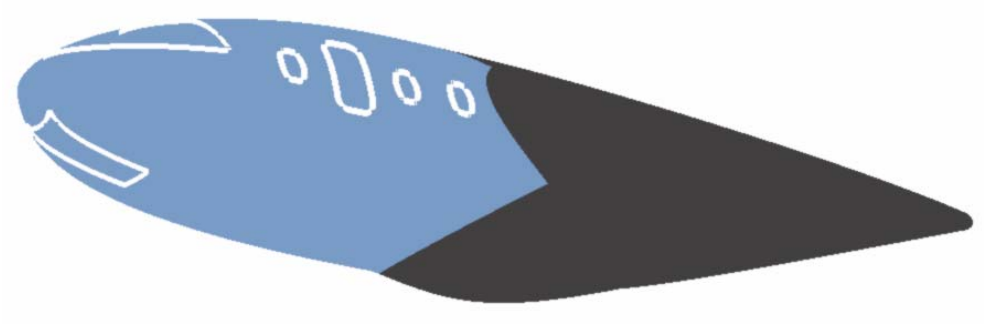

Figure 108. Advanced Fuselage with Active Suction

Using information from "Hybrid Laminar Flow on Wings and Fuselages" by John C. Lin (Reference 30), estimates were made for the power required to provide active suction to either preserve or re-establish the natural laminar flow. The equivalent suction drag is given by the expression:

$$C_{ds} = \int_0^{x/c} (C_q / \eta_p)(1 - C_{ps}) d(x/c)$$

Where: C_q is the local suction coefficient (.0007 to .0009)
η_P is the compressor efficiency (.80 to .85)
C_P is the local suction coefficient.

A sensitivity analysis was performed to determine the range of power requirements. The suction coefficient range comes from Reference 30, and typical values for compressor efficiencies. Representative values for the local pressure coefficient are used for the specific location on the airplane.

Table 38 shows the lengths and power estimates to provide suction to preserve and re-establish laminar flow. Future research will need to determine the width and extent of the required lines of active suction. For this feasibility assessment, 4 inch strips are used around each window, escape hatch, and the windscreen. A five inch strip of 63 ft. in length is assumed for suction at or near lifting surface leading edge attachment joints.

The power estimates for suction shown in Table 38 are well within a range of feasibility that motivates a need for detailed systems design and integration studies. For the preservation of laminar flow Table 38 show less than 9 Hp for either active suction on the fuselage areas shown in Figure 108 or on 63 ft of lifting surface leading edges. A total of 17 Hp is small enough to neglect the impact on aircraft fuel burn. Table 38 shows a total of 156 Hp for a system with enough suction to re-establish laminar flow after the flow has been tripped. This amount of power is measurable, but still within one or two percent of total aircraft fuel burn. The analysis suggests that the feasibility or value of an active system will be driven by the weight and cost of the system components necessary to perform the suction.

Table 38. Lengths and Power Required Estimates to Provide Suction to Preserve and Re-Establish Laminar Flow

Aircraft Component	Preserve Laminar Flow (Hp)		Re-Establish Laminar Flow (Hp)		Length Around Component (in)
	M=0.6, 25,000 ft	M=0.6, 41,000 ft	M=0.6, 25,000 ft	M=0.6, 41,000 ft	
Nose Gear Door	0.65	0.31	6.06	2.89	162
Seven Windows	1.33	0.63	12.46	5.95	239
Left Escape Hatch	0.42	0.20	3.97	1.89	106
Right Escape Hatch	0.49	0.23	4.56	2.18	121
Windshield	1.24	0.59	11.67	5.57	312
Total - All except lifting surfaces (4 inch strip)	8.26	3.94	77.44	36.97	941
5" X 63' Lifting Surface Strip	8.40	4.01	78.72	37.58	756
Aircraft Total	**16.66**	**7.95**	**156.16**	**74.55**	**1,697.00**

Several assumptions were necessary to estimate the weight of additional systems, and additional fuel burned to provide suction for active laminar flow. From analysis of bleed air systems for similar Cessna aircraft, a weight of 0.0948 lbs/inch of protected area was developed. This weight includes bleed air tubes and brackets along with 75% of the pre-cooler weight to condition bleed air to approximately 400 deg. F. A system that performs all of the suction identified in Table 38 is expected to weigh approximately 160.9 lb. Aircraft sizing sensitivities with this extra weight and the fuel burn associated with the required horsepower extraction from the main engines should be performed on the final 2035 concept vehicle.

6.1.2.3 Wing, Tails, Goldschmied Propulsors and Wetted Area

Another approach to reducing the lift dependent viscous drag is simply to reduce the wetted area of the air-vehicle to the absolute minimum. In the context of tail surfaces, this frequently leads to the exploration of tailless and flying wing configurations. Large wing areas are frequently needed for field length requirements, initial climb altitude requirements, and the fuel storage. High-lift systems can be used to support field length requirements. For any given high-lift system the appropriate relationship between engine thrust and wing area is required for both initial climb altitude and field length. Goldschmied propulsors have also been proposed for shortening fuselages without creating flow separation at the aft end.

6.1.2.3.1 Wings, High-Lift Systems, & High Altitude Cruise

A trade off between wing area, high-lift system complexity, cruise altitude, and engine thrust is anticipated for the optimum 2035 aircraft. As shown in Appendix E, the Cessna Citation CJ2+ experiences significant reductions in fuel burn for cruise altitudes of 45,000 ft. versus 35,000 ft. On a 1000 nm mission the CJ2+ consumes 30% less fuel at 45,000 ft that it does at a cruise altitude of 35,000 ft. Even for missions as short as 250 nm, a 17% reduction in fuel burn is experienced for a cruise altitude of 45,000 ft.

A significant portion of this benefit is simply caused by a reduction in air density and therefore the friction drag of the aircraft. However, the capability to climb to altitude is primarily a function of wing area and engine thrust. These same parameters are critical for takeoff from short runways. This becomes an interesting design trade, since NASA has aggressive goals for both fuel burn and field length. New technology high lift systems will enable an aircraft to satisfy field length requirements with a smaller wing and engine, but limit the aircraft's initial cruise altitude. A large wing enables both field length and high altitude cruise, but forces the aircraft to

fly with a larger wetted area for the entire flight. Minimum fuel burn for the 2035 vehicle will require the best wing area and engine thrust for the cruise flight condition.

It is recommended that cruise altitude remain a critical design variable for the optimization and sizing of the 2035 vehicle. Since the baseline 20 passenger aircraft satisfied field length requirements with simple high-lift systems, it is reasonable to anticipate the optimization of engine and wing technologies for optimum cruise performance. This should enable minimum fuel burn without the weight or cost of complicated high lift systems.

6.1.2.3.2 Tail Sizing

Appendix D documents a fundamental review of the issues and challenges associated with tail sizing. This document discusses the requirements for a vehicle's lifting surfaces (1) to lift the vehicle weight, (2) to trim the loads so that the vehicle maintains level flight, (3) to provide stability so that the vehicle natural returns to level flight if perturbed, and (4) to provide the ability to control the vehicle. These requirements lead to tails or aft portions of lifting surfaces that are responsible for producing pitching moment or stability, but not lift.

Figure 109 shows how a vehicle's need for both trim and stability leads to wetted area in a variety of air-vehicle configurations. It should be noted that there is some wetted area penalty for trim and stability functions even in tailless and flying-wing aircraft. Traditionally, aircraft have minimized this wetted area penalty by placing a very small tail as far aft of the aircraft center of gravity as possible. This is particularly true for competition sailplanes.

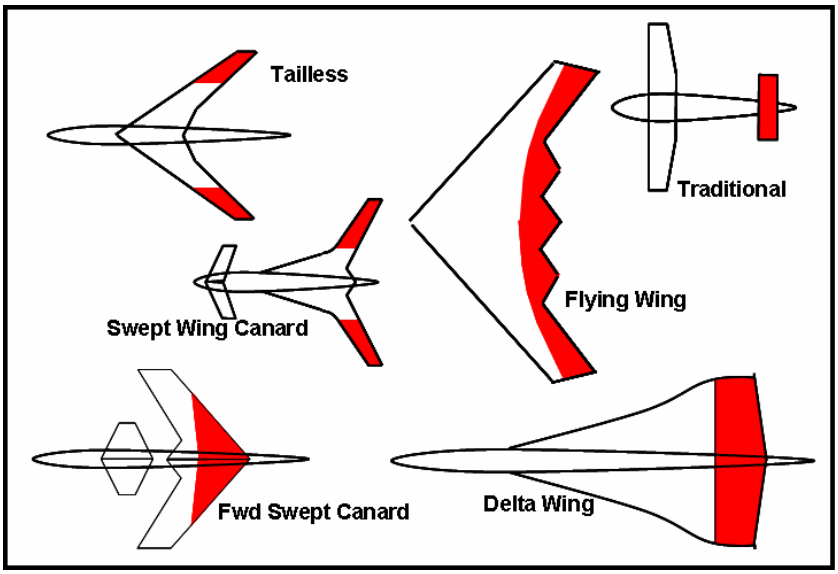

Figure 109. Aft Portions of Lifting Surfaces with Responsibility for Trim or Stability.

A tail's contributions to trim and pitch control (see Appendix D) are particularly important for airliners that must operate with a wide range of center of gravity positions. The reduced fineness ratio and 4 abreast seating from the previous section reduce the operating range of center of gravity some, but a small aft tail is still a desirable feature. It should also be noted from Figure 109, that tailless configurations require some wing sweep to move the stabilizing or controlling surface aft of the aircraft center of gravity. As noted in the previous section, wings without sweep are desirable for natural laminar flow.

6.1.2.3.3 Goldschmied Propulsors

Goldschmied propulsors were investigated briefly for their potential contribution to the reduction of fuselage wetted area. These flow control devises enable the truncation of the fuselage tail cone without flow separation and the associated increase in drag. More than half of the tail cone is used to store passenger bags and secondary systems (see Figure 169). Consequently a reduction in wetted area associated with truncating the tail cone is small. This improvement would also be offset by the addition of twin booms to support a tail that provides the control authority necessary for airline operations that create a wide range of center of gravity locations. Figure 110 shows an example of a configuration with a truncated tail cone and a tail that is supported by twin booms.

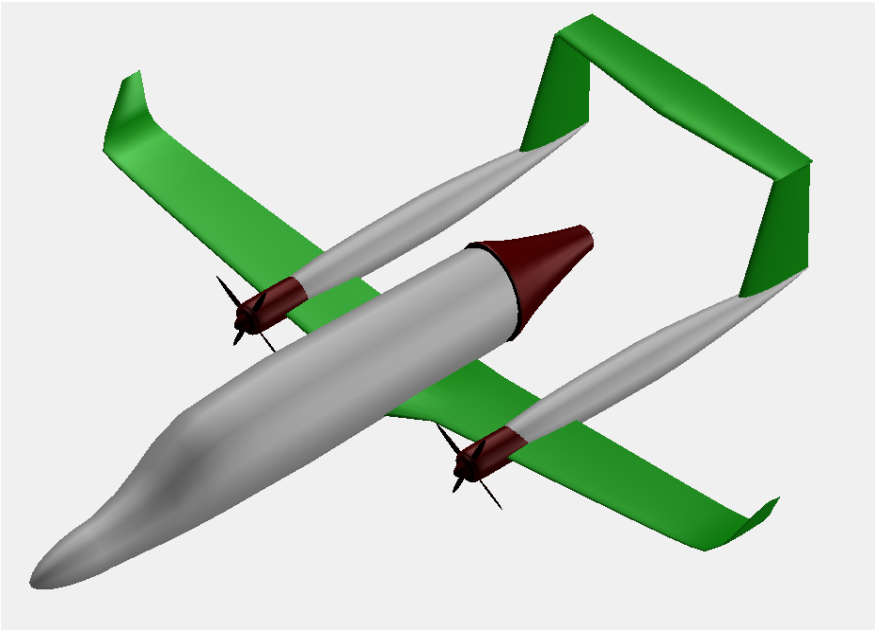

Figure 110. A shortened tail cone, and twin boom tail configuration

Preliminary analysis of the configuration wetted area in Figure 110 was larger than that of a conventional aft-tail aircraft configuration. Figure 111 shows an alternative tailless configuration with a Goldschmied propulsor and a swept wing. This configuration requires a positive wing sweep to place some trim and stabilizing surface aft of the aircraft center of gravity. Given the desire for controllability for a large range of center of gravity locations and the desire for a wing with natural laminar flow, this may not be the best choice. It should also be recognized that the Goldschmied propulsor requires the weight, cost, and fuel burn of the boundary layer suction and propulsive fan that keeps the flow attached to the aft end of the fuselage. One would need a significant reduction in wetted area for this additional machinery to be beneficial.

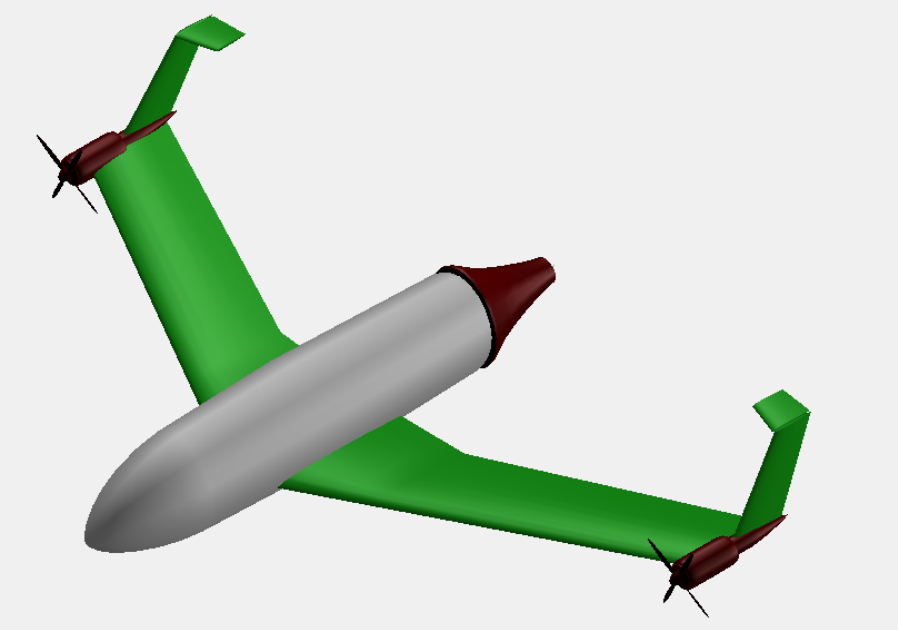

Figure 111. Tailless, Swept Wing with Goldschmied Propulsor.

6.1.2.4 Induced Drag and Wing Morphing

Approximately 30-50% of the drag of the advanced vehicle configuration is anticipated to be lift-dependent or induced drag. Induced drag is directly related to the weight of the aircraft and a function of the aircraft span lift distribution. It is well known that minimum induced drag is associated with an elliptical lift distribution. Consequently the obvious strategy for an advanced vehicle is to have an elliptical lift distribution on as large a wing span as is possible without a structural weight penalty.

Wings with zero degrees of quarter chord sweep that have been recommended for minimum compressibility drag and laminar flow are ideal for minimum induced drag. The un-swept wing enables the design of a wing twist distribution that maintains an elliptical lift distribution for all angles of attack and phases of flight. With this characteristic a wing that has the ability to morph or change its twist distribution in flight has little benefit. It should be noted however that small cruise flaps or limited wing morphing could be used to enable the vehicle to maintain an angle of attack of zero degrees for the vehicle fuselage. This has potential benefit for maintaining laminar flow on the fuselage.

6.1.2.5 Recommendations for Aerodynamic Design

The fundamental characteristics of vehicle configuration choices and their impact on compressibility drag, induced drag, and lift-independent viscous drag have been reviewed. Particular attention was given to the development of laminar flow, the reduction in vehicle wetted area, and the elimination of compressibility drag. The following strategy is recommended for the development of the 2035 vehicle:

- Maintain a cruise speed that is less than or equal to a Mach number of 0.60,
- Make sure that the wing and engine are sized for cruise,
- Keep the cruise altitude as a vehicle design variable,

- Limit lifting surface sweep to zero degrees (laminar flow & compressibility drag),
- Use a low fineness ratio fuselage to reduce wetted area and increase the percent of the fuselage that is available for natural laminar flow,
- Design all surfaces for as much natural laminar flow as possible,
- Explore limited use of active flow control to maintain laminar flow, and
- Explore the use of self cleaning surfaces to help maintain laminar flow in operational environments

6.1.3 Advanced Aircraft Structures and Systems

Ever since the advent of powered flight, aircraft weight has been a primary challenge for aircraft designers and fabricators. Through the years, more and more innovative materials have been created and used in aircraft production. As aircraft grew larger, both in physical size as well as available power plant output, designs transitioned from wood and fabric structures to include metallic components. Painful lessons were learned relative to fatigue in aluminum structures as those materials gained wider and wider acceptance as the material of choice for aircraft fabrication. As aircraft shape evolved, it became harder and harder to manufacture all parts out of metallic materials and other competing program needs led to the introduction of composite materials into the aircraft market.

At first comparison, composites are a natural fit for aircraft fabrication due to their advantages with specific strength and/or specific stiffness when compared to typical aerospace metallic alloys. However, their highly orthotropic nature requires that they be stacked up in a sequence of layers to provide the necessary strength or stiffness that a particular design requires. As a result, the overall structure does not typically yield a reduction in weight that is in line with direct volumetric and specific gravity computations. Certainly there are a number of experimental, home-built composite aircraft that tout weight reductions as compared to their certificated counterparts. These aircraft are not subjected to the same rigorous certification process, may not be as robust as certificated airframes.

Many advances in composite utilization on commercial aircraft designs have been dependant on material and process development that is driven by the needs of military programs, which are not as sensitive to short development program cycles and funding limitations as commercial development programs are. Examples of successful composite implementation in military programs include extensive use of composite materials on the B-2, F-117, F-14, F-18, F-22, F-35, V-22 and C-17 programs. Through the use of composites on these programs, advancements have been made in design criteria, analysis techniques, test program development, and data analysis methodologies. These advancements eventually work there way into the public domain through published research papers, industry conferences and/or migration of personnel from one company to another and further allow composite implementation in broader arenas, such as commercial aviation.

There have been a number of attempts at certifying commercial composite aircraft, some have been successful and some have not. In the late 1960's, the FAA certified the Windecker Eagle, a 4 place aircraft built from fiberglass and epoxy materials. In the 1970's, Bill Lear started the design of the LEAR FAN. It was built with a 100% carbon-epoxy airframe and relied heavily on bonded joints rather than fasteners as used in metallic structures. It was reported to have an empty weight approximately 2,000 pounds less than similarly sized metallic designs. Despite first flight in the end of 1980, the aircraft failed to be certified, mainly due to issues with the complexity of the twin engine, single driveshaft concept that powered it. Hawker Beechcraft

developed the Starship with help from Burt Rutan and Scaled Composites. It was built using large scale fiber placement concepts and laid the ground work for the now certified Premier IA and Horizon designs, as well as the upcoming Premier II aircraft. Despite gaining certification, the programs were oft delayed and had to overcome several major technical issues to achieve certification. Several smaller GA companies have developed composite aircraft that have achieved FAA certification, including various small GA designs from Adam Aircraft, Cessna, Cirrus and Diamond Aircraft. Several other smaller composite designs are currently in development, including the Bombardier Learjet 85, the HondaJet, the Spectrum 33 Independence and 44 Freedom. At the other end of the design spectrum are the upcoming designs from Boeing and Airbus. The 787 is revolutionary in its use of composites, pushing the concepts it learned from the use of composites on the 777 program to much broader application on the 787, replacing metallic structure in most of the airframe. Likewise, the A350 design from Airbus will incorporate additional composites as compared to their historical designs, but not to the extent that the 787 will achieve.

In some cases, the primary driver for the use of composites was primarily for weight savings, but often times, especially for new start-up companies, it was to avoid having to spend the capital necessary to set up a shop for metallic part production. Whether or not all of the aircraft above were able to achieve the estimated weight savings due to their composite designs is subject to debate since it is unclear what a similar design from metallic structure would have weighed, and/or how much extra contingency weight was carried in the first published performance numbers for the various aircraft. It is likely however, that these programs did not achieve the hoped for reductions that are dreamed about when people first start discussing the replacement of metallic structures with composite structures.

This report summarizes the materials, fabrication concepts, and technologies related to weight reduction, target weight savings, and risks associated with an advanced structural concept as compared to a baseline metallic structure for a conventional low wing aircraft with a tubular fuselage and aft-mounted engines. Target weight savings are established for both structures and subsystems weight groups. Weight savings in subsystems weight groups are based on a synergistic relationship with a multi-function structures concept or on an assumption of the subsystems state-of-the art in the 2035 time frame. Appendix G provides a detailed review of composite structures technologies and a ranking of these technologies with respect to their value to a 20 passenger airliner that is planned for entry into service in 2035.

6.1.3.1 Technical Approach for Weight Reduction

As described above there are current material systems and fabrication methods that enable the design, development, and manufacture of advanced composite aircraft structures. These current technology materials have also been shown to enable significant weight reductions in the load bearing structure of military aircraft. The technical approach for weight reduction in a 2035 aircraft needs to focus on those issues that have either prevented the use of composite structures in commercial aircraft or prevented these structures from realizing the weight savings that can be claimed from improvements in material strength.

This section discusses the opportunities and challenges in the areas of (1) the application of new, higher strength materials, (2) the selection of fabrication techniques, (3) the impact associated with elevated temperature, wet environments, (4) the need to design for damage tolerance, (5) the benefits of structural health monitoring, and (6) the use of multi-function integration of subsystem functions into the aircraft structure. Each of these technology areas is considered a promising area for weight reduction in a 2035 aircraft.

6.1.3.2 Composite Material Selection & Design Data

6.1.3.2.1 Current Composite Materials Baseline

There are many options when selecting materials for an advanced composite airframe structure. Selection of appropriate matrix systems, fiber types, and product forms requires consideration of data availability, structural needs, cost, manufacturability and reparability concerns. Not only are the primary structural composite materials of concern, but ancillary materials such as surface films, lightning strike protection materials, film and paste adhesives, potting compounds, corrosion protection materials, specialty fasteners, and finishing systems such as primers and topcoat paints must also be carefully considered.

Because it is difficult to predict how the primary structure composite materials developed between now and the program timeframe may improve, first attempt weight estimates where based on using structural materials that are commercially available in the present timeframe with adjustments applied to account for the reductions associated with the challenges presented in the section of this report that deals with technologies for weight reduction. Further improvements over the current weight reduction estimates could be achieved if further material developments in continuous fiber or matrix materials yield better baseline mechanical properties as compared to existing products.

The suggested concept for this effort is to use a commercially available toughened epoxy resin system for the majority of the airframe components. A traditional 350°F curing epoxy is currently being chosen because it allows for continuous use up to 200°F and has significantly improved mechanical properties when limited to use at 160°F. Although other resin systems can be found that cure in the 250°F-270°F range, continuous use at 160°F requires increases in design factors of safety and weight relative to 350°F cure systems.

Supporting materials will be conventional commercial aerospace products compatible with epoxy composite matrix systems and tailored to co-cure or secondary cure operations. Advanced coatings of material are planned for lightning strike protection. A detailed study of coating alternatives is presented in Appendix G. Different configurations of materials may be used in different areas of the aircraft, depending on the thickness of the underlying structure, proximity of underlying systems that need to be protected, and/or zone of the aircraft.

6.1.3.2.2 Application of New Advanced Materials

All new materials need to go through an extensive amount of testing and evaluation prior to their application. Appendix G provides a review of the current industry approach to the development of the material databases that are needed to design, certify, and deliver an aircraft with composite structures. The current approaches to either shared consortium databases or proprietary databases are time consuming and expensive. It should be noted that the NCAMP consortium is developing a shared database for composite materials that were first applied to military aircraft in the late 1980s.

Breakthrough weight reduction based on new materials for aircraft that are delivered in the 2035 time frame will be dependent methods and approaches to the development of material property and design databases. Furthermore, rapid prediction of the characteristic of a new material system at the structural assembly level will facilitate meaningful decisions regarding the selection of a new material system and the associated investment in the design, qualification, and certification databases.

It is recommended that an investment roadmaps be developed for the creation of

1. an industry standard, shared database for generic composite materials that could be applied to parts that are either not load critical or protected from extreme environments
2. new analytical methods and test techniques that enable rapid, low cost development of material properties and design data.

The intent behind these two efforts is to enable multiple aircraft and material manufactures to be able to afford the development of a new material system just prior to or during the development of a new aircraft program. Typically, this means that the new material and design database should take no more than 1 year to develop.

6.1.3.3 Fabrication Techniques

Many of the historical composite aircraft designs such as the Adam Aircraft A500, the Hawker Beechcraft Premier IA and Horizon, the Cessna Corvalis, the Cirrus and Diamond use core stiffened panel designs. Whether reinforced with honeycomb or foam core, the principal is the same, to arrive at a highly stiff structural concept with a minimal amount of weight per square foot of coverage. While this appears to be a best path forward, when consideration is made for all of the concessions and design features that must be added to facilitate attachment of high point loads such as wing and landing gear attachments, systems, secondary structures, and interior components, the benefits of core stiffened construction compared to conventional stringer and frame stiffened concepts are quickly eroded. Additionally, core stiffened structures require a minimum gage of material on the face sheets to prevent excessive impact and/or lightning strike damage from occurring. Further consideration for field repair of core stiffened structures yield further issues that must be dealt with in the design and certification program.

Boeing has chosen a skin, stringer, and frame concept for the 787. Honda utilizes a similar concept for the main sections of the HondaJet fuselage barrel. This fabrication technique has several advantages over core stiffened concepts, in that they are composed of discrete components that can be manufactured, inspected and/or repaired with minimal impact to surrounding structures. While the skill sets necessary to produce the composite elements that comprise the primary structure are specialized, the personnel that will be completing the rest of the aircraft fabrication and system installations will only require a minimum of additional training to learn how to work with composite assemblies.

Based on these concepts, the fabrication concept for this airframe is a conventional stringer and frame stiffened skin configuration rather than a honeycomb sandwich configuration airframe. The tooling concept utilizes single sided female tools for a fuselage that will be split down the length of the aircraft with joints at or near butt line zero. Cure will be through traditional autoclave heat and pressure arrangement utilizing vacuum bag techniques. The skin, stringers, and frames will be constructed using a variety of manufacturing methods that may include hand lay-up, machine placement of tow or slit tape products, resin transfer molding, and/or press curing. Which options will be used for which components will be determined through design optimization and the resulting trade-offs that are made based on weight, cost, manufacturability and other concerns.

Similar to the fuselage, the wing will be of traditional design utilizing skins, stringers, spars, and ribs. Individual detail components will be individually tooled and manufactured prior to final assembly of the wing structure. The wing skins will be laid-up and autoclave cured on female

single sided tooling using vacuum bag techniques. Assembly of the wing structure will consist of a combination of mechanical fasteners and bonding techniques to join the individual components into a consolidated structure.

6.1.3.4 Reduction of Factors for Environmental Concerns

6.1.3.4.1 Current design approaches for environmental concerns

One of the perceived major hurdles in any aircraft design and certification efforts has been the material property reductions due to environment, fatigue, and damage that are used with composite materials as compared to metallic structures. Different methodologies have been used by various companies on different programs, but it is commonplace for knock down factors to be used to compensate for actual material and process variation, fatigue scatter effects as compared to static test data scatter, as well as to offset environmental degradation due to moisture levels and temperature. These knock down factors are multipliers that are used to offset as-computed material allowables for one or more of the listed effects. An example of the use of one of these knock downs would be as follows. If lamina level coupon data showed a drop between room temperature ambient compression strength and elevated temperature wet compression strength of 35%, a full scale test article that is critical in the compression strength case and tested at room temperature ambient conditions would need to pass 135% to offset the reductions for the elevated temperature wet scenario.

More recent qualification efforts through AGATE and NCAMP have brought industry standards of moisture conditioning for wet testing by placing samples in an environmental chamber set at 160°F ± 5°F and 85% ± 5% relative humidity until moisture equilibrium has been reached. While this method has brought standardization into how samples should be conditioned, there are still some questions about how this environment correlates to real world airframe moisture absorption. In real world examples, higher temperature environments tend to have lower humidity levels, making the potential for these extreme exposures highly unlikely.

A more realistic real world scenario might consist of a lower temperature exposure with high humidity, for example, 90°F and 85% RH for an extended period. Studying percent weight gain due to moisture at this environment and comparing it to the equilibrium moisture content levels based on 160°F and 85% RH may provide for a reduced amount of moisture to be seen in a real world structure and could result in even less of a design value reduction for moisture effects.

An additional topic in this area that needs to be further studied and better understood is how moisture uptake occurs in relatively thick composite structures. If it could be shown that through the life cycle of an aircraft, only the outermost layers take on the majority of the moisture and that they do not stay saturated through normal operations that may result in desorption of the moisture, such severe penalties may not need to be applied to the composite material design values.

From a design and certification standpoint, understanding the nature of moisture absorption and desorption relative to relatively thick structures and how changing the conditioning temperature and relative humidity may become a key issue. To date, Fick's Law has most often been used to model moisture uptake in composite structures. Validation of this model relative to moisture levels through the thickness of relatively thick composite structures would be beneficial to design allowable coupon moisture levels moving forward. If it can be shown that a lower percent moisture equilibrium will be attained at real world worst case conditions than at the elevated temperature and humidity conditions that we are using today, there is still an issue with

the significantly longer conditioning times that would be required to condition samples at the lower temperature range. If it could also be shown that the same percentage moisture uptake driven at higher temperatures and humidity would have the same through the thickness moisture levels, then conditioning could be performed faster at these elevated conditions, making sub-element, element or full-scale testing of conditioned test articles more feasible and reducing the need for computed reduction factors which may result in unnecessary conservatism in existing structures.

6.1.3.4.2 Risks with reducing penalties for environmental concerns

Risks associated with reducing knock down factors for composite materials involve not resolving some of the potential differences between conditioning at elevated temperature and humidity vs. long term moisture uptakes at worst case real world temperature and humidity combinations. In the worst case, full structural test articles are designed and tested for certification using an overly conservative combination of temperatures and humidity to shorten the moisture uptake time, but artificially increase the moisture uptake percentages to levels that would never be seen in real world conditions over the life of an airframe. While this does not lead to a safety concern, it does raise the potential of resulting in over designed structures that are heavier than they need to be and result in less efficient airframes and increased fuel burn scenarios.

Even if a more realistic moisture percentage concept can be developed, an accelerated conditions scenario that mimics it will likely be required by OEMs for their certification program timelines. Real world condition at ambient temperatures and worst case humidity levels will require extremely long conditioning programs that will not make the approach feasible to the OEM. It would become more likely that increase load factors would be used on as-fabricated airframe structures, again leading to less than optimally designed structures that are heavier than they need to be in order to meet the certification requirements.

6.1.3.5 Airframe Health Monitoring, Fatigue, and Damage Tolerance

Airframe health monitoring has the potential to reduce or eliminate some current design requirements for fatigue and damage. Regulatory guidance material today dictates that an aircraft have certain fatigue and damage tolerant characteristics. In today's environment, it is typical to discuss damage as falling into the following 5 categories:

- Category 1: Damage consisting of barely visible impact damage and/or allowable manufacturing defects and damage that can be expected and is permissible through typical manufacturing operations. This category would be shown to meet ultimate load requirement of 1.5 times the limit load.
- Category 2: Visible impact damage that would be captured during normal inspection processes and would be repaired at that time. This category may result in failures below ultimate load, but would remain above limit load capability.
- Category 3: Obvious damage that needs to be repaired when found, typically within a few flights of the occurrence that caused it. This category is required to meet limit loads.
- Category 4: Damage caused by a discrete source that would be obvious to the flight crew. This category of damage would result in failure below limit load, but should allow for continued safe flight. Damage in this category would require repair operations to be completed after the flight in which the damage occurred and prior to being placed back into service.

- Category 5: Anomalous damage not considered in design but known to operations. This category of damage requires immediate repair.

Based on these criteria, the airframe manufacturer has to evaluate and make trade-offs on increased utility for the end user vs. optimization and weight reduction in the structure. By assigning larger and larger amounts of damage into the lower categories, the airframe becomes more and more robust, pushing the allowable damage limits and critical damage thresholds higher and higher, but all at the cost of weight. A robust airframe health monitoring system may allow for a reversal in this trend by allowing an airframe design to be optimized by effectively changing how each damage category is defined. Certainly the effect of certain damage types and sizes does not change the airframes ability to meet safety criteria relative to flight, but shifting the focus from regular maintenance inspections and/or obvious visual indications to a system based monitoring and indication system should allow for smaller and smaller defects to be captured and dealt with in a more reliable fashion.

Technologies relative to structural health monitoring to date seem to be revolving around embedded wires or grids to sense local strains, acoustic sensor arrays, and vacuum monitoring systems. Future growth is anticipated in the area of nanotechnology implementation in structural health monitoring, either as secondary embedded strain sensors or potentially as a dual use applications for carbon nanotube reinforced materials. These technologies appear to be progressing at a rate that would allow implementation in the concept aircraft timeframe. What is unclear, and a potential risk, is how much weight can be saved by being able to better monitor airframe health and/or watch damage growth around potential “hot spots” in an airframe design. Initial applications are likely to be limited to new approaches to airframe certification for damage and maintenance inspections.

6.1.3.6 Multi-Functional Structures

Traditional aircraft design has arrived at a mixture of unique single use components being married together to arrive at a functional aircraft end product. An example would be an airframe made of structural members such as skins, stringers, and frames that is then stuffed with ventilation ducting, pneumatic and hydraulic lines, electrical wire bundles, sound and temperature insulation materials, etc. By incorporating dual use materials and/or structural design concepts, significant weight savings may be able to be achieved.

Introduction of these multi-functional structures may bring an undesirable effect of system integration complexity that could lead to functional and/or reliability issues, so it is not an area that should be taken on without significant forethought and planning for worst case scenarios. Some technologies that are under considered for multi-functional integration include the following topics:

- Use of conductive materials integrated into laminates for lightning protection, EMI shielding, ice protection systems
- Use of traditional airframe stiffening structure for acoustic damping by tailoring shapes and spacing
- Use of closed section stiffening elements as ECS air ducts
- Use of thermal and acoustic insulation materials as EMI shielding materials
- Use of select metallic structural components as electrical ground planes for systems installations

- Use of lightning strike protection systems as health monitoring system relative to lightning strikes and/or potential impact events

Further review and development of these integrated, multi-functional structure concepts would be required before they could be considered feasible for the concept aircraft. These tests would include purpose built structures consisting of representative concepts that would be subjected to functional and reliability testing for their intended purposes. Evaluation of these test articles would also include review for unforeseen consequences or issues that might arise from their configuration. An example would include how a lightning strike and any associated repair to the system may negatively impact the ability to use the installation as an airframe health monitoring system. Another example would be to understand the inefficiencies associated with routing air through dual purpose stiffening elements / ducts that are outboard of the thermal insulation systems that are installed inboard of the ducts. A final example would be to understand the structural inefficiencies that might arise from sizing and placement of frames and stiffeners based on acoustic damping criteria. In each of these studies, it is likely that simulation models would need to be developed and confirmed such that future work could be done by simulation outside of the immediate inference space of the test articles.

Multi-functional structures also pose some risks relative to implementation. At first look, multi-functional structures seems like it would be a relatively easy evolution of current design practices, and has potential for significant weight savings in several areas. However, on a more in depth review, the specific requirements of optimum structural design criteria may be in conflict with placement of stringers and frames for acoustic dampening performance, and as such, a delicate balance of the various input parameters would need to be performed. Further implementation of concepts like embedded ductwork using features of existing stringers, frames and skins further complicates the design issues. A further risk of such multi-use integrated structures is in how they may impact field service, inspection and repair of the primary structure or system side of the installations. The complexity of these issues will need to be further researched and investigated through smaller scale development articles to prove out some of the concepts. Development of design optimization software that can tie together inputs from aerodynamic models, structural member models, acoustic models, and space management models for routing of systems, ducts, cabling, etc. with associated output parameters may be required for realistic best case design scenarios to be arrived at.

6.1.3.7 2035 Concept Airframe

A 2035 concept vehicle may take advantage of advanced structures and systems technology to save 33% in empty weight. From a structures perspective, approximately 22% in empty weight savings is a result of (1) the use of a frame and stringer stiffened shell structure to simplify the integration and installation of subsystem components, (2) the use of advanced coating materials to protect against lightning strikes and electromagnetic interference, (3) the use of a protective and health monitoring external skin, and (4) the integration if ice protection, environmental control system air ducts, and antennas into the protective skin. Careful design of the protective external skin eliminates the need the paint, thermal, and acoustic damping materials used in current technology aircraft. This protective skin is intended to absorb impact damage, distribute the current of a lightning strike, reflect electromagnetic energy, and limit the negative impact of atmospheric heat and moisture on the load caring capability of the primary structure. An additional 11% in sub-systems weight is a combination of observed weight reductions in current avionics and electrical systems and an assumed reduction in sub-system component weight as results of continued development of and transition to electrical systems.

Figure 170 and Figure 171 show the new concept for a protective outer skin. For a current technology composite aircraft the size of the B20 (see left half of Figure 170) 952 lbs is accounts for

- some protection against impact damage,
- material used to increase strength in hot and wet environments,
- fill, fair, prime and paint materials,
- lightning strike protection materials,
- acoustic damping, and
- thermal insulation.

Typical polymer (Mylar) film weights are 0.15 to 0.30 lb/ft^2 and current technology foam weights are 0.125 to 0.25 lb/ft2. With these assumptions and the wetted area of the B20, the novel protective skin in the right half of Figure 170 will weight approximately 371 lbs. This leads to a savings of 581 lbs caused mostly by the elimination of everything in the above list except acoustic damping and thermal insulation. It is reasonable to assume a future external layer of foam and film could protect against both lightning and EMI, since typical acoustic treatment materials are already include a layer of aluminum foil. Even if some of the weight savings is eliminated when considering protection against impact damage a layer that reflects sunlight and seals out moisture is bound to reduce the impact of hot and wet environments on material strength.

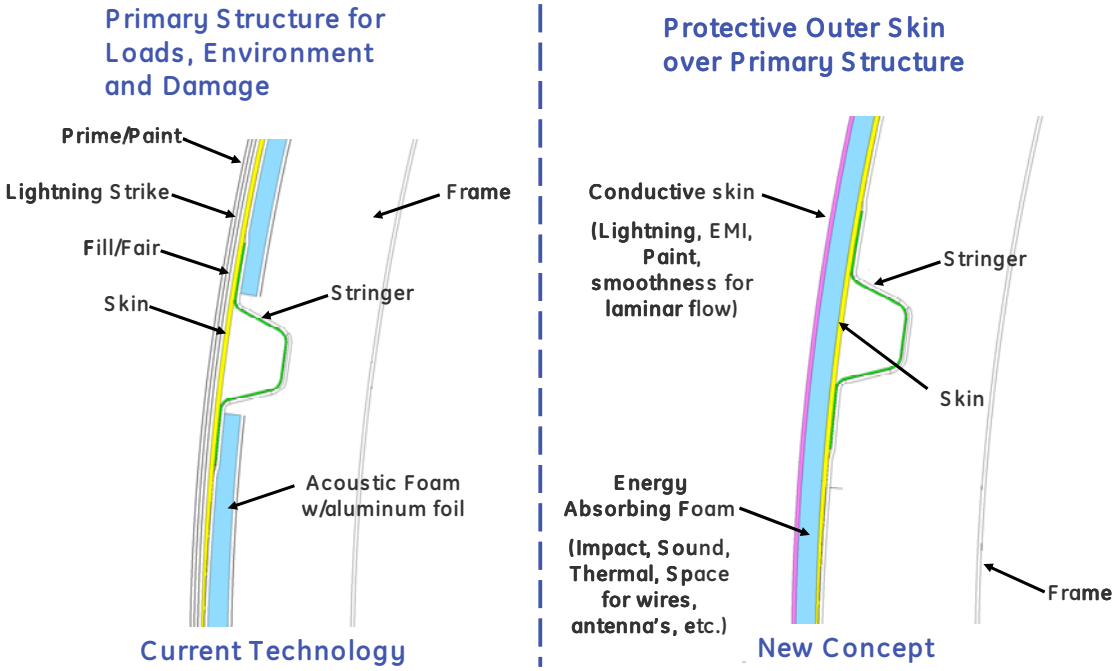

Figure 112. Protective Outer Skin in Advanced Composite Structure

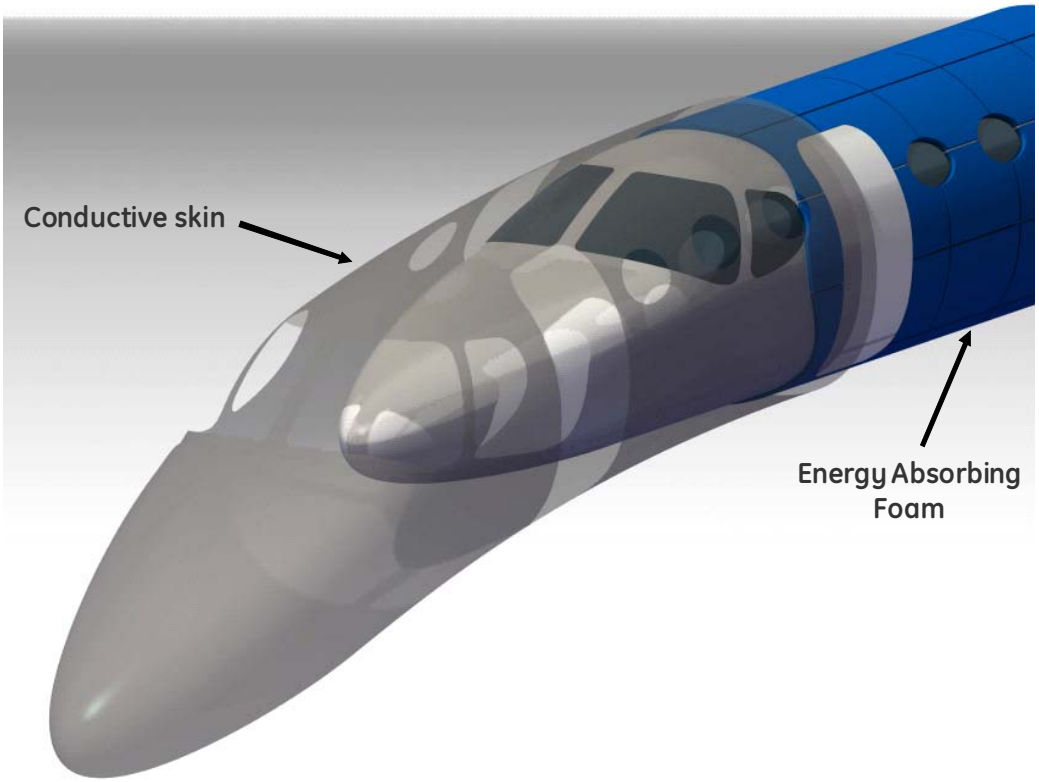

Figure 113. Energy Absorbing Foam and Conductive Film Provide Protective Coating

With careful design this external protective skin will show visible damage as a result of impacts that force repairs in current technology aluminum structure without impacting the primary structure's ability to support flight loads. This visible damage forces a repair of the external protective skin and an inspection of the primary structure. An active health monitoring system attached to the primary structure could facilitate this inspection and measure the temperature and moisture content of the structure. Knowledge of the moisture and temperature of the structure could be used to limit flight speeds and the associated loads or to force a maintenance procedure to dry and cool the structure.

6.1.3.8 Target Structure and Systems Weight Savings

Composite airframe structures have always provided a material strength that enables significant reductions in the weight and complicates the integration of subsystems. The complications typically show up in the requirement to protect the aircraft from lightning, to protect aircraft electronics from electromagnetic interference (EMI), in the establishment of an electrical ground plane, and in the installation of system components. A core-stiffened composite structure provides few, if any, places for fastening components or for transferring actuator or component loads into the structure. Core-stiffened composite structures also require unique acoustic treatment to ensure a quiet cabin.

Table 39 quantifies these challenges in a notional aircraft certified in 2010, but based on materials and technologies available from 1990 through 2005. It is common for current day commercial composite aircraft to show little, if any, reduction in aircraft empty weight.

Table 39. Roadmap for Weight in Advanced Airframes

Aircraft Weight Groups	% of B-20 Empty Weight	2010 Composite Aircraft - Materials from 2000s	2015-2020 Composite Aircraft - Materials from 2010s	2030-2035 Composite Aircraft - Materials from 2020s	Technical Approach to 2035 Aircraft
Wing	15.60%	30.00%	35.00%	39.20%	New conductive skin reduces risk & supports accoustic, thermal, and some ice protection functions
Tail	5.16%	30.00%	35.00%	44.00%	
Fuselage	24.16%	25.00%	30.00%	34.00%	
Propulsion	18.98%	0.00%	0.00%	29.67%	Advanced engines reduce weight & fuel burn
Landing Gear	5.49%	0.00%	0.00%	15.00%	Systems, landing gear, & nacelles benefit from transition to electric systems, application of new materials, and optimized integration & installation concepts
Nacelle & Air Induction	2.71%	0.00%	0.00%	20.00%	
Surface Controls	1.88%	-15.00%	0.00%	15.00%	
Hydraulics	1.28%	-15.00%	0.00%	100%	
Electrical	5.41%	-35.00%	0.00%	15.00%	
Avionics and Instruments	3.95%	-35.00%	30.00%	60.00%	Avionics & instruments benefit from panel mount integration & continued breakthroughs in commercial electronics
Furnishings & Equip	10.48%	-60.00%	0.00%	29.19%	Some functions for accoustic damping, thermal insullation, ice protection, & paint moved to wing, tail, and fuselage weight groups (New Conductive Skin)
Air-conditioning & Anti-Ice	4.06%	-15.00%	0.00%	26.34%	
Paint	1.12%	0.00%	0.00%	100%	
Total % Savings	**0**	**1.60%**	**15.47%**	**33.11%**	
Risk	Application of aluminum structure & system integration technology	Application of current composite & system integration technology	Improved Materials, EMI, Lightning, & Sys. Integration	Conductive, Protective, & Health Monitoring Skin	

A 2015-2020 commercial aircraft based on materials from 2005 – 2015, integrally stiffened structures that simplify system installations, and conductive coatings to reduce the penalties associated with EMI, Lightning, and the requirement for an electrical ground plane is presented in column 4 of Table 39.

This aircraft solves most of the systems integration challenges present in current technology aircraft and enables approximately 15% reduction in overall aircraft empty weight. It should be noted that both the current day and the 2015-2020 composite aircraft experience a benefit of 30-35% reduction in the weight of load bearing structure.

To accomplish the 33% savings in aircraft empty weight necessary to meet NASA's goal of a 70% reduction in fuel burn a novel protective outer skin is used (1) to protect the aircraft from EMI, and lightning, (2) to provide energy absorbing protection and passive health monitoring for the primary structure, (3) to eliminate the need for paint while ensuring the smooth surface necessary for the maintenance of laminar flow, and (4) to simplify the integration of ice protection, antennas and other systems into the surface of the aircraft.

Table 39 also shows that this 2035 vehicle depends on an advanced propulsion system and the weight reductions associated with the miniaturization and integration of electronics. Since the protective outer skin also provides the acoustic damping and thermal protection functions, these weights are eliminated from the furnishings and equipment group. An active gust-load alleviation system is also intended to improve ride quality and mitigate the risk of achieving

weight reductions in the lifting-surface weight groups. A 10-15% reduction in subsystem component weights is based on (1) continued industry development of and transition to electrical systems and (2) continued use of light weight materials in these components.

6.1.4 Advanced Reference Aircraft Mission and Technology Sensitivities

The B-20 baseline airliner with current technology has been developed, and investigations have been conducted into potential technologies in air vehicle configuration and systems, engine and propulsion system, aerodynamics, and structures. The next step is a parametric approach which uses estimates from the technologies reviewed to determine that the mission parameters are still a good match with the anticipated new technology configuration and to determine the sensitivities of the B-20 to the relative effects of the technologies. The team took two approaches to the sensitivity studies: Georgia Tech used their FLOPS models and data to develop a parametric environment which allowed rapid investigation of sensitivities while the Cessna team used MAPS to run point optimizations for each of the conditions. Both teams used minimum mission fuel as their figure of merit. The two approaches and their results will be described in this section.

Technologies studied include an advanced turbofan engine, 60% laminar flow on the fuselage, wing, horizontal tail, and vertical tail, and 24% empty weight reduction. Before applying the technologies, Cessna also conducted a study of the sensitivity of the B-20 to mission parameters of design range, cruise altitude, cruise speed, number of passengers, and propulsive efficiency (engine weight and Thrust Specific Fuel Consumption). Both teams used minimum mission fuel as their figure of merit. The two approaches and their results will be presented in the following sections section.

6.1.4.1 B-20 High Lift Considerations

Before beginning to investigate sensitivities, the team needed to determine a strategy for dealing with high lift. Figure 114 shows the level of achieved maximum lift coefficient for various high lift systems. Initial studies showed that flaps only or flaps and slats high lift technology would be sufficient for a 20-passenger airliner. There is no need for investigation and development of advanced high lift technologies such as blown flaps or wing morphing to meet the NASA field length requirements for this class of aircraft.

Initially the baseline B-20 was designed with plain flaps which yield moderate maximum lift coefficients; the baseline B-20 had a BFL of 4,000 ft with a relatively low C_{Lmax} of 1.685 (based on the nominal C_{Lmax} of the Cessna Citation Sovereign which has plain flaps). BFL was an active constraint in the optimization, and performance was compromised since top of climb and cruise performance may not have been at their optimum values. As a reminder, the BFL calculation for this level of analysis fidelity is:

$$BFL = \frac{34.71(W/S)}{C_{L_{\max}}(T/W - 0.05)}$$

Increasing C_{Lmax} to 2.45, representative of slats and double slotted flaps as shown in Figure 114, reduces the BFL for the B-20 to 2,754 ft. In order to eliminate BFL as a constraint and an impact on sizing during the sensitivity studies, C_{Lmax}=2.45 was used for all of the sensitivity studies. All BFL's shown in this following section, in the section on sensitivities the 2035 Final Configuration, and in the One-Off Technology sections will be based on 2.45. However, the

BFL for the final 2035 Configuration is based on C_{Lmax} of 1.685. This means that the wing will be aerodynamically clean, and there will most likely be no noise penalty in the flaps deployed configuration.

If a condition arises where the BFL is greater than 4,000 ft with plain flaps, two options can be employed: 1) increase C_{Lmax} by using a more complex high lift system and suffer a noise penalty; or 2) increase the wing size and suffer a slight performance penalty. In future work, attention must be paid to the details of wing, high lift system, and noise integration and trades.

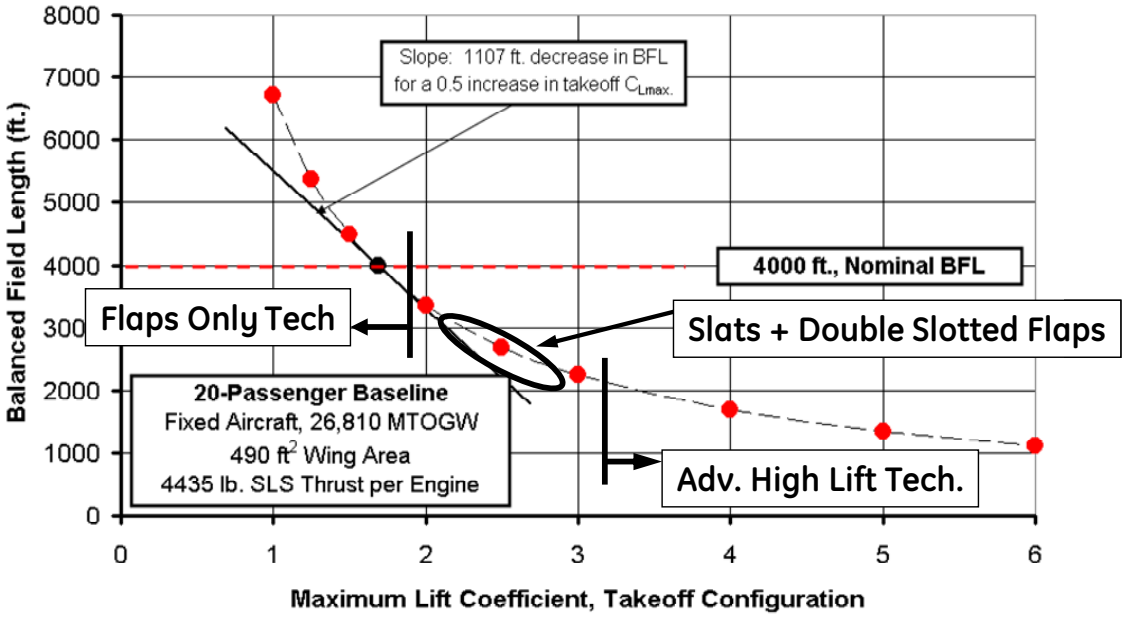

Figure 114. High Lift Technology Impact on Balanced Field Length

6.1.4.2 Parametric Analysis

The Georgia Tech team developed a FLOPS model of the baseline aircraft, referred to as the B-20, and used it to generate a parametric analysis environment. This parametric environment was meant to facilitate rapid trade studies of the entire design space around the notional B-20, allowing the researchers to quickly assess the impact of notional technologies. In addition, the environment allows the investigation of geometric trades on the aircraft, as well as nominal changes in mission and performance.

6.1.4.2.1 Methodology

The parametric environment was built using the Design Space Exploration process, shown in Figure 115. The DSE process uses a Design of Experiments formulation to facilitate the creation and implementation of surrogate models. Surrogate models are, in effect, models of a model. They allow the statistical capture of most, if not all, significant effects of a more complex model. Because surrogate models are in the form of equations, they may be easily manipulated for optimization and analysis.

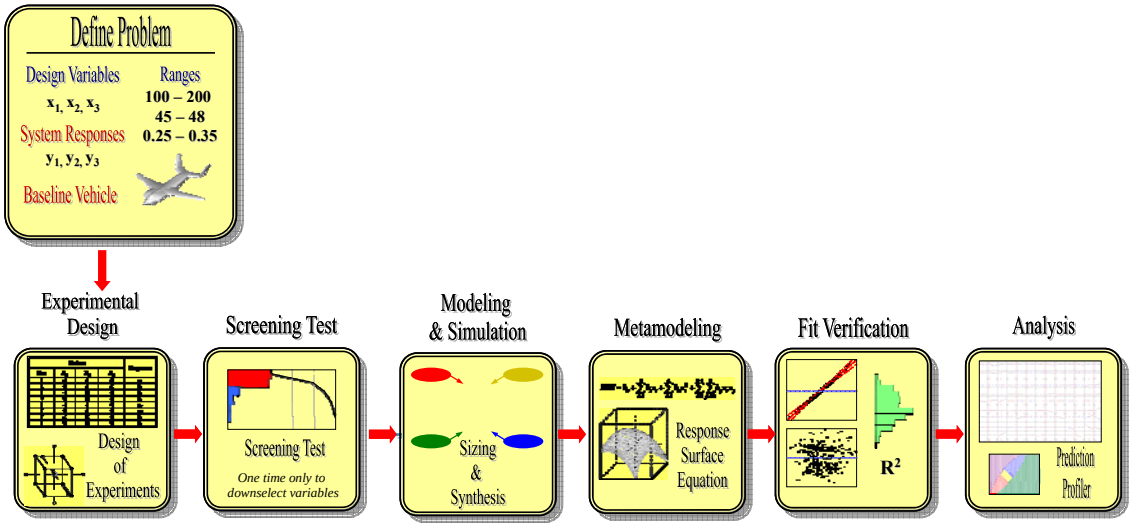

Figure 115. Creation Methodology for Parametric Environment

The first step in the DSE process is to define the problem, which involves defining the dimensions and range of the problem. Then, the baseline, around which the parametric space is to be constructed, is established. In this case the configuration around which the perturbations take place is the B20 baseline. The number of dimensions of the problem is defined by the actual variables that comprise the study. These variables are typically those parameters that the analyst or designer has control over. For example, “wing aspect ratio” is a typical geometric variable. The parametric space is defined by the ranges associated with each of the variables. Finally, the last aspect of defining the problem is to identify the metrics or responses of interest, which are the outputs of the simulation program. These outputs are usually the key analysis metrics associated with the aircraft, such as “takeoff gross weight” or “mission fuel burn”.

A Design of Experiments (DoE) is then chosen to represent the problem. A DoE is a subset of a full factorial combination of variables that imposes as much orthogonality (and thus variable effect independence) as possible. For this study, a Latin Hypercube with space filling technique is used to generate the DoE, which is used to create the input files to the sizing and synthesis code, FLOPS. The metrics/outputs are then parsed and stored for each case of the DoE. The resulting dataset is then used to train an artificial neural net (ANN) to best capture the non-linear space. Part of the resulting dataset is reserved to perform model representation tests. Rigorous statistical analysis is performed to ensure that the resulting surrogate models are adequate to approximate the non-linear parametric space. For instants, model fit error (MFE) is calculated in terms of standard deviation to determine how well does the ANN predicts the points that are used in its training. A good MFE is a standard deviation under 1. Another more conclusive test to perform to determine the “goodness” of a surrogate is to calculate the model representation error (MRE), also expressed in terms of standard deviation. The MRE measures how well the ANN predicts points that were not used in its training. Again, a good MRE is a standard deviation under 1.

6.1.4.2.2 Creating the Baseline Parametric Environment

The methodology described above was used to create a parametric environment around the B20 configuration described baseline aircraft definition. The variables and ranges chosen for this study are shown in Table 40. Thrust to weight ratio (TWR) and wing loading (WSR) were chosen as variables to examine the vehicle design space. Design range was chosen as a mission level variable along with cruise Mach number and cruise altitude. Geometric variables of interest included wing aspect ratio, wing sweep, and fuselage length. Fuselage length was used to estimate a first order impact of number of passengers. "Cd Subsonic" parameter was used to assess notional aerodynamic technologies. To model improvements in engine technology, a fuel flow factor (FACT) and an engine weight technology factor (WPMSC) were used. The weight technology factors were determined by using weight reduction goals provided by Cessna. Normally, the parametric environment would include variables for propulsion system design, however, since GE is responsible for all propulsion system modeling, the environment is constructed around a specific GE engine design characterized by its engine performance deck, engine weight, diameter, and length. The scaling laws for engine performance, weight, diameter, and length as the vehicle grows and shrinks in the synthesis and sizing process were provided by GE, and modifications were made to FLOPS to accommodate these new scaling relationships.

Table 40. Variables for Creating Baseline Parametric Environment

	INPUTS	Var Name	Low	High
	Wing Loading	WSR	50	95
	Thrust to Weight	TWR	0.28	0.45
Geo	Fuselage Length	XL	0%	20%
Geo	Aspect Ratio	AR	5	10
Geo	Wing Sweep	SWEEP	0	20
Geo	Max Nacelle Diameter	DNAC	-10%	10%
Geo	Max Nacelle Length	XNAC	-10%	10%
Aero	Cd subsonic	FCDSUB	0.86275	1.09275
Mission	Maximum Cruise Altitude	CRALT	25000	42000
Mission	Maximum Cruise Mach	VCMN	0.5	0.69
Mission	Range	DESRNG	720	880
Prop	Fuel Flow Factor subsonic	FACT	-10%	15%
Tech	Engine Wt Technology Factor	WPMSC	-400	400
Tech	Wt wing	FRWI	-35%	5%
Tech	Fuselage Weight	FRFU	-30%	5%
Tech	Horizontal Tail Weight	FRHT	-35%	5%
Tech	Vertical Tail Weight	FRVT	-35%	5%
Tech	Nacelles and/or Air Induction	FRNA	-10%	5%
Tech	Surface Controls Weight	FRSC	-10%	5%
Tech	Electrical Controls Weight	WELEC	-50%	5%
Tech	Weight Avionics	WAVONC	-5%	5%
Tech	Furnishings Weight	WFURN	-10%	5%
Tech	Air Conditioning Weight	WAC	-20%	5%

The responses/metrics chosen for this study are shown in Table 41. The three primary aircraft weights (takeoff gross, operating empty, and fuel) are tracked. In addition, takeoff and landing field lengths are noted. Engine thrust, engine scale factor, and wing area are tracked as a convenience, linking to the thrust to weight ratio and wing loading inputs. Note that in this particular environment, there is no capability to calculate noise or emissions; therefore, guidance provided by this parametric environment can only be from the fuel burn perspective.

Table 41. Outputs for Baseline Parametric Environment

OUTPUTS
Takeoff Gross Weight
Fuel Weight
Operating Empty Weight
Reserve Fuel
Takeoff Field Length
Landing Field Length
Engine Thrust
Engine Scale Factor
Wing Area

The B-20 aircraft was modeled in FLOPS and calibrated to match Cessna's baseline as closely as possible. As indicated before, a space-filling Latin Hypercube design of experiments was then created, resulting in roughly 6000 simulations cases being conducted in FLOPS. The outputs were then parsed from each run, and a neural net trained. The resulting neural net surrogate models are used to create the parametric environment shown in Figure 116.

This interactive environment allows the user to manipulate the variables in real time, by either typing in a desired value (of, say, fuselage length) or by simply moving the hairlines to the correct value. All outputs are then updated in real time, as are the slopes of the lines that indicate the relationships between the input variables and the outputs. In this way, the user can very quickly conduct trade studies, as well as rapidly assess the impact of design variable changes.

The interactive environment was primarily used by the team to assess the likelihood of meeting NASA goals, using extrapolated evolutionary technology gains. For example, the Cessna members of the team provided weight goals for the 2035 timeframe that they believed to be realistic, given the current state of technology and extrapolating forward. By including these weight goals as variables in the parametric environment, the team could get a very quick feel for the impact of these weight savings on the overall vehicle. More importantly, the team could quickly assess the first order effects of combining technologies, such as weight savings as well as a reduction in subsonic drag. The impact of changing wing loading and thrust to weight ratio of the vehicle is also visually depicted in order to guide the team to appropriately selecting them to minimize a particular metric or response. Since mission parameters, such as cruise Mach number, cruise altitude, and design range, are also included as parametric variables, one can clearly see how these variables affect fuel weight, for example.

Since one of the NASA goals is to achieve a 70% reduction in fuel burn, fuel weight becomes an obvious metric/response to focus. The idea is to inspect Figure 116 to identify technology factors that would reduce fuel weight. These technology factors are the variables in Table 40 with the label "TECH". Among the technology factors, the reducing the fuselage and

wing weight factors provides the greatest benefit of reducing fuel weight, followed by electrical and furnishing weight factors. Therefore, the team is recommended to investigate technologies to reduce weight in the fuselage, wing, electrical system, and furnishings.

Examining Figure 116 one can also gain insight into impact of vehicle sizing parameters, thrust to weight ratio and wing loading. For the B20 baseline configuration with the baseline turbofan engine, lower vehicle thrust to weight ratio and lower wing loading will result in reduced fuel weight. Finally, examining the impact of mission parameters, cruise Mach number and cruise altitude, on fuel weight indicates that for this combination of airframe and engine, a cruising altitude around 40,000 ft and cruise Mach above 0.6 will result in a more favorable fuel burn.

A similar approach was taken to create another parametric environment around the B-20 with an advanced reference turbofan provided by the GE members of the team. A third parametric environment was also created using the same advanced turbofan in combination with an advanced airframe consisting of component weight reduction and laminar flow. All three parametric environments were examined and the trends discuss above did not change.

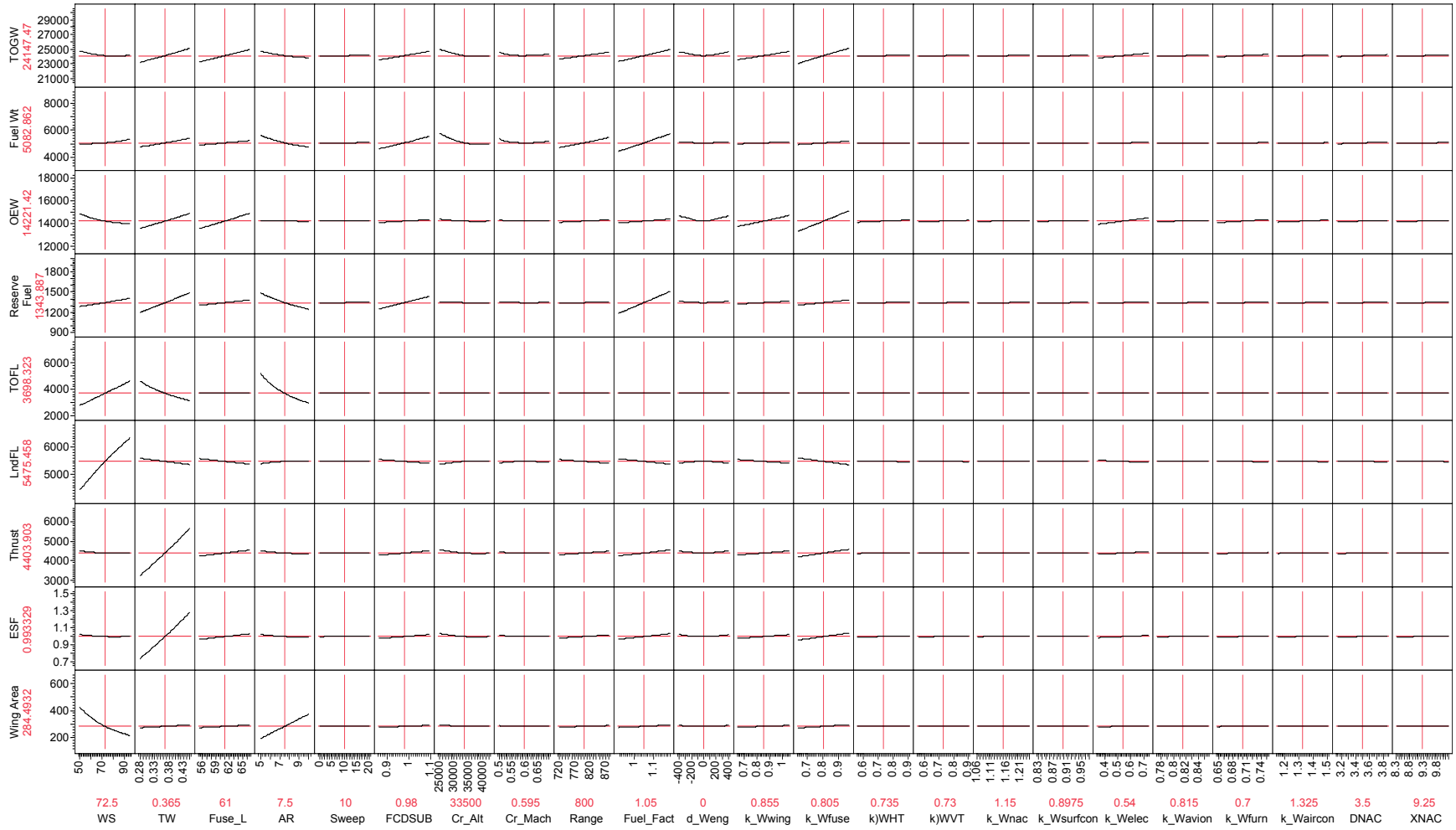

Figure 116. Prediction Profile Parametric Environment for B-20

6.1.4.3 Point Optimization Technology Sensitivities

The Cessna approach to optimization was to define a matrix of conditions of interest and run detailed optimizations at each of those points using a Model Center wrapper with Cessna's MAPS genetic algorithm optimizer. All sensitivities represent the results of an aircraft sizing optimization with the objective to minimize the sum of maximum takeoff gross weight plus mission fuel. The design variables for this optimization are wing area, sea level engine thrust, and available fuel. Constraints are placed on cruise speed, cruise altitude, and balanced field length. This approach enables the comparison of "optimum" aircraft that correspond to either technology assumptions or mission constraint parameters.

6.1.4.3.1 B-20 Mission/Payload Sensitivities

Payload and mission sensitivities are explored by re-optimizing the B-20 with different mission requirements or constraints. Variations in the required range, the cruise speed, the cruise altitude, and the number of passengers are presented. For all of these mission/payload sensitivity cases, C_{Lmax}=1.685 and the BFL constraint is active. Examination of the change in range to changes in engine weight and thrust specific fuel consumption for a fixed configuration without resizing was also examined.

The change in mission fuel as a function of range is shown in Figure 117. The dashed line represents the mission fuel for a configuration resized to meet the corresponding range. The solid line represents the mission fuel required when the baseline B-20 flies the reduced range. The relationships are nearly linear. Resizing the B-20 results in a 6.3% decrease in the mission fuel required for 200 nm range compared to the baseline B-20 with sufficient fuel to go only the 200 nm plus reserves (a difference of 76 lbs).

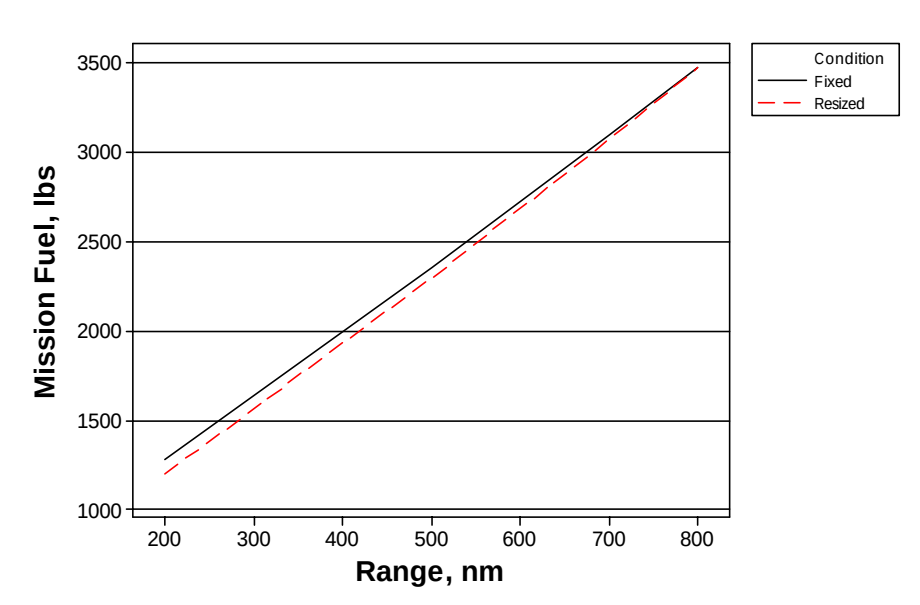

Figure 117. B-20 Sensitivity to Range

The sensitivity of the B-20 mission fuel to cruise altitude is shown in Figure 118. The minimum mission fuel is around 40,000 ft cruise altitude, consistent with the Georgia Tech results. One of the limitations of MAPS is that cruise altitudes are restricted to odd thousands of

feet (such as 39,000 ft or 41,000 ft). A cruise altitude of somewhere between 39,000 ft and 41,000 ft will minimize mission fuel.

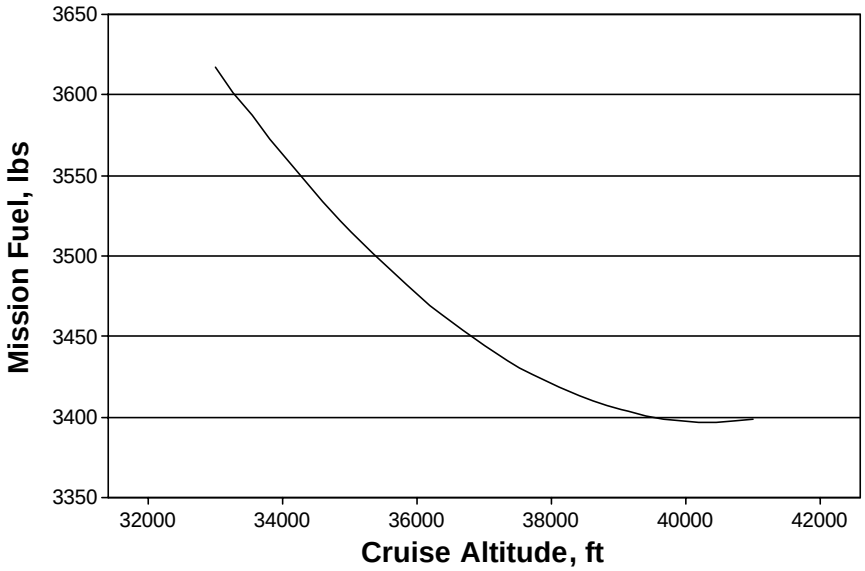

Figure 118. B-20 Mission Fuel Sensitivity to Cruise Altitude

Figure 119 shows the sensitivity of the B-20 mission fuel to cruise speed. The minimum fuel burned occurs at Mach 0.6; much above Mach 0.6 the fuel burned increases rapidly due to increases in compressibility drag. Below Mach 0.6 the mission fuel also increases because even though the fuel flow rate decreases with decreasing Mach number, the extra time spent flying the mission overcomes the fuel flow reduction.

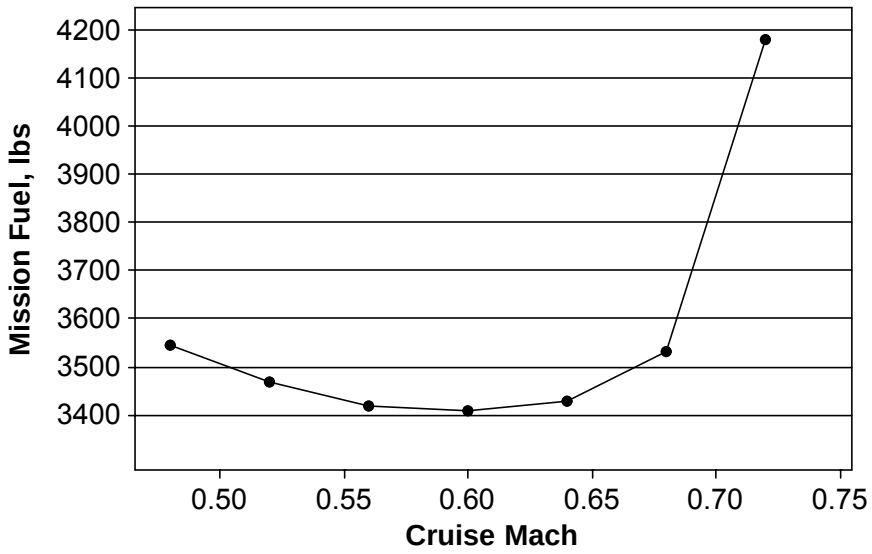

Figure 119. B-20 Mission Fuel Sensitivity to Cruise Speed

The B-20 was resized for 29 and 38 passengers by adding three and six additional rows of seats, respectively, as shown in Figure 120. Each configuration was optimized for minimum fuel. A summary of the results is shown in Table 42. Adding a passenger adds 241 lbs to the payload (195 lb passenger with 30 lbs checked baggage and 16 lbs of carry-on baggage). The resulting increase in MTOGW is about 700 lbs per passenger and the increase in mission fuel is about 75 lbs per passenger to maintain the 800 nm range and meet the other design requirements and constraints. Virtually constant thrust and wing area per passenger must be added to allow the configurations to meet the requirements.

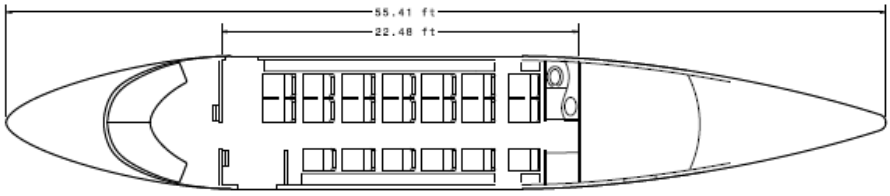

20 Passenger Floor Plan

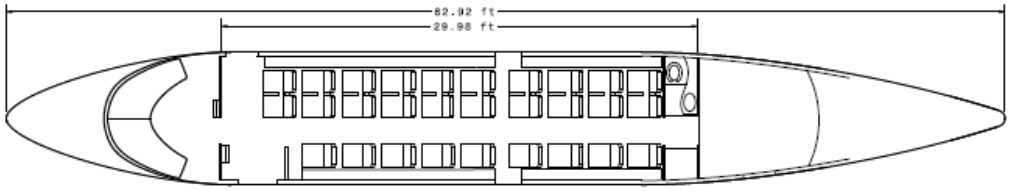

29 Passenger Floor Plan

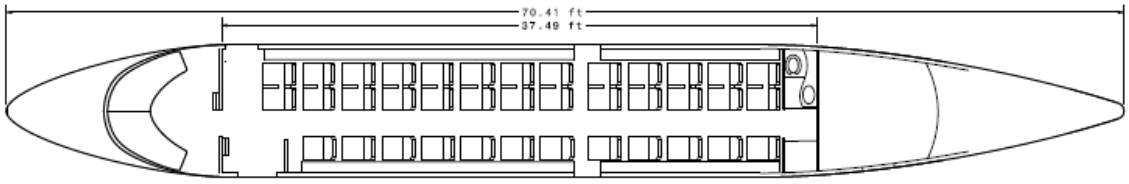

38 Passenger Floor Plan

Figure 120. 20-, 29-, and 38-Passenger Airliner Layouts

Table 42. B-20 Sensitivity to Number of Passengers

Parameter	From 20 to 29 passenger	From 29 to 38 passenger	From 20 to 38 passenger
Δ MTOGW, lb/pass	688	703	696
Δ Mission Fuel, lb/pass	65	69	67
Δ Thrust, lb/pass	116	116	116
Δ Wing Area, sq ft/pass	12	13	13

In order to investigate the sensitivity of the B-20 to changes in engine weight and engine efficiency (as measured by Thrust Specific Fuel Consumption or TSFC), the baseline B-20 was run as a fixed configuration with fixed MTOGW, fixed empty weight (except for the varying engine weight), and fixed engine performance (resizing to meet the 800 nm mission did not take place). An engine weight factor (which equates directly to a reduction or increase in the weight of the engines) was run between 0.75 (engines weigh 25% less than the baseline engines) and 1.05 (engines 5% heavier than the baseline engine). The total engine weight savings at each weight reduction was added completely back as pounds of additional fuel, with a resulting increase in range; the amounts of fuel considered here could be accommodated in the existing wing fuel tanks and did not result in any penalties for additional fuel tanks in the fuselage. Similarly, engine weights increases reduced the amount of fuel available on a pound for pound basis with a resulting decrease in range.

The TSFC was varied between 0.75 (the engines burn 25% less fuel at all points to generate the same thrust as the baseline engines) and 1.05 (the engines burn 5% more fuel at all points to generate the same thrust as the baseline engines). The modified TSFC also applied to calculation of the reserve fuel required. The improved fuel efficiencies resulted in increases in range while the fuel efficiency degradation resulted in a decrease in range.

The results of the propulsion sensitivity study are shown in Figure 121, Figure 122, and Figure 123. The effects of reductions in TSFC have a larger impact on range than the same percentage reductions in engine weights. For example, as shown in Figure 121 with the TSFC held constant, a 100 lb decrease in engine weights (4.8% decrease) results in a 3.9% increase in range (from 800 nm to 831 nm). Figure 122 shows that a 5% decrease in TSFC results in a 9.1% increase in range (from 800 nm to 873 nm). Contours of constant range for varying engine weights and TSFC are shown in Figure 123. The steep slope of the contour lines shows once again that percentage changes in TSFC have about double the impact of the same percentage changes in engine weights. These percentage changes for both engine weights and TSFC cover wide ranges and do not match the ease of achieving or physical reality, but do serve the purpose of showing the sensitivity of the B-20 changes in the parameters.

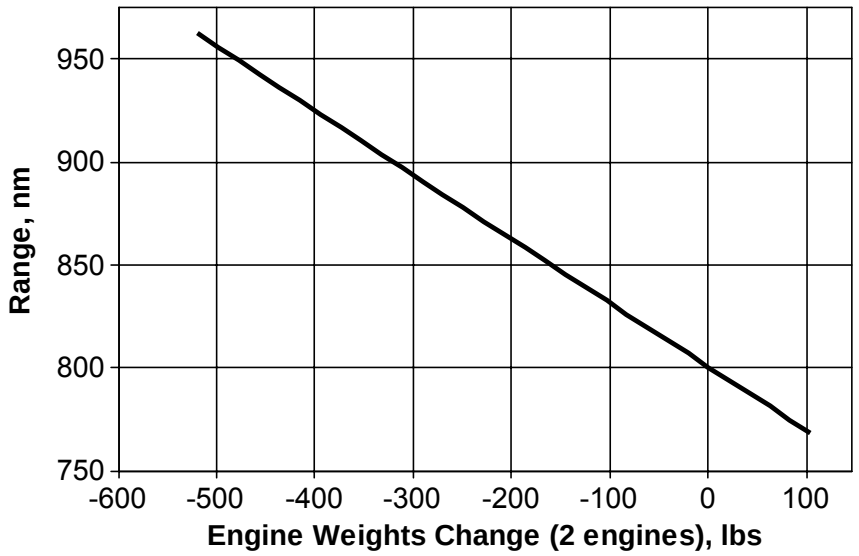

Figure 121. B-20 Sensitivity of Range to Change in Engine Weights (TSFC Constant)

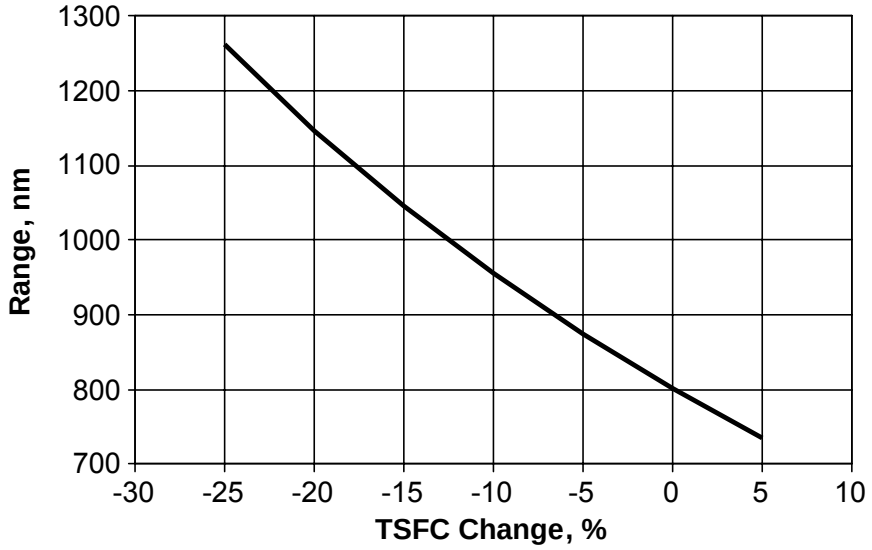

Figure 122. B-20 Sensitivity of Range to Change in TSFC (Engine Weights Constant)

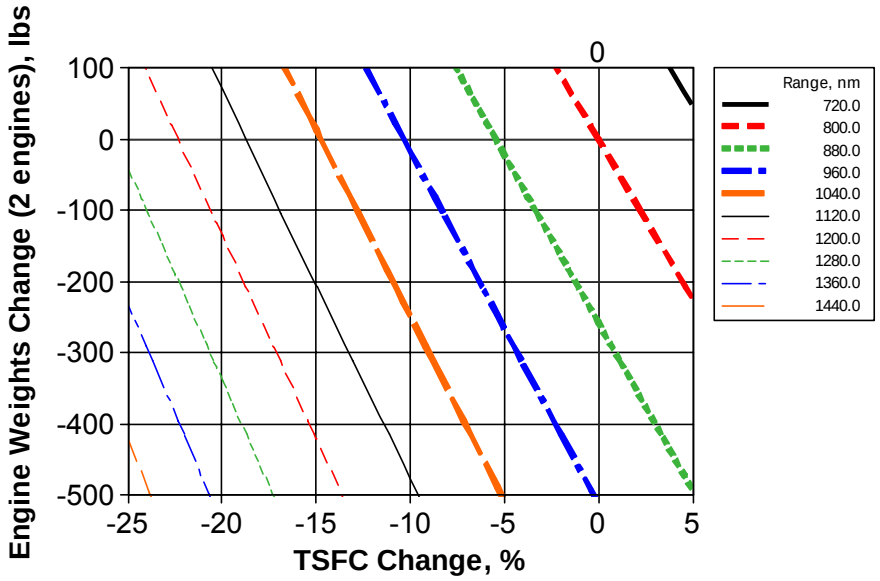

Figure 123. B-20 Range Sensitivity to Changes in Engine Weights and TSFC

6.1.4.3.2 B-20 Advanced Reference Aircraft Sensitivity to Cruise Mach Number

A hypothesized set of new technologies was applied to the B-20 to determine the sensitivity of the configuration to the mission requirements cruise Mach number and cruise altitude. These technologies included an advanced technology turbofan engine, achievement of laminar flow 60% of the distance aft on the fuselage, wing, and tails, and 24% reduction in empty weight. Mach numbers of 0.5 and 0.6 and 0.6 were examined. Cruise altitudes of 25,000 ft, 33,000 ft, and 41,000 ft were also examined. The graphs in this section are all looks at different characteristics of the resulting seven configurations when optimized to meet the B-20 requirements.

The mission fuel for the baseline B-20 and for the B-20 with the new technologies described above optimized for Mach 0.5 and 0.6 at 25,000 ft, 33,000 ft, and 41,000 ft is shown in Figure 124. The results for the M 0.5 and M 0.6 cruise Mach numbers are nearly identical. The minimum fuel burned appears to be around 41,000 ft and Mach 0.6. This is confirmed in Figure 125 which shows the percent reduction in mission fuel compared to the B-20 baseline. All of the configurations are short of the NASA goal of 70% reduction in fuel burned, but do show reductions between 50% and 60%. The resolution of Figure 125 is sufficient to see that the Mach 0.6, 41,000 ft design is still the right choice when advanced technologies are applied.

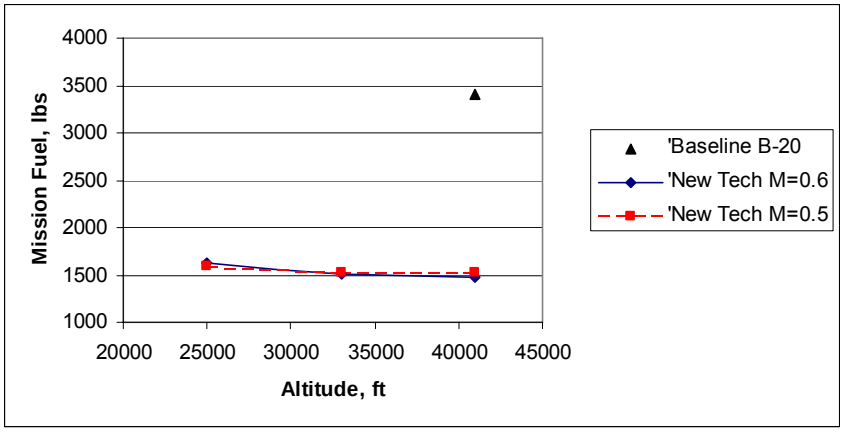

Figure 124. B-20 Turbofan with Advanced Technologies Mission Fuel Sensitivity to Cruise Mach Number and Altitude

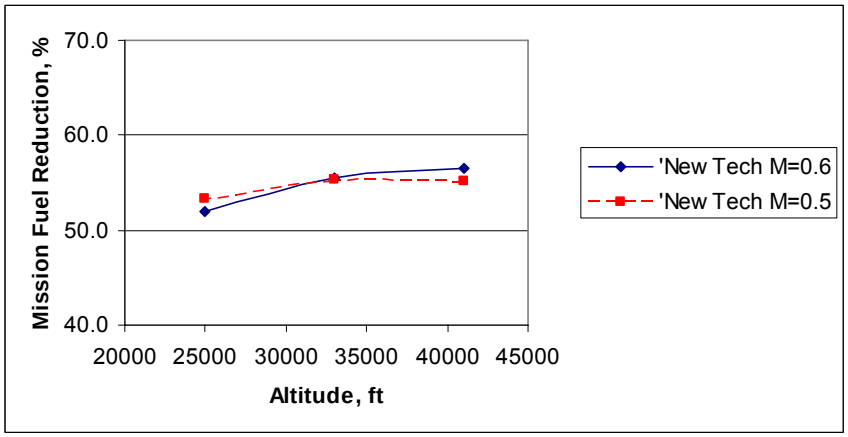

Figure 125. B-20 Turbofan with Advanced Technologies Mission Fuel Reduction Compared to Baseline B-20

Figure 126 shows the sensitivity of MTOGW of the B-20 to changes in cruise Mach number and cruise altitude. The MTOGW is less for the Mach 0.6 cases. The 25,000 ft cruise altitude at Mach 0.6 has the lowest MTOGW. Minimum MTOGW is not an objective for the NASA N+3 activities.

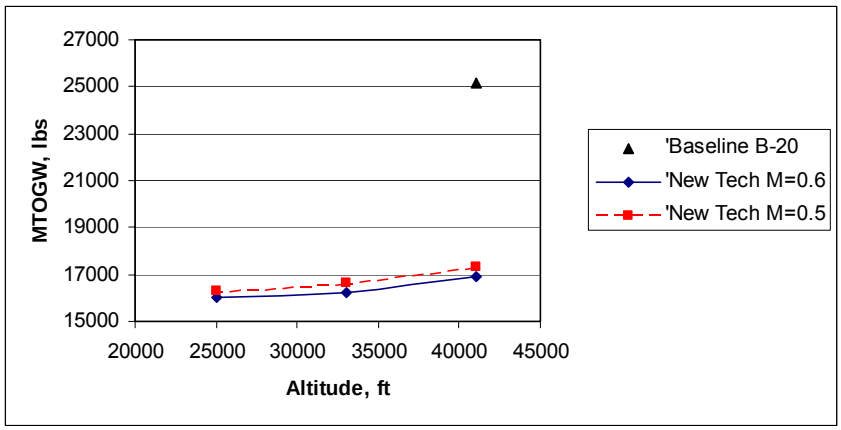

Figure 126. B-20 Turbofan with Advanced Technologies MTOGW Sensitivity to Cruise Mach Number and Altitude

The sensitivity of Basic Operating Weight (BOW) of the B-20 with advanced technologies to cruise Mach number and cruise altitude is shown in Figure 127. Similar to MTOGW, the Mach 0.6 cases have lower BOW than the Mach 0.5 cases while the 25,000 ft cruise altitude at Mach 0.6 has the lowest BOW.

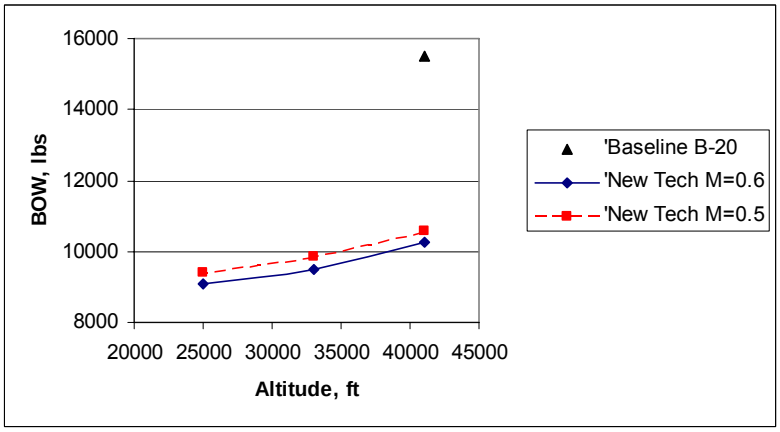

Figure 127. B-20 Turbofan with Advanced Technologies BOW Sensitivity to Cruise Mach Number and Altitude

Figure 128 shows the sensitivity of reserve fuel for the B-20 with advanced technologies configuration to cruise Mach number and altitude. In these cases, the reserve fuel is set at 28% of mission fuel, so, like the mission fuel, the difference due to cruise Mach number is very small. Also like before, the 41,000 ft case has the smallest reserve fuel.

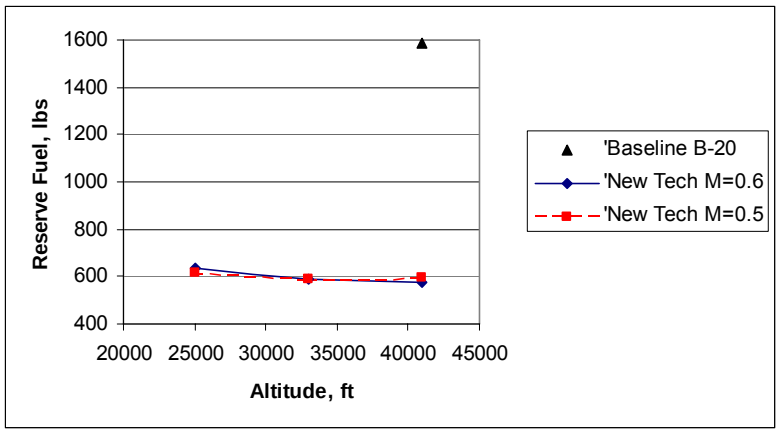

Figure 128. B-20 Turbofan with Advanced Technologies Reserve Fuel Sensitivity to Cruise Mach Number and Altitude

The sensitivity of thrust for the B-20 with advanced technologies configuration is presented in Figure 129. As cruise altitude increases, the thrust required increases. There is almost no difference between the thrust required at Mach 0.5 and Mach 0.6. The sensitivity of wing area to cruise altitude and Mach number is shown in Figure 130. Wing area increases with cruise altitude. The trend for increasing wing area with increasing altitude is similar but the higher cruise Mach number has a smaller wing area in all cases.

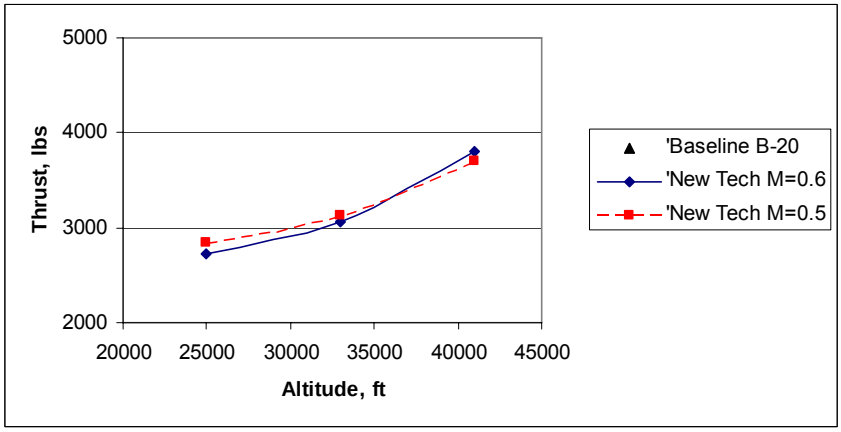

Figure 129. B-20 Turbofan with Advanced Technologies Thrust Sensitivity to Cruise Mach Number and Altitude

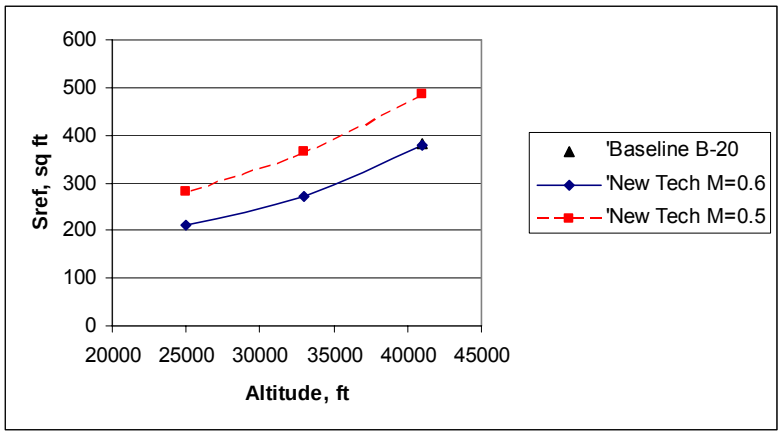

Figure 130. B-20 Turbofan with Advanced Technologies Wing Area Sensitivity to Cruise Mach Number and Altitude

Balanced Field Length is shown in Figure 131. BFL decreases with increasing cruise altitude (these configurations have larger wings and greater thrust). BFL also decreases with decreasing Mach number (larger wings). In all cases, the BFL is less than 4,000 ft and is not a constraint in the optimizations. As noted in the high lift discussion, C_{Lmax}=2.45 for these cases.

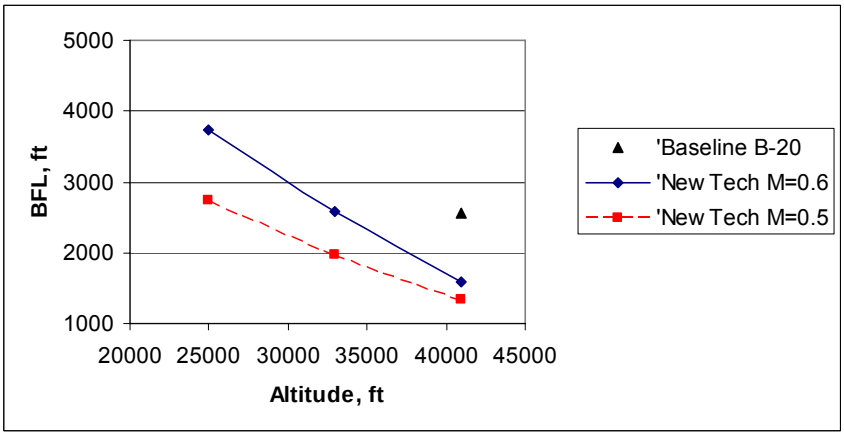

Figure 131. B-20 Turbofan with Advanced Technologies BFL Sensitivity to Cruise Mach Number and Altitude

Based on these results, for the advanced turbofan engine, a cruise Mach number of 0.6 and a cruise altitude of 41,000 ft is recommended.

6.1.4.3.3 Impact of Individual Technologies

The final step in this sensitivity study was to examine the effects of each technology applied separately. The impact of the individual technologies on the B-20 is shown in Table 43. Each case represents an optimization run with the identified technologies applied. Column 1 is the baseline B-20 with no advanced technologies. Column 2 is the B-20 with all of the technologies applied (advanced turbofan engine, 60% laminar flow on the fuselage, wing, and tails), and 24% empty weight reduction.

The B-20 with only the advanced turbofan engine (no laminar flow and no weight reduction) is shown in Column 3. The propulsion system technology has the biggest impact, with a reduction in mission fuel of 33.9%. Column 4 shows the B-20 with laminar flow only (no advanced turbofan engine and no empty weight reduction). Laminar flow technology has the second largest impact, with a reduction in mission fuel of 25.1% compared to the baseline B-20. Finally, the impact of a 24% reduction in empty weight only (no advanced turbofan engine and no laminar flow) is shown in Column 5. The empty weight reduction has the smallest impact at 11% reduction in mission fuel. When these three technologies are combined, the maximum impact is 56.5% reduction in mission fuel compared to the baseline B-20.

Table 43. Impact of Individual Technologies on B-20

	1	2	3	4	5
Summary	B-20, M=0.6 41K'	All New Tech Turbofan, M 0.60 41K'	Advanced Turbofan Only M=0.6, 41K'	Laminar Flow Only M=0.6, 41K'	Weight Reduction Only M=0.6, 41K'
MTOGW, lbs	25119	16939	22154	23208	20589
BOW	15488	10239	14387	15026	11737
Mission Fuel, lbs	3402	1480	2248	2547	3029
Reserve Fuel, lbs	1584	575	874	990	1178
Thrust, lbs	5165	3798	5318	3935	4903
Wing Area, sq ft	383.4	377.5	361.3	464.8	344.2
BFL, ft	2569	1596	2020	2447	1988
Max Fuel, lbs	4986	2055	3122.00	3537	4207
Wing Loading	65.52	44.87	61.32	49.93	59.82
Thrust to Weight	0.41	0.45	0.5	0.34	0.48
% Fuel Reduction from Baseline	0.0	56.5	33.9	25.1	11.0

6.1.4.4 Mission and Technology Sensitivity Conclusions

The results of Cessna's point optimizations and Georgia Tech's parametric environment exploration led to similar conclusions. Georgia Tech recommends a cruise Mach number of about 0.6 and a cruise altitude of about 40,000 ft. Mach 0.6 was the recommended cruise speed from MAPS. MAPS is limited to odd thousands of cruise altitude; altitudes of 25,000 ft, 33,000 ft, and 41,000 ft were examined. From those choices 41,000 ft was the best for the turbofan configuration. Within the limitations of the tools, the results are similar. The team chose to move ahead with Mach 0.6 and 41,000 ft as the mission requirements for the B-20 advanced turbofan.

Examination of the impact of the individual technologies on the B-20 showed that propulsion and engine systems has the greatest impact, laminar flow has the next greatest impact, and empty weight reduction has the smallest impact. For the propulsion system, decreases in TSFC have about twice as much impact as the same percentage decrease in engine weight. The results also show that the technology levels assumed here are not sufficient to achieve the NASA N+3 goal of 70% weight reduction. Additional work and application of technology beyond that of the Advanced Referent Turbofan Aircraft is required.

6.1.5 Advanced 2035 Aircraft Configuration Selection Process

The configuration down select process was facilitated using a Multi-Attribute Decision-Making (MADM) technique called TOPSIS, which is the Technique for Order Preference by Similarity to Ideal Solution. TOPSIS is based on the notion that the best alternative amongst a finite set should have the shortest distance to the ideal solution and farthest from the negative-ideal solution. TOPSIS provides a preference order of the deterministic values obtained in the decision matrix, at a given confidence level, resulting in a ranking of the best alternative

concepts. TOPSIS begins with the decision matrix (DM) for "n" metrics and "m" alternatives. From this matrix, each element of a metric vector (i.e., a given column) is non-dimensionalized by the Euclidean norm of that metric vector. If so desired, subjective weights may be placed on each metric to establish a relative importance. Next, each metric vector must be classified as a "benefit" or a "cost" whereby a maximum of a benefit and a minimum of a cost are desired. Positive and negative ideal solution vectors are then established. The positive vector elements consist of the maximum value of the "benefit" metrics and the minimum value of the "cost" metrics. The negative vector is the compliment of the positive vector. Next, the distance of each alternative from the positive and negative ideal solution is measured by the m-dimensional Euclidean distance, where "m" is again the number of alternatives. Finally, each alternative is ranked from "best" to "worst" based on the closeness to the positive solution and distance from the negative ideal solution. These rankings can change depending upon the level of confidence and metric weightings assumed.

The metrics used in the configuration are presented in Table 44 below. These metrics were derived based on the project goals and interaction with NASA.

Table 44. TOPSIS Metrics

Metrics	Description
Noise	Noisier concepts get lower scores. Assess noise at airport boundaries.
Simplicity	Complex concepts get lower scores.
Cost/Ticket Price	Higher ticket prices get lower scores. Assess any part of configuration that would translate into ultimately higher ticket prices for passengers
Environmental Impact	Lower impact gets higher scores. Includes all environmental impact except noise and NOx (such as water vapor, etc)
Fuel Burn/Energy Consumed	Better fuel burn gets higher scores. Assess primarily drag, somewhat propulsion (since we have different propulsor options for many concepts)
LTO Nox Emissions	Higher emissions get lower scores.
Passenger Acceptance	A more readily accepted configuration gets higher scores.
Safety	A safer configuration gets higher scores.
TOFL & Metroplex Compatibility	If concept appears able to meet 4000 foot runway constraint, and/or helps enable the metroplex concept, it gets higher scores

6.1.5.1 Alternative/Configuration Description

Five configurations were considered for downselect. These configurations are the alternatives considered in the TOPSIS procedure described in the previous section. Each configuration is accompanied by a *notional* picture that depicts the general arrangement. These pictures are not to be construed as actual designs.

The first alternative configuration is an advanced tube and wing powered by turbofans (see Figure 132). This notional configuration is representing configurations with weight and drag reduction technologies. Some of the design options are conventional tail, propulsor location, distributed propulsion, and fuel cells or hybrid propulsion.

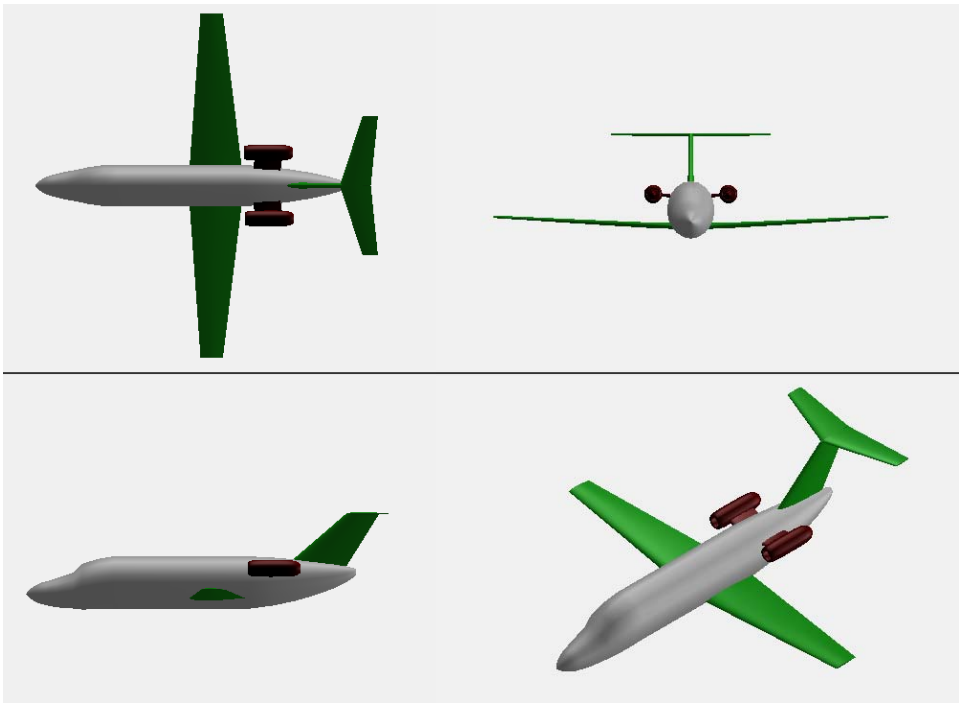

Figure 132. Notional Advanced Tube and Wing Configuration

The second configuration alternative is a strut braced wing powered by turboprops (see Figure 133). This notional configuration represents configurations with weight and drag reduction technologies including a high aspect ratio wing. Some of the design options are t-tail, propulsor location, distributed propulsion, and fuel cells or hybrid propulsion.

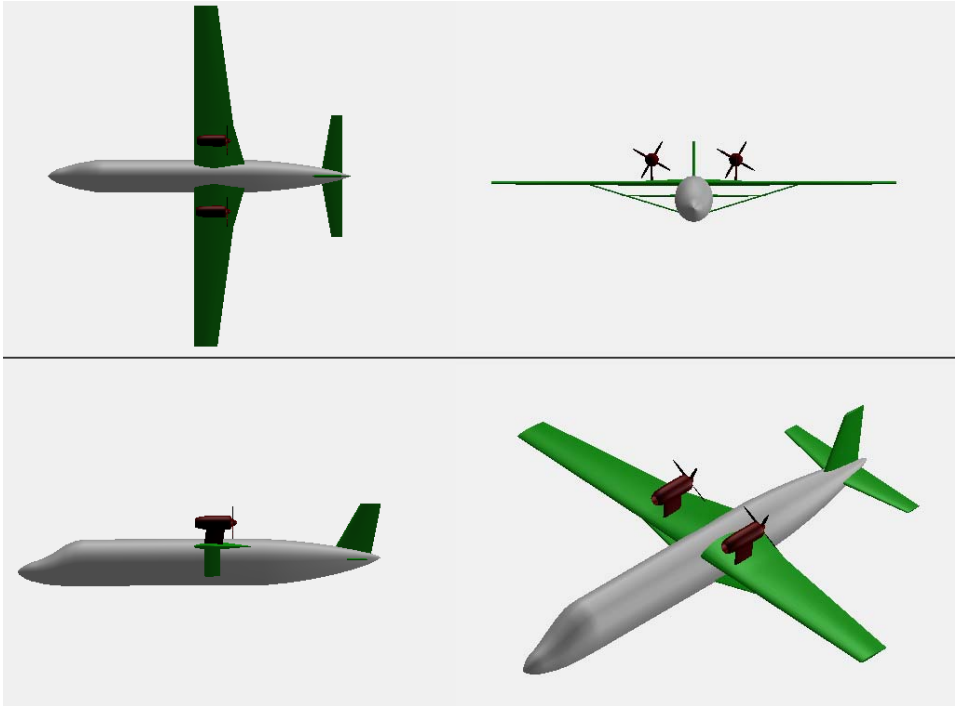

Figure 133. Notional Strut Braced Wing Configuration

The third configuration is a blended wing body powered by turbofans (see Figure 134). This notional configuration represents configurations with weight reduction technologies and embedded propulsion for noise reduction. Some of the design options are canard and fuel cells or hybrid propulsion.

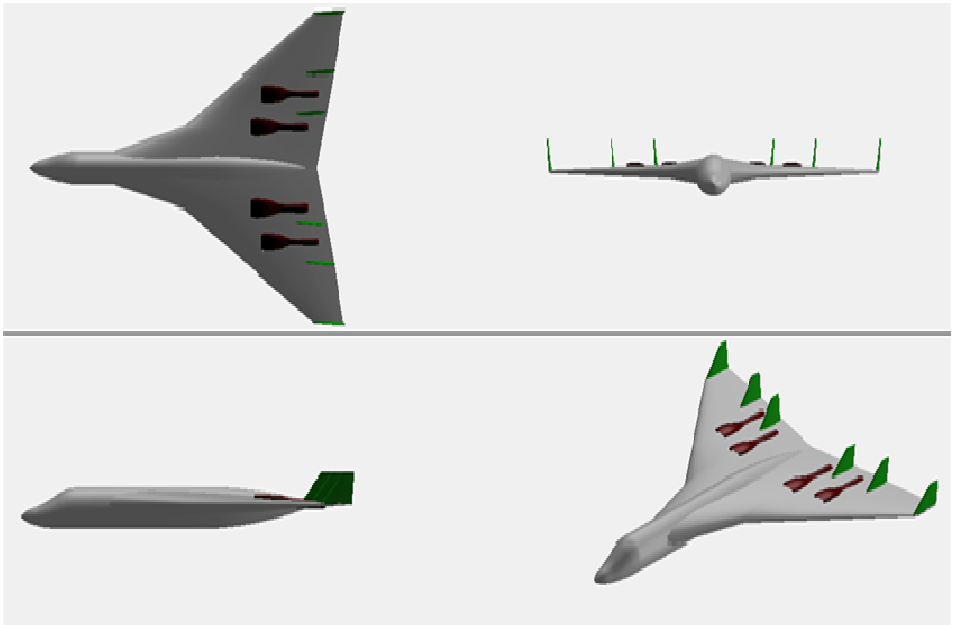

Figure 134. Notional Blended Wing Body Configuration

The forth configuration is a twin boom powered by turboprops (see Figure 135). This notional configuration is representing configurations with weight and drag reduction technologies including a laminar flow fuselage. Some of the design options are boom mounted propulsors, pusher or tractor, Goldschmied propulsor, winglets, wingtip mounted propulsors, propulsor type, and fuel cells or hybrid propulsion.

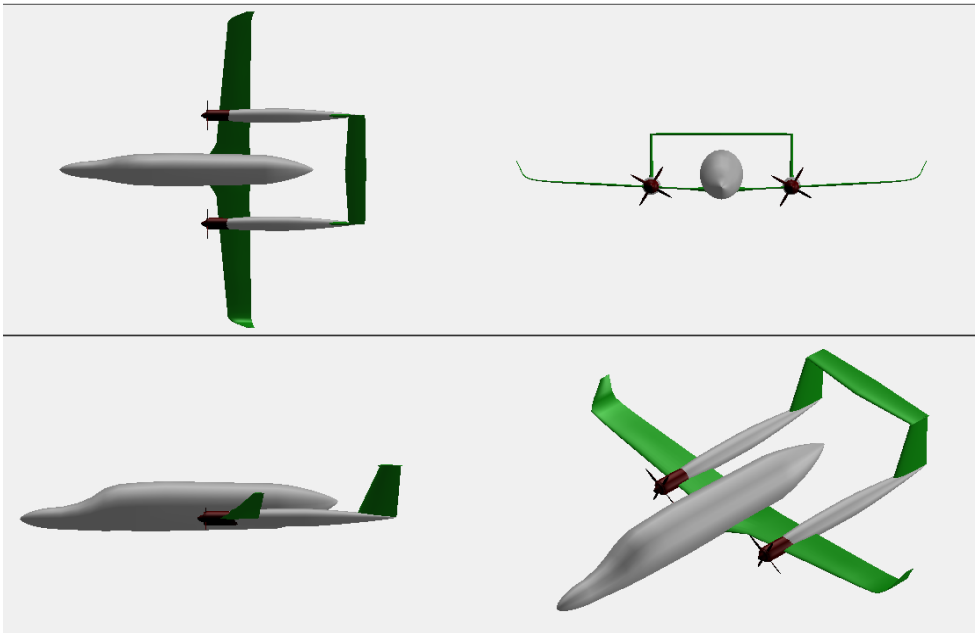

Figure 135. Notional Twin Boom Configuration

The fifth configuration is a laminar flow fuselage powered by turboprops (see Figure 136). This notional configuration represents configurations with weight and drag reduction technologies including a laminar flow fuselage. Some of the design options are boom mounted a conventional tail, propulsor location, turbofan, no canard, and fuel cells or hybrid propulsion.

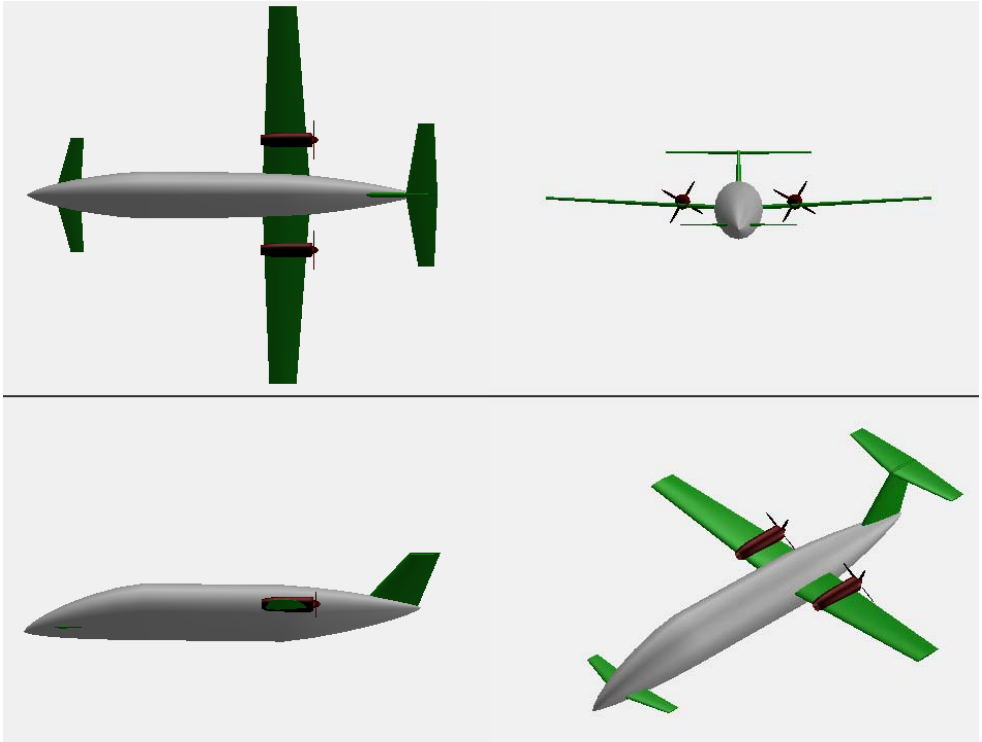

Figure 136. Notional Laminar Flow Fuselage Configuration

6.1.5.2 Initial Down Selection

The TOPSIS procedure previously described was used to rank each of the initial five configurations; the ranking of the configurations was done by fifteen professional in different disciplines ranging from propulsion to aircraft design. The guideline given to the professionals was to rank the concepts *relative* to each other, not with respect to any baseline. The rankings of the configurations were averaged based on the compiled results of the professionals ratings for each configuration based on the metrics, the rating ranged from 1 to 9, where 9 is the best. Each metric was also weighted based on the agreement of the goals set by NASA, so noise, cost, and fuel burn were ranked higher than the other metrics and were considered over the other metrics if there was a tie between configurations. The initial five configurations averaged rankings are shown below in Table 45.

Table 45. Initial TOPSIS Results

	Noise	Simplicity	Cost/Ticket Price	Environmental Impact	Fuel Burn and/or Energy Consumed	LTO NOx Emissions	Passenger Acceptance	Safety	TOFL & Metroplex Compatibility	
Config. # / Weightings	**7**	**0**	**5**	**0**	**9**	**5**	**3**	**3**	**5**	**Rank**
Strut Braced Wing	5	6	5	4	5	5	5	5	7	**3**
Blended Wing Body	2	2	3	4	4	3	3	3	4	**5**
Twin Boom	3	4	6	6	6	6	4	5	7	**4**
Laminar Fuselage	3	4	6	7	7	7	5	6	6	**1**
Adv Tube/Wing	5	8	7	5	5	3	8	7	7	**2**

Based on the results of the rankings, *the blended wing body configuration was removed* since it scored the lowest overall and the lowest in the metrics of the most importance. As a result of the finding it was requested that the laminar fuselage configuration be altered and an additional concept be created, these configurations were shown in the previous section.

After initial ranking of the configuration in TOPSIS additional modified configurations were added for further consideration. The modified configurations are based on the laminar flow fuselage and the strut braced wing.

6.1.5.3 Additional Configurations

The first modified configuration considered is a laminar flow fuselage with turboprops (see Figure 137). This notional configuration is representative of the initial configuration with the weight and drag reduction technologies including a laminar flow fuselage, but the wing is moved forward and down while removing the canard. Some of the design options are a conventional tail, propulsor location, turbofan, and fuel cells or hybrid propulsion.

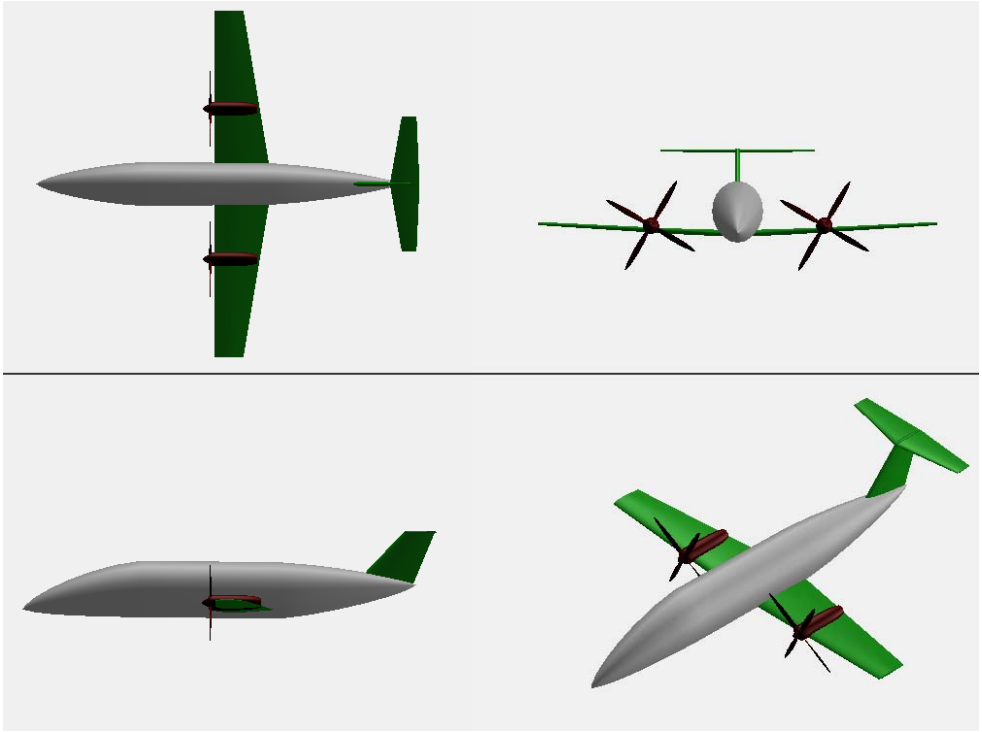

Figure 137. Notional Laminar Flow Fuselage Configuration

An additional configuration to be considered as a result of the initial downselect is a high aspect ratio tractor powered by turboprops (see Figure 138). This notional configuration has the weight and drag reduction technologies with a high aspect ratio wing. Some of the design options are a conventional tail, turbofan, distributed propulsors and fuel cells or hybrid propulsion.

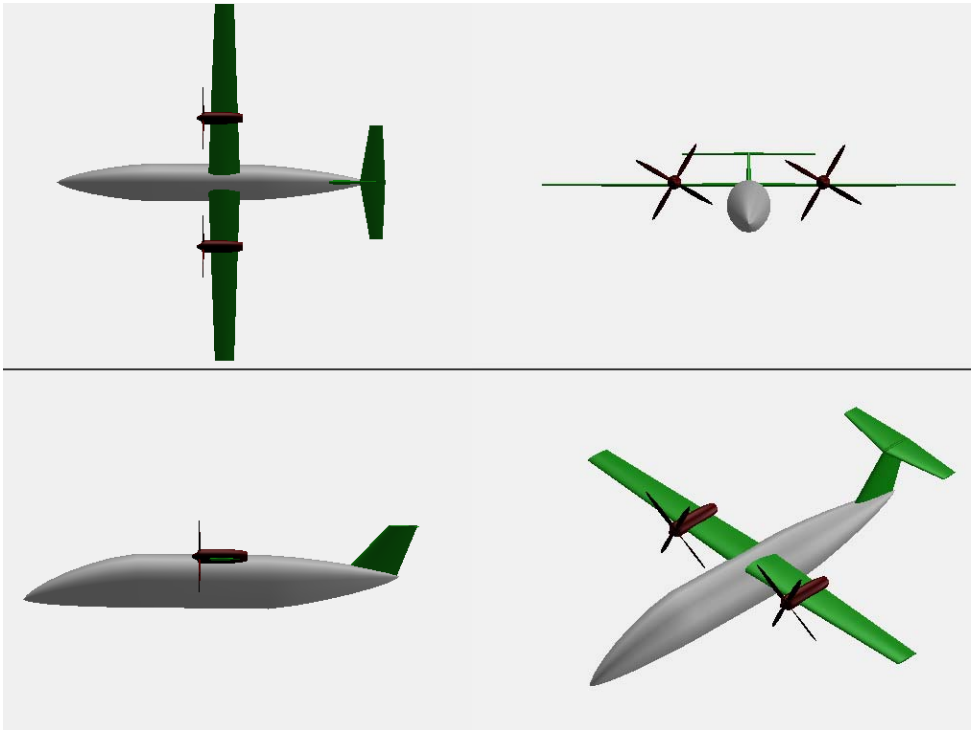

Figure 138. Notional High Aspect Ratio Tractor Configuration

6.1.5.4 Configuration Down Selection

The TOPSIS procedure previously described was once again used at the workshop for configuration selection which took place at Cessna on November 12, 2009. The metric rankings were not changed for this second round, maintaining the emphasis on metrics directly related to NASA goals. The results of the discussion are shown below in Table 46.

Table 46. Down Selected TOPSIS Results

	Noise	Simplicity	Cost/Ticket Price	Environmental Impact	Fuel Burn and/or Energy Consumed	LTO NOx Emissions	Passenger Acceptance	Safety	TOFL & Metroplex Compatibility	Rank
Configuration/Weighting	5	0	3	0	7	0	0	0	0	
1. Adv Tube and Wing	6	9	4	3	3	3	9	9	4	**4**
2. Hi AR Pusher	3	5	6	7	8	7	3	5	8	**2**
3. Laminar Fuselage	5	7	4	5	5	5	6	5	6	**3**
4. Twin Boom Laminar Fuse	5	1	1	4	4	4	1	5	5	**5**
2a. Hi AR Tractor	4	5	6	7	7	7	5	5	8	**1**

The ranking of the individual configurations was based on discussions from the workshop. The discussion on the configurations was structured around their impact on each of the metrics.

The Goldschmied propulsor technology was discussed in detail since it would significantly affect configuration choices. To implement the Goldschmied propulsor it was determined that the design would have to be tailless and use a delta wing configuration or a twin boom configuration. Concerns were voiced regarding the impact of lots of intersections on laminar flow goals and the effect on wetted area, both important to the fuel burn objective. The addition of a possible extra propulsor also made the technology not very favorable from a fuel burn and cost perspective. Further, potential development and maintenance costs of the new system

were considered to make this concept too risky and led the team to remove it from further consideration

The discussion on noise considered which configuration would be the noisiest or produce more noise in comparison with the other configurations. The team determined that the pusher would be noisier than the puller configuration due to the impact of the wing wake on the propeller. For propulsion the turbofan would be noisier, but offers the ability to be shielded unlike the turboprop. The conclusion that propellers have lower frequency noise made turboprops less of a concern when weighting the configurations.

The discussion on fuel burn and NOx emissions led to the determination that a higher aspect ratio wing along with a configuration with a turboprop would be a good choice. For the engine, a pusher verses a tractor when considering laminar flow verses prop efficiency is most likely indifferent.

The discussion on the metric of cost, revolved mostly around the different propulsion types. Of note, the Goldschmied propulsor was thought to require significant development and optimization cost, and have much higher acquisition and maintenance cost due to the additional engine or propulsor and control system.

The result of the ranking with the TOPSIS procedure found that the **high aspect ratio tractor configuration** was the best based upon the metrics and their weightings of importance. However, additional studies were carried out to consider turboprop vs. turbofan and tractor vs. pusher trades.

6.1.6 Advanced Turbofan and Turboprop Aircraft Sensitivity Studies

While workshops and debates were occurring about the final configuration, parallel work took place on more realistic considerations of the incorporation of the propulsion, aerodynamics, and structures technology. Cessna documented a set of comparisons of advanced turbofan and advanced turboprop sensitivities; Georgia Tech provided complementary analyses to validate the results. The Cessna documentation is presented in the next section.

After the workshops were completed and final configuration decisions were made, projections of advanced technologies along with specific actions to achieve those technologies were completed (for example, fuselage layout for laminar flow and multi-function fuselage with protective skin). The results of the decisions and design actions were combined into the 2035 advanced reference vehicle. Georgia Tech and Cessna conducted sensitivity studies to determine the best cruise Mach number and altitude for the 2035 advanced reference vehicle and hence the 2035 final configuration. Those results are presented in the final section.

6.1.6.1 Cessna Turbofan vs. Turboprop Sensitivity Studies

Cessna trade studies once again defined a matrix of conditions to run as separate optimizations in MAPS. Initial studies compared the B-20 with advanced technologies (including an advanced turbofan engine) to a B-20 with advanced technologies including an advanced turboprop configuration. The sensitivities were run at altitudes of 25,000 ft, 33,000 ft, and 41,000 ft, and at Mach 0.60 for the advanced turbofan and Mach 0.55 for the advanced turboprop.

Figure 139 shows the mission fuel comparison for the two configurations. The advanced turboprop uses less mission fuel than the advanced turbofan, and the sensitivity of the turboprop to changes in altitude is less than the sensitivities of the advanced turbofan to altitude. The 33,000 ft cruise altitude has the smallest mission fuel burned, although the difference between mission fuel at 33,000 ft and 41,000 ft is only 64 lbs.

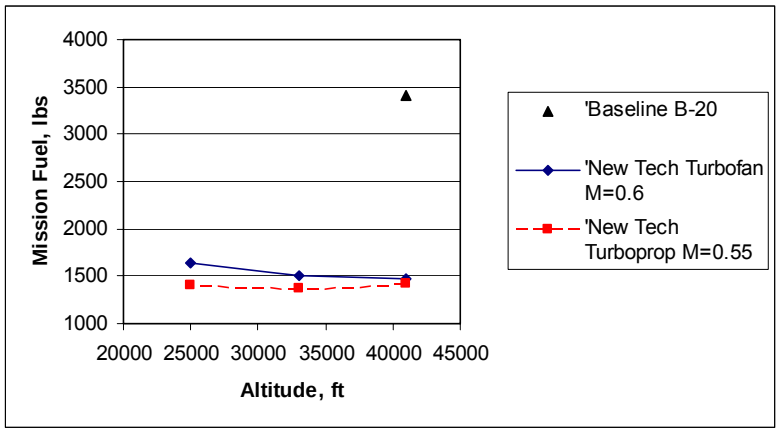

Figure 139. B-20 with Advanced Technology Mission Fuel Sensitivity to Propulsion System Type

The reduction in mission fuel for these advanced configurations compared to the baseline B-20 is shown in Figure 140. The advanced turboprop provides greater mission fuel reduction than the advanced turbofan. The greatest reduction occurs at 33,000 ft cruise altitude.

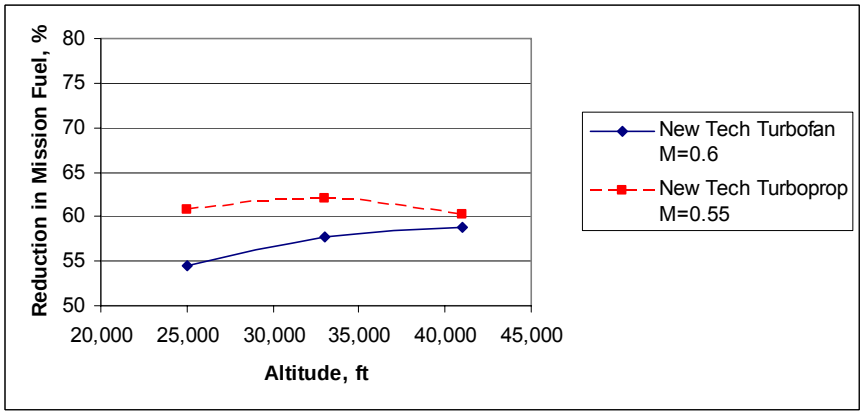

Figure 140. B-20 with Advanced Technology Mission Fuel Reduction Sensitivity to Propulsion System Type

MTOGW is shown in Figure 141. Sensitivity of MTOGW of the advanced turboprop to changes in cruise altitude is slightly larger than sensitivity of the advanced turbofan. The advanced turboprop has a slightly larger MTOGW at 41,000 ft than the advanced turboprop.

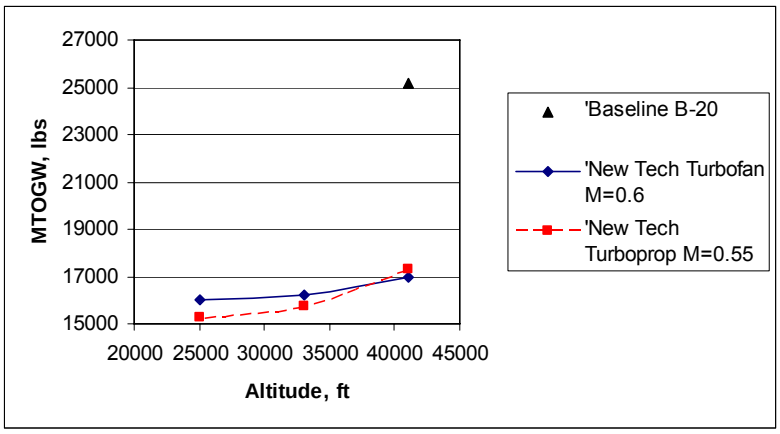

Figure 141. B-20 with Advanced Technology MTOGW Sensitivity to Propulsion System Type

Sensitivity of the turbofan and turboprop configurations to cruise altitude is shown in Figure 142 and Figure 143. Wing areas for both configurations are essentially the same. The turboprop's engine size, as indicated by its nominal sea level thrust, is much more sensitive to altitude than the turbofan engine. This is because the top of climb thrust requirement sizes the engines, and the turboprop thrust lapses more with altitude than a turbofan. The turboprop's mission fuel burn, however, is fairly flat with altitude, as seen in Figure 140. Being able to fly above weather and large commercial traffic, however, would be an advantage that might favor flying at higher altitudes. Cruise altitude was reevaluated by Georgia Tech with more advanced technologies incorporated into the design. Results are shown in the following sections.

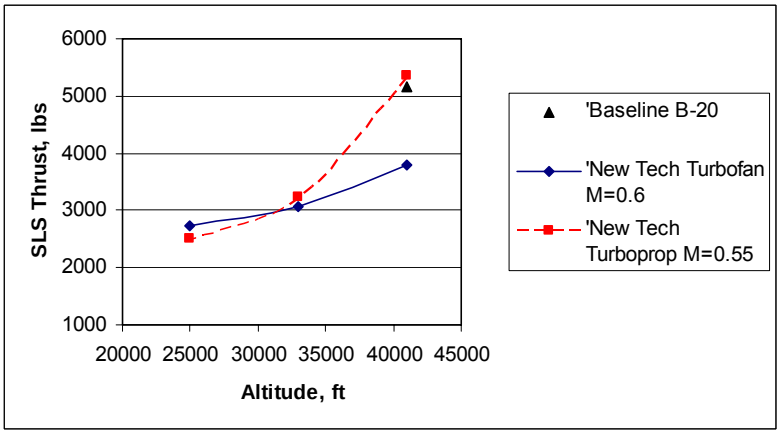

Figure 142. B-20 with Advanced Technology Thrust Sensitivity to Propulsion System Type

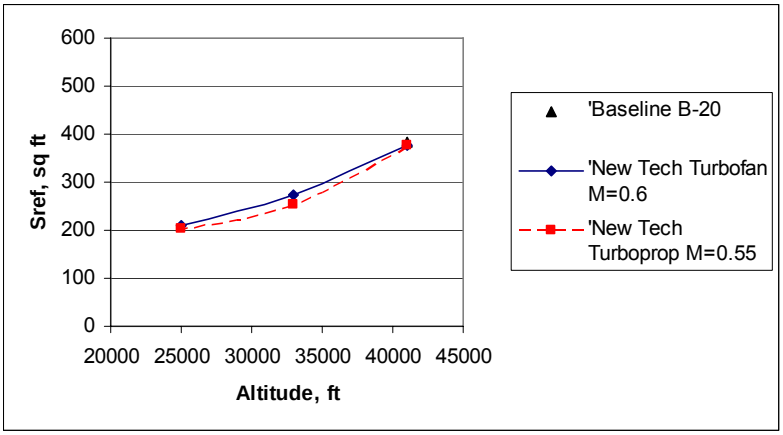

Figure 143. B-20 with Advanced Technology Wing Area Sensitivity to Propulsion System Type

Sensitivity of the two configurations' BFL is shown in Figure 144. As before, these results are for the higher (2.45) C_{Lmax}. At the 41,000 ft altitude, the advanced turboprop BFL is even less than the advanced turbofan. In fact, the BLF is approaching 1,000 ft. Using a plain flap system to minimize noise and risk of disturbing laminar flow would still provide a BFL well under 4,000 ft.

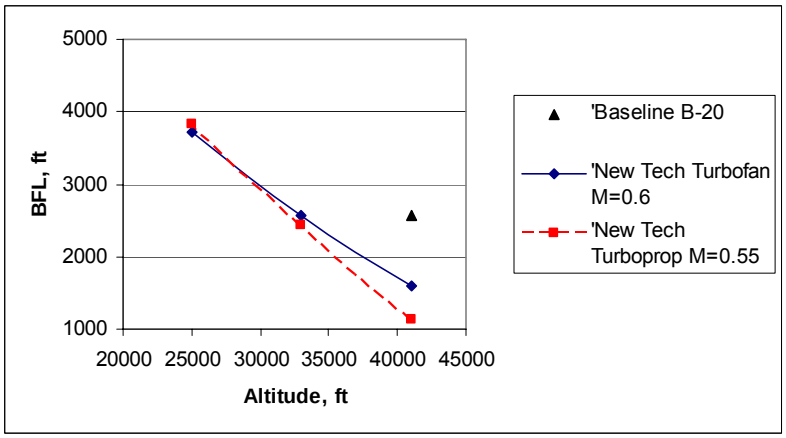

Figure 144. B-20 with Advanced Technology BFL Sensitivity to Propulsion System Type

6.1.6.2 Georgia Tech Turbofan versus Turboprop Trades

In the previous sections, technology investigation of the combined effect of vehicle weight reduction, laminar flow, and advanced turbofan are analyzed and presented. The resulting vehicle of combining these three technologies is referred to as the 2035 advanced reference vehicle. The initial approach to find an optimal combination of thrust to weight (T/W), wing loading (W/S), cruise Mach number, and cruise altitude was to use the parametric environment created around this 2035 reference vehicle. The idea is to use the dynamic environment in Figure 145 to dial in the variable settings for minimum fuel weight (see second prediction profiler of Figure 145). This was a very visual and quick way to find a potential configuration to satisfy

the NASA fuel reduction goal. However, this approach does not account for a crucial top of climb (TOC) constraint of 200 fpm rate of climb (ROC). After analyzing the TOC ROC data gathered to create this parametric environment, it was determined that an accurate surrogate could not be created. Therefore the potential solution obtained from the dynamic environment had to be checked to see if the TOC ROC constraint was satisfied by running the mission analysis, (e.g. FLOPS). If the constraint was not met, then a series of sensitivity cases were performed using the solution from the dynamic environment as the starting point to find a solution that would give the lowest fuel weight while maintaining a TOC ROC of 200 fpm or better. This initial approach was repeated for the advanced reference turboprop puller and pusher configurations (see Figure 146 and Figure 147). The main difference in modeling the advanced turbofan and the two turboprop configurations are summarized in Table 47. The engine deck distinction also carries the GE SFC, weight, diameter, and length scaling rules which are difficult to capture in a table summary. In other words, appropriate SFC scaling, engine weight, diameter and length scaling are embedded in the program switches coded to the mission analysis program, FLOPS.

Table 47. Turboprop Modeling Distinctions

	Turbofan	Turboprop Puller	Turboprop Pusher
Engine Deck	GE3800AR	GE5000ATP	GE5000ATP
SFC Impact	GE3800AR Scaling	GE5000ATP Scaling	5% Penalty Relative to GE5000ATP Scaling
Drag Delta due to Propeller	No	Yes	Yes
Fuselage Laminar Flow (%)	60%	60%	60%
Wing Laminar Flow (%)	60%	10%	50%
Horizontal Tail Laminar Flow (%)	60%	60%	60%
Vertical Tail Laminar Flow (%)	60%	60%	60%
Nacelle Laminar Flow (%)	60%	0%	0%

This initial approach to find an “optimal” configuration with the best fuel weight was very tedious and time consuming so the GT team developed an optimization scheme using Phoenix Integration’s ModelCenter®. Basically, the mission analysis program, FLOPS, was coupled with an internal optimizer within ModelCenter® (see Figure 148). The main advantage of setting up this optimization environment is that the TOC ROC constraint is always satisfied. However, one of the main caveats of this optimization environment is that it is very prone to FLOPS failures. Once the mission analysis fails, the optimizer cannot automatically restart another run. The other probably more important caveat is that the solution is highly dependent on the starting guess. In other words, the solution space is highly multi-modal containing potentially many local optimums. Therefore, for every optimization run, several initial guesses were used and successful solutions were recorded and presented to the entire team to select the “best” solution.

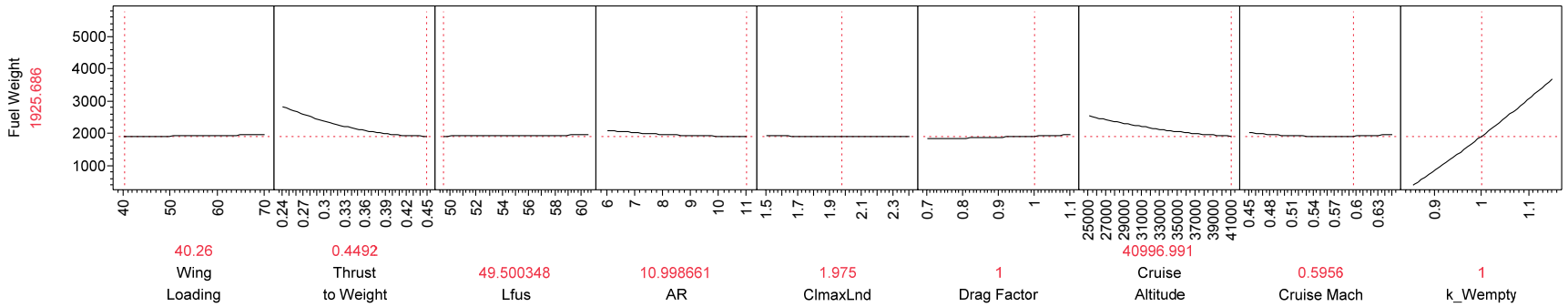

Figure 145. Parametric Environment for Advanced Reference Turbofan with Weight Reduction and Laminar Flow

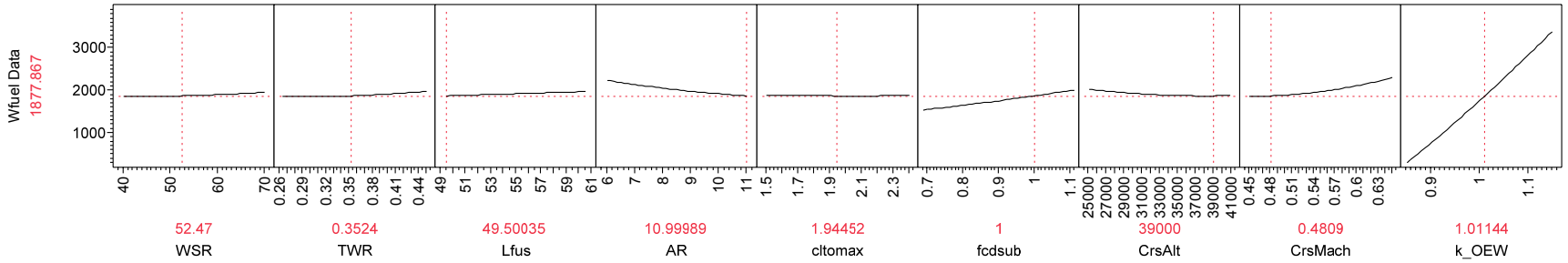

Figure 146. Parametric Environment for Advanced Reference Turboprop (Puller) with Weight Reduction and Laminar Flow

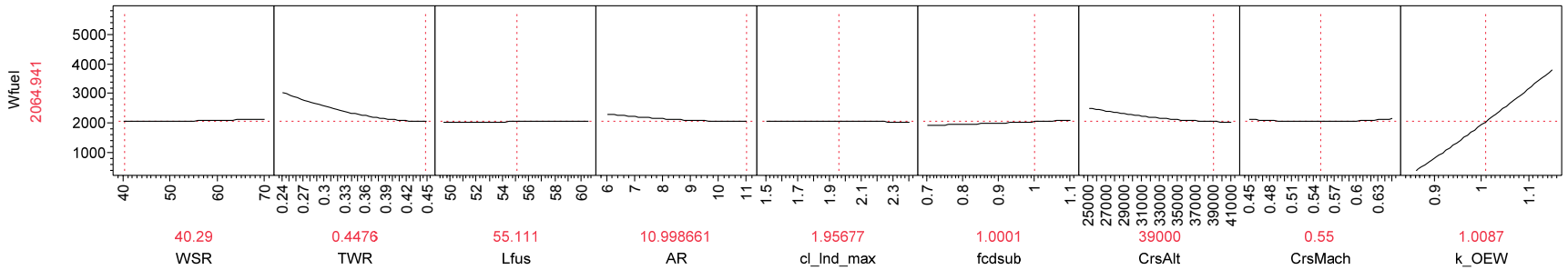

Figure 147. Parametric Environment for Advanced Reference Turboprop (Pusher) with Weight Reduction and Laminar Flow

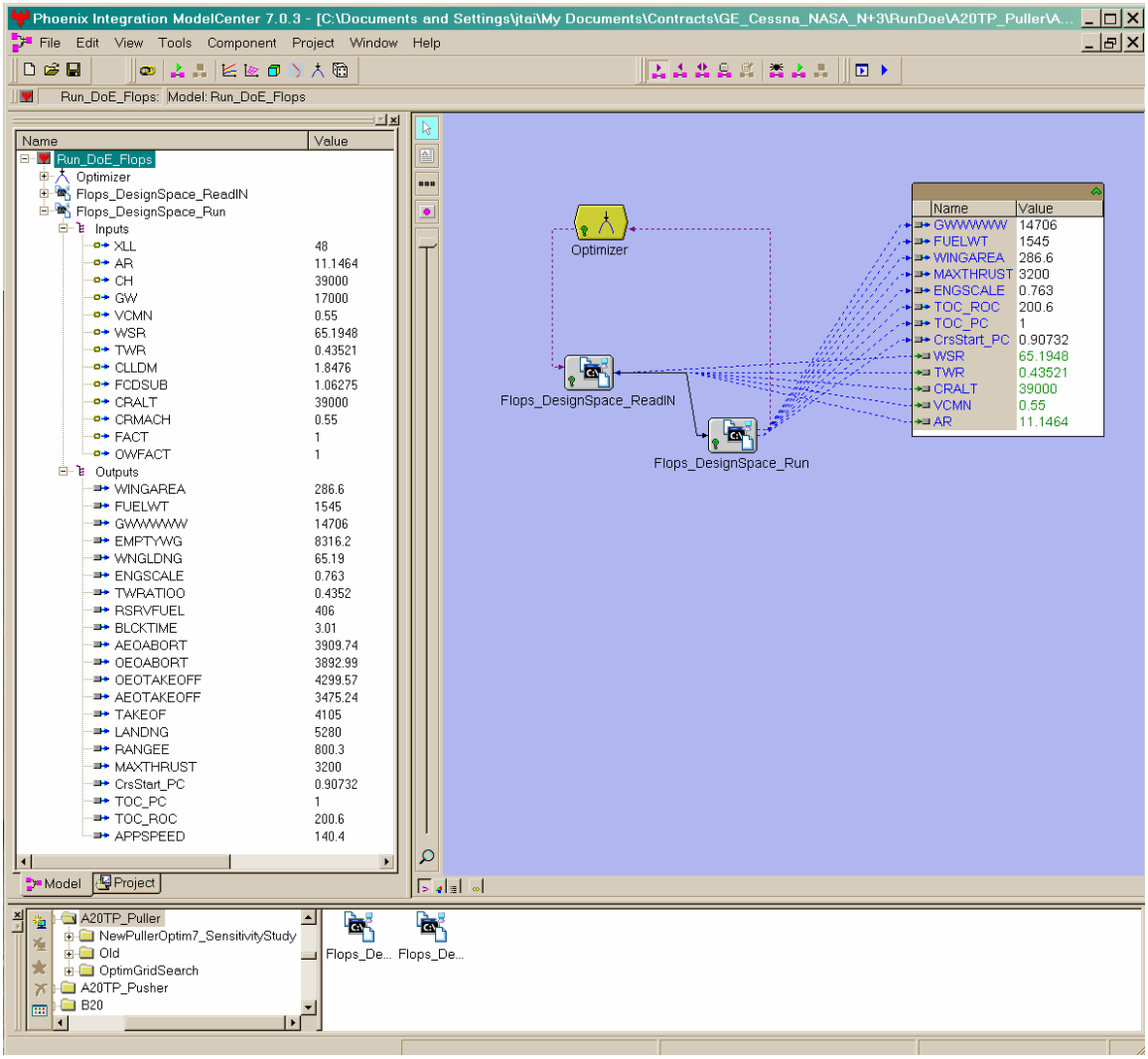

Figure 148. Optimization Environment Using ModelCenter®

The optimal solutions for the advanced reference turbofan are shown in Table 48. In this optimization exercise, the objective is to minimize fuel weight with a constraint of 200 fpm TOC ROC by varying the thrust to weight ratio, wing loading, wing aspect ratio, cruise Mach number, and cruise altitude. Examining the mission fuel weight for these three configurations shows that they are all within 20 pounds of each other. The second solution was not selected to be compared to the turboprop solutions because of the slower cruise Mach number; therefore, the first solution is selected due to a lower mission fuel weight. Similar optimal solutions were obtained for the turboprop puller and pusher configuration, and they are presented in Table 49 and Table 50, respectively. For the turboprop puller configuration, the choice came down between the second and third solution due to the higher mission fuel weight of the first solution. The third optimal solution was selected for the turboprop puller configuration due to the larger engine, balanced field length (BFL), and slightly better TOC ROC. The selection for the turboprop pusher configuration is easier since there are two solutions, and they are very similar. The selection of the turboprop pusher was solution 2 based on mission fuel weight.

Table 48. Advanced Reference Turbofan Optimal Solutions

	Adv. Turbofan A20v3_Optim1	Adv. Turbofan A20v3_Optim2	Adv. Turbofan A20v3_Optim3
Engine Deck	GE3800AR	GE3800AR	GE3800AR
MTOGW, lbs	17625	17253	17789
Mission Fuel, lbs	1348	1347	1366
ESF	0.9273	0.6808	0.9359
Wing Area, sq ft	391.7	431.3	444.7
BFL, ft	1822	2267	1619
TOC ROC, ft/min	212.8	565.1	696.9
Aspect Ratio	11	11	11
Cruise Mach	0.65	0.5	0.6
Cruise Altitude, ft (ending)	44152	40000	41000
W/S	45	40	40
T/W	0.4	0.3	0.4

Table 49. Advanced Turboprop Puller Optimal Solutions

	Adv. Turboprop PullerOptim_1	Adv. Turboprop PullerOptim_2	Adv. Turboprop PullerOptim_3
Engine Deck	GE4200ATP	GE4200ATP	GE4200ATP
MTOGW, lbs	14804	14551	14664
Mission Fuel, lbs	1113	1088	1095
ESF	0.8213	0.7645	0.7996
Wing Area, sq ft	223.7	195.9	203.6
BFL, ft	2257	2694	2505
TOC ROC, ft/min	200.1	200.6	202.9
Aspect Ratio	13.01	14.0	14.0
Cruise Mach	0.55	0.55	0.55
Cruise Altitude, ft (ending)	39000	39000	39000
W/S	66.17	74.29	72.03
T/W	0.465	0.441	0.457

Table 50. Advanced Turboprop Pusher Optimal Solutions

	Adv. Turboprop PusherOptim_1	Adv. Turboprop PusherOptim_2
Engine Deck	GE5000ATP	GE5000ATP
MTOGW, lbs	17200	17186
Mission Fuel, lbs	1260	1249
ESF	0.7227	0.7221
Wing Area, sq ft	430.0	429.6
BFL, ft	1619	1619
TOC ROC, ft/min	413.5	297.9
Aspect Ratio	11.0	11.0
Cruise Mach	0.45	0.46
Cruise Altitude, ft (ending)	50000	40123
W/S	40.00	40.00
T/W	0.400	0.400

The selected solutions for all three configurations, advanced reference turbofan, turboprop puller, and turboprop pusher, are summarized in Table 51; this table was used to determine the final 2035 selected configuration. Again, using mission fuel weight as the discriminator, one can obviously see that the turboprop puller is the selected concept.

Table 51. Advanced Aircraft Optimal Solutions

	Adv. Turbofan A20v3_Optim1	Adv. Turboprop PullerOptim_3	Adv. Turboprop PusherOptim_2
Engine Deck	GE3800AR	GE4200ATP	GE5000ATP
MTOGW, lbs	17625	14664	17186
Mission Fuel, lbs	1348	1095	1249
ESF	0.9273	0.7996	0.7221
Wing Area, sq ft	391.7	203.6	429.6
BFL, ft	1822	2505	1619
TOC ROC, ft/min	212.8	202.9	297.9
Aspect Ratio	11	14.0	11.0
Cruise Mach	0.65	0.55	0.46
Cruise Altitude, ft (ending)	44152	39000	40123
W/S	45	72.03	40.00
T/W	0.4	0.457	0.400

6.1.6.3 Cessna 2035 Advanced Reference Vehicle Sensitivities

Modeling the 2035 advanced reference vehicle in MAPS involved many of the same considerations just described in the Georgia Tech section. Updating the fuselage dimensions for the laminar flow fuselage design, adjusting laminar flow to account for the puller (tractor) turboprop configuration, adding a propeller drag increment, and adding the Year 2035 Advanced Turboprop Concept engine deck prepared MAPS to run the new configuration. Once again a matrix of runs was defined (cruise Mach number of 0.55 and cruise altitudes of 25,000 ft, 33,000 ft, and 41,000 ft), and configurations were optimized at each of the selected points. The optimization did not provide reasonable configurations at 41,000 ft due to the large engine thrust required; exploration of the design space below 41,000 ft showed 39,000 ft to be a good cruise altitude. The results of the optimizations are described here.

The mission fuel for the 2035 advanced reference vehicle is shown in Figure 149. The change in mission fuel as a function of altitude is very flat, with the minimum occurring at 39,000 ft. The difference between the mission fuel for 25,000 ft and 39,000 ft is only 83 lbs or 7.7% of the mission fuel. The mission fuel is significantly reduced from the B-20.

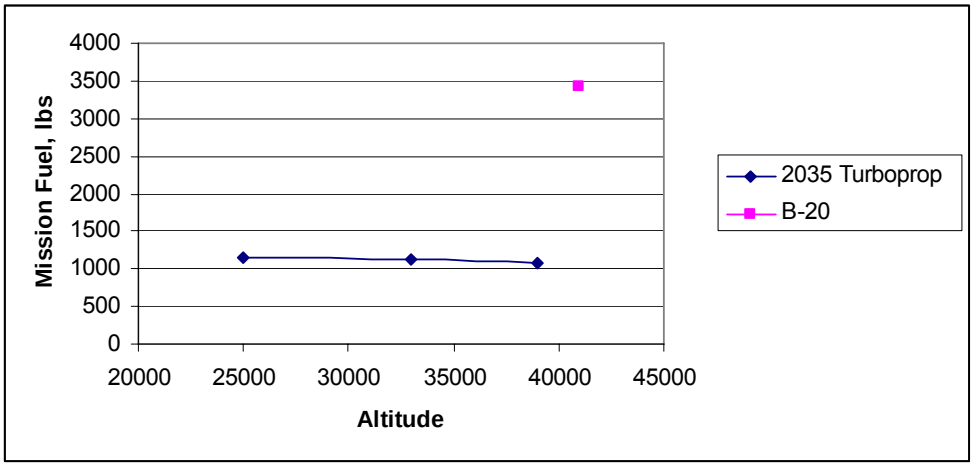

Figure 149. Mission Fuel for the 2035 Advanced Reference Vehicle

The percent reduction in mission fuel compared to the B-20 baseline airliner is shown in Figure 150. The maximum reduction is nearly 69%, which is within the realm of the NASA N+3 target of 70% given the fidelity of this analysis.

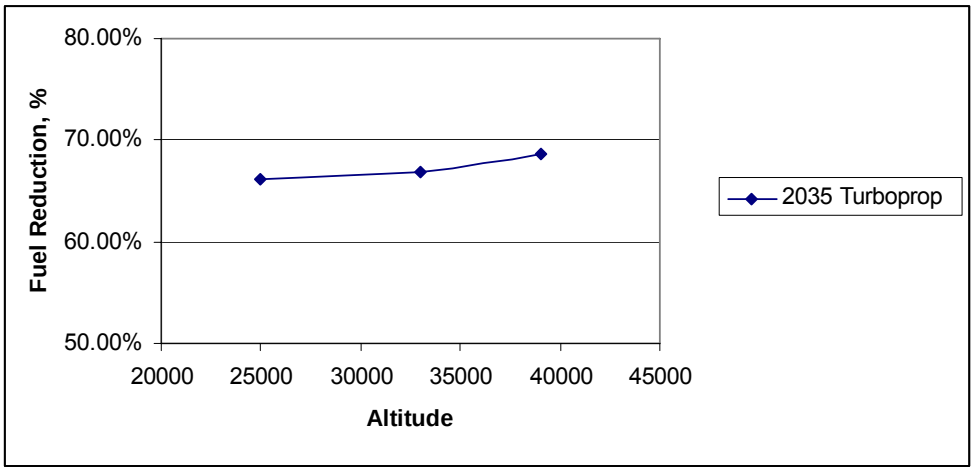

Figure 150. Mission Fuel Reduction for the 2035 Advanced Reference Vehicle Compared to the Baseline B-20

Figure 151 shows the MTOGW for the Year 2035 Advanced Reference Vehicle as a function of cruise altitude. Again the trend is very flat, with only a 933 lb difference between the configuration optimized for 25,000 ft and the configuration optimized for 39,000 ft. That represents a 6.3% change in MTOGW. The heaviest MTOGW also corresponds to the configuration with the least mission fuel. The Year 2035 Advanced Reference Vehicles' MTOGW is about 60% of the MTOGW of the B-20.

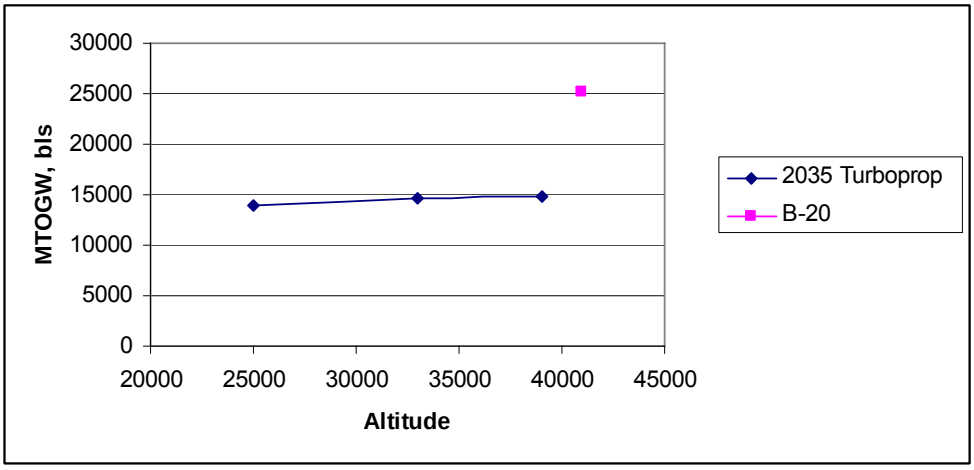

Figure 151. MTOGW for the 2035 Advanced Reference Vehicle

Thrust for the Year 2035 Advanced Reference Vehicle increases from 25,000 ft cruise altitude to 33,000 ft altitude and then remains about constant on up to 39,000 ft as seen in Figure 152. Since the baseline advanced turboprop engine is sized at 4200 lbs thrust, the engines for the 2035 Advanced Reference Vehicle are scaled down anywhere from 20% to 50%.

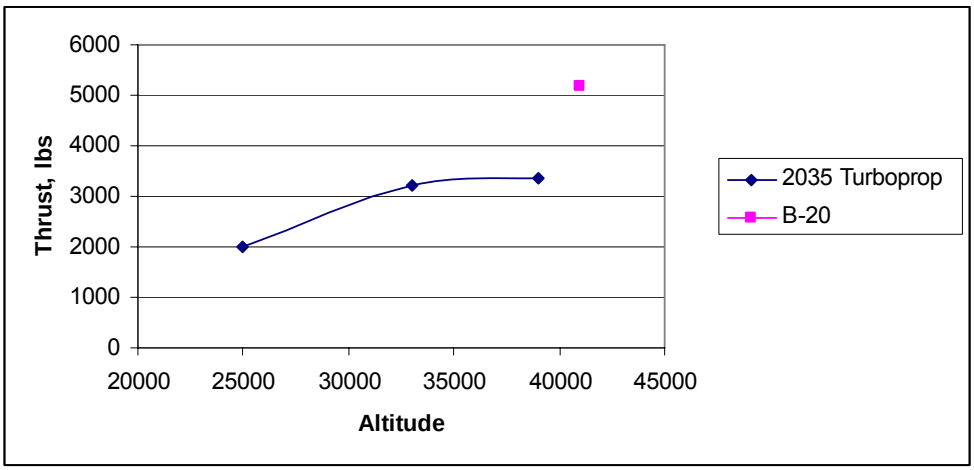

Figure 152. Thrust for the 2035 Advanced Reference Vehicle

Wing area for the 2035 Advanced Reference Vehicle is shown in Figure 153. The wing area is fairly constant as a function of cruise altitude, with the largest wing occurring for the aircraft optimized for a cruise altitude of 33,000 ft. The maximum difference between the areas for the 33,000 ft and 39,000 ft airliners is 32 square feet or about 13%.

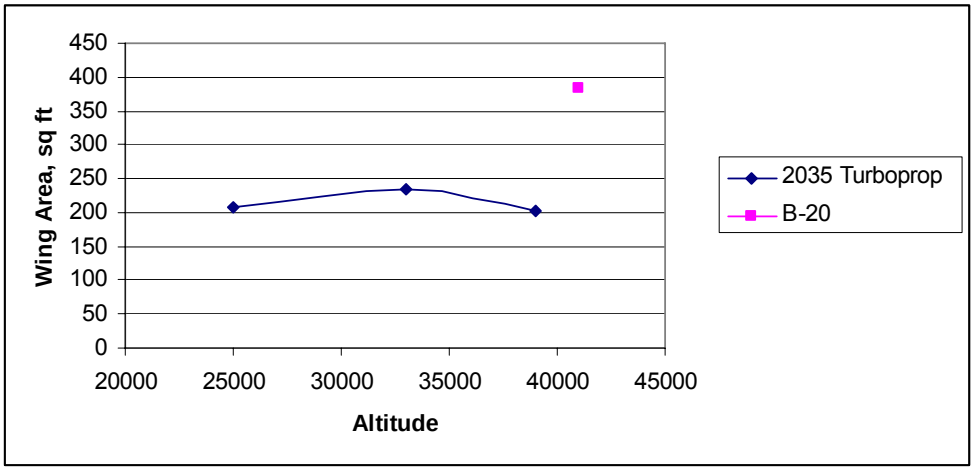

Figure 153. Wing Area for the 2035 Advanced Reference Vehicle

Based on the results of this sensitivity analysis, the Year 2035 Final Configuration selected cruises at Mach 0.55 and 39,000 ft. The analysis conclusions are consistent between Georgia Tech and Cessna. The 2035 Final Configuration results from both groups will be compared in the section describing the 2035 Final Configuration.

6.1.6.4 Comparison of Georgia Tech and Cessna "No Laminar Flow" Result

During the course of this project, Cessna and Georgia Tech personnel coordinated closely on agreement between the results produced by the different tools. Differences could always be attributed to differences in aerodynamics, differences in weights, and/or differences in mission modeling. As experience modeling and matching was acquired, the team became increasingly efficient at producing similar results.

As an example, the Georgia Tech FLOPS results are compared to the Cessna MAPS results for the 2035 selected configuration with laminar flow removed. The full Georgia Tech results will be presented in the selected technology sensitivity and ranking section, but are borrowed to be compared here with the Cessna results. Table 52 compares the main characteristics of the two configurations. Agreement in performance parameters is outstanding, with a 0.26% difference in MTOGW, a 0.86% difference in BFL, and a 4.36% difference in mission fuel.

The comparison of results highlights another interesting point about this class of aircraft. The FLOPS results consist of higher thrust (4,589 lbs) compared to the MAPS result of 3,858 lbs with lower wing area (195 sq ft compared to 233 sq ft). The optimization space is fairly flat, making it possible to increase thrust and decrease wing area to meet takeoff distance requirements or to decrease thrust and increase wing area. This allows another option besides a complex high lift system to meet any increased BFL requirements.

Table 52. Comparison of FLOPS and MAPS Results for 2035 Selected Configuration with No Laminar Flow

Parameter	FLOPS	MAPS	Difference, %
Mission Fuel, lbs	1,308	1,251	4.36
MTOGW, lbs	15,557	15,517	0.26
Thrust, lbs	4,589	3,858	15.93
Wing Area, sq ft	195	233	-19.69
BFL, ft	2,099	2,081	0.86
W/S, lbs/sq ft	80.0	66.7	16.63
T/W	0.59	0.50	15.25

6.1.6.5 2035 Vehicle Aircraft Sensitivities Conclusions

Results from studies of the 2035 advanced reference vehicle by both Georgia Tech and Cessna show that a cruise Mach number of 0.55 and a cruise altitude of 39,000 ft will give the minimum mission fuel burn for an Advanced Turboprop Aircraft. It also shows a significant fuel burn advantage for an advanced tractor turboprop vs. a pusher or turbofan configuration. With the selected configuration NASA's N+3 goal of a 70% reduction in fuel burn is likely achieved, given the level of fidelity of this analysis. Results also show that the penalty for flying at lower altitudes is relatively small. Comparison of the Cessna MAPS and Georgia Tech FLOPS results show that there is excellent agreement between the tools and that thrust/wing area trades to meet the requirements can be used to help open the design space.

6.2 Propulsion System Trade Studies and Analysis Report

The fuel burn, LTO NOx, and community noise goals for this study are extremely challenging. The small size of the aircraft, and relatively short-range missions present some significant additional challenges. For the short range missions (<800 nmi) of the advanced N+3 network, mission fuel burn amounts to <10% of aircraft weight, so SFC improvements do not compound into much greater fuel burn savings as they do in longer range aircraft. The very small engine size limits the many normal avenues for reducing fuel consumption and emissions. And blended-wing-body or delta wing designs that would allow superior noise shielding or benefit from distributed propulsion, would result in higher drag in this size and speed class.

Propulsion system trade studies were conducted to determine the configuration and technologies with the greatest potential for meeting the study goals and achieving commercial viability in 2030 timeframe. GE's Aviation and Global Research divisions identified advanced propulsion system technologies, components, and engine configurations as potential candidates for our Advanced 2035 Airliner. These concepts were first reviewed at the study team's technology identification workshop. Additional technologies were added as the study progressed. GE simulated the advanced engine technologies and concepts, and then developed scalable performance and installation data for Cessna and Georgia tech to use in their advanced aircraft studies. A TOPSIS ranking was used to help select the best advanced propulsion system concept for the selected advanced 2035 airliner.

GE conducted an advanced propulsion design space exploration to better quantify the impact of advanced technologies, and to understand the issues and challenges to achieving the

study goals for this class of aircraft. An advanced, very-high bypass turbofan was defined to explore the potential of advanced propulsive and thermal efficiency technologies for this application. It was used as the reference point for evaluating the impact of cycle pressure ratio, turbine temperature, and bypass ratio on the study metrics. The Advanced Reference Turbofan was also used as the baseline for evaluating other more unconventional propulsor and power generator configurations. Multiple, distributed fans, counter-rotating ducted and open rotors, and advanced propellers/propfans concept were considered versus the Advanced Reference Turbofan. Constant volume topping cycles (such as a pulse detonation combustor) were evaluated for potential to improve core thermal efficiency in this small engine size. Electric motor driven propulsors powered by batteries, fuel cell, and hybrid fuel cell/turbomachinery concepts utilizing hydrogen or jet fuel were also evaluated.

6.2.1 Advanced Reference Turbofan

The Advanced Reference Turbofan engine concept incorporates all the advanced materials, aero, acoustic, mechanical systems, and combustion technologies we have defined for the 2030-2035 timeframe, including those listed below. This engine was used to explore the propulsion challenges in meeting the N+3 goals for this future small commercial airliner market. A scalable performance, noise, and installation data package was developed for the Advanced Reference Turbofan and provided to Georgia Tech and Cessna for their advanced aircraft studies. Technologies incorporated into the Advanced Reference Turbofan include:

Advanced materials/cooling

- Higher temp/strength Next Generation CMC airfoils and combustor/flowpath liners
  - Next Generation environmental barrier coatings
- Higher temp/strength disk/shaft materials
  - Dual Alloy Turbine Disk and Dual alloy Hi-Temp Ti Impeller
  - Next Gen High temp GE1014 shafts
- Advanced Composite Fan, OGV, Nacelle, Front frame, Core Cowl, AGB

Advanced mechanical systems

- Advanced seals and improved rotor/stator flow discouragers
- Advanced air bearings and Hybrid ceramic bearings
- Advanced active clearance control including impeller shroud. (Enabling high efficiencies w/ small components)

Advanced aero/operability/manufacturing

- Improved airfoil & end wall contour, min thickness for high efficiencies with small components
- Active stall/surge prediction/detection/control
- Variable A18 for operability and performance optimization for low FPR designs

Figure 154 shows a cross-section of the Advanced Reference Turbofan in it nominal thrust size. It is a 10:1 BPR separate flow turbofan, with a 1.6 pressure ratio direct-drive fan which is ~29 inches in diameter. The engine is sized to produce ~630 lb of thrust at its max cruise rating at 41K/0.6M. The engine overall pressure ratio and turbine temperatures would be considered moderately high for a much larger engine, but are very high for and engine of this size. Overall pressure ratio is adjusted to maintain minimum airfoil dimensions as the engine size is scaled to meet the thrust requirements of the studied aircraft.

Engine component performance at the critical 41K Max Cruise rating is shown in Figure 154. Significant development in aero, manufacturing, and systems technologies would be required to achieve this level of component performance given the extremely small airfoils and ultra-low Reynolds numbers. Figure 155 shows some of the mechanical systems technologies required to attain this level of performance.

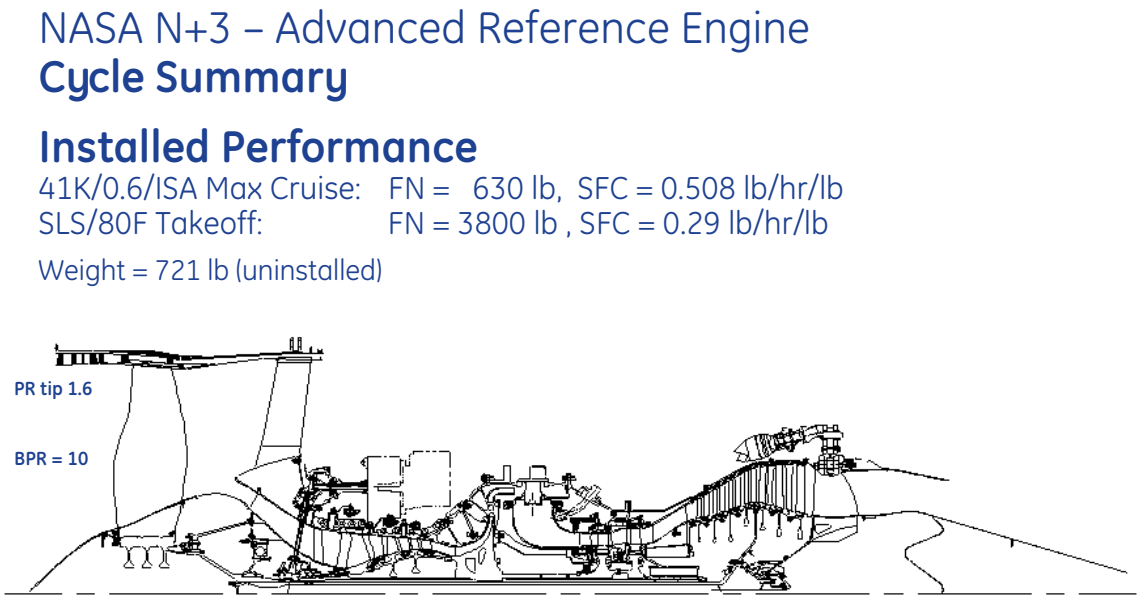

Figure 154. Advanced Reference Turbofan Overall & Component Performance

Figure 156 shows the material technologies that enable the engine to achieve this level of OPR and T41 with fewer stages and far lower secondary flows than today's engines. CMC airfoils and combustor liners, advanced integrated composite structures, and high-temperature titanium alloy technologies will be require to achieve the engine weight goals.

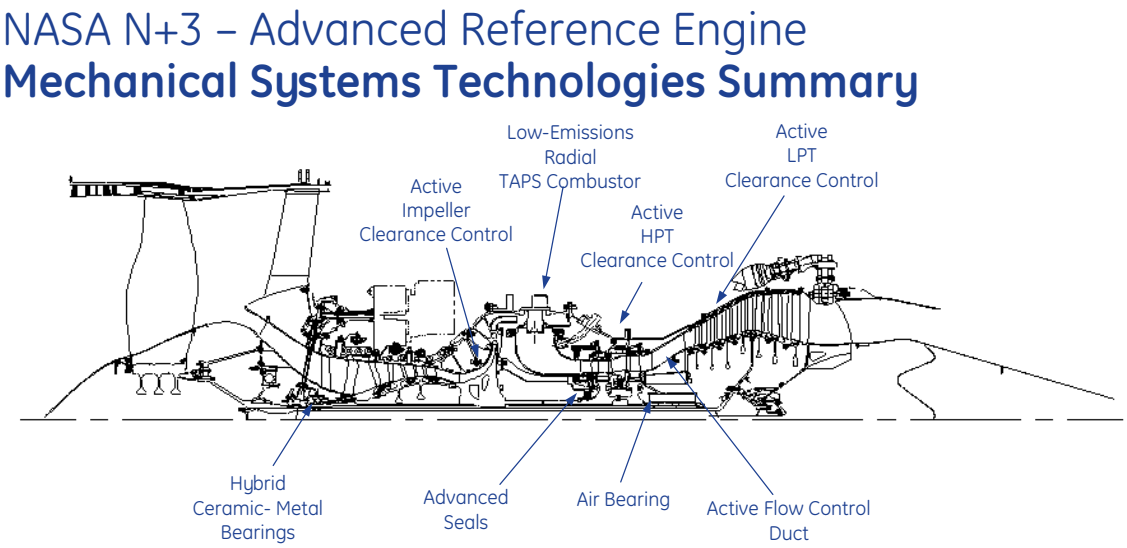

Figure 155. Advanced Performance-Enabling Mechanical Systems Technologies

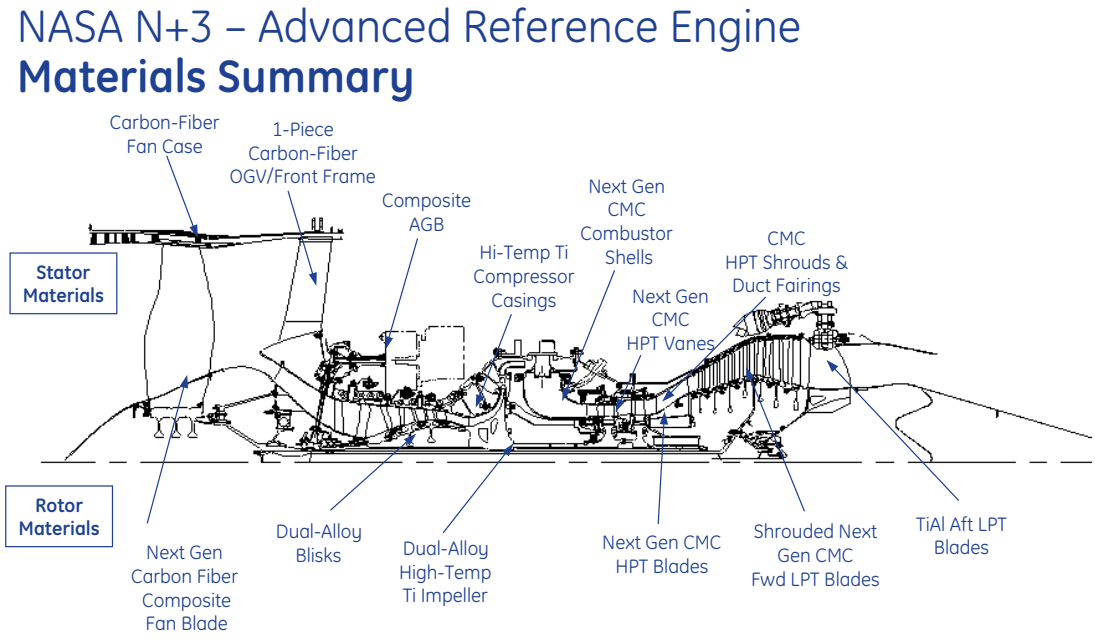

Figure 156. Advanced Reference Turbofan Materials Technologies

The Advanced Reference Turbofan's very high bypass ratio cycle alone results in noise levels 30 to 40 EPNdB cum below regulations. Advanced noise suppression technologies and airframe shielded can provide further reduce community noise levels. Figure 157 shows some of the integrated nacelle and acoustic technologies evaluating in these studies.

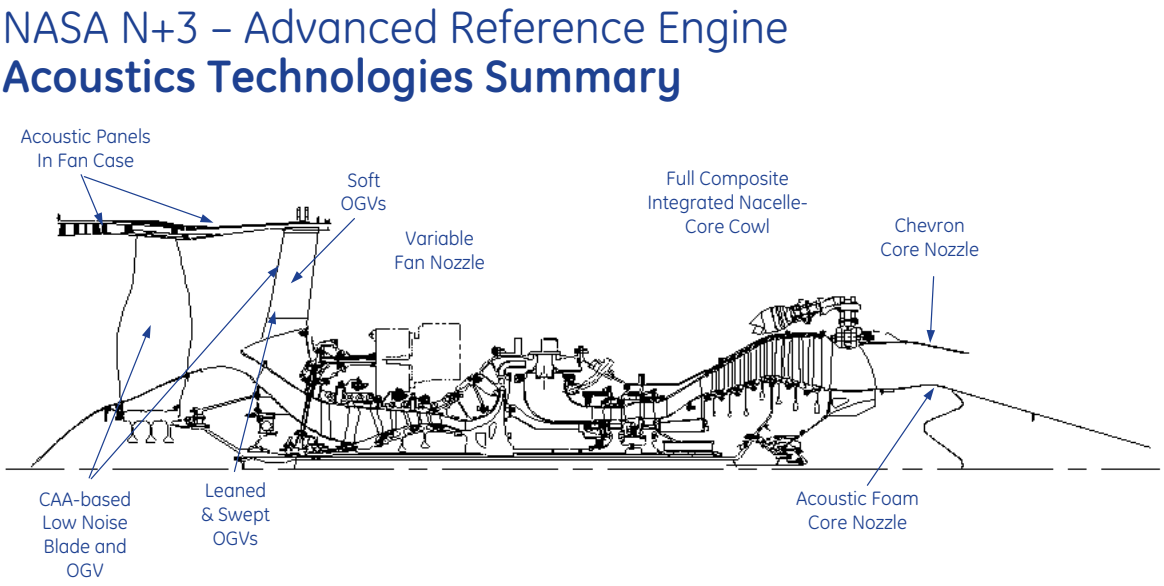

Figure 157. Advanced Reference Turbofan Integrated Nacelle, Acoustics Technologies

6.2.2 Thermal Efficiency Studies

Findings from the advanced reference turbofan studies indicated several areas of challenge. First was the extreme challenge of engine size on performance and emissions. Due to the reductions in drag and weight brought about by the technologies of the advanced aircraft, thrust requirements are significantly reduced from the baseline engines. To properly explore issues related to engine size, the advanced engine was assumed to have a cruise thrust requirement more than 30% lower than the baseline aircraft. Parametric studies were performed to assess the impact of fan and overall pressure ratio, bypass ratio and turbine temperature on engine size, weight, SFC, NOx, and noise. The effects of airfoil size on component efficiencies, and the effects of T3 and T41 on cooling flow and emissions, were taken into account.

Figure 158 shows the impact of turbine temperature and overall pressure ratio on bypass ratio and SFC for Advanced Reference Turbofan. Even with very aggressive airfoil size ameliorating technologies, there appears to be small SFC benefits of ultra-high overall pressure ratio cycles in this thrust class. Similarly, ultra-high turbine temperatures allow higher engine bypass ratios and reduced core size, but no real added benefit in SFC. This is partly due to the impact of size effects on the high-pressure turbomachinery. Even at the moderately high overall pressure ratio and turbine temperature of the Advanced Reference Turbofan, the high-pressure compressor and turbine corrected flows, and therefore airfoil dimensions, are smaller than any current high performance turbomachinery. Significant manufacturing and clearance control technology development will be required to attain this level of performance at the miniature airfoil dimensions implied by these corrected flows. Increasing overall pressure ratio beyond the Advanced Reference Turbofan's level also has little SFC benefit, due to airfoil size effects. An additional 25% pressure ratio improves SFC by only 1%, but would add significant engine weight, cost, manufacturing and performance risk, and NOx emissions. Similarly, further increasing turbine temperature also reduces the size of the engine core turbomachinery (Figure 159), with the expected impact on component efficiencies. Pressure ratios and T41's higher than the Advanced Turbofan in this thrust class will result in airfoil dimensions inconsistent with high performance turbomachinery.

Impact of T41 and OPR on SFC and BPR

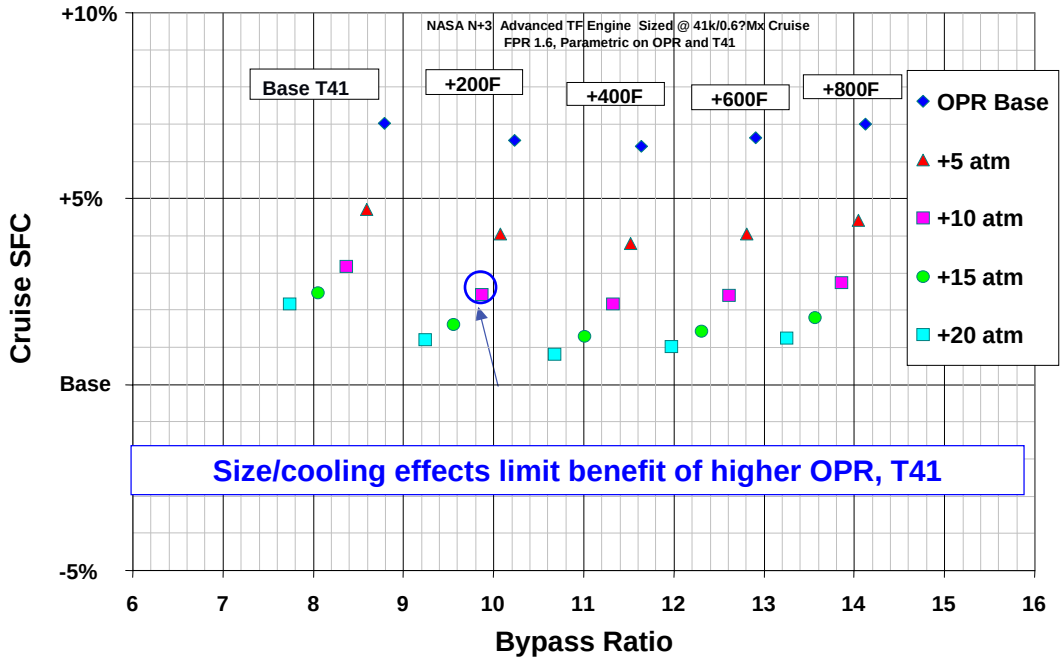

Figure 158. Impact of Pressure Ratio and T41 on SFC and Bypass Ratio

Impact of T41 and Pressure Ratio on Turbomachinery Size

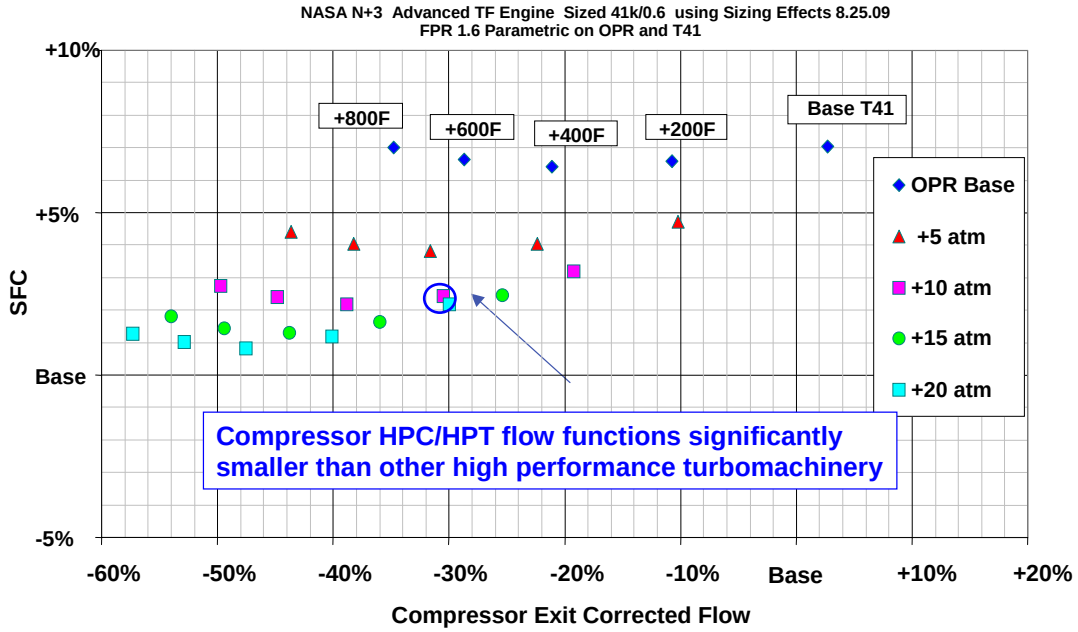

High T41, High OPR, High BPR Reduce Airfoil Sizes & Increase Losses

Figure 159. Impact of T41 and Pressure Ratio on High Pressure Turbomachinery

The negative impact of higher turbine temperatures on performance in this thrust class goes beyond considerations of minimum airfoil size or cooling. The advanced engine will be significantly smaller in thrust and ~3 times higher bypass ratio than the baseline engine, resulting in core flows that are a small fraction of the baseline. Yet the customer offtakes required for the N+3 future airliner do not scale down, as future passengers will require the same amount of cabin bleed air as today. For these small, advanced engines, customer offtakes will consume more than 20% of core airflow and power at cruise, negatively impacting SFC by at least 10%. Further increases in T41 would drive the core smaller, resulting in increased fuel consumption.

Limiting T41 has other benefits in this application. With significant development in CMC material and manufacturing technology, moderately high turbines temperatures may be achievable with uncooled HPT blades in this timeframe. Combined with advanced thermal and environmental barrier coatings, minimally cooled CMC combustion liners could also be achievable at this level of T3 and T41. Dramatic reductions in turbine and combustor cooling, and combustion temperatures, would allow very lean fuel/air ratios in the combustor front end, greatly reducing NOx emissions. Additionally, as CMC a fraction of the density of turbine alloys, the lighter airfoils reduce turbine rotor weights by about half.

Limiting redline T41 and overall pressure ratio to maintain certain minimum compressor and turbine airfoil heights appears to be the best strategy for positively impacting fuel burn and NOx in this size class. As the Advanced Reference Turbofan was scaled to meet the thrust requirements of the various studied aircraft, redline T41 was maintained and overall pressure ratio set to maintain minimum turbomachinery airfoil dimensions.

6.2.3 Propulsive Efficiency Studies

Another avenue to reduce fuel consumption and emissions is to increase bypass ratio to increase propulsive efficiency. Turbofan, distributed propulsion, and single- and counter-rotating open rotor propulsors were considered for their impact on fuel burn, emissions, field length, and noise through increased effective bypass ratio.

Reducing fan pressure ratio (to increase BPR) generally reduces specific fuel consumption, as well as the dominant sources of engine noise; fan tip mach numbers and exhaust velocity. Figure 160 shows the impact on cruise SFC of reducing fan pressure ratio at a constant overall pressure ratio and T41. Increasing bypass ratio and reducing FPR reduces SFC, at the expense of specific thrust. Reducing cruise fan pressure ratio below 1.6 increases the Advanced Reference Turbofan's engine weight and drag by at least 4% for every 1% gain in SFC, due to the larger fan. The aircraft fuel burn sensitivity studies indicate that a 1% improvement in SFC can only offset about 2.3% engine weight gain. This indicates that much lower fan pressure ratios will not necessarily benefit mission fuel burn. Fan pressure ratio may be reduced to improve noise, however, at some slight expense in fuel burn. Reducing FPR from 1.6 to 1.45 (which increases BPR from 10:1 to 13) results in ~7 EPNdB cumulative noise margin improvement.

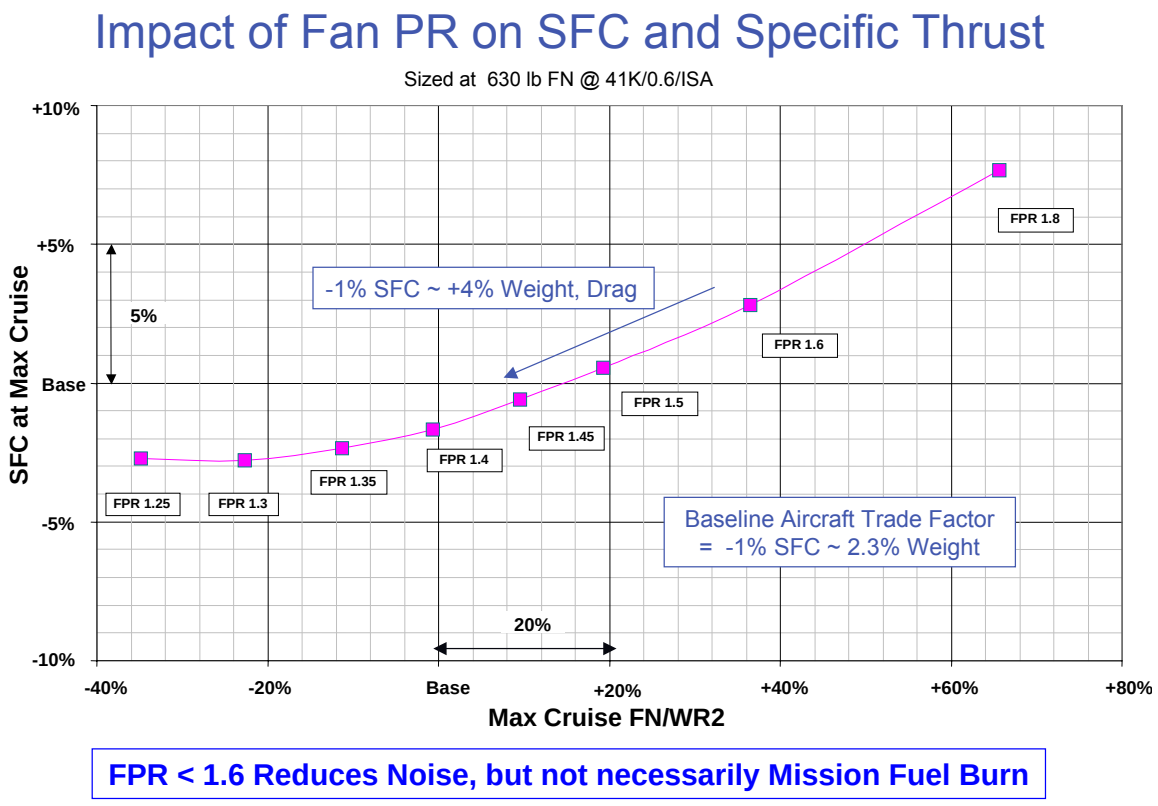

Figure 160. Impact of Fan Pressure Ratio on Cruise SFC and Specific Thrust

Our studies indicate that with the advanced materials assumed in this study, bypass ratio would be limited to ~13:1 for a moderately high OPR *front-drive* turbofan in this size class. The engine core's small airflow and high-pressure ratio dictates the need for an axi-centrifugal compressor design. This results in inherently low turbomachinery radius ratios and core bores than an all-axial compressor design. The small core bore diameter limits the fan shaft diameter and therefore its torque carrying capability. Large diameter (higher BPR) fans turn more slowly, and therefore generate more torque for a given fan power, so the core bore diameter limits the diameter of the fan.

A geared fan, driven by a high-speed LP turbine, does not appear viable option for achieving ultra-high bypass ratios for this particular application. The high-speed LP shaft actually requires a *larger* shaft diameter than the direct drive fan. The much higher speed of the geared fan's LP shaft requires a large diameter to attain the stiffness required to tune critical speeds out of its dynamic operating range. High stiffness LP shaft materials capable of providing an operating range free of critical speeds are not anticipated to have adequate strength in this timeframe. Various bearing arrangements were also considered, along with advanced bearing concepts with dynamically variable stiffness, without any desirable solutions. At the restricted core bore mandated by a small, high performance axi-centrifugal core design, It does not appear possible to achieve a dynamic operating range free of critical speeds with an UHB front-drive geared fan. Offset cores, rear-drive fans, distributed fans, or unconventional topping cycles would be required to achieve higher bypass ratios.

Variable pitch open rotor systems allow much higher bypass ratios, while eliminating the LP shaft dynamics issues and the weight of the fan cowl. Both single rotating (turboprop) and

counter-rotating open rotor systems were considered for this application. Counter-rotating systems allow the elimination of the losses due to exit swirl. This is critical at higher Mach numbers (> 0.7), and allows efficient cruise at Mach numbers competitive with turbofans. This application cruises at much lower Mach numbers (<0.6) in order to minimize aircraft wave drag and maximize aircraft laminar flow. At these speeds, the additional propulsive efficiency benefit of a counter-rotation is relatively small, but the interaction noise penalty large. Counter-rotating open rotors do not appear to be the best solution to meeting the –71 EPNdB noise metric.

A more detailed propulsive efficiency study was developed to assess the impact of turbofan fan pressure ratio, and compared to an open rotor propulsor. Table 53 shows the results of this study. An advanced turboprop was developed for comparison to the Advanced Reference Turbofan. Three advanced engine concepts were defined to the same level of technology, turbine temperature, minimum airfoil size, and cruise thrust. The propulsive and thermal efficiency improvements of the 1.6 FPR advanced turbofan yields a 28% improvement in cruise SFC vs. the baseline engine. The Advanced Reference Turbofan's lower fan pressure ratio, higher BPR, and smaller size would also result in noise reductions equivalent to a 12 EPNdB improvement in cumulative margin vs. the baseline engine. Optimization and application of GE's advanced noise reduction concepts would yield significant further improvement. Reducing the fan pressure ratio to 1.45 would improve SFC by an additional 3%, takeoff thrust by 7%, and noise margin by an additional 7 EPNdB, at the expense of adding 100 lbs to engine weight due to the larger fan. An advanced turboprop could yield an additional 21% SFC improvement over the higher bypass turbofan, and even greater takeoff thrust, at the expense of >>50% propulsion system weight increase. The superior takeoff trajectory and lighter disk loading of the propeller allow for even greater noise reduction with a properly optimized design.

An aircraft system sizing study was performed to assess whether the SFC improvement of the turboprop outweighed its weight disadvantage compared to the turbofan. Scalable propulsion system performance, weight, and dimension data tables were developed for both the turbofan and turboprop. Both pusher and tractor prop configurations were evaluated. Nacelle drag and impact of the propulsor on aircraft drag were also modeled. This study showed the tractor turboprop configuration to have ~20% fuel burn advantage over the turbofan. The pusher prop configuration was also superior to the turbofan, but higher fuel burn than the tractor configuration due to higher exhaust losses, lack of inlet supercharging by the propeller, and impact of the wing wake on propeller performance. The wing wake was also predicted to have a significant negative impact on propeller noise. The tractor prop configuration is also safer, as emplaning passengers would be pushed away, rather than towards, a running propeller. These factors indicated that a tractor propeller configuration is the superior choice for this relatively low speed application.

Table 53. Propulsive Efficiency Impact on Weight, SFC, and Noise

Propulsive Efficiency Study

Impact of Fan PR at Constant T41, Min Airfoil Size

	Baseline 2008 Turbofan	Advanced Turbofan	Advanced Turbofan	Advanced Turbopop
Fan tip PR	**1.69**	**1.6**	**1.45**	η_{prop} 90% η_{gb} 98.5%
41K/0.6/ISA Mx Cr				
Thrust	920	630 (-32%)	630	630
SFC	0.705	0.508 **(-28%)**	0.494 **(-30%)**	0.391 **(-45%)**
Dfan	30"	28.9"	32.1"	12.4 ft
BPR	3.5	10.2	13.1	
SLS/80F Take Off				
Thrust	4400	3800	4050	5500
TSFC	0.47	0.29	0.26	0.17
Weight	1030	721	820	1290
Thrust/Wt	**4.3**	**5.3 (+23%)**	4.9 **(+16%)**	**4.3**
Cum Noise EPNdB (w/o technology or trajectory benefits)	251	238.4	231.7	~220

Turboprop's superior SFC, Emissions, Noise vs. Weight Penalty

6.2.4 Impact of Cycle and Advanced Technology on LTO NOx.

For a given level of combustor technology, LTO NOx is largely a function of SFC, T3, and T41. The advanced engine's SFC improvements, due to increased BPR (propulsive efficiency) and reduced losses and cooling (thermal efficiency), dramatically reduce NOx vs. the baseline engine. While the OPR and T41 of the advanced engine are significantly higher than the baseline engine, higher compressor efficiency and improved hot section materials and cooling yield reasonable T3's and T4's. The impact of these combined effects on the advanced reference turbofan is shown in Table 54. The advanced turbofan, with RQL combustor technology similar to the baseline engine, would produce 57% fewer grams of LTO NOx per trip compared to the baseline engine. The advanced turbofan's LTO emissions would be about ~60% below the CAEP/6 requirement for a 6000 lb FN turbofan. While this is a dramatic improvement, meeting this study's goal requires and additional 38% reduction in LTO NOx beyond RQL combustor technology.

Advanced combustor technology is required to meet the aggressive N+3 LTO NOx goal. GE has studied the development of an Innovative, Radial Twin Annular PreSwirl (TAPS) Combustor to bring this advanced, low emissions combustor technology to this size class. Our studies indicated that this technology has the potential to reduce LTO emissions to meet the N+3 goals. The selected advanced propulsion system description and Radial TAPS technology roadmap in this study describe the significant challenges to scaling this technology down to this very small size class.

Table 54. Reduction in LTO NOx due to Improved Propulsive & Thermal Efficiency

Emissions Goal: -75% LTO NOx vs. CAEP/6

LTO NOx is a Function of SFC, OPR, and T41

> Reducing fuel burn via improved propulsive efficiency helps

> Reducing fuel burn via reducing losses/cooling (thermal efficiency) helps

> Reducing fuel burn via increased OPR (T3) and T41 increases NOx

Advanced Engine LTO NOx with RQL Technology

	2008 Baseline	Advanced TF Cycle
Flat Rated Thrust (lb)	4400	3801 (-14%)
BPR	4	10
OPR	22	Higher
T41 R/L	2300F	Higher
LTO NOx vs. CAEP/6 (g/kN FN) **(relative to 6000 lb FN req't)**	-25%	**-60%**
LTO NOx (g/cycle)	825	352 (-57%)

Improved Prop & Thermal Efficiency and Reduced Thrust Req't

Additional Technologies Needed to Achieve –75% LTO NOx

6.2.5 Noise Trades: Key to community acceptance.

The 2030 network studies indicate that the demand for the direct point-to-point travel offered by the N+3 network could increase fourfold by the Year 2030. But the number of community airports willing to tolerate this increased traffic may be limited unless it has minimal impact on community noise. Most community airports are already far louder than NASA's goal of 55 LDN at the airport boundary. Adding commercial service to these airports is likely to encounter resistance if there is a significant noise increase for the local community. NASA's current N+3 metric of 71 EPNdB cumulative margin to Stage 4 appears appropriate to use as a goal to keep community noise impact to acceptable levels. Figure 161 shows the cumulative noise levels relative to the Stage 4 requirement for currently certified small airplanes.

It can be seen that turboprops are generally quieter than turbofans, and that existing turboprops would be able to meet Stage 4 requirements. The B20 baseline aircraft for this study has good noise performance due to its modern mixed flow turbofan, but is only about 20 EPNdB below the Stage 4 limit. Increasing bypass ratio to as high as 13:1 could potentially reduce noise to levels approaching the N+2 goal levels, even without the use of advanced noise suppression technologies. Achieving the extremely challenging N+3 goals will require advanced propulsion and airframe technologies, and an innovative ultra-quiet propulsor.

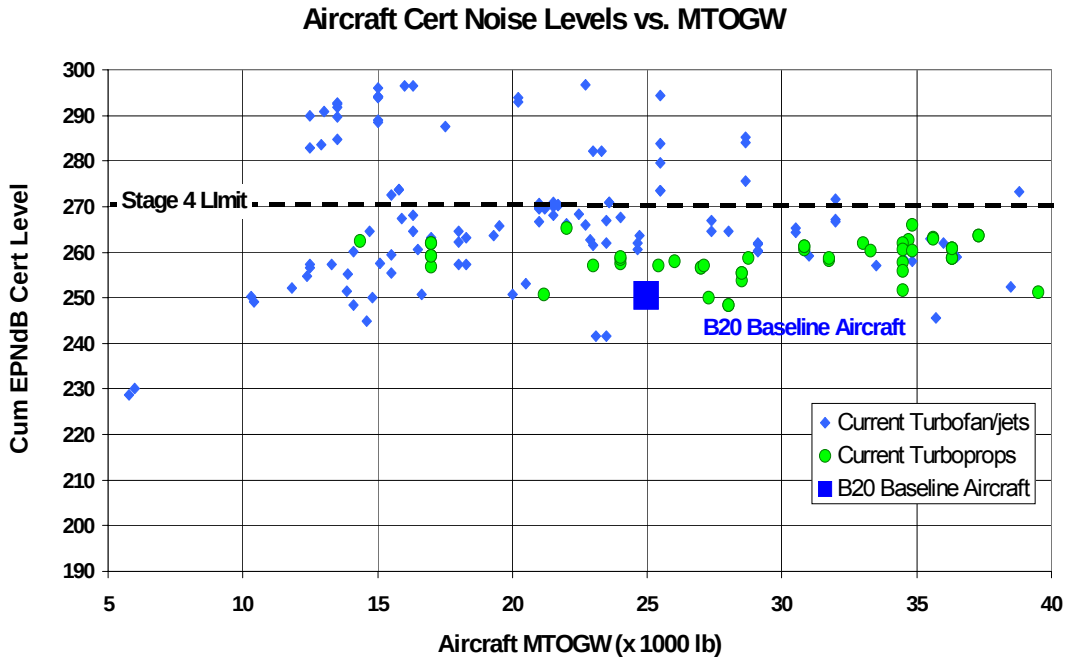

Figure 161. Aircraft Certification Noise Levels vs. Weight

Turbofan, turboprop, and open rotor engine architectures were considered from a noise perspective. Turbofan predictions were made using ANOPP, based on performance estimates generated by the cycle model and WATE and trajectories calculated by FLOPS. The noise certification levels shown for the turbofan engines in this report were calculated based on the dominant noise contributions of the jet, fan, and airframe sources. No predictions were initially calculated for turbine, core/combustor, or compressor noise, as these typically are not major contributors in modern high bypass or turboprop engine configurations.

6.2.5.1 Advanced Turbofan Noise Estimates

Initial estimates of the airframe noise for the baseline aircraft were 60.84, 63.44, and 73.71 EPNdB for the cutback, sideline, and approach observers, respectively. These estimates included wing, tail, flaps, and gear noise as calculated by the Fink module in ANOPP. Slat noise was not included as slats were not present on any of the aircraft considered. The reduced weight of the advanced aircraft and improved aerodynamics allowed a reduction of the flap size and complexity to a small simple flap. Further, the changes made to the airframe to enable laminar flow also help noise. With laminar flow over much of the forward half of the aircraft, it can be considered aerodynamically clean, producing an 8 dB reduction in the wing noise component. With these improvements, the airframe noise calculated by ANOPP for the advanced aircraft is 54.5 EPNdB at the cutback observer, 57.5 at the sideline observer, and 69.9 at the approach observer.

Noise estimates for the advanced turbofan engine were calculated based on the methods described. From a noise perspective, the best turbofan concept was a high bypass ratio engine, with a fan pressure ratio reduced to approximately 1.45. This concept was used for all noise estimates to follow, even though performance considerations might dictate the selection of a

different option. To calculate the noise levels at the three certification observers, the engine characteristics were computed for a standard acoustic day, and the noise certification trajectory was computed in FLOPS using the new airframe and engines. The combination of aerodynamic, structural, and propulsive technologies combined to bring the noise down to 222 EPNdB, cumulatively for the three observers, due to the use of quieter engines at higher altitude. The combination of jet and fan technologies shown in Table 55 were applied at this point. The effect of each technology at each observer location was estimated, and the result was a reduction of 3 dB in jet noise at each of the takeoff observers. Fan inlet noise was reduced by 3 dB at the takeoff locations and 6 dB at approach, while fan exhaust noise was reduced by 2 dB at takeoff and 4 dB at approach. A sensitivity study of the total level at each observer location against reductions in each source component allowed an accurate estimation of the combined effect of the component reductions. The improvements to airframe noise were already included in the noise levels used as a starting point for the sensitivity study. The combined reductions of 3.17, 3.35, and 4.24 EPNdB at cutback, sideline, and approach respectively were then applied to the levels for the corresponding observer. The final results for the advanced turbofan engine on the advanced airframe are shown in Table 56, indicating a cumulative level of 211.22 EPNdB, 59.78 dB below Stage 4.

6.2.5.2 Advanced Turboprop Noise Estimates

Previous research has clearly established that counter-rotating propellers are noisier than single rotating propellers due to the interaction effects. Once it was established that a cruise Mach number of 0.6 or less was optimal for this N+3 aircraft, the efficiency of a propeller at these speeds was sufficient to allow the elimination of the open rotor designs on the basis of noise and performance. Prediction capability for advanced turboprop engines was quite limited given the fidelity of the propeller modeling in this phase of the study. Without detailed blade shapes or aerodynamic loads, only one well-established, publicly available method was appropriate, an empirical approach detailed in SAE AIR-1407[26]. This method provides an estimate for the full flyover metrics (such as EPNL) based on a basic list of inputs, including number of blades, RPM, diameter, number of propellers, input power, flight speed, ambient temperature, and distance to the observer. Because the AIR-1407 method was expected to perform best with the propeller at full power, only the level at the sideline observer was calculated in this manner, with a result of 73.38 EPNdB. This full power level was used as a reference point to identify a noise-power-distance curve (NPD) from the AEDT database that could be considered representative of the new aircraft. Only turboprop aircraft in the AEDT database were considered under the assumption that the scaling laws for extrapolating to different power settings would be more appropriate with the same type of engine. Because of the technology level of the advanced aircraft, the identified aircraft was much smaller, a Beech Mentor. The NPD was modified slightly to match the output from the SAE method. The error associated with the process is clearly not ideal, but most of the assumptions were made in a manner such that the results would err on the high side, hopefully producing a conservative estimate of the noise benefits. Use of the modified Beech NPD resulted in estimated levels of 54, 73, and 70 dB at the three observer locations.

The NPD inherently includes all of the noise produced by the aircraft, not just the noise from the propeller. Thus, the levels reported are for the turboprop (propeller and engine noise sources) and the airframe. For a very quiet engine operating close to idle during approach, one would expect that the airframe noise would dominate for this observer. As mentioned earlier, the airframe noise estimate for the advanced airframe is 69.94 dB at approach, which corresponds quite well with the 70 dB estimated from the NPD. Thus, the prediction for the turboprop on approach is assumed to be dominated by airframe noise with a level of 70 dB.

Similarly, the cutback trajectory calls for the turboprop to operate at 55% power, and the estimated level from the NPD is 54 dB. The airframe noise is slightly higher, at 54.46 dB, but it is possible that the engine noise would also be a factor once the propeller noise has been reduced this far. As a result, an estimate of the exhaust jet noise was made based on exhaust conditions from the cycle analysis. At all three certification points the estimated jet noise was approximately 20 EPNdB below that estimated from the propeller, thus jet exhaust noise can be neglected. The noise from the turbomachinery was not estimated due to the level of study of the program but it is assumed that with the 'S'-duct inlet to the core and the inclusion of the noise reduction technologies already discussed in Table 55 for fan noise, these noise components would also not be significant factors in the overall system noise. Assuming the worst case for approach noise, the 54 dB from the NPD can be assumed as propeller noise, and when combined with the airframe levels, the resulting noise at approach is about 57 dB. Propeller technologies could only be applied for the takeoff observers, where the propeller noise is dominant. The technologies listed in Table 55 were estimated to produce a combined 3 dB reduction at sideline and 1 dB at cutback, resulting in levels of approximately 70 and 56 EPNdB, respectively. Combining the estimates for the three observers produces a cumulative level of 196 dB, 75 dB below Stage 4.

6.2.5.3 Noise Comparison between Turbofan and Turboprop Engines

Sideline estimates of the noise from the advanced turboprop and the best advanced turbofan were similar, with the turbofan around 73 EPNdB and the turboprop around 70 EPNdB. The noise levels predicted for the advanced aircraft with the 13:1 bypass ratio advanced turbofan engines, including the application of technologies, are shown in Table 56. The noise certification levels for the advanced turboprop aircraft, calculated as discussed above, are shown in Table 57. Estimates of the noise produced by the turboprop at off-design conditions were substantially lower than predicted for the turbofan. This improvement was achieved through the use of a propeller designed for noise reduction, with a large diameter and many blades, resulting in a quieter source operating at a low tip speed. The extra power available from the turboprop proposed herein allows a steeper departure trajectory, which passes over the cutback observer at a higher altitude. As would be expected for an extremely quiet engine, the airframe noise becomes dominant during approach. The airframe noise was reduced for both engines through the introduction of aerodynamic improvements to minimize the size and weight of the aircraft and to improve the flow over the necessary control surfaces.

Based on the above noise prediction methodology, the advanced turboprop is estimated to be 15 EPNdB cumulatively lower than that achievable with an advanced turbofan. The superior noise performance of the advanced turboprop, combined with its superior fuel consumption, make it the obvious choice for the Advanced N+3 Air Vehicle.

Table 55. Noise Technologies Applied to the Engine Concepts

Jet Noise
3D Integrated Propulsion Systems (Installation effects)
Shape Memory Alloy / Variable shape Chevrons (Fan & Core)
Non-axisymmetric/Beveled Nozzles
Offset High Speed Stream
Fan Noise
CAA based Low Noise Blade / OGV Design
Soft / Active OGV
Zero splice lip, inlet & fan case liners
Optimized Zone Nacelle Liners
Scarfed Inlet
Inlet Blowing
Active Rotor Wake Control
Propellor Noise
CAA based Low Noise Prop
Active Pitch Control
Active Flow Control
Non-uniform Blade Arrangements
Tip Speed Optimization

Table 56. Noise Certification Levels for the Advanced Turbofan Concept

Advanced Turbofan Aircraft Noise Levels		
Takeoff	59.62	EPNdB
Sideline	73.21	EPNdB
Approach	78.39	EPNdB
Cumulative	211.22	EPNdB
Cum Below Stage 4	59.78	EPNdB

Table 57. Noise Certification Levels for the Advanced Turboprop Concept

Advanced Turbofan Aircraft Noise Levels		
Takeoff	56	EPNdB
Sideline	70	EPNdB
Approach	70	EPNdB
Cumulative	196	EPNdB
Cum Below Stage 4	75	EPNdB

6.2.6 Unconventional Propulsion Concepts

Due to the extremely challenging N+3 fuel burn, emissions, and noise goals, unconventional and integrated propulsion/air vehicle technologies were evaluated for their potential to meet the study metrics. Distributed propulsion, unconventional topping cycles, fuel cells and alternate fuels were studied for their potential to address this metric.

6.2.6.1 Multiple, Distributed Propulsors for Reduced Noise and Increased Propulsive Efficiency

Distributed propulsion concepts use a large number of ultra-low pressure ratio fans (or fan ducting slots) to efficiently re-energize the aircraft boundary layer, with the goal of achieving high effective propulsion efficiency. This small, low speed N+3 application, however, does not lend itself to the types of configurations (delta wing, blended-wing-body) that would benefit most from distributed propulsion. Advanced technologies have significantly reduced the size of the N+3 airliner, but not the height of its passengers. A delta wing or hybrid wing body design combined with the minimum passenger cabin height would result in a very thick and high drag wing. For this low speed application, a very high aspect ratio, short chord wing is most desirable to minimize drag and takeoff field length. The Advanced Airliner's calculated boundary layer height on the fuselage of the selected advanced concept is on the order of magnitude of an inch. The boundary layer on the wings is predicted to be much less than an inch. Distributed propulsion would increase aircraft weight, with minimal if any benefit in effective propulsive efficiency when the ducting drag and losses are included. While the lower fan pressure ratio and airframe shielding could dramatically reduce noise, it would come at a significant penalty in fuel burn and emissions.

6.2.6.2 Pulse Detonation Combustion (PDC) Topping Cycle

Pulsed Detonation Combustion can have significant performance benefits when employed for topping gas turbine engine cycles. A pulse detonation combustor integrated into an advanced turbofan was studied for this application.

A conventional turbine engine employs a deflagration combustor that generates a temperature rise at the expense of a small pressure loss. Detonation combustion actually results in a significant pressure rise from the heat addition (see Figure 162). The pulsed detonation combustion cycle of filling, ignition, detonation, expansion, purging, and filing again is somewhat analogous to that of an internal combustion engine (Figure 163).

What is a detonation?

- Detonation is one of several possible modes of combustion
- Key feature: pressure-rise combustion

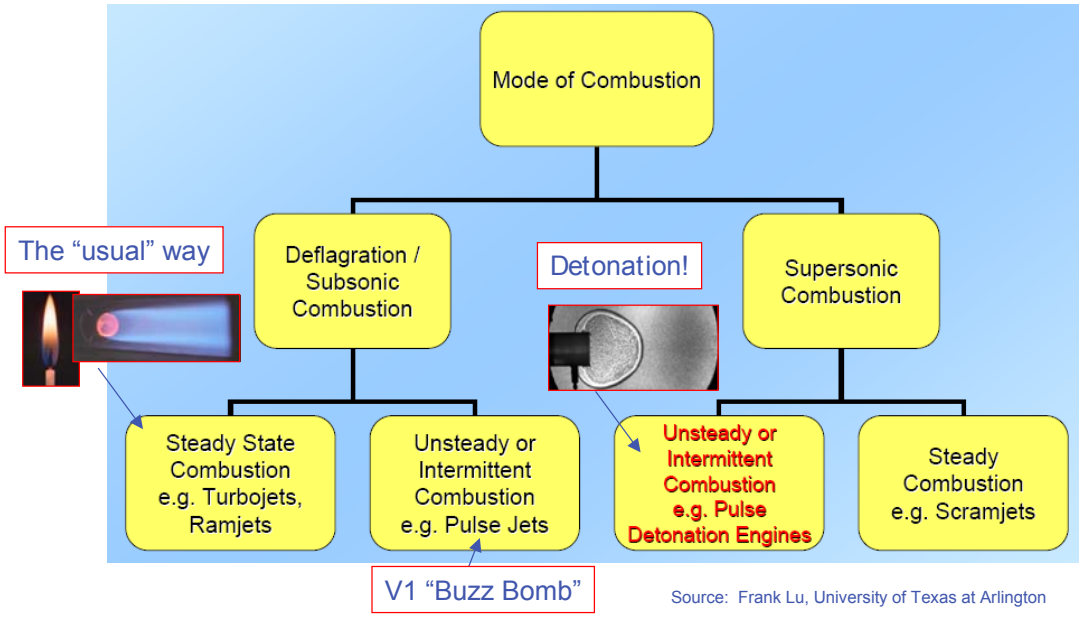

Figure 162. Pulse Detonation Combustion Results in a Pressure Rise

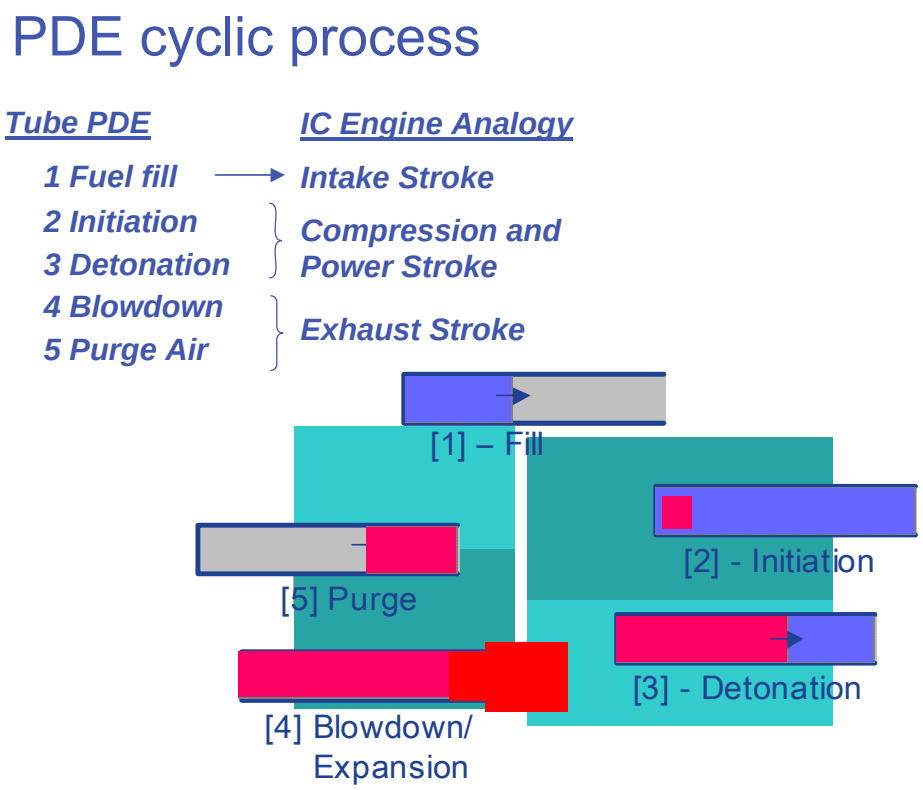

Figure 163. Pulse Detonation Combustion Cycle Analogous to IC Engine

A pulse detonation combustion topped turbofan was studied in the same nominal thrust size as the Advanced Reference Turbofan. The advanced turbofan's combustor was replaced with a pulse detonation combustor, and effective cycle pressure ratio was varied to find the optimum for fuel burn. The strength of the detonation and the associated time-average pressure rise increases with the temperature rise across the combustor. Conversely the benefits of PDC topping are more limited if the base cycle is already a high pressure ratio design, as the delta T across the combustor will be small. Compared to the moderately high pressure ratio advanced reference turbofan, there was a significant SFC gain at the max cruise operating condition. SFC improvement was somewhat larger at reduced powers and smaller at higher powers. However, the SFC improvement due to PDC topping does not appear to offset the significant added weight of the Pulsed Detonation Combustor and associated hardware for this application. The increase in propulsion system weight outweighs the SFC benefits for the N+3 airliner, as this short-range aircraft's fuel burn is very sensitive to aircraft weight. Additionally, the high peak temperatures and pressures of the detonation combustion are likely to result in levels of NOx production higher than the N+3 goals. Other constant volume topping cycles such at internal combustion engines also have high peak temperatures and pressure and poorer power to weight ratios compared to gas turbine cores.

Pulse detonation combustion as a topping cycle to enhance SFC appears to be better suited to longer range aircraft that are less sensitive to weight, or to ground applications.

6.2.6.3 Fuel Cell Propulsion

Both Proton Exchange Membrane (PEM) and Solid Oxide Fuel Cells (SOFC) prolusions systems were evaluated for this application. Figure 164 shows the high level characteristic of both types of fuel cells.

Solid oxide fuel cells require preheating of the inlet air to the 600°C to 1000°C range. They also consume only about 80% of the fuel processed. For these reasons, they are generally thought to work best as part of a hybrid system with a gas turbine, where the resulting combined cycle can theoretically achieve thermal efficiencies in the 70% range. Rough estimates for performance and weight of a SOFC/gas turbine hybrid engine were generated using liquid hydrogen as a fuel. Weight and performance estimates were also generated for a system with a reformer that would allow the SOFC/GT powerplant to run of aviation fuel.

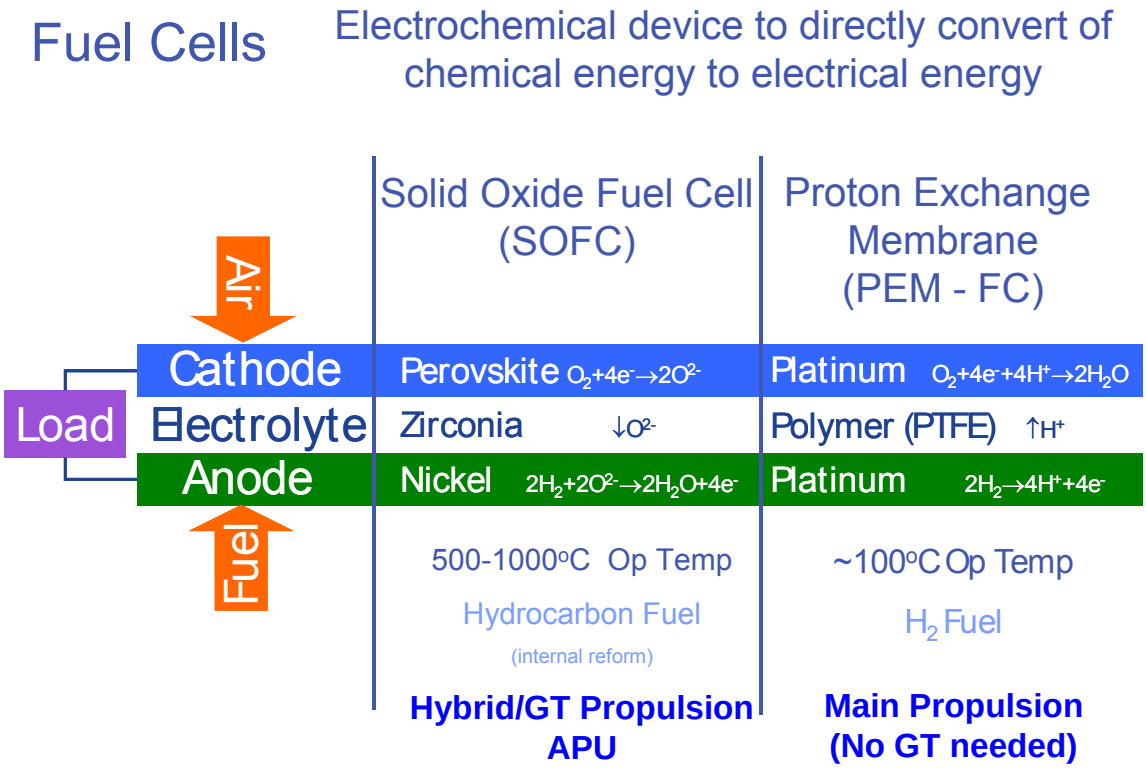

Figure 164. High Level Characteristics of SOFC And PEM Fuel Cells

A PEM fuel cell operating on liquid hydrogen (LH2) was also evaluated as the total power source for the propulsion system. PEM-FC's operate at relatively low temperature and pressure, and therefore do not require high pressure and temperature turbomachinery. PEM fuel cells are currently at a higher stage of development than SOFC's, and a higher rate of improvement in thermal efficiency and power-to-weight as well (see Figure 165).

Projected Power Density of PEM FC For In-Flight Operation at Altitude

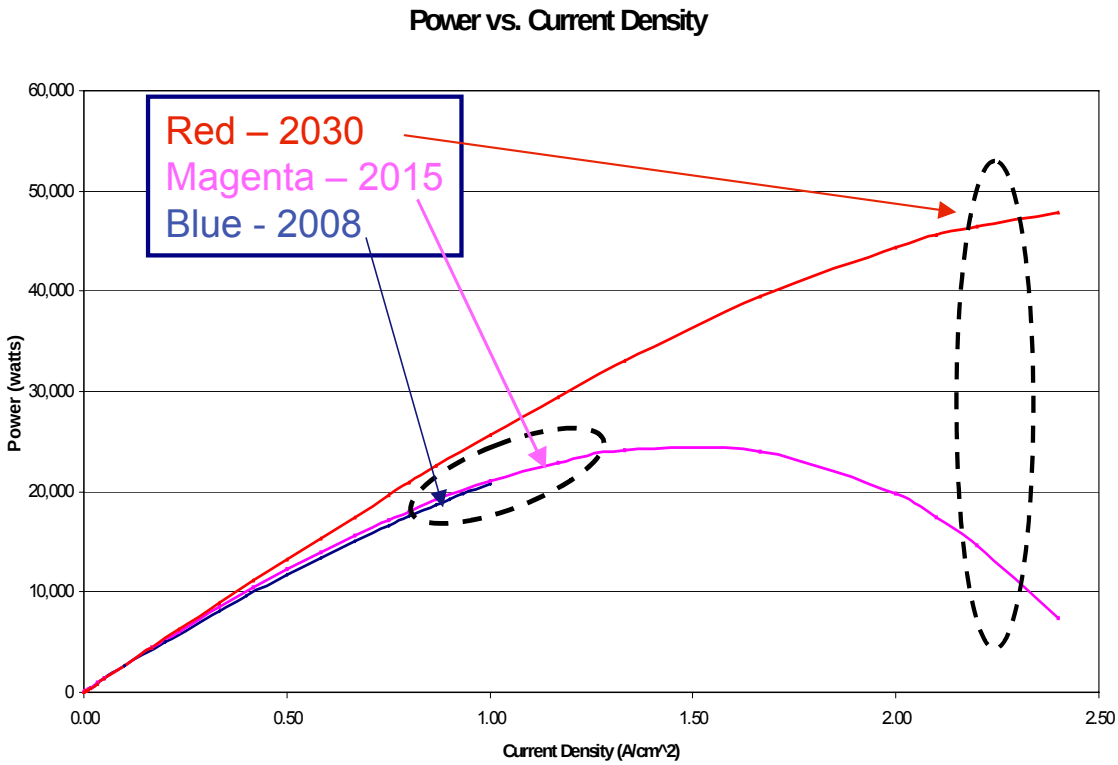

Figure 165. Rate of Improvement in Power vs. Current Density for PEM Fuel Cells

Figure 166 shows that PEM-FC's operate most efficiently at lower powers and currents densities. For our application, cruise is ~1/3 of takeoff power. This results in a potential fuel cell stack efficiency of 71% in cruise and takeoff stack efficiency of ~59%. This makes it well suited for our application as cruise fuel consumption is of greatest importance to mission fuel burn.

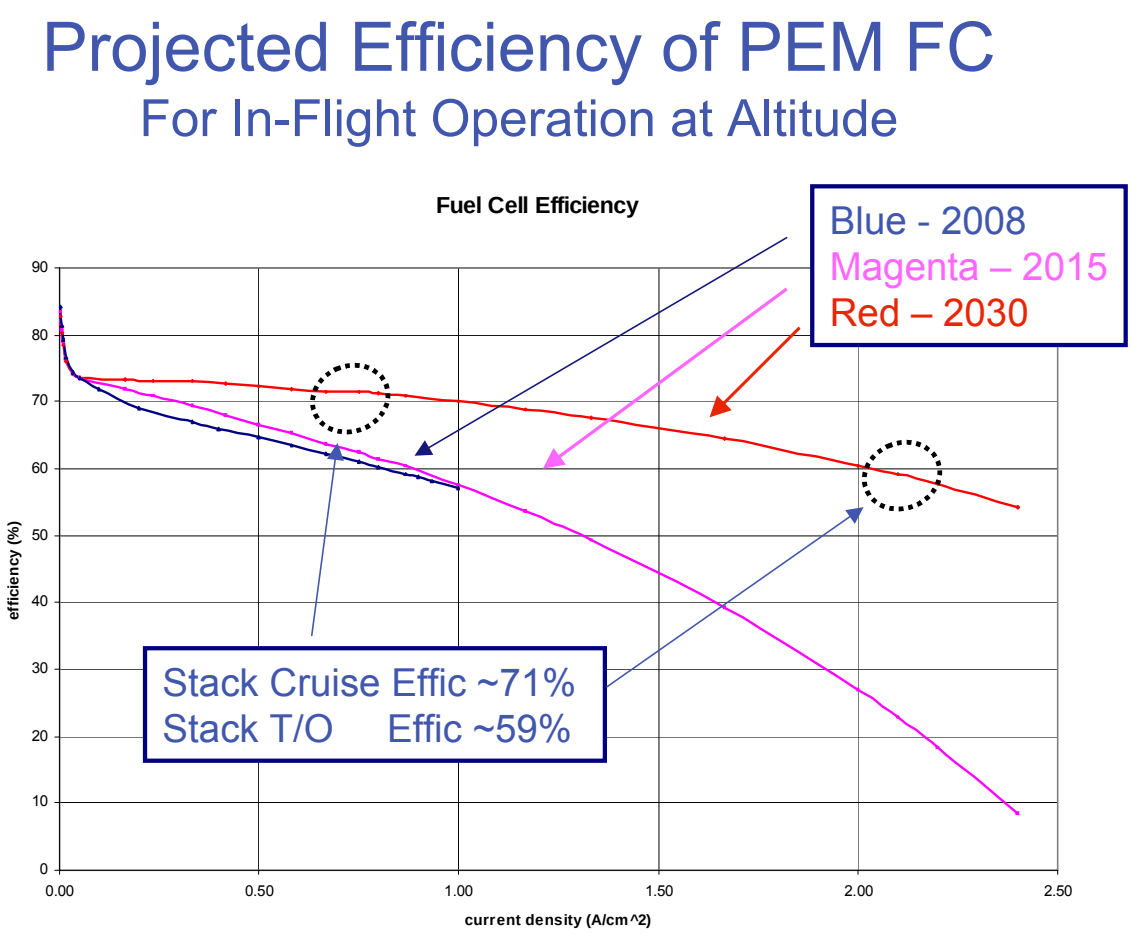

Figure 166. PEM Fuel Cell Stack Efficiency at Takeoff and Cruise

A complete PEM fuel cell power plant was sized to provide power to an electrically driven propulsion fan, and a compressor to provide customer bleed air. Table 58 compares the total fuel cell propulsion and fuel system performance, weight, and volume to the Advanced Reference Turbofan with a similar fan. When both systems are sized to the same thrust requirement, the fuel cell system's cruise thrust SFC (lbm/hr/lbf) is 75% less than the advanced reference turbofan. Compared on an energy consumption basis, the fuel cell system consumes ~55% less energy per unit thrust (Btu/hr/lbf) than the advanced reference turbofan. Essentially zero emissions, with the exception of water vapor, is another major benefit.

The actual mission fuel burn improvement of the fuel cell propulsion is expected to be far less due to the significant increase in propulsion system weight and volume. Table 58 shows that the total fuel cell power plant and fuel system is about 5000 lbs heavier and 300 cubic feet larger than that of the advanced turbofan system. A liquid hydrogen powered SOFC/Gas Turbine hybrid powerplant offered somewhat greater fuel savings, but at a higher weight and system volume. Reduced propulsor power requirements, or further improvements in technology, are needed to make this fuel cell turbofan concept more attractive for this application.

Table 58. PEM Fuel Cell Propulsion System vs. Advanced Turbofan

PEM Fuel Cell vs Advanced Reference Turbofan
Sized to Produce the Same Cruise Thrust

Cruise Performance	***Adv Turbofan***	***PEM FC TF***
FPR	1.6	1.6
FN (lb) @ 41K/0.6 Mx Cr	630	630
SFC @ Mx Cr (lbm/hr/lbFN)	0.509	- 75%
SFC @ Mx Cr (BTU equiv)		- 55%
Fuel Weight + Tank (lb)	~2800	~750
Power Plant Weight (lb)	721 x 2	~4300 x 2
Total Weight (lb)	~4250	~9350
PP + Fuel Volume	80 cu ft	375 cu ft
LTO NOx	325g	0 g

- Fuel Cell SFC improvement smaller at higher powers (Climb, Takeoff)
- Fuel Cell Propulsion system weight/volume >> Adv Reference Turbofan
  - Would result in much higher thrust requirement and Aircraft size/weight
  - Increased aircraft size would increase cost and reduce fuel savings

In order to minimize the size of the fuel cell powerplant, propulsion systems with propeller propulsors were also studied and compared to an advanced 2035 turboprop. Table 59 shows the propulsion system weight and volume of fuel cell propulsion systems sized to produce the same thrust as an advanced 4200 lb thrust turboprop. Also shown is the estimated liquid hydrogen fuel tank volume for a propulsion system sized for these powerplants. These numbers would be doubled for a 2 engine aircraft. Due to their large volume, the fuel cell powerplants would need to be located in the fuselage, with electric motors on the wing driving the propellers. Liquid hydrogen, due to the spherical, insulated high-pressure tanks, would also be stored in the fuselage. Aggressive estimates were made for year 2030 fuel cells and cryogenic motor power-to-weight ratios, and transmission efficiencies. No weight or power loss was book kept for the power lines required to bring the electric power out to the wing mounted propellers.

Table 59. Fuel Cell Powerplants Sized to Produce 4200 lb of Takeoff Propeller Thrust

	Mission SFC Scalar	Propulsion System Weight	Fuel Cell Powerplant Volume	Hydrogen Fuel Volume	Fuselage Length Increase for Fuel Cell, LH2
Advanced Gas Turbine Turboprop	1	1045 lb	-	-	-
LH2 PEM Fuel Cell	0.3	3458 lb	42 cu ft	67 cu ft	+7.7 ft
LH2 SOFC/GT Hybrid	0.25	3774 lb	81 cu ft	55 cu ft	+9.6 ft
Jet A SOFC/GT Hybrid w/ Reformer	0.55	3774 lb + 3857 lbr Reformer	81 (PP) + 97 (reformer) cu ft	0	+12.7 ft

An aircraft mission analysis assessed the impact of these advanced propulsion concepts on the study metrics and aircraft and engine size. The advanced air vehicle and propulsion systems were optimized to minimize fuel burn, and propulsions system weights and volumes scaled with the aircraft thrust requirements. Table 60 shows the results of these studies. The details of this mission sensitivity modeling are shown in Appendix I.

Table 60. Mission Evaluation of Fuel Cell Propulsion System vs. Advanced Turboprop

	Aircraft TOGW	Aircraft Empty Weight	Takeoff Thrust per Engine	Mission Fuel Burn (lbs)	Mission Energy Usage (Btu)
Advanced Gas Turbine Turboprop	14550 lb	7636 lb	3353 lb	1088 lb	Base
LH2 PEM Fuel Cell	+41%	+86%	+21%	-55%	-19%
LH2 SOFC/GT Hybrid	+41%	+87%	+21%	-60%	-28%
Jet A SOFC/GT Hybrid w/ Reformer	+136%	+250%	+114%	+21%	+21%

An can be seen in Table 60, liquid hydrogen fuel cell systems show potential for reducing mission energy usage by 20% to 30% compared to an advanced gas turbine powerplant. Additionally, NOx emissions would be zero for a hydrogen fueled fuel cell system. Aircraft empty weight for the LH2 fueled aircraft would increase by well over 80% compared to an advanced gas turbine turboprop powered aircraft. This would represent a very large increase in aircraft acquisition cost. This could have significant negative impact on ticket price, which has a strong impact of the N+3 network's ability to capture market share. Thrust requirements would scale to about 20% larger than an advanced gas turbine turboprop. The added propeller thrust and aircraft size would result in an aircraft ~ 6 EPNdB cum louder than an advanced turboprop powered aircraft during the landing and takeoff cycle. Adding the weight of a reformer to the fuel cell powerplant to enable the use of jet fuel would result in an extremely large aircraft that burned more fuel than an advanced gas turbine turboprop.

Even in this extremely weight sensitive, short-range aircraft, fuel cell propulsions systems show some potential for reducing energy consumption, with the added advantage of eliminating ground emissions. It may also be optimistic to assume that the infrastructure of all the small community airports in the N+3 network will be upgraded to support and maintain LH2 fueled aircraft by Year 2030. At the assumed technology level, the increased aircraft cost, community

noise, and field length requirements appear to make fuel cells appear to be less attractive than an advanced turboprop for this short range, cost sensitive application.

Fuel cell systems merit further study for longer-range applications, or if fuel cell and electric propulsion technology advances beyond that projected here for the 2030 timeframe.

6.2.7 Advanced Propulsion System Configuration Selection

The study team reviewed the various propulsion concepts studied and their associated aircraft studies to select the propulsion system configuration with the greatest potential for enhancing this new mode of commercial aviation. A TOPSIS ranking was used as an aide in selecting the best engine configuration for the 2035 airliner. The propulsion concepts were ranked for their impact on the study metrics: fuel burn, LTO NOx and noise, and field length/compatibility with small community airports relative to the Advanced Reference Turbofan. The ranking was on a typical 1, 3, 5, 7, 9 scale, with the Advanced Reference Turbofan represented by ratings of 5 in all categories. Feasibility for entry into service in the Year 2030 timeframe, and perceived costs impacting ticket price were also screening criteria. Fuel burn and LTO noise were given higher weighting due to the importance of environmental impact and community acceptance. The results of the ranking are shown in Table 61.

Table 61. Propulsion System Configuration Selection TOPSIS

	Fuel Burn	LTO NOx	Noise	Small Airport Compatibility/ TOFL	Feasibility for 2030 EIS	Aircraft Acquisition Cost/Ticket Price	Ranking
Weighting	**3**	2	**3**	2	2	3	
Adv Noise Optimized TF	5	5	5	5	5	5	4
Adv Noise Optimized TP	**7**	**7**	**9**	**7**	**7**	**5**	**1**
Open Rotor	7	7	1	7	5	5	6
Geared Fan > 13 BPR	3	3	7	5	1	5	6
Distributed Propulsion	3	3	9	5	5	3	5
Pulse Detonation	3	1	3	5	3	3	8
Battery Propulsion	5	9	3	1	1	1	9
PEM Fuel Cell TP (LH2)	9	9	7	3	3	3	2
SOFC/Hybrid TP GT (LH2)	9	9	7	3	3	3	3
SOFC/Hybrid TP GT (JP Fuel)	5	7	5	3	3	1	7

Table 61 shows the Advanced, Noise Optimized Turboprop is the most promising propulsion concept for meeting the study goals. It shows the potential for meeting the extremely challenging N+3 fuel burn and LTO NOx metrics. Its excellent takeoff thrust allows it to take off from short runways and climb quickly, minimizing community noise and real world ground emissions. This concept also minimizes aircraft and engine size for lost acquisition cost. The low noise propeller shows the potential for meeting the N+3 noise with far less technical risk to achieving acceptable levels of community noise than the other concepts.

The TOPSIS study also shows that fuel cell powered systems may have potential for aviation propulsion applications. With the best fuel consumption, and water vapor for emissions, fuel cells appear to have the lowest environmental impact. However, the weight of these fuel cell powerplants would drive up airplane weight, cost, and noise. The risk of shortfall

of study metrics is far greater for the aggressive fuel cell technologies than the selected Advanced Turboprop concept. Fuel cell systems definitely merit further study for longer-range applications that are less sensitive to propulsion weight and more sensitive to specific fuel consumption. Cheaper hydrogen, higher fossil fuel prices, tighter environmental regulations, or severe carbon taxes would make these fuel cell concepts more attractive. And fuel cell and electric propulsion technology could progress well beyond that projected here for the Y2030 EIS timeframe. For this reason, a technology risk assessment and roadmap is included in this study to show the most important development needs for fuel cell powerplants for aviation propulsion.

7.0 Selected Advanced 2035 Airliner Configuration

7.1 Advanced Airliner Design Philosophy

A 20-passenger airliner (see Figure 167) has been developed for 2030-2035 transportation scenario that includes a combination of distributed point-to-point transportation between small communities, between small communities and the suburban airports of large communities, and the suburban airports of two large communities. This transportation concept enables economic development in smaller communities where land and labor are affordable, links these communities with existing businesses in large communities, and provides a transportation service that offloads the traffic at hub airports without the infrastructure investment required for additional large hub airports. Infrastructure investment in trains or bus service that connects current hub airports to nearby suburban airports enables a direct connection between this new distributed network service and the traditional hub and spoke transportation system.

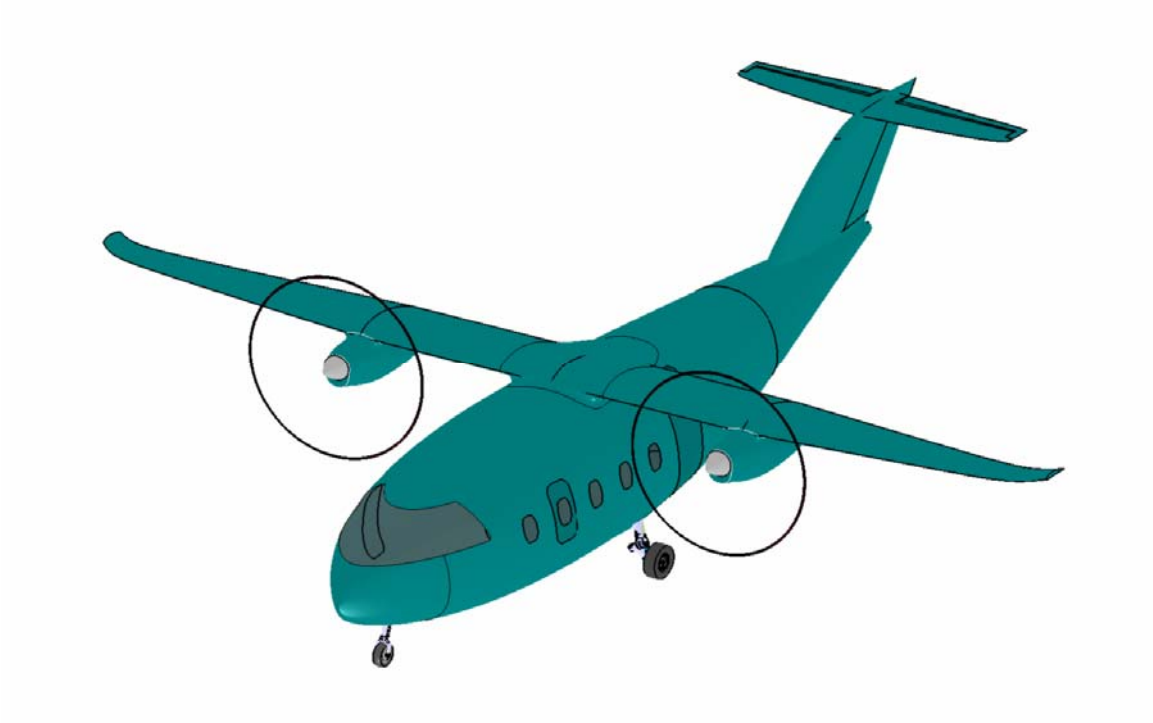

Figure 167. Advanced 20 Passenger Turboprop Airliner for Y2035

Key focus areas in this study include (1) a short range mission with a cruise speed that eliminates compressibility drag and enables the formation of natural laminar flow, (2) advanced turboprop engines with reduced noise and superior fuel economy, (3) an airframe shape that enables low drag through laminar flow and high aspect ratio wings, and (4) a new approach to the application of composite structures that both reduces weight and facilitates the integration of aircraft systems into the airframe structure.

7.2 Mission, Payload, FAA Regulations

Demand studies have confirmed a design mission and payload that is identical to that used for the baseline 20-passenger airliner. Nearly 80% of current day airline trips are less than 800 nm with an even distribution between 200 and 800 nm. A 200nm trip begins to attract traditional automobile customers and 800nm links together most population centers. These studies also confirmed a payload of 20 passengers and their luggage. The payload also includes two crew members, one attendant, and the equipment necessary for current day FAR Part 25 certification regulations and for Part 21 airline operations. These regulations also require air vehicle configurations to have at least two engines. As the airspace system accepts unmanned air vehicles and health monitoring systems mature, there is the potential for some relief from the requirement for multiple crew members. The associated reduction in payload would further improve the performance and fuel burn of the 2035 vehicle presented in this report.

As for the baseline 20 passenger aircraft, an 800 nm IFR range supports the customer demand and a balanced field length of 4000 ft. enables operation from more than 1,000 non-hub airports in the U.S. (see Table 62). These demand studies support cruise Mach numbers less than 0.60 that eliminate compressibility drag and the challenges associated with laminar flow on swept wings. A maximum operating altitude of 41,000 ft enables flexibility for all weather operations and for optimum climb profiles, optimum descent profiles, and point-to-point clearances in the future air-traffic system. The design cruise altitude of 39,000 ft is actually an optimum result from the simultaneous design of the vehicle and the cruise altitude.

Table 62. Mission Specifications

IFR Range (200 nm alternate)…….. Maximum Takeoff Weight, Full Fuel, Optimal Climb and Descent, Maximum Cruise Thrust at 39,000 ft	800 nm
Cruise Speed…….. Top of Climb, 39,000 ft, ISA (Optimized for Fuel Burn)	Mach = 0.50 to 0.60
Maximum Operating Altitude…….. Cruise Altitude & Aircraft Optimized for Fuel Burn	41,000 ft
Takeoff Runway Length …… Maximum Takeoff Weight, Sea Level, ISA, Balanced Field Length per Part 25	3,650 ft
Climb Performnance……. Maximum Takeoff Weight, Sea Level, ISA	30 min. to 39,000 ft
Landing Runway Length……. Maximum Landing Weight, Seal Level, ISA, per Part 25	2,750 ft
Certificated Noise Levels	
Takeoff……	56 EPNdB
Sideline……..	70 EPNdB
Landing……..	70 EPNdB
Cumulative……..…..……	196 EPNdB
Margin to Stage 4 Requirement……..	75 EPNdB
LTO NOx vs. CAEP/6 Standard for 6000 lb FN (Modified Idle)	77% Margin

7.3 Advanced Airliner Configuration & Associated Technologies

7.3.1 Aerodynamic Configuration

The vehicle configuration was driven by the need to provide a comfortable space for 20 passengers and to minimize the drag of the vehicle. As described in the Aerodynamic Configurations and Technologies for Drag Reduction section, particular focus was given to fuselage wetted area and the ability to maintain laminar flow on the fuselage, which for the advanced reference aircraft is responsible for 63% of the wetted area of the vehicle. In contrast, the wing is sized for cruise performance and is responsible for 19% of the total wetted area. Flying wings, Goldschmied propulsors, turbofans, and advanced propeller or prop-fan configurations were considered for their potential to enable natural laminar flow and for their impact on wetted area.

Trade studies with fineness ratio and careful lofting to ensure favorable pressure distributions for laminar flow led to fuselage shapes with continuously varying surface curvature.

Figure 168 shows the regions of potential laminar flow on a 2035 turboprop configuration. The 2035 vehicle has the same comfort, space, baggage volume, entry, and exit accommodations at the baseline 20 passenger aircraft. Hence this new vehicle is anticipated to provide passenger comfort that is similar to a current day Boeing 737. Figure 169 shows both top and cross-sections views of the 4-abreast cabin that was selected for its support of laminar flow and reduced fuselage wetted area. A rear location for the cabin entry door supports laminar flow on the forward fuselage and forces the selection of a high-wing vehicle configuration. Windows and the cockpit windscreen can be virtual (LED screen), camera based, or installed without gaps or steps in the exterior surface. Emergency escape hatches are placed in the forward section of the fuselage to allow a smooth installation with a semi-permanent or breakable seal that eliminates any steps or gaps in the outer surface. Baggage volume aft of the cabin and next to the entry door enables the loading of bags as the passengers enter the aircraft. The flight attendant seat has moved to the aft bulkhead wall. The main landing gear is located in the fuselage aft of the projected region of laminar flow.

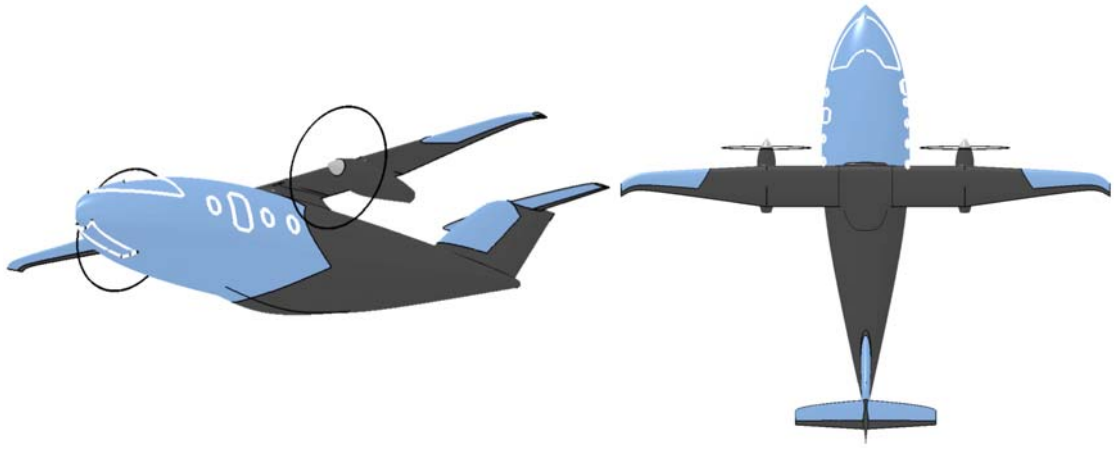

Figure 168. 2035 Final Configuration with Laminar Flow Regions

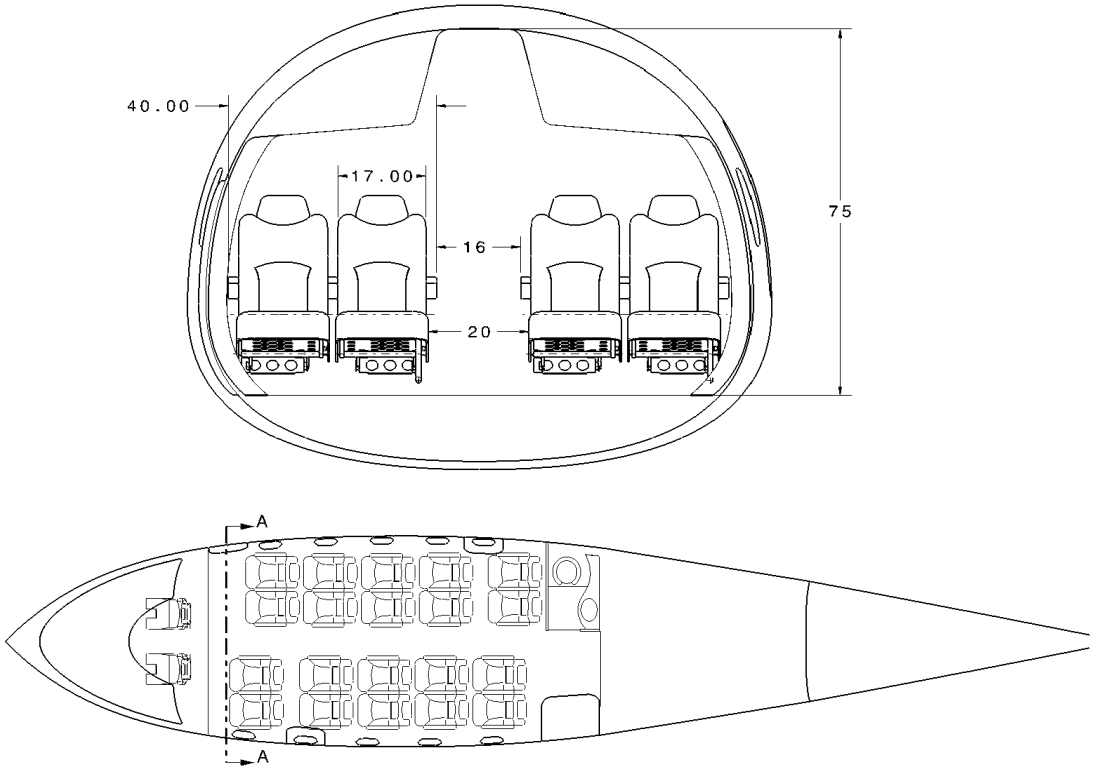

Figure 169. Top and Front View of Cabin Layout

Wing and engine mount locations were selected to maximize laminar flow and propulsive efficiency. The large propeller diameters required for propulsive efficiency essentially force the use of a high wing with wing-mounted engines. Pusher configurations would maximize laminar flow by minimizing propeller disturbance of flow over the wing. However, tractor propeller installation produced five percent better thrust specific fuel consumption, which was enough to produce better fuel burn than pusher configurations that have more wing laminar flow. A tractor configuration also avoids the noise generated by a propeller operating in the wake of the wing. Since the current Bombardier Dash-8Q-400, (Reference 32) commercial turboprop has a wing aspect ratio of 12.8, it is reasonable to expect an aspect ratio 14 wing with the application of advanced materials and gust-load alleviation. A detailed structural optimization study could also be focused on the benefits, if any, associated with the addition of a wing strut.

High aspect ratio lifting surfaces are used to reduce the impact of lift dependent drag. Zero sweep wings maintain their cruise lift distribution at all angles of attack and eliminate any benefit that might be associated with cruise flaps or wing morphing. However, some cruise flaps may help promote fuselage laminar flow by keeping the fuselage angle-of-attack near zero as the payload or fuel load changes.

7.4 Advanced Airframe & Systems

The 2035 vehicle achieves a 33% reduction in empty weight relative to current technology. Advanced composite materials, a conductive health monitoring skin, advanced engine technology, modern electronics, and attention to subsystem optimization enable this breakthrough reduction in aircraft empty weight. Of particular interest is the protective skin that solves many of the issues that have prevented weight reduction in traditional composite structures.

7.4.1 Advanced Airframe

A 2035 concept vehicle may take advantage of advanced structures and systems technology to save 33% in empty weight. From a structures perspective, approximately 22% in empty weight savings is a result of (1) the use of a frame and stringer stiffened shell structure to simplify the integration and installation of subsystem components, (2) the use of advanced coating materials to protect against lightning strikes and electromagnetic interference, (3) the use of a protective and health monitoring external skin, and (4) the integration if ice protection, environmental control system air ducts, and antennas into the protective skin. Careful design of the protective external skin eliminates the need the paint, thermal, and acoustic damping materials used in current technology aircraft. This protective skin is intended to absorb impact damage, distribute the current of a lightning strike, reflect electromagnetic energy, and limit the negative impact of atmospheric heat and moisture on the load caring capability of the primary structure. An additional 11% in sub-systems weight is a combination of observed weight reductions in current avionics and electrical systems and an assumed reduction in sub-system component weight as results of continued development of and transition to electrical systems.

Figure 170 and Figure 171 present a new concept for a protective outer skin. Figure 170 shows how a layer of acoustic and thermal insulation can be moved to the outside of the primary structure, thereby providing a protective skin for the primary structure. A crushable, conductive, energy-absorbing layer enables the primary structure to use as few as 3 or 4 layers of high strength composite material. Since the protective skin is designed to crush, impact damage will be easy to identify visually. The thickness of the protective skin can be varied as necessary for potential damage events or for the installation of ice protection systems, wires, antennas or other sensors. Figure 171 shows an installation concept for the energy absorbing foam and for the final conductive layer. Application of the film layer can also facilitate the establishment of a smooth surface that supports natural laminar flow or some surface texture that helps structure a turbulent boundary layer. Easy removal and replacement of the outer protective skin enables maintenance, repair, and inspection of the airframe throughout its useful life.

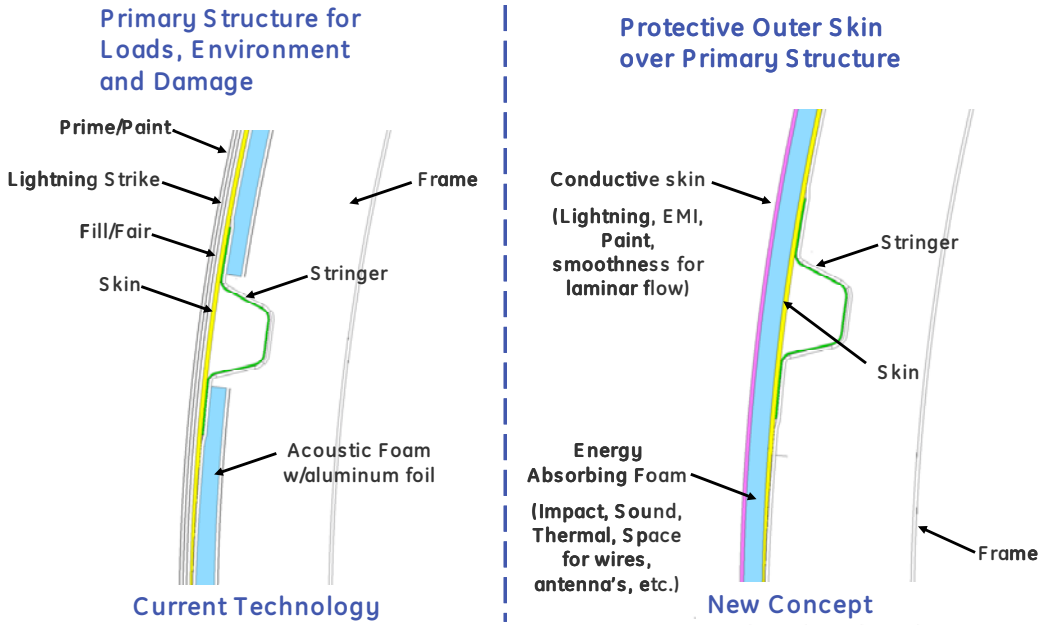

Figure 170. Protective Outer Skin in Advanced Composite Structure

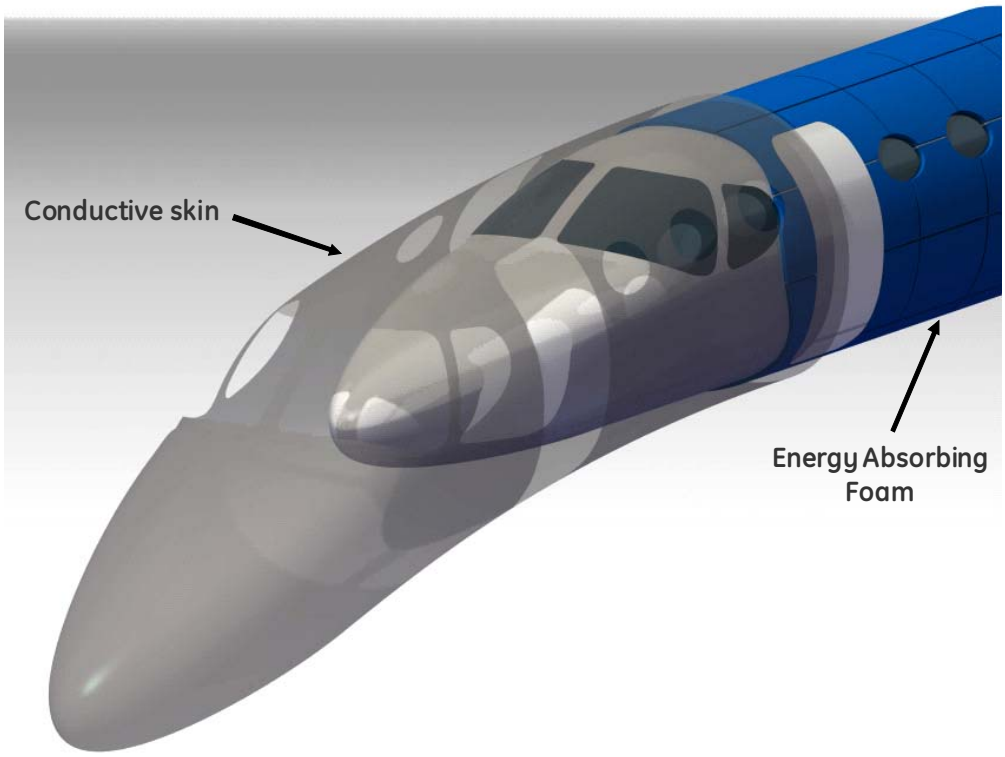

Figure 171. Energy-Absorbing Foam and Conductive Film Provide Protective Coating

7.4.2 Landing Gear

The landing gear is a tricycle configuration; consisting of two, single tire, trailing link main landing gear assemblies, and a single tire, nose landing gear assembly. Extension, retraction and breaking are powered electrically. A detailed structural design study is recommended for future work. The benefits of advanced materials, detailed design, and integration are indented to support the 15% reduction in weight relative to the baseline technology. The integration study should include the impact on wing and fuselage structure of landing gear that is attached to the wing nacelle (see Bombardier Dash 8Q-400) or attached to the fuselage as shown in Figure 172. Some consideration should also be given to the addition of a wing strut.

7.4.3 Surface Controls

A fly-by-wire system is envisioned in all axes to support gust load alleviation, ride control, and if necessary autonomous flight in the event of an emergency. Small cruise flaps enable continuous operation of the fuselage at an angle of attack that promotes laminar flow. All surface controls are expected to be actuated electrically. However, manual and electro-hydraulic actuations are options for the future vehicle. Single-slotted fowler flaps or plain flaps with a continuous mold like seal are sufficient to provide the maximum lift capability needed for a 4000 ft. balanced field length. The current trend in flight control technologies for military and unmanned air vehicles is expected to lead to the 15% reduction in weight relative to the baseline aircraft.

7.4.4 Auxiliary Power Unit (APU)

The APU is an advanced turbine or piston engine of appropriate size. During ground operation, this unit provides electricity for heating, cooling, lighting, and avionics. The APU is the primary source of electricity to start the main engines and for emergency power in flight. Certifying the APU as “essential” (i.e., operation required during flight) enables the elimination of emergency ram-air turbines or batteries for emergency power. APU weight reduction relative to the baseline aircraft is associated with a reduction in the load requirements of advanced systems and advanced engine technology.

7.4.5 Hydraulics

No hydraulic system in envisioned for the advanced 2035 vehicle. However local applications of hydraulic power packs and electric-hydraulic actuators should not be ruled out during detailed subsystem optimization.

7.4.6 Electrical

Electrical generators producing high voltage power (115 or 270V) are envisioned for both main engines and for the APU. A split bus electrical architecture with the appropriate power control units provides power in the voltage and type necessary for subsystem components. Two Lithium-Ion batteries of the appropriate capacity are used to provide power to start the APU and for emergency power.

7.4.7 Avionics

The 2035 vehicle will benefit from the continued breakthroughs in modern electronics. The functionality of the system is expected to improve relative to current day Honeywell Epic,

Rockwell Collins Pro-Line, and Garmin 1000 systems. Give the recent migration of panel mount glass cockpits into Cessna 172 class aircraft, it is not unreasonable to assume that 2035 electronics and fiber optic communication systems will lead to a weight reduction of up to 60% relative to the year 2000 system of the B-20 baseline aircraft. The 2035 vehicle is also expected to have antennas integrated into the structure's protective skin.

7.4.8 Environmental Control

Vapor-cycle cooling is anticipated for the 2035 vehicle because the power requirements are approximately ½ those of current day air-cycle systems. Electrical heat or main-engine bleed-air systems provide cabin heating and pressurization. There are separate flow paths and temperature controls for the cockpit and the cabin.

7.4.9 Ice protection

The wing, horizontal stabilizer, and engine inlet leading edges are protected from ice using an electrical resistance, an electrical induction, or an electrical expulsive system. These systems support integration into the vehicles protective skin. The air data probes and windshield are protected with electrical resistance heaters. Modern hydrophobic coatings should be investigated for their potential to eliminate the need for active ice protection. Integration of advanced power distribution wires into the aircraft's protective skin provide most of the weight savings claimed for the ice protection.

7.5 Advanced Airliner Geometry

A three-view solid model of the 2035 turboprop is shown in Figure 172. Geometric parameters for the aircraft geometry are called out in Table 63. The wing is somewhat tapered and un-swept with an aspect ratio of 14. The wing span is 53.39 ft. The horizontal tail is un-swept and tapered. Horizontal tail area is 19.4% of wing area, and horizontal tail span is 15.52 ft. The vertical tail (at 24.3% of the wing area) is highly swept and tapered. The fuselage, with an overall length of 48.0 ft, has a fineness ratio of 5.4. The nacelle fineness ratio is 2.04. Overall configuration length is 50.99 ft, and overall height is 16.49 ft.

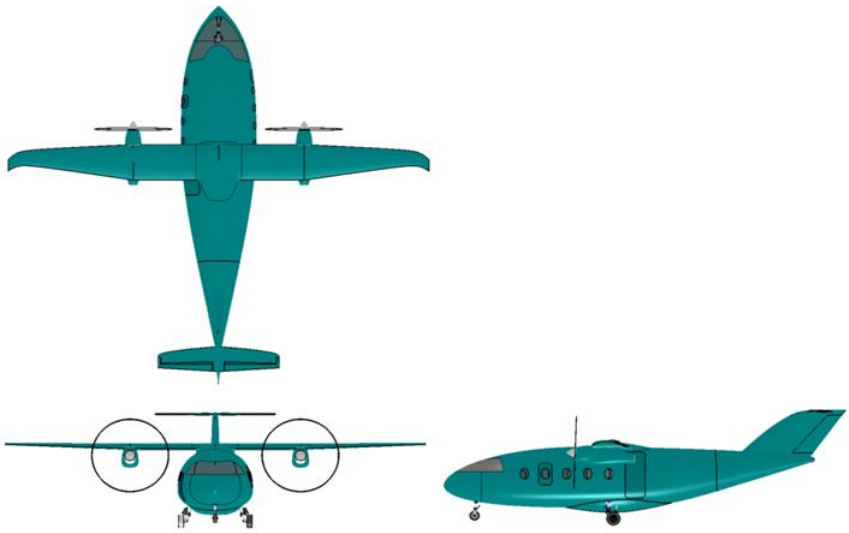

Figure 172. Three-View Solid Model of Y2035 Advanced Airliner Concept

Table 63. Y2035 Advanced Airliner Geometric Data

	Wing	Horizontal Tail	Vertical Tail
Aspect Ratio	14	6.11	0.872
Taper Ratio	0.318	0.425	0.6
Sweep (c/4) (°)	0	20	49
Thickness-to-chord (%)	0.1375	0.0921	0.12
Reference Area (sq ft)	203.6	39.43	49.56
	Fuselage	**Nacelle**	
Length (ft)	48.0	5.54	
Maximum Width (ft)	9.6	2.71	
Maximum Height (ft)	8.2	2.71	

7.6 Advanced Propulsion System Description and Performance

The Propulsion Group includes the weight of the entire propulsion system including the turboprop engine, the propulsor, prop gearbox, shafting and torque mount tube, engine systems and fuel system. General Electric provided scalable performance, weight, and dimensions for advanced Ultra-Quiet and Efficient Turboprop propulsion system for aircraft sizing and mission analysis. The final aircraft sizing required 3353 lbs of net system installed thrust at SLS conditions. This advanced propulsion concept is described in sections to follow.

7.7 Advanced Air Vehicle Performance

The mission requirements for the advanced air vehicle (Table 62) are as the same as those for the B-20 baseline aircraft, except the cruise Mach number is reduced to 0.55 and the cruise altitude to 39,000 ft based on optimization studies. The mission profile (Figure 173) is also the same as the B-20 except for the noted cruise altitude differences. The reserve fuel calculations are identical to those made for the B-20 baseline.

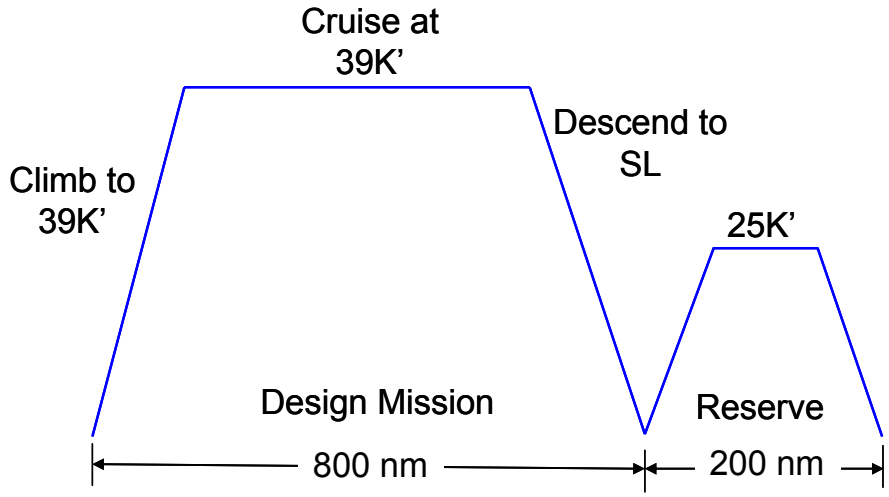

Figure 173. Y2035 Advanced Airliner Mission Profile

The cruise drag polar for the 2035 turboprop at Mach 0,55 at 39,000 ft is shown in Figure 174. Start of cruise at Mach 0.55 and 39,000 ft takes place at a lift coefficient of 0.81.

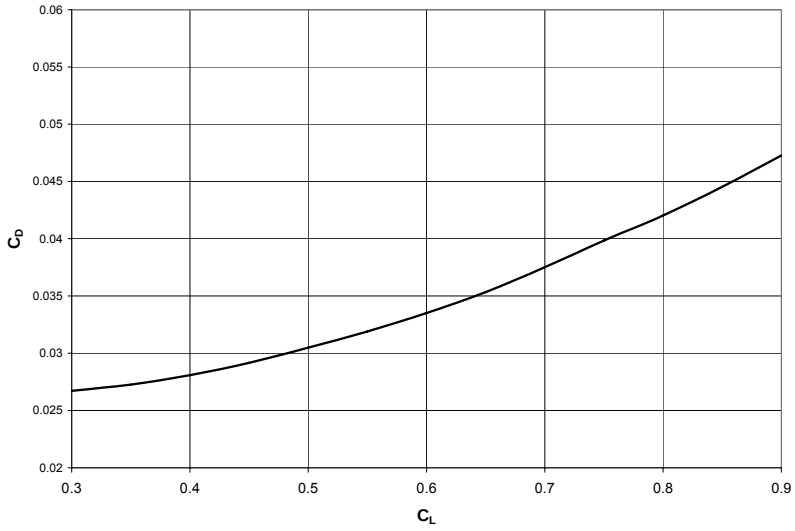

Figure 174. Advanced Airliner Cruise Drag Polar (M=0,55)

The takeoff and landing drag polars are shown in Figure 175. As with the B-20 described earlier, the BFL is 2,538 ft with double-slotted fowler flaps, and 3,642 ft with a single slotted flap system. Since the optimum aircraft is relatively insensitive to reductions in wing loading from 72 lb/sq. ft. to 50 lb/sq. ft. the final flap configuration (if any) can be optimized for airframe noise.

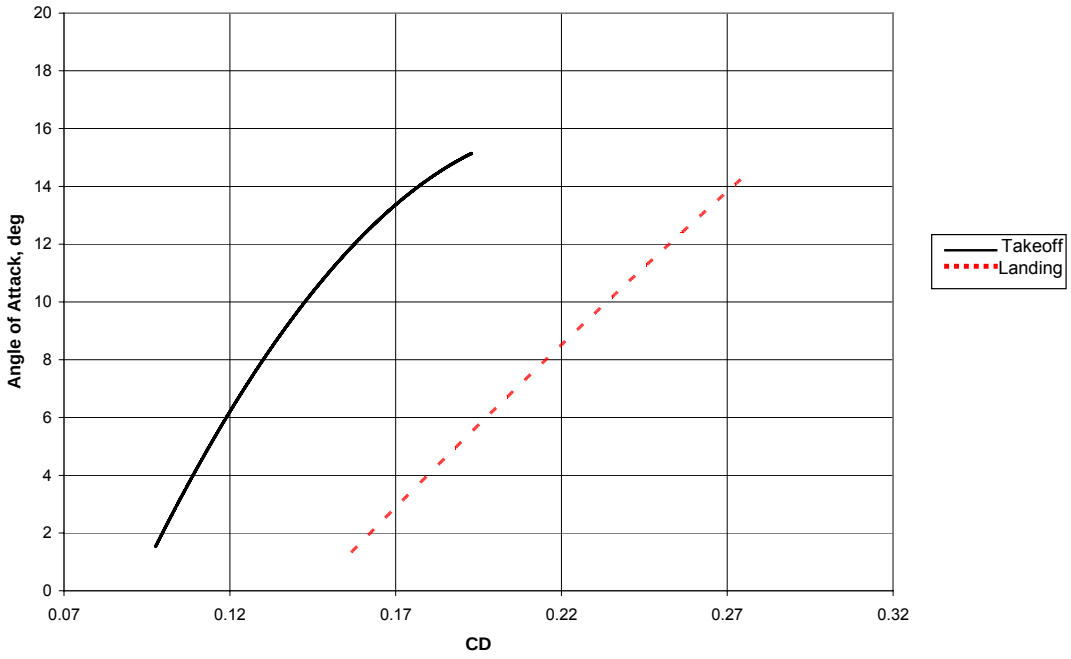

Figure 175. Advanced Airliner Low Speed Drag Polars

Component weights for the 2035 Final Configuration as calculated by both FLOPS and MAPS are shown in Table 64. Agreement between the two codes is excellent, with only 0.6% error in MTOGW and about 5% difference in fuel burned. Advanced composite structures, a protective health monitoring skin, ultra-efficient engines, and all-electric systems characterize the aircraft technologies. Fuel volume is small enough and wing volume large enough to include all of the fuel in the wings. The MTOGW, at 14,664 lbs, is 59% of the MTOGW of the B-20 baseline aircraft.

Table 64. Advanced Airliner Weight Statement

Component	FLOPS Weight, lbs	MAPS Weights, lbs
Wing	830	905
Horizontal Tail	59	99
Vertical Tail	94	87
Fuselage	1,989	1,989
Landing Gear	456	462
Surface Controls	136	140
Nacelle and Air Induction	168	204
Propulsion Group	1,831	1,846
Hydraulics	0	0
Electrical	386	387
Avionics and Instruments	161	163
Furnishings and Equipment	1,028	1,031
Air Conditioning and Anti-Ice	310	312
Auxilliary Power	109	109
Unusable Fuel and Fluids	79	87
Empty Weight	**7,636**	**7,821**
Option Allowance	0	0
Crew	690	690
Basic Operating Weight	**8,325**	**8,510**
Mission Fuel	1,013	1,076
Reserve Fuel	399	418
Total Fuel	**1,412**	**1,494**
Full Fuel Payload	4,845	4,845
Ramp Weight	**14,582**	**14,849**
Taxi/Takeoff Fuel	82	95
Max TO Gross Weight	**14,664**	**14,754**

Fuel usage for the mission as calculated by both FLOPS and MAPS is shown in Table 65. Total fuel is 1,494 lbs, with 1,095 lbs of the total being used for the mission (fuel fraction of 0.10). The MAPS estimation of fuel is within a remarkable 2 lbs of total fuel, even though there are some small differences in the individual mission segments for reasons previously discussed.

A summary of the mission and configuration characteristics is shown in Table 66, again with a comparison between FLOPS and MAPS. The agreement between FLOPS and MAPS is again excellent. The slightly higher wing loading and slightly lower thrust-to-weight ratio of the final configuration in MAPS gives a 114 ft longer BFL. The 2035 turboprop weighs 14,644 lbs, just over 10,000 lbs less than the B-20. The wing area is half that of the B-20 at 203.6 sq ft, giving a higher wing loading of 72.03 psf. Each engine has 3,353 lbs of flat-rated SLS thrust, giving a thrust-to-weight ratio of 0.46. Most importantly, the mission fuel is 31.1% of that of the B-20 baseline, very close to the NASA goal of 70% fuel reduction. The MAPS calculation of 31.5% of the B-20 mission fuel is a slightly smaller reduction due to the slightly smaller mission fuel requirements for the B-20 (3,402 lbs in MAPS compared to 3,516 lbs in FLOPS).

Table 65. Advanced Airliner Mission Fuel Usage

Mission Phase	FLOPS Fuel, lbs	MAPS Fuel, lbs
Taxi/Takeoff	82	95
Climb	214	230
Cruise	608	633
Descent/Landing	191	116
Mission Fuel	**1,095**	**1,074**
Reserves	399	418
Total Fuel	**1,494**	**1,492**

Table 66. Advanced Airliner Performance

Parameter	FLOPS	MAPS
Wing Area, sq ft	203.6	203.6
Thrust per Engine, lb	3,353	3,353
Engine Size Factor	0.7996	0.7996
Wing Loading, psf	72.03	72.93
Thrust-to-Weight ratio	0.46	0.45
Total Fuel	1,494	1,492
Fuel Fraction	0.10	0.10
BLF, ft for Clmax=1.685	3,642	3,756
Range, nm	800	800
Cruise Mach	0.55	0.55
Cruise Altitude, ft	39,000	39,000
MTOGW, lb	14,664	14,849
Fuel reduction compared to baseline B-20, %	68.9	68.6
Cert Noise: Cum Margin Below Stage 4	75 EPNdB	75 EPNdB
LTO NOx: Margin to CAEP/6 6000 lb FN Req't	77% margin	77% margin
Field Length: Margin N+3 Airport Req't, ft	358.0	244.0

7.8 Landing and Takeoff Noise

The noise certification levels for the advanced aircraft were calculated as discussed in the Trade Studies section. Based on the available information, the aircraft is estimated to be 75 EPNdB below Stage 4, an improvement of 55 dB below the baseline aircraft's levels, as seen in Table 57. This improvement was achieved through the introduction of innovative noise and aerodynamics technologies, resulting in a quieter source, which passes over the observers at a higher altitude (other than sideline). Figure 176 shows that the Advanced Turboprop is radically quieter than currently certified aircraft and even the noise levels possible with advanced turbofans. The Ultra Quiet and Efficient Propulsor is one of the key technologies to reducing noise and tuning it out of the objectionable range.

The sensitivity study introducing between 6 and 36 new N+3 operations at the notional airport was once again carried out using the expected 2030 baseline air traffic and the noise characteristics of the selected advanced air vehicle concept. As expected, the impact of the additional advanced aircraft operations was almost eliminated with the advanced ultra-quiet aircraft. As seen in Figure 177, the contours for the added advanced N+3 aircraft traffic (color lines) plot virtually on top of those for the notion airport baseline traffic (black lines). The additional 24 flights per day of N+3 traffic projected for the notional airport in Year 2030 would increase the 55dB contour area by only 0.018 nmi^2. The additional noise introduced by the

advanced N+3aircraft operations is minimal, making community acceptance of this convenient new service very likely.

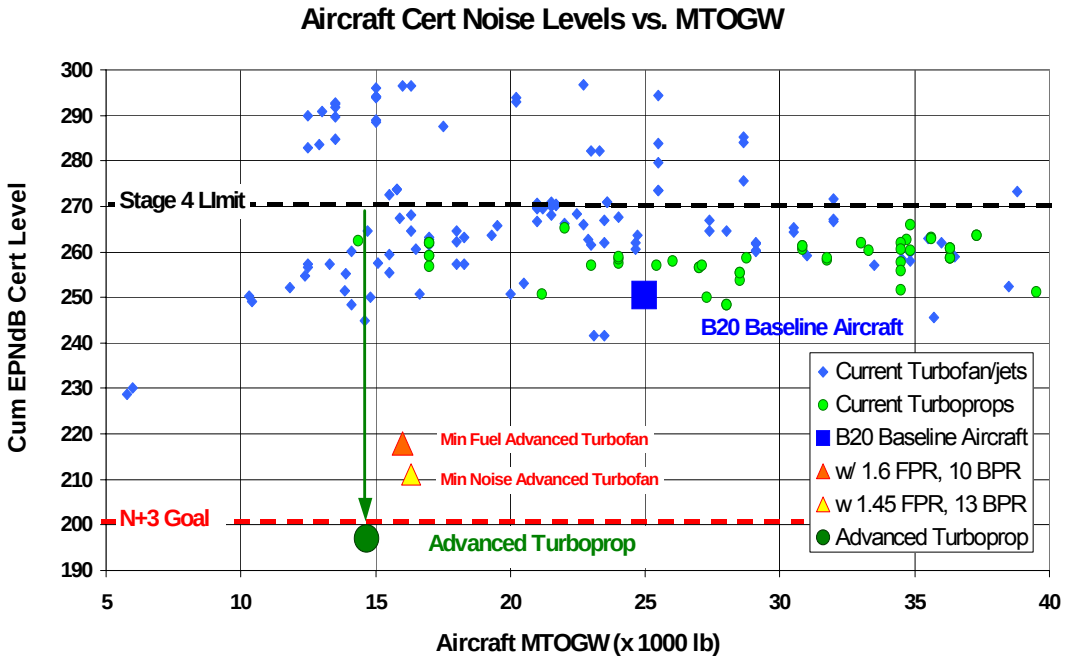

Advanced Turboprop Noise Technologies Mitigate Increase In Future N+3 Traffic

Figure 176. Advanced Turboprop Cert Noise versus Other Aircraft

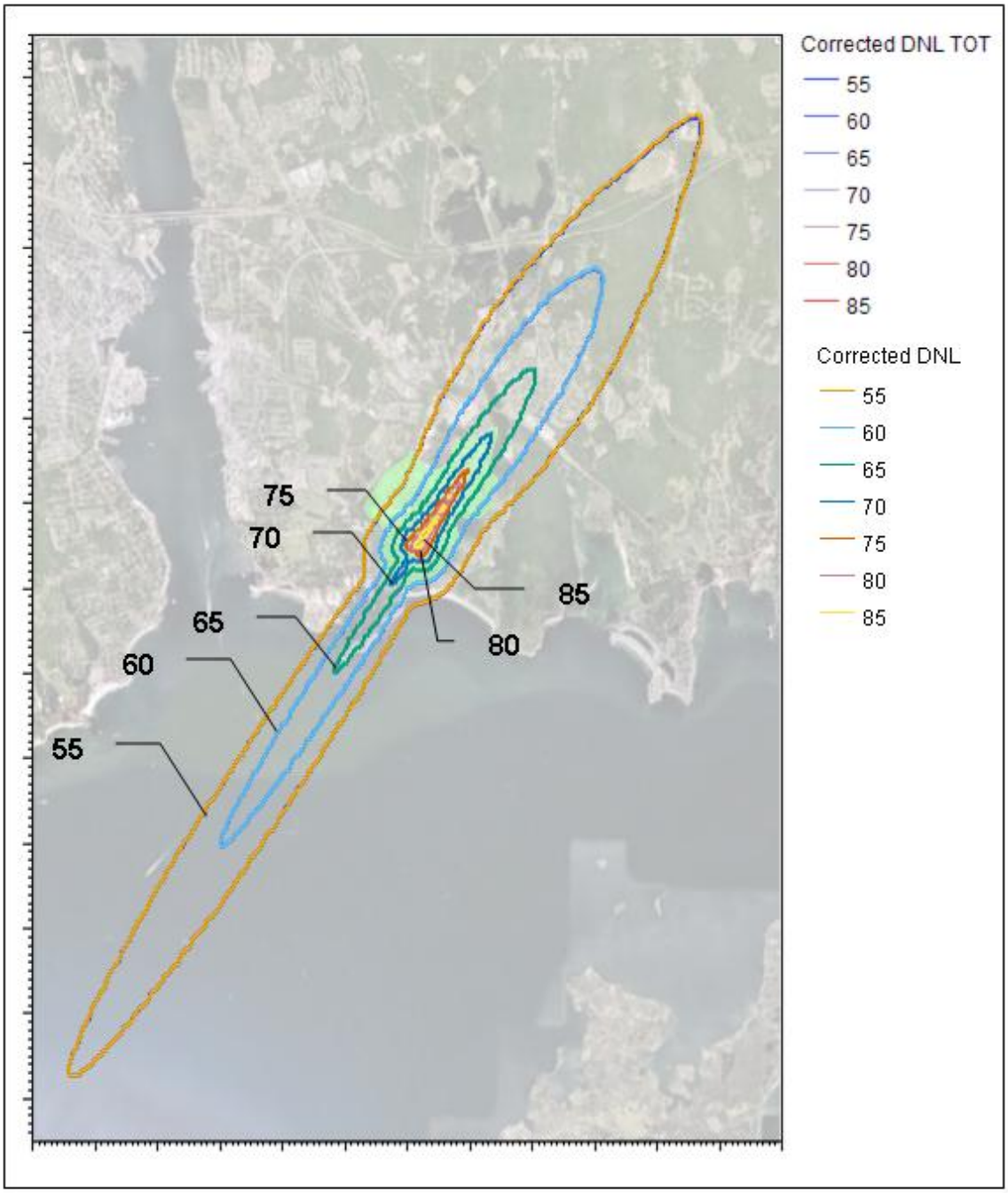

Figure 177. Impact of Advanced Airliner Traffic on Airport Noise

8.0 Advanced Quiet and Efficient Propulsion System Concept

GE has developed an innovative Year 2030-2035 propulsion concept to enable extremely efficient point-to-point air travel utilizing small community airports, while minimizing negative impact on the environment and surrounding community. The GE Ultra Quiet and Efficient Turboprop (UQETP) Concept (Figure 178) combines an efficient, noise-optimized propeller with advanced, low emissions turbomachinery and a performance- and quiet-enhancing control system. This innovative propulsion concept meets the spirit of NASA's N+3 goals, and is defined to maximize the potential for community acceptance and economic viability needed to enable this future mode of travel.

The UQETP Advanced Turboprop, combined with the advanced aircraft technologies, has the potential to exceed NASA's N+3 goals for LTO NOx and certification noise. The excellent low speed thrust characteristics of the propeller enable the advanced aircraft to takeoff and land from the small airports in the N+3 network without the drag, noise, or expense of complex lift devices. Mission fuel burn reduction is within 1 percentage point of NASA's goal. A small amount of fuel burn performance has been sacrificed in order to reduce community noise, to make the added N+3 traffic virtually unnoticed by the local airport community. Further propulsion system and flight trajectory optimization may exist sufficient to exceed the fuel burn goal. This propulsion concept also emphasizes affordability and compatibility (fuels, maintainability) with the small airport infrastructure.

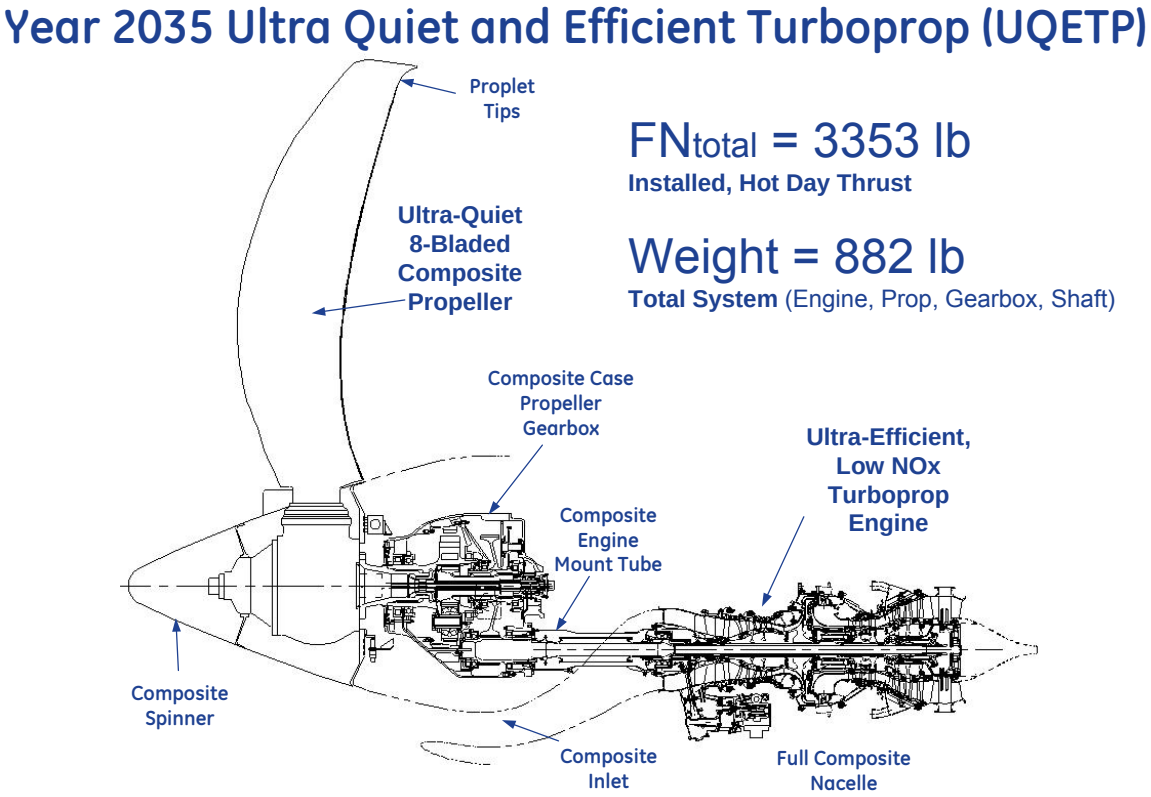

Figure 178. Year 2030 N+3 Ultra Quiet and Efficient Turboprop Concept

8.1 Ultra Quiet and Efficient Propulsor: Key to Community Acceptance

The propulsion system trade studies show that a turboprop has superior fuel burn, emissions, and noise characteristics for the relatively the low cruise speed (M < 0.6) requirement of the Advanced Airliner. Turboprops also have excellent takeoff field length performance, and enhancing our ability to add airports the future N+3 travel network with shorter than 4000 ft runways. Minimizing aircraft noise for community acceptance, without significantly compromising mission fuel burn, is the key to maximizing the number of airports served by the N+3 network, and therefore the economic viability of this new mode of travel. As propeller noise dominates the propulsion system's contribution to aircraft noise, propeller design studies were conducted to trade noise versus performance and weight.

Typically for a commercial turboprop aircraft, propeller diameter, blade count, tip speed and activity factor would be selected as the best trade between weight, performance, and *cabin noise at cruise*. Currently certified commercial turboprops meet Stage 4 noise requirements (see Figure 161), and as they are generally quieter than turbofans operating out of commercial airports. Operators are under little pressure to reduce takeoff noise, so ground noise is not generally given much consideration in designing commercial airliner propellers. But as our N+3 concept hopes to expand commercial air service to small airports that currently have none, the goal is to reduce community noise impact to nearly unnoticeable levels.

Minimizing propeller noise during the landing and takeoff cycle would drive a propeller to a very large diameter and many airfoils, essentially a large, variable-pitch propfan. However, a variable pitch propeller's weight scales nearly linearly with number of blades, and by approximately the square of the diameter. Additionally, cruise performance at M= 0.55 is hurt by excessive blade count or chord, due to blockage effects.

A design trade study was performed to study the impact of propeller blade count, activity factor, and diameter on takeoff noise, weight, and cruise performance. Detailed propulsor airfoil design is beyond the scope of this Phase 1 contract. GE's expertise in the design of high bypass fans, turboprops and open rotor systems was used to develop estimates of advanced propulsor performance, weight, and noise. The following paragraph describes our methodology for estimating propulsor noise, weight, and performance.

First, a proprietary advanced propeller performance model was used to assess the impact of propeller diameter, blade count, and activity factor on cruise and takeoff performance and tip speed. Weights of these various designs were estimated by applying scaling equations for tip speed, diameter, blade count, power loading, and activity factor to a modern composite propeller. A 12% challenge was added on weight for advanced technologies including thinner airfoils and improvements in the spinner, hub, and pitch control. Next, the methods described previously were used to translate the propeller diameter, blade count, power loading, and tip speed into a takeoff noise estimate for a conventional propeller. Estimates of the impact of potential advanced noise suppression technologies were then applied to the selected propeller configuration. (See Table 55.)

Using this methodology, a propeller configuration with 8 blades, a moderate 105 activity factor, and a diameter of 9.84 feet proved to be the best balance between reducing takeoff noise and minimizing negative impact on mission fuel burn. An 8 bladed configuration reduced takeoff noise by ~50% at the expense of ~1% in mission fuel burn versus a lower blade count design. Cruise efficiency of 90% should be achievable, even with a blade count and activity factor that is biased for low takeoff noise. The thrust requirement at max takeoff gross weight is

predicted to be achievable at a prop tip speed of only 600 ft/sec, about 20% lower than typical in this class. Cruise tip speed is only 590 ft/sec, which also should result in low cabin noise and passenger fatigue.

This near constant design tip speed design would allow an advanced propulsion control system the freedom to seek the optimum propeller speed, pitch, and power loading to minimize noise for any given mission or flight condition. Propeller rotational speed could be allowed to vary over a 20% range with almost no penalty in engine performance or propulsion system design weight. The pilot would simply set the power level and the integrated propulsion system control would actively adjust pitch, speed, and power loading to minimize noise at the desired thrust. The control system would follow a base map and algorithms developed via prediction and test, but actively adjust pitch, speed, and power based on nacelle noise sensor feedback.

The detailed engineering process could further reduce noise and improve performance through detailed 3D aerodynamic, mechanical and aero-acoustic design optimization. Advanced mechanical, blade material and manufacturing considerations drive toward minimal blade thicknesses (and hence associated thickness noise) that ensure suitable structural integrity for safe and reliable operation.

Detailed Computational Aero-Acoustic (CAA) analysis using GE's cutting-edge prediction tools would ensure the multi-disciplinary design optimization process includes noise assessments at a fidelity level that is able to adequately distinguish between 3D blade design features of interest, with a particular focus on balancing aero performance at cruise with aero-acoustic noise at takeoff flight conditions.

Advanced propeller noise reduction features would be applied and developed with particular interest in optimizing these features for the selected turboprop configuration and cycle, which is substantially different than what has been typically employed to date. For example, it is anticipated that application of circumferentially non-uniform blade design approaches will yield greater benefits at the advanced propulsor's lower tip speeds by redistributing a fraction of the dominant acoustic power into lower frequencies, and take advantage of favorable perceived noise weighting effects.

Advanced tip geometries such as proplets can be employed to provide performance benefits. Proplets could allow additional noise reduction by further reducing tip speeds at the required takeoff thrust, while improving cruise efficiency. In addition, proplets offer a means to implement circumferential non-uniformity at the propeller tip region while maintaining uniformity at the hub to minimize pitch control weight and complexity by designing blades with alternating dihedral (i.e., towards either the pressure-side or suction-side of the propeller). Figure 179 illustrates this concept.

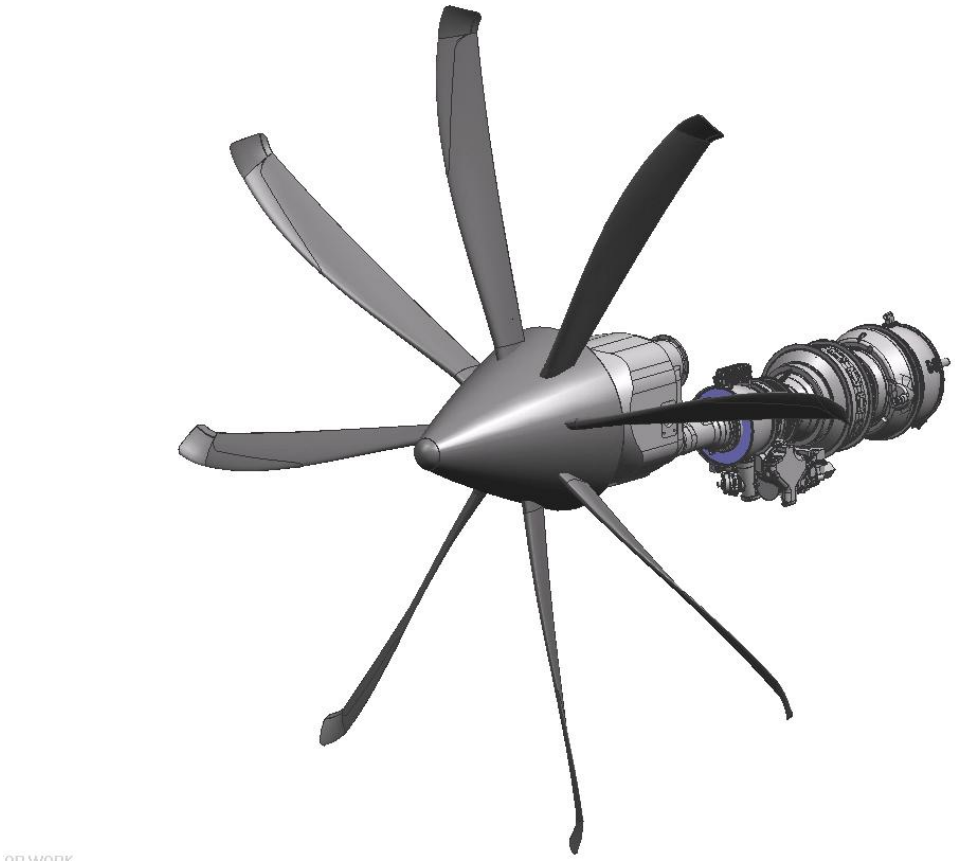

Figure 179. Year 2035 N+3 Ultra Quiet and Efficient Propulsor

Advanced flow control concepts are another possible approach to improve takeoff noise and performance with significantly less performance penalty at cruise than fixed airfoil geometry designs. Typically, airfoil design for good high speed cruise efficiency look very different than those designed to optimize takeoff thrust and noise. Most propeller designs are a compromise between cruise and takeoff requirements. An advanced fluidic propeller could have an airfoil shape highly biased for cruise efficiency, and be blown at takeoff to minimize noise (and maximize thrust). Under most takeoff conditions, substantial engine bleed flow could be made available for takeoff noise optimization.

Finally, advanced aero performance and aero-acoustic analytical capabilities can be applied to evaluate and improve installation effects associated with propulsion-airframe integration. Correctly capturing the detailed aero-acoustic interactions for the complete aircraft system is enormously complex, but is now becoming possible with current modeling capabilities and availability of high-performance computing facilities. The future use of this capability will be instrumental in identifying and clarifying the details of the installation noise effects such that an improved low-noise system-integrated design will ensure an ultimately successful realization of the N+3 aircraft configuration.

8.2 High Efficiency/Low Emissions Engine: Minimizing Environmental Impact

The GE UQETP advanced turboprop concept represents major advances in small gas turbine engine performance, weight, and emissions. It's innovative design features enable the Advanced Airliner to reduce mission fuel burn by nearly 70% and LTO NOx emissions to more than 75% below CAEP 6 standards. Yet it's basic design is selected to minimize cost and ensure compatibility with the infrastructure (fuel, maintainability) of the small community airports in the N+3 network.

This advanced, small gas turbine is optimized to minimize fuel burn and emissions, while producing the substantial customer offtakes expected for the comfort of the passengers paying a premium ticket price for this convenient mode of travel. Advanced technology allows the engine's physical airflow to be less than one fifth that of the baseline engine, yet produce the same generous customer offtakes efficiently. At cruise, 31% of the engine power and 13% of the fuel is consumed in producing the customer offtakes.

The UQETP engine core is comprised of an advanced, axi-centrifugal compressor, an innovative radial inflow combustor, and an uncooled CMC high-pressure turbine. It is a front-drive configuration, powered by a lightweight CMC free-shaft power turbine. It is sized to produce a flat-rated 3353 pounds of net system installed thrust (prop + engine). The engine can deliver 1591 shaft horsepower to the propeller with full installation and offtakes, flat-rated to a ISA+28C day. Significant temperature margin is available for emergency power and hot day operation. An average new engine would have significant additional turbine temperature margin under all conditions for production variation and field deterioration. Generous SFC/Fuel margin has been added to the predicted average engine performance for production variation.

8.2.1 Innovative Aero, Materials, and Mechanical System Technologies

Next generation CMC high pressure turbine airfoils allow high turbine temperatures without the need for blade cooling, resulting in dramatic reduction in engine size. The engine's overall pressure is set to minimize SFC, consistent with the technologies identified to achieve high efficiencies at small high-pressure compressor and turbine blade dimensions. The corrected airflows of these high-pressure components are a fraction of other engines in this class. Innovative technologies focused on achieving high component efficiencies and low emissions with very small turbomachinery are key to meeting the N+3 goals. Some of the performance, weight, and emissions enabling engine technologies and features are shown below and in Figure 180.

Advanced Radial TAPS: Compact, Ultra-Low Emissions Combustor

- Dramatically reduced emissions in a compact, easy to maintain design

Advanced lightweight material technologies

- High temp/strength Uncooled Next generation CMC airfoils
- Next generation CMC combustion liner with EBC coating for low cooling/emissions
- Higher temp/strength disk/shaft materials
  - Dual Alloy Turbine Disk and Dual alloy Hi-Temp Ti Impeller
  - Higher temp shaft materials
- Advanced Composite Propeller, Nacelle, Torque tube, and Propeller and Accessory Gearboxes

Advanced mechanical systems

- Advanced seals and innovative rotor/stator gap flow discouragers
- Air bearings and Hybrid ceramic bearings
- Advanced active clearance control, including impeller shroud. (High eta's w/ small airfoils)

Advanced aero/operability/manufacturing

- Advanced airfoil and flowpath aero designs, and the manufacturing technologies required to achieve these geometries in small airfoils.
- Active stall/surge prediction/detection/control to ensure safe operation at maximum compressor efficiency
- Innovative impeller concept for higher efficiency and lower cooling air temperature

NASA N+3 – UQETP Advanced Turboprop Concept **Component and Systems Technologies**

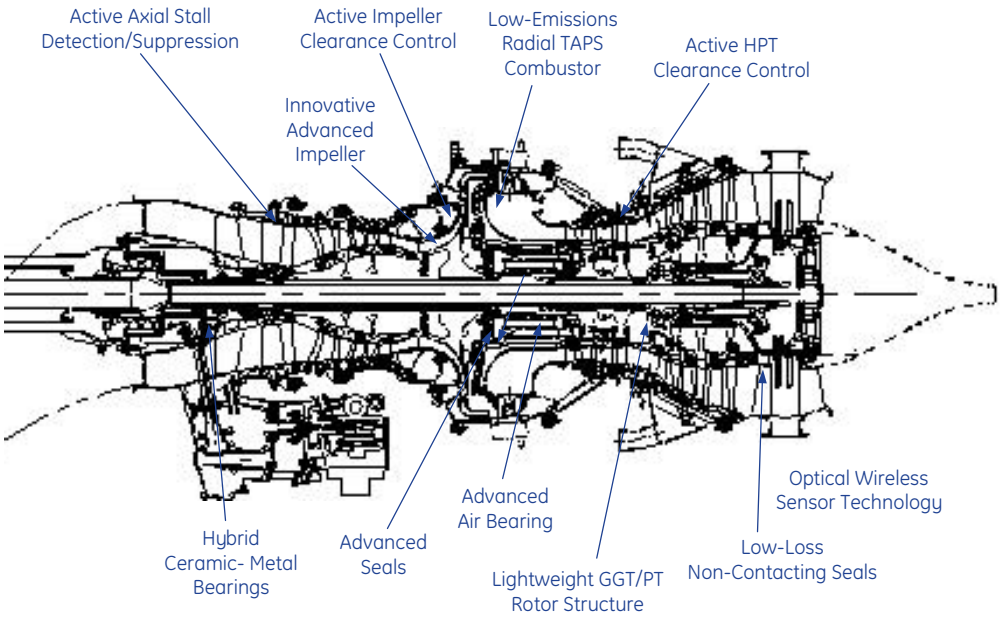

Figure 180. Innovative N+3 Engine Technologies

Advanced manufacturing technologies will be employed to allow fine 3D aero features on the airfoils as well as flowpath contouring to help achieving high performance at these small airfoil sizes. Thin and smooth advanced ceramic erosion coatings will help maintain axial compressor performance over time. Active stall detection and suppression will allow safe operation near the compressor peak efficiency with less required stall margin.

The centrifugal compressor has several innovative performance and weight enhancing features. A lightweight titanium design is made possible at these cycle temperatures by an advanced dual-alloy high-temperature Ti configuration. The GE's advanced, innovative impeller concept not only significantly improves performance at reduced tip speed, but also provides an excellent, low temperature source for power turbine purge air. GE's concept for Active Impeller

Shroud Clearance Control has the potential for reducing impeller tip clearance by as much as 75%. And GE's advanced diffuser/deswirler concept would not only reduced engine diameter and weight, but enhance compressor performance as well.

An innovative Radial-Inflow Twin Annual PreSwirl (TAPS) Combustor concept will give the opportunity for generation-after-next TAPS technology to be scaled to this size class. This novel radial inflow design would allow a dramatically larger combustor front end to enable execution of the advanced, lean burn TAPS technologies. The radial configuration would also shorten the engine significantly, and allow extremely easy fuel injector removal and replacement. A minimally cooled CMC combustor liner with advanced environmental barrier coating (EBC) would enable further leaning of the combustor front end for low emissions.

The high pressure and power turbine blades made of next generation CMC material will allow uncooled HPT blades at these moderately high turbine temperatures, and allow generous temperature margins for production variation and deterioration. As CMC's are a fraction of the weight of turbine alloys, the turbine disk weights are reduced by half.

As the CMC airfoils eliminate all chargeable turbine blade cooling, advanced seal technology is the major avenue for further secondary flow reduction. Most advanced seal technology concepts identified to date do not have the combination of durability and speed, temperature, and delta P capability demanded by the advanced commercial turboprop, or cannot be scaled down to this size class. Several advanced seal concepts under consideration show potential to work in this size and environment, with the potential to reduce leakage flows by half compared to labyrinth seals, with excellent durability.

Other mechanical improvements would include hybrid ceramic bearings and actively controlled air bearings to reduce weight, losses, and clearances. Optical, wireless sensor technology would reduce weight, improve measurement accuracy, and allow reduction of temperature margins. Composite nacelles, propeller blades and hubs, gearbox casings, and torque mount tube would significantly reduce weight over today's design.

Material selections are illustrated in Figure 178 and Figure 181. The propulsion system weight breakdown is shown in

Table 67. Table 68 further breaks down the GE UQETP turboprop engine weight by component. These weight savings contribute significantly to mission fuel burn improvements, as weight is a strong contributor to fuel burn on this short range aircraft.

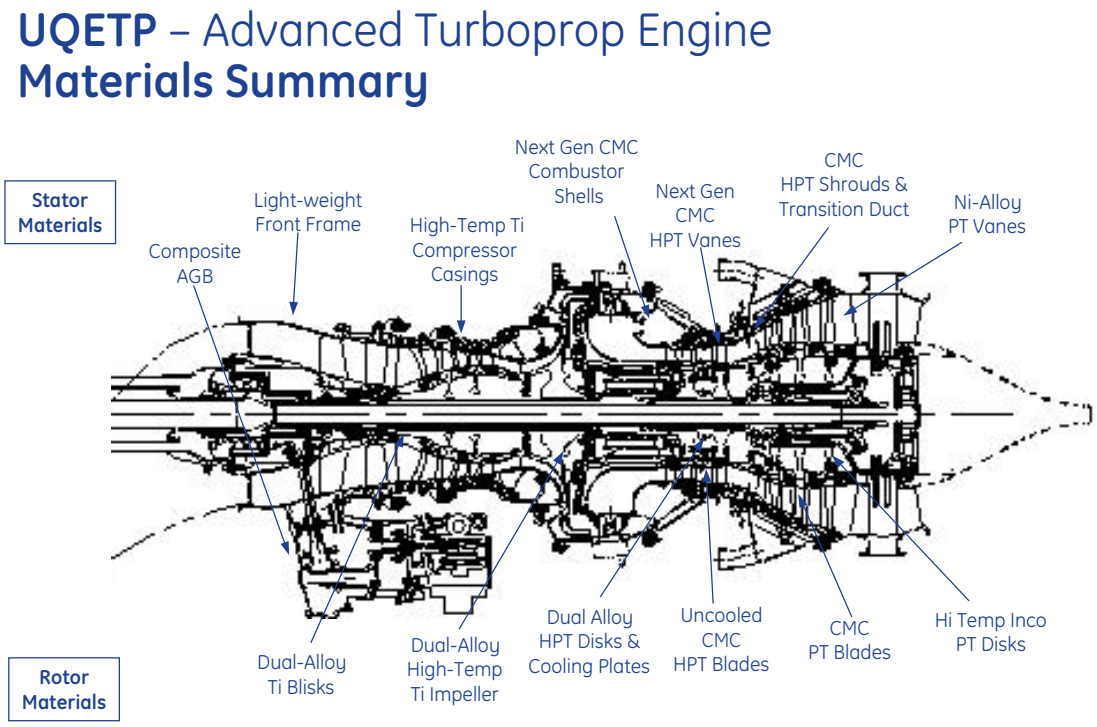

Figure 181. Advanced UQETP Engine Materials Summary

Table 67. Overall Advanced UQETP Propulsion System Weight Breakdown

Advanced Propulsion System
Uninstalled Weights

Component	Weight (lbs)
Propeller	292
Propeller Gearbox	215
PGB Mounting	28
Engine	347
Total	**882 lb**

Table 68. Advanced Turboprop Bare Engine Weight Breakdown

GE UQETP – Advanced Turboprop **Engine Weight**

Front Frame - Compressor Module	**76**
Midframe - Combustor Module	**46**
High Pressure Turbine Module	**25**
Low Pressure Turbine Module/Exhaust Frame	**67**
Controls, Lube System, Accessory Gearbox, Configuration Hardware	**133**
Total Weight	**347 lb**

8.2.2 Engine Cycle, Performance, and Fuel Burn

Table 69 shows the installed performance and detailed cycle breakdown of the Year 2035 UQETP Advanced Propulsion Concept. Takeoff, Takeoff Roll, Top of Climb, and Initial Cruise operating conditions are shown, along with the nominal 39K/0.55M/ISA Max Cruise Design Point. The aforementioned technologies allow the extremely small turbomachinery to achieve very high efficiencies at the cruise operating conditions, and throughout the mission. Overall pressure ratio is similar to the baseline engine, but it is achieved at a small fraction of the core airflow of the baseline engine. The propulsion and thermal efficiency improvements of the advanced turboprop result in cruise TSFC 41% better than the baseline engine. Added to the weight and aerodynamic improvements of the advanced air vehicle, cruise fuel burn is reduced by 71% compared to the baseline aircraft. The advanced technologies of GE's Ultra Quiet and Efficient Turboprop Concept have the potential to dramatically reduce fuel burn and environmental impact.

Table 69. Advanced Propulsion System Installed Performance

GE UQETP Installed Performance

	Parameter	Units	SLS/ ISA SLS TAKEOFF (flat rated)	SL / 0.25 MN ROLLING TAKEOFF (flat rated)	39K/ .55 TOP OF CLIMB (run to FN req'ment)	39K/ .55 INITIAL CRUISE (run to FN req'ment)	39K / .55 DESIGN POINT Max Cr 100% N2r
ALT	Aircraft altitude	ft	0	0	39000	39000	39000
XMP	Aircraft Mach number		0	0.25	0.55	0.55	0.55
DTAMB	Delta ambient temperature	deg R	0	0	0	0	0
TAMB	Ambient temperature	deg R	518.7	518.7	390.0	390.0	390.0
WB24	Customer bleed	lb/sec	0.402	0.402	0.402	0.402	0.402
ZPWXHP	Customer horsepower extraction	hp	34	34	34	34	34
PCNSD	Power turbine speed	%	101.7	101.7	101.7	100	100
FNTOT	Total thrust	lbf	3353	2548	515	412	473.8
TSFC	Thrust SFC	lb/h/lbf	0.189	0.247	0.408	0.418	0.406
WFT	Margined fuel flow	lb/h	634.4	628.4	210.3	172.4	192.4
FN	Engine net thrust	lbf	171.1	102.8	24.6	13.2	19.6
FRAM	Ram drag	lbf	0	69.178	40.673	37.754	39.935
FNPROP	Propeller thrust	lbf	3182	2445	490	399	454
PWSD	Delivered shaft horsepower	hp	1591	1591	532	429	489
SFC	Shaft power SFC	lb/h/hp	0.399	0.395	0.395	0.402	0.394
EPWSD	Equivalent shaft horsepower	hp	1677	1658	559	443	510
ESFC	Equivalent SFC	lb/h/hp	0.378	0.379	0.376	0.389	0.377

8.2.3 Innovative, Radial TAPS Combustor to Meet Aggressive NOx Reduction Goals

The Advanced Turboprop's dramatically reduced fuel burn, due to the highly efficient propulsor and reduced losses and cooling (thermal efficiency), also dramatically reduces NOx vs. the baseline engine. The vastly superior fuel efficiency (over 40% better SFC than the baseline engine) is not sufficient to meet this study's NOx reduction metric. With a modern rich-quench-lean (RQL) combustor, the Advanced Propulsion System would have LTO Emissions ~ 59% below the CAEP/6 requirement for a 6000 lb FN turbofan. This is a dramatic improvement, but meeting this study's goal requires an additional 39% reduction in LTO NOx beyond RQL combustor technology.

An advanced lean-burn combustor concept based on GE's Twin Annual PreSwirl (TAPS) technology is the best approach to meeting the remaining challenge to NASA's NOx metric. As shown in Figure 182 the TAPS is a staged combustion design, with a premixing main stage and a concentric pilot. Only the pilot is fueled at ignition and low power, and it is optimized for good stability and low power CO and HC emissions. The main stage, which is fueled above approach power, is a lean, cyclonic premixing design for ultra-low NOx emissions. The very lean, well-mixed main stage results in ultra-low emission at high power, as shown in Figure 183. Table 70 shows that TAPS technology can cut takeoff and climb NOx by more than half compared to a modern RQL design, and the potential for exceeding NASA's LTO NOx goal. In addition, cruise NOx emissions are only 1030 grams/hour for the GE UQETP with a TAPS combustor, vs. 3584 grams/hours for the baseline engine, a 71% reduction in cruise emissions.

There are some significant technical challenges, however, in inserting TAPS technology into are N+3 propulsions system. The main challenge will be scaling the extremely large fuel injectors and front end down to the very small core size of the advanced engine. An innovative radial inflow TAPS configuration would allow significantly larger (and fewer) fuel injectors by increasing the effective diameter. This would also shorten the length of the engine and dramatically improve access to the fuel injectors for easy maintenance. Substantial technical challenge still remains to scaling down this technology to this size, and the feasibility must be further explored.

Another potential NOx reduction opportunity would be to focus technology development on low power emissions. A TAPS combustor runs only on its central pilot at lower power operations, and therefore it offers no real improvement in NOx emissions over RQL combustors during the taxi or approach portions of the LTO cycle (see Table 70 and Figure 183). Airblast atomization technology, applied to the central pilot, could bring significant NOx reductions during these operations.

The N+3 network itself is also likely to bring substantial real world reductions in LTO NOx that is not captured by the NOx certification testing. In reality, the N+3 community airports are likely to have significantly reduced taxi time and ground delays, reducing the emissions at the ground level.

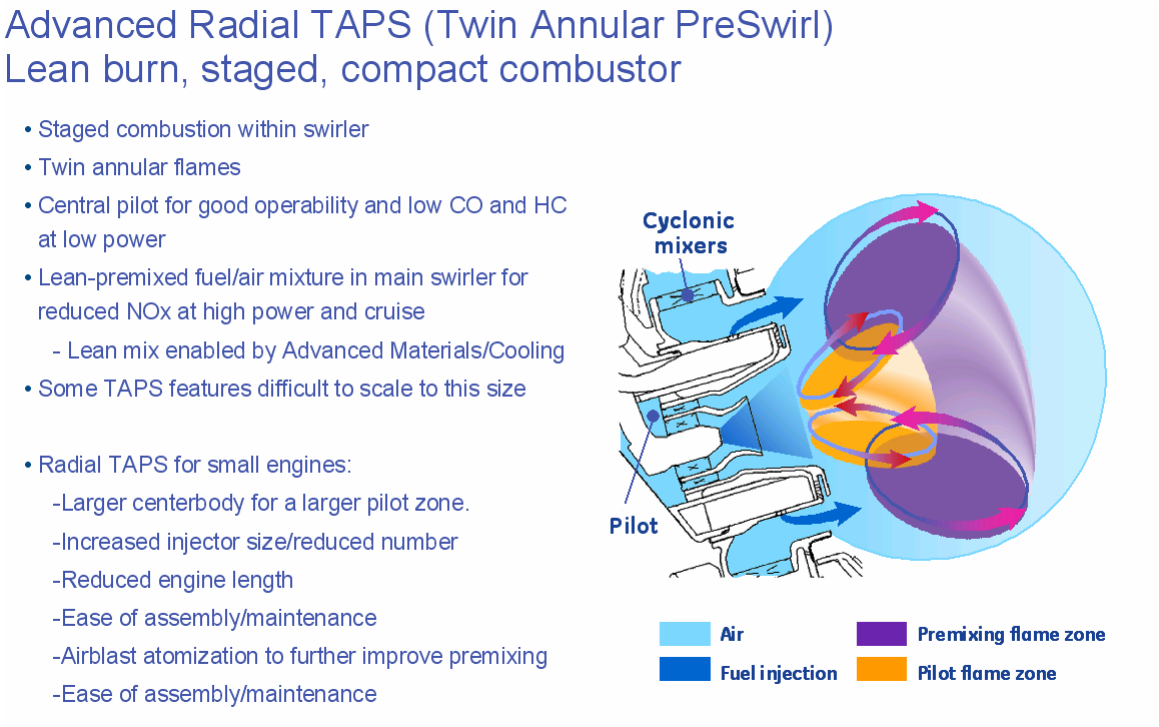

Figure 182. Advanced Twin Annular PreSwirl Combustion

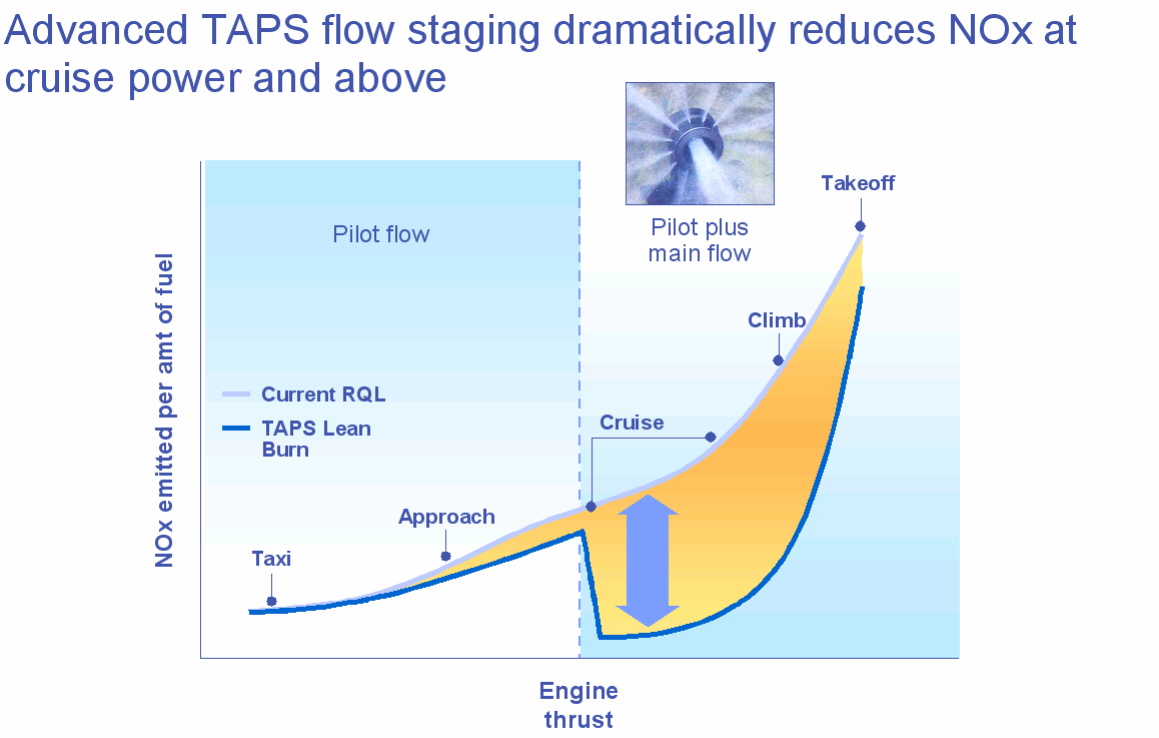

Figure 183. TAPS Technology Dramatically Reduces NOx at High Power

Table 70. Impact of Advanced TAPS Technology on LTO NOx

LTO NOx IMPROVEMENT vs. BASELINE

Advanced UQETP Turboprop LTO NOx vs. Baseline Engine

	w/ RQL	w/ Adv Radial TAPS
Takeoff	- 66%	- **89%**
Climb	- 64%	- **90%**
Approach	- 52%	- 59%
Idle	- 40%	- 55%
Total LTO NOx (**g/cycle**)	- 56%	- **74%**
LTO NOx vs. CAEP/6	- 59%	- **77%**

(vs. 6000 lb FN Requirement. Turboprop Idle = 4%SHP, 80% prop speed)

- **NOx Goals Achievable w/ Improved Cycle + Mat'ls + Advanced Radial TAPS**
  - Scaling TAPS technology to this size, however, is a significant challenge
- **Low Power Emissions are biggest opportunity**
  - Focus on Pilot for further improvement
- **Reduced N+3 ground operation time is additional real world benefit**

In short, almost all the N+3 technologies contribute to NOx reduction by reducing fuel burn, temperatures, and cooling flow requirements. Additional technologies are required to meet the challenging goal of reducing LTO NOx 75% below future requirements. An innovative radial inflow combustor employing advanced TAPS technologies has the potential to meet or exceed the study metrics, and reduce cruise emissions by 71% vs. the baseline aircraft. Significant development effort will be needed to scale the TAPS technology down to this engine thrust class. Premixing and stability at the Advanced Turboprop's relatively low T3's will also be an area of technology focus. Incorporating airblast atomization technology is another key development need.

9.0 Advanced 2035 Airliner Metrics and Key Technologies

The ultra quiet and efficient Advanced 2035 Airliner concept defined here effectively meets the N+3 goals for noise, fuel burn, emissions, and compatibility with the more than one thousand small community airports of this new air transport network. The novel technologies focus on the metrics that maximize the potential for community acceptance and affordability, the keys for commercial viability of the future ultra-convenient air transport system.

9.1 Advanced 2035 20 passenger Airliner Concept vs. Baseline and Metrics

The Advanced 2035 Airliner Concept meets or exceeds the essential goals to enable the future N+3 air travel network. The following is a brief review of the Advanced Airliner's performance vs. the baseline B-20 airliner and the study metrics:

Field Length: 4000 ft to Satisfy Small Airports in N+3 Network

- Light weight aircraft and high propulsor thrust result in a takeoff BFL of only **3650**

-70% Fuel Burn Metric vs. Current Technology Baseline Aircraft

- Advanced Airliner Concept weight, aero, and propulsion technologies result in a **69.1%** improvement vs. the Baseline Aircraft.
- Further opportunities for improvement:
    - Optimization of cruise altitude/mission profile/trajectory
    - Re-regulation to allow electronic co-pilot
    - Technologies beyond TRL 6 in Year 2025

-75% LTO NOx vs. CAEP/6 Requirement

- Efficient Aircraft and Propulsion System, Innovative Radial TAPS Combustor yield **77%** Margin vs. CAEP/6 LTO NOx 6000 lb thrust requirement.
- 75% Reduction in LTO Cycle NOx vs. Baseline on a grams/Trip basis
- Cruise emissions are < 1030 NOX g/hr, a 71% improvement vs. Baseline Aircraft
- N+3 Point-to-Point travel inherently lower LTO emissions than Hub & Spoke due to single Takeoff and Landing. Reduced idle/taxi at small airports also reduces LTO NOx

71 dB Cum Margin to Stage 4 Noise Requirement or 55 LDN at Airport Boundary

- Small, Clean Aircraft and Innovative Ultra-Quiet Propulsor have potential to reduce Noise to **75 dB** Cum Margin below Stage 4
- Noise increase of only 0.015 dB LDN at the airport boundary due to added N+3 traffic. Increase in traffic should be virtually unnoticeable to local community.

This innovative selected Advanced Turboprop Airliner employs technologies that are anticipated to be affordable in the 2030 timeframe, a key factor in making this new, time-saving and stress-reducing mode of transport available to a large portion of the traveling public.

9.2 Impact of Advanced Aircraft and Propulsions System

It is important to identify the major contributors to the Advanced Airliner Concept's dramatic improvements in fuel burn, noise, and emissions versus current technology aircraft. As a first step, a study was performed to determine how much of the improvements are due to: 1) propulsion vs. airframe technologies, and 2) advanced technologies versus unconventional or innovative approaches. The Year 2035 A20 Advanced Airliner Concept was evaluated against:

1) Year 2008 Baseline Aircraft (B20 with Year 2008 Baseline Turbofan)
2) Year 2035 Advanced Reference Aircraft (advanced, but conventional tube & wing design w/ Advanced Reference Turbofan)
3) Year 2008 Baseline Aircraft with Year 2035 Ultra Quiet and Efficient Turboprop
4) Year 2035 Advanced Airliner Concept with Year 2008 Baseline Turbofan

An aircraft mission analysis study was used compare the various aircraft configurations. All aircraft concepts were optimized to minimize mission fuel burn, and therefore CO2 emissions. Engine scale factor was set to meet the requirement of a 200 ft/min rate of climb at top of climb for the max range and payload mission. Other metrics were allowed to float, including field length. All concepts could be made to meet the 4000-foot field requirements of the small community airport network, at some expense to either fuel burn or LTO noise. LTO NOx is evaluated on a grams per passenger basis, a better metric for evaluating the impact on the local community than simple certification values. The results of this study are shown in Table 71. Aircraft modeling and optimization details are shown in Appendix I.

The Advanced Reference Aircraft (AR20), for the purposes of this sensitivity study, is defined to show the significant improvements that advanced, Year 2035 technologies could bring to an aircraft of conventional configuration. The aircraft defined here has the advanced weight saving structural technologies of our Advanced Airliner, but without the novel protective skin, multi-functional structures, or aircraft systems. Its conventional tube and wing configuration does not allow for the extensive laminar flow of the Advanced Airliner. The Ultra-High Bypass Advanced Reference Turbofan engine has all the performance and weight enhancing technologies of the UQETP Advanced Turboprop, but is shown here without the innovative noise technologies and radial TAPS combustor. Table 71 shows the impressive improvement in the study metrics brought about by the advanced technologies incorporated in the Advanced Reference Aircraft. Fuel burn is reduced 53% compared to the baseline aircraft. An ultra-high bypass (~13:1 BPR) variant of the Advanced Reference Turbofan reduces noise to nearly N+2 goal levels. With the application of all the innovative noise technologies defined in this study, noise levels approaching 60 EPNdB below Stage 4 are possible. LTO NOx with a modern RQL combustor is almost 60% lower than the baseline aircraft. It should be possible to achieve N+3 goals with the advanced Radial TAPS technology.

The Ultra Quiet and Efficient A20 Airliner is able to reduce fuel consumption by an additional third compared to the AR20 Advanced Reference Airliner. This is achieved through a combination of an innovative laminar flow design, novel protective skin and multifunctional structures, and a highly efficient and noise optimized turboprop. The noise optimized propeller reduces ground noise 15 EPNdB cum below what is possible for a 13:1 bypass ratio turbofan with advanced noise reduction technologies. The A20 Advanced Airliner is also significantly smaller and requires much smaller engines, which has excellent implications for aircraft acquisition cost and ticket price.

Table 71. Impact of Advanced Airframe and Propulsion System

	TOGW lb	Thrust lbf	Fuel Burn lb/mission	LTO NOx g/LTO/Pax	LTO Noise EPNdB Cum	Field Length Landing, T/O
Baseline Airliner	24973	4557.5	3516	43	-20	4000
B20 w/ 2008 TF	**BASE**	**BASE**	**BASE**	**BASE**	**BASE**	**BASE**
Advanced Airliner	14550	3203.8	1088	10.5	-74	
A20 w/ 2030 ATP	**-42%**	**-30%**	**-69%**	**-75%**	**-54**	**-9%**
Adv Reference Airliner	17511.1	4090.4	1669	17.3	-41	
AR20 w/ 2030 ARTF	**-30%**	**-10%**	**-53%**	**-59%**	**-21**	**-8%**
Advanced Propulsion Only	22267	5197	1800	20.6	-62	
B20 w/ 2030 ATP	**-11%**	**+14%**	**-49%**	**-52%**	**-42**	**+23%**
Advanced Airframe Only	16437.6	3287.8	2135	31.9	-32	
A20 w/ 2008 TF	**-34%**	**-28%**	**-39%**	**-25%**	**-12**	**+6%**

To evaluate the impact of propulsion technologies, a current technology aircraft, with the same level of technology as the baseline aircraft, was optimized with scaled versions of the GE UQETP Advanced Turboprop. The improvements to the baseline aircraft fuel burn and LTO NOX due to the Advanced Turboprop alone are nearly as great as all the technologies of the Advanced Reference Aircraft combined. Additionally LTO noise is improved more than 40 EPNdB cum compared to the baseline aircraft, and might be sufficiently quiet for the future N+3 network.

The A20 Advanced Airliner was also sized with scaled 2008 technology GE4600B baseline turbofan engines. The advanced aircraft alone reduced fuel burn almost 40% versus the baseline aircraft, and reduced LTO emissions by 25%. Noise was also improved 12 EPNdB cum versus the baseline aircraft because of the much aerodynamically cleaner design, and the reduced thrust requirements of the lighter, lower drag aircraft. These improvements are smaller than those afforded by the Advanced Turboprop. However, the advanced weight and aero improvements of the A20 Airframe result in a much smaller aircraft, which has excellent implication for aircraft acquisition cost.

9.3 Technology Sensitivity Studies

9.3.1 Technology Sensitivity and Ranking of Key Technologies

A one-off technology sensitivity study was conducted in order to capture the impact of individual technology categories on the study metrics. The idea behind the one-off approach is to start with the selected configuration, the 2035 AR20 Advanced Airliner, remove one technology at a time, and assess the impact on the metrics. With each removal, the delta from the 2035 Airliner is reported. Essentially, the one-off technology trade study allows the quantification of each technology in terms of how much is it worth in delta fuel burn, delta noise and delta emissions. Once the quantification is assessed then the technologies can be ranked based on much they contribute to each of the metrics.

In order to maximize the impact of each technology, an optimization is required after the removal of each technology. The optimization objective is again mission fuel weight by varying thrust to weight ratio and wing loading subject to 200 fpm top of climb (TOC) rate of climb (ROC) or better constraint. Takeoff field length was allowed to float to show some impact on

this metric. In reality, if the actual field length exceeded that of the future network's runways, the aircraft would be re-optimized to a 4000 ft field length at some expense to noise or fuel burn.

Table 74 shows the individual impact of key technologies on the study metrics and the size of the Advanced Airliner and Propulsion system. Some of the technologies are also arranged in groups where their integration or co-development may make for greater synergistic improvements. These two categories can be described as a propulsion system weight and performance group, and an aircraft structural or weight reduction group weight reduction group.

Table 72. One-Off Impact of Removing Technologies from A20 Advanced Airliner

	TOGW	Engine Size	Fuel Burn	LTO NOx (g/PAX)	LTO Noise (EPNdB cum)	Field legth
Advanced A20ATP	**BASE**	**BASE**	**BASE**	**BASE**	**BASE**	**BASE**
Advanced Propulsion Mech Systems	1%	2%	7%	10%	~ same	2%
Advanced Propulsions Aero	1%	-5%	**14%**	10%	~ same	11%
Adv Propulsion Materias/Manufacturing	4%	~ same	**13%**	**40%**	~ same	4%
Advanced Radial TAPS	~same	~same	~same	**75%**	~same	~same
Noise Optimized Turboprop	~same	~same	~same	~same	**+29 dB**	**15%**
AF Structural Technologies	**20%**	9%	**10%**	**15%**	**+3dB**	4%
Advanced Airframe Systems	5%	-1%	2%	~same	+1dB	~same
Multifunction AF Structure	1%	0%	~same	~same	~same	~same
Novel Protective AF Skin	7%	1%	3%	2%	+1dB	7%
Novel AF Laminar Flow Technologies	7%	**43%**	**20%**	**65%**	**+9dB**	**4%**

The results of the one-off technology study shown in Table 74 were then used to inform a TOPSIS ranking of the technology categories to identify the technologies with the biggest impact on the studies metrics and the chance for enabling viability of this new mode of air transportation. The technologies were ranked on a typical 0,1,3,5,7,9 scale for their impact on the study metrics or perceives aircraft cost (based on aircraft/engine size, etc.). Once again, fuel burn and noise were given 50% higher weighting than the other metrics because of their impact on the environment and community acceptance.

Table 73. TOPSIS Ranking of Most Influential Technologies

	Fuel Burn	LTO NOx	LTO Noise	Field Length	A/C Cost/ Ticket Price	Ranking
Weighting	**3**	2	**3**	2	2	
Propulsion Techs (Mat'ls, Aero, Systems)	**9**	**7**	0	**7**	1	2
Advanced Radial TAPS	0	**9**	0	0	0	4
Efficient, Noise Optimized Propeller	0	0	**9**	**7**	0	3
A/C Materials/Structure/Systems	5	3	1	5	5	3
A/C Laminar Flow Technologies	**5**	**7**	3	1	5	1

The Aircraft Laminar Flow Technologies have the biggest impact on the most metrics. The reduced drag allows for a smaller aircraft and much smaller engine (cost), significant reductions in fuel burn and emissions, and a moderate noise benefit due to reduced airframe noise and engine size.

The Propulsion Technology Package has by far the largest impact on fuel burn and very high impact on LTO NOx and field length. The performance and weight enhancing technologies of the Propulsion group have very little influence on noise.

The Airframe Materials, Structures, and Systems Group and the Noise Optimized Propeller had similar overall benefits to the future N+3 network. The weight saving airframe technologies reduced fuel burn, emission, field length, and potentially aircraft cost. The Noise Optimized Propeller's strong impact on LTO noise and field length would help determine the number of small community airports in the point-to-point travel network, and therefore, its commercial viability.

Finally, the innovative Advanced Radial Taps Combustor would bring large engine advanced emissions technologies down to small size. Its strong impact on NOx and other emissions may be key as more stringent emission requirements are brought to this previously unregulated size class.

10.0 Technology Risk Assessment Report & Technology Roadmaps

Risk and technology roadmaps have been identified for the key enabling aircraft and propulsion technologies identified in Section 9. A technology risk assessment and roadmap for fuel cell technologies is also contained in this section, as these concepts also showed promise to dramatically reduce the environmental impact of future aviation.

10.1 Advanced Low NOx Radial TAPS Combustor

10.1.1 Goals and Objectives

1. Develop a small scale premixing combustor with enhanced premixing capable of achieving 30 to 50% reduction in LTO NOx compared to a current RQL combustor with acceptable stability and performance
2. Develop advanced materials and cooling technologies applicable to small engines to minimize cooling requirements, enabling higher operating temperatures without increased NOx emissions
3. Evaluate and develop advanced pilot systems to reduce low power emissions, with acceptable ignition and stability characteristics

10.1.2 Technical Description

The primary approach to meet the aggressive N+3 emission goal of LTO NOx 75% below CAEP6 standards will be the Twin Annular Premixed Swirler (TAPS) combustor. The TAPS combustor mixer uses a lean-premixing main stage to reduce NOx and particulate matter emissions at high power operating conditions, and a concentric pilot stage to provide stability and low CO and HC emissions at lower power. Two key challenges for the TAPS mixer are (1) to achieve excellent main stage fuel air mixing effectiveness at high power operating conditions to substantially reduce NOx formation by reducing flame temperatures and virtually eliminate soot particulate matter formation by avoiding rich regions where soot is formed, and (2) to establish a robust pilot stage recirculation zone at low power operating conditions to provide excellent ignition capability, flame stability, and low CO and HC emissions. A third challenge is to minimize cooling flow required for the whole combustor structure so that enough combustion air is available to provide the lean fuel air mixtures needed to reduce flame temperature to levels needed to achieve the NOx requirements.

The initial TAPS combustor has already been certificated at levels less than 50% of CAEP6 standards in the GEnx engine, which will provide thrust for new wide body aircraft including the Boeing 787 and 747-8. Some key future technical challenges are:

1. Further improve TAPS main stage mixing to reduce NOx to less than 75% of CAEP/6 in current engines.
2. Implement advanced materials and cooling designs to increase the amount of combustor airflow available to the TAPS mixer in order to achieve NOx less than 75% of CAEP/6 in future, higher temperature cycles.
3. Develop innovative pilot concepts to reduce NOx formation during pilot only operation at approach and idle, while maintaining current ignition, stability and emissions capabilities.
4. Develop methods to scale key technologies across the whole spectrum of engine thrust

Plans to meet challenges 1 through 3 above for large engines are currently being implemented under GE's NASA N+2 projects. In parallel, efforts are underway under GE internal projects and FAA CLEEN efforts. It is anticipated that these N+1 and initial N+2 efforts will be completed in the 2016 timeframe.

Once technologies and scaling methodologies are in place based on current NASA N+2 and CLEEN Programs, the next step will be to apply those technologies to engines in the 3000 lb thrust-class. Specific challenges and required technology development for small engines include:

- Reduced inlet pressure and temperature at high power make fuel vaporization more difficult and increase the challenge of maintaining a stable lean flame with high combustion efficiency. Improved fuel atomization and increased residence times for vaporization and combustion will have to be evaluated, analytically and in flame tube testing.

- Increased surface-to-volume increases the challenge of minimizing air used to cool the combustor structure. Cost effective structures constructed with advanced materials will have to be developed to minimize cooling air.

- Reducing the diameter of the TAPS pilot fuel injector will require scaling or reconfiguration of thermal protection and fuel-staging features. Moreover, the volume of the recirculation zone behind the pilot injector will be reduced, increasing the challenge to meet low power emissions and stability requirements. Initial work to quantify the effect of reduced fuel injector diameter will include mechanical and heat transfer analyses of scaled down thermal protection and staging features, coupled with state-of-the-art CFD analyses. Flame tube and sector testing will be executed to systematically evaluate emissions and combustion stability.

If promising results are obtained in these initial tests, full annular tests would be used to bring the concept to TRL 5. If we encounter practical scaling limits with respect to emissions, performance or cost/benefit during this initial effort, alternatives to TAPS would be investigated.

10.1.3 Risk Assessment

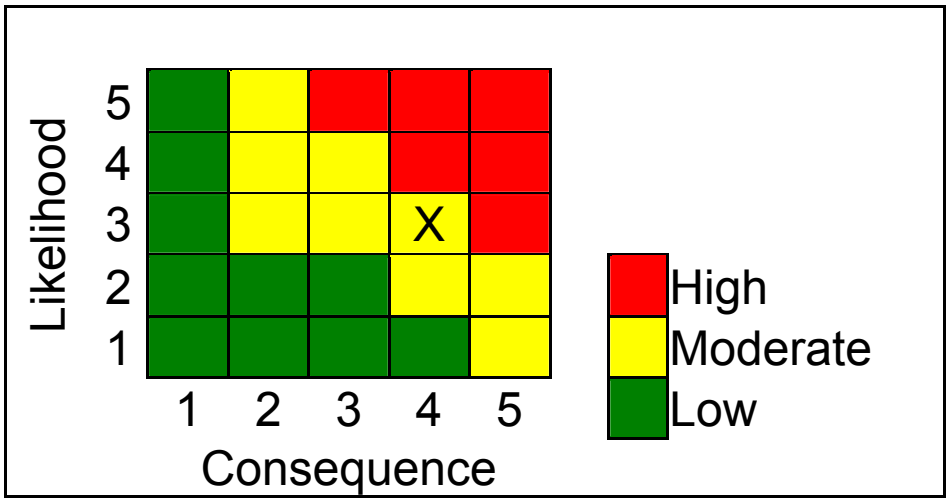

10.1.4 Milestones

From a technical standpoint GE recommends that development of TAPS technology for small engines should begin after features and attributes of advanced TAPS technologies have been defined under N+1 and N+2 efforts. For that reason, we have assumed an October 2015 start for work on this N+3 combustor. Key milestones and completion dates would then be:

1. June 2016 - Systems analysis and conceptual design
2. January 2017 - Main stage mixing studies and flame tube tests
3. January 2017 - Mechanical and thermal design and analysis of combustor structure with minimum cooling flow
4. June 2017 - Small diameter pilot stage CFD studies, flame tube and sector tests

10.1.5 Deliverables

1. Combustor conceptual design drawing and analysis summary
2. Preliminary combustor mechanical design description
3. Flame tube component rig hardware and test and analysis results

10.1.6 Long Term Schedule

1. June 2018 - Full annular rig design
2. June 2019 - Full annular rig test (TRL 5)

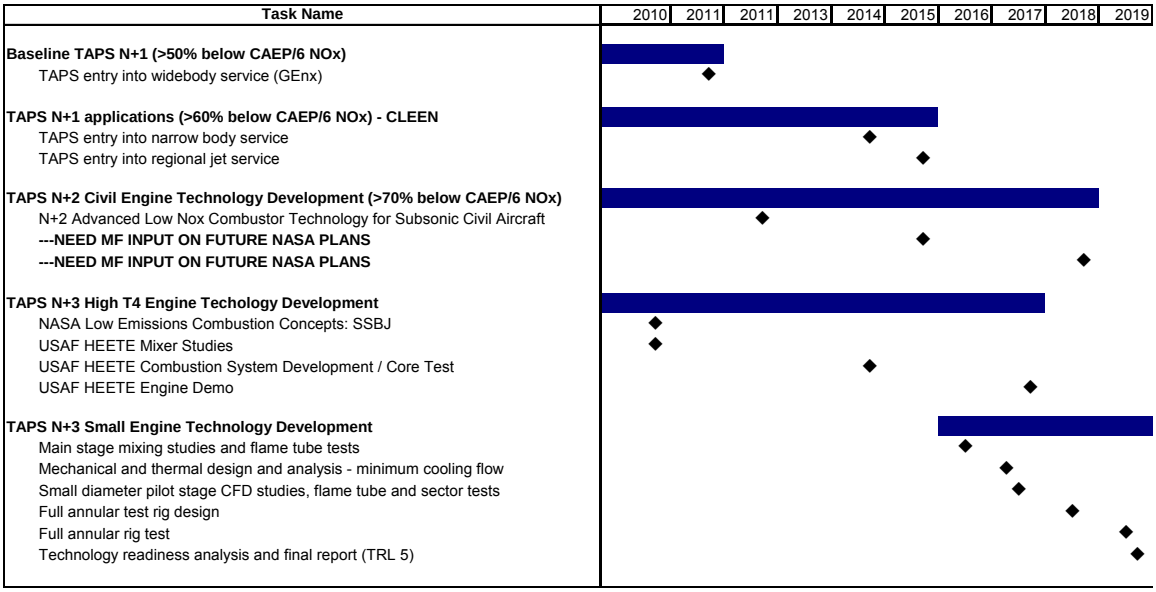

10.1.7 Performance Area impact

Fuel Burn	none
LTO Emissions	meet 75% reduction below CAEP 6
Cumulative Noise	none
Fuel Efficiency	enable higher temperature operation within NOx limits

10.2 Low Noise/High Performance Propeller

10.2.1 Goals and Objectives

1. Propeller with high cruise efficiency
2. Propeller with low noise
3. Light weight, high reliability

10.2.2 Technical Description

The propeller generates the majority of the noise propagated to the farfield in turbo-prop engines. An advanced technology low noise/high performance propeller is a critical component of the Ultra Quiet and Efficient Propulsion and a large contributor to the noise and fuel efficiency. System studies must be conducted to determine the best combination of number of props, diameter, and tip speed to balance the mission requirements.

To make a leap in the technology level of the aero-acoustic propeller design advanced high fidelity tools will be utilized to balance the system requirements between acoustics and aerodynamics of the basic blade design. Next various technologies of potential value to reduce the noise production of the propeller will be evaluated, including concepts such as non-uniform circumferential spacing and tip treatments as discussed in Reference 33, and fluidics. Scale model rig tests will be used to validate designs and technologies ultimately leading to an engine demonstration.

10.2.3 Risk Assessment

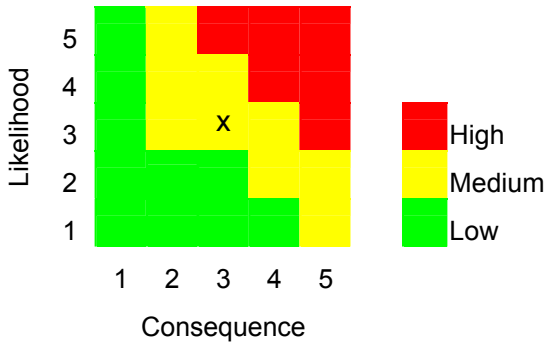

10.2.4 Milestones

1. GEN1 Scale Model Test
2. Non-Uniform Spacing, Tip Features, Fluidics assessment
3. GEN2 Scale Model Test
4. Engine Test

10.2.5 Deliverables

1. GEN1 Prop Design
2. Scale Model Hardware
3. GEN2 Prop Design
4. Scale Model Hardware
5. Engine Hardware

10.2.6 Long Term Schedule

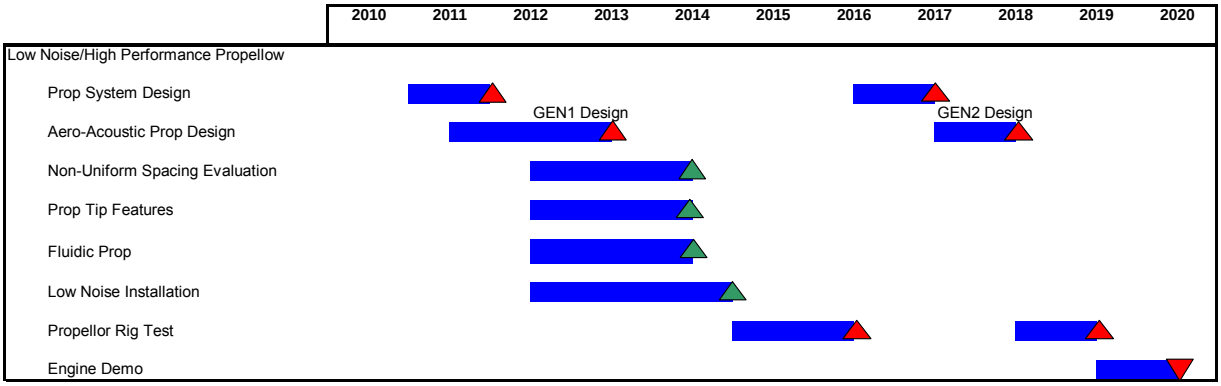

10.2.7 Performance Area impact

Emissions	reduced fuel burn
Cumulative Noise	reduced takeoff/landing noise
Field Length	reduced field length
Fuel Efficiency	high efficiency

10.3 Advanced Propulsion Materials, Manufacturing, Mechanical Systems

10.3.1 Goals and Objectives

- Improved manufacturing and materials for reduced weight and increased performance and durability
- Advanced mechanical systems for reduced weight and increased performance and durability

10.3.2 Technical Description

Advanced disk, shaft, and airfoil materials and manufacturing processes will allow higher temperatures, higher tip speeds, and more complex airfoil shapes and flowpath counters for lower weight and higher performance.

High temperature flowpath, combustor, and structural materials reduce the need for cooling.

Lightweight composite structures reduce weight in accessory and propeller gearboxes, and other low-temperature static structures.

Advanced bearing, seals, and axi-centrifugal core clearance control technologies improve performance and durability and reduce weight and emissions.

10.3.3 Risk Assessment

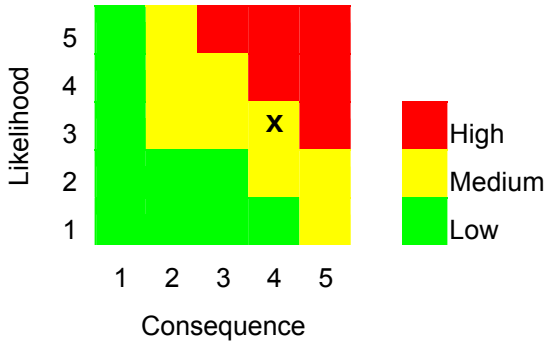

10.3.4 Milestones

Subscale material development process
Full scale material development
Final material ready for engine use
Man tech milestones --- TBD
Tests of gen1,2,3 CMC Components
Tests of seal and bearing components
Test of modulated cooling components
Test of advanced axi-centrif core clearance control concepts

10.3.5 Deliverables

Slave Hardware for Engine Demo Test
Integrated Engine Build-up
Full scale engine tests (repeated builds/test of dedicated test assets)
Test Reports

10.3.6 Dependencies

Need suitable mule engine(s) to use as a dedicated engine test asset
Base engine could be off-the-shelf or a current technology demonstrator engine
Need contingency plan for backup hardware in case of a catastrophic failure during testing

10.3.7 Performance Area impact

Fuel Burn	Significant reduction
Emissions	Significant reduction
Cumulative Noise	Little or no impact
Field length	moderate reduction

10.4 Risk and Development of Practical Laminar Flow

10.4.1 Aero 1.1: Step and Gap Requirements in Favorable Pressure Gradients

10.4.1.1 Statement of Need

To meet long term goals for a large reduction in fuel usage by future airplane designs, a significant drag reduction will be required by extensive reliance on laminar flow. Detail design of airplane components where laminar flow is to be preserved using natural methods requires specific tolerances for steps and gaps. These tolerances will be used to specify material and manufacturing requirements.

10.4.1.2 Goals and Objectives

Develop a database that can be used for detail design of components depending on local Reynolds number, pressure gradient, and geometry.

10.4.1.3 Technical Description

Design for Natural Laminar Flow (NLF) requires great attention to detail in the design and manufacture of airplane surfaces. Current methods and data available can help to define these requirements based on surface waviness or to design surface shapes to prolong the NLF run by maintaining a favorable pressure gradient over the maximum chordwise extent. These methods assume smooth surfaces, but airplanes will always need to have joints in places where components connect. These joints are never perfectly smooth, especially if there are doors, windows, or access panels which are required for operation or maintenance. It is also likely that the step or gap size could change after time in service.

Boundary layer theory predicts that the flow will transition from laminar to turbulent if the velocity profile through the boundary layer contains an inflection. A general favorable pressure gradient will delay the occurrence of a velocity inflection, but a local imperfection will cause a pressure oscillation containing an adverse gradient. The flow will transition if the general favorable gradient is not strong enough to keep the flow laminar.

To progress beyond the preliminary design stage, an airplane concept which requires extensive runs of NLF will need quantitative specifications for step and gap allowables so that detailed part design and manufacturing approach can be defined.

Information for use by designers needs to be parametric in nature, so that requirements can be tailored to the specific location on the airplane. If the local Reynolds number and/or pressure gradient is more favorable, then the size and/or tolerance can be relaxed and a less stringent method can be used. Conversely if the location is less favorable, then strict methods must be enforced. The type of database required does not exist.

The data required includes both 2D and 3D configurations, such as airfoil/wing and fuselage nose shapes. It would be most useful if a range of Reynolds numbers is tested, but at the least the test must include the full scale flight regime. A progressive series of test shapes will provide the desired variation in pressure gradients, and each shape would test several step and/or gap sizes. Transition would be measured with a suitable technique such as sublimating chemicals, liquid crystals, infrared, etc.

Current analytical and computational techniques are insufficient to predict boundary layer transition in the presence of imperfections such as steps and gaps in the presence of pressure gradients. The required data must be gathered experimentally using a suitable technique, either wind tunnel or flight testing. Wind tunnel is likely preferred due to the ability to control independent variables; however a pressure tunnel would be required to achieve the required Reynolds number. The National Transonic Facility at NASA Langley Research Center or the Onera F1 in Toulouse, France would be suitable candidates.

10.4.1.4 Milestones

1. Survey and document complete
2. Test methodology established and documented
3. Determination of test facility/hardware requirements, budget, and schedule
4. Construct hardware and conduct test.
5. Data analysis and development of design database.

10.4.1.5 Demonstrations and Deliverables

Aero1.1.1: Conduct a survey and document relevant theoretical and experimental work in the field of boundary layer transition and in the presence of imperfections. Deliverable is a report.

Aero1.1.2: Establish a methodology to investigate the effect of step and gap size on transition for various pressure gradients. Consider the desirability of a consortium approach. Deliverable is a report and an action to establish a consortium if that proves to be desirable.

Aero1.1.3: Determine requirements for test facility and test hardware. Develop schedule to construct hardware and conduct test. Deliverable is a document describing the requirements, schedule, and budget.

Aero1.1.4: Construct hardware and conduct test. Deliverable is the hardware and raw data.

Aero1.1.5: Reduce the data and cast in format for use by designers. Deliverable is the final report documenting the methods and data.

10.4.1.5 Schedule

The schedule shown in Figure 184 is typical of a single iteration attempt at (1) establishing a current baseline for the technology and the preferred approaches for further development, (2) building test articles, (3) conducting some engineering experiments, and (4) processing and reporting on the data. This schedule does not include delays associated with a phased funding of the effort. It also doesn't account for a likely need to re-test and re-analyze after the initial set of data is interpreted. Two or three iterations may be necessary to be confident that design data for steps, gaps, and contours is accepted by the manufacturing process and product design customers.

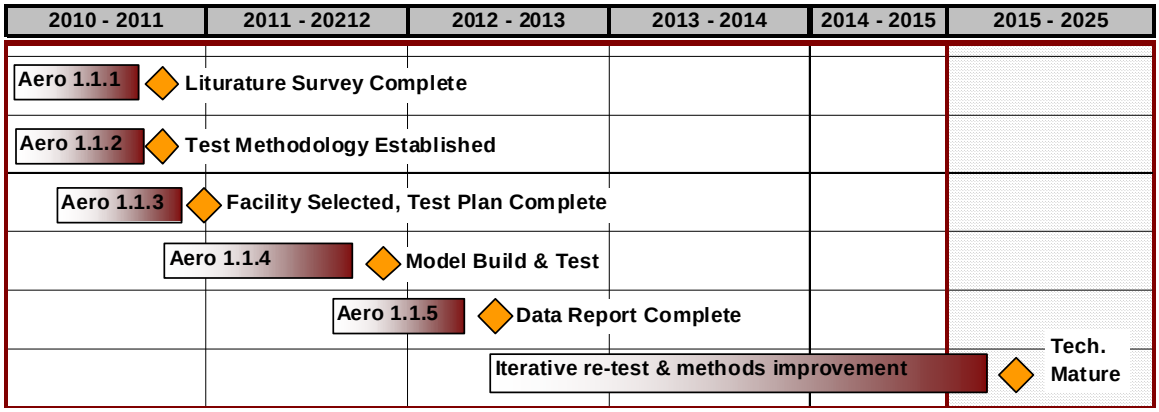

Figure 184. Development Schedule for Aero 1.1

10.4.2 Aero 1.2: Suction Requirements to Reestablish Laminar Flow

10.4.2.1 Statement of Need

To meet long term goals for a large reduction in fuel usage by future airplane designs, a significant drag reduction will be required by extensive reliance on laminar flow. Detail design of airplane components where laminar flow is to be preserved using active methods requires quantitative suction requirements to preserve and reestablish laminar flow. These requirements will be used to correctly size and design suction systems.

10.4.2.2 Goals and Objectives

Develop a database that can be used for detail design of active suction systems intended to reestablish or preserve laminar flow.

10.4.2.3 Technical Description

Design for Natural Laminar Flow (NLF) requires great attention to detail in the design and manufacture of airplane surfaces. Some areas of the aircraft surface cannot be designed to preserve laminar flow naturally regardless of the design or manufacturing approach. Examples of these areas would be near doors, windows, or access panels. In some cases the location of a door may be forward of an area which could otherwise take advantage of laminar flow but because the flow is tripped a turbulent boundary layer would exist. In this case, application of suction could reestablish laminar flow which would then be naturally sustained downstream.

This concept is the basis for Hybrid Laminar Flow which has been tested successfully in previous studies. Further work is needed to determine quantitative suction requirements for various disturbance sizes and local pressure gradients.

To progress beyond the preliminary design stage, an airplane concept which requires extensive runs of HLF will need quantitative specifications for suction requirements for the variety of applications that may be encountered. With this data a detailed system design and manufacturing approach can be defined.

Information for use by designers needs to be parametric in nature, so that requirements can be tailored to the specific location on the airplane. If the local Reynolds number and/or pressure

gradient is more favorable, then the suction requirement can be relaxed and a less stringent method can be used. Conversely if the location is less favorable, then stronger suction would be needed. The type of database required does not exist.

The data required includes both 2D and 3D configurations, such as airfoil/wing and fuselage nose shapes. It would be most useful if a range of Reynolds numbers is tested, but at the least the test must include the full scale flight regime. A progressive series of test shapes will provide the desired variation in pressure gradients, and each shape would test several step and/or gap sizes and suction levels. Transition would be measured with a suitable technique such as sublimating chemicals, liquid crystals, infrared, etc.

Current analytical and computational techniques are insufficient to predict suction requirements to reestablish laminar flow downstream of imperfections such as steps and gaps and in the presence of pressure gradients. The required data must be gathered experimentally using a suitable technique, either wind tunnel or flight testing. Wind tunnel is likely preferred due to the ability to control independent variables; however a pressure tunnel would be required to achieve the required Reynolds number. The National Transonic Facility at NASA Langley Research Center or the Onera F1 in Toulouse, France would be suitable candidates.

10.4.2.4 Milestones

1. Survey and document complete
2. Test methodology established and documented
3. Determination of test facility/hardware requirements, budget, and schedule
4. Construct hardware and conduct test.
5. Data analysis and development of design database.

10.4.2.5 Demonstrations and Deliverables

Aero1.2.1: Conduct a survey and document relevant theoretical and experimental work in the field of boundary layer transition and in the presence of imperfections. Deliverable is a report.

Aero1.2.2: Establish a methodology to investigate the effect of step/gap size on suction requirements to delay transition and/or reestablish laminar flow for various pressure gradients. Consider the desirability of a consortium approach. Deliverable is a report and an action to establish a consortium if that proves to be desirable.

Aero1.2.3: Determine requirements for test facility and test hardware. Develop schedule to construct hardware and conduct test. Deliverable is a document describing the requirements, schedule, and budget.

Aero1.2.4: Construct hardware and conduct test. Deliverable is the hardware and raw data.

Aero1.2.5: Reduce the data and cast in format for use by designers. Deliverable is the final report documenting the methods and data.

10.4.2.6 Schedule

The schedule shown in Figure 185 is typical of a single iteration attempt at (1) establishing a current baseline for the technology and the preferred approaches for further development, (2) building test articles, (3) conducting some engineering experiments, and (4) processing and reporting on the data. This schedule does not include delays associated with a phased funding of the effort. It also doesn't account for a likely need to re-test and re-analyze after the initial set of data is interpreted. Two or three iterations may be necessary. However, in this area many of the iterations are likely to be in the systems development roadmap. This other effort is focused on designing and testing suction systems that create the amount of suction that is defined in the report from Aero 1.2.5.

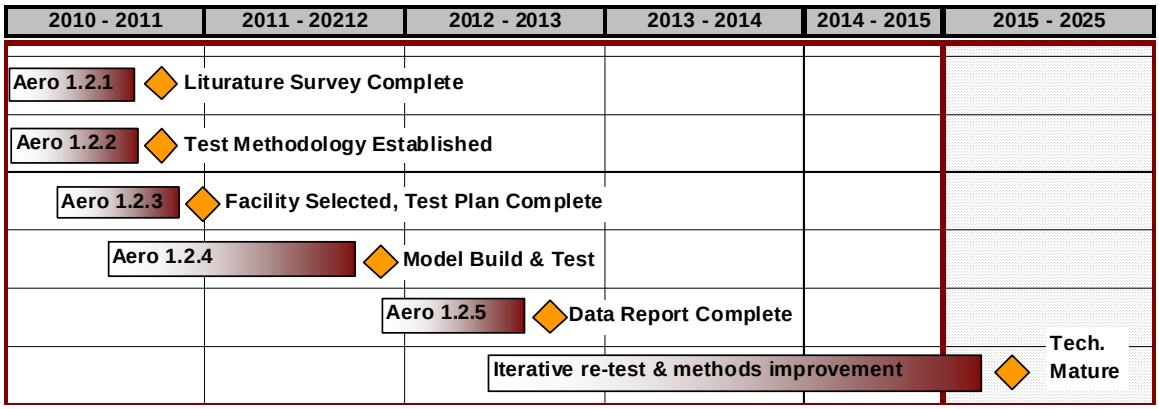

Figure 185. Development Schedule for Aero 1.2

10.4.3 Aero 2.0: Self Cleaning Surfaces

10.4.3.1 Statement of Need

For laminar flow surfaces, regardless of the method used to design or manufacture to achieve the required surface shape and smoothness, there will be times when the operational environment contaminates the surface with ice, dirt, or insect debris. This has been shown to trip the flow and the laminar flow drag improvement will be lost. Some method to prevent contamination or to clean it promptly afterward will be needed if laminar flow is to be relied upon in an operational environment.

10.4.3.2 Goals and Objectives

Test the performance of self cleaning surfaces and their ability to prevent contamination or to shed it after a contamination event.

10.4.3.3 Technical Description

All aircraft must perform in an environment which can impose a variety of contaminants, including dirt, rain, ice, and insects. These elements can hinder flight performance in many ways even on conventional aircraft. Transport airplanes are designed with systems which enable them to operate safely within this environment. A good example is icing, where a system is designed to melt or remove ice contamination from leading edges and mitigate the increased drag and reduced lifting ability which would otherwise occur.

For aircraft designed to operate with significant amounts of laminar flow, the level of protection must be increased significantly. In addition to an ice protection system described above, a system must be devised to prevent or remove even the slightest amount of roughness from the leading edge. Otherwise the boundary layer will transition from laminar to turbulent, drag will increase dramatically, and the airplane will not perform as designed. The requirement to keep surfaces clear of contaminants is present regardless of whether a passive or active system is used to achieve laminar flow.

Two basic approaches may be considered. First is to prevent the contamination from reaching the leading edges. The Boeing 757 Hybrid Laminar Flow testing planned on using a Krueger flap to deflect insects from the leading edge during low altitude phases of flight. A second approach is to devise a system to remove the contaminants from the leading edges after the fact. This could be achieved through a type of self cleaning surface coating which would keep contaminants from sticking, or by excreting a cleaning fluid from the surface to carry the contaminant away.

It is the second approach that is the subject of this study. The “Lotus Effect” describes a surface which is super-hydrophobic and repels water to a very high degree. Dirt particles are then picked up by water droplets due to their higher affinity for the dirt than the surface. In theory, after a contaminating event, the dirt could be carried away by water from a yet to be determined source.

In an interesting contrast, super-hydrophilic surfaces can have a similar cleaning effect. This approach also requires water which then spreads smoothly across the surface, carries away the dirt, and dries quickly leaving a clean surface. A commercially available treatment is in use to keep windows clean on large buildings.

The testing of these surfaces would best be done on a flight article which could be exposed to a variety of contaminants. It is not necessary to establish laminar flow or detect transition. The test would concentrate on measurement of contamination and the performance of the coating in removing the contaminant.

10.4.3.4 Milestones

1. Survey and document complete
2. Test methodology established and documented
3. Determination of test facility/hardware requirements, budget, and schedule
4. Construct hardware and conduct test.
5. Data analysis and development of design database.

10.4.3.5 Demonstrations and Deliverables

Aero 2.1: Conduct a survey and document relevant theoretical and experimental work in the field of boundary layer transition and in the presence of imperfections. Deliverable is a report.

Aero 2.2: Establish a methodology to investigate the feasibility of approaches to keep surfaces clean. Consider the desirability of a consortium approach. Deliverable is a report and an action to establish a consortium if that proves to be desirable.

Aero 2.3: Determine requirements for test facility and test hardware. Develop schedule to construct hardware and conduct test. Deliverable is a document describing the requirements, schedule, and budget.

Aero 2.4: Construct hardware and conduct test. Deliverable is the hardware and raw data.

Aero 2.5: Reduce the data and format for use by designers. Deliverable is the final report documenting the methods and data.

10.4.3.6 Schedule

The schedule shown of Figure 186 is typical of a single iteration attempt at (1) establishing a current baseline for the technology and the preferred approaches for further development, (2) building test articles, (3) conducting some engineering experiments, and (4) processing and reporting on the data. This schedule does not include delays associated with a phased funding of the effort. It also doesn't account for a likely need to re-test and re-analyze after the initial set of data is interpreted. Two or three iterations may be necessary. This entire work package could be completed with the experimental application of self-cleaning materials to experimental test fixtures

Maturity of this capability for airline operations will depend on manufacturing and installation trials and on in-service tests. It may be a challenge to find willing partners and to acquire meaningful in-service data.

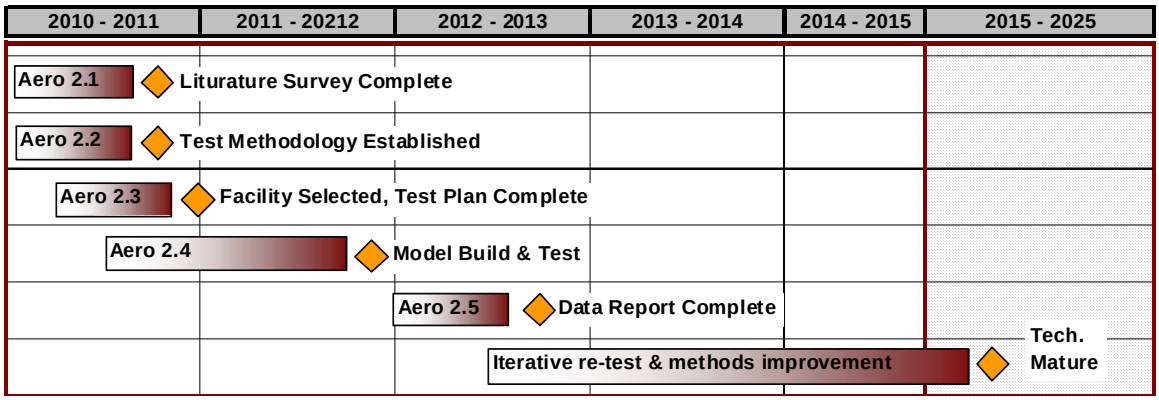

Figure 186. Development Schedule for Aero 2.0

10.4.4 Laminar Flow Development Risk

The risk assessment for technologies that enable laminar flow is developed from a combination of (1) an estimate of the current technology or analysis readiness level, (2) an assessment of the difficulty associated with technology development tasks, and (3) an estimate of the impact or consequence to the 2035 vehicle's compliance with NASA's goals (Fuel burn, Noise, NOx, & Field Length). Appendix H presents some standard definitions for technology readiness level (TRL), some standard definitions for analysis readiness level (ARL), and the use of likelihood and consequence ratings for a technology development risk assessment in this report.

Table 74 indicates that the extent and quality of data for step, gap, and contour requirements in favorable pressure gradients is immature and inadequate for design and manufacturing process trade studies. However, the state-of-the-art of analytical and experimental methods necessary to develop this data is relatively well understood. An investment in either Aero 1.1 or 1.2 is anticipated to lead to a successful outcome.

Table 74. Analysis Readiness Levels for Aero 1.1 and Aero 1.2

New Technology Development Risks					
Task #	Technology Work Package Description	Rationale for Analysis Readiness Level	ARL	Technical Challenges, Development Approach	Development Difficulty Rating
Aero 1.1	Step and gap requirements in favorable pressure gradients. Semi-emperical estimation method.	Some correlation data exists, but not sufficient for required design projects.	3	Testing methodolgy is fairly well established but required data is a novel application	5
Aero 1.2	Suction requirements for laminar flow control. Semi-emperical estimation method.	Some correlation data exists, but not sufficient for required design projects.	3	Testing methodolgy is fairly well established but required data is a novel application	5

Table 75 suggests that the application of self-cleaning coatings to the development and maintenance of laminar flow on aircraft surfaces is quite immature and that little work has been done to explore this concept. Without any experience and little research literature on this topic, the task difficulty rating becomes high. However, the application of these coatings to windows on skyscrapers is relatively mature. Consequently, this relatively high risk investment also has the potential for large benefit in a relatively short period of time.

Table 75. Technology Readiness Level for Aero 2.0

New Technology Development Risks					
Task #	Technology Work Package Description	Rationale Technology Readiness Level	TRL	Technical Challenges, Development Approach (to get to a TRL=6)	Development Difficulty Rating
Aero 2.0	Self-cleaning aircraft surfaces.	Some related types of surfaces have demonstrated for other uses. Not anything for Aero.	2	Significant technology advances will be required to achieve a TRL=6. No clear delvelopment path exists.	8

Table 76 and Table 77 show estimates of the likelihood that investments in Aero 1.1, Aero 1.2, and Aero 2.0 will fail to produce results that are sufficient to transition the technology into a production environment. The relatively well understood nature of the tasks in Aero 1.1 and Aero 1.2 suggests that most of the risk in this effort is in the execution and in the appropriate application of resources. The unknown nature of the work in Aero 2.0 leads to a high likelihood

that this technology will fail to mature in time for application on a 2035 vehicle. One of the challenges associated with this effort is the fact that the market size for a specialized material coating is relative small.

Table 76. Likelihood of Development Challenges in Aero 1.1 and 1.2

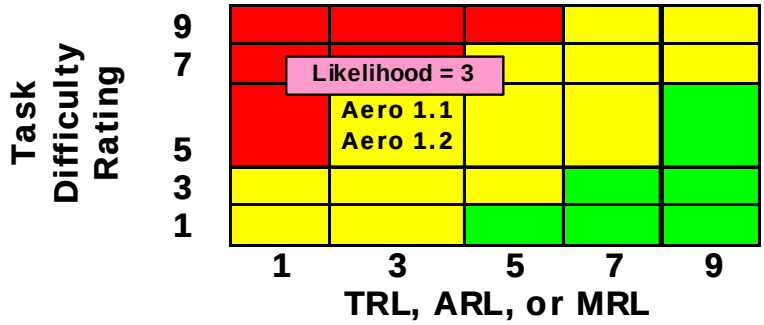

Table 77. Likelihood of Development Challenges in Aero 2.0

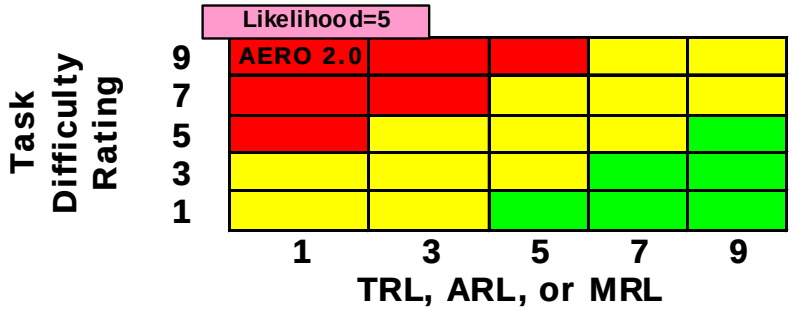

It should be no surprise that Table 78 and Table 79 show a high consequence for failure to mature laminar flow technologies. Laminar flow contributes to approximately 1/3 of the fuel burn benefits in the 2035 vehicle. The risk cube of Table 79 is the results of coupling these high consequence ratings with the likelihood of failure ratings from Table 76 and Table 77. Both the investments in Aero1 and Aero2 are enablers for this valuable laminar flow capability, but Aero2 is perhaps the least well understood. Solving the problem of low cost cleaning or surface smoothness maintenance for airline operations is consider a crucial enabler and could clear the way for private investment in other laminar flow enabling technologies.

Table 78. Technology Risk Assessment for Operational Laminar Flow

Technology Categories	Consequence	Rationale	Likelihood	Rationale
Requirements data base for step, gap, & suctions specifications. Semi-emperical methods that enable design trade studies that include variations in suction, steps, & gaps (Aero1)	4	If the required database is not available then there is a large risk to achieving the desired goals.	3	The required technology to test and aquire the data are fairly well established, so there is only an average liklihood that the data won't be acquired.
Self cleaning aircraft surfaces (Aero2)	5	If the required self cleaning surface cannot be developed n there is a very large risk to achieving the desired goals.	5	There are a very limited number of coatings that have been developed and/or tested, and none of them have been used for aerospace applications.

Table 79. Risk Cube for Laminar Flow Development

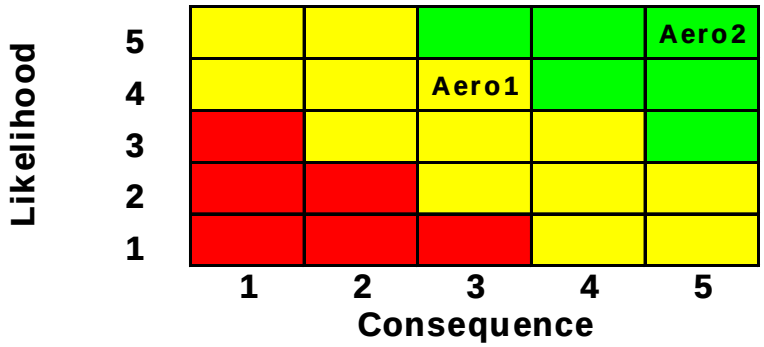

10.5 Composite Airframe Risks and Roadmaps

A 33% weight reduction in empty weight is critical to achieve the goals of the 2035, 20 passenger airliner. Conventional composites are known for their ability to be formed to complex shapes and can provide higher strength with lower weights; history has shown that successful incorporation of composite materials has been a challenge. To better understand the complexity of these issues, reference 1 provides an overview of current types of composite fibers, resins, and tooling methodologies, explores their applications and discusses new innovations in conductive coatings. Reference 2 presents the challenges related to composites by defining current structural weight penalties due to design allowables, environmental issues, fatigue, and damage tolerance. Savings in weight can only obtained with ideal selections of fibers, resins and tooling methodologies.

Most current day composite airframe structures have benefited from the increased material strength but suffered penalties during the integration of sub-systems. Additional penalties have resulted from the addition of lightning strike protection material and from an increase in design factors of safety to account for degradations in strength associated with extreme temperature and moisture environments. The sub-system integration issues typically show up in the requirement to protect the aircraft from lightning, to protect aircraft electronics from electromagnetic interference (EMI), in the establishment of an electrical ground plane, and in the attachment of system components to the airframe structure. A core-stiffened composite structure provides few, if any, places for fastening components or for transferring actuator or component loads into the structure. Core-stiffened composite structures also require unique acoustic treatment to ensure a quiet cabin.

The development roadmaps presented in this report enable a 2035 advanced structure based on the properties of composite materials that are available in 2020 to 2025 and described in Section 6.0 (Advanced Air Vehicle Trade Studies and Analysis Report). This aircraft also benefits from a novel protective skin that enables the use of very thin walled, integrally-stiffened structures. Integrally-stiffened structures simplify the installation and attachment of subsystem components The protective skin changes the paradigm for composite airframe development by allocating requirements for durability, damage tolerance, lightning strike, electromagnetic interference, thermal insulation, acoustic damping, and aesthetic appearance to a set of materials that are not directly responsible for supporting primary loads. This new concept is a direct result of the observation that current day composites that are designed to support pressure and flight loads only are too thin and vulnerable to impact damage, lightning, and extremes in atmospheric temperature and humidity.

This report describes the issues and basic testing needed to establish basic material data including the reductions related to the environment. It then describes the additional “design specific” testing needed to substantiate the base data on structural shapes and testing for damage tolerance. Further details are presented for an outer “protective” layer that may redefine design methodologies by reducing damage tolerance structural weights, eliminate additional materials for thermal and acoustic treatment and provide of a thin conductive outer layer that eliminates the need to paint while providing protection form lightning and electromagnetic interference. Finally development roadmaps and a risk assessment associated with each these roadmaps is presented.

10.5.1 A Roadmap of Weight Savings

As reported in Section 7.0 (Selected Advanced 2035 Airliner Configuration), the performance of the 2035 vehicle depends on a 33% reduction in empty weight that is enabled by technology improvements in engines, sub-systems and airframe structure. Table 80 shows how the additions of key technologies for structures and systems lead to reductions in the empty weight of a current technology aircraft.

Table 80. Roadmap for Empty Weight Savings in 2035 Aircraft

Aircraft Weight Groups	% of B-20 Empty Weight	2010 Composite Aircraft - Materials from 2000s	2015-2020 Composite Aircraft - Materials from 2010s	2030-2035 Composite Aircraft - Materials from 2020s	Technical Approach to 2035 Aircraft
Wing	15.60%	30.00%	35.00%	39.20%	New conductive skin reduces risk & supports accoustic, thermal, and some ice protection functions
Tail	5.16%	30.00%	35.00%	44.00%	
Fuselage	24.16%	25.00%	30.00%	34.00%	
Propulsion	18.98%	0.00%	0.00%	29.67%	Advanced engines reduce weight & fuel burn
Landing Gear	5.49%	0.00%	0.00%	15.00%	Systems, landing gear, & nacelles benefit from transition to electric systems, application of new materials, and optimized integration & installation concepts
Nacelle & Air Induction	2.71%	0.00%	0.00%	20.00%	
Surface Controls	1.88%	-15.00%	0.00%	15.00%	
Hydraulics	1.28%	-15.00%	0.00%	100%	
Electrical	5.41%	-35.00%	0.00%	15.00%	
Avionics and Instruments	3.95%	-35.00%	30.00%	60.00%	Avionics & instruments benefit from panel mount integration & continued breakthroughs in commercial electronics
Furnishings & Equip	10.48%	-60.00%	0.00%	29.19%	Some functions for accoustic damping, thermal insullation, ice protection, & paint moved to wing, tail, and fuselage weight groups (New Conductive Skin)
Air-conditioning & Anti-Ice	4.06%	-15.00%	0.00%	26.34%	
Paint	1.12%	0.00%	0.00%	100%	
Total % Savings	**0**	**1.60%**	**14.00%**	**33.11%**	
Risk	Application of aluminum structure & system integration technology	Application of current composite & system integration technology	Improved Materials, EMI, Lightning, & Sys. Integration	Conductive, Protective, & Health Monitoring Skin	

From an aircraft structure perspective, this roadmap of capability and benefit is shown in Figure 187. As shown in Figure 187, and described later in this report, it can take 5 years to develop the qualification and design data for a new material system. For a 2020 aircraft Figure 187 shows an overlap in the development of design and material development with the design and development of the new aircraft. This typical overlap leads to either high risk in the aircraft development program or conservative assumptions in the material data and failure criteria used to design the aircraft. Current approaches to the development of composite aircraft require some of this overlap because the aircraft shape influences the element and sub-assembly tests required to certify the final structure. Some of this test data requires assumptions and requirements based on things like impact damage and repair. For example, it is common for the design strain levels of some assemblies to be based on data from test panels that have been repaired and then subjected to impact damage.

The 2030 to 2035 aircraft shown in Figure 187 benefits from analytical methods that accelerate the development of material property and design data as well as structural assembly concepts that reduce the dependency or de-couple the structural design properties from the approach to repair, inspection, and impact damage. For the 2035 aircraft, the stress and strain characteristics of the primary structure need not be as dependent on repair techniques and impact damage if a protective skin is responsible for absorbing the anticipated impacts. A health monitoring system that measures the temperature, moisture content, and strength of the primary structure can be used to schedule inspections and repair or to reduce the operational flights speeds and associated loads. This approach enables material development and selection for either impact damage or tensile strength requirements, but not both.

Clearly, the speed and cost associated with the development of material qualification and design databases have a significant impact on the materials that are selected for new air vehicles. Since the novel, protective skin reduces the impact of moisture, heat, and lightning on the primary structure, it has the potential to add some flexibility in the selection if materials for the primary structure of the 2035 vehicle. Early development of the protective skin concept, followed by the rapid development of the qualification and design database for a new material system provides the best potential for weight reduction in the 2035 vehicle.

Although conceptually quite appealing the potential weight reduction associated with multi-functional structures concepts is small compared to the benefit associated with the materials used for primary structure. In this study, multi-functional structures concepts were limited to ice protection, the environmental control system, and the antennas of the navigation and communication system. Small to medium weight reductions in the structure-like portions of these systems leads to a small (1-2 %) reduction in overall aircraft empty weight. The need to integrate sensors and ice-protection systems into the protective skin is primarily driven by the need to create a smooth exterior surface that will promote and enable natural laminar flow.

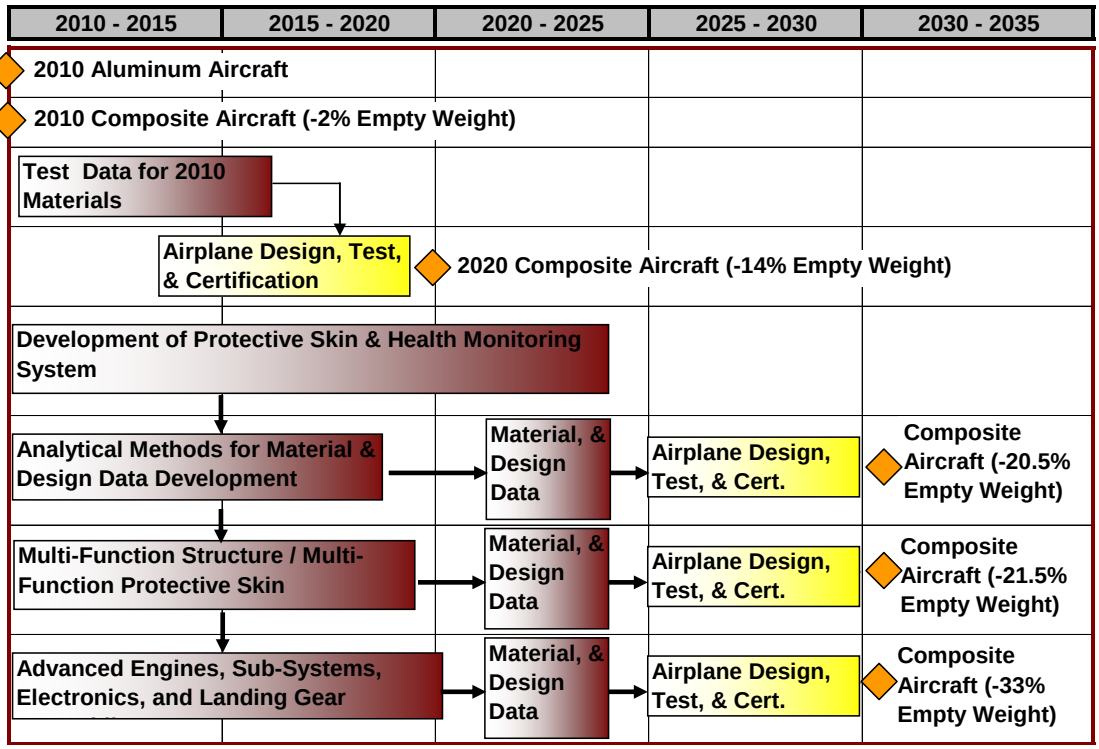

Figure 187. Impact of Structures Research on 2035 Vehicle Empty Weight

The novel protective skin with a health monitoring system, and the rapid development of material qualification and design databases are the critical technologies for aircraft weight reduction. An on-going refinement in the weight of subsystem weight is anticipated to make a significant contribution, but may be associated with the industry's current investment in electronic systems rather than any new initiative required by NASA.

10.5.2 Composite Development Roadmap for a 2015 to 2020 Aircraft

A detailed discussion of composite aircraft development processes that are typical of current technology (2010 – 2020 aircraft) is presented in this section to emphasize the importance of the more detailed technology development programs discussed later in the report. Figure 188 shows the typical timeline for the development of a composite aircraft and the associated materials, component, and assembly databases. The overlap between material and design data development and aircraft design is primarily in the areas of environmental protection, damage tolerance, repair and rework, and manufacturing processes. This overlap adds risk to the aircraft development program and leads to conservative assumptions about the anticipated performance of a material system's response to damage, repair, and harsh environments. Decreasing this risk is critical to widespread application of advanced composite structures on commercial aircraft.

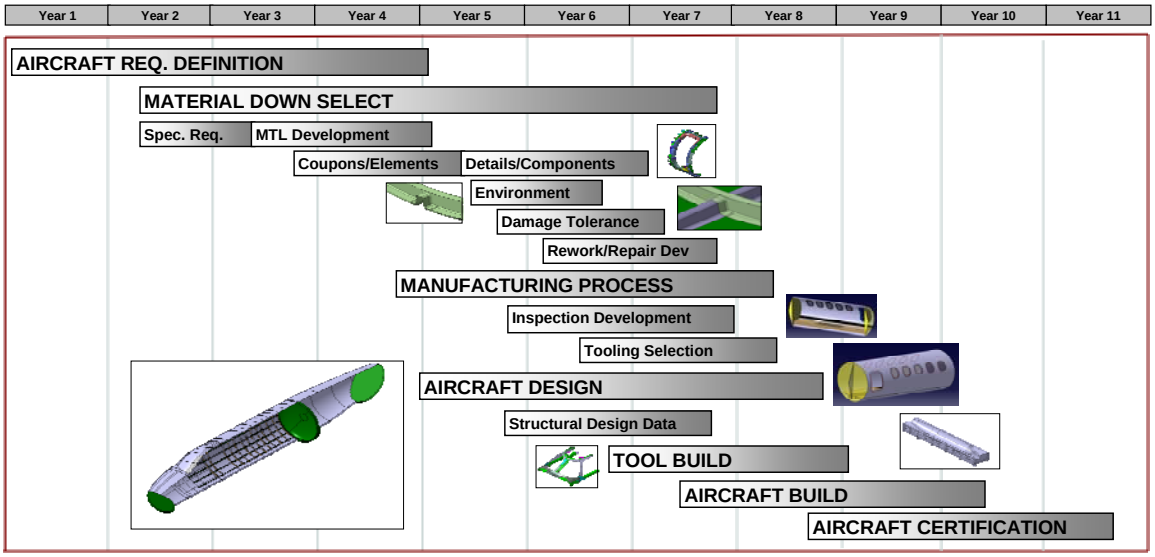

Figure 188. Conventional Process Time Frame

10.5.2.1 Material Selection

Basic material selection may be one of the first decisions after initial development of the requirements for any new aircraft. Performance, aerodynamic shapes, operation temperatures, cost and weight can all be impacted. Seldom are the "best" or most "ideal" materials in production before the start of a project and the search for materials leads to products which are still under development. A challenge for any new effort is concurrent materials development program with aircraft design effort.

It may take several years to perform the required tests to provide the statistical database needed for structural coupons and elements (see Figure 189). Several additional years and design specific configurations are needed for testing the details, sub-components and components (assemblies). Outcome of these tests may provide additional data and impact the design criteria. Frequently this drives multiple test cycles before a final test configuration and the associated design criteria agree.

Material characteristics will impact the configurations in the detail, sub-components and component tests. Programs may encounter delays and higher cost to implement new materials and/or test failures due to assumptions on immature materials. Every effort is a balance between potential performance lost due conservative material selection and the risk of a new better performing material.

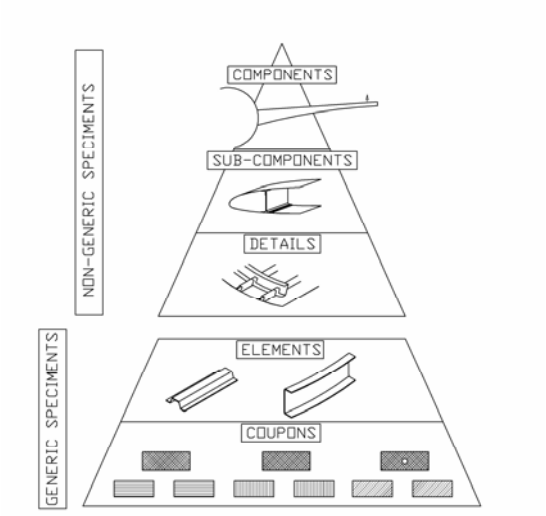

Figure 189. Building Block Design Data Development

Design criteria are driven by material design allowables, section stability, modulus stiffness, damage tolerance, reparability and fatigue. These numbers can be defined and tested at room temperature, but are not well understood how these variables impact design considerations under differing environmental conditions (see Figure 190). An example is a part sized by damage tolerance in a dry condition, but might require sizing for compression load under hot/wet conditions or stiffness in cold conditions. These critical design considerations could also be dependent on specific areas of the aircraft.

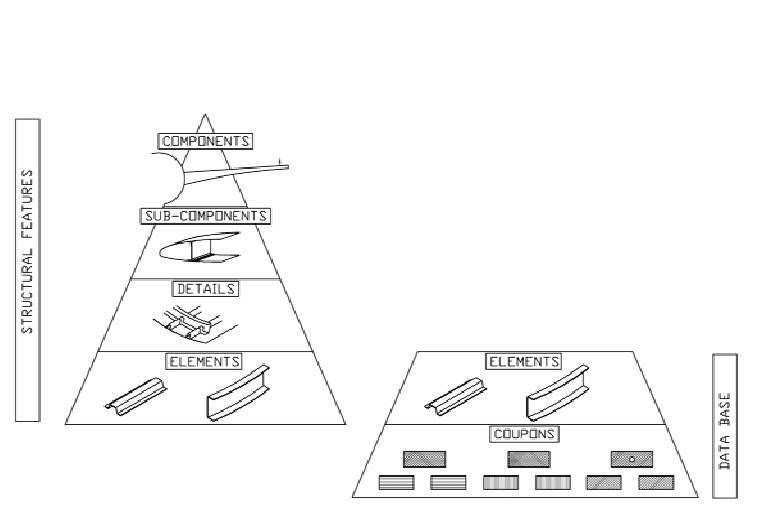

Figure 190. Non-Specific and Specific Design Data

NASA should consider investing in a more robust, streamlined, and analytic approach to testing to and design database development.

10.5.2.2 Manufacturing Process

Fabrication techniques are driven by the materials selections. Epoxy resins are currently the easiest to use, accommodates the most variety of fabrication methods and have been selected for this effort. Hand lay-up, automated tape lay-up, filament wrapping, pressure resin transfer (RTM), vacuum resin transfer (VARTM), and resin transfer utilizing prepreg (SQRTM) all can be used with epoxy resins.

Bismaleimides and Polyimides resins offer higher temperature performance advantages to epoxies, but are greatly limited in their high tooling and manufacturing cost. The year 2035 solution may involve limited use of these materials and will require manufacturing research for tooling and process requirements.

Design for Manufacturing and Assembly (DFMA) practices should be utilized for any design effort. Fabrication methodology needs to focus on the elimination of production steps and reduction in secondary operations. Process variations must be controlled within reasonable design constraints. Hand operations need to be eliminated or reduced in skill level. A road map for any composite implementation should include a focus on design that does not limit the ability to fabricate large assemblies.

10.5.2.3 Inspection, Rework and Repair

The ability of any of these structures to be inspected, reworked, in-process repaired, and field repaired is critical and may become a driving requirement in the selection of materials and fabrication techniques. One must be insured that the design goals have been met during manufacturing by inspecting or testing for voids and flaws. The manufacturing process can not be limited by lack of in-process repair causing unacceptable scrap rates. An aircraft must allow for certain levels of field diagnostic and field repair to avoid unrealistic flight restrictions. Increase in weight due to Impact damage is defined by detectable limits and can be reduced through comprehensive heath monitoring and inspection systems.

Tooling concepts will become critical in all future development efforts. Surface control, expansion rates, ability to handle material variations, ability to accept automation, cure temperatures, cure pressures, cycle times, turn times, tool life, and costs all impact tooling selections. Future aircraft are expected to depend on multiple manufacturing methods. Additional study in the decision processes used to select these methods for an individual aircraft would be valuable.

10.5.3 Composite Development Roadmap for a 2030 to 2035 Aircraft

As presented in the previous sections, rapid development of material and design data basis, a de-coupling of the damage tolerance and environmental protection functions from the primary load bearing structure, and the development of material standards that define material properties in terms of fiber and resin chemistry have the potential to make significant contributions to the performance of air-vehicles in 2035. This section presents the advanced structures development roadmaps for methods and standards (STC 1.1 through 1.3) and for new airframe concepts (STC 2.1 and 2.2).

STC 1.1: Composite Material Standards

STC 1.2: Analytical Methods for Base Material Properties

STC 1.3: Analytical Tools for Design Properties

STC 2.1: Start-C2 Protective Skins

STC 2.2: Structural Health Monitoring

Figure 191 shows how an original equipment manufacturer might spend a couple of years getting comfortable with the processes and technologies developed through investment in STC 1.1 through STC 2.2. With these technologies in place the design data necessary to develop and certify the aircraft is mostly available at the start of the aircraft design phase. Figure 191 shows some small efforts to validate the use of generic design data for a specific product. Although the overall period of time may look similar to that shown in Figure 188 for current technology composite aircraft, the risk has been reduced such that the 4-5 year period for aircraft design and certification is virtually assured. Furthermore, the company commitment to product development is significantly reduced by moving most of the material data development outside the program. Access to certification quality data of this type will enable more commercial companies to sponsor the development of advanced composite aircraft.

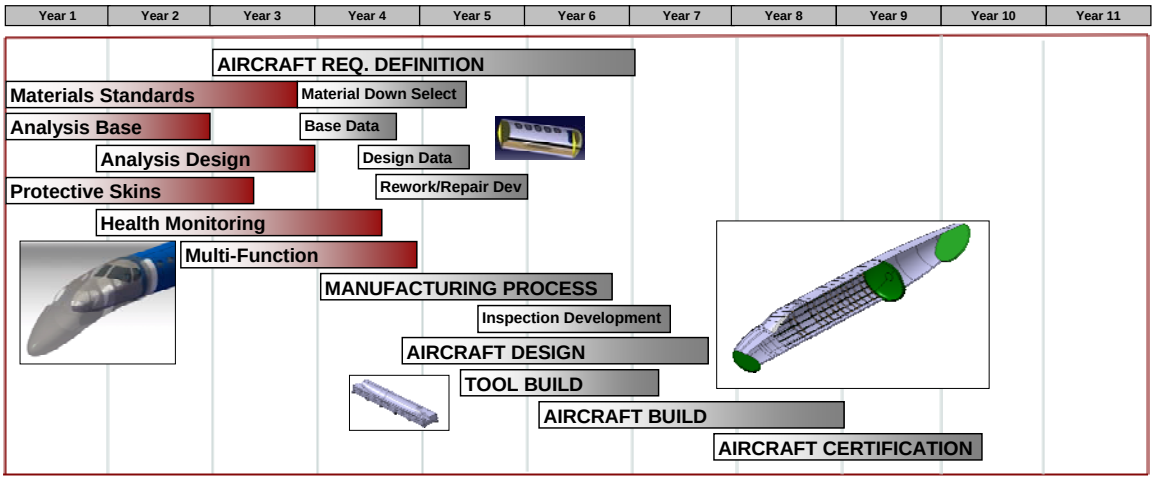

Figure 191. Composite Airframe Timeline for 2035 Vehicle.

10.5.4 STC 1.1 Composite Material Standards

10.5.4.1 Statement of Need

Widespread use of composite materials in the commercial aircraft industry would benefit significantly from a set of industry standard materials. These standard materials would have known material properties for generic coupons and elements. The ability to purchase commodity materials from multiple suppliers without an extensive investment in material qualification would enable all aircraft manufactures to use composite materials without the risk and investment in a material qualification program.

Examples of this approach come from two high temperature polyimide systems, PMR-15 and AFR-PE-4 that were developed at NASA Lewis Research Center and the Air Force Research Labs respectively. The formulations for these resins were made available to several material suppliers, which has enabled them to provide these materials without an extensive internal investment for the development and qualification activities.

10.5.4.2 Goals and Objectives

The goals for this effort are to (1) define and publish specific formulations for a suite of composite materials, (2) develop the coupon and element test data for composite materials based on these formulations, (3) complete statistical evaluation of variations in material properties caused by variations in the formulations or process parameters, and (3) document the standard material formulations and material property data in a standards document that would be accepted industry wide.

10.5.4.3 Technical Description

Specific formulations for a suite of commonly used product versions, i.e. out-of-autoclave 270°F curing resin, 250°F autoclave cured intermediate toughness resin, 350°F autoclave cured highly toughened resin, need to be established and published. A method should be set up that would allow multiple manufactures to show compliance to those requirements. Building block data through the lamina and laminate level should be completed on these resins combined with commercially available fiber types through industry supported qualification programs. The qualification programs would need to include resin manufactured at multiple suppliers, and statistical evaluation would be required to show equivalency between the various sources before a commodity approach would be appropriate. Composite materials that are qualified in this way could be purchased as a commodity with accepted published design data. Proper execution could save years and allow more manufactures, reduce development costs, reduce recurring costs.

10.5.4.4 Milestones

- Basic chemical formulations defined
- Generic material coupon and element test data completed
- Standard material specifications and processing methods documents

10.5.4.5 Deliverables

- Standard specification report
- Material properties test data report
- Composite material standards document

10.5.4.6 Schedule

Given the continued development of new materials, one would expect that the industry could benefit from a continuous update and expansion of standard composite materials. However, it is reasonable to expect the development of standards for 3-5 fiber and resin systems in a 3 to 5 year period. Figure 192 shows a potential timeline for the development a composite material standards document.

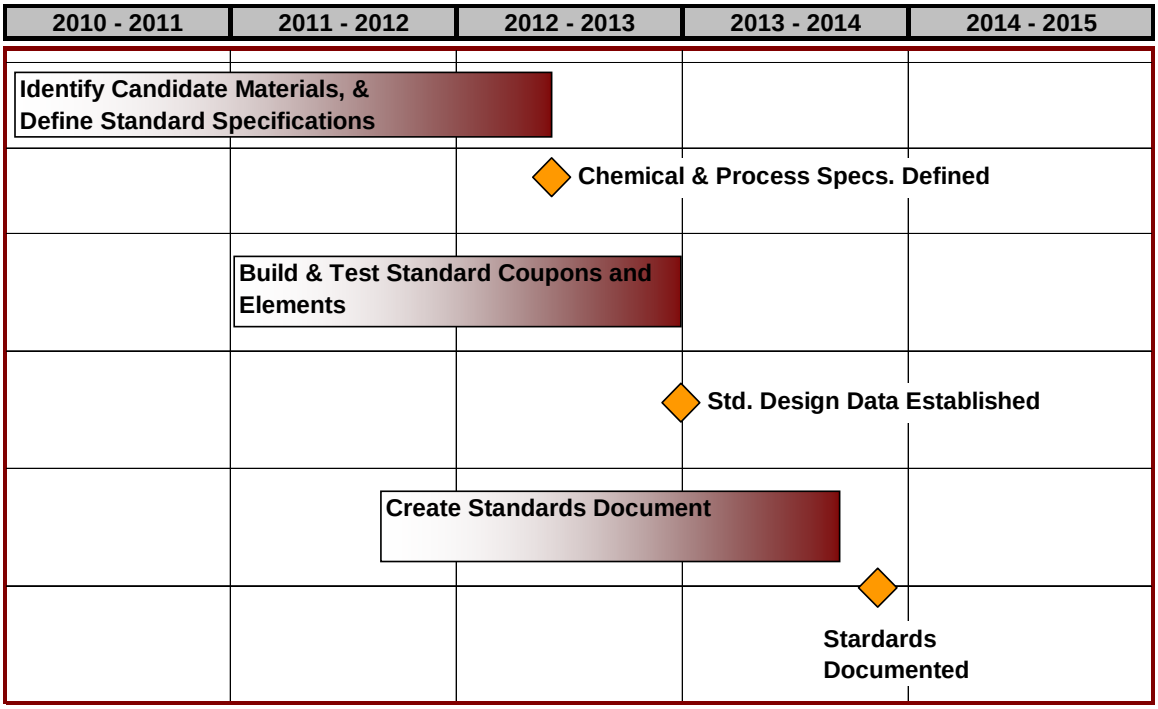

Figure 192. Schedule for Composite Material Standards Development

10.5.5 STC 1.2 Analytical Methods for Basic Material Properties

10.5.5.1 Statement of Need

Test verified analytical tools or semi-empirical methods are needed to reduce the time and cost associated with the development of basic coupon and element material data. From an aircraft certification perspective some testing will always be required. However, the current reliance on extensive test databases for every material that is considered is sufficiently expensive and time consuming to eliminate consideration of many promising materials. Analytical methods that allowed detailed structural design trade studies with new materials would be valuable, even if some follow-up testing was required for certification. These methods would reduce the risk of an investment in coupon and element data for a new material.

10.5.5.2 Goals and Objectives

The goal of this effort is to develop, test, and validate a set of analytical and or semi-empirical tools that estimate basic coupon and element properties from a set of standard material specifications. A secondary objective would be to quantify some of the sensitivities associated with variations in the material specifications and processes.

10.5.5.3 Technical Description

Current state-of-the-art methods allow from prediction of lamina level properties, but there do not appear to be generally accepted approaches for the prediction of laminate level properties. The research proposed here is intended to focus on methods that can predict both lamina and laminate level properties with access to limited test data. Verification of these methods can be facilitated with the test database developed in STC 1.1.

Figure 193 lists the typical input quantities and desired output results for the semi-empirical tools that are to be developed in this research effort. The impact of variations in input properties is also desired so that design data (allowables) can be developed from these new tools. Particular attention should be given to the time, people, and test resources that are needed to generate a design database for a new material system.

Inputs	Outputs
Resin Matrix Properties	**Lamina Level Properties**
Density	Tensile Strength
Tensile Strength	Tensile Modulus
Tensile Modulus	Compression Strength
Compression Strength	Compression Modulus
Compression Modulus	Interlaminar Shear Strength
Shear Strength	Short Beam Shear Strength
Shear Modulus	
Fracture Toughness	
Thermal Properties	
(rheology, Tg curves)	
Fiber Properties	**Laminate Level Properties**
Density	Unnotched Compression
Fiber Diameter	Unnotched Tension
Tow Size	Open Hole Compression
Tow Yield	Filled Hole Compression
Tow Style (twist)	Open Hole Tension
Tensile Strength	Filled Hole Tension
Tensile Modulus	Single Bearing Shear
Elongation at Break	Interlaminar Tension
	Compression After Impact
Composite Properties	
Fiber content	
Resin Content	
Cured Ply Thickness	
Maximum Porosity Level	
Fluid Exposures	
Use Temperature	

Figure 193. Inputs and Outputs for Semi-Empirical Tools

10.5.5.4 Milestones

- Mathematical models defined
- Predictive capability demonstrated
- Software verification completed
- Software and manual released

10.5.5.5 Deliverables

- Mathematical modeling report
- Software capability verification report
- Software application & users manual

10.5.5.6 Schedule

Figure 194 shows a potential schedule for the development of a set of analytical tools that estimate coupon and element material data. The start of this schedule is delayed so that the test data from STC 1.1 can be used in both the development and validation of these tools. Another approach would be to use existing material databases for initial tool development this would enable a project start in 2010. In either case, extensive customer trials with different material sets is anticipated. Published reports of the results and experience would enable others to use the tools with confidence.

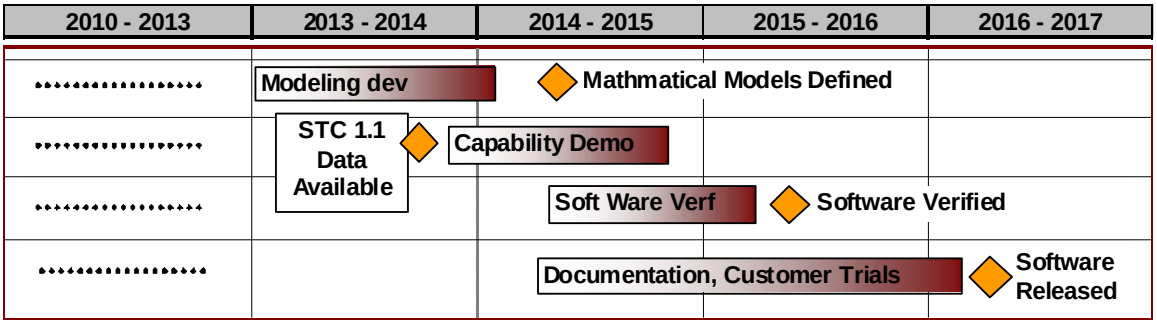

Figure 194. Schedule for Analytical Tools for Basic Material Data

10.5.6 STC 1.3 Analytical Tools for Design Properties

10.5.6.1 Statement of Need

Analytical tools are needed to predict the stress and strain characteristics of structural sub-components and components. This predictive capability needs to include the effects of damage, repair, and hot plus wet environments. This new capability should enable evaluation of the strain performance of structures based on new materials without either very conservative assumptions or a significant amount of testing.

Progress has been ongoing for several years. Several companies offer analytical software for multiple applications including aircraft, automobiles, wind turbines, jet engines, and marine requirements. This offers a multitude of variations and the output is generic and guidance in nature. Within aircraft design, differences in integral and core stiffened structures can present challenges for one software package. These challenges come from complexity of individual layer interactions, defects, failure theories, etc have been either too complex or computer intensive to be applied to entire structural models. .

The trend is to use output to define tests matrix for future “tweak” of software to closer match the actual outcome. This is an iterative aircraft section specific process to substantiate use of the software for use in future analysis.

10.5.6.2 Goals and Objectives

The goal is to develop finite-element type tools and integrated models that allow detailed analysis of the stress and strain behavior of composite assemblies that have experienced damage or are subjected to very hot and wet environments.

10.5.6.3 Technical Description

This research task is intended to develop finite-element or similar tools that have been verified, supported, or improved by access to test data. As described above the need for test data should be reduced to a minimum and the results of STC 1.1 and 1.2 should contribute to this effort. These new or improved tools shall be appropriate for a high performance desktop computer and be capable of estimating the performance of structural assemblies in (1) room temperature dry conditions, (2) in elevated temperature, wet conditions, and (3) after specified damage or repair events. The current generation of software tools that address these issues are either too dependent on a large and expensive experimental database or are too computationally intensive to evaluate the impact of a new and unknown material system on a structural assembly.

Figure 195 shows a typical list of the input and output quantities that are intended for the tools planned for this research effort. As mentioned above, it is anticipated that some experimental test data will be required for the tools to provide sufficient accuracy to be useful at estimating the impact of a new material system on the weight of an aircraft structure. These new tools are also intended to quantify the variation in output quantities that results from variations in input quantities. These variations shall be used along with the output quantities of Figure 195 to create and output design data (allowables) that are appropriate for a new material system.

Inputs
Lamina Level Properties
Tensile Strength
Tensile Modulus
Compression Strength
Compression Modulus
Interlaminar Shear Strength
Short Beam Shear Strength
Laminate Level Properties
Unnotched Compression
Unnotched Tension
Open Hole Compression
Filled Hole Compression
Open Hole Tension
Filled Hole Tension
Single Bearing Shear
Interlaminar Tension
Compression After Impact
Structure Properties
Skin Properties (Materials / Layup)
Stiffening Elements
Core Density
Core Thickness
Core Cell Size
Core Wall Thickness
Stringer Geomoetry
Stringer Materials / Layup
Stringer Locations
Frame Geometry
Frame Materials / Layup
Frame Locations
Fastening / Bonding
Fastener Type
Fastener Size
Fastener Locations
Bonding Method
Bonding Strength
Bonding Modulus
Allowable Manufacturing Defects
Typical Damage Sites
Typical Repair Methods
Typical Repair Allowables

Outputs
Bearing Behavior
Skin / Panel Buckling
Column Crippling / Buckling
Overall Structural Stability
Impact Damage Models
Analysis of Shear Panels
Identification of potential hot-spots
Strucutural performance predictions at environmental extremes
Performance of damage, damaged-repaired structure

Figure 195. Typical Inputs and Outputs for Sub-Assembly Analysis Methods

10.5.6.4 Milestones

- Mathematical models defined
- Predictive capability demonstrated
- Software verification completed
- Software and manual released

10.5.6.5 Deliverables

- Mathematical modeling report
- Software capability verification report
- Software application & user's manual

10.5.6.6 Schedule

Figure 196 shows a potential schedule for the development of a set of analytical tools for sub-assemblies in extreme operating conditions. The start of this schedule is delayed so that the test and analysis data from STC 1.2 can be used in both the development of these tools. Another approach would be to use existing design databases for initial tool development this would enable a project start in 2010. In either case, extensive customer trials with different material sets is anticipated. Published reports of the results and experience would enable others to use the tools with confidence.

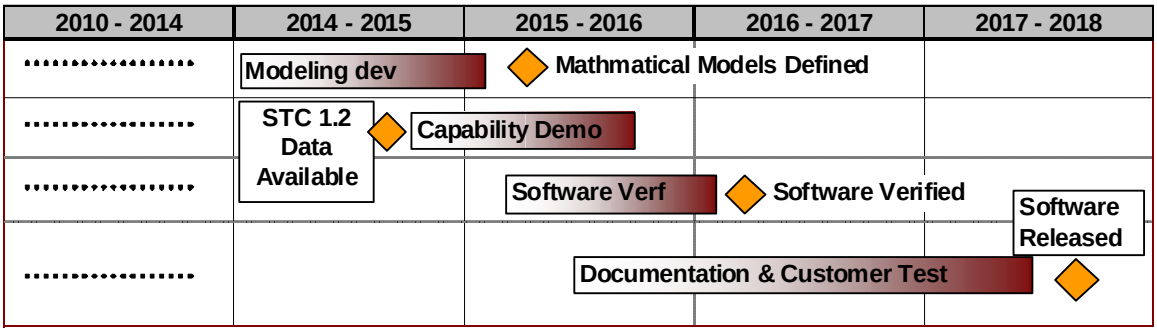

Figure 196. Schedule for Development of Analytical Design Tools

10.5.7 STC 2.1. STAR-C², Damage Tolerant Skins

10.5.7.1 Statement of Need

An external skin or airframe surface is needed to absorb impact damage and to provide environmental protection. This skin should be responsible for Smoothing out bumps or gaps, providing Thermal insulation, Absorbing impact and acoustic energy, Reflecting ultraviolet radiation, Conducting large amount of electrical current, and providing a Cosmetically appealing appearance (STAR-C²).

10.5.7.2 Goals and Objectives

The objectives of this development effort are to (1) establish the technical requirements for the STAR-C² skin, (2) identify appropriate materials for this protective skin, (3) develop an appropriate installation and repair process for the skin, (4) build representative test panels that

include both structure and skin, and (5) verify through test the effectiveness of the selected materials at satisfying the technical requirements.

10.5.7.3 Technical Description

There are very established reasons to follow the building block methodology for selection and achieving structural design data needed for composites aircraft. One has to look into the final aircraft requirements to be able to properly evaluate areas where there could be innovative reductions. Interior thermal and acoustic materials serve a singular function of cabin passenger comfort. They also utilize critical space needed for systems. These materials, if located externally rather than internally, have the potential to absorb energy that could reduce impact damage structural weights. Electrical requirements for lightning strike and EMI could be combined with Health Monitoring, reduce skin heat, provide UV protection, and address exterior cosmetic requirements. A combination of all of these requirements, a **STAR-C² Skin** (**S**moothing, **T**hermal, **A**bsorbing, **R**eflective, **C**onductive, **C**osmetic) into one protective layer system may reduce weight penalties related to flush fasteners, surface fillers and primers and paint. This same system could address skin gaps, door/window seals, external antennas and impact the aircraft smoothness and low drag performance.

These features could also allow the use of non-flush fasteners, cover previous protruding features, allow for heath monitoring zone wiring, and provide a visual standard for previously undetected damage. A review of these requirements provides a decision path between the merit in a simple large easily replaceable exterior skin panels and a “dual” system of a protective material covered by a conductive external skin. Installation, performance, maintenance requirements, customer color options, and replacement costs may drive the final decision. A single or combination external skin could fundamentally change how we address aircraft structures and aerodynamic smoothness.

Tests are needed to establish acceptable STAR-C² detectable damage. Baseline could be metallic skin/structures or at a higher defined level prior to damage of the composite structure. Test would represent delectability with different colors and lighting conditions. Specific testing is needed to understand how external STAR-C² impact loads are shared by the internal skins.

Skins properties requirements need to be defined and material search preformed. Large scale testing will be needed to identify issues related to performance, durability, practical section sizing, splicing/joint, and repair methodologies.

Research will include integral health monitoring and aerodynamic features such as antenna integration.

10.5.7.4 Milestones

- STAR-C² technical requirements established
- Candidate materials selected
- Installation & repair concept documented
- Test panels (EMI/LS/Acoustic/Impact/Cosmetic) constructed
- In-service demonstrations complete

10.5.7.5 Deliverables

- STAR-C² requirements document
- Material selection & concept definition document
- STAR-C² test data reports
- STAR-C² concept verification report
- Flight & In-service test report

10.5.7.6 Schedule

Figure 197 shows a notional schedule for the development, test, and demonstration of the STAR-C² skin. It is reasonable to expect some initial experience and test data for candidate materials in a 3-5 year period. Acceptance of this form of passive protection is likely to depend on some in-service testing. It may make sense to perform this testing on a single aircraft that has been modified with a STAR-C² on the surface of the fuselage. One would also expect the initial test program to generate some lessons learned and motivate the use of slightly different materials for the skin.

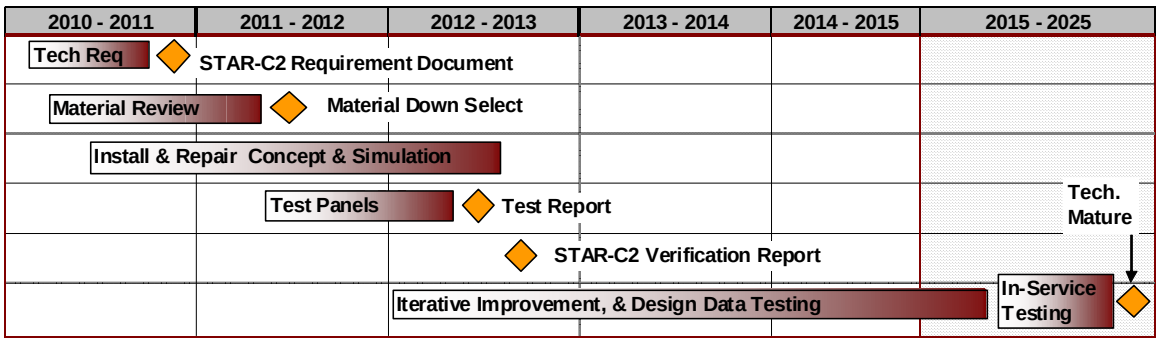

Figure 197. Schedule for STAR-C² Damage Tolerant Skins

10.5.8 STC 2.2. Structural Health Monitoring

10.5.8.1 Statement of Need

The STAR-C² skin developed in STC 2.1 provides passive health monitoring for impact damage and surface wear. This protective skin is expected to absorb any impact damage that doesn't leave visible damage without any impact to the underlying structure. Once the STAR-C² skin shows visible impact damage, then an inspection and or repair would be required.

An active health monitoring system that could replace or eliminate the need for a factory or service center inspection in the event of visible damage to the STAR-C² skin is desired. This system could either identify damage during an impact event or evaluate the integrity of the structure after the event.

A health monitoring system should measure current operating environment, loading information needed for gust alleviations actions, as well as provide rapid detection of damage or failure in an aircraft structure. This technology should incorporate devices that include, but are limited, temperature sensors, humidity sensors, strain sensors, accelerometers, and light or motion sensors. The recorded information could provide the data needed for maintenance and repair.

The weight and cost penalties related to damage tolerance and environmental exposure is due to what the pilot does not know or can not inspect within a reasonable effort (preflight). Current composite aircraft can be 20-40% stronger as related to their aluminum counterparts when parked on a dry runway on a 60-70F day. Observations indicate that it can take months for a composite structure to absorb enough moisture to degrade its performance, yet design guidelines force the structure to support ultimate loads while in this moist condition on the hottest potential day. An ability to measure moisture, temperature, and to track the trends in these parameters over time would enable a pilot to continue operation at reduced airspeed or to schedule a maintenance operation to dry out the structure.

Future aircraft must rely less on pilot walk around preflight inspections which are often restricted on what areas they can see, decisions impacted by external conditions; rain, cloudy or bright days, and vary by training and experience. They must rely on systems that provide in-depth structural and system health monitoring. In-flight, this same system would provide safe operating limits for any given condition. Past attempts have offered challenges for mounting and connecting of the sensors. The STAR-C²skin concept offers a unique medium for installation.

10.5.8.2 Goals and Objectives

The objectives of this development effort are to (1) establish the technical requirements for the health monitoring system, (2) develop concept architectures for the system, (3) develop test articles and procedures that simulate appropriate impact events and environment conditions, (4) test the effectiveness of the monitoring system at identifying critical conditions or reporting on the health of the structure, and (5) propose a flight demonstration program to test the effectiveness and reliability of the system .

10.5.8.3 Technical Description

Systems will need development for temperature, humidity, conductivity, damage detection, NDI, and load monitoring and be incorporated into a prognostic algorithm. Output will be a real time system to support safe flight and provide maintenance guidance.

10.5.8.4 Milestones

- Monitoring system technical requirements established
- Concept architecture defined
- Test articles and test plans completed
- Flight demonstration Test Plan

10.5.8.5 Deliverables

- Monitoring system requirements document
- Concept definition report
- Concept test articles report
- Flight demonstration

10.5.8.6 Schedule

Figure 198 shows a notional schedule for the development, test, and demonstration of an active health monitoring system. It is reasonable to expect some initial experience and test data for a concept monitoring 3-5 year period. However, the complexity of this system that requires sensors, electrical information processors, and integration with primary structures suggests that several iterations will be necessary. Each of these iterations is expected to lead to a more reliable system and easier to certify. Acceptance of such a system will also require some field service tests that show the system can be counted on for dispatch reliability, and for performing its intended function.

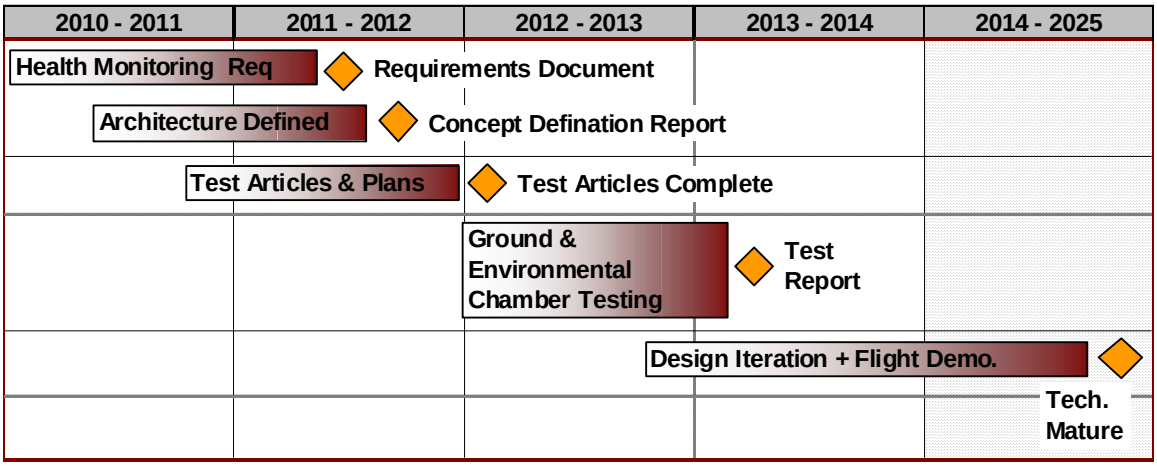

Figure 198. Schedule for Health Monitoring

10.5.9 Airframe Structures Development Risk

The risk assessment for the structural technologies and development roadmaps is developed from a combination of (1) an estimate of the current technology or analysis readiness level, (2) an assessment of the difficulty associated with the technology development task, and (3) an estimate of the impact or consequence to the 2035 vehicle's compliance with NASA's goals (Fuel burn, Noise, NOx, & Field Length). Appendix H presents some standard definitions for technology readiness level (TRL), some standard definitions for analysis readiness level (ARL), and the use of likelihood and consequence ratings for a technology development risk assessment in this report.

Table 81 shows that the methods technologies presented in this report range in readiness from a basic principals or back of the envelop method to methods that currently provide good qualitative trade studies. The perceived difficulty for the development of these technologies ranges from a relatively straightforward development task with a rating of 3 on a scale of 1 to 9 to a very difficult task that is associated with no known technical approach or solution. Development of this group of technologies to a level that could be used for airframe certification with a limited or reduced test matrix would enable widespread commercial use of advanced composite materials and lead to significant reductions in the empty weight of future aircraft structures.

Table 81. Analysis Readiness Level for Structural Methods Technologies

New Technology Development Risks					
Task #	Technology Work Package Description	Rationale for Analysis Readiness Level	ARL	Technical Challenges, Development Approach	Development Difficulty Rating
STC 1.1	Composite Material Standards	Material properties are available from material suppliers, but chemical formuation is considered proprietary	5	It should be a strateforward task to develop material properties from a known chemistry in the lab. It may be a challenge to motivate material suppliers to manufacture an industry-standard material	3
STC 1.2	Analytical Methods for Material Base Properties	There is no known analysis method or approach to capability	1	There are no known methods that use variations in chemical formuations to predict material strength or toughness properties	9
STC 1.3	Analytical Toods for Design Properties	Finite element methods exist for undamaged materials in standard environments. Analysis for the deflection and strain of damaged or environmentally degraded assemblies	5	One would expect a wide variation in the performance of damaged components. Mathematical models for damaged components are likely to imprecise	7

Table 82 shows that the structural concept technologies presented in this report have technology readiness levels of 2 to 3 and represent the definition of a potentially beneficial application concept. Both development tasks are considered difficult to very difficult. The Star-C2 skins have the potential to be quite easy to develop, but a detailed investigation of currently available materials in the context of this application is required before this can be established. There are many approaches to structural health monitoring currently under development, but the complexity and maturity is far from something that a commercial operation would rely on for the dispatch of an airliner. Developing this level of reliability and confidence typically takes years of in-service experience. It is recommended that the initial health monitoring systems be used to reduce the time and cost of scheduled and un-scheduled structural inspections. If the Star-C2 skin shows visible damage, then a structural inspection shall be required prior to the next flight. Can the health monitoring system provide this inspection or will the aircraft need to be moved to a repair facility?

Table 82. Technology Readiness Level for Structural Technologies

New Technology Development Risks					
Task #	Technology Work Package Description	Rationale Technology Readiness Level	TRL	Technical Challenges, Development Approach	Development Difficulty Rating
STI 2.1	Star C^2 Skins	Cessna has defined the application concept based on observations of current technologies materials in similar applications	2	Testing for performance that ie equal to that of current technology aluminum skins is straightforward, but it is unkown if the appropriate materials or manufacturing processes for the desired skin are available	7
STI 2.2	Structural Health Monitoring	It is anticipated that current active health monitoring systems can be adapted to the Star CS skin and structural concept quickly	3	Demonstrating an active health monitoring system that is reliable enough to be counted on for aircraft dispatch is a significant challenge	9

Table 83 and Table 84 show that the structural technology groups are either likely or very likely to still be in development in 2025 to 2030. This suggests that a significant effort by NASA and collaboration with industry will be required to accelerate this development and enable the 33% reduction in empty weight claimed for the 2035 turboprop in this report.

Table 83. Likelihood Assessment for Structural Methods Technologies

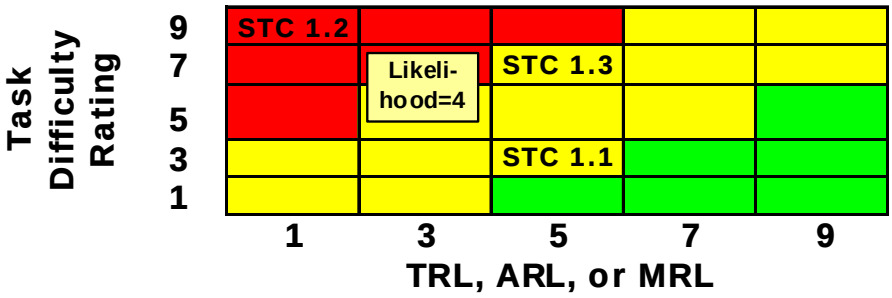

Table 84. Likelihood Assessment for Advanced Composite Technologies

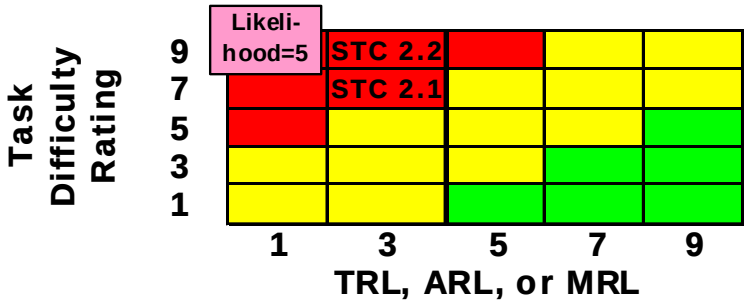

Table 85 and Table 86 show how the task difficulty and technology maturity assessment are combined to establish a technology risk assessment for the methods and hardware technologies proposed for an advanced airframe structure in this report. Rapid development of material and design databases for composite structures that are based on commodity materials nearly ensures widespread use in commercial aircraft by 2035 and enables approximate 15% reduction in the empty weight of these aircraft. The consequence of not having the Star-C2 skin is even greater because this skin is also considered an enabler for the natural laminar flow that contributes approximately 1/3 of the fuel burn savings in the 2035 turboprop. Table 86 shows that both the structural methods and hardware related technology groups are in the high-risk corner of the risk cube and indicate some development collaboration between NASA and industry is warranted.

Table 85. Rationale for Airframe Technology Risk Assessments

Technology Categories	Consequence	Rationale	Likelihood	Rationale
Composite Materials & Design Data (STC1)	4	This group of technologies are responsible for approximately half of the weight savings in the 2035 vehicle and become an enabler for the widespread use of advanced composite structures in commercial vehicles.	4	It is unlikely that composites materials will become commodities by 2025, but some methods improvement and wider use by commercial companies is very likely.
Star-C2 Skins & Active Health Monitoring (STC2)	5	The star-C2 skins are an enabler for natural laminar flow, contribute to 6% in empty weight savings for the advanced vehicle, and significantly reduce the risk associated with design for damage tolerance in thin-walled composite structures.	5	This is a paradigm shifting concept that will be difficult to implement by 2035, but it is likely that the required materials either exist or can be developed quickly.

Table 86. Structural Technologies Risk Assessment.

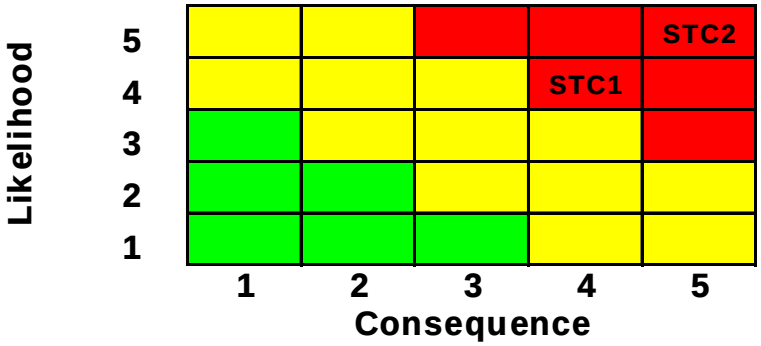

10.5.10 Subsystem and Multi-Function Structures Roadmaps

10.5.10.1 Sys 1.0: Structural Ice Protection for Laminar Flow

10.5.10.1.1 Statement of Need

The natural laminar flow (NLF) requirements necessary to meet the fuel burn requirements established for 2035 vehicles lead to fuselage shapes with large forward facing regions that will collect ice. These fuselage surfaces will need some form of ice protection to prevent large ice shapes from separating from the fuselage and impacting aft sections of the aircraft.

An ice protection system needs to be integrated into the STAR-C^2 to satisfy the performance requirements of 2035 vehicles. Electric heaters, electro-expulsive systems, and TKS-fluid type systems are all compatible with the STAR-C^2 concept. Since the self-cleaning surfaces are required for the maintenance of natural laminar flow, a TKS-fluid system may have the potential for preventing ice accumulation and for cleaning the aircraft surface. In all cases the ice protection system needs to be installed such that it doesn't leave steps, gaps, or other protuberances that might trip the boundary layer.

10.5.10.1.2 Goals and Objectives

The goals of this effort are (1) to identify the best ice protection system for integration into the STAR-C2 skin and (2) to design a representative system, and (3) to test the ice protection performance of this system in an icing tunnel.

10.5.10.1.3 Technical Description

Design for Natural Laminar Flow (NLF) requires great attention to detail in the design and manufacture of aircraft surfaces. Current ice protection systems based on hot bleed-air, pneumatic boots, TKS-fluids, electro-expulsive actuators, and electric heater-mat systems are all installed into the leading edges of lifting surfaces with fasteners, steps, or gaps. All of these disturbances have been shown to force laminar to turbulent transition in the boundary layer. The outer layer of the STAR-C2 skin has the potential to cover up or smooth out these installation disturbances. However the effectiveness of the resulting ice protection system would need to be tested in both an icing tunnel and a flight environment.

All of the current technology ice protection systems could be compatible with a STAR-C2 skin concept. However each system provides a different set of installation challenges. The flexible surface of a pneumatic boot type system would require a flexible outer surface to the aircraft that may not meet the lightning and damage tolerance requirements of the STAR-C2 skin. The heat based systems are probably the easiest to integrate, but add a high thermal conductivity requirement to the external layer of the STAR-C2 skin. A TKS-fluid system has the added benefit of supporting a self-cleaning operation, but adds the complexity of placing holes in the skin. An electro-expulsive system forces the integration of skin actuators into the outer foam surface.

An integration trade study followed by a design, build, and test program is recommended. The trade study is intended to define several integration concepts that are compatible with the STAR-C2 skin concept and quantify the relative weight, power, and reliability numbers for the installed system. After a system down-select, a detailed design shall be created for both icing tunnel and flight test demonstrations of the new ice protection system.

10.5.10.1.4 Milestones

- Ice protection technology selected
- System integration design completed
- Icing tunnel test of new design completed
- Data report and recommendations complete
- Roadmap to production readiness complete

10.5.10.1.5 Demonstrations and Deliverables

Sys 1.1.: Conduct a technology assessment and detailed trade study for the selection of an ice protection technology that can be integrated into or become part of the STAR-C^2 skin.

Sys 1.2: Design ice protection system with a STAR-C^2 skin for test in an icing tunnel.

Sys 1.3: Build model and conduct test in icing tunnel test.

Sys 1.4: Analyze and document icing tunnel test results

Sys 1.5: Develop roadmap for remaining development and transition to certification

10.5.10.1.6 Schedule

The schedule shown in Figure 199 is typical of a subsystem development program that begins with architecture trade studies and ends with critical demonstration tests. A follow-on design and test iteration is expected, since it is anticipated that integration with the STAR-C^2 will provide some unknown challenges.

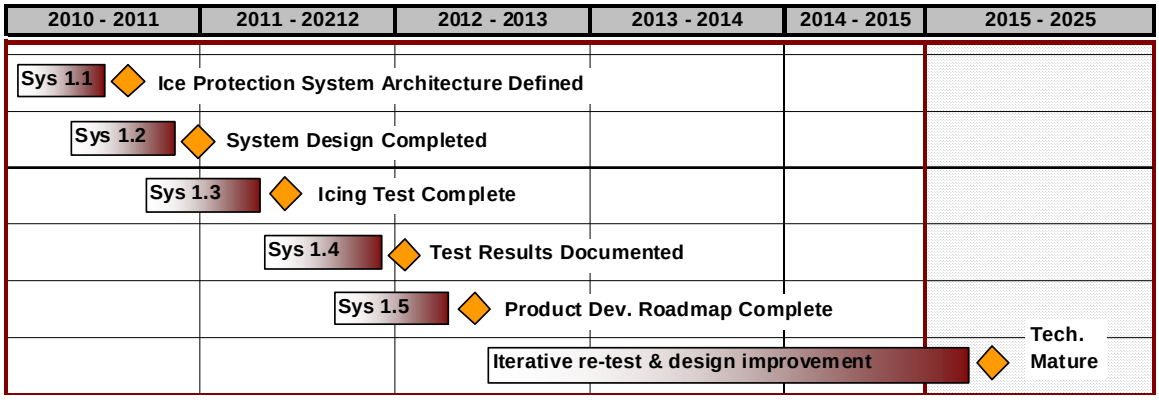

Figure 199. Development Schedule for Sys. 1.0

10.5.10.2 Sys 2.0: Multi-Function Structure for Environmental System Air Distribution and Acoustic Damping

10.5.10.2.1 Statement of Need

The need to reduce the empty weight of the 2035 configuration drives a desire to take advantage of every piece of hardware for as many functions as possible. The need for weight reductions drives a design to optimize the shape and arrangement of fuselage skins and stringers to (1) address the traditional skin stiffness, fuselage bending, and panel buckling requirements, to (2) use the stringers or frames to distribute cabin air, and to (3) minimize the impact of structural vibration on cabin noise and the requirement for additional damping material.

10.5.10.2.2 Goals and Objectives

The objective of this research is to conduct high-fidelity structural optimization studies that minimize structural weight with the functional requirements for environmental air distribution and a reduction in interior noise.

10.5.10.2.3 Technical Description

This research involves several overlapping structural optimization studies and some environmental control system architecture development. As stated above, the primary objective is the reduction in overall aircraft empty weight. However, it is recognized that the use of fuselage skin stiffeners as air-distribution ducts provides an opportunity to reduce the cost and part count of the aircraft system.

In the first phase of work is to optimize the fuselage structure to support pressure loads, bending loads, and to deal with other traditional structural functions. This result provides a baseline for measuring the value of a multi-function concept. During this phase a traditional approach to the addition of acoustic damping material and to the installation of air ducts for the distribution of cabin aircraft will be used to define baseline systems.

In the second phase of work stringers and frames are defined that meet the needs of the air-distribution system. With this definition the location and shape of the remaining stringers and frames is optimized to produce a minimum weight structure.

In a third phase the need to minimize structural vibration in frequencies that lead to undesirable tones in the cabin is considered during the optimization of the structure for minimum weight.

Finally, all of the optimized concepts are compared and evaluated from the perspective of minimum weight, cost, repair, and in-service maintenance.

10.5.10.2.4 Milestones

1. Minimum weight fuselage defined
2. Minimum weight fuselage with ECS ducts is defined
3. Minimum weight fuselage with ECS ducts & vibration tuning is defined
4. Optimization results report
5. Concept trade study evaluation report.

10.5.10.2.5 Demonstrations and Deliverables

Sys 2.1: Perform a structural optimization study for the composite fuselage

Sys 2.2: Perform a structural optimization study for a composite fuselage that uses stiffeners to distribute cabin air.

Sys 2.3: Optimize a composite fuselage that uses stiffeners to distribute cabin air for both weight and the tuning of specific vibration frequencies.

Sys 2.4: Document the optimization methods and results of Sys 2.1 through 2.2.

Sys 2.5: Perform concept evaluation studies for the results of 2.4 and recommend the best approach for multi-function use of structural components.

10.5.10.2.6 Schedule

Figure 200 show a notional schedule for the optimization of multi-functional fuselage structures. If necessary, the schedule could be reduced by approximately 6 months by performing Sys 2.1, 2.2, and 2.3 simultaneously. The sequential order shown in Figure 200 provides the opportunity to learn from the optimization model developed in Sys. 2.1

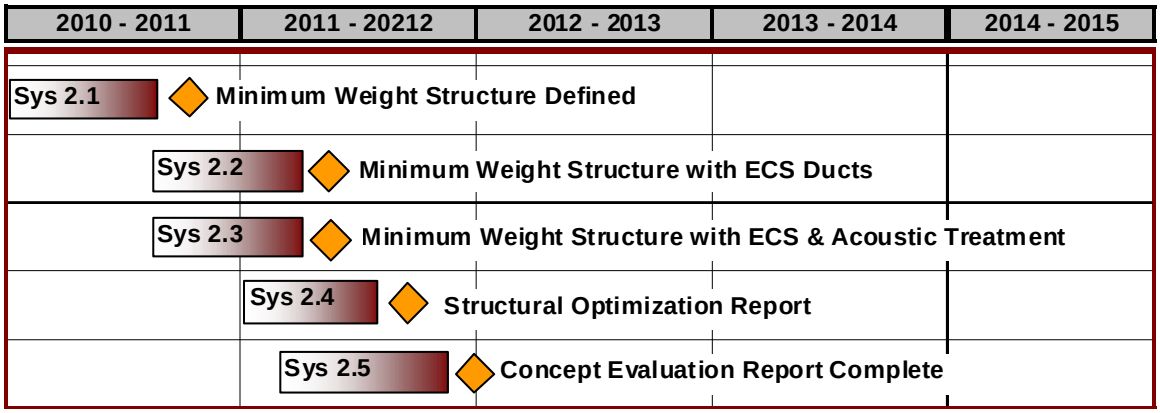

Figure 200. Development Schedule for Sys. 2.0

10.5.10.3 Sys 3.0: Suction Systems for Active Laminar Flow

10.5.10.3.1 Statement of Need

The 2035 vehicle presented in this report depends on the development and maintenance of laminar flow on more than 50% of the aircraft surface. A limited amount of active suction is needed to either re-establish or maintain laminar flow in regions where joints or doors are unavoidable. An obvious location for the application of active systems is near or around the door opening for the noise landing gear.

10.5.10.3.2 Goals and Objectives

The objective of this development task is to design an active suction system that is both compatible with the STAR-C2 skin concept and minimizes the weight, the power, and the number of parts.

10.5.10.3.3 Technical Description

A detailed architecture trade study will be conducted to determine the best way to extract power from the main engines and use this power to run a compressor that provide the necessary suction. Since the potential suction tubes are distributed in many different aircraft locations, it is reasonable to anticipate the use of distributed electric motors and compressors

The installation or integration of suction tubes with the STAR-C2 skin is also a interesting challenge. For easy installation and repair the final layer of the STAR-C2 skin is anticipated to be thin and flexible. One would expect suction tubes to be thick and rigid. However, there may

be several options for a transition from the normal STAR-C2 skin concept to the suction surface near or in a joint or door opening. The challenge will be to make that transition without creating any surface disturbance that trips the boundary layer

Once the system architecture is defined, a prototype system shall be designed and tested either on a flight vehicle or in a low turbulence wind tunnel. This task shall be coordinated with the laminar flow suction tests identified in Aero 1.2. In Aero 1.2, the objective is to define suction requirements and effectiveness at establishing and maintaining laminar flow. In this task, suction control, power management, system diagnostics are issues to document during prototype testing.

Finally, an evaluation of the final system and test results shall be used to recommend an desirable design changes and develop the roadmap of additional investments necessary to mature the technology for product introduction.

10.5.10.3.4 Milestones

- System architecture defined.
- Installation and manufacturing processes identified.
- System design completed.
- Prototype hardware assembled.
- Prototype test completed.
- System Evaluation Documented

10.5.10.3.5 Demonstrations and Deliverables

Sys 3.1: Conduct a suction system architecture trade study.

Sys 3.2: Conduct a manufacturing process and component installation study.

Sys 3.3: Design the suction system and define the parts list of bill of materials.

Sys 3.4: Build a prototype suction system for a nose landing gear system.

Sys 3.5: Test the prototype system in support of a laminar flow suction requirements and effectiveness test.

Sys 3.6: Document system performance and develop roadmap for remaining development.

10.5.10.3.6 Schedule

The schedule shown in Figure 201 is typical of a subsystem development program that begins with architecture trade studies and ends with critical demonstration tests. A follow-on design and test iteration is expected, since it is anticipated that integration with the STAR-C^2 will provide some unknown challenges.

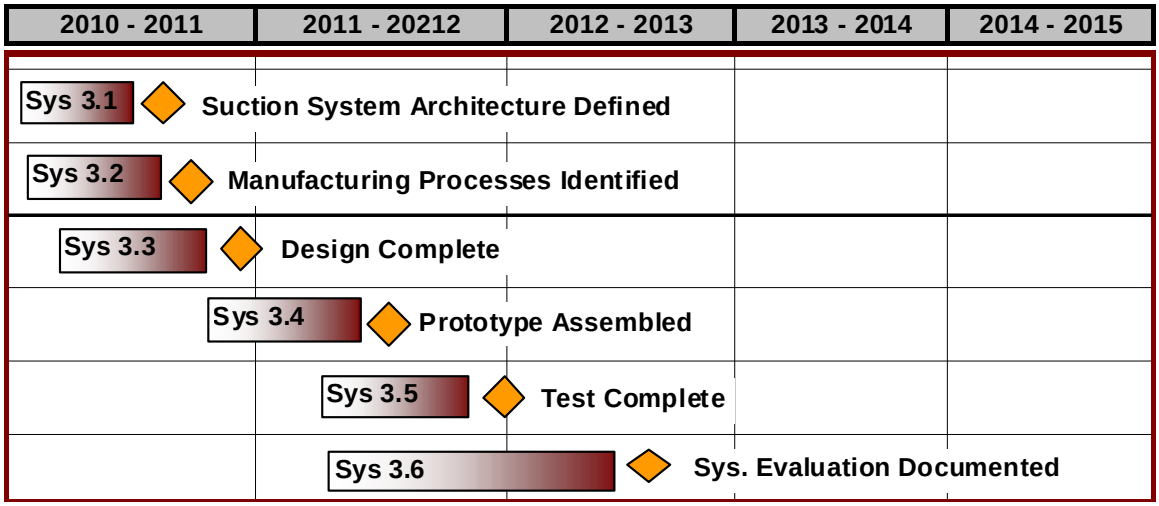

Figure 201. Development Schedule for Sys. 3.0

10.5.10.4 Subsystems Development Risk

The risk assessment for technologies that enable laminar flow is developed from a combination of (1) an estimate of the current technology readiness level, (2) an assessment of the difficulty associated with technology development tasks, and (3) an estimate of the impact or consequence to the 2035 vehicle's compliance with NASA's goals (Fuel burn, Noise, NOx, & Field Length). Appendix H presents some standard definitions for technology readiness level (TRL), some standard definitions for analysis readiness level (ARL), and the use of likelihood and consequence ratings for a technology development risk assessment in this report.

Table 87 shows a TRL level of 3 for the ice protection system because the laminar flow fuselage presents a large water impingement zone that will require ice protection. This large area for ice protection will provide challenges in weight and power consumptions. However, current ice protection technologies have the potential to satisfy the functional needs. This development effort should be able to be completed with current technology tools and materials

Table 87. Technology Readiness Levels for Sys 1.0.

New Technology Development Risks					
Task #	Technology Work Package Description	Rationale for Analysis Readiness Level	TRL	Technical Challenges, Development Approach	Development Difficulty Rating
Sys 1.1	Ice Protection Technology Trade Studies	Current technology ice protection systems are compatible with the STAR-C2 skin. Performance with self cleaning surfaces is unknown. The power requirements are large for extensize fuselage impingment zones	3	Trade study methods and current ice protection technologies are mature. Developing a system that without extensive increases in power will be challenging	5
Sys 1.2	Design of ice protection system with STAR-C2 skin	STAR-C2 skin may drive application of new materials and manufacturing methods	3	Existing materials and methods will be used if possible. Any new materials or processes with drive difficulty	6
Sys 1.3	Build Icing Tunnel Model	Existing model build technologies will be used for this effort	4	Existing experimental model manufacturing techniques should eliminate model build issues	6
Sys 1.4	Analyze and document icing tunnel results	Existing tunnels and test techniques are planned for this task	7	Analysis and documentation of icing tunnel performance results is well understood	2
Sys 1.5	Roadmap for remaining development	The test data and design experience is expected to provide insight into any existing technical maturity issues	7	Roadmap development is a known process	1

Table 88 shows little difficulty in completing this development effort and a relatively high TRL for the maturity of the concept. Structural optimization methods are reasonably mature and the multi-functional goals of this task do not contribute significantly to the weight goals of the 2035 vehicle.

Table 88. Technology Readiness Level for Sys 2.0

New Technology Development Risks					
Task #	Technology Work Package Description	Rationale for Analysis Readiness Level	TRL	Technical Challenges, Development Approach	Development Difficulty Rating
Sys 2.1	Fuselage structure optimization for minimum weight	Advanced composites leads to light weight without optimization	6	Structural optimization methods are reasonably well developed.	2
Sys 2.2	Fuselage structure and ECS duct optimization for minimum weight	Advanced composites leads to light weight without optimization. Integration with ECS ducts in conceptually simple	5	Structural optimization methods are reasonably well developed.	2
Sys 2.3	Fuselage structure and ECS duct optimization for minimum weight and specified vibration characteristics	Advanced composites leads to light weight without optimization. Integration with ECS ducts in conceptually simple. Optimization for vibration characteristics provides some challenges	3	Structural optimization methods are reasonably well developed.	4
Sys 2.4	Document optimization results	Risk of obtaining weight savings in final multi-fuction structure is low. Most of the savings are generated by the composite material	6	A thorough set of optimization trade studies should enable support for the best approach to multi-fuction structural design	2
Sys 2.5	Concept Evaluation Report	Risk of obtaining weight savings in final multi-fuction structure is low. Most of the savings are generated by the composite material	6	A thorough set of optimization trade studies should enable support for the best approach to multi-fuction structural design	2

Table 89 indicates that suction systems that satisfy the system weight goals and provide the necessary function will be a challenge. New materials and manufacturing processes may need to be developed to provide the suction function within acceptable cost and weight targets.

Table 89. Technology Readiness Level for Sys 3.0.

New Technology Development Risks					
Task #	Technology Work Package Description	Rationale for Analysis Readiness Level	TRL	Technical Challenges, Development Approach	Development Difficulty Rating
Sys 3.1	Suction system architecture design study	Although conceptually simple, the manufacturing and installation methods required to install suction pipes in the STAR-C2 skin are unkown	2	Success is dependent on developing an understanding of the required manufacturing and installation processes	7
Sys 3.2	Installation and Manufacturing Process Review	Although conceptually simple, the manufacturing and installation methods required to install suction pipes in the STAR-C2 skin are unkown	2	A review of available technologies is straightforward. The availability of the required processes is unknown	9
Sys 3.3	Detailed Design of Suction System	Although conceptually simple, the manufacturing and installation methods required to install suction pipes in the STAR-C2 skin are unkown	2	Once the materials and manufacturing processes have been defined, the design task should be relatively straightforward	4
Sys 3.4	Build prototype suction system	Although conceptually simple, the manufacturing and installation methods required to install suction pipes in the STAR-C2 skin are unkown	2	The precision for hole spacing and surface contours may drive difficulty into this task	9
Sys 3.5	Document System Performance and Technical Maturity	Although conceptually simple, the manufacturing and installation methods required to install suction pipes in the STAR-C2 skin are unkown	2	Documentation is a well understood task	2

An assessment of the likelihood that the technologies of Sys 1.0, Sys 2.0, and Sys. 3.0 will not mature in time for a 2035 vehicle is presented in Table 90, Table 91, and Table 92. The suction system is considered the most challenging with a likelihood of 4. An ice protection system should be feasible based on variations of current solutions. It is anticipated that viable solutions for Sys 3.0 should be available with the application of current technology structural optimization tools.

Table 90. Likelihood of Development Challenges in Sys 1.0.

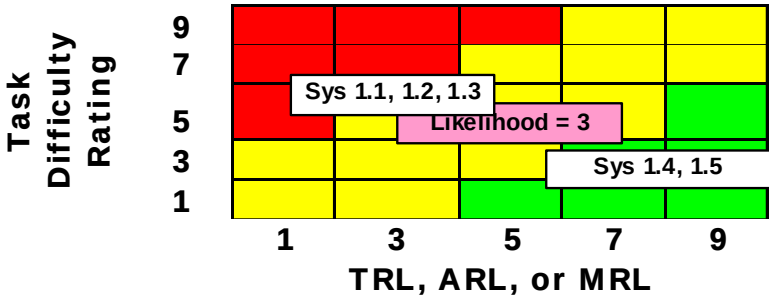

Table 91. Likelihood of Development Challenges in Sys 2.0.

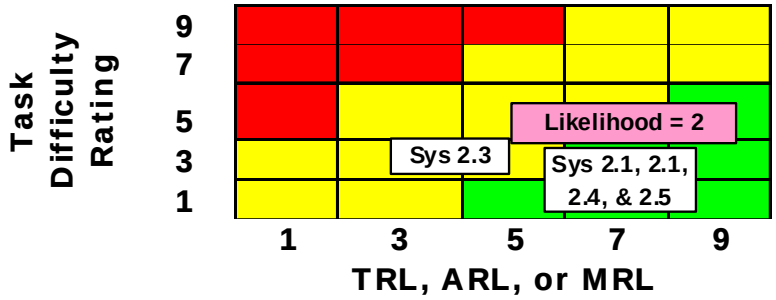

Table 92. Likelihood of Development Challenges in Sys 3.0.

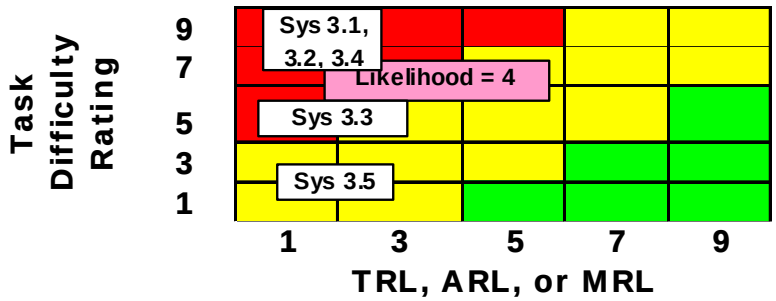

It should be no surprise that Table 93 and Table 94 show a high consequence for failure to mature the systems technologies that enable laminar flow. Laminar flow contributes to approximately 1/3 of the fuel burn benefits in the 2035 vehicle. The risk cube of Table 94 show how the high consequence rating for Sys 1.0 and Sys 3.0 puts these technology development tasks into a the high-risk corner of the cube. In contrast, Sys 2.0 is considered a low risk development effort.

Table 93. Technology Risk Assessment for Aircraft Subsystems

Technology Categories	Consequence	Rationale	Likelihood	Rationale
Ice Protection for Star-C2 Skins	5	Without Laminar Flow the 2035 Fails to Meet its Range Goals	3	Current ice protection technologies can protect the fuselage. The challenge will be in the required power and weight of the system.
Multi-Function Structure for ECS and Interior Noise	2	Failure to accomplish this multi-function goal has little impact on final empty weight of the 2035 vehicle	2	Structural optimization methods are relatively mature.
Suction System for Laminar Flow	5	Without Laminar Flow the 2035 Fails to Meet its Range Goals	4	System weight and compatability with the Star-C2 skin are expected to be challenging goals

Table 94. Risk Cube for Subsystems Development.

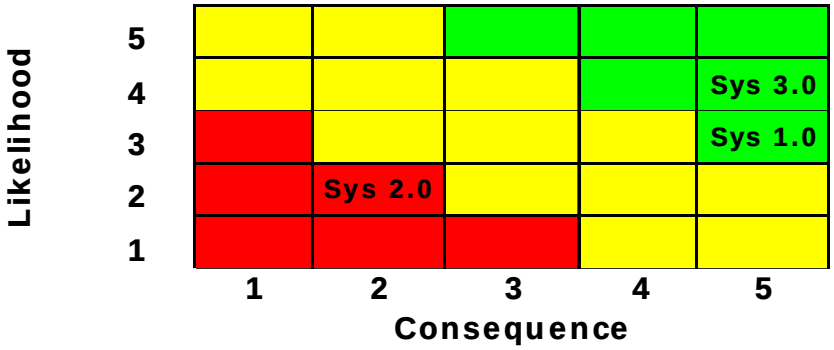

10.6 SOFC/GT Hybrid Electric Aircraft Propulsion

10.6.1 Goals and Objectives

1. Hybrid propulsion system to meet fuel efficiency, emissions, and noise goals.
2. Identify optimized system design and configuration for SOFC/GT hybrid propulsion aircraft, including specific power requirements for SOFC
3. Develop advanced SOFC stack technology to meet specific power requirements dictated by system optimization results

10.6.2 Technical Description

Solid Oxide Fuel Cell (SOFC) / Gas Turbine (GT) hybrid systems offer several advantages over conventional jet propulsion for aviation applications. These advantages include increased energy efficiency, reduced emissions, fuel savings, noise reduction and efficient integration to the auxiliary power demand. However, to maximize these advantages, systems optimizations must be modeled and analyzed and resulting component requirements met through innovation.

A key disadvantage of using SOFCs for aviation applications is that they have not specifically been designed for high specific power. Traditionally, SOFC development has focused on low-cost, high efficiency stationary power, with less emphasis on weight and volume. Recent developments in the materials sets for SOFCs have shown entitlement of 2-3X improvement in power density. In addition, a relaxation of cost constraints on packaging shows entitlement of 2-3X decrease in specific mass. Thus, a 2X improvement in performance, coupled with a 2X decrease in mass yields a 4X improvement in specific power. To take advantage of these opportunities in specific power improvement, a breakthrough SOFC fabrication technology must be developed. Nano-enabled spray manufacturing technologies offer great promise for low-cost manufacturing of engineered architectures for fuel cells.

10.6.3 Milestones and Deliverables

Milestone: Define basic requirements for components / subsystems

Deliverables: Define major components and the process flow

Risk Assessment:

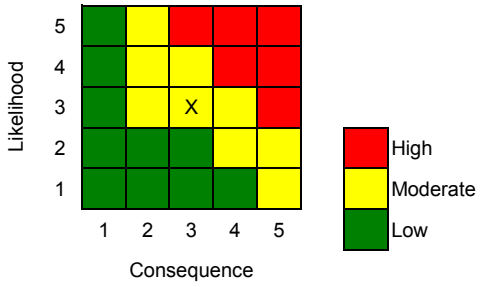

Milestone: Demonstrate 3 kW, 3-cell SOFC short stack with required specific power

Deliverables:

- Double power density to 2 W/cm^2 on button cells
- Develop lightweight interconnect and packaging for 50% mass reduction
- Scale advanced fabrication technique to 100 cm^2 cells
- Develop cell architecture to deliver 1.5W/cm^2at 80% fuel utilization
- Demonstrate 3-cell lab short stack (0.5 kW) with required specific power

Risk Assessment:

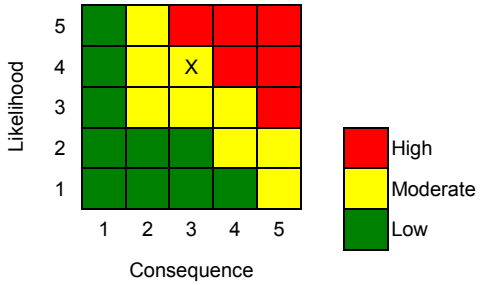

Milestone: Component validation

Deliverables:

- Start communication with airframers
- Detailed component designs
- Component level prototypes

Risk Assessment:

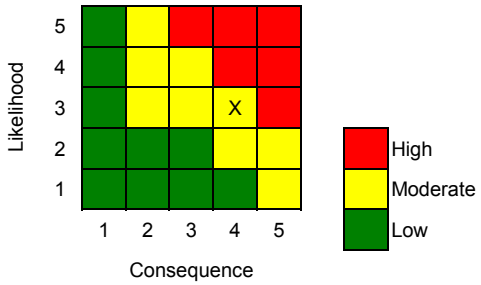

Milestone: Demonstrate integrated 200 kW SOFC / GT system

Deliverables:

- Demonstrate 25 kW SOFC system w/ required specific power
- Demonstrate 200 kW SOFC system w/ required specific power

Risk Assessment:

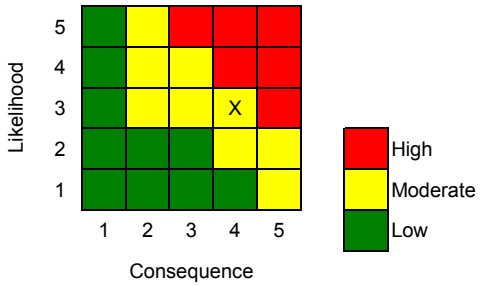

Milestone: System level test validation

Deliverables: Subsystem test validations

Risk Assessment:

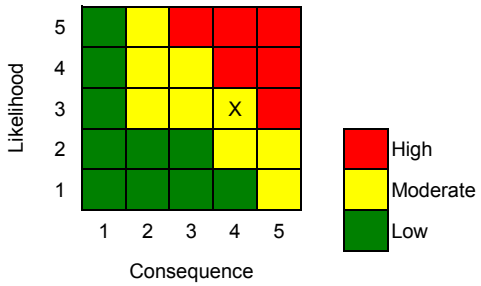

10.6.4 Schedule

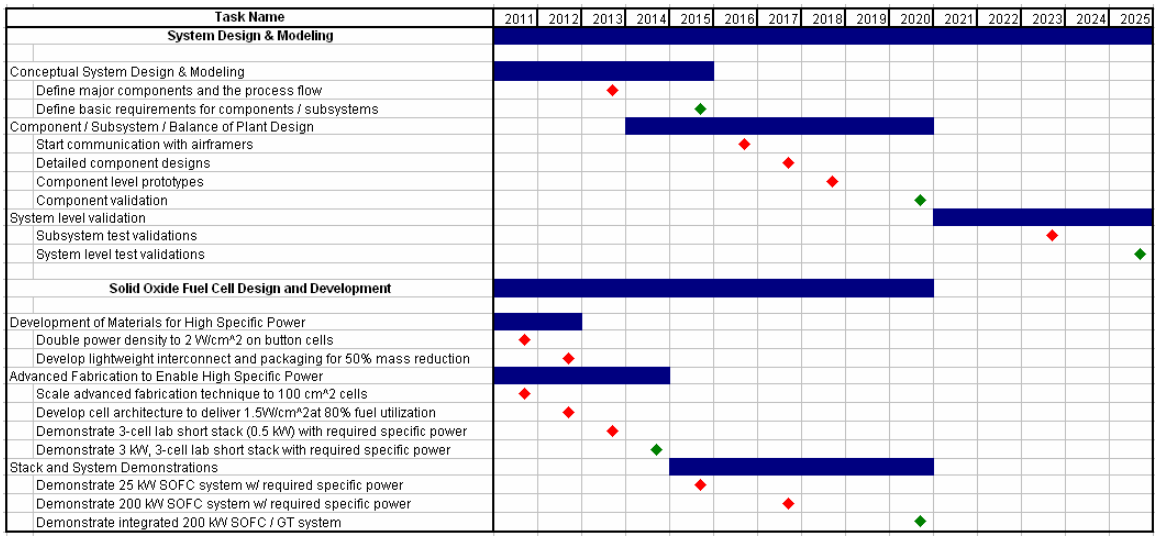

10.6.5 Performance Area Impact

Emissions	Reduced emissions
Fuel Efficiency	Reduced fuel burn
Noise	Reduced core exhaust noise

11.0 Summary

This study indicates the clear potential for an exciting new mode of air travel that could dramatically reduce travel time and stress by enabling direct point-to-point air travel from local community airports. This new air transport network would allow for greater growth in commercial air travel by adding ~1000 underutilized small airports to augment the saturated major hubs. The advanced and innovative technologies of the Year 2035 Ultra Quiet and Efficient Airliner could make this rapid, premium mode of travel available and affordable to a large percent of travelers. This can be accomplished without negative environmental impact, and bring economic benefit to the local airport community.

The Advanced Airliner developed here meets the spirit of the N+3 goals of dramatic reductions in fuel burn, environmental impact, and community noise. The ultra low noise turboprop design is targeted at maximizing the potential for community acceptance, a key to expanding the N+3 airport network. This new, small airliner concept incorporates technologies that minimize the size of the aircraft and engines, reducing acquisition cost, and improving affordability for the traveling public.

The innovative technologies of the Advanced Airliner dramatically reduce ground emissions and noise in an aircraft size where they are currently unregulated. Without these improvements, small airliners won't gain the community acceptance needed to bring commercial air travel to these small airports. The technology roadmaps outlined in this report are key to the commercial and environmental viability of the point-to-point travel network. These unique technologies are targeted at bringing large commercial airliner fuel efficiency to the small, quiet, short-range aircraft needed for this future, convenient air travel network.

References

1. Lewe, J.-H., “Active Control Algorithms of the Air Transportation Network”, Presentation in 16th Annual External Advisory Board Review, Aerospace Systems Design Laboratory, Georgia Institute of Technology, 2008.
2. Yang, E.-S., Lewe, J.-H., & Mavris, D.N., “Demand-Centric Analysis of the Air Transportation System,” in Proceedings of AIAA 8th Aviation Technology, Integration and Operations (ATIO) Conference, AIAA Paper 2008-8889, Anchorage, AK, September 2008.
3. Lewe, J.-H. et al., “An Agent-based Forecasting Tool for NASA’s SATS Program,” Tech. rep., 2nd Place Entry in 2002 University Competition, NASA/FAA, 2002.
4. Lewe, J.-H. et al., “Identification of Design Requirements Through Agent-based Simulation for Personal Air Vehicle System,” AIAA Paper 2002-5876, 2002.
5. Lewe, J.-H., Eric, U.G., Mavris, D.N. & Schrage, D.P., “An Agent-Based Framework for Evaluating Future Transportation Architectures,” AIAA Paper 2003-6769, 2003.
6. Lewe, J.-H., An Integrated Decision-Making Framework for Transportation Architectures: Application to Aviation Systems Design, Ph.D. thesis, School of Aerospace Engineering, Georgia Institute of Technology, Atlanta, GA, 2005.
7. Lim, C.G., Lewe, J.-H. & Mavris, D.N., “An Agent-Based Approach for Modeling the Commercial Air Transportation Network System,” Air Transport Research Society World Conference, Berkley, CA, June 2007.
8. Lim, C.G., An Integrative Assessment of the Commercial Air Transportation System via Adaptive Agents, Ph.D. thesis, School of Aerospace Engineering, Georgia Institute of Technology, Atlanta, GA, 2008.
9. “The 1995 American Travel Survey: Microdata file,” Data CD-ROM, Bureau of Transportation Statistics, 1999.
10. U.S. Department of Transportation, Bureau of Transportation Statistics, “NHTS 2001 Highlights Report,” BTS03-05, Washington, DC, 2003.
11. General Aviation Manufacturers Association, General Aviation Statistical Databook, Available at <http://www.gama.aero/ media-center/industry-facts-and-statistics/statistical-databook-and-industry-outlook>
12. U.S. Department of Transportation and Federal Aviation Administration (FAA), “Report to Congress - National Plan of Integrated Airport Systems (NPIAS) (2007 - 2011),” Tech. rep., U.S. Department of Transportation and Federal Aviation Administration (FAA), 2006.
13. Gillen, D.W, Morrison, W.G. & Stewart, C., Air Travel Demand Elasticities: Concepts, Issues and Measurement, Department of Finance Canada. Modified 2008-10-6. Available at < http://www.fin.gc.ca/consultresp/Airtravel/airtravStdy_-eng.asp> Accessed 14 September 2009.
14. Ahmadi, S., Boeri, L., Jimenez, H., & Mavris, D. “Design of a Light Eco-Friendly Aircraft for 2030-2035 using a Visual Tradeoff Environment,” AIAA’s 9th Aviation Technology, Integration, and Operations Conference, September 2009.
15. “ECAC Doc No. 29 3rd Edition Report on Standard Method of Computing Noise Contours Around Civil Airports Volume 1: Applications Guide.”
16. “ECAC Doc No. 29 3rd Edition Report on Standard Method of Computing Noise Contours Around Civil Airports Volume 2: Technical Guide.”
17. Horonjeff, R. and F.X. McKelvey, Planning and design of airports. 4th ed. 1994, New York: McGraw-Hill. xiii, 829 p.
18. Federal Aviation Administration, Planning and Design of Airport Terminal Facilities at Nonhub Locations, Advisory Circular 150/5360-9,Department of Transportation, 1980: Washington, D.C.

19. Federal Aviation Administration, Planning and Design Guidelines for Airport Terminal Facilities, Advisory Circular 150/5360-13, Department of Transportation, 1988: Washington, D.C.
20. Markovich, M., Airport Costs, Florida Department of Transportation, Editor. 2008.
21. Karlsson, J., et al., Airport economic impact methods and models. ACRP synthesis,. 2008, Washington, D.C.: Transportation Research Board. 67 p.
22. Texas Department of Transportation, Commercial Aviation Airport Economic Impact. [cited 2010 February 8]; Available from: http://www.dot.state.tx.us/txdot_library/publications/commercial_aviation_impact.htm.
23. Smith, W., Iowa Economic Impact on Aviation, Wilbur Smith Associates, Editor. 2009.
24. Brueckner, J.K., Airline Traffic and Urban Economic Development, U. Studies, Editor. 2003, University of Illinois: Champaign.
25. Federal Aviation Administration, The Economic Impact of Civil Aviation on the U.S. Economy, Air Traffic Organization, 2008.
26. Society of Automotive Engineers, Aerospace Information Report 1407, "Prediction Procedure for Near-Field and Far-Field Propeller Noise," May, 1977.
27. Torenbeek, Egbert, "Synthesis of Subsonic Airplane Design," Delft University Press, Martinus Nijhoff Publishers, Copyright, 1982.
28. McCullers, Linwood A.: Flight Optimization System (FLOPS) Release 6.12 User's Guide. October 2004.
29. Feagin, Richard C. and Morrison, William D., Jr.: Delta Method, An Empirical Drag Buildup Technique. NASA CR-151971, December 1978.
30. Sommer, Simon C. and Short, Barbara J.: Free-Flight Measurements of Turbulent-Boundary-Layer Skin Friction in the Presence of Severe Aerodynamic Heating at Mach Numbers from 2.8 to 7.0. NACA TN-3391, 1955.
31. Lin, John C.: Hybrid Laminar Flow on Wings and Fuselages. Truss Braced Wing Synergistic Efficiency Technologies Workshop. August 11, 2009.
32. Jackson, Paul (edited by), "Jane's All the World's Aircraft 2007-2008," Jane's Informational Group Inc., Delft University Press, 2007.
33. Metzger, F.B., "A Review of Propeller Noise Prediction Methodology 1919-1994," NASA Contractor Report 198156, June 1995.

Appendix A: Benchmarking the Tools: Modeling the CJ2+

Appendix A: Benchmarking the Tools: Modeling the CJ2+

In order to quantify the effects of technologies on NASA goals, several notional aircraft and technologies need to be modeled in appropriate sizing and synthesis tools. Usually these tools are physics-based legacy codes that often include empirical relationships. Because the Cessna and Georgia Tech teams each have their own in-house set of tools, the first step in the modeling tasks was to ensure that both tools agreed analytically, within reason. To that end, the team chose the CJ2+ aircraft to model with both set of tools, and then to compare the results. This would, in effect, benchmark the tools going forward.

The aircraft sizing and analysis tools planned for use in this research contract include NASA's FLOPS software (Ref. 1) and Cessna's internal aircraft sizing and configuration analysis suite. Both sets of analysis and design tools use sets of mathematical relationships similar to those found in References 2 and 3. Any differences in the results are anticipated to be in the assumptions or approximations used to estimate drag, weight, engine performance or in the statistical correlation to real data from production aircraft. Cessna's fleet of business jets is quite similar in size and complexity to a small 20 passenger airliner. Therefore the correlation with real data is anticipated to be slightly better for the Cessna tool set than for the FLOPS tool, which is a physics-based analysis tool. Most of the published applications for FLOPS have focused on either military aircraft or large commercial transports.

A Cessna Citation CJ2+ will be used in this study to identify key differences in the analysis results from FLOPS and those that Cessna might calculate for a similar aircraft. The Citation CJ2+ is a little smaller in size, but similar in weight and complexity to that anticipated for a highly efficient 10-30 passenger airliner for the 2035 time period. References 4-9 describe the aircraft in detail and provide aircraft weight, performance, and systems description data. The tuning and validation of NASA's FLOPS aircraft analysis tool with data from aircraft flight and operating manuals (Refs. 4-6) provides a credible tool for the development of small airliners for 2035.

This section provides a description of the Cessna Citation CJ2+ and the performance characteristics for a representative evaluation mission. An overview of size, weight, materials, and technologies that make up the CJ2+ is presented. The weight and geometric description of the CJ2+ is then provided in the format required by the FLOPS analysis tool. Mission performance as established in flight test for the production aircraft is presented in a form that is appropriate for a direct comparison with results generated by the FLOPS analysis tool. Some recommendations are made with respect to an approach that could be used to tune and validate the FLOPS analysis tool with the data provided in this report.

General Description of Cessna Citation CJ2+

The Cessna Citation CJ2+ is an all-metal, pressurized; low-wing business jet with retractable tricycle landing gear and a T-tail (see Figure 202Figure 202). A pressurized cabin has provisions for up to eight passengers, a crew of two, luggage, and optional equipment. Two Williams International Co., LLC FJ44-3A-24 turbofan engine are pylon-mounted on the rear fuselage. Also known as Model 525A, the Citation CJ2+ is certified to the requirements of U.S. Federal Aviation Regulation Part 23 including day, night, VFR, IFR, single pilot, and flight-into-known-icing conditions.

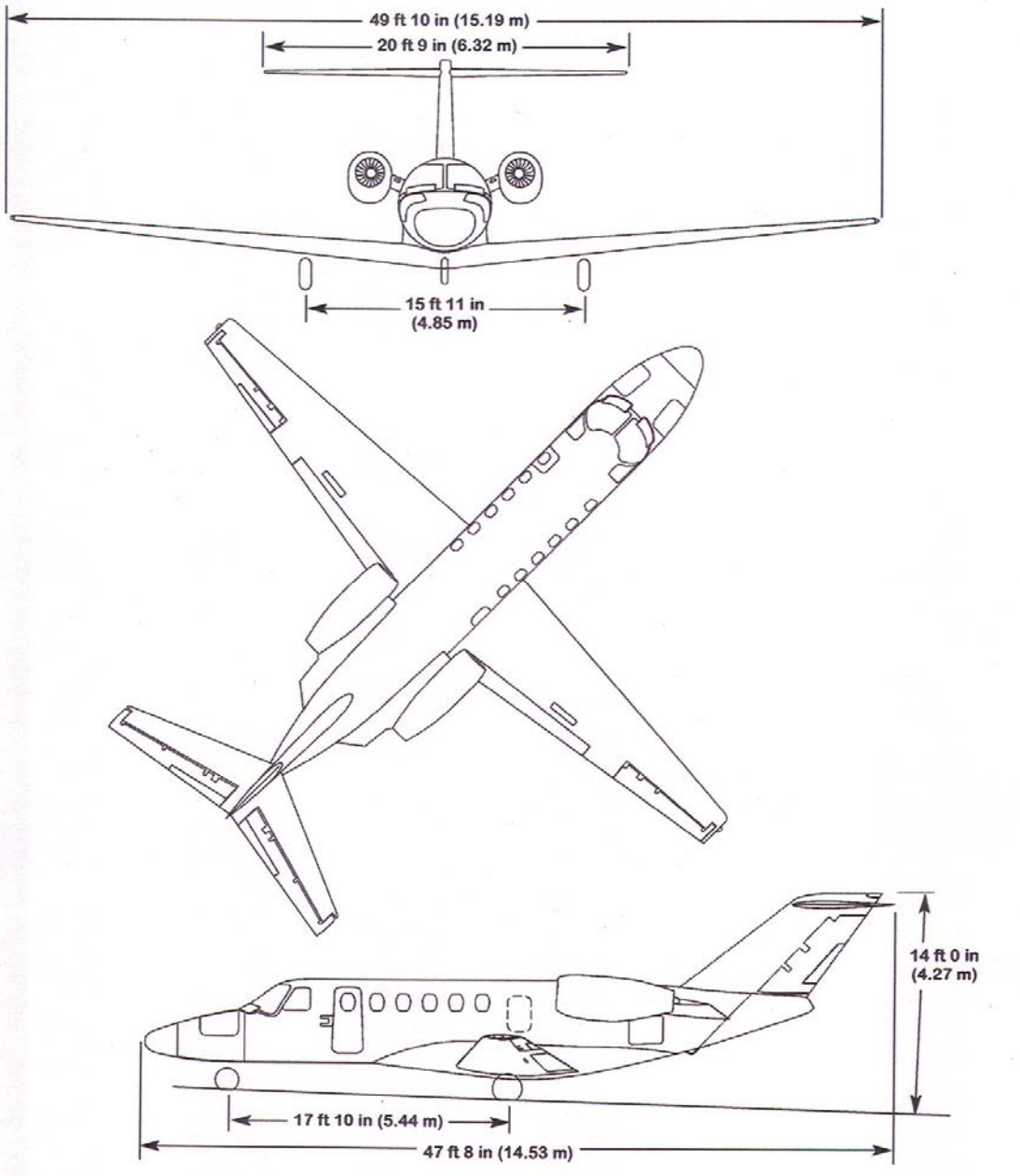

Figure 202. General Description and External Dimensions for Cessna Citation CJ2+

Figure 203 and Figure 204 present the interior dimensions of the CJ2+ and show the most typical 7-passenger seating arrangement. Pilot and co-pilot seats are fully adjustable and include a five-point restraint system. Passenger seats are mounted on a pedestal with the ability track forward, aft, and laterally. Each seat may also be reclined up to 45 degrees. Natural lighting throughout the cabin is provided by 12 elliptical windows. Overhead lights with full dimming capability are also available. Individual air outlets and reading lights are available above each passenger. 110 volt AC power is provided in the side wall near seats #5 and #6. The lavatory in the rear of the aircraft also serves as an extra passenger seat and a coat closet.

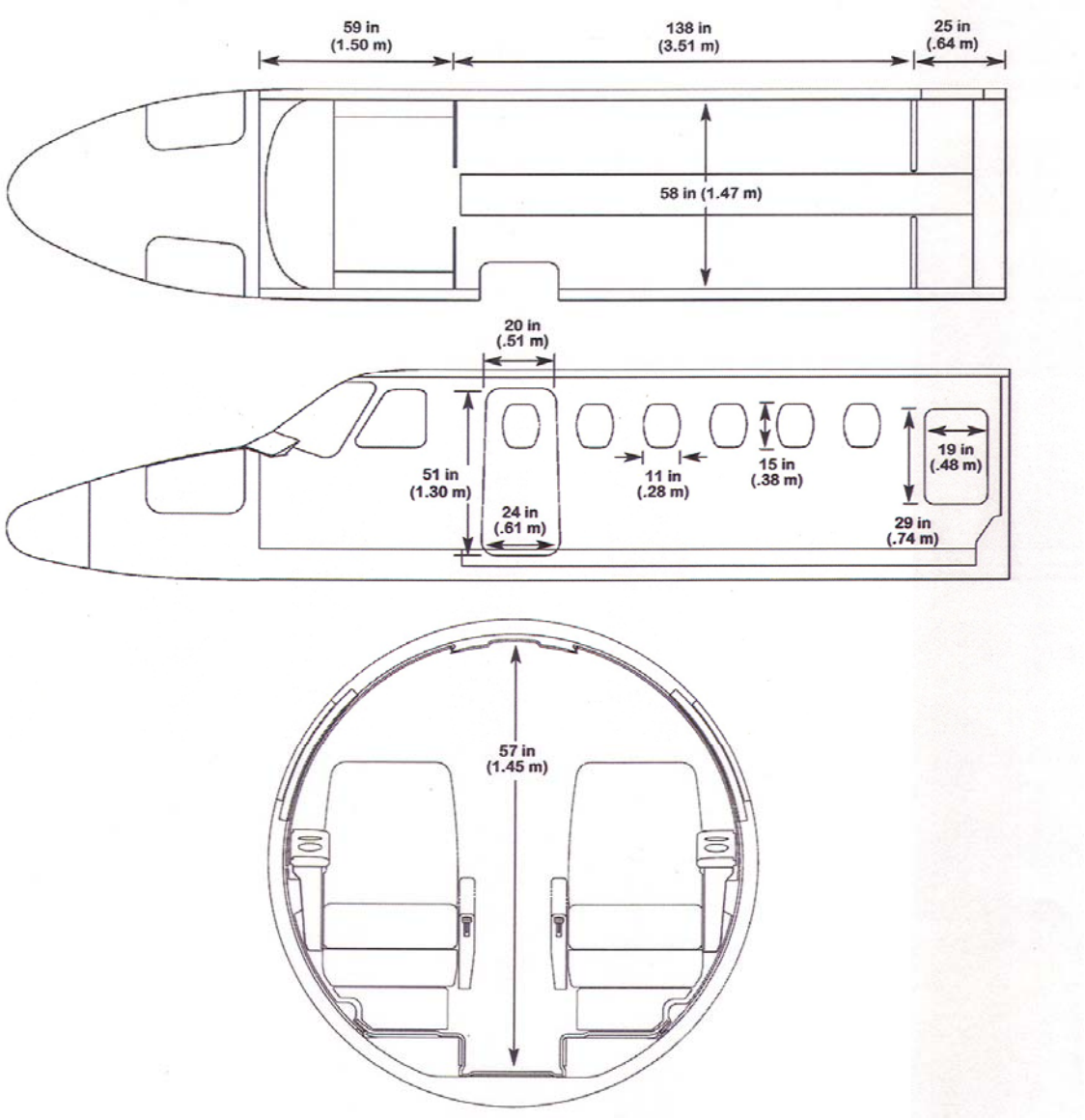

Figure 203. Interior Dimensions for Cessna Citation CJ2+

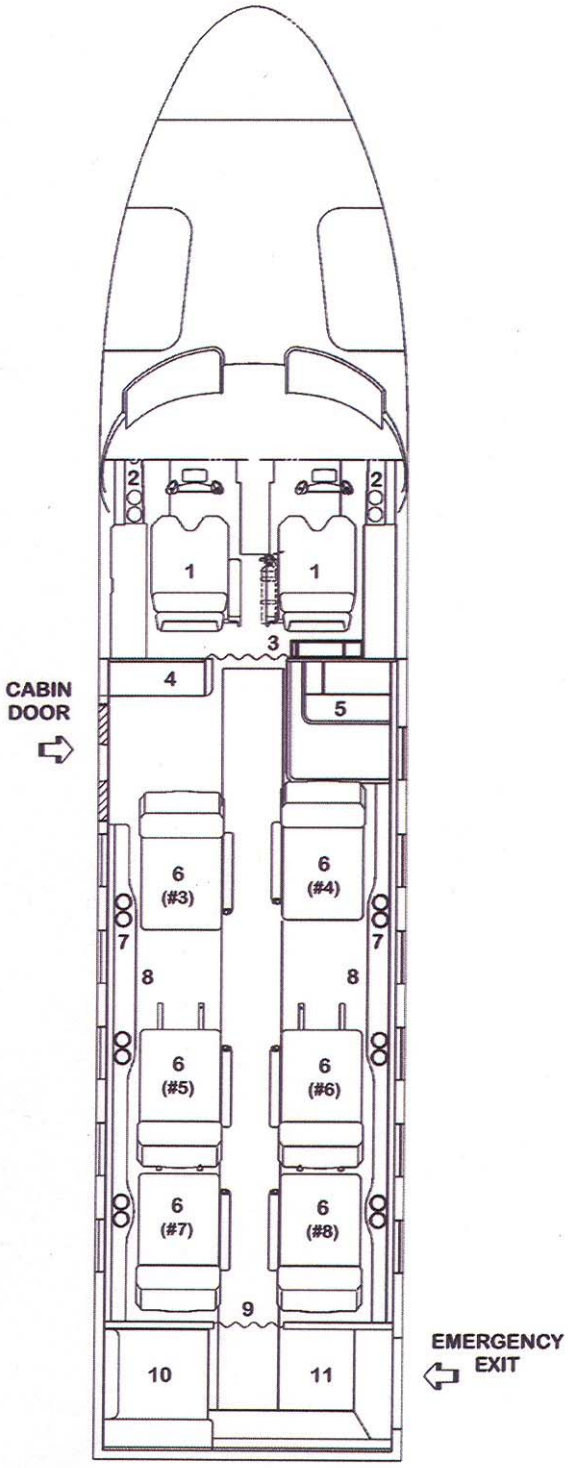

Figure 204. Standard seating arrangement for the Cessna Citation CJ2+

Basic aircraft payload, weights, and performance capability are presented in Table 95 and Table 96. Table 95 presents a maximum takeoff weight of 12,500 lb, a standard empty weight of 7,650 lb, and a useful load of 4,975 lb. Full fuel payload is 1,045 lb with a fuel capacity of 3,930 lb. As shown in Table 96, a maximum take of weight mission starts with a FAA, part 25 balanced field length of 3360 ft and completes a 1613 nm mission with 100 nm of National Business Aircraft Association (NBAA) instrument flight rules (IFR) reserve fuel. Table 96 also shows a maximum cruise altitude of 45,000 ft and a maximum cruise speed of 418 knots.

Table 95. Basic Aircraft Weights

Maximum Ramp Weight	12,625 lb
Maximum Takeoff Weight	12,500 lb
Maximum Landing Weight	11,525 lb
Maximum Zero Fuel Weight	9,700 lb
Standard Empty Weight	7,650 lb
Useful Load	4,975 lb
Fuel Capacity (useable) at 6.70 lb/gal	3,930 lb

Table 96. Basic Aircraft Performance

Takeoff Runway Length …….. Maximum Takeoff Weight, Sea Level, ISA, Balanced Field Length per Part 25, 15 deg. Flaps	3,360 ft
Climb Performnance…… Maximum Takeoff Weight, Sea Level, ISA	28 min. to 45,000 ft
Maximum Altitude……	45,000 ft
Maximum Cruise Speed…… Mid-Cruise Weight, 31,000 ft, ISA	418 KTAS
NBAA IFR Range (100 nm alternate)…… Maximum Takeoff Weight, Full Fuel, Optimal Climb and Descent, Maximum Cruise Thrust at 45,000 ft	1613 nm
Landing Runway Length…… Maximum Landing Weight, Seal Level, ISA, per Part 25	2980 ft
Certificated Noise Levels	
Takeoff……	75.5 EPNdb
Sideline……	86.1 EPNdb
Landing……	89.7 EPNdb

Airframe Structure

The Citation CJ2+ is a conventional design that incorporates advanced aluminum metal bond assemblies, steel and other materials as appropriate. Table 97 shows the structural design and limit speeds. Design maneuver limit load factors are -1.52 Gs to +3.6 Gs. Ultimate loads are defined as 1.5 times the limit loads. The maximum cabin pressure differential is 8.9 psi.

Table 97. Structural Design and Limit Speeds

Limit Speeds	
V_{MO} at 8,000 to 29,123 ft …….	278 KIAS
M_{MO} at 29,123 ft ……..……..	0.737
Flap Extension Speeds	
V_{FE} 0 ° to 15° Extension ……..…	200 KIAS
V_{FE} 15 ° to 35° Extension …..…	161 KIAS
Landing Gear Extended Speeds	
V_{LO} retracting ……..……..….	200 KIAS
V_{LO} extending ……..……..……	200 KIAS
VL_E ……..……..……..……	200 KIAS

Propulsion

Two Williams FJ44-3A-24 power the Citation CJ2+ and provide the secondary power for the hydraulic, pneumatic, and electrical systems. This engine is a mixed-flow turbofan with a twin-spool design, with 5 compression stages and 3 turbine stages, and produces 2490 pounds of takeoff thrust at sea level, static conditions. Dual channel Full Authority Digital Engine Controls (FADECs) provide automation and efficiency in engine management.

Figure 205 show the primary flight controls for the Citation CJ2+. The primary flight controls (rudder, ailerons, and elevators) and nose wheel steering are totally mechanical, and require no hydraulic or electric power. Trim systems are all mechanically-driven trim tabs, actuated manually through knobs or wheels in the cockpit. Pitch trim may be actuated electrically as well as manually. Flaps, speed brakes, and landing gear are actuated hydraulically. Low idle thrust settings eliminate the need for thrust reversers or thrust attenuators.

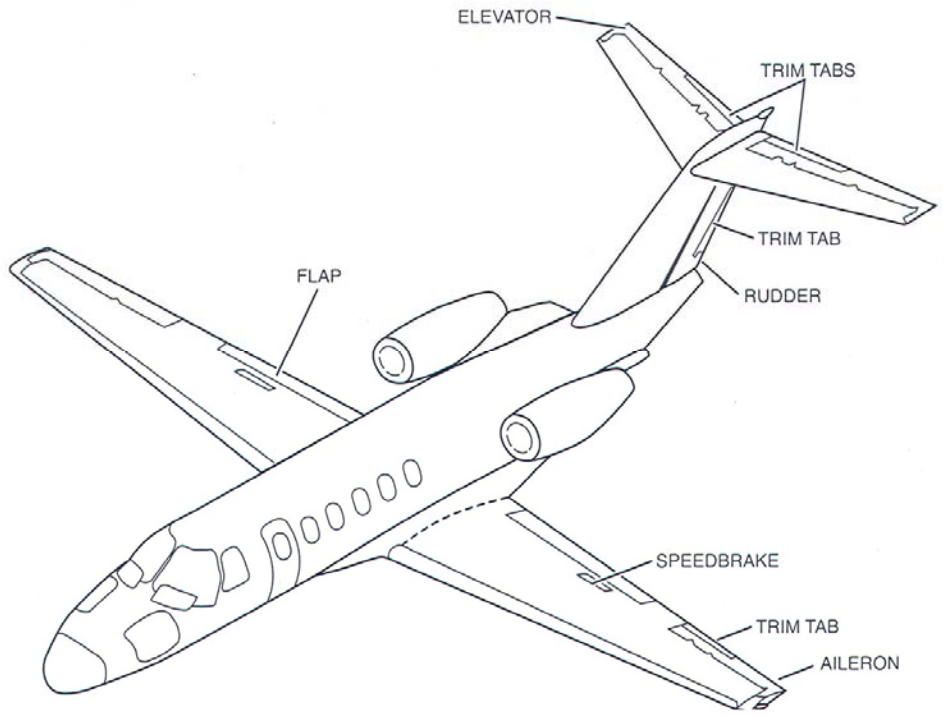

Figure 205. Citation CJ2+ Flight Control Surfaces Systems

Primary systems for the Citation CJ2+ include a fuel system, a hydraulic system, an electrical system, a pressurization system, an environmental control system, an oxygen system, and an ice and rain protection system. Each of these systems either supports other aircraft systems or provides for a healthy and comfortable cabin and cockpit environment. Power for all of these systems is generated by the aircraft's main engines.

Mechanical power is extracted from the main engines to support the hydraulic system, the generation of electrical power, and for fuel system pumps. The fuel system supports the main engines with two integral fuel tanks, one per wing, providing a total of 3,930 pounds of usable fuel. The open-center hydraulic system provides 1,500 psi of on demand power for landing gear, speed brake, and flap actuators. Electrical power for both the cabin and cockpit is provided by two 300 amp, 29 volt, DC starter-generators. Each of these starter-generators is used both for turbine engine start and to provide aircraft electrical power.

Engine bleed air at differential pressure of 8.9 psi provides cabin pressurization for the environmental control system. This pressure permits a sea level cabin altitude up to 23,586 ft and an 8,000 ft cabin altitude at the maximum cruising altitude of 45,000 ft. Engine bleed air is also used to heat the cabin, defog the windows. A vapor cycle air conditioning systems provides cabin cooling and a 50 cubic foot oxygen bottle provides for flow to masks, as necessary.

A combination of engine bleed air and electrical power is also used for the aircraft ice protection system. Hot bleed air provides anti-ice protection for engine inlets, pylon inlet ducts, wings and windshields. Lower temperature air is used for pneumatic boots that provide de-ice protection to the horizontal tail. A back-up alcohol anti-ice system is used for the windshields.

Electrical heaters provide anti-ice protection for the pitot tubes, static ports, and the angle of attack sensors. Windshield rain removal is accomplished with engine bleed air.

Flight Compartment, Instrumentation, and Avionics

The Citation CJ2+ is delivered with the Collins Pro Line 21 Avionics System. These avionics include an integrated flight director, autopilot, and electronic flight information system (EFIS). Capabilities and equipment in the CJ2+ instrumentation and avionics system include but are not limited to the following:

- Flight Guidance System
- Attitude Head Reference System (AHRS)
- Air Data Computer (ADC)
- Integrated Flight Information System (IFIS)
- Integrated Electronic Checklist
- Fight Management System (FMS)
- Global Positioning System (GPS)
- Radio Tuning Units (RTUs)
- Terrestrial Navigation Receivers
- Distance Measuring Equipment (DME)
- Radio Altimeter
- VHF Communication Transceivers
- Transponders
- Traffic Collision Avoidance System (TCAS I)
- Terrain Awareness Warning System (TAWS)
- Weather Avoidance Radar
- Electronic Standby Instrument System (ESIS)
- Emergency Locator Transmitter (ELT)
- Maintenance Diagnostic Computer

Primary flight displays (PFDs), multi-function displays (MFS) and instrument panels features are show in Figure 206.

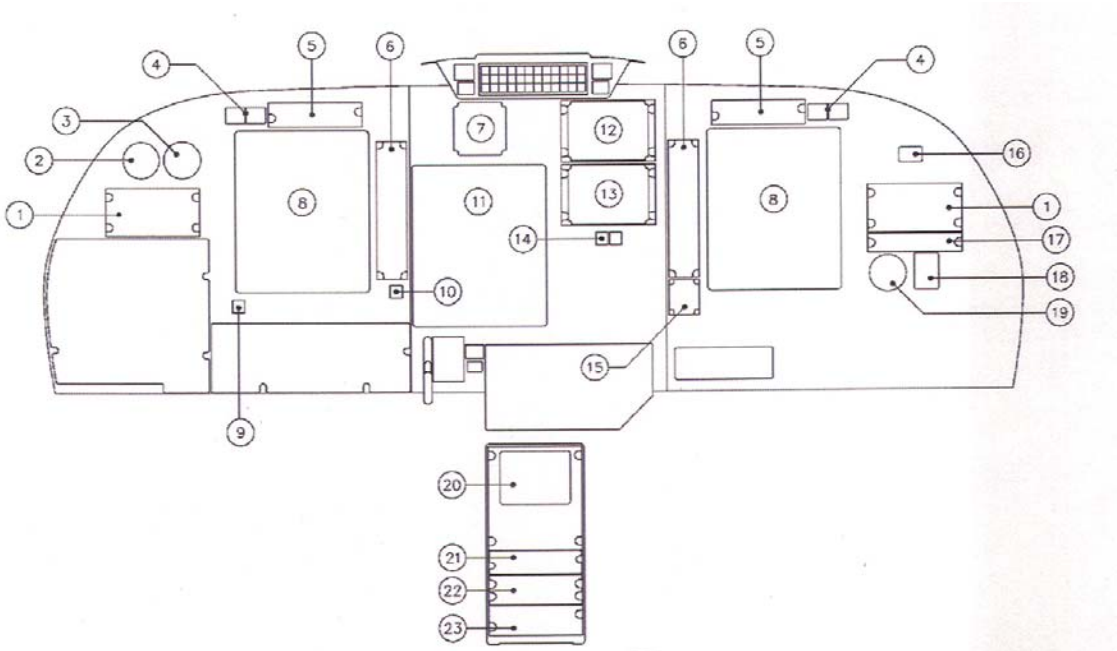

1. Audio Control Panel
2. Davtron Clock
3. Angle of Attack Indicator
4. Master Caution/Warning Annunciators
5. Autopilot Mode Selection Panel
6. Display Control Panel
7. Electronic Standby Instrument System
8. Primary Flight Display (PFD)
9. Avionics Dispatch Switch
10. Cockpit Speaker Mute Switch
11. Multi-Function Display (MFD)
12. Radio Tuning Unit No. 1 (RTU) with EHSI
13. Radio Tuning Unit No. 2 (RTU)
14. TAWS Annunciators
15. Copilot Course Knob Panel
16. Flight Hour Meter
17. Provisions for Cockpit Voice Recorder (CVR) Control Panel
18. ELT Remote Control
19. Oxygen Pressure Indicator
20. Flight Management System (FMS) CDU
21. Course / Altitude / Heading Control Panel
22. Cursor Control Panel
23. Autopilot Panel

Figure 206. Flight Compartment Instrument Panel and Pedestal Layout

This comprehensive communication, navigation, and cockpit control system enable single-pilot operation of the CJ2+ in the modern airspace system anywhere in the world. More detailed descriptions of the system components and capabilities can be found in references 4-6.

Evaluation Mission

A maximum payload mission is provided for evaluation, verification, or tuning of the NASA FLOPS aircraft performance analysis and sizing code (see Figure 207). This mission includes climb, cruise, descent, and reserve segments. The climb segment is further characterized by a 230 KIAS climb at constant power setting to 10,000 ft altitude. A Mach = 0.55 constant power climb brings the aircraft to a cruise altitude of 43,000 ft. The cruise segment is flown at maximum cruise power setting. The rate of descent is 3000 ft/min or is established by a flight speed that is 10 knots slower than the maximum operating Mach number (see Table 97).

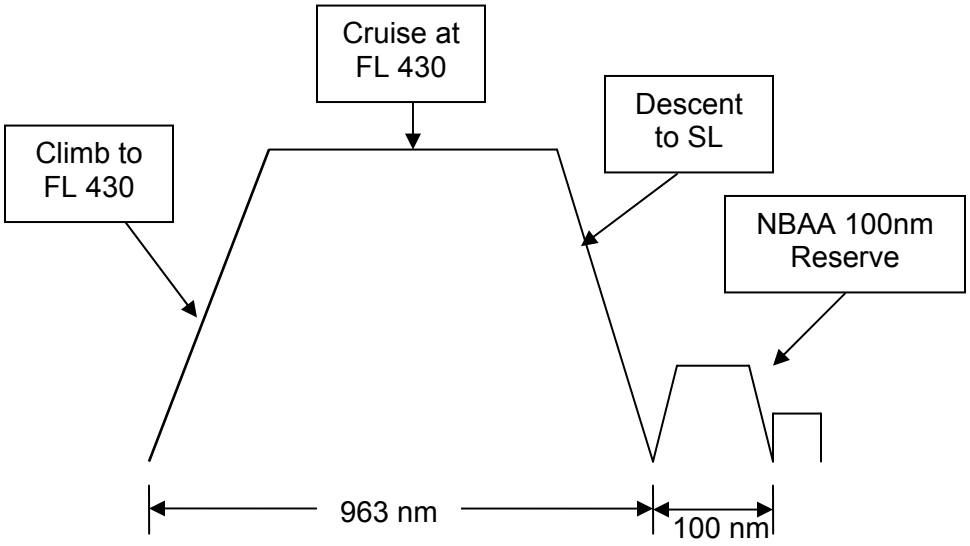

Figure 207. Representative Maximum Payload Mission for the Citation CJ2+

The reserve segment is defined by National Business Aircraft Association (NBAA) 100nm reserve mission. This mission consists of a 5 minute loiter at sea level, a climb to 5000 ft, a hold for 5 minutes, a climb to 17,000 ft, a cruise at long range cruise setting, a descent to sea level for a total of 100 nm with enough additional fuel to loiter at 5000 ft for 30 minutes.

Table 98 shows the performance results for a CJ2+ mission with a maximum payload of 1750 lbs and a take off weight of 12,500 pounds. This assumes a basic operating weight (BOW) of 7931.5 pounds. This BOW includes the crew, miscellaneous equipment, and options. This 962.8 nm mission consumes 1992.4 pound of fuel after taxi and takeoff and requires a reserve fuel allocation of 826.1 pounds. The table shows that a direct climb to 43,000 ft is accomplished in 23 minutes, and cruise segment of 118.7 minutes, and a descent of 14.6 minutes.

Table 98. Distance, Fuel Burn and Time for CJ2+ Maximum Payload Mission

Segment	Distance (nm)	Fuel Burn (lbs)	Time (min)
Taxi-Takeoff	0	125	0
Climb	117.4	500.4	23
Cruise	759.8	1404.7	118.7
Descent	85.6	87.3	14.6
Reserve	100	826.1	53.6*

A maximum take off weight condition can be used to validate the field length calculations in FLOPS. A Citation CJ2+ is capable of a balanced field length of 3,360 ft from a maximum take off weight condition at sea level with 15 degrees of flaps and a standard atmosphere (see Table 96).

FLOPS Data & Input Files

In order to support the collaboration with Georgia Tech, General Electric, and NASA, data for the CitationJet 2+ described in this report has been formatted to be compatible with NASA's FLOPS performance analysis tool. FLOPS users at Georgia Tech were able to use this data to start from to create input files and to analyze the CitationJet 2+ for the evaluation mission described above.

Table 99, Table 100, and Table 101 present the data required to analyze the CJ2+ with FLOPS on the evaluation mission shown in Figure 207. Geometric data that represents the CJ2+ shown in Figure 202Figure 202 is presented in Table 99. Each line in the table shows the FLOPS input parameter, a description of the parameter, a value, and the appropriate units.

Table 99. Aircraft Geometric Input for NASA FLOPS Aircraft Analysis Tool

FLOPS Parameter	Description	Value	Units
DIH	Dihedral	5	deg
FLAPR	Flap Ratio	0.121205702	
XL	Fuselage Length	47.66666667	ft
WF	Fuselage Width	14	ft
DF	Fuselage Depth	14	ft
XLP	Length of passenger compartment	13.75	ft
XMLG	main landing gear (oleo) length	8.046	in
XNLG	nose landing gear (oleo) length	7.437	in
SHT	Horizontal tail area	70.678	ft2
SWPHT	Horizontal Tail ¼ chord sweep angle	20	deg
ARHT	Aspect Ratio Horizontal Tail	6.112	
TRHT	Taper Ratio Horizontal Tail	0.425	
TCHT	Thickness to chord Horizontal tail (@ MAC)	0.088229	
SVT	Vertical tail area	46.84	ft2
SWPVT	Vertical Tail ¼ chord sweep angle	49	deg
ARVT	Aspect Ratio Vertical Tail	0.87	
TRVT	Taper Ratio Vertical Tail	0.6	
TCVT	Thickness to chord Vertical tail	0.12	
TR	main wing taper ratio	0.319	
SWEEP	¼ chord main wing sweep	0.793	deg
TCA	main wing thickness to chord ratio (@ MAC)	0.128421	
AR	main wing aspect ratio	8.772	
SW	main wing surface area	264.344	ft2
XNAC	Average length of baseline engine nacelles	7.37327381	ft
DNAC	Average diameter of baseline engine nacelles	2.663650794	ft
WHGT	wing height above ground	2.07	ft

Aircraft weights and mission parameters that are appropriate for the FLOPS analysis tool are shown in Table 100 and Table 101. This data can be used directly for a performance evaluation of the mission described in this report.

Table 100. Aircraft Mission Parameters

FLOPS Parameter	Description	Value	Units
	Total Number of Passengers	9	
NPF	Typical Number of First Class passengers	4	
NPT	Typical Number of Tourist (Coach) Passengers	N/A	
CH	Maximum Cruise Altitude	45000	ft
CRMACH	Cruise Mach Number	0.71	M
CRALT	Cruise Altitude	41000	ft
VMMO	Maximum operating Mach number	0.737	M
DESRNG	Design Range	1613	nmi
PAYLOD	Design Payload	1750	lb

Table 101. Basic Aircraft Operating Weights

FLOPS Parameter	Description	Value	Units
OEW	Operational Empty Weight (no crew)	7685.66	lbs
MZFW	Maximum Zero Fuel Weight	9700	lbs
MTOGW	Maximum Takeoff Gross Weight	12500	lbs
FULWMX	Maximum Wing Fuel Weight	3930	(lbs)
FULFMX	Maximum Fueselage Fuel Weight	0	(lbs)
WLDG	Design Landing Weight	11525	(lbs)

This concludes the description of the Cessna CitationJet 2+ including sufficient data for an aircraft performance analyst to simulate a representative mission. This simulation can be compared with the flight performance data provided for a maximum payload mission. Fuel burn for each segment of this mission along with the takeoff, landing, and climb performance numbers provided enables the development of a model that approximates the production aircraft. Development of this type of model should help tune the NASA FLOPS analysis tool and identify any improvements in the FLOPS methods that may be required for the development of 2035 airliners.

Calibrating the Models

The model calibration was done in two steps. First, the CJ2+ model was calibrated in the FLOPS tool used by Georgia Tech, and then evaluated as compared to the Cessna in-house tools. The goal of this work was to identify modeling best practices and areas of concern when working with the Baseline 20 airliner. The Cessna CJ2+ results consist of flight test data and outputs from Cessna's Mission Analysis and Performance System (MAPS), drag, and weights codes along with other design tools. The Cessna tools have already been calibrated to reproduce the CJ2+ characteristics. A representative maximum payload mission is used for comparison. After the CJ2+ calibration was completed, a similar analysis was conducted for the B-20 aircraft.

The data for the CJ2+ was obtained from a combination of Cessna flight test data and the airplane manuals. This data was reproduced when using the Cessna weight estimating relationships, the Cessna aerodynamics software (FSDRAG), and the Cessna aircraft performance code (MAPS).

The goal of this study is to compare the outputs of MAPS (which closely models the CJ2+ performance) and FLOPS. The version of FLOPS used for this comparison is a Georgia Institute of Technology (Georgia Tech) modification of Version 6.12 (Reference 10). The modification adds the ability to include aeroelastic effects and includes one extra input variable. As a check, input files were run in the Georgia Tech Version 6.12 and in the NASA Version 7.40 (Reference 11). The results from both versions of FLOPS were identical, since the aeroelastic capability is not used in this study.

FLOPS Modeling Methodology

Figure 208 shows the flowchart for calibrating a small aircraft in FLOPS. First, the aircraft geometry must be defined. Next, an engine deck must be supplied. (Although FLOPS does have the capability to generate an engine deck, in this particular study, the engine decks were provided by the GE team members). Finally, a design mission must be specified. FLOPS is then executed to calculate weights, fuel burn, and performance. FLOPS has the ability to either accept a given drag polar, or to use internal physics-based algorithms to generate aerodynamics, given the geometry. In this particular case, tuning factors within FLOPS were used to match the given CJ2+ drag polar. An iterative process is then used to change the multiplicative factors within FLOPS in order to match the given data.

FLOPS does have the capability of exactly matching a given aircraft and its performance. However, this involves “hardwiring” certain factors into the input. By doing so, an exact match is virtually guaranteed. However, the aircraft may not then be perturbed, thus limiting parametric trade studies. FLOPS use of multiplicative tuning factors allows a parametric analysis of the aircraft, at the slight, if any, cost in accuracy.

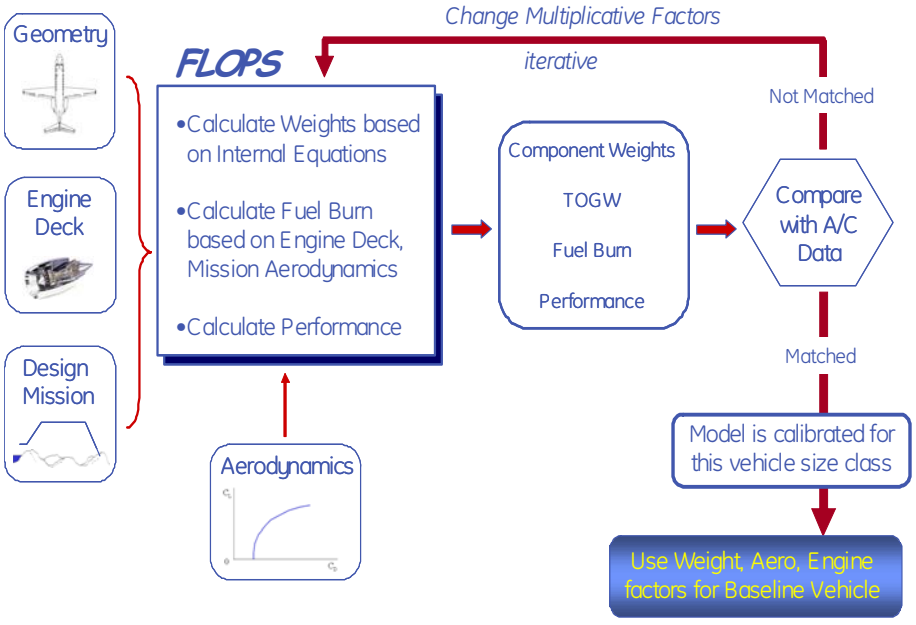

Figure 208. FLOPS Calibration Methodology

CJ2+ Evaluation Mission

A maximum payload mission is provided for evaluation, verification, and tuning of the FLOPS aircraft performance analysis and sizing code. The mission profile (which was already shown in Figure 207) includes climb, cruise, descent, and reserve segments. The FLOPS mission inputs are shown in Table 3. The climb segment is composed of a 230 KIAS climb to 10,000 ft altitude and a Mach = 0.55 climb to 38,000 ft along a specified Mach/altitude schedule (shown in Table 102). FLOPS completes the climb at a minimum fuel to climb to the cruise altitude of 43,000 ft. The cruise segment is flown at a constant Mach number of 0.67 at 43,000 ft. The descent is flown along the Mach/altitude schedule shown in Table 103. The descent schedule equates to a 3,000 ft/min rate of descent or is established by a flight speed that is 10 knots slower than the maximum operating Mach number.

The reserve segment is defined by National Business Aircraft Association (NBAA) 100 nm reserve mission. This mission consists of a 5 minute loiter at sea level, a climb to 5,000 ft, a hold for 5 minutes, a climb to 17,000 ft, a cruise at long range cruise setting, a descent to sea level for a total of 100 nm with enough additional fuel to loiter at 5,000 ft for 30 minutes. Rather than modeling this reserve mission completely, the missed approach time, distance to an alternate airport, and fixed fraction of reserve fuel (0.028) were used to model the reserve mission. This matched the CJ2+ MAPS-calculated reserve mission.

Table 104 shows a comparison of the MAPS and FLOPS results by segment for distance, fuel burn, and time. A comparison of the climb, cruise and descent mission legs is shown in Figure 209. The FLOPS analysis tool didn't enable detailed modeling of the NBAA IFR 100 nm reserve mission, so 28% of total mission fuel was added to the FLOPS reserve mission fuel. This forces both MAPS and FLOPS to carry the same reserve fuel load throughout the primary mission. It is recognized that a simplified reserve mission will be necessary for the sizing and trade studies intended for small airliners.

Table 102. CJ2+ Climb Profile for FLOPS Model

Mach Number (VCTAB)	Altitude, ft (ACTAB)
0.3477	0.
0.3602	2,000.
0.3733	4,000.
0.3870	6,000.
0.4014	8,000.
0.4166	10,000.
0.4324	12,000.
0.4491	14,000.
0.4667	16,000.
0.4851	18,000.
0.5045	20,000.
0.5249	22,000.
0.5464	24,000.
0.55	26,000.
0.55	28,000.
0.55	30,000.
0.55	32,000.
0.55	34,000.
0.55	36,000.
0.55	38,000.

Table 103. CJ2+ Descent Profile for FLOPS Model

Mach Number (VDTAB)	Altitude, ft (ADTAB)
0.3931	0.
0.4071	2,000.
0.4217	4,000.
0.4371	6,000.
0.4532	8,000.
0.4825	10,000.
0.5007	12,000.
0.5197	14,000.
0.5397	16,000.
0.5606	18,000.
0.5826	20,000.
0.6057	22,000.
0.6299	24,000.
0.6554	26,000.
0.6822	28,000.
0.6953	30,000.
0.6943	32,000.
0.6932	34,000.
0.6920	36,000.
0.6907	38,000.

Table 104. Comparison of MAPS and FLOPS Maximum Payload Mission

	Distance (nm)		Fuel Burn (lbs)		Percent Mission Fuel		Time (min)	
Segment	**MAPS**	**FLOPS**	**MAPS**	**FLOPS**	**MAPS**	**FLOPS**	**MAPS**	**FLOPS**
Taxi-Takeoff	0	0	125	125	5.9	6.0	0	0
Climb	117.4	122.8	500.4	514	23.63	24.66	23	23.95
Cruise	759.8	763.7	1404.7	1414	66.34	67.85	118.7	119.5
Descent	85.6	56.7	87.3	31	4.12	1.49	14.6	10.08
Total Mission (no reserve)	962.8	943.2	2117.4	2084	100	100	156.3	153.53
Reserve	100	N/A	826.1	826.1*	39.01	39.64	53.6	N/A

*The reserve fuel weight was matched in FLOPS by setting the RESTRP variable to 0.28.

The match between MAPS and FLOPS results is excellent, with a difference of only 1.6 percent more total fuel in the MAPS mission (2117.4 lbs in MAPS compared to 2084 lbs in FLOPS). The CJ2+ burns slightly less fuel during climb and slightly less fuel in cruise in MAPS; shorter distances are associated with those lesser fuel amounts.

The most significant difference between the MAPS and FLOPS results is during descent. The descent schedule from MAPS was used in FLOPS to try to improve the fidelity of the match, but there was still a 33.8% difference in distance and 64.5% difference in fuel burn during descent. In spite of the large differences in descent characteristics, there is only two percent difference in the range and 1.6 percent difference in fuel for the overall mission (very acceptable for this type of analysis). These differences in range can be seen visually in Figure 209.

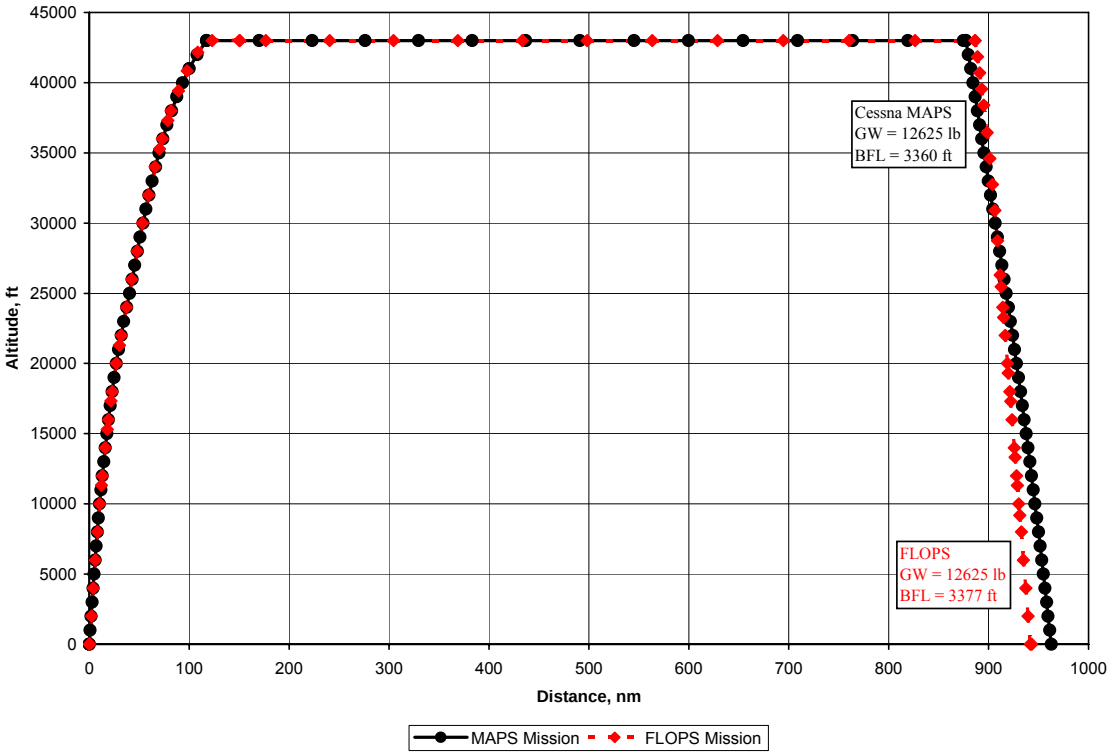

Figure 209. Comparison of MAPS and FLOPS Results for the Citation CJ2+

Field Length Analysis

A maximum take off weight condition can be used to validate the field length calculations in FLOPS. A Citation CJ2+ is capable of a balanced field length (BFL) of 3,360 ft from a maximum take off weight condition at sea level with 15 degrees of flaps and a standard atmosphere. The variation of BFL with TOGW is shown in Figure 210. FLOPS shows excellent agreement from about 11,500 lbs through the maximum TOGW (12,500 lbs). FLOPS slightly over predicts BFL between about 10,000 lbs and 11,500 lbs. Below 9,700 lbs, FLOPS starts to underestimate the BFL. The FLOPS relationship for BFL appears to be linear, and as TOGW decreases, the actual BFL does not decrease linearly.

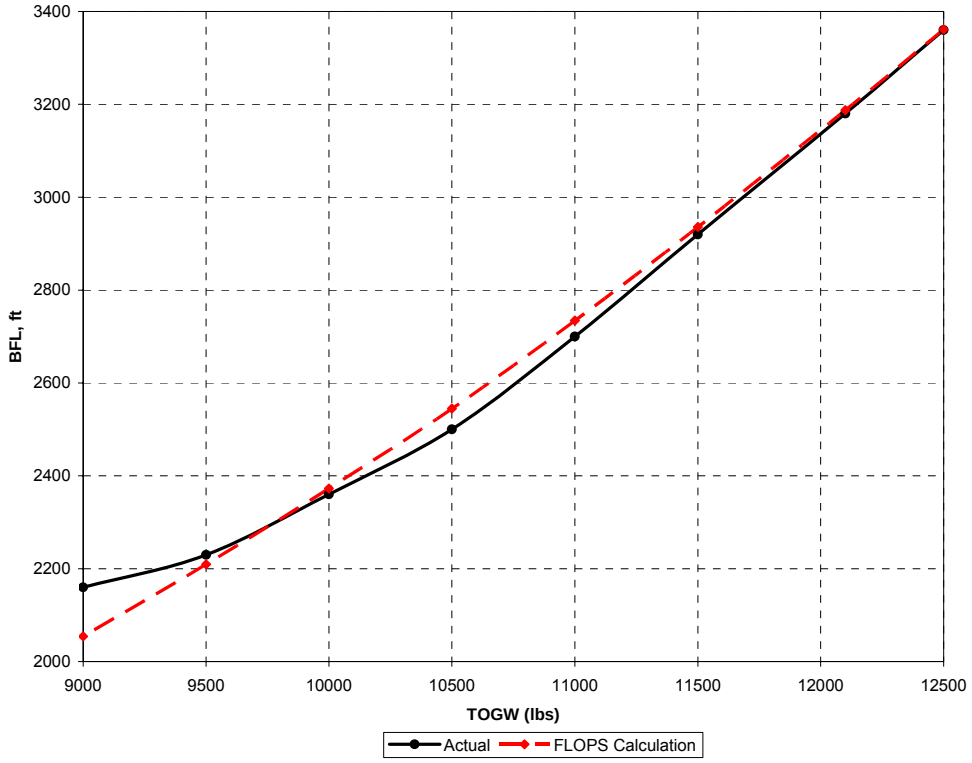

Figure 210. BFL Sensitivity to Takeoff Weight

Weights Calibration

In order to match the CJ2+ mission, the CJ2+ component weights were used as FLOPS inputs. The Cessna weight equations were derived from empirical data compiled on eight production model Citation aircraft and predict the CJ2+ weights needed for FLOPS with two exceptions: 1) avionics (WAVONC) and instrumentation (WIN) are lumped into one value in the Cessna weights equations; and 2) air conditioning (WAC) and anti-ice systems (WAI) are lumped into one value in the Cessna weights equations. For the purposes of tuning weights in FLOPS, actual weights from the CJ2+ weight statement were used for the individual weights. This will be an issue when using the Cessna weight equations to generate B-20 component weights and tuning factors in FLOPS.

After determining that the performance calculations were good, then FLOPS was allowed to calculate the weights. FLOPS uses statistical/empirical equations to predict the weight of each item in a group weight statement (Reference 10). According to Reference 12, the FLOPS weight equations are based on weight and technical data collected and analyzed for 19 commercial and seven military transport aircraft.

There are equations in FLOPS which are based on a small set of general aviation (GA) aircraft for the wing, fuselage, horizontal tail, vertical tail, fuel systems, and surface controls. When the GA weight equations option is selected, these component weights are calculated using the GA equations. The remaining component weights are calculated from the transport weight equations.

The engine weight (WENG) does not scale like other weight factors, and is fixed for now. It is computed by default as:

$$WENG = \frac{THRUST}{5.5}, \& W_{Engine} = WENG\left(\frac{THRUST}{THRSO}\right)^{EEXP}$$

(In subsequent modeling of the B-20, FLOPS was modified to scale the engine weight based on a relationship provided by the GE team members). FLOPS was run, and the FLOPS-calculated weights were compared to the Cessna-component weights. Results are shown qualitatively in Table 105 where the "+" indicates that FLOPS over predicted the component weight, and the "-" indicates a component weight under predicted by FLOPS. The number of "+" or "-" signs indicates the magnitude of the over or under prediction.

Table 105. Correlation Between FLOPS and Cessna Weights

	Correlation GA	Correlation Transport
Wing	-	-
Horizontal Tail	++	--
Vertical Tail	++	--
Fuselage	+	-
Fuel System	++	+++
Surface Controls	++	+++
	Correlation Transport	
Nacelle	--	
Landing Gear	--	
Instruments	+++	
Avionics	+	
Hydraulics	++	
Electrical	++++	
Furnishings & Equipment	++	
Air Conditioning	-	
Total	**+ (10%)**	**+ (18%)**

KEY	
FLOPS over (+) or under (-) predicts weight by:	
+ or -	0-20%
++ or --	21-40%
+++ or ---	41%-100%
++++	>100%

Results show that FLOPS does an excellent job in estimating the wing and fuselage weight. The GA weight estimation for the wing is nearly perfect. For the tails, the GA equations somewhat over predict the weights while the transport equations somewhat under predict the weights. The fuel system and surface controls weights are dramatically overestimated by the transport weight equations and only significantly overestimated by the GA weight equations.

For the remainder of the components, the avionics and air conditioning weights are closest to the actual values. Nacelle and landing gear weights are significantly under predicted while furnishings and equipment weight and hydraulics weight are significantly over predicted (21-40%). Weight of the instruments is dramatically over predicted by FLOPS.

It is reasonable to expect significant errors in component weight prediction, since FLOPS primarily uses empirical fits to weight data from large transport and military aircraft. This is

particularly true for electrical, instrument, and hydraulic system weights. General aviation aircraft typically have manual rather than hydraulically-powered flight controls. It is also typical for general aviation aircraft to have simple systems with fewer and more modern instruments. The large difference in the electrical system weight is probably caused by the large airliner weight equation's use of the number of passengers to size the electrical system. Smaller jets typical serve 8 or fewer passengers and have electrical systems that are driven by system architecture decisions rather than the number of passengers. Some, but not all, of these differences will remain for the development of small airliners.

FLOPS prediction of the total configuration weight is very good (within 10%) using the GA equations and good (within 18%) using the transport equations. The conclusion from this weight analysis is that the GA weight equations should be used for CJ2+ type aircraft.

Drag Calibration

As stated in the FLOPS Users Manual (reference 10), the aerodynamics module uses a modified version of the EDET (Empirical Drag Estimation Technique, reference 13) program to provide drag polars for performance calculations. Modifications include smoothing of the drag polars, more accurate Reynolds number calculations, and the inclusion of the Sommer and Short T' method (reference 14) for skin friction calculations. Alternatively, drag polars may be input and then scaled with variations in wing area and engine (nacelle) size.

A Cessna flight-test data derived drag polar for the CJ2+ was input in FLOPS to match the mission, as shown previously. That drag polar was also computed by Cessna's FSDRAG routine; the FSDRAG polar matched the actual. The next step was to allow FLOPS to compute the drag. When comparing FLOPS computed drag to FSDRAG, the following observations were made: 1) FLOPS-predicted CD_0 (zero-lift drag) varied 2-60% from Cessna FSDRAG values across major components, and is 91% of FSDRAG total; FLOPS-predicted $\partial CD_i/\partial CL^2$ (induced drag) is closer to an elliptic lift distribution than the Cessna FSDRAG value; and FLOPS-predicted CD_C (compressibility drag) is less than half of Cessna values at the design C_L.

Adjustments can be made to wetted area and or form factor calculations in FLOPS to improve the zero-lift drag analysis. FLOPS also enables the use to tune the span efficiency and resulting induced drag with an input parameter.

Calibration Conclusions for the CJ2+

Cessna data has been used to model the CJ2+ in the Georgia Tech version of FLOPS for the purposes of comparing the results with measured performance data and Cessna's comparable tool MAPS. The exercise provided insight into the similarities and differences between the two tools. Mission profiles were close when climb and descent paths from MAPS were used in FLOPS; there was more variation in the descent path. Overall mission fuel burned predictions were very close when using actual drag polars and aircraft weights.

Results from NASA's Flight Optimization System were compared with data for the Cessna Citation CJ2+ to identify best modeling practices and areas of concern for the development of small airliners. Flight test derived data and Cessna's performance tools that have been tuned to this data enabled a direct comparison of mission performance. The Flops mission analysis agreed with actual data within 2% for both range and fuel burn. FLOPS estimates for field length were also in excellent agreement with actual aircraft performance. FLOPS predictions for drag and some component weights remain areas of concern for modeling of small airliners.

Having confirmed that the tool sets used were appropriate and can be calibrated for this size of aircraft, the next step was to develop a notional, current technology baseline aircraft. This aircraft was used to benchmark the NASA goals in current day. The design goals for the aircraft were derived from the conclusions of the network studies.

References

1. "FLOPS," Cessna Aircraft Company, Wichita, KS, August 2008, Revision E.
2. Torenbeek, Egbert, "Synthesis of Subsonic Airplane Design," Delft University Press, Martinus Nijhoff Publishers, Copyright, 1982.
3. Shevell, Richard S., "Fundamentals of Flight," Prentice Hall, Englewood Cliffs, New Jersey 07632, Copyright, 1989.
4. "Citation CJ2+ Specification and Description (Units 525A-0439 to 525A-TBD)," Cessna Aircraft Company, Wichita, KS, August 2008, Revision E.
5. "Operating Manual Citation CJ2, Original Revision, Serial 525A-0001 and On," Cessna Aircraft Company, Wichita, Ks., November 2000.
6. "Airplane Flight Manual Citation CJ2, Revision 6, Airplanes 525A-001 through -0299," Cessna Aircraft Company, Wichita, Ks., June 2000.
7. Anderson, John D., Jr.: Aircraft Performance and Design, WCB/McGraw-Hill, 1999, pp. 221-226.
8. Ensign, Thomas: Sensitivity Studies of Electric Systems on Business Jet Range, AIAA Paper 2008-147, presented at the 46th AIAA Aerospace Sciences Meeting and Exhibit, 7-10 January 2008, Reno, Nevada.
9. Ensign, Thomas, Levy, David, and Gallman, John W.: Suggested Configurations and Technologies, Cessna Work Element 2.3, NASA N+3 Contract, September 12, 2009.
10. McCullers, Linwood A.: Flight Optimization System (FLOPS) Release 6.12 User's Guide. October 2004.
11. McCullers, Linwood A.: Flight Optimization System (FLOPS) Release 7.40 User's Guide. August 2008.
12. Beltramo, Michael N.; Trapp, Donald L.; Kimoto, Bruce W.; and Marsh, Daniel P.: Parametric Study of Transport Aircraft Systems Cost and Weight. NASA CR 151970, April 1977.
13. Feagin, Richard C. and Morrison, William D., Jr.: Delta Method, An Empirical Drag Buildup Technique. NASA CR-151971, December 1978.
14. Sommer, Simon C. and Short, Barbara J.: Free-Flight Measurements of Turbulent-Boundary-Layer Skin Friction in the Presence of Severe Aerodynamic Heating at Mach Numbers from 2.8 to 7.0. NACA TN-3391, 1955.

Appendix B: Configuration and Technology Brainstorming

Appendix B: Configuration and Technology Brainstorming

A team of Cessna employees met several times in early 2009 to discuss NASA's aggressive goals for 2035 airliners, to brainstorm aircraft configuration concepts, and to assess the ability of these concepts to satisfy one or more of the goals. Introductory discussion emphasized NASA's goals for fuel burn, NOx, Noise, and field length. The team's overall strategy to satisfy these goals with 10-30 passenger airliners on short (1000 nm or less) point-to-point routes was also discussed. Once a thorough list of configuration concepts was developed, the team agreed to categorize the concepts based on engine type, installation philosophy, lifting surface arrangement, and finally by the teams assessment of the potential benefit to one or more of NASA's N+3 goals.

A more comprehensive list of candidate technologies was generated by subject matter experts at The Georgia Institute of Technology and improved upon during the IRMA workshop in the spring of 2009. These brainstorming discussions identified a number of configurations were assessed in more detail at a second team workshop later in 2009. The intent was also to develop unique synergistic relationships between technologies, lifting surface arrangements, and engine installation concepts that would combine to satisfy NASA's N+3 goals. The configurations and technology concepts that were identified and discussed in these meetings are listed below.

Configuration Concepts for Fan or Ducted Fan Engines

1. Twin engine, aft fuselage mount configurations (left & right engines)
    - Conventional T-Tail
    - Tail below engines
    - H-Tail similar to A-10
    - Conventional joined wing
    - High-wing strut-brace with engine/strut-brace integration
    - 3-surface configuration – may facilitate gust load alleviation & ride control
2. Twin engine, wing mount configurations
    - Fuselage mount, but engine over wing or under wing
    - High wing – upper or lower engine mount
    - Lower wing – upper or lower engine mount
    - Upper wing engine mount could include upper surface blowing; lower engine mount could include externally blown flaps
    - Engine/Wing integration concepts could include various tail configurations (canard, conventional, T-tail, 3-surface, or no-tail)
3. Twin engine, aft fuselage mount – upper & lower engines
    - DC-10 plus 727 type installation
    - Lower engine plume shields noise from upper engine
    - Buried engine fuselage concepts could include various tail configurations (canard, conventional, T-tail, 3-surface, or no-tail)
    - Vectored thrust for control – eliminate need for tail
4. Single engine configurations
    - Aft pusher
        - Similar to DC-10 or 727 with conventional or T-tail
        - Could include various wing-tail configurations (canard, conventional, T-tail, 3-surface, V-Tail, or no-tail)
    - Aft engine configurations could use conventional or V-Tail for noise shielding

- o Nose mount concept – needs work on exhaust/fan exit concept
- o Vectored thrust for control – eliminate need for tail

Configuration Concepts for Open Rotor or Turboprop Propulsion Concepts

1. Same configuration as fan concepts (see 1, 2 above), except can't fury an open rotor in fuselage.
2. Nose tractor, and tail pusher concepts typical of modern turboprops
   - Tail pusher configuration may need twin boom/tail arrangement for airframe

Distributed Propulsion Configurations

1. 4 engine concept similar to BAe 146
2. 3 engine concept similar to Boeing 727
3. Distributed propulsion could facilitate powered lift
4. Thoughts on noise & small or many engines
   - Might be easier to shield engines
   - SFC is probably better on larger engines
   - Noise really scales with thrust, so other than structural shielding small engines don't really help

Configurations for NASA's N+3 Goals

1. Noise Goals
   - Aft-Fuselage Twin Fan Engine over H-tail
   - Aft-Fuselage Single Engine over V-Tail
     i. Consider neutrally stable configuration
     ii. Add canard as necessary for control
   - Tube Fuselage with Aft wing & canard
     i. 2 upper surface, but wing trailing edge engines
     ii. Use some wing sweep and trailing wing surfaces for pitch & roll
     iii. Use winglets at tip of swept wing for yaw control
     iv. Could consider flying wing if CG envelope could be managed
2. Fuel Burn, and CO2
   - Conventional wing-tail configuration
     i. Twin aft mount engines
     ii. Twin wing mount engines
   - Tube Fuselage with Aft wing & canard
     i. 2 pusher wing mounted open rotor engines
     ii. Use some wing sweep and trailing wing surfaces for pitch & roll
     iii. Use winglets at tip of swept wing for yaw control
     iv. Could consider flying wing if CG envelope could be managed
3. Field Length
   - Tube Fuselage with single flying wing
     i. High wing with low mount twin engines & blown flap
     ii. Low wing with upper mount engines and upper surface blowing
   - Any of the other configurations with modern large airliner slat + flap high lift systems – this suggests a higher wing loading and lower cruise altitude

4. Cost (Purchase Price * DOC)
    - Conventional T-Tail with twin aft fuselage mount fan engines
    - Conventional T-Tail with twin aft fuselage mount open rotor engines
    - Single engine tractor turboprop or open rotor configuration
        i. High strut-braced wing to reduce wing weight
        ii. Conventional low-wing to provide for landing gear retract
        iii. Single engine pusher turboprop configuration

Downselected Technology Concepts for All Configurations

1. Active or passive laminar flow
2. Composite engine and airframe structure
3. Integration of airframe and systems functions in airframe
    - Wires & wire routing
    - Acoustic treatment
4. 4-D trajectories for mission fuel optimization
5. Chevrons on engine for noise control
6. Seamless nacelle liners
7. More electric aircraft subsystems
8. Airframe shielding for propulsion noise
9. Unstable or neutrally stable concept that enable elimination of tail surface for drag saving
10. Gust load alleviation for lighter weight lifting surface structure
11. Ride control for comfort with light weigh loading aircraft

Appendix C: Regulatory Requirements for Commuter Aircraft

Appendix C: Regulatory Requirements for Commuter Aircraft

The following appendix explores the presently existing federal regulations regarding commuter aircraft. Of particular emphasis is how the rules change depending on cruise altitude and number of passengers. Also included are rules that determine the minimum crew and minimum number of engines.

Transitional requirements for a new scheduled commuter service aircraft have been reviewed to determine the impact of crossing altitude and seating boundaries. The regulatory basis for these conclusions is on the following pages.

Before 1996, commuter operations up to 30 passenger seats fell under Part 135 rules. The proliferation of commuter jets, increased market segment usage, and high accident rates lead to a call for "one level of safety" for all airline operations. As a result, a number of rules were substantially rewritten or outright added. This extensive change is documented in the Federal Register, Vol. 60, No. 244, December 20, 1995, pages 65831-65940.

Among the changes was the creation of Part 119, with new definitions of commuter operation and more specific guidance as to which Part governs a given operation. It should be noted that "Commuter" in the operational sense no longer has any relationship to "Commuter Category" in Part 23 aircraft certification standards.

Since these new rules went into effect in 1996, almost all commuter operations must be conducted under Part 121, the same as larger airline operations. Less stringent safety requirements apply to propeller driven aircraft with 9 or fewer passenger seats (ref. 119.3), which can be operated under Part 135 (ref. 119.21a4). This threshold was considered reasonable and necessary to allow economical air service in very small markets in remote areas where alternative transportation options were limited and even more hazardous.

Air carrier operations with jet aircraft or more than 9 passenger seats must be conducted under Part 121 (ref. 119.21a1 & a2), which strictly prohibits single pilot (ref. 121.385c) and single-engine aircraft (ref. 121.159). For a single-engine single-pilot aircraft with 19 passenger seats to operate under Part 121, these basic rules will need to be waived. With no historical precedent to do so, it is unlikely such a path is feasible.

At least one flight attendant is required if payload exceeds 7500 or passenger seats exceed 19, resulting in a weight and space penalty. Assuming a folding seat in the vicinity of the main cabin door the space penalty is small and the weight penalty is about 220# (200# required crewmember weight and 20# for seat).

Also, if passenger capacity exceeds 19 seats:

- Two additional emergency exits of increased size are required
- Access to exits requires more space (seat pitch/longer cabin)
- Lower aisle must be wider (increases barrel diameter)

The exits and improved access will add about 100 lbs.

Thus the 20th passenger seat comes with an additional 320 lb weight penalty, most of which is the weight of an extra crew member and emergency exits. Weight spiral is not included in

this, as the aircraft is larger to accommodate the additional seating, but also needs to be larger to carry this extra weight.

If certified altitude exceeds 25,000 feet, there may be minor weight impacts in some systems and structure for redundancy. Double pane windows would be the most substantial differential, with an estimated weight penalty about 1 pound per passenger crossing 25,000'.

To maintain an equivalent stress level, the pressure vessel weight will increase by 3.5% for every 1000' increase in maximum aircraft/cabin altitude differential. For a 40-seat commuter (estimated 8' diameter x 40' long vessel) of primarily aluminum construction, this is about 20 lb per 1000' feet of altitude increase.

If certified for flight at RVSM altitudes (FL290-FL410), there is a small development penalty to demonstrate compliance, but no weight penalty.

Altitudes above 40,000' (soon to be 45,000') have substantial certification challenges for little benefit on an aircraft with this short mission profile.

All other altitude delineators have essentially no effect, thus any altitude from 25,000 to 40,000 that is within the climb performance limitations of the aircraft should be acceptable. Fuel economy benefits likely justify any weight penalty of going to higher altitudes.

Supporting Regulatory Issues for Commuter Aircraft

Transitional requirements: Part 121/135, Part 23/25, 19 passengers, 25,000' Altitude

Sections of the Federal Aviation Regulations (FARs) are provided in this appendix along with the comments that enable an interpretation for airliners for 2035.

Operational Rules

Part 121 governs Air Carrier operations, while Part 135 governs Air Taxi operations. In general, scheduled airline service falls under 121, while on-demand service is usually 135.

121.9 previously force all operations of aircraft with 30 or less passenger seats and a maximum payload capacity of 7,500 pounds or less to operate under 135 rules. This no longer applies (unknown transition date, but suspect early 1996), and all commuter flights should now be conducted under Part 121.

Aircraft Category requirements:

All Air Carrier (121) operations using new or recent designs must use multi-engine aircraft certified to Part 25 Transport Category standards (recent Part 23 Commuter Category aircraft can *not* operate under 121).

121.157 Aircraft certification and equipment requirements.

(h) Newly type certificated airplanes. No person may operate under this part an airplane for which the application for a type certificate is submitted after March 29, 1995, unless the airplane is type certificated under part 25 of this chapter.

121.159 Single-engine airplanes prohibited.

No certificate holder may operate a single-engine airplane under this part.

Minimum Flight Crew:

Minimum 2 pilots, unless <10 passenger seats AND operating under 135.

121.385(c) The minimum pilot crew is two pilots and the certificate holder shall designate one pilot as pilot in command and the other second in command.

135.99(b) No certificate holder may operate an aircraft without a second in command if that aircraft has a passenger seating configuration, excluding any pilot seat, of ten seats or more.

Flight Attendants:

Minimum 1 flight attendant if:
>7,500# payload AND 10-50 passenger seats (121 ops),
≤7,500# payload AND 20-50 passenger seats (121 ops), OR
>19 passenger seats (135 ops)

121.391 Flight Attendants.

(a) Each certificate holder shall provide at least the following flight attendants on each passenger-carrying airplane used:

(1) For airplanes having a maximum payload capacity of more than 7,500 pounds and having a seating capacity of more than 9 but less than 51 passengers--one flight attendant.

(2) For airplanes having a maximum payload capacity of 7,500 pounds or less and having a seating capacity of more than 19 but less than 51 passengers--one flight attendant.

135.107 Flight attendant crewmember requirement.

No certificate holder may operate an aircraft that has a passenger seating configuration, excluding any pilot seat, of more than 19 unless there is a flight attendant crewmember on board the aircraft.

NOTE: 121.391(a)(1) did NOT have the 7500# weight limit when 121.9 was in effect, forcing 135 ops.

Regulatory Requirements by Seating Capacity

Only 2 Emergency Exits required for <20 passenger seats. 4 Exits, some larger, required for >19 passenger seats, with even larger exits required >40 seats (and then additional exits >110 seats, which is beyond the scope of this analysis).

Access to exits must be fully unobstructed for >19 seats; minor obstructions may be allowed for <20 seats.

Lower portion of aisle may be 3” narrower with <20 seats.

25.807 Emergency exits.

(g)(3) For a passenger seating configuration of 10 to 19 seats, there must be at least one Type III or larger exit in each side of the fuselage.
(4) For a passenger seating configuration of 20 to 40 seats, there must be at least two exits, one of which must be a Type II or larger exit, in each side of the fuselage.

25.813 Emergency exit access.

(2) In addition to the access—

(i) For airplanes that have a passenger seating configuration of 20 or more, the projected opening of the exit provided must not be obstructed and there must be no interference in opening the exit by seats, berths, or other protrusions (including any seatback in the most adverse position) for a distance from that exit not less than the width of the narrowest passenger seat installed on the airplane.
(ii) For airplanes that have a passenger seating configuration of 19 or fewer, there may be minor obstructions in this region, if there are compensating factors to maintain the effectiveness of the exit.

25.815 Width of aisle.

The passenger aisle width at any point between seats must equal or exceed the values in the following table:

Passenger seating capacity	Minimum passenger aisle width (inches)	
	Less than 25 inches from floor	25 inches and more from floor
10 or less----------	[1]12	15
11 through 19----------	12	20
20 or more----------	15	20

Regulatory Requirements by Altitude

For Certification above 25,000', have additional requirements:

Slightly more stringent Vibration and Buffeting analysis.

More stringent pressurization requirements:

Higher system redundancy

Higher structural redundancy (dual-pane windows)

Time-history exposure limits for occupants

More comprehensive failure analysis

More stringent oxygen system requirements

Oxygen dispensing must be located at the occupants

Diluter or pressure masks for flight crews

For Operation above 25,000' additional crew training for high altitude physiology.

For Operation at FL290-FL410 Reduced Vertical Separation Minimum airspace, crew and aircraft must meet additional RVSM requirements and approvals.

For Certification above 30,000':

Oxygen dispensing units must automatically deploy when needed

For Certification above 34,000':

Pressure mask with diluter regulator for flight crew.

For Operation above FL350: >1 pilot wears oxygen mask, unless quick-donning masks available and >1 pilot at the controls

For Certification above 40,000':

Can not allow cabin altitude to exceed 40,000' for any length of time

Note: In work to raise this requirement to 45,000'

For Operation above FL410: >1 pilot wears oxygen mask

Sec. 25.251 Vibration and buffeting.

(e) For an airplane with MD greater than .6 or with a maximum operating altitude greater than 25,000 feet, the positive maneuvering load factors at which the onset of perceptible buffeting occurs must be determined with the airplane in the cruise configuration for the ranges of airspeed or Mach number, weight, and altitude for which the airplane is to be certificated. The envelopes of load factor, speed, altitude, and weight must provide a sufficient range of speeds and load factors for normal operations. Probable inadvertent excursions beyond the boundaries of the buffet onset envelopes may not result in unsafe conditions.

25.841 Pressurized cabins.

(a) Pressurized cabins and compartments to be occupied must be equipped to provide a cabin pressure altitude of not more than 8,000 feet at the maximum operating altitude of the airplane under normal operating conditions.

(1) If certification for operation above 25,000 feet is requested, the airplane must be designed so that occupants will not be exposed to cabin pressure altitudes in excess of 15,000 feet after any probable failure condition in the pressurization system.
(2) The airplane must be designed so that occupants will not be exposed to a cabin pressure altitude that exceeds the following after decompression from any failure condition not shown to be extremely improbable:

(i) Twenty-five thousand (25,000) feet for more than 2 minutes; or

(ii) Forty thousand (40,000) feet for any duration.

(3) Fuselage structure, engine and system failures are to be considered in evaluating the cabin decompression.

25.1447 Equipment standards for oxygen dispensing units.

(b) If certification for operation up to and including 25,000 feet is requested, an oxygen supply terminal and unit of oxygen dispensing equipment for the immediate use of oxygen by each crewmember must be within easy reach of that crewmember. For any other occupants, the supply terminals and dispensing equipment must be located to allow the use of oxygen as required by the operating rules in this chapter.

(c) If certification for operation above 25,000 feet is requested, there must be oxygen dispensing equipment meeting the following requirements:
(1) There must be an oxygen dispensing unit connected to oxygen supply terminals immediately available to each occupant wherever seated, and at least two oxygen dispensing units connected to oxygen terminals in each lavatory. The total number of dispensing units and outlets in the cabin must exceed the number of seats by at least 10 percent. The extra units must be as uniformly distributed throughout the cabin as practicable. If certification for operation above 30,000 feet is requested, the dispensing units providing the required oxygen flow must be automatically presented to the occupants before the cabin pressure altitude exceeds 15,000 feet. The crew must be provided with a manual means of making the dispensing units immediately available in the event of failure of the automatic system.

(2) Each flight crewmember on flight deck duty must be provided with a quick-donning type oxygen dispensing unit connected to an oxygen supply terminal. This dispensing unit must be immediately available to the flight crewmember when seated at his station, and installed so that it:

(i) Can be placed on the face from its ready position, properly secured, sealed, and supplying oxygen upon demand, with one hand, within five seconds and without disturbing eyeglasses or causing delay in proceeding with emergency duties; and

(ii) Allows, while in place, the performance of normal communication functions.

(3) The oxygen dispensing equipment for the flight crewmembers must be:

(i) The diluter demand or pressure demand (pressure demand mask with a diluter demand pressure breathing regulator) type, or other approved oxygen equipment shown to provide the same degree of protection, for airplanes to be operated above 25,000 feet.

(ii) The pressure demand (pressure demand mask with a diluter demand pressure breathing regulator) type with mask-mounted regulator, or other approved oxygen equipment shown to provide the same degree of protection, for airplanes operated at altitudes where decompressions that are not extremely improbable may expose the flight crew to cabin pressure altitudes in excess of 34,000 feet.

(4) Portable oxygen equipment must be immediately available for each cabin attendant. The portable oxygen equipment must have the oxygen dispensing unit connected to the portable oxygen supply.

121.417 Crewmember emergency training.

(e) Crewmembers who serve in operations above 25,000 feet must receive instruction in the following:

(1) Respiration.

(2) Hypoxia.

(3) Duration of consciousness without supplemental oxygen at altitude.

(4) Gas expansion.

(5) Gas bubble formation.

(6) Physical phenomena and incidents of decompression.

91.211 Supplemental oxygen.

(ii) At flight altitudes above flight level 350 unless one pilot at the controls of the airplane is wearing and using an oxygen mask that is secured and sealed and that either supplies oxygen at all times or automatically supplies oxygen whenever the cabin pressure altitude of the airplane exceeds 14,000 feet (MSL), except that the one pilot need not wear and use an oxygen mask while at or below flight level 410 if there are two pilots at the controls and each pilot has a quick-donning type of oxygen mask that can be placed on the face with one hand from the ready position within 5 seconds, supplying oxygen and properly secured and sealed.

(2) Notwithstanding paragraph (b)(1)(ii) of this section, if for any reason at any time it is necessary for one pilot to leave the controls of the aircraft when operating at flight altitudes above flight level 350, the remaining pilot at the controls shall put on and use an oxygen mask until the other pilot has returned to that crewmember's station.

G91.1 Section 1. Definitions.

Reduced Vertical Separation Minimum (RVSM) Airspace. Within RVSM airspace, air traffic control (ATC) separates aircraft by a minimum of 1,000 feet vertically between flight level (FL) 290 and FL 410 inclusive. RVSM airspace is special qualification airspace; the operator and the aircraft used by the operator must be approved by the Administrator.

Appendix D: Considerations for Arrangement of Wing and Tail Surfaces

Appendix D: Considerations for Arrangement of Wing and Tail Surfaces

Nomenclature

d	=	differential of [the parameter that follows]
ℓ_h	=	Distance from center of gravity to horizontal tail
ℓ_W	=	Distance from center of gravity to wing
L	=	Aircraft lift force (in pitch axis considerations)
=		Aircraft rolling moment (in roll axis considerations)
L_h	=	Horizontal tail lift force
L_w	=	Wing lift force
M	=	Aircraft pitching moment
M_o	=	Pitching moment of an aerodynamic surface (wing)
N	=	Aircraft yawing moment
S_h	=	Horizontal tail area
S_{hl}	=	Portion of the horizontal tail area that lifts
S_{hs}	=	Portion of the horizontal tail area that stabilizes
S_w	=	Wing area
W	=	Aircraft weight
α	=	Angle of Attack
β	=	Angle of sideslip
δ_a	=	Angular aileron deflection
δ_e	=	Angular elevation deflection
δ_r	=	Angular rudder deflection
Δ	=	Change in [the parameter that follows]
Φ	=	Angle of roll

Introduction

In the history of aviation, a wide variety of aircraft configurations has been proposed. Several configuration types have been built and tested. However, the vast majority of aircraft designs that have proven successful for their builders and operators may be described as a "traditional" configuration, that is, with one or more lifting surfaces near the center of gravity of the aircraft, and tail assembly consisting of a horizontal and vertical surface, mounted a considerable distance aft of the center of gravity. These tail surfaces are non-lifting, in that they do not contribute to supporting the airborne aircraft, and may, in some cases, provide a downward force.

The search for untraditional or "advanced" configurations is as old as aviation itself. Greater efficiency, through a superior configuration (or any other means) implies greater performance for the dollar, and an aircraft product that is more profitable to the builder and owner. This has driven an ever-increasing state-of-the-art, as attested by a comparison of the Wright Flyer and the space shuttle. The Flyer's first flight lasted 12 seconds, with a range of 120 feet, and a ground speed of just over walking speed, while the space shuttle has stayed aloft for over a week, covering millions of miles, and re-entering the Earth's atmosphere at over 25 times the speed of sound. It is interesting to note that both of these aircraft may be categorized as

advanced configurations. The Flyer is a relaxed stability (in fact, unstable) canard configuration. The space shuttle is a lifting body, in which the fuselage provides the significant portion of lifting force, and the "wings" provide the remainder of the necessary lift, along with pitch-stabilizing moments of a non-lifting, horizontal tail.

Because of today's unprecedented cost of aviation fuel and environmental concerns of burning such fuel, contemporary interest in aircraft efficiency and, in turn, advanced configurations has redoubled. In particular, questions have arisen regarding the most efficient configuration of lifting and stabilizing surfaces. A thoughtful person might conclude that *some* of the proposed advanced configurations do not meet all the functional requirements of a lifting surface and tail combination, and therefore are not a practical avenue toward reduced fuel consumption. In this report, the basic requirements of lifting and tail surfaces are discussed, in order to allow the reader to differentiate which configurations have the potential to burn less fuel and cause less stress to the environment.

Lift and Pitch Stability

The function of an aircraft configuration may be evaluated in three axes: pitch, yaw, and roll..[1] Each of the three axes requires a balance of forces and moments, plus some method to provide controllability in that axis. The pitch axis is the most complicated in that it also must generate a lifting force equal to the weight of the aircraft. Since lift generation usually implies the considerable profile and induced drag of a wing, the pitch axis of an advanced configuration is the most critical to efficiency, and generally receives the most attention. In this report the pitch axis is considered first, followed by a brief and simpler treatment of yaw and roll axes.

Table 1 shows four simple requirements of the pitch axis of an aircraft configuration. Requirement 1) is a balance of forces in the vertical direction, which indicates that a lifting force must be generated, equal to the weight of the aircraft (but opposite in direction). Requirement 2) indicates that the total moments in the pitch axis must sum to zero. Requirement 3) suggests that the derivative of pitching moment to angle of attack should be negative, which is to say that a configuration should acquire a negative pitching moment opposite in direction to a change in angle of attack. Requirement 4) indicates that the moment balance in Requirement 2) should be altered by a deflecting the elevator surface from some neutral position. These requirements use a sign convention that angle of attack and moments are positive in the nose up direction, and elevator deflection is positive in the trailing edge down direction. These rules and sign conventions are derived from Reference 1. The requirements in Table 106 should be familiar to anyone involved in aircraft preliminary design. However, the implications and application of these rules might be surprising to some.

Table 106. Pitch Axis Requirements

1)	$L = W$	(Lift)
2)	$M = 0$	(Trim)
3)	$\frac{dM}{d\alpha} < 0$	(Stability)
4)	$\frac{dM}{d\delta_e} < 0$	(Controllability)

It should be kept in mind that the rules in Table 106 apply to a configuration with any number of surfaces that extend horizontally. Therefore, L and M are understood to indicate the *total contribution* of all surfaces to lift and pitching moment. Further, these rules are understood to apply to straight and level cruise conditions for an aircraft, and are not strictly correct for climbing, descending, pitching, or turning flight. In this report, the implications of Requirements 1) through 3) will be considered first, which indicate the ability of an aircraft to cruise in an acceptable manner. Following this, the additional controllability necessary to perform maneuvering (climbing, descending, pitching, or turning) flight will be considered by examining Requirement 4).

It is usually assumed that the forces and moments in Table 106 are generated with one or more wings, and one or more horizontal tails, each with fixed positions on the aircraft, and an elevator that is controllable in pitch. It is *imperative* that all the forces and moments in Table 106 exist as shown, but they need not be generated by aerodynamic surfaces. For example, in Requirement 1), instead of using a wing, lift may be generated by a rotor (as in a helicopter) or by a jet or rocket engine blasting downward (AV-8 Harrier in hover flight). Controllability and trim (Requirements 4) and 2)) may be achieved by relocating weight within the aircraft, such as fuel (B-1, Concorde).

In cases where aerodynamic stability (Requirement 3) of a configuration is inadequate, stability can be enhanced with a horizontal stabilizer that moves in response to angle of attack (F-16), or by vectoring engine thrust upward or downward as proposed for several future fighter aircraft concepts. Theoretically, stability could also be enhanced by transfer of fuel within the aircraft. For any of these schemes to be effective, the generated force must be a distance from the aircraft center of gravity, and must be modulated faster than the aircraft is capable of pitching. Furthermore, the force must *always be available* in flight, which might not be the case if there is a flight control system failure, the engines were idled, or if all fuel in the aircraft is burned. Since this report is concerned with advanced configurations and their effect on aircraft efficiency, it is assumed that the forces and moments in Table 106 are developed with fixed wings and horizontal tail surfaces, but keeping in mind that there are alternatives to achieving these forces and moments.

Requirements 1) through 3), Lift, Trim, and Stability

When considering advanced configurations for aircraft, a natural choice is to have all surfaces provide the same lift per area (or, the same lift coefficient). A sketch of this architecture is shown in Figure 211. The lift forces, L_w and L_h, are placed at the center of pressure of their respective surface. For ease of understanding, this diagram is labeled as a familiar, traditional configuration, but can, in fact, represent all configurations. For example, Figure 211 represents a canard if the horizontal tail area (S_h) is greater than the wing area (S_w). Multiple wings (or horizontal tails) may lumped together to provide the effect of one wing (or horizontal tail) in the figure. Tail area or tail arm (ℓ_h) may be reduced to near zero to represent a flying wing configuration.

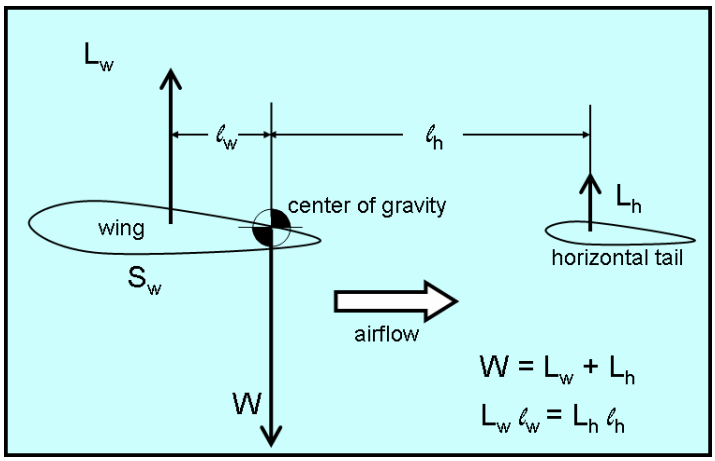

Figure 211. A Neutrally Stable Configuration

It may be shown that Requirement 1) is met in Figure 211 if $L_w + L_h = W$. Similarly, Requirement 2) is met if the center of gravity is placed such that $L_w \ell_w = L_h \ell_h$. However, if the lift curve slopes of the wing and horizontal tail[2] are equal, then it can be shown that for a change of angle of attack, $\Delta L_w \ell_w = \Delta L_h \ell_h$, and the pitching moment from the horizontal and wing exactly counter each other. Hence, $dM/d_\alpha = 0$, Requirement 3) is unmet, and the aircraft is neutrally stable in the pitch axis.

[2] A configuration may be stabilized by forcing the lift curve slope of the lifting surface to be much less than that of the horizontal tail. This generally forces the lifting surface to be of very low aspect ratio and efficiency. Such is the case with the space shuttle, in which part of the lift is generated by the fuselage, with an aspect ratio of much less than one. However, the space shuttle lift-drag ratio of about three (compared to about fifteen for a typical airliner) suggests that this does not improve configuration efficiency.

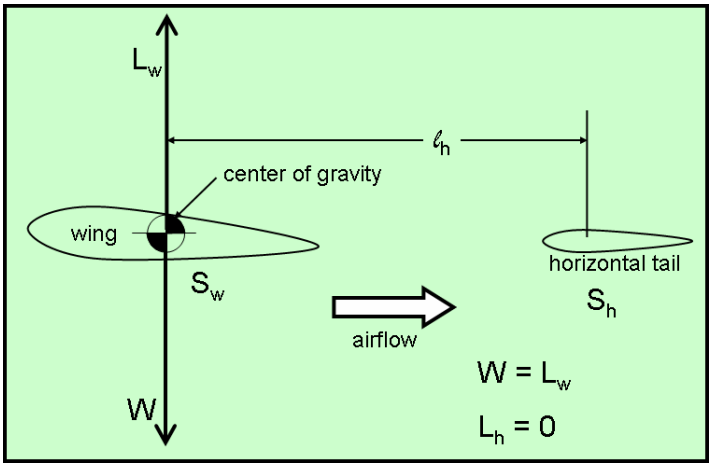

Figure 212. A Traditional Configuration that Meets Requirements 1) through 3).

The neutral stability in Figure 211 can be remedied if the horizontal tail *contributes* to the pitching moment of the aircraft, but *does not contribute to lifting the aircraft*. A diagram of this architecture is shown in Figure 212. Requirement 1) is met when $L_h = 0$ if $L_w = W$, and Requirement 2) is met if the center of gravity is placed at the center of pressure of the wing. It may be shown that for a positive increase in angle of attack, the change in pitching moment is proportional to $- S_h \ell_h$, giving $dM/d_\alpha < 0$, and Requirement 3) is met. Clearly, this configuration is stable, and the degree to which it is stable depends on the magnitude of S_h and ℓ_h.

It should be recognized that the horizontal tail lift need not be zero for Requirements 1) through 3) to be met. If the horizontal tail lifts some, but less than the wing (on an area basis), it may be thought of as two separate surfaces: one lifting with the same lift coefficient as the wing, and the other with zero lift. The lifting portion of the horizontal may be added to that of the wing, producing a position for net lift and center of gravity somewhere between the centers of pressure of the wing and horizontal tail as shown in Figure 213. Notice in Figure 213 that stability is decreased since ℓ_h is now shorter, the wing contributes a destabilizing moment as L_w changes. Figure 213 becomes a canard if wing is much smaller than the horizontal tail, the destabilizing moment arm ℓ_w becomes large, the stabilizing arm ℓ_h becomes small, and the center of gravity is located about midway between the surfaces.

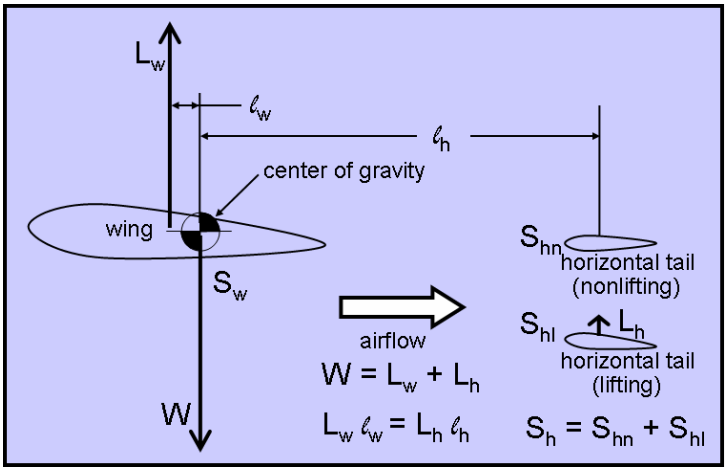

Figure 213. A Configuration with Low, but Positive Horizontal Tail Lift

This loss of stability in Figure 213 may be countered with greater horizontal tail area, S_h, but with an increase in tail weight and drag. Similarly, stability can be enhanced, or horizontal tail area decreased if the tail has a download. Hence, a reasonable downward force on the horizontal tail reduces tail area (for the same level of stability). A special case of this is considered in the next paragraph.

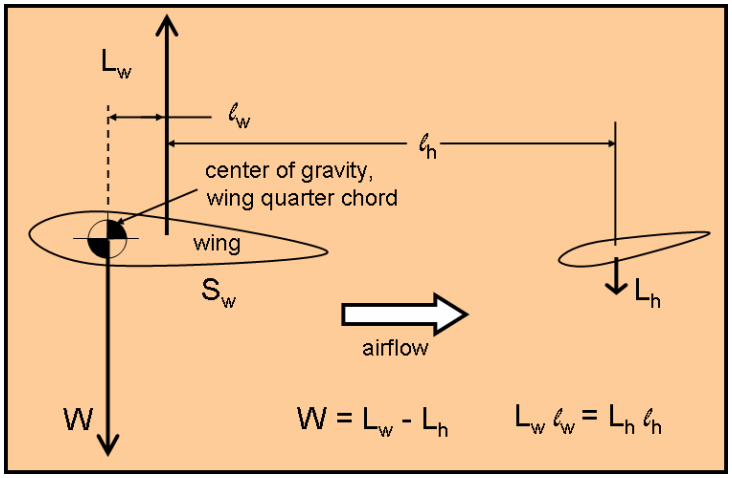

Figure 214. A Configuration with the Center of Gravity at the Wing Quarter Chord

For real aircraft, the center of gravity of the aircraft is never *exactly* at the center of pressure of the wing, and is usually forward of the center of pressure, somewhere near the quarter chord of the wing. In this case, Figure 212 would change to look like Figure 214. For Requirement 2) to be met, the horizontal tail would have a negative (downward) lift, which counteracts the moment between the lift and weight. This configuration is more stable (for the same size tail) than Figure 212 since the moment arm for the tail is increased to ($\ell_w + \ell_h$), and because the wing contributes a stabilizing moment.

In Figure 211 through Figure 214, no mention was made of pitching moment generated by wing and horizontal tail airfoils. This is because the lift forces were placed at the *centers of pressure* of the airfoils. It may be recalled from basic aerodynamics that the center of pressure

for an airfoil is the point around which the aerodynamics is manifest as a single force (*with no moment*). For symmetric airfoils, the center of pressure is at or near the quarter chord, but for modern, cambered airfoils, the center of pressure is at a point somewhere aft of the quarter chord. Since this point moves with angle of attack and Mach number, analysis is simplified if the aerodynamic force is moved to the quarter-chord of the airfoil, and a resulting pitching moment is included, which is zero for symmetric airfoils, and a constant, negative moment coefficient for most cambered airfoils. This is shown in Figure 215. Traditionally, no moment is shown for the horizontal tail. Most horizontal tails have a symmetric airfoil, and hence, L_h is not moved and does not cause a moment. However, if a cambered airfoil is used, the moment exists, but is small compared to that of the wing, and is usually neglected. Notice that ℓ_h and ℓ_h' are not equal, but this difference is generally neglected, as well. It should be kept in mind that airfoil pitching moment is not a reality, but rather, an artifact of placing aerodynamic forces and weight at the quarter chord.

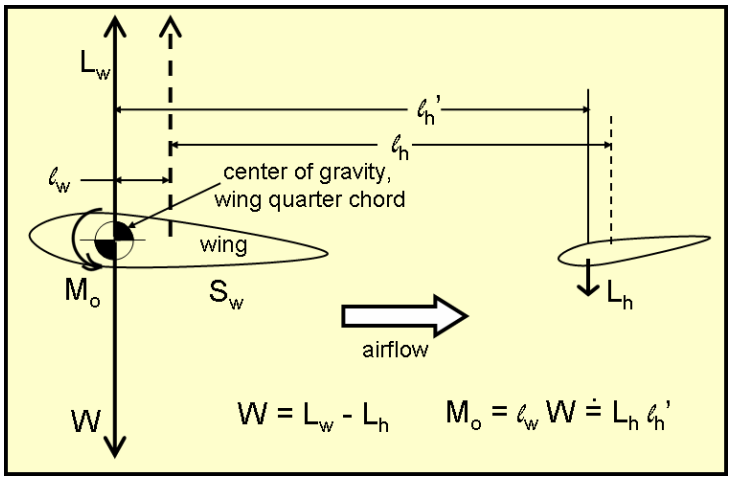

Figure 215. A Traditional Configuration

Like Figure 211, Figure 215 represents all configurations, since the aerodynamic surfaces of any configuration may be lumped together to produce one lifting (wing), and one stabilizing (*or non-lifting*) surface. Requirement 1) is always met if the total lift is equal the total weight. Requirement 2) is met if the center of gravity is placed such that all moments add to zero. And Requirement 3) is met if there is some portion of the horizontal tail has no lift, other than to counteract airfoil pitching moment. From this discussion it may be concluded that for all configurations with fixed aerodynamic surfaces that meet Requirements 1) through 3) of Table 106, *there must be some horizontal area, some distance aft of the aircraft center of gravity, that contributes to pitching moment, but not to lift*.

Many attempts have been made to get around having non-lifting, or stabilizing area on the aft part of the aircraft. In many cases, some (or all) of the lifting area is combined with the non-lifting area, on one aerodynamic surface. As a unit, the surface is actually lifting, but it nevertheless has additional area that serves a stabilizing function, making the surface *lift less* than if stability was not an issue. An example of this is a flying wing with little or no sweep. With symmetric airfoil sections, the aircraft can be no more than neutrally stable. A reflexed trailing edge is added to provide stability (an aft-positioned, non-lifting area) and also to account for the pitching moment of cambered airfoil sections. Similarly, highly swept flying wing or tailless aircraft may use wing twist to wash out all lift on the wing tips, which extend toward the aft end of the aircraft. Canard aircraft (that are stable) have a significantly higher wing loading

on the canard than the main wing, indicating that a portion of the main wing is non-lifting. Figure 216 shows a variety of aircraft configurations. Marked in red is the portion of the aerodynamic surfaces that may be asserted to be non-lifting. As a side comment, Figure 216 suggests that when analyzing advanced configurations, failing to consider the portion of a "wing" that is non-lifting can lead to serious miscalculations in effective wing area and aspect ratio.

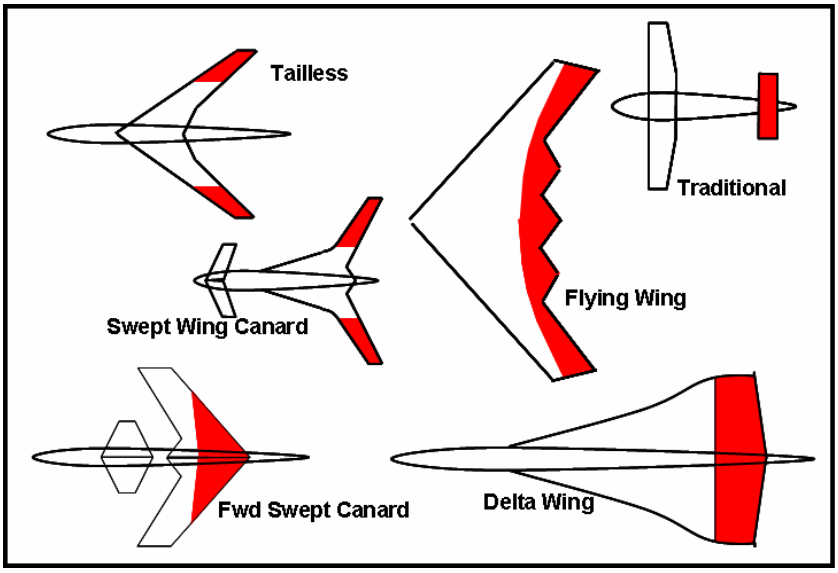

Figure 216. Differing Aircraft Configurations and their Non-lifting Areas

It is insightful to recall that the stabilizing moment produced by a non-lifting surface is proportional to the product of the non-lifting area and the distance between the center of gravity and the center of pressure of the non-lifting surface. Within reasonable limits, the amount of non-lifting area (and hence, its profile drag and weight) can be minimized by placing it as far aft of the lifting surface as possible. Looking at Figure 216, centers of pressure may be imagined for the combined lifting surfaces and combined non-lifting surfaces. Doing so suggests that some advanced configurations place the lifting and non-lifting surfaces very close together, and therefore may not optimize surface area or profile drag. Furthermore, the discussion regarding Figure 213 suggests that non-lifting area might be further reduced with a reasonable download (in addition to airfoil pitching moment). The ideas in this paragraph do not indicate that, for example, the Concorde or B-2 would fulfill their missions better with a traditional configuration. Rather, this paragraph suggests that efficiency is compromised to attain extremely high speed (in the case of the Concorde) or low observability (B-2). At first glace these configurations appear to be synergistic, but are not optimal for aircraft that are designed for more ordinary utilization and high efficiency.

Some outtakes from this discussion follow:

- There must be some horizontal area, some distance aft of the aircraft center of gravity, which contributes to pitching moment, but not to lift.
- Farther aft placement (within reason) of this nonlifting area allows it to be smaller (with less drag and weight).
- Greater download (within reason) on this surface also allows it to be smaller (with less drag and weight).

Requirement 4), Controllability

To this point, the implications of Requirements 1) through 3) have been discussed. Fulfilling these requirements provides an aircraft that flies properly at a single flight condition. Of course, aircraft are required to fly properly at a wide variety of conditions, hence the need for Requirement 4), controllability. Table 106 does not state the required level of controllability (that is, the magnitude of $dM/d\delta_e$). Several considerations for pitch axis controllability are listed below:

❶ Pitch maneuverability (momentary excursions from L = W and/or M = 0). (Includes takeoff rotation and landing flare.)
❷ Variations in weight and center of gravity position
❸ Variations in flap settings
❹ Variations in speed
❺ Variations in Mach number
❻ The need to counteract turbulence (attempting to maintain L = W amid changes in angle of attack)
❼ Jammed or runaway controls

Many of the variations in the list can (and occasionally do) occur at the same time. During a takeoff, the aircraft may have to compensate for the worst case of ❶ + ❷ + ❸ + ❹ + ❻. Similarly, the aircraft might compensate for the worst case of ❶ + ❷ + ❹ + ❺ + ❻ + ❼ during climb, cruise, and descent, and the worst case of ❶ + ❷ + ❸ + ❹ + ❻ + ❼ during landing. The minimum controllability (Requirement 4)) is the worst case of the takeoff, cruise, and landing cases (each with the sum of the worst case components), while at the same time accomplishing Requirements 1) through 3).

It should be understood that pitch axis controllability involves creating a pitching moment, normally through the deflection of the elevator (or stabilator, canard, or the incidence of the non-lifting surface). This moment can also be provided by other methods, such as pitch thrusters (space shuttle, and AV-8 Harrier), but since this report deals with the merit of configurations, this unpopular and inefficient solution will be overlooked. To the extent that the moment is unopposed, it will cause the aircraft to pitch, which in turn modulates lift and causes a vertical force on the aircraft as well. Creating such a moment requires that the elevator be located some distance from (before or after) the lifting surface. Minimizing the size of the elevator (and its associated drag and weight) suggests that the elevator should be as far as practical from the center of gravity. Placing the elevator a distance in front of the lifting surface destabilizes the aircraft and causes the non-lifting area to increase. Placing the elevator aft of the lifting surface, and in conjunction with the non-lifting area, has two synergistic effects: To the extent that the elevator is not allowed to move with a disturbance in angle of attack, it adds to stability and serves as a portion of the non-lifting area. And, as the elevator is deflected, it will cause aerodynamic forces on the non-lifting surface, allowing the non-lifting area to serve as a portion of the elevator area. Both of these effects tend to reduce surface area (drag and weight). To the outtakes in the previous section, three additional observations may be added:

- The controllability requirement in the pitch axis is a sum of several worst case factors, and is in addition to the requirements for lift, trim, and stability.
- Controllability considerations require a movable surface (elevator) that must be mounted forward or aft of the center of gravity.

- A forward location for an elevator surface has a detrimental effect on aircraft stability, drag, and weight; an aft location has several synergistic effects, especially in conjunction with the nonlifting surface.

Yaw Stability

Requirements for the yaw axis are similar to those of the pitch axis, but much simplified since side forces (analogous to lift and weight, in the pitch axis) do not normally exist during cruise flight. Hence, no vertical surface corresponding to a wing is needed, and there are no requirements similar to Requirement 1) and 2) of Table 106 for this axis. Yaw axis requirements are shown in Table 107.

Table 107. Yaw Axis Requirements

1)	$\frac{dN}{d\beta} < 0$	(Stability)
2)	$\frac{dN}{d\delta_r} < 0$	(Controllability)

Requirement 1) suggests that when an aircraft encounters a change in sideslip angle, it should respond with a yawing moment to counter the sideslip change. As in the pitch axis, such a disturbance might be countered with split ailerons, side facing propellers, jet engines or rockets, or other active force generators, which must be located some distance from the wing center of pressure. But since the value of advanced configurations is under consideration, it is assumed that such a force will be provided by the configuration itself, that is, a fixed, vertical, non-lifting surface. This surface must be located aft of the center of gravity. Within reasonable limits, the area of this surface (as well as weight and drag) is minimized by placing it as far aft as possible. Such is the single yaw axis requirement for an aircraft to cruise at a single condition.

Requirement 2) suggests that the aircraft should have controllability in the yaw axis. This is generally achieved through the use of a movable vertical control surface, or rudder. As in the pitch axis this surface should be a distance from the wing center of pressure, and achieves synergism when used in conjunction with the vertical non-lifting surface. This discussion assumes the sign convention of yawing moments and sideslip angles are positive with the nose to the right, and rudder deflections are positive with the trailing edge to the left.[1] Some conditions affecting the size of the rudder are shown below.

❶ Yaw maneuverability (momentary excursions from side force and/or N = 0)
❷ The need to counteract adverse yaw
❸ Dutch roll damping
❹ Counteracting yawing moments during engine out (on the ground and in flight)
❺ Sideslips, or skidding turns

❻ The need to counteract engine torque and p-factor, for a propeller aircraft
❼ Roll maneuverability, in case of an aileron failure
❽ Jammed or runaway controls

All the above conditions could conceivably occur at the same time, although not all of the conditions apply to all configurations. As in the pitch axis, the control surfaces in the yaw axis should be sized to accommodate all the controllability considerations that apply, while simultaneously maintaining yaw stability. Similar to the elevator in the pitch axis, the rudder must be placed a distance fore of aft of the center of gravity. A forward position reduces stability, while an aft location, in conjunction with the vertical stabilizer, is synergistic. Some outtakes from this discussion follow:

- There must be some vertical area, some distance aft of the aircraft center of gravity, in order to stabilize the aircraft in yaw.
- Farther aft placement (within reason) of this surface allows it to be smaller (with less drag and weight).
- The controllability requirement is a sum of several worst case factors, and is in addition to the requirements for stability.
- Controllability considerations require a movable surface (rudder) that must be mounted forward or aft of the center of gravity.
- A forward location for a rudder surface has a detrimental effect on aircraft stability, drag, and weight; an aft location has several synergistic effects, especially in conjunction with the non-lifting surface.

Roll Stability

Considerations for the roll axis are very similar to those in the yaw axis, in that there are normally no forces and moments to be generated during cruise flight. The roll axis is different in that there is no passive aerodynamic surface that can prevent an aircraft from rolling. For this reason, virtually all aircraft are slightly unstable in roll (with the autopilot deactivated). This is to say that if an aircraft were to encounter a disturbance in roll, its tendency is to continue to roll in the direction of the disturbance. Hence, $dL/d\Phi$ is not a design criterion or a differentiator of configurations.

Table 108. Roll Axis Requirements

1)	$\frac{dL}{d\beta} < 0$	(Stability)
2)	$\frac{dL}{d\delta_a} > 0$	(Controllability)

However, if the aircraft should encounter a disturbance in roll, it is desirable that it should have a tendency to maintain *coordinated flight*, that is, flight in which sideslip angle is zero and the net force on the aircraft (and passengers) is vertical with respect to the aircraft. This is expressed as "dihedral stability", or $dL/d\beta$. If $dL/d\beta$ is negative, then when an aircraft experiences a sideslip it should provide a rolling moment. This property, in combination with other stability considerations, promotes an aircraft whose response to an excursion in roll angle is a coordinated turn (or coordinated spiral) in the direction of the roll angle. Hence, $dL/d\beta < 0$ is the stability parameter in the roll axis, as shown in Table 108. This discussion uses a sign convention of roll angle and rolling moment to the right are positive, sideslip with the nose to the right is positive, and aileron deflections with the right aileron up and the left aileron down are positive.[1]

Dihedral stability can be enhanced through a number of configuration choices: wing and horizontal tail dihedral angle, vertical tail height, wing sweepback, wing position on the fuselage, and others. Dihedral stability generally has little effect on the efficiency of an aircraft, and therefore is usually not a great differentiator of configurations.

As in the other axes, the aircraft must be controllable in roll. As shown in Table 108, roll control is represented by the derivative $dL/d\delta_a$. The degree of controllability is the worst case combination of the items shown below:

❶ Roll maneuverability (momentary excursions from $L = 0$)
❷ The need to produce a sideslip (for example, in a crosswind landing)
❸ Controlling the aircraft for minimum drag during an engine out
❹ The need to counteract a flap asymmetry
❺ Recovery from stalls or spins
❻ The need to counteract the instability in $dL/d\Phi$. (This is evident during a steep turn in which aileron deflection opposite the turn is required to maintain L = 0.)

In order for ailerons (or roll spoilers) to produce a rolling moment, they must be located some distance laterally from the center of gravity. This can become an issue for aircraft with a low wing aspect ratio and a large demand for roll rate. In case of an aileron asymmetry (for example, if one aileron is inoperative), it is desirable for the ailerons to be located near the center of gravity in a fore and aft direction. As with the elevator and rudder, placing the ailerons in conjunction with the wing has some synergistic effects: The aileron can contribute to the area and lifting force of the wing, and the aerodynamic forces generated by a deflected aileron also impinge on the wing, enhancing the rolling moment.

Upward extending winglets on swept wings can magnify the adverse yaw effect of aileron deflection, while downward extending winglets can alleviate adverse yaw. A horizontal aerodynamic surface a short distance above or below an aileron will reduce the effectiveness of an aileron, unless both surfaces have an aileron. This can be pictured by imagining a biplane in which the wings are unusually close together, and only the top wing has ailerons. A downward deflection of an aileron causes a higher pressure area between the wings that pushes upward on the top wing, but downward on the bottom wing, and therefore produces a disappointing roll response. Similarly, an upward deflection causes a low pressure area between the wings, with opposite forces and a similarly disappointing roll response.

Some outtakes from this discussion follow:

- The stability requirement for motion in the roll axis is different than the other two axes. There is no non-lifting surface to achieve stability in roll. Various features can be added to cause the aircraft to respond to a disturbance in roll with a coordinated turn. These features have little effect on the stability of the aircraft.
- The controllability requirement is a sum of several worst case factors.
- Controllability considerations require movable surfaces (ailerons) that must be mounted some distance laterally from the center of gravity, but preferably near the center of gravity in a fore and aft direction.
- Locating the ailerons in conjunction with the wing is synergistic. Other aerodynamic surfaces near the ailerons can affect the stability and controllability of the aircraft.

Recommendations: Tail Sizing for 2035 Airliners

Recent increases in fuel prices and concerns regarding environmental risks have redoubled the search for novel aircraft configurations that promise increased efficiency. Some of these configurations may be lacking in their ability to lift their own weight, to eliminate unwanted moments, and fly with acceptable stability and controllability in three axes. This report provides the basic requirements for stable and controllable flight, with the intention that the reader can sort out for himself which configurations have merit, and which are lacking.

The history of aviation shows that the forces and moments specified as basic requirements may be supplied by relatively simple aerodynamic surfaces, or by more active devices such as reaction control rockets, jet or propeller thrusters, or even by helicopter rotors. In order to differentiate the utility of configurations, it is assumed that all basic requirements are met by aerodynamic forces alone; configurations that do not meet the basic requirements aerodynamically, while not necessarily useless, will achieve controlled and stable flight by providing the same forces and moments in some other (and perhaps, more complicated) way. Some outtakes from this report are as follows:

- In order for a configuration balance weight with lift, without creating an unopposed pitching moment, and while providing stable flight, some horizontal, non-lifting (stabilizing) surface must be located aft of the center of gravity.
- In order for a configuration to be stable in yaw, it must have some vertical, non-lifting (stabilizing) surface located aft of the center of gravity.
- The non-lifting surfaces in the previous outtakes may be minimized in area, weight, and drag if placed as far aft as practical. This generally implies separate surfaces from the lifting surface.
- To achieve control in the pitch and the yaw axes, a horizontal and vertical movable surface is necessary. These surfaces must be placed at a distance ahead of, or behind the center of gravity. Synergism occurs if they are placed aft, in conjunction with the non-lifting surfaces.
- Sizing of non-lifting and control surfaces is a worst case sum of several factors.
- The roll axis has no non-lifting (stabilizing) surface, comparable to those in the pitch and yaw axes. For this reason, roll stability considerations generally have little effect on the viability of an advanced configuration.

- Controllability in the roll axis is achieved with control surfaces which must be located some distance laterally from the center of gravity, but preferably near the center of gravity in the fore and aft direction.
- Synergism occurs if the roll control surfaces are located in conjunction with the lifting surface. Similar to the control surfaces in other axes, these surfaces are sized by a worst case sum of several factors.

References

[1] Roskam, Jan, "Airplane Flight Dynamics and Automatic Flight Controls," Roskam Aviation and Engineering Corporation, 1979.
[2] Anderson, John D., "Introduction to Flight," McGraw-Hill Book Company, 1978.
[3] Keuthe, Arnold M., and Chow, Chuen-Yen, "Foundations of Aerodynamics: Bases of Aerodynamic Design," John Wiley and Sons, 1976.

Appendix E: High-Lift Systems and Optimum Cruise Altitudes

Appendix E: High-Lift Systems and Optimum Cruise Altitudes

Cessna experience indicates that transportation value and utility to the customer is generally enhanced by aircraft with moderate wing loading, relatively short runway requirements, simple flap systems, and high cruise altitudes. These factors are not independent. Short runway capability means access to a much wider variety of convenient, uncongested airports. Moderate wing loading (as compared to typically higher wing loading of airliners) reduces the runway requirements, and at the same time, allows the capability to climb to higher altitudes. Higher cruise altitude means fuel saving for a specified mission length, or greater range for a specified fuel load. In most cases, a complicated flap system is unnecessary; retaining a relatively simple flap system further enhances value and utility through cost and weight reduction, allowing more of the wing internal volume to be devoted to fuel, and decreasing the risk and cost of mechanical problems.

Generally, business jets that have low wing loading and high thrust-to-weight ratio sufficient to takeoff in less than 4000 feet of runway also have low wing loading and high thrust-to-weight ratio sufficient to cruise well above 40,000 feet of altitude. Consider the Citation CJ2+, which takes off in 3360 feet. Figure 217 shows a 1000 nm mission flown in the Citation CJ2+ at a variety of cruise altitudes. Completing the mission at 35,000 feet altitude burns 2735 pounds of fuel, while using 45,000 feet altitude requires only 1933 pounds, a reduction of 30%. These figures include the entire 1000 nm mission, which is to say that the fuel expended, and distance covered during climb and descent are included. Citation CJ2+ cruise speeds vary somewhat with altitude, but a comparison of enroute time suggests that the speed variation is not a significant differentiator.

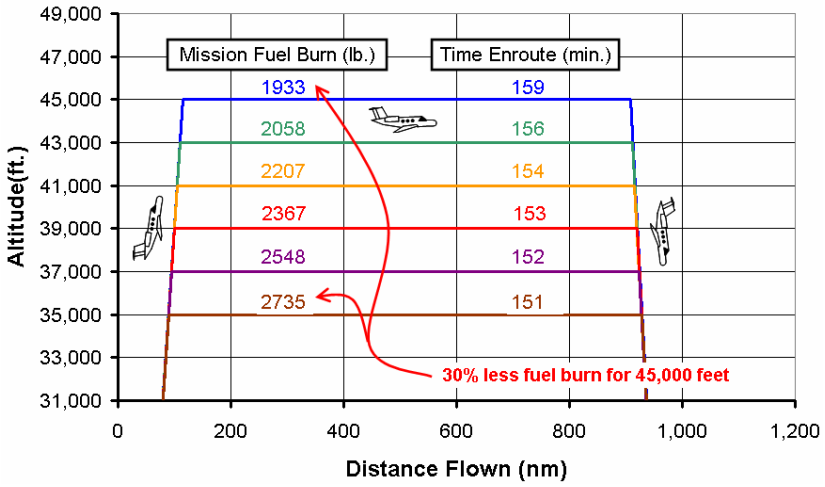

Figure 217. On a 1000 nm Mission, Citation CJ2+ Uses 30% Less Fuel at 45,000 Feet Altitude, Compared to 35,000 Feet Altitude

Figure 218 and Figure 219 are similar to Figure 217, except for 500 nm and 250 nm missions, respectively. Fuel saving is 25% for 500 nm and 17% for 250 nm. These figures suggest that business jets that are designed for relatively short takeoff runway requirements will burn less fuel, or cruise farther, if allowed to cruise at higher altitudes, even for relatively short mission lengths. This matches with Cessna's experience in designing business jets.

It should be kept in mind that the figures are drawn using performance data from the Citation CJ2+, a design which includes systems sophistication and fuselage strength required to cruise at 45,000 feet. If the CJ2+ were designed for a lower certified ceiling altitude, the additional fuel burn in the figures might be reduced slightly by lighter, simpler pressurization and oxygen systems, and perhaps a thinner skin gage on the pressurized portion of the fuselage. It is believed that the effect of this change to the figures would be small or insignificant.

It is possible that there are disadvantages to choosing a certified altitude that is too high. As mentioned in the previous paragraph, higher altitudes can cause an increase in systems and structural weight. Additionally, certification standards become incrementally more stringent at a several altitudes, and most notably at 45,000 feet. This might make additional altitude capability prohibitive from a cost or complexity perspective. Also, certifying to an altitude above the service ceiling of the aircraft has little value.

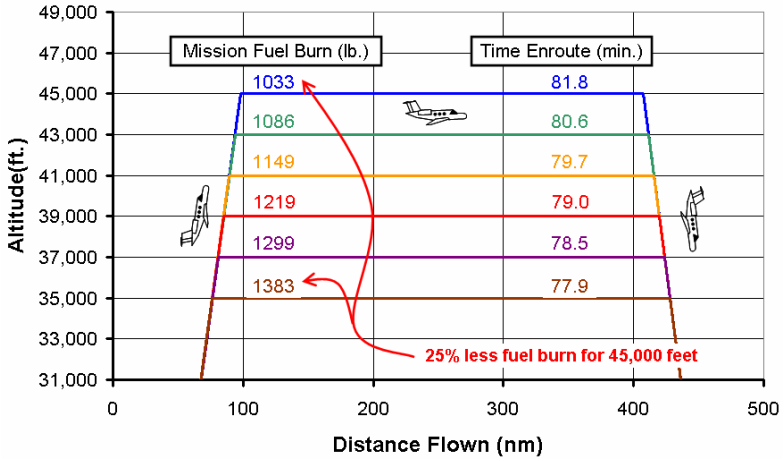

Figure 218. On a 500 nm Mission, Citation CJ2+ Uses 25% Less Fuel at 45,000 Feet Altitude, Compared to 35,000 Feet Altitude

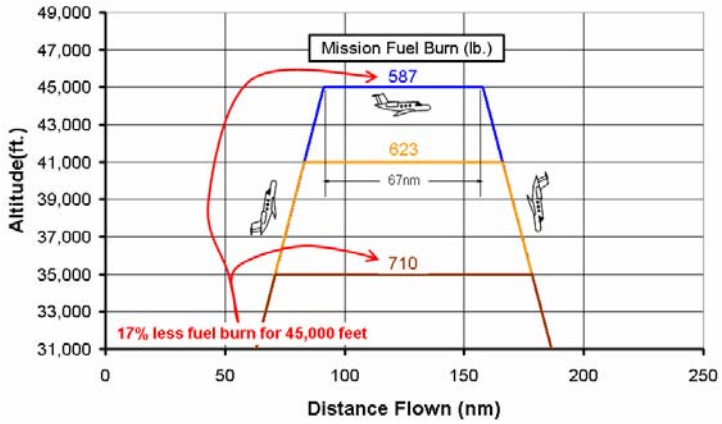

Figure 219. On a 250 nm Mission, Citation CJ2+ Uses 17% Less Fuel at 45,000 Feet Altitude, Compared to 35,000 Feet Altitude

Since the N+3 study includes advanced engines, such as high bypass turbofans, open rotors, and turboprops, the question as been raised as to whether aircraft with these engines also benefit from higher altitudes. In terms of bypass ratio, turboprops represent the opposite end of the spectrum from today's business jet engines. It is desired to replicate Figure 217 through Figure 219 for pressurized business turboprops, but insufficient data is available. However, specific range (nautical miles flown per pound of fuel burned) may be computed from the operating manuals for the Pilatus PC12, the Cessna 425, and Cessna 441. This data is shown in Figure 220. Two lines are shown for each aircraft, the upper line representing cruise at best range airspeed, and the lower representing high speed cruise. The rightmost data for each aircraft represents the certified ceiling for that aircraft. In all cases, the specific range shows an increasing trend up to the certified ceiling, suggesting that turbine powered business aircraft, regardless of bypass ratio, can cruise more efficiently at higher altitudes.

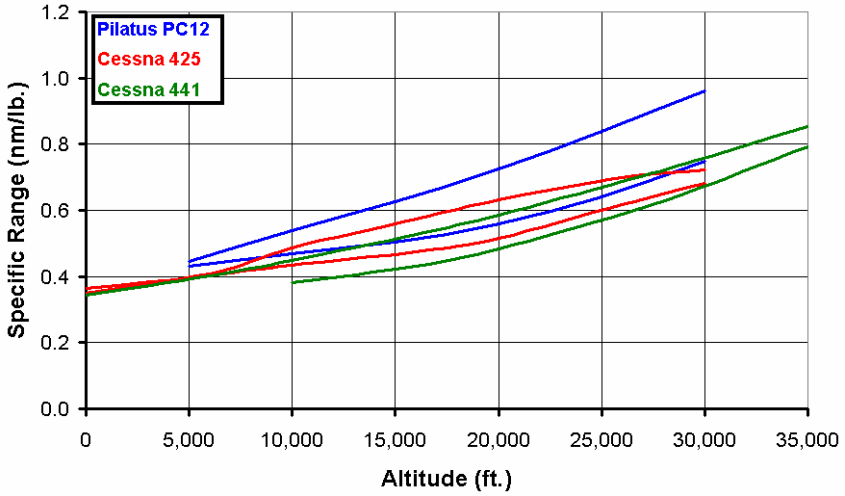

Figure 220. Specific Range of Three Pressurized Business Turboprop Aircraft

On paper, any of the aircraft mentioned in this section might be redesigned with high-lift flaps and a smaller wing, and thus keeping the takeoff runway requirement near that of the N+3 airliner. Doing so would cause the fuel volume in the wing to decrease, but because of the relatively conservative range of the 20-passenger baseline aircraft, this may not be a problem. However, the service ceiling of the aircraft would undoubtedly decrease. This, along with the greater weight of the high lift flaps, tend to increase the fuel consumption of the aircraft. This fuel increase might be offset by a decrease in weight and drag because of the smaller wing.

At the time of writing this section, it is unclear if the redesigned aircraft with high lift flaps and a smaller wing would burn less fuel than the original design. This is a question that may be investigated, to determine if high lift systems have any promise for the 2035 N+3 airliner. It appears clear, however, that high altitude cruise is beneficial. The best altitude, and the weight penalty that goes with it, may also be determined through research under the N+3 contract.

Appendix F: Laminar Flow in Theory and Practice

Appendix F: Laminar Flow in Theory and Practice

Introduction

Throughout the modern history of airplane design, the quest for improved performance has led directly to the desire to reduce drag. There are many ways to achieve this goal, such as great attention to detail to minimize excrescence drag, or wing design optimization to reduce induced and/or wave drag. One area that has held great promise for decades is to design for laminar flow in the boundary layer to reduce skin friction drag. The allure is great: Locally skin friction would be reduced by 75%, and with an average of 60% laminar flow over the entire aircraft, skin friction drag would be reduced by half.

The basic theory behind laminar boundary layers and transition has been known since the 1930s, and engineers have been designing airplanes attempting to take advantage of it ever since then. The NACA developed laminar flow airfoils which have been in operation since World War II and are currently in use on several aircraft types. There have been many active and hybrid laminar flow control demonstration projects conducted since the 1950s, most of which have been successful at achieving laminar runs over various parts of the aircraft surface. With modern aerodynamic design methods, several new airfoils have been developed that are capable of laminar runs up to 60-70% chord. However, the performance improvements resulting from these capabilities have been limited due to practical or operational considerations, which to date have been proven difficult to overcome for an aircraft with laminar flow to a significant extent.

This paper provides a brief discussion of the theory behind laminar flow boundary layers, and gives examples of research and production applications for subsonic airplanes. In addition to the theoretical basis, however, there are many practical considerations. In reality, the design for laminar flow – whether natural or produced by active control – presents inherent design compromises. Laminar flow does not come for free. An airplane design that is to be put in service must be manufactured, which provides other limitations. There may be operational considerations, such as leading edge contamination by insects, debris, ice, or rain. To be built and sold as a commercial product, an airplane must be certified by the governing regulatory authority, such as the FAA in the US and EASA in Europe.

To understand the true potential of laminar flow, research is needed which quantifies these practical considerations and compromises. For active control, the true weight and power requirements need to be determined for a full size aircraft system which is certifiable and meets operational and maintenance requirements.

Basic Theory and Research

Background

The derivation of the differential equation describing a laminar boundary layer (BL) on a flat plate with zero pressure gradient was first derived by Blasius, and the solution described by Prantl [1]. Laminar BL's have been observed and measured in a variety of applications, and are reasonably well understood. The average skin friction coefficient for a flat plate laminar BL is given by [1,2]:

$$C_f = \frac{1.328}{\sqrt{\mathrm{Re}_l}}$$ **Laminar Boundary Layer**

Since that time, a tremendous amount of study has been oriented towards the tendency of the laminar BL to become unstable, and transition to become turbulent. A laminar BL will transition to a turbulent BL naturally at a critical Reynolds Number, the specific value depending on the application. The transition is caused by the fundamental instability of the Navier-Stokes equations, whereby small disturbances become amplified. The details of experimental observations into transition, and the derivation of the Orr-Sommerfeld stability equation are well described in [3] and will not be repeated here.

There is no analytical derivation for the characteristics of a turbulent BL. However multiple experimental observations have resulted in the following well known formula for average skin friction [1,2]:

$$C_f = \frac{0.72}{\mathrm{Re}_l^{1/5}}$$ **Turbulent Boundary Layer**

With these formulas, the lure of laminar flow becomes readily apparent as shown in Figure 221. In much of the region of interest for commercial aircraft, RE=10,000,000 – 50,000,000, the skin friction reduction is approximately 75%. Also shown is the theoretical stability limit for ideal flow, and most of the range is above the limit. So a turbulent BL and the associated drag level should be expected.

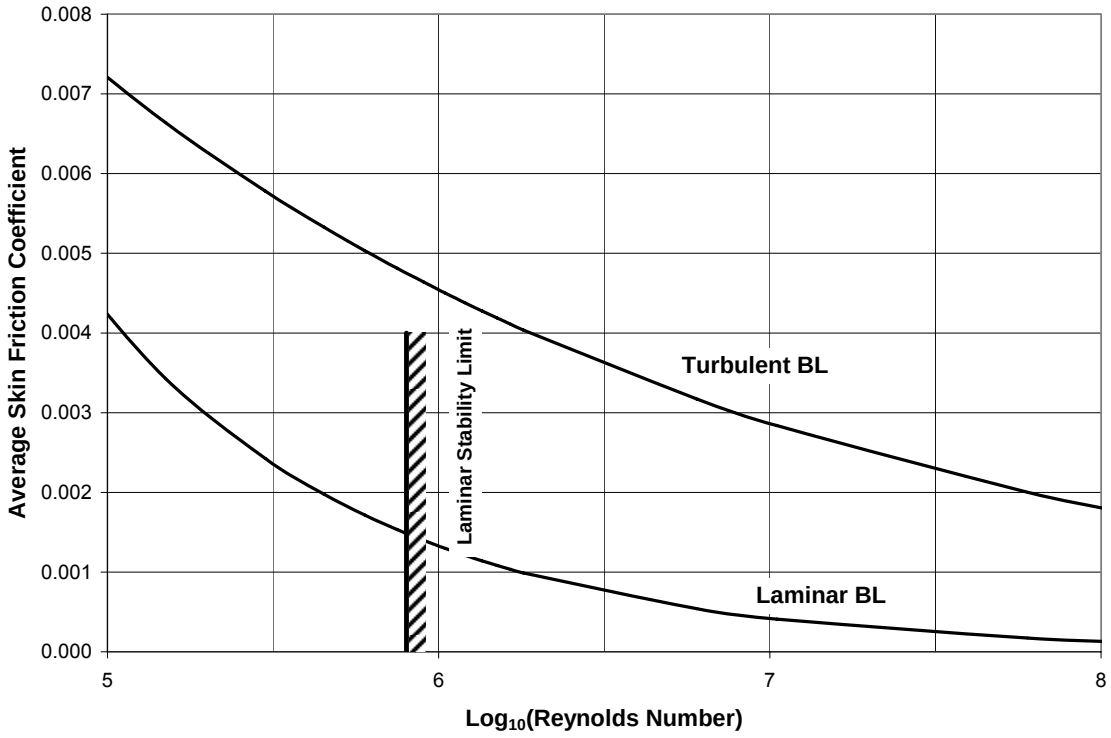

Figure 221. Average Skin Friction for Flat Plate Laminar and Turbulent Boundary Layers.

In the study of laminar to turbulent transition, it has been observed that a variety of factors can either promote or delay transition. The Orr-Sommerfeld equation describes amplifications of waves of infinitesimal strength. That is the ultimate limit for a flat plate that is perfectly smooth in a freestream that has no disturbances. Surface roughness or freestream turbulence will cause early transition.

The presence of a pressure gradient has a strong influence on transition location. If the velocity profile in the BL contains an inflection, the flow will become unstable [3]. An adverse (increasing) pressure gradient will cause an inflection due to back pressure on the BL, resulting in early transition. A proverse (decreasing) pressure gradient can delay transition. This is a fundamental aspect of Natural Laminar Flow (NLF) airfoil designs.

Transition will be delayed at high subsonic Mach numbers. Compressibility will have a stabilizing effect on the BL due to the damping effect of density gradients on the two-dimensional Tollmien-Schlichting waves [4]. Airfoils designed for higher speeds can have a more relaxed proverse pressure gradient to achieve the same transition location. This is beneficial as an optimum supercritical design will have a flat, “rooftop”, pressure profile. The proverse gradient present in low-speed airfoil design may behave poorly in transonic flow, with low critical Mach number and rapid increase in wave drag. Note that the presence of a shock wave, with its obvious adverse pressure gradient, will always cause BL transition.

The considerations above all apply to two-dimensional flow. For a three dimensional wing, sweep angle will have a destabilizing effect on the BL from two main effects [5,6]. First, crossflow instability due to spanwise pressure gradients can cause early transition from the

amplification of Tollmien-Schlichting waves. The second source is from attachment line contamination.

Airfoil Designs

In the late 1930s, the NACA began an effort to design airfoil sections with extended regions of laminar flow [7]. These sections had regions of proverse pressure gradient over the forward half of the chord for a moderate range of lift coefficients. The first successful designs are the NACA six-series airfoils, and they saw fairly widespread use. To achieve the desired pressure distribution, the sections used a leading edge radius more narrow than the four- and five-digit sections and had the maximum thickness relatively far aft. The narrow leading edge radius led to relatively low maximum lift coefficient, and the thinner sections have more abrupt stall characteristics due to the sharp stall break.

The evolution of modern 2D inverse design methods in the 1970s resulted in further efforts to design airfoils with extended regions of laminar flow. These airfoils achieved longer runs of Laminar flow, up to 60% chord. Maximum lift was also increased relative to the NACA 6-series airfoils, although $C_{L\,MAX}$ was still somewhat lower than modern high lift airfoils. Both low (e.g. NLF(1)-0414F) and high speed (e.g. HSNLF(1)-0213) versions were designed [8,9] during this timeframe.

With the current availability of inverse 2D design methods that can run on modern PCs and workstations, many other NLF airfoils have been designed. Some of them are for special purpose aircraft, while others are used on amateur built models. Some are found on certified aircraft. More information can be found at [10,11].

The bulk of design research has been oriented towards wings and airfoils, however some studies have been conducted on fuselages and nacelles [4,16]. All application of natural laminar flow are dependent on smooth aircraft surfaces without steps, gaps, or other protuberances.

Boundary Layer Control Methods

Active

Early research revealed that active methods could be used to delay BL transition and increase the run of laminar flow. The stabilizing effect of BL suction has been shown analytically and confirmed experimentally starting from the late 1930s [3]. Numerous wind tunnel and flight tests have shown extensive runs of laminar flow, up to and including full chord on the wing [12, 13]. The basic method is to install a porous or slotted surface with ducting to a powered suction source. The required suction level can be kept reasonably low, however the complexity and weight of the system can be substantial.

The success of these experiments begs the question: Why haven't any of these systems found their way onto successful commercial or military aircraft? The implied answer is that they were determined to be too complicated, too heavy, and take up too much volume to "buy" their way onto the airplane. In other words, an airplane equipped with such a system would weigh more and be more expensive to own and operate than an equivalent airplane without them, despite the advantage that a laminar BL would provide. Lacking the basic research on BLC techniques, suction system architectures, data on failure modes and effects and certification rules, industry has been reluctant to invest in development programs with configurations

requiring BLC to be successful. The availability of such data may provide industry the opportunity to determine if such vehicles would be or could be commercially viable.

Hybrid

A promising approach tested in the late 1980s and early 1990s is hybrid laminar flow control system. The concept used suction on the first 10-20% of the wing chord. In this way the BL can be stabilized past the LE devices, skin joints, and pressure suction spike if present. Once past the LE region, a lengthy run of NLF would result. The size and weight of the system could be greatly reduced as compared to suction over the full surface. The concept was demonstrated on a Dassault Falcon 50 and a Boeing 757 [12, 13]. Laminar runs were measured to 35% chord for the Falcon 50 and to the rear spar on the 757. Unfortunately, these tests have not been well documented, and no information is available regarding the weight savings of the system.

Leading Edge Roughness Elements

Recent research by Dr. Helen Reed at Texas A&M University has shown that transition can be delayed on swept wings by the careful placement of small roughness elements on the leading edge. The elements function by creating waves which cancel out the spanwise Tollmien-Schlichting instability [14]. This research is only in its early stages, but delayed transition has been demonstrated in flight test. One very promising feature of this approach is that the roughness elements do not have an active mechanism in the same sense as a suction system. However, the height of the roughness elements is very small, on the order of 50 μm. Manufacturing, maintenance, and operational aspects have yet to be addressed.

Applications

Perhaps the first application of a laminar flow airfoil on a production airplane is the North American P-51 during WWII. It used the NACA 66-(1.8)15.5 [10]. While the airplane was very successful, it is believed that the manufacturing methods used at the time could not produce a wing with sufficient smoothness to sustain laminar flow [15]. Many commercial aircraft developed after WWII used NACA 6-seres airfoils [10]. These aircraft can be expected to obtain varying amounts of laminar flow depending on the smoothness of the production configuration.

One area where a definite success can be claimed is on high performance sailplanes, where laminar flow airfoils such as those by Wortman are in common use. The low speed range results in low Reynolds number so extensive runs of laminar flow are achieved. In the case of sailplanes, the demand for performance outweighs the compromises imposed by NLF airfoils. Production rates are fairly low and therefore sailplanes are conducive to a custom built environment. Since the wing loading is usually very low due to very high wingspans, low takeoff and landing speeds are achieved without reliance on high lift coefficients. Composite construction is very common, so a smooth surface finish is easily achieved with no gaps or joints. They are generally not flown in bad weather, so ice and rain are not an issue. LE contamination due to insects is an operational reality, but the consequences of the resulting loss in performance are understood.

In the 1980s Cessna Aircraft Company embarked on a research program with NASA LaRC to measure laminar flow extent on a variety of aircraft [5, 16, 17]. A special wing was

constructed utilizing an NLF(1)-0414F section and fitted to a Cessna Centurion for flight testing. While the tests confirmed the performance of an appropriately smooth NLF wing, perhaps the most important component of the research was the handling qualities implications both with and without laminar flow [18]. This experience led to the application of a modified HSNLF(1)-213 on the Cessna CitationJet. The design of the wing utilized a thick-skin approach to minimize surface waviness, which did add a small structural weight penalty but achieved an overall mission weight reduction. Development testing showed that laminar flow was achieved as long as the structural joint between the heated leading edge anti-icing system and the downstream wing skin was constructed in a consistent manor. Certification testing of the CitationJet was performed on an airplane whose leading edges' cleanliness was representative of an airplane in normal operational service.

The Piaggio Avanti [19] twin turboprop aircraft uses a proprietary laminar flow airfoil specially designed by Gerry Gregorik at Ohio State University. It also uses a unique three lifting surface arrangement to move the main wing back and allow it to pass through the middle of the fuselage. This arrangement reduces interference drag. Another unusual aspect to the design is the fuselage nose, which is shaped to allow laminar flow over the forward fuselage. While the general shape definitely promotes laminar flow, the presence of the canard, radome seam, and windshield joints will generally result in boundary layer transition. The typical amount of laminar flow on the fuselage attained in practice is not known.

The Honda R&D HondaJet utilizes a 15% thick specially designed NLF airfoil for the main wing [20]. Wind tunnel and Flight tests (on a modified T-33 aircraft) show laminar flow on the upper surface to around 45% chord. Data for the prototype aircraft has not been published. The airplane is not yet certified, so the performance advantages of the final configuration are not known.

Use of NLF airfoils has made significant inroads into the amateur built airplane industry. Many of these aircraft use composite construction, as with gliders, and avoid seams, steps, and gaps which trip the BL. Also as with gliders, these aircraft are hand built and enjoy the luxury of performance taking precedence over all other criteria. Wind tunnel and flight test results for the Rutan VariEze and LongEZ [5] showed significant runs of NLF. Also documented was a change in the handling qualities of the VariEze when the canard BL was intentionally tripped early. The canard showed a loss of lift with a turbulent BL, resulting in a significant nose down pitching moment. Flight experience with these aircraft in rain, which tripped the BL on the canard, had shown pitch control difficulties. Later versions used a redesigned NLF airfoil which retained good lift characteristics even when turbulent.

Aircraft Design Compromises

Because of the compromising nature of airplane design, it is very unusual for any one discipline to dominate a configuration. Most airplanes are a balance of competing elements which must in the end work together. It can be observed from the history of airplane design that new technologies must always "buy their way" onto the airplane. It is reasonable to believe that, based on the length of time that the theory of natural and active laminar flow has been well understood and the relative lack of successful applications, that the costs have not been consistently shown to justify the benefits. It is clear that additional fundamental research on methods for reducing the impact of the design compromises would allow the technology to find its way onto more commercial products.

Aerodynamic Compromises

Even solely within the discipline of aerodynamics, the choice to design for NLF imposes compromises. It is very difficult, if not impossible, to design for NLF and high lift at the same time. A typical high lift airfoil designed with modern methods will have a $C_{L\ MAX}$ advantage of at least 0.15 as compared to an airfoil designed for NLF. This difference is due to the narrow LE radius required to sustain the proverse pressure gradient and delay transition. The delta is still present with trailing edge flaps deflected, since the LE suction peak is still the limiter for $C_{L\ MAX}$ with flaps down.

A further decrease in $C_{L\ MAX}$ results if leading edge (LE) devices are appropriate for the design. The inevitable contour discontinuity that will be present for a slat or other device will always cause transition at or shortly downstream of the discontinuity. It may be possible to define a drooped LE using morphing structure technology, but the un-drooped position must meet the rigorous profile and waviness constraints of the NLF airfoil. A design such as this has never been demonstrated. A drooped LE cannot achieve the same $C_{L\ MAX}$ as a slatted LE.

Any decrease in $C_{L\ MAX}$ will result in a larger wing area required to meet a given field length requirement. The larger wing will increase skin friction drag, thus compromising the gain made from the NLF.

As discussed above, wing sweep angle will have a destabilizing effect on a laminar BL. If the airplane is designed for high speeds, then a swept wing is desirable to reduce wave drag. A tradeoff will exist between drag reduction for NLF and wave drag. No detailed study has been published which examines this trade.

Note that this discussion applies to NLF, and active or hybrid systems can sustain laminar flow past large radius LE's with devices. They will also help to stabilize the BL on swept wings. However, an active system presents other issues, discussed below.

Weight, Power, and Volume Requirements for Active Systems

Experimental testing of active and hybrid laminar flow control (LFC) systems have always been restricted to demonstrations, where a small portion of the aircraft is fitted with a glove or other added device and the needed suction is provided to the test area [12, 13, 16]. These experiments have been very successful at achieving laminar flow, but an aspect that is not published are the system weight, power, and volume requirements. Obviously, the weight of airplane systems is a critical design parameter, and the addition of the suction system will cause a significant impact. Not only will the basic compressor and ducting systems add weight, but there may be a structural impact due to the addition of porous or slotted skins. It may be possible to use the ducting system for structural stiffening of the skin. The suction system must be powered in some way – such as engine driven or electrical - which takes power from the propulsion system and decreases efficiency. Finally, these systems must take up volume as well. In addition to the volume of the pumping system, the ducting system in the wings will take up critical space used for fuel storage and/or other systems.

The weight and power requirements of these systems will offset the advantages gained by laminar flow to some degree. No published data show the weight and power requirements for a fully functional system designed to promote laminar flow over entire wings, nacelles, and/or fuselages. The consequences could be substantial, and a very real risk is present that the estimates during preliminary design could be in significant error.

Manufacturing Challenges

The manufacturing requirements to promote and sustain natural laminar flow are fairly well documented. To comply with requirements to control waviness, a thick skin construction approach is usually required. Otherwise normal imperfections that creep in during assembly will cause surface imperfections that will cause the boundary layer to transition to turbulent. Bonded aluminum or composite construction can also help. Very few commercial aircraft have been certified with composite primary structure.

Modern metal aircraft construction creates many joints with steps or gaps in the surface that, without special attention during the design and construction process, will prevent natural laminar flow. A common situation where this exists is at the wing LE where the ice protection system must be integrated. Current manufacturing methods lead to a joint at generally 10% chord on the upper and lower surface. This joint is difficult to control during manufacture and service. Methods to control the size and shape of the gap must include the paint application as well.

While aerodynamicists always like to think of the aircraft as having a smooth exterior, the reality is that the surface is full of joints, access panels, doors, windows, antennas, control surfaces, etc. These are all items required to perform the mission or inspect and maintain the structure. New approaches to these joints, panels, and protuberances will be required for laminar flow on future aircraft. These have yet to be developed.

While manufacturing requirements in general may not add a significant weight penalty, they may add to the airplane manufacturing cost. This must be considered as part of the total life cycle cost.

Operational Considerations

Airplanes commonly operate in a variety of environmental conditions which could potentially contaminate the laminar flow. The primary requirement is to keep the LE clean so the boundary layer is not tripped.

Previous studies have looked at two methods to keep the LE clear of insect contamination [16]: one is to use a Krueger flap as a deployable shield to deflect insects away from the LE, and the second is to incorporate a liquid purge system into the LE to keep it clean. Both systems are intended to operate at low altitudes, and are retracted or discontinued during cruise. The liquid purge system can be incorporated into the LE suction system; however storage of the liquid and the additional piping required adds weight and complexity to the system.

Since successful transport aircraft must be certified for operating safely in icing conditions, any successful design must have a certifiable ice protection system (IPS) on board. As described above, the IPS is integrated into the leading edge and must be compatible with the design for laminar flow whether active or passive. None of the documented active systems were integrated with an IPS, and the author is not aware of any research into compatible systems.

Typical operations in rain or the accumulation of ice on leading edges will trip a laminar BL. This is not likely to be a significant issue, as these events are mainly limited to approach and departure and not to cruise, at least for turbofan powered aircraft. For these aircraft, cruise

operations are generally conducted far above the weather where laminar flow can be reestablished.

After many years of operations the surfaces of all aircraft will suffer from erosion and may no longer be smooth enough to sustain laminar flow. No long term studies have been conducted in this area, so it is not known how long typical surfaces will last. Certainly the replacement of significant portions of the aircraft which have roughened would need to be factored in to maintenance costs.

Maintenance requirements for active systems are not well understood. Porous or slotted systems may need periodic cleaning to remove debris, and the suction equipment will also suffer breakdowns. While methods may exist that are used on existing systems, the added costs must still be accounted for.

Recommendations for Laminar Flow in 2035 Vehicles

This essay has presented a brief history of the motivation, theory, and research behind the application of laminar flow technology to subsonic airplanes. While the potential benefits are great, there are substantial obstacles to the successful application to certified airplanes. These obstacles include:

- Aerodynamic penalties in high lift performance for natural laminar flow designs
- Manufacturing tolerances for gaps and steps
- Overall weight, power, and volume impact for active laminar flow control systems
- Design for reliability of active systems
- Operational and maintenance impact

It is recommended that future work include an accurate accounting of the aerodynamic compromises and system requirements. These studies might include:

- Accounting of the aerodynamic limitations such as $C_{L\ MAX}$ reduction and low speed un-swept wings on mission capabilities and sizing.
- System design studies that enable an accurate accounting of weight, power, and volume requirements for a full airplane active or hybrid laminar flow control system.
- Operational studies to determine reserve requirements for partial or total loss of laminar flow.
- Development of new manufacturing and monitoring techniques to eliminate joints and inspection panels.

References

1. Prantl, L., **The Mechanics of Visous Fluids**. In W.F. Durand: Aerodynamic Theory III, 1935.
2. Kuethe, K.A. and Chow, C.Y., **Foundations of Aerodynamics**, John Wiley and Sons, 1976.
3. Schlichting, H., **Boundary Layer Theory**, McGraw-Hill Book Co., 1979.
4. Vijgen, P., Dodbele, S.S, Holmes, B.J., and van Dam, C.P., "Effects of Compressibility on Design of Subsonic Fuselages for Natural Laminar Flow," *J. Aircraft* Vol 25 No 9 p776, 1988.
5. Holmes, B.J., Obara, C.J., and Yip, L.P., "Natural Laminar Flow Experiments on Modern Airplane Surfaces", NASA TP 2256, 1984.
6. Beasley, J.A., "Calculation of the Laminar Boundary Layer and Prediction of Transistion on a Sheared Wing," R&M No. 3787, British ARC, 1976.
7. Abbott, I.H. and Von Doenhoff, A.E., **Theory of Wing Sections**, Dover Publications, Inc., 1959.
8. McGhee, R.J., Viken, J.K., Pfenninger, W., Beasley, W.D., and Harvey, W.D., "Experimental Results for a Flapped Natural-Laminar-Flow Airfoil with High Lift/Drag Ratio," NASA TM 85788, 1984.
9. Sewall, W.G., McGhee, R.J., Viken, J.K., Waggoner, E.G, Walker, B.S., and Millard, B.F, "Wind Tunnel Results for a High-Speed, Natural Laminar-Flow Airfoil Designed for General Aviation Aircraft," NASA TM 87602, 1985.
10. Lednicer, D. The Incomplete Guide to Airfoil Usage, http://www.public.iastate.edu/~akmitra/aero361/design_web/airfoil_usage.htm.
11. Selig, M., The UIUC Airfoil Data Site, http://www.ae.uiuc.edu/m-selig/ads.html
12. Braslow, A.L. "A History of Suction-Type Laminar-Flow Control with Emphasis on Flight Research," NASA Monographs in Aerospace History Number 13, 1999.
13. Joslin, R.D., "Overview of Laminar Flow Control," NASA TP-1998-208705, 1998.
14. Saric, S.S., Carpenter, A.L., and Reed, H.L., "Laminar Flow Control Flight Tests for Swept Wings: Strategies for LFC," AIAA Paper 2008-3834 Presented at the 38th Fluid Dynamics Conference and Exhibit, Seattle, WA, 2008.
15. Laminar Flow Airfoil, http://www.aviation-history.com/theory/lam-flow.htm
16. Hefner, J.N. and Sabo, F.E., "Research in Laminar Flow and Laminar-Flow Control," NASA CP 2487, 1987.
17. Ahmed, A., Wentz, W. H., Jr., and Nyenhuis, R., "In-Flight Boundary Layer Transition Measurements on a Swept-Wing," *J. Aircraft* Vol. 26, No. 11, p979, 1989.
18. Manuel, G.S. and Doty, W.A., "Flight Test Investigation of Certification Requirements for Laminar-Flow General Aviation Airplanes," *J. Aircraft* Vol. 28, No. 10, p652, 1991.
19. McClellan, J.M., "Fuel Miser: Piaggio Avanti II Flies Biggest Cabin the Fastest for the Least Fuel Burn," *Flying Magazine*, December 2008.
20. Fujino, M., Yoshizaki, Y., and Kawamura, Y., "Natural Laminar Flow Airfoil Development for a Lightweight Business Jet," *J. Aircraft*, Vo. 40, No. 4, p609, 2003.
21. Liddle, S.C., and Crowther, W.J., "Systems and Certification Issues for Active Flow Control Systems for Separation Control on Civil Transport Aircraft," AIAA Paper 2008-158 presented at the 46th AIAA Aerospace Sciences Meeting and Exhibit, 2008.

Appendix G: Composites for Light Weight and Environmental Protection

Appendix G: Composites for Light Weight and Environmental Protection

Overall, this research project covers a number of potential concepts dealing with a future air travel concept developed for the 2035 timeframe. Separate work elements deal with topics ranging from the rationale for the point to point passenger model, the overall aircraft configuration concepts, new enabling engine technologies, gains that can be achieved through enhanced laminar flow technologies, etc.. This particular work element focuses on the task of achieving a 30% weight savings, as compared to a baseline 20 passenger aircraft built with current day methods and materials. The project includes a review of currently available technology concepts, a summary of various research topics currently underway that will help to enable some of the proposed weight savings, and a look into next generation materials and methods that will need to be developed to make the weight savings estimates a reality.

While there are examples of composite implementations that have been somewhat successful, none have provided the anticipated weight savings improvements envisioned when the programs have started. Certainly, there are examples of smaller, general aviation aircraft fabricated from composites, but there are no commercially viable commuter category aircraft with extensive use of composites. While there are examples of successful military aircraft and larger transport category aircraft, such as the Boeing 787, in the works, they often have design requirements that make composites feasible. An example is that the skin thickness required to carry the structural loads on a 787 fuselage barrel is sufficiently thick that impact damage from items such as a dropped toolbox are not likely to be catastrophic, whereas a minimum thickness fuselage on a 20 passenger commuter aircraft may not be capable of withstanding the same impact.

In order to achieve the prescribed 30% weight reduction targets, the 2035 advanced airframe concept will not only have to be able to withstand the structural requirements of meeting all limit and ultimate load conditions, but it will have to do so while addressing all of the required environmental (temperature, humidity, and corrosion), repeated load, and damage tolerant requirements. Above and beyond the structural aspects, the airframe will also have to permit all of the required lightning strike and high intensity radiated fields (HIRF) / electromagnetic interference (EMI) requirements to be met for all of the installed systems. Additionally, the airframe needs to provide a platform for installation of all systems and sub-system equipment in ways that are not detrimental from a weight standpoint. Finally, the airframe concept must not only be structurally sound and systems and equipment friendly, it must also be conducive to field service and withstand the rigorous environment that commercial commuter air service requires.

This report gives a high level review of current structural design concepts, current day resins and fibers, and composite fabrication technologies including material forms and tooling concepts. A brief review of current day methods for dealing with environmental effects such as heat and humidity, impact damage, and noise is also presented, with further development of those topics in the Trade Studies and Analysis Report. A review of current day lightning strike protection and EMI shielding techniques is given, followed by a more in depth review of current state-of-the-art research activity in enhancing the conductive nature of composite materials. Finally, a down selection to arrive at the technologies chosen to develop the 30% weight reduction is presented. Further discussion on the weight savings estimates and the technology

development roadmaps required to make these concepts a reality are discussed in the Technology Roadmaps report.

Composite Structural Concepts

Core Stiffened Construction

Because core stiffened sandwich structures exhibit very high specific stiffness values, they are an attractive configuration for aircraft design. However, there are a number of issues associated with these sandwich panel constructions that need to be considered. Although there are other options, the majority of core stiffened structures are typically reinforced by either foam core products or honeycomb core products.

Foam core products can be further separated into structural foam cores that are designed to carry applied loads and non-structural foam cores that act more as captive tooling materials and stay with the part after it is fabricated.

Honeycomb cores are available in a variety of base materials, wall thicknesses, and cell sizes, allowing for a multitude of core density options. Typical aerospace core materials are constructed of either aluminum sheets or aramid paper that has been coated with resin. Aramid based honeycomb cores tend to be hydroscopic, and if not adequately protected, will readily absorb moisture from the air they are stored in. The pre-bond moisture is released during elevated temperature cure temperatures and can create issues by either inhibiting cure on the bonding adhesives or creating enough encapsulated gas pressure to keep the face sheets from bonding to the core materials.

Core stiffened structures exhibit other challenges as well when it comes to interface and/or attachment with other features in an airframe. In honeycomb stiffened core structures, it is common to pot attachment points with potting compound that can address the high compressive loads, but carries a penalty of high density values when compared to the native core. Core structures also pose issues for field repair, in that application of local heating to cure repair patches can often result in further delaminations between the adjoining skin and core. Drying and cleaning core in structures to be repaired is very tricky and chances of having a successful repair are often not as high as they might be with a discrete element stiffened structure. Core designed structures divide the required layers between the inner and outer surface. If done to the ideal structural sizing, inadequate material is left on the outer layer for protection of impact damage. Additional layers drive up weight.

Skin / Stringer / Frame Construction

Traditional skin, stringer and frame construction for airframe structures is a fairly well understood science. In house design tools for traditional sizing and placement of conventional material structural elements has been fairly well developed and manufacturing techniques to fabricate and construct aircraft with these kinds of structures have been fairly well optimized. Modifying these techniques to methods that are applicable to composite materials has had mixed success. Many attempts at making composite aircraft have resulted in “black aluminum” designs where composites are used to replace metallic components on a 1-for-1 basis, resulting in a less than optimized composite structure. Nevertheless, utilizing the lessons learned from skin, stringer and frame construction techniques should result in a more optimized, serviceable

airframe when compared to a sandwich construction, especially in the size of aircraft that is being considered for this study.

Joining / Fastening Concepts

One of the problem areas that have hindered increased implementation of composites in airframe applications is relative to the joining and fastening of the various parts and assemblies. Historically, the bearing strength of composites has been a large hurdle to overcome, especially in relatively thin gage structures. In order to get the bearing stresses down to manageable levels, it is often necessary to build up edge bands with additional plies of material to increase the bearing areas. These build ups are detrimental from both an overall weight perspective as well as from a manufacturability standpoint. While there are some publicly available empirical models, such as BJSFM (bolted joint stress field model) that help in the design and analysis of bolted joint configurations, there is typically still a need to do a significant amount of laminate, sub-element and higher level building block pyramid type tests to fully understand the interactions that occur in fastened and bolted joints.

In addition to the material issues of bearing strength of the composites materials themselves, traditional fasteners that have been created for use in composites tend to be very expensive compared to their analogs for the metallic world and also often require specialized installation equipment. Machining equipment that can stand up to the difficult environment of machining composites while being able to maintain the necessary hole quality and tolerance requirements as well as provide adequate tool life has proven to be a difficult balancing act.

Another method of fastening adjacent / adjoining assemblies is through primary adhesive bonding. In these joining methods, the two surfaces to be bonded are carefully prepared for bonding, a bonding adhesive is put in place, the two (or more) adherends are placed together and through careful application of pressure and/or heat, the surfaces are permanently bonded together. While this joining technology has a lot of apparent advantages as compared to traditional installation of fasteners, it does require consideration of secondary load paths in the event that the primary bond surface fails. It also tends to be very labor intensive in both surface preparation and bond adhesive mixing and application, and ultimately is viewed as a special process that requires a great deal of control over the materials, processes, and tooling.

Composite Materials

Fiber Reinforcements

While composite materials can be made from any mixture of two or more separate and distinct materials, for the sake of this effort, the term composite is exclusively used to refer to fiber reinforced polymer matrix materials. With a few exceptions for carbon-carbon composites and metal matrix composites, the bulk of composites used in fabrication of aircraft structures and components are fiber reinforced plastics. These product forms can contain any of a number of fiber types embedded in any of a number of various polymer technologies. While the variety of the fibers and polymers used are large, this report will provide a brief overview of the technologies that are widely available on a commercial basis and make up the vast majority of what is used in current applications.

Fiberglass

Fiberglass fibers come in several classes of product, each based on differing mixes of the constituent materials that are used to produce them. They are produced by melting a mix of blended oxide materials and then drawing the resulting product through a heated bushing and spinning die arrangement at temperatures near 1250°C. The typical used aerospace fiberglass products are “E” glass and “S” glass. E-glass is formulated from calcium alumino-borosilicate and has relatively low dialectric constant and high electrical resistivity. S-glass is formulated from magnesium alumino-silicate and has higher strength and stiffness as compared to E-glass.

Because glass is very sensitive to abrasion at the fiber levels, various materials are applied during the production process. These products may include binders, lubricants, and finishes, each added for unique processing improvements. Binders aid in holding the assembled individual fibers into tow bundles, improving handleability and processing of fiber bundles into other material forms. Lubricants are typically applied to reduce abrasive damage to the fiber bundles that result in follow-on processes such as weaving of glass fabric broadgoods. Finishes, which are typically organo-silane based, are used to improve adhesion between the fibers and the matrix materials used.

Due to its low cost and relatively high specific strength properties as well as its availability, fiberglass is an attractive option for some structures.

Aramid

Aramid fibers are produced from an aromatic polyamide polymer chain. They have specific strengths similar to fiberglass fibers but have specific strengths on the range of two to three times as high. Aramid fibers exhibit high strain to failure capabilities which allow them to absorb large amounts of energy. This phenomenon makes them ideally suited for applications such as engine containment rings and ballistic protection.

Aramid fibers are not without their drawbacks however. They tend to be hydroscopic, readily absorbing significant amounts of water from the ambient environment. Because of their unique energy absorption tendencies as the fibers rupture, they also tend to be more difficult to machine without using very specific tools and processes tailored toward machining of aramid fiber products.

Carbon

Similar to fiberglass and aramid fibers, carbon fibers come in a variety of different kinds. The first separation in carbon fibers is based on the precursor material used to produce them. One class of products, and the one most often used in structural applications, is produced from a polyacrylonitrile (PAN) precursor. The PAN precursor is drawn through a fiber spinning head in either a dry spinning or wet spinning process during which the resultant fibers are stretched to improve their mechanical properties through alignment of the polymer chains. The stretched fibers are stabilized through an oxidation step in an air oven at approximately 250°C. The fibers then undergo varying degrees of carbonization and graphitization at temperatures between 1200 and 2500°C, depending on the particular product being produced. The resulting fibers can either be left unsized or may be treated with one of a variety of sizing materials that help protect them from damage in further manufacturing operations such as weaving and also help promote adhesive with the selected matrix resin material.

A second class of carbon based fiber products is based on a pitch precursor. These fibers are produced by heating the pitch precursor and melt spinning into fiber form. The follow on process of stabilization, carbonization and graphitization are similar to PAN base fibers. In general, pitch based fibers do not have as attractive mechanical properties as PAN based fibers, and as such, they are not widely used for aircraft component production. Some pitch based fibers do exhibit specific tensile stiffness values much higher than those that can be obtained with PAN based technologies, but at the cost of compression and shear strengths. As such, unless there is a specific design need for them, pitch based fibers are generally not used in aircraft structural applications.

As previously noted, there are a number of different commercially available PAN based structural fibers. The differences are based on the dry or wet spinning technique used to produce them, as well as differences in the proprietary fabrication process used to convert the precursor fibers into the final form. There are a variety of well known, widely characterized fibers commercially available, including standard modulus fibers such as T300, T650, AS4, G30-500 and intermediate modulus offerings such as IM7 and T-800, There are a number of high and ultra high modulus fibers available as well, but they have not found much market exposure beyond niche applications in high end military and UAV markets. The high and ultra high modulus fibers tend to have reduced strengths and or deficiencies in other mechanical properties, as well as relatively higher price points that make them less attractive for commercial aviation applications.

Boron

Boron fibers have been studied in the past and are often used in metal matrix composite forms at this time. They are relatively large diameter fibers compared to the other fibers discussed in this report and are very hard. Due to their hardness, they are difficult to drill and machine. Production of the boron fiber itself involves a process of chemical vapor deposition of boron onto a tungsten or carbon carrier in a reactor. The process is expensive and time consuming. The resulting fiber product is relatively expensive and likely not within the price point of commercial aircraft applications, at least not for ongoing production parts. Boron fibers have shown some promise when used in repair applications as patch materials on existing metallic structures.

Quartz

Quartz fibers are a specialty fiber that is most commonly used in structures associated with covering antenna or radome structures. It has a significantly lower dielectric constant than any of the other fiber products, making it ideal for these kinds of structures. The lower dielectric properties come at a cost though, with quartz fibers being significantly more expensive than the other options. As such, the extent of their use should be considered carefully and be limited to those options where a suitable E-glass based product will not work.

Thermoset Matrix Materials

The first of the two major families of polymeric matrix materials are the thermoset materials. These materials can be provided in one or two part systems and consist of base chemistries that are modified for a particular end use. These materials can generally be obtained in a totally uncured state or a value added partially cured state that is then held in a B-stage product form that can later be processed to final cure state with additional application of heat. This family of

products differs from the thermosets in that the cure reaction is not reversible, so once cured, the products can not be reverted back to a form that can be reprocessed. The cure mechanism of this family of products is based on relatively low molecular weight polymers that build in molecular weight during the cure reaction and ultimately create covalent cross-link bonds. These cross-link bonds tend to make the materials brittle in nature and additives are generally added to raise the resulting product toughness.

Epoxies

The family of polymers that makes up the bulk of the composite materials used in aircraft applications is based on epoxy formulations. Epoxies are widely used due to their relatively easy process requirements, their ability to be tailored for specific applications through additive packages to address issues such as toughness, fire resistance, end use temperature, moisture absorption, compression strength, etc. Often times, the addition of these modifiers and additives are detrimental in other characteristics, so finding a product that satisfies a given end use is an on purpose trade-off between the various properties.

Epoxies have a wide range of process requirements, with two-part systems that will cure at room temperature, to high end prepreg systems that cure at temperatures as high as 350°F. Historically, most aircraft composites were 350°F curing systems based on diaminodiphenyl sulfone (DDS) curative packages, more recently, 250°F curing epoxies have been formulated, most of which are based on dicyandiamide (DICY) curative packages. Some epoxies have been formulated to cure at a wide range of temperatures from as low as 180°F all the way up to 350°F. Generally, these products require a post-cure operation at a higher temperature if the original cure was done at the lower end of the range.

Epoxies hold an advantage over many of the other thermoset systems in that they are easier to process and pose less risk from a environmental, health, and safety standpoint. They also exhibit less shrinkage as compared to other lower temperature thermoset materials such as polyester and vinylester based systems. They are relatively easy to bond, exhibit good chemical resistance, and are well understood.

Bismaleimides

Certain applications require higher continuous use temperatures that can generally be addressed by epoxies. Typically, the next thermoset polymers reviewed when epoxy can not handle the temperature requirements of an application are the bismaleimides (BMI). While not as easy to process as epoxies, they can be used in long term temperature exposures up to 450°F and up to 600°F in short term applications. BMIs require dwell temperatures around 550°F for several hours. As a result, tooling associated with BMI part production tends to be significantly more expensive and/or tool life is drastically shortened when compared to typical epoxy tooling concepts.

Part production with BMI also tends to be more difficult than when using epoxies, as the material tends to be less tacky and can be difficult to work with, especially in larger parts with complicated geometries.

Polyimides

When bismaleimide technology does not provide adequate continuous use temperatures, the next step up in thermoset technology are the polyimides. These resins become even harder

to process than bismaleimides and further raise costs and complications with tooling concepts. Several of the polyimides are based on technologies based on in-situ polymerization of monomer reactants (PMR). PMR-15, arguably the most widely known commercialized PMR resin, contain methylenedianiline (MDA), a known carcinogen, which requires exposure control until the part has been processed through an imidization step that removes the threat of the free MDA.

Processing of polyimide resins tends to be very complicated, time consuming, and expensive. Very specific cure cycles are generated to tailor the evolution and removal of solvent gases. It is not uncommon to require a lengthy step cure process, then remove the part from the cure device and re-bag it for the next stages of the cure. The cure processes tend to be very sensitive to ramp rates, dwell temperature and hold times, and a blown bag or slight mis-step in the cure process can easily result in a scrapped part.

Significant effort has been spent over the years to develop non-MDA polyimides, with some success and commercially available polyimides available today are pushing upwards of 900°F continuous use temperatures. In fact, in many applications, the resin technologies are moving beyond the capabilities of the reinforcement fibers for long term use at the elevated temperatures.

Due to the complications and cost associated with polyimides, they are generally used only when one of the other thermoset materials will not meet the needs of the program.

Cynate Esters

Cyanate Esters are another group of resins that have thermal and strength properties superior to epoxies. While not as good as BMI resin in thermal and strength properties, cyanate esters have found special applications because of their superior dielectric loss properties and low moisture absorption. The major uses are radomes, skins covering phase array antennae, advanced stealth composites, and space structures.

Thermoplastic Matrix Materials

The second major category of polymer composites is the thermoplastic materials. As opposed to the thermoset materials previously discussed, these are higher molecular weight resins that are not cross-linked and do not undergo further chemical changes during follow-on part processing operations. Because they are not cross-linked, they tend have higher toughness properties than unmodified thermoset materials and because they do not undergo further chemical changes in processing, the process time to fabricate parts is significantly shorter than that for the traditional thermoset materials. Additionally, since the chemical reactions are essentially completed in the end user raw material state, there are fewer health concerns relative to thermoset materials with their various unreacted chemical components. They also provide for long term stable shelf life at room temperature conditions. Generally, thermoplastic matrices do not absorb moisture at the levels of the thermoset matrices. Furthermore, because of their lack of cross-linked structures, they do not suffer the same hot/wet degradation as thermoset matrices; however, the thermoplastics are much more susceptible to damage from exposure to a variety of solvents and fluids that are commonly used in the aerospace industry.

PEI

Polyetherimide is an amorphous thermoplastic matrix that has processing temperatures around 700°F range and glass transition temperatures around 420°F.

PEEK

Polyetheretherketone is a semi-crystalline thermoplastic that has a melt temperature of approximately 650°, a processing temperature of approximately 700°F and a glass transition temperature around 290°F.

PPS

Polyphenylene Sulfide is a semi-crystalline thermoplastic that has a melt temperature of approximately 550°F, a processing temperature of approximately 625°F and a glass transition temperature of approximately 190°F.

Product Forms

Regardless of the particular fiber and matrix options chosen, the materials are available for purchase in a number of product forms. These product forms tend to be a trade off between more basic material forms such as dry fiber performs and liquid resins and products that have value added services added to them, such as the pre-impregnated offerings. A brief description of each of them, including potential pros and cons will be discussed in this section. For the most part, this section will assume thermoset resin matrices, although some of the product form discussion could be applicable to both thermoset and thermoplastic product forms.

Dry Fiber Preforms

Dry fiber performs can come in a variety of product types, some generic in form so they can be used in an endless array of part fabrication operations, and some specifically tailored to a unique and particular production article. In the simplest form, a dry fiber preform is a two dimensional woven fabric consisting of the chosen fiber type, woven to a predetermined areal weight at a given width. Weaving of aerospace fibers is directly linked to other textile weaving operations, using many of the same kinds of looms, creels, and concepts to determine how a given fabric construction can be made. In the fiberglass product lines, there are industry standard weave styles that are commonly accepted such as style 108, 120, 1581, 7781, etc. Each style is clearly defined in weave pattern, number of tows in the warp and fill direction, areal weight ranges, etc.. Similarly, aramid fiber fabrics can be obtained in industry standard styles such as style 281 and style 285. While there is not an industry standard specification that dictates carbon fabric weave patterns, the fabric suppliers have standard product forms such as a plain weave fabric manufactured with 3K carbon fiber tows at an areal weight of approximately 195 grams per square meter. Similarly, there are standardized weave patterns for satin harness and twill patterns in various combinations of tow sizes and areal weights.

Preforms are not limited to flat two dimensional weaving of a single material however. Options exist to have two and three dimensional braided performs made, as well as more intricate fabrics woven from 2 or more fiber types, making hybrid fabrics available if a design requires them. Not all performs are braided or woven either, a number of stabilized, stitched, and/or non-crimp knitting techniques are available that allow for products to be stacked and

combined into double bias tapes and multi-axial unidirectional products pre-stacked and held together for quick buildup of relatively heavy areal weight fiber performs. Other production methods for preform creation also exist for non-continuous fiber preform creation. These techniques include the use of pneumatically blown chopped fibers onto molds with performs that are stabilized with powdered binders to dip processes that allow for preform creation from short fibers floating in solution beds.

Regardless of the technology chosen to manufacture dry preforms, consideration needs to be given to the potential for contamination of the preform, shelf life and storage conditions if binders or sizings are applied, compatibility with the matrix products that will be used, and damage that may be imparted from the preform creation process. Examples would include having a fiberglass preform for a radome application that contains random carbon fiber contamination from a weaving loom that weaves both carbon and fiberglass fabrics, preforms that are shape stabilized with a heat set binder that has a limited shelf life that can not be extended, or high modulus carbon fibers that are difficult to weave without significant fuzzing issues of the carbon fiber.

Liquid Resins

Liquid resin products come in a variety of product forms from single component pre-mixed to multiple component kits that need to be mixed at the end user location. Pre-mixed resins generally require controlled storage conditions to keep the mixed resin from continuing its cure reaction, and generally have limited shelf life even if kept in controlled storage. Pre-mixed resins are an attractive choice for high volume material users that do not want/have the necessary facilities, labs, and/or manufacturing equipment to measure and mix the multiple component resins on site.

On the other hand, multiple component resins have an advantage in that they typically have more stable shelf storage and life properties. The increased flexibility in storage comes at a price of additional manufacturing steps that need to be addressed at the end user location in the form of individual component measuring and mixing operations. Depending on the size of the manufacturing operation it may be worthwhile to investigate automated meter and mix equipment that would mitigate some of the human error potential in the resin component measuring and mixing operations.

Resin Films

Resin films are essentially pre-mixed and catalyzed resin products that have been processed through some sort of film coater equipment (as either hot-melt or solvated resin) and are then stabilized and sold as a raw material. The areal weight and tolerances of the resin film is controlled by the customer specifications and the end product is used in resin film infusion processing where it is placed in a mold with a fiber preform and will flow and infuse the preform during the ensuing manufacturing operations. Resin films have an advantage over liquid resins in some applications, relative to the ability to create product stackups and process parts without having to perform the liquid resin infusion step which can be rather time consuming. If a pre-made kit configuration is implemented, it also allows for ease of manufacturing and inventory control. The downside of resin films are that as B-staged products they require controlled storage and have relatively short shelf lives. Resin film infusion processing is also not widely used at present, so options for part processing may be somewhat limited.

Pre-impregnated Materials

The majority of currently used composites in aerospace applications are in the form of pre-impregnated materials, or prepregs for short. These products incorporate a broad range of product forms from wide width broadgood woven fabrics and unidirectional tapes to slit tape or towpreg product forms that are formed from individual fiber tows or slit tape products at widths down to 1/8" in width used for fiber placement or tape winding operations. The common trait of all these products is that they consist of a dry fiber form that is impregnated in resin in a value added process. Prepregs tend to be made in one of two methods that are ultimately linked to the resin formulation.

These two methods are hot-melt coating and solvated resin coating. In hot-melt coating, a resin film is produced from a resin mix at elevated temperature. This resin film is consolidated into the fibers by passing it through a combination of heat and pressure then cooling it prior to rolling it up and packaging it for delivery to the customer. Hot-melt prepregs can be easily manufactured in one side or both side tacky configurations. Solvated resin coating processes involve pre-mixed resin chemistries that contain higher solvent content to lower their viscosities. The lower viscosity resin is used in either a resin bath or applied through a roller application onto the fiber form and is then run through a carefully controlled heated tower operation to drive off the excess solvents before the prepreg is rolled up and packaged for delivery.

Composite Fabrication Technologies

When producing a product from fiber reinforced polymer materials, consideration needs to be given to the product forms of the raw materials that will be used to fabricate the part. While similar mechanical properties could be obtained from coupons produced in any of these following production methods, consideration should be given to manufacturability of a part, repeatability, number of parts in the expected life of the program, etc. By weighing all of these factors, an optimized mix of product form and manufacturing methods can be arrived at to deliver the best compromise in part fabrication.

Pre-impregnated Materials

Hand Layup

Hand layup operations in aerospace applications generally uses prepreg materials, but could also include wet layup where a dry fiber form is worked together with a liquid resin and the ensuing wet impregnated material is then placed onto the tool. In hand layup, the individual plies that make up the component are placed into a tool by hand. Each ply is individually placed and worked into any existing geometry or features that require additional operations to get the ply to conform to the part shape.

Automated Tape Layup

In automated tape layup, pre-impregnated unidirectional materials are produced and then further processed into custom widths materials depending on the equipment that will be used to produce the final parts. Typical widths of unidirectional tape used in automated tape layup are in the 6" range. In this production method, a multi-axis robot is used to place layer after layer of the unidirectional tape onto a tool, building up the plies of the final part with each pass. The benefits of automated tape layup include higher throughput as compared to hand layup, as well

as highly repeatable part production once the programming is established. The downsides of automated tape layup are the limitations associated to ply buildup concepts, including when and where plies can start and stop and the fact that structures have to be designed to accommodate full width passes of the tape material form. Additionally there are constraints on overall part geometry due to the limitations of robot head design.

Fiber Placement

Fiber placement is a further evolution from automated tape layup, in that the unidirectional tape is further slit down to typical sizes of 1/4" to 1/8" width. Unlike automated tape layup, there are fewer limitations on customizing ply build-up as individual slit tape segments can be stopped and restarted on the move, allowing for much more precise design and fabrication concepts. Similar to automated tape layup, fiber placement also has limitations on the contour of parts that can be produced based on limitations of robot head design. Additionally, the increased flexibility as compared to automated tape layup often comes at a decrease in the amount of material that can be placed per hour. The complexities of a fiber placement head as compared to an automated tape layup head also imply that there may be increased maintenance cost and associated down time for fiber placement equipment as compared to automated tape layup equipment. The technology relating to both automated tape layup and fiber placement has made great strides in recent years and the throughputs achieved on modern equipment are advertised as far surpassing those achieved on machines that were built within the last few years. It is likely that capital acquisition and maintenance costs of this kind of equipment will continue to decrease over time to the point that it is easier to justify the purchase and upkeep of these kinds of capabilities.

Separate Raw Materials

Fiber Preforms

Generally, fiber preforms are used in any of the wet resin types of processes such as liquid resin transfer, resin film infusion, wet layup, etc. The fiber preforms can either be individual tows of reinforcement fibers, woven fabrics, braided preforms, pre-stitched stackups, or partially consolidated pre-cut plies that are held together through the use of a spray or powder binder material. The preforms are typically placed on a mold, and resin is introduced through one of the methods mentioned below. Air is removed from the preform as the resin is introduced and the resulting assembly is cured to produce a finished part.

Resin Film Infusion

In resin film infusion, the resin, in film form is placed strategically with a fiber preform in a mold. The mold is either closed or the assembly is bagged, depending on the configuration of the tool, and heat and pressure application is used to melt the resin film. At the lower viscosity, the resin will flow through the preform to impregnate the fibers and consolidate the composite. The part is held at adequate temperature until the resin finishes curing and the composite part can be removed from the tool. Resin film infusion is related to resin transfer molding, in that separate resin and dry fibers are used to fabricate the finished part, but includes the value added step of having the resin either cast or produced in film forms that are appropriate for the part to be produced. The configuration of how to stack the resin and film and the proper amounts of each to use for a particular application take a fair amount of up front work and development, but once completed, should lead to a very repeatable process.

Resin Transfer Molding

Similar to resin film infusion, resin transfer molding utilizes a dry fiber preform that is placed into the molding tool. Rather than insert resin in film or block form, the resin is introduced a liquid product through resin injection sites. The preform is typically covered with a flow medium or membrane, that helps distribute the resin through the entire part, allowing for adequate wetout of the preform and removal of entrapped air. Resin transfer molding can be done through a number of slightly different processes, many of which are patented, but all of them share the introduction of wet resin to a dry preform. Pressure can be applied through use of multiple piece closed mold tools, vacuum pressure only under a bag, application of external presses, hydrodynamic pressure caused by continuing to push resin while the outlet is closed, or some combination of these factors. Understanding the characteristics of the resin being used, the flow front characteristics of the tool in use, the location of resin injection and outlet points and process parameters are all key to successful implementation of resin transfer molding techniques for composite part production.

Tooling Concepts

Single Sided Female Tooling

In aircraft related composite part production, single sided female tools are most often used for the production of parts with very finely controlled outer mold lines. The tools are fabricated to provide smooth external surfaces to the parts that are fabricated on them. Most often, the tools have relatively shallow curvature and are appropriate for hand layup of either wet layup systems or prepregs, but can also accommodate automated tape or fiber placement, as long as the material applicator head can reach the tool surface. Likewise, single sided female tooling can be used for a variety of vacuum assisted resin transfer molding or resin film infusion manufacturing techniques.

Single Sided Male Tooling

Similar to single sided female tooling, single sided male tooling also provides one surface to layup and cure a composite part on. The difference between the two is the nature of the tool, with male tooling generally being convex in nature vs. concave for the female tooling concepts. The advantage to male tooling is apparent when trying to produce parts with narrow geometry and/or tight radii that would make it near impossible to work material into the far reaches. The disadvantage of male tooling is that the outside surfaces are generally not the same surface quality as if they were built on the tool interface side. Often times the bag side surfaces on male tooling are either an external surface for the aircraft, or a mating surface for a subsequent bonding or fastening interface. Various methods do exist to try to provide better surface finish for these areas, mostly through the use of rigid or semi-rigid caul sheets, but all of them make fabrication and bagging of the part more complex. Similar to female tooling, male tooling can be used for all kinds of hand layup operations, most automated tape layup and fiber placement, as well as resin transfer molding and resin infusion methodologies.

Dual Sided Tooling

Unlike the single sided tooling concepts discussed above, dual sided or multi-piece tooling concepts provide for a tooled surface on both sides of the fabricated part. Fabrication of parts on these kinds of tooling involves placement of the prepreg, wet layup materials, or dry fiber preform and possibly resin film on a portion of the tool, then entrapping it with the other portions

of the tool to completely envelope the part geometry with hard tooling. For resin transfer molded parts, the resin is injected once the tool is closed, but for all other methods, all of the material has to be in the tool before closing it. As can be imagined, the bulk factors of composites make tooling in this manner complex, as usually high pressures have to be applied to get the tool to close properly without shifting or pinching the materials.

Despite the tooling complexities involved, the advantage of double sided tooling is that overall part geometry is very consistent from part to part, although some forethought and balancing needs to be done to develop material charges based on actual resin content and fiber volume percentages of the incoming materials. For resin transfer molded parts, the injected resin fills up the remainder of the tool cavity, so this tooling concept is more advantageous to that production technique, although it also has uses in heated press cure processes for relatively thick parts, on the order of several inches thick.

Tooling Materials

Tooling for composite part fabrication can be made from a variety of materials spanning from simple plaster splashes and tooling foams to more complex hybrid structures constructed of Invar facesheets assembled onto composite backing structures. The tooling concepts and materials chosen are dependant on a variety of factors including but not limited to program budget, anticipated life of the program, engineering requirements for part dimensions or surface quality, and production methodology. For the most part, simple plaster, wooden or foam tooling concepts are good for lower temperature, limited production run development work, but are not suitable for typical serial production environments. For these applications, most part fabricators use either metallic or composite technologies.

Metallic tooling for composites range from simple shapes stretched or machined into aluminum or steel, to very complex large tooling produced from Invar. Aluminum and/or steel can be used in lower temperature curing parts, or where the thermal expansion mismatches do not create significant problems for the finished part geometry. Aluminum has found wider application in lower temperature cure assemblies because of its lower density and ease of machining and manufacturing. The downfall of aluminum is that it is relatively easy to damage, such as gouges that can occur when cleaning excess resin off of the tool between operations.

On the other end of the metallic spectrum is Invar, a nickel steel alloy with very low coefficient of thermal expansion (CTE) values compared to the other metallic solutions. The CTE of Invar is typically very close to that of the composite materials used in part production, and as such, makes it easier to build large composite details or assemblies with fewer dimensional issues that are caused by mismatched CTE values between the tool and composite materials. Invar tools also tend to be more expensive than aluminum or steel tools, but are more robust than aluminum tools and have extended service lives by comparison.

Aside from metallic tooling, composites can also be used to fabricate tooling. There are a variety of tooling grade composite materials commercially available, most utilizing either epoxy or BMI resin technologies partnered with heavier weight commercial grade woven fabrics. Epoxies are often chosen for lower temperature curing part production, because they are easier to produce and can provide adequate tool life when used at lower temperature ranges. If higher cure temperatures are required, or the program has a longer life that would mandate a longer tool life, BMI often becomes a more likely option, despite being more difficult to process than epoxy based options. Regardless of which resin system is used, making composite tools can

be an involved operation utilizing several interim steps to go from a first stage master to a finished composite tool.

Despite the complexities involved in fabrication of composite tooling, there are several advantages to consider. A primary advantage of composite tooling is that of weight. Most composite tools can be designed with significantly lower weights than their metallic counterparts. While not always a consideration, tool handling and movement through a plant or the size of the gimbals required for a fiber placement machine may drive the need to consider lighter weight composite tooling. Another potential advantage of composite tooling is that if the program dictates the use of rate tooling to meet the program demand, the follow-on composite tool fabrication can take advantage of the interim steps used on the first tool and savings may be generated in overall tooling cost when compared to the metallic solutions. Furthermore, composite tooling may accommodate shapes and curvatures that would be difficult, if not impossible, to achieve in traditional metallic tooling.

Environmental Protection

Temperature and Humidity

Current day practices for polymer matrix based composite aircraft structural design require that mechanical property values be reduced to account for reduction in properties that are exhibited by the materials when exposed to elevated temperatures and elevated humidity levels. Further explanations of these reductions and means of accommodating them are given in Trade Studies and Analysis Report.

Overall protection of aircraft structure from humidity is accomplished through application of topcoat paints and in certain instances, moisture barriers such as bondable tedlar. Exterior protection and cosmetic enhancement through the use of paints brings its own associated complications, as traditionally, dark pigmented paints absorb solar heat, raising the temperature of the structure. Existing methodologies to mitigate risk with this phenomenon include limiting paint choices on upward facing horizontal structures to certain reflectance values. Current research is being conducted to create solar heat reflective topcoat technologies that will help overcome these heat related issues, and may permit for smaller reductions in mechanical properties due to temperature related issues in the future.

Moisture uptake in thermoset resin systems has been a historical problem for composites. The effects of the moisture absorption and current methods of dealing with them are more thoroughly developed in the Trade Studies and Analysis Report. Development of epoxy based resin systems into the current day has not solved the issue of their tendency for moisture absorption, and it does not seem likely that this fundamental issue will ever be overcome. In light of that, novel design methods which isolate the composite structure from being exposed to moisture may be a path forward. Application of new hydrophobic barrier materials on the exposed surfaces of the composite parts may enable reduction or elimination in the knockdowns that are often associated with these structures.

Impact Damage

As previously identified, relatively thick gage structures tend to overcome issues that thin gage structures would have relative to levels of impact damage for a given impactor diameter and energy level. Regardless of other structural requirements that drive the structural sizing,

impact damage resistance must also be considered and designed for. Current day methods include sizing the structure for other considerations, then impacting representative panels to see that amount of damage that is imparted. It is believed that to achieve the maximum weight savings targets, impact damage resistance may become the overall design driver, if traditional construction techniques are used. If novel methods can be developed to provide protection from impact damage through means other than direct contact of impactors with the structural portion of the fuselage itself, significant weight savings may be realized.

Lightning Strike and Electromagnetic Interference

Conductive Composites

Conductivity of composite materials has always been an issue when they are implemented in applications that require them to be resistant to potential lightning strikes and/or have specific EMI shielding properties. For the most part, these kinds of requirements have been addressed through the use of parasitic conductive layers that are built into or are placed onto the composite parts in secondary applications. The downfall of the current approaches is that they are expensive from a weight and cost standpoint, require careful control of the thickness of dielectric products such as paint that are put on top of them, and typically need to be repaired after being exposed to an event such as a lightning strike.

Current industry trends for the protection of carbon fiber reinforced aircraft assemblies from lightning strike revolve around the extensive use of metallic screens, expanded metallic foil products suspended in a polymer layer, or metallic wires that are interwoven with the structural fibers in a layer of prepreg. These protection layers are typically located on the outer-most layer of the composite buildup. The metallic portion of these protection materials can be made from a number of different materials that can be obtained in various areal weights. The material and weight of products used are generally selected based on a compromise between the amount of protection required, material cost, material workability, and life-cycle considerations that must be made due to potential for degradation due to issues such as galvanic corrosion. Commercially available products in use today generally utilize aluminum, copper, nickel, titanium, or phosphorous bronze, although other more exotic combinations can be found as well.

When a lightning bolt strikes a panel protected with these materials, the intent of the protection scheme is to allow for a larger lightning attachment area so that the current can flow into the panel, spread across the surface and then through the rest of the aircraft structure, rather than allowing for arcing through the panel into underlying systems and/or structures. Careful consideration needs to be given to ensure that these panels are electrically connected to the surrounding structure or ground plane through the use of adequate electrical bonding straps. Likewise, the thickness of dielectric materials, such as surface fillers and cosmetic topcoats, outboard of the protection material create issues in how much damage is done due to the initial attachment of the lightning bolt to the panel. Thick dielectric layers tend to make small attachment zones that create significant damage to the panel, whereas thinner dielectric layers are usually accompanied with larger attachment zones that exhibit smaller amounts of burn through or delamination.

The overall construction of the panel also plays a role in the phenomena related to lightning strikes. Different weights or alloys may be selected for core stiffened panels than are used for solid laminate panels, although the facesheet thickness on core stiffened panels as well as type of reinforcing fiber and stacking sequence likely also has some effect on performance in lightning strike tests. Regardless of which protection scheme is used, a thorough understanding

of design requirements and certification issues is required to ensure that the correct levels of protection are used for each application. In some instances, a complete burn through or large delamination may be acceptable for a panel, whereas in other areas, no penetration or arcing to the underlying equipment may be tolerable.

In addition to the issue of lightning strike, there are additional issues that need to be addressed concerning electro-magnetic interference relative to composite aircraft. This kind of interference is not only caused by indirect effects of lightning strikes, but can also be encountered when exposed to various electromagnetic wave sources such as radar or radio antennae. Typical metallic aircraft construction techniques are fairly good at providing protection against these electromagnetic sources, especially if care is taken during the design phase to shield equipment and keep the influence of opening in the structure in mind. However, due to their nature, composite assemblies do not provide the level of EMI protection that metallic structures exhibit naturally. The current industry trends to provide protection for electromagnetic interference are based largely on the same materials that are used to provide lightning strike protection. Generally, metallic foils, or embedded screens are used on composite structures to provide some protection, and additional shielding of equipment and cable bundles can be done at their respective installation levels in order to satisfy certification requirements.

Carbon Nanotubes

Carbon nanotubes have been under investigation at the academic level for some time. They receive such a large amount of attention because of their promise for great performance gains in electrical conductivity, thermal conductivity, mechanical properties, and other features as compared to the materials that are in wide use today. For the purposes of this review, we are mainly focused on the electrical property improvements that nano-scale materials may bring as enhancements to the existing materials in use.

As discussed above, the majority of lightning strike protection currently used relies on metallic screens or expanded foils that have raw material electrical resistivity values in the order of 1.7×10^{-8} Ω–m for copper and 2.6×10^{-8} Ω–m for aluminum [Ref. 1]. Comparatively, micro scale pan-based bulk carbon fibers have resistivity values in the order of 1.7×10^{-5} Ω–m [Ref. 2] and neat buckypaper has values reported at 4.9×10^{-5} Ω–m [Ref. 3]. These resistivity values for bulk micro and nano-scale carbon fiber materials are several orders of magnitude higher than their existing metallic counterparts and are still significantly lower than the values that are reported for these product forms once they are embedded in a polymer matrix which by their natures are electrical insulators. For example multi-walled carbon nanotubes embedded in a typical epoxy resin, epox 862, exhibited resistivity values in the range of 0.39 to 2.25 Ω–m depending on the aspect ratio and percent weight loading used [Ref. 3]. Composite panels that utilize carbon nanotube forests as nano-stitch reinforcements between unidirectional carbon/epoxy prepreg plies have exhibited resistivity values of 0.57 Ω–m in-plane and 53.4 Ω–m through the thickness [Ref. 4]. An additional concept under study is to grow the carbon nanotubes in-situ on the reinforcement fibers. Panels produced from reinforcement fabrics enhanced this way and then impregnated through follow-on processes result in resistivity values in the range of 1×10^{-2} to 1×10^{-1} Ω–m [Ref. 5].

Functionalization and incorporation of these carbon nanotubes has been investigated extensively over the last decade, with a great deal of advancement being made. Three interesting methods of incorporating nanotubes into end use products are through incorporating

bulk nanotubes directly into the polymer matrix, growing the nanotubes directly on the reinforcing fiber product, or creating an interim product form such as non-woven mat from nanotubes that can then be incorporated into a final product.

Many early attempts at incorporating nanotubes into polymer matrices were made through the use of mechanical mixing through the use of high shear mixers. Attempts to use these methods were not very successful due to the high Van der Waal forces causing agglomeration of the nanotubes, resulting in non-homogeneous mixes. Additionally, the low bulk density of bulk nanotubes tend to drive the polymer matrix viscosity very high at very low weight percentage loadings, resulting in products that are very difficult to mix and use in follow-on process steps. Additional methods of creating carbon nanotube enhanced products include the use of ultrasonication and microfluidic processors to create dispersions in interim product mixes that are then incorporated into the end use matrix through additional process steps. Ultrasonication appears to be the most widely used method, but due to the process, has a downside of causing damage to the carbon nanotubes. Dispersion through microfluidic processes appear to be less damaging and loadings as high as 15% of nanotubes by weight have been exhibited [Ref. 3].

A second method of incorporating nanotubes into composites is by incorporating nanotube forests directly into existing composite manufacturing technology and product forms. In this method, aligned carbon nanotube forests are grown on a substrate, harvested, and placed at the interply region between two layers of typical carbon/epoxy unidirectional tape. The nanotubes are wet out through capillary action during the ensuing curing process and become integrated into the assembly. A similar approach is to grow the carbon nanotubes in-situ on the reinforcing fiber or fabric. Follow-on processing follows typical current production methods and results in the nanotubes being incorporated into the end product. Presently, these techniques are being performed routinely at a lab scale, but efforts are underway to investigate and overcome issues related to production scale up.

Finally, another approach to incorporating nanotubes into composites is through the creation of mat or veil products that could substituted for the non-woven carriers and scrims currently used in film adhesive and surface film product forms used in composite processes. Nanocomp and Nanolab are examples of companies that have begun to commercialize the production and sales of nanotube based paper or mat products. These products are generally produced by floating a network of carbon nanotubes on a fluid medium and then removing them from the fluid bed with a filtering process that results in a non-woven paper or mat product being created. These are prime examples of processes that were being done at a lab scale just a few years ago, but have been scaled up in order to meet an anticipated future production demand.

Other Nano-enhancements

In addition to carbon nano-tubes, other research initiatives are underway to investigate nano-scale particles of various clays, metallic alloys and other exotic materials to enhance conductivity and electrical shielding properties either by themselves, or by implementing them in conjunction with carbon nano-tubes. Similar to the carbon nano-tubes, there is a lot of academic research being performed in this area, but no significant commercially available products have come to market or been adopted yet. Furthermore, the conductive nano-scale metallic work such as nickel nano-strands being investigated for lightning strike protection and EMI shielding are being proposed as add-on layers, similar to the existing metallic screen products already in use, so while they may provide more or better protection, they do not appear to overcome the manufacturability concerns and limitations. For comparison purposes, nickel

nano-strand materials have exhibited resistivity values of 1 x 10^{4} to 5 x 10^{-3} Ω–m when mixed in polymer resins and 1 x 10^{-3} to 8 x 10^{-5} Ω–m when introduced into polymer materials in a veil format [Ref. 6]. The lowest resistivity values were obtained at high volume loadings of 20%, and more realistic values where in the 1 x 10^{-1} to 1 x 10^{-4} Ω–m range.

The fact that the literature review showed only moderate improvements for nickel nano-strand based solutions as compared to carbon nanotube based solutions, coupled with the fact that the manufacturing methodology was not an improvement over today's state of the art, more attention was given to the carbon nanotube based solutions.

Conductive Resin Additives

Aside from nano-enhanced materials, a review of more traditional materials used for lightning strike and EMI protection was undertaken. While traditional metallic woven screens, expanded foils and interwoven wires have been used extensively for protection of non-conductive aircraft structures, research has also been ongoing on altering traditional polymer matrix materials through the inclusion of metallic powders and flake materials. Research aimed at studying EMI shielding effectiveness has demonstrated that copper, zinc and aluminum used as powder fillers in the matrix resin do not establish a sufficient network to act as a faraday cage for shielding [Ref. 7]. Likewise, because they do not form a network and are embedded in polymer matrix, they would likely be ineffective as lightning strike protection materials when used at loading levels that would be economically feasible and conducive to manufacturing operations.

Although use of metallic fillers has been shown to not work well for EMI shielding at lower percent weight values, it is in fact possible to load enough filler into the polymer to become conductive enough to work. Unfortunately, homogeneous loading of the polymer at high enough percentages to reach the percolation threshold are accompanied by an unacceptable increase in product cost, loss of manufacturability, or loss of mechanical properties. Recent research has shown that it is possible to create chemistries that, when processed correctly, result in heterogeneous structures resulting in highly conductive networks of metallic flake fillers that combine and result in resistivity values on the order of 1 x 10^{-4} Ω–m and lower. These values easily exceed those that can be achieved with homogeneous loaded polymers, while only using a fraction of the loading by weight [Ref. 8]. This research does have interesting potential both for lightning strike protection and EMI shielding concepts.

Conductive Polymers

An interesting area of research at the moment is in the area of intrinsically conductive polymers. One such resin that is getting a lot of attention is poly(3,4-ethylenedioxythiophene) or PEDOT for short. While not used as a bulk thermoset polymer as most of the typical structural composite materials in current use, this polymer is most often applied to an underlying structure through a wet process such as spraying, dip coating, or spin coating. More recently, methods to apply the PEDOT through chemical vapor deposition processes have allowed for better adhesion to the substrate. Recently, the use of PEDOT on top of a shape-memory, polymer foam has been studied as a potential concept for a morphing UAV wing [Ref. 9]. The PEDOT is suggested to be used as a resistive heater that will allow the activation temperature of the coated shape memory foam to be achieved, allowing for the wing shape to morph depending on mission demands. While the literature review did not reveal surface resistivity values for the PEDOT coated materials, it is possible that they could be used in a system to enhance lightning

strike protection and/or EMI shielding concepts. Furthermore, they have been demonstrated to be able to achieve upwards of 100°C temperatures in shape memory foams, and may provide interesting options for use in advanced leading edge anti-ice concepts.

Technology Selection for Advanced Composites

The previous sections of this report provide a general overview of the state-of-the-art materials and processes used in fabrication of complex high performance composite assemblies today. In order to down-select from the various choices above, a scorecard was created that helped provide relative rankings for airframe structural fabrication techniques, the various fiber types and the various resin types. Each of these components was ranked for their impact to meeting a variety of key goals including the ability to achieve a 30% targeted weight reduction compared to a current day baseline metallic aircraft, low cost manufacturing, improved dispatch reliability, ability to be serviced in the field or in a repair depot, damage tolerance, resistance to humidity effects, ability to withstand lightning strike and ability to meet HIRF requirements. While there are likely other design drivers that could be considered, these were considered to be sufficient enough in number and breadth of coverage that they should be able to discriminate a clear leader in each of the categories. In order to drive stratification in the results, factors of 0, 1, 3 and 9 were used to help differentiate between the options. Table 109 shows the results of the ranking evaluation for the construction techniques, fiber and resin selections. No ranking was done for the other topics discussed in this report, such as raw material forms, manufacturing method for detailed parts, tooling concepts or tooling materials. While these factors are all perceived as important concepts for how a composite solution would be implemented, they are not considered primary drivers for the weight savings goal of this activity.

Table 109. Composites Technology Assessment.

	30% Reduction in Weight to B20 Config	Low Cost Manufacturing	Increased Dispatch Reliability	Easy to service / repair in field	Damage Tolerant	Resistant to Humidity Concerns	Withstands Lightning Strikes	Meets HIRF Considerations	
Importance (1 is low, 10 is high)	10	3	5	5	7	7	9	9	Total
Fuselage Construction									
Core Stiffened	3	3	1	1	3	0	3	3	124
Stringer / Frame	9	3	1	3	3	3	1	3	197
Fastened Assy	1	1	1	9	1	3	1	0	100
Bonded Assy	3	1	1	3	1	0	1	0	69
Materials - Fiber									
Glass Fibers	1	9	1	9	9	3	3	3	225
Aramid Fibers	1	3	1	3	3	0	3	3	114
Carbon Fibers	9	3	1	9	9	3	3	3	287
Boron Fibers	9	0	1	3	9	3	3	3	248
Quartz Fibers	9	0	1	3	9	3	3	3	248
Materials - Matrix									
Epoxy	9	9	3	9	3	3	3	3	273
BMI	9	3	3	1	9	3	3	3	257
Polyimide	3	1	3	1	1	3	3	3	135
Cynate Ester	3	3	3	1	1	3	3	3	141
PEI	3	9	3	3	9	9	3	3	267
PEEK	3	9	3	3	9	9	3	3	267
PPS	3	9	3	3	9	9	3	3	267

Based on this ranking score card, the suggested advanced composite airframe would consist of a discrete stiffened, stringer and frame configuration fabricated from carbon fiber reinforced epoxy matrix materials. It will likely consist of a mix of fastened and bonded assembly techniques depending on the overall manufacturing process chosen.

Given this configuration, there are a number of areas that will pose potential issues and need to be researched and resolved in order for this concept to allow for the potential weight savings targets to be met. For thin walled, discretely stiffened airframe structure of this class, there are two issues that are impacted by the relatively thin part thickness. These two concerns are the sensitivity to humidity absorption and impact damage. It is unlikely that new advances will be made in epoxy resin chemistries that will result in eliminating their reduction in mechanical properties when exposed to moisture. It is possible that better techniques will be developed to model or measure the actual moisture level that an airframe has been exposed to, which could lead to some weight savings gains over today's techniques, but would likely not result in the total reductions that are targeted here. Likewise, thicker composite designs, such as those seen on larger commercial aircraft naturally bring a resistance to impact damage at typical impact energies that are expected from normal operations. In thin walled structures, it is very likely that impact resistance will become a design driver if new methods of protecting the structures from the impact can not be developed. A potential solution to both the moisture

absorption and impact resistance issues would be a newly developed outer covering that would provide protection through both impact absorption properties as well as act as a moisture barrier to keep moisture out of the structural components underneath.

While not discussed in the ranking matrix above, a carbon fiber/epoxy matrix composite solution will also need to be protected from lightning strikes and be designed to meet the various EMI criteria. There are current day materials that can meet these needs, but at the cost of potentially not meeting the weight targets established here. At present, nano-scale methods of enhancing conductivity / resistivity in composites are several orders of magnitude off of the performance of current day materials. Further development of nano-enhanced or novel use of non-homogenous materials should be monitored for potential breakthroughs that would enable their use as replacements for today's materials and processes, but successful replacement of current state-of-the art protection schemes seems questionable at best. Additional work to satisfy these criteria with a new novel external covering described above for impact and moisture absorption should also be investigated.

Material Properties Data for Advanced Structures

Current Vision for Shared Material Properties Data

The availability of publicly available design allowable information has hindered the introduction of composite materials into airframe structures. Initial attempts at overcoming this problem were made through MIL-HDBK-17, but most airframe design and manufacturers were unwilling or unable to share the materials data that they had developed internally because it was either a competitive advantage from a business standpoint, or were unable to share them because of restrictions placed on them by the funding source. Some raw material manufacturers and a few end users did make their databases available to MIL-HDBK-17 for inclusion. However, the data submitted often did not follow any particular set of guidelines on how many lots of product were included or what the mix of resin and fiber/fabric lots were to manufacture those lots. Additionally, the fabrication techniques were often not documented or made publicly available and a variety of industry standard and company specific test methods were used in the testing phase. Due to these issues, it was very difficult for a new end user to pick up the data from MIL-HDBK-17 and use it for their own internal design.

Starting in 1995 the NASA funded AGATE program created a new potential to further establish the concept of a shared database for the lowest level building block material properties, as well as provided guidance on how an end user could leverage the available shared database by testing a smaller subset of coupons and based on statistical analysis for equivalency, be allowed to use the established shared database as their own. After the AGATE program ended in 2001, the FAA continued supporting the development of several guides regarding how to write material and process specifications, as well as how to deal with various changes in constituent raw materials and/or process relative to the manufacture of the raw materials.

While the AGATE effort established a firm framework for how a shared database system of composite allowables should function, it had some limitations, in that once the program ended, no additional materials could be added to the AGATE database. There were also some differences in how the statistical analysis was performed when compared to the longer established MIL-HDBK-17/CMH-17 statistical methods. In 2005, NCAMP was formed to further develop the shared database concepts, include new and improved statistical analysis

techniques and provide additional opportunities for more shared databases to be created. The concept was changed slightly, to increase the pool of coupons that are tested at the creation of the shared database, so a larger sample of the composite population can be evaluated. Additionally, the NCAMP test programs do not stop at the lamina level, but include testing at the laminate level, moving further up the building block pyramid. This additional testing will provide yet more shared design allowables, making it even more attractive to look at composites for new airframe designs.

NCAMP is also working very closely with the CMH-17 Data Review Working Group in an effort to harmonize how the resultant test data is reviewed so that all NCAMP tested materials can be submitted for inclusion into the CMH-17 datasets. By marrying the output of the NCAMP effort with CMH-17, the shared database concept will hopefully be available to a wider audience, both aircraft related and others. NCAMP is taking the further step of publishing material and process specifications for each of the products being analyzed, further driving commonality into the manufacture of these composite products.

Having a shared set of design allowables at the lower level building blocks will help in opening up the potential application market for these composite materials. As more companies take on the task of using these materials in their designs, the skill set of the workforce should increase in the areas of composite design and optimization. Likewise, the available computational tools necessary to design and analyze these structures will become more widely available. Development of these tools and the skill sets to use them is seen as key to further insertion of composites into airframe structures in the future.

At present, NCAMP and CMH-17 are making adequate progress in the area of materials database development and sharing; however with the recent economic downturn, there is potential that participation by industry partners may be reduced due to funding issues. The vision of NCAMP appears to be that one day it becomes self-sustaining either through payment for development of additional materials databases by material manufacturers and/or OEMs or by payment for testing of materials for certification in a lab for hire scenario.

At the present time, CMH-17 is mainly supported by the FAA and DoD. It appears that the hope is that commercial sales of the published handbooks and any profits made from offered tutorials and/or conference fees will allow CMH-17 to be economically viable on its own. Until that happens, it is imperative that appropriate levels of funding and support are given to keep the current movement of the effort underway.

In addition to NCAMP and CMH-17, additional efforts such as the FAA funded JAMS (Joint Advanced Materials and Structures) which is comprised of CECAM (Center of Excellence for Composites and Advanced Materials, Wichita State University) and AMTAS (Advanced Materials in Transport Aircraft Structures, Washington State University) are key to development of new design methodology and technology maturation and their associated transfer into the public domain through interaction between OEM end users and the university level where the work is being done.

As can be seen, most of these efforts are currently being supported heavily by the FAA through their safety mandate. Any changes to the funding levels and/or personnel support of these programs would be extremely detrimental and may derail the development and implementation of these materials into future aircraft designs.

Risks to Current Shared Data Vision

Ground work for material design allowable creation has steadily gained ground in the industry sector, first with AGATE, and now with NCAMP. As more companies get on board with the concept of shared databases and with continued support from regulatory agencies such as FAA and EASA, as well as other funding sources, such as NASA and the material suppliers, it seems likely that more and more materials allowable data will become publicly available and the means to access it and use it will be better defined and understood by airframe design and manufacturing companies.

There are a few risks associated with this concept. The first of these risks is in regards to a scenario where the industry does not support or embrace the shared database initiative after the existing NCAMP activities are completed. Shared database concepts are not new to the composites industry as CMH-17, previously MIL-Handbook-17, historically has contained a section of shared materials databases, although adoption in use by end users was complicated at best. Unlike metallic materials, the final properties of composite materials are influenced just as much by how they are processed into final form as they are by their constituent raw materials and the process of making them into usable materials. Because of this, it has been industry practice to have individual material and process specifications at each design / fabrication company. Once individual, proprietary specifications are put in place at each end user, the possibility of what was once a common material ceases to exist and the scenario exists for each end user to have small, but important, differences in their own material and/or process specification, all which make the material unique and potentially no longer part of the population of the shared database. NCAMP has addressed many of these issues through their issuance of NMS specifications, which sets the stage for a shared material specification tied to a shared process specification which is tied to a shared database. However, until OEMs are willing to link their products and development to specifications that are not entirely in their control, adaptation may be tenuous at best.

A second risk of the shared database concept is that it is not financially viable on its own and becomes a static set of materials data once the original effort is completed. AGATE laid the ground work for future directions taken on by NCAMP, but once the program was over, the databases generated became static. NCAMP is furthering the cause and mechanisms of how to create share and maintain materials databases, but once the funding is over, it will become the responsibility of the material suppliers and end users to step up and fund further qualification testing programs and share the data with the general public. Historically, OEMs have been reluctant to share data, either because it is a competitive advantage to keep the data proprietary or because the funding associated with the qualification program has restrictions that do not allow for public sharing of the data that was generated. Material suppliers have typically been willing to fund some qualification programs, and may continue to do so in the future, although without linking the funding to a particular program with associated cost/benefit analysis, they may not be as willing to openly fund new material qualifications. To be sure, material qualifications could continue to be done either with OEM internal budgets or material supplier budgets without making them publicly available shared databases, but the scrutiny and level of review that a shared database receives through an organization such as NCAMP by participating members, or through CMH-17 through an industry related volunteer data review group should not be discounted.

Finally, there is a risk with the shared database concept as related to export compliance and ITAR issues. Several of the more advanced materials being qualified may fall into the export compliance and/or ITAR category. Interpretation of regulations and rules relative to the

classification of property data, material specifications, process specifications, or data reports are subject to interpretation by each end user, and may vary from one company to the next. The potential implication of being in violation of the regulations is severe enough that many companies may choose not to make their data public for fear of reprisal for inadvertently releasing information that should have been controlled.

Future Vision for Material Properties Data

Standards for Commodity Composites

Widespread use of composite materials in the commercial aircraft industry would benefit significantly from a set of industry standard materials. These standard materials would have known material properties for generic coupons and elements. The ability to purchase commodity materials from multiple suppliers without an extensive investment in material qualification would enable all aircraft manufactures to use composite materials without the risk and investment in a material qualification program.

Examples of this approach come from two high temperature polyimide systems (PMR-15 and AFR-PE-4) that were developed under government contract and whose chemical makeup are openly published. This situation has enabled multiple suppliers to provide these materials without extensive investment in qualification programs by either the supplier or the manufacturer.

New Methods for Rapid & Inexpensive Material and Design Data

Test verified analytical tools or semi-empirical methods are needed to reduce the time and cost associated with the development of basic coupon and element material data. From an aircraft certification perspective some testing will always be required. However, the current reliance on extensive test data bases for every material that is considered is sufficiently expensive and time consuming to eliminate consideration of many promising materials.

Analytical tools are needed to predict the stress and strain characteristics of structural sub-components and components. This predictive capability needs to include the effects of damage, repair, and hot plus wet environments. This new capability should enable evaluation of the strain performance of structures based on new materials without either very conservative assumptions or a significant amount of testing.

Analytical methods that allowed detailed structural design trade studies with new materials would be valuable, even if some follow-up testing was required for certification. These methods would reduce the risk of an investment in coupon and element data for a new material.

Recommendations for Advanced Structures Development

In order to meet the targeted improvement in fuel burn and the associated emissions for a 2035 timeframe, 20 passenger commuter aircraft, an estimated weight savings of approximately 30% as compared to a baseline metallic aircraft was targeted. Historically, composite implementations on non-military aircraft have not shown the large weight savings that are desired. This report has provided an overview of advanced composite airframe construction techniques, fiber types, polymer thermoset and thermoplastic matrix materials, raw material forms, and associated composite manufacturing techniques. Additionally, an overview of tooling

concepts and materials was discussed. A review of current state-of-the-art concepts and ongoing research for how to handle the issues of lightning strike protection and EMI protection were covered, with emphasis on various nano-enhanced material developments.

A ranking matrix was developed to down select from the major manufacturing concepts, fibers and resins, and a recommendation for each of those areas was presented. The major shortcomings and issues associated with the down selected configuration were discussed. A technology development roadmap that addresses the impact of each of these concepts to the overall weight savings, as well associated risk and technology development needs to allow for the implementation of these concepts in a 2035 aircraft is presented later in this report.

A case is presented for continued development of composite material data bases. A industry standard set of minimum performance materials that could be manufactured by multiple suppliers would enable wide spread use of composites. New methods that reduce the time and cost of material testing and qualification will enable rapid introduction of breakthrough materials.

Finally, it is suggested that a research effort be developed to understand the requirements of and evaluate materials that can be used as a novel exterior protection concept. The concept would incorporate energy absorbing materials covered in a smooth external layer. The energy absorption materials would allow for impact damage requirements to be decoupled from the structural requirements of the underlying composite structure. The outer layer would allow for enhanced laminar flow, as well as provide protection of the underlying structure from degradation due to environmental concerns such as UV exposure and moisture uptake.

References

1. The Engineering Toolbox, Resources, Tools, and Basic Information for Engineering and Design of Technical Applications (http://www.engineeringtoolbox.com/resistance-resisitivity-d_1382.html)
2. Hexcel Corporation, Carbon Fiber Data Sheet (http://www.hexcel.com/NR/rdonlyres/5659C134-6C31-463F-B86B-4B62DA0930EB/0/HexTow_AS4.pdf) (2009).
3. Ying Tian et. al., 2009. "Dispersion of Short and Long Nanotubes Using Microfluidic Method for Composite Applications," SAMPE Fall Technical Conference Proceedings: Global Material Technology: Soaring to New Horizons, Wichita, KS, October 19-22, 2009. Society for the Advancement of Material and Process Engineering, CD-ROM—10 pp.
4. Megan S.Tsai, Megan S., Guzman de Villoria, Roberto, Wardle, Brian L., 2009. "Towards Multifunctional Enhancement of Composite Aerostructures via the Incorporation of Aligned Carbon Nanotubes," SAMPE Fall Technical Conference Proceedings: Global Material Technology: Soaring to New Horizons, Wichita, KS, October 19-22, 2009. Society for the Advancement of Material and Process Engineering, CD-ROM—12 pp.
5. Barber, Derreck M., Wicks, Sunny S., Wardle, Brian L., 2009. "Health Monitoring of Aligned Carbon Nanotube (CNT) Enhanced Composites," SAMPE Fall Technical Conference Proceedings: Global Material Technology: Soaring to New Horizons, Wichita, KS, October 19-22, 2009. Society for the Advancement of Material and Process Engineering, CD-ROM—9 pp.
6. Hansen, George, "High Aspect Ratio Sub-Micron and Nano-Scale Metal Filaments," *SAMPE Journal,* Vol. 41, No. 2, March/April 2005, pp. 2-11
7. Morgan, Alexander B., Stonecash, T. Jared, Pierce, Jennifer L., 2009. "Integrated EMI Coatings for Composites Through Engineered Use of Nanofillers," SAMPE Fall Technical Conference Proceedings: Global Material Technology: Soaring to New Horizons, Wichita, KS, October 19-22, 2009. Society for the Advancement of Material and Process Engineering, CD-ROM—15 pp.
8. Fornes, Timothy D., Huffman, Nicolas D., Carruthers, Seth B., 2009. "Elminating Tradeoffs in Conductive Composites via Novel Heterogeneous Structures," SAMPE Fall Technical Conference Proceedings: Global Material Technology: Soaring to New Horizons, Wichita, KS, October 19-22, 2009. Society for the Advancement of Material and Process Engineering, CD-ROM—12 pp.
9. Handy, Erik S., Sanderson, Terry M., Justice, Ryan S., 2009. "Electrically-Conductive Skins for Morphing UAVs," SAMPE Fall Technical Conference Proceedings: Global Material Technology: Soaring to New Horizons, Wichita, KS, October 19-22, 2009. Society for the Advancement of Material and Process Engineering, CD-ROM—13 pp.

Appendix H: Risk Analysis Rating Definitions

Appendix H: Risk Analysis Rating Definitions

The technology development risk analysis presented in this report is based on industry standard approaches. This approach includes an estimate of the likelihood that a technology will be developed to a level of maturity in the desired time frame and an assessment of the consequence to the 2035 vehicle if the technology maturity is not achieved. Table 110 shows some definitions for technology readiness level, manufacturing readiness level, and analysis readiness level that are both used in this report and expected to be in agreement with industry accepted approaches to the assessment of technology maturity. Table 111 shows how an assessment of current technology maturity and an assessment of the difficulty required to development the new technology can be used to estimate the likelihood that application maturity will be established in the 2025 to 2030 time frame. Table 112 shows how the consequence and likelihood ratings are development for the risk cube analysis for each of the technology categories proposed for future work in this report.

Table 110. Technology, Manufacturing, and Analysis Readiness Levels

Technology Readiness Level (TRL)	Definition of TRL Rating	Manufacturing Readiness Level (MRL)	Definition of MRL Rating	Analysis Readiness Level (ARL)	Definition of ARL Rating
1	Basic principals observed with analytical or experimental methods	1 to 2	Basic material properties have been observed and couples with candidate manufacturing approaches	1	Simple first principals analysis with no verification or validation (Back of the envelope analysis)
2	Application concept proposed for new technology	2 to 3	Preliminary manufacturing concepts and strategy have been defined	2	Analysis correlates roughly with simple tests
3	Technical approach for development and evaluation of new concept defined	3 to 4	Materials, machines, & tooling demonstrated in laboratory environment	3	Analysis method provides some guidance, but prediction track record is poor (coarse, qualitative, product trade studies)
4	Component or breadboard validation in laboratory environment	4 to 5	Initial productivity assessment of component technology complete. Component form, fit, & function constraints defined.	4	Predicts trends in a controlled environment, but not reliable in a relevant environment
5	Component or breadboard validation in relevant environment	5 to 6	Materials, machines & tooling demonstrated in relevant environment. Manufacturing processes are in development	5	Predicts trends reliably enough to discriminate between designs (good qualitative trades are possible)
6	System or subsystem model or prototype demonstrated in a relevant environment	6 to 7	Pilot manufacturing processes set-up and in test. Raw materials in production & available. Processes and procedures demonstrated in a production environment	6	Trends are very reliable, but absolute value must still be calibrated with testing (quantitative trades are possible after calibration)
7	System or prototype demonstrated in operational environment	7 to 8	Components in advanced development and ready for low rate production. Physical & functional interfaces defined	7	Process predicts absolute value - no development testing is required (quantitative trades are possible)
8	Product completed and flight qualified through test and demonstration	8 to 9	Low rate production. All manufacturing processes established & controlled in production to 3 sigma quality levels	8	Process predicts absolute value - certification & qualification authorities accept analytical results with reduced testing
9	Product proven through successful customer operations and field support	9 to 10	Full rate production. All materials, manufacturing processes & procedures, inspection and test equipment controlled in production to Six Sigma quality levels	9	Certification / qualification authorities accept analytical results without testing

Table 111. Estimate of Likelihood Rating with TRL, ARL, MRL.

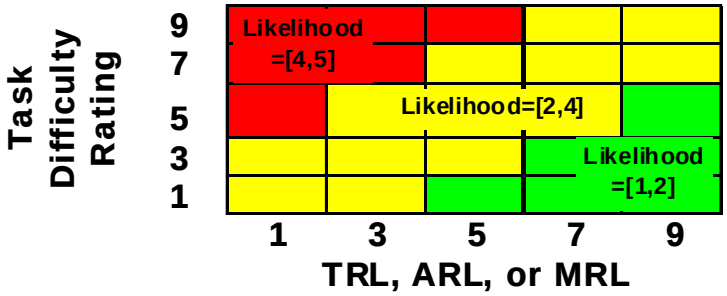

Table 112. Consequence and Likelihood Risk Ratings.

Consequence Ratings	Rationale = Impact on One or More of NASA's Metrics if development fails to mature technology by 2025	Likelihood Ratings	Rationale = Likelihood that development will fail to mature technology by 2025
1	None	1	Very Unlikley
2	Small	2	Unlikely
3	Average	3	Average Likelihood
4	Large	4	Likely
5	Very Large	5	Very Likely

Appendix I: Aircraft Technology Sensitivity Modeling Details

Appendix I: Aircraft Technology Sensitivity Modeling Details

Technology Sensitivity Study (One-Off Analysis Study)

Technology Sensitivity Methodology and Modeling Inputs

In order to capture the individual technology impact on the metrics of interest, fuel burn, noise, emissions, and field length, a one-off approach is selected. The idea behind the one-off approach is to start with the selected configuration, the 2035 advanced turboprop puller and remove one technology at a time. With each removal, the delta from the 2035 advanced turboprop puller for each metric is reported. Essentially, the one-off technology trade study allows the quantification of each technology in terms of how much is it worth in delta fuel burn, delta noise and delta emissions. Once the quantification is assessed then the technologies can be ranked based on much they contribute to each of the metrics.

In order to maximize the impact of each technology, an optimization is required after the removal of each technology. The optimization objective is again mission fuel weight by varying thrust to weight ratio and wing loading subject to 200 fpm top of climb (TOC) rate of climb (ROC) or better constraint. Because of multimodal nature of the technology space, resulting in many local optima, it was necessary to execute 200 random cases of different T/W and W/S combination, and chose the best of the mission fuel solution that satisfy the TOC ROC constraint as the starting point for gradient based optimizer. Ideally, these 200 cases should be randomly and evenly distributed throughout the design space considered as seen in Figure 148. One, of course, can choose to run as many of these cases to search the technology space more thoroughly, but the idea is to get in the region of global optimum and use the optimizer to get to the final solution. In order to execute this grid search plus optimization exercise, again a ModelCenter® environment is developed as in seen in Figure 223. A VBA script was developed to loop through the mission analysis program, FLOPS, using the grid search points contained in the Excel “DoE” file, and write the results directly an Excel “OutputFile”. The resulting dataset is then used to filter out the failed cases, and the remaining set of solutions is then next sorted by TOC ROC. The cases that have at least 200 fpm TOC ROC are then sorted by mission fuel weight. The case with the lowest mission fuel weight is then chosen to be used as the starting point of the gradient-based optimizer.

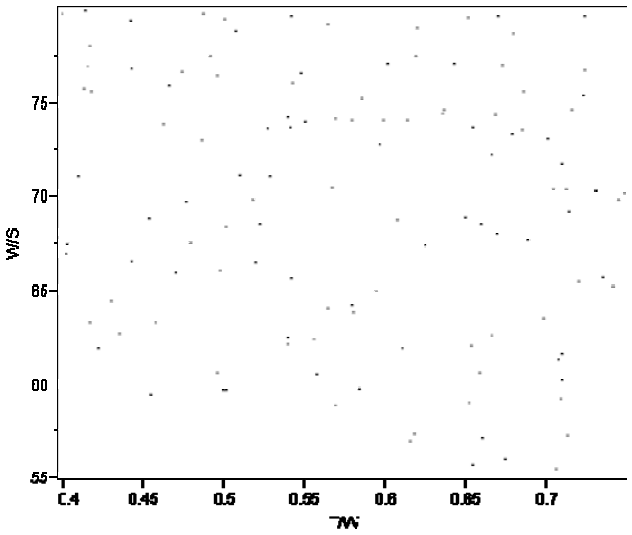

Figure 222. Random Optimization Seeding of Thrust to Weight and Wing Loading

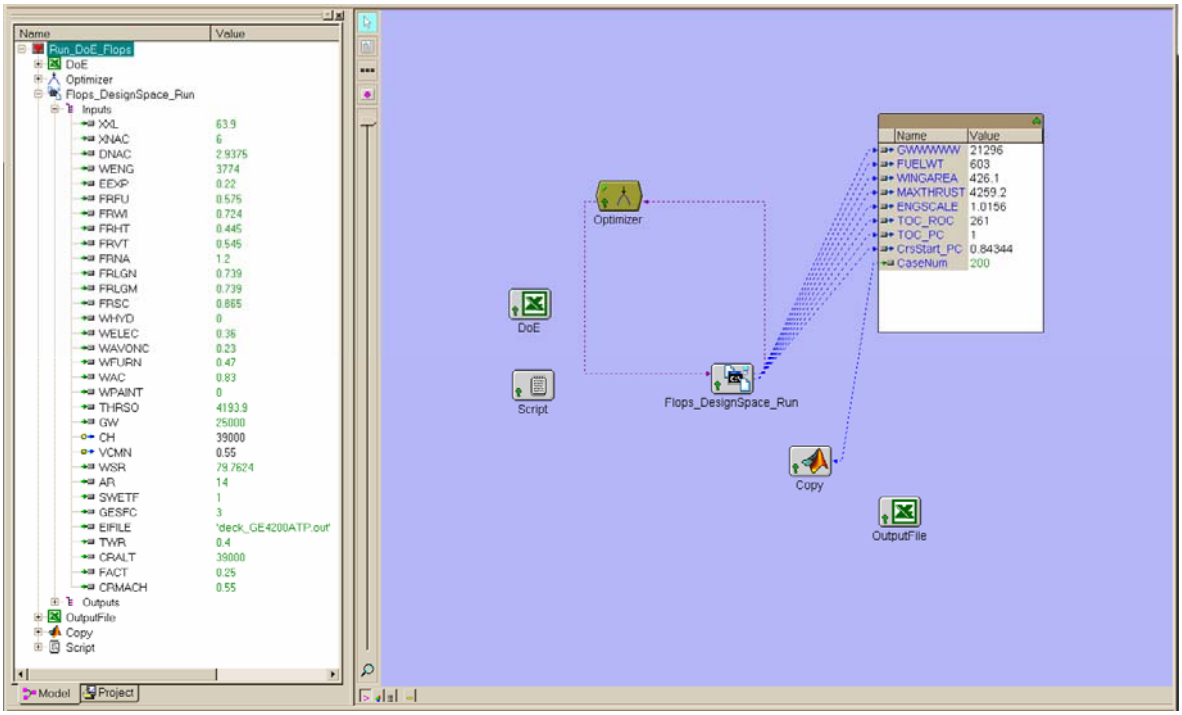

Figure 223. Grid Search and Optimization ModelCenter® Environment

The technologies analyzed in the one-off analysis are broken down into airframe and propulsion. The airframe technologies are further broken down into structures, subsystems, and aerodynamic technologies. The propulsion technologies are broken down into advanced mechanical systems, advanced component aero, advanced propulsion material and manufacturing, advanced combustor, engine noise, and noise optimized propeller.

The technologies that impact mission fuel weight are analyzed in this on-off technology study, and they are summarized in Table 113 below.

Table 113. Technologies with Mission Fuel Weigh Impact

Technology Group	Technologies
Airframe	Structures
Airframe	Advanced Systems
Airframe	Multi-function Structures
Airframe	Novel Protective Skin
Airframe	Advanced Aerodynamics
Propulsion	Advanced Mechanical Systems
Propulsion	Advanced Component Aero
Propulsion	Advanced Material and Manufacturing

The inputs into mission analysis program, FLOPS, to simulate the airframe structures and advanced systems technologies are summarized in Table 114. The modeling inputs to simulate the airframe multi-function and novel protective skin technologies are summarized in Table 115. The modeling inputs to simulate the airframe aerodynamic technology (laminar flow) are summarized in Table 116. The modeling input to simulate the propulsion advanced mechanical systems and advanced component aerodynamics are summarized in Table 117. The modeling input to simulate the propulsion advanced materials and manufacturing technologies are summarized in Table 118.

Table 114. Airframe Structures and Systems Technologies Modeling Inputs

Modeling Factors	2035 Adv. Systems Only (Remove all Structural Technologies)		2035 Adv. Airframe (Remove Adv. Systems Technologies)	
Configuration No.	1		2	
	Remove %	Value	%	Value
FACT (SFC Factor)	0.00%	1.0000	0.00%	1.0000
XNAC (Engine Length)	0.00%	6.0000	0.00%	6.000
DNAC (Engine Diameter)	0.00%	2.9375	0.00%	2.9375
XL (Fuselage Length)	0.00%	48.00	0.00%	48.00
SWETF (Fuselage Wetted Area)	0.00%	962.00	0.00%	962.00
WENG (Engine Weight)	0.00%	1045	0.00%	1045
EEXP (Engine Wt. Expon. Factor)	n/a	n/a	n/a	n/a
FRFU (Fuselage Wt. Factor)	34.00%	0.8712	0.00%	0.5750
FRWI (Wing Wt. Factor)	39.20%	1.1908	0.00%	0.7240
FRHT (Horizontal Tail Wt. Factor)	44.00%	0.7946	0.00%	0.4450
FRVT (Vertical Tail Wt. Factor)	44.00%	0.9732	0.00%	0.5450
FRNA (Nacelle Wt. Factor)	0.00%	1.2000	0.00%	1.2000
FRLGN (Nose Lndg Gear Wt. Factor)	0.00%	0.7390	15.00%	0.8694
FRLGM (Main Lndg Gear Wt. Factor)	0.00%	0.7390	15.00%	0.8694
FRSC (Control Surface Wt. Factor)	0.00%	0.8650	15.00%	1.0176
WHYD (Hydraulics Wt. Factor)	0.00%	0.0000	100.00%	0.5900
WELEC (Electrical Wt. Factor)	0.00%	0.3600	15.00%	0.4235
WAVONC (Avionics Wt. Factor)	0.00%	0.2300	60.00%	0.5750
WFURN (Furnishing Wt. Factor)	26.09%	0.6359	0.00%	0.4700
WAC (AC Wt. Factor)	23.64%	1.0870	0.00%	0.8300
WPAINT (Paint Wt. Factor)	100.00%	0.0670	0.00%	0.0000
FCDO (Drag Reduction Factor)	0.00%	1.1861	0.00%	1.1861
TRUW (%NLF Upper Surf. Wing)	0.00%	24.0	0.00%	24.0
TRLW (%NLF Lower Surf. Wing)	0.00%	24.0	0.00%	24.0
TRUH (%NLF Upper Surf. HT)	0.00%	59.0	0.00%	59.0
TRLH (%NLF Lower Surf. HT)	0.00%	59.0	0.00%	59.0
TRUV (%NLF Upper Surf. VT)	0.00%	41.0	0.00%	41.0
TRLV (%NLF Lower Surf. VT)	0.00%	41.0	0.00%	41.0
TRUB (%NLF Upper Surf. Fusel.)	0.00%	48.5	0.00%	48.5
TRLB (%NLF Lower Surf. Fusel.)	0.00%	48.5	0.00%	48.5
TRUN (%NLF Upper Surf. Nacelle)	0.00%	0.0	0.00%	0.0
TRLN (%NLF Lower Surf. Nacelle)	0.00%	0.0	0.00%	0.0
Engine Deck	GE4200ATP		GE4200ATP	

Table 115. Airframe Multi-Functions and Novel Skin Protection Technologies Modeling Inputs

Modeling Factors / Configuration No.	2035 Adv. Airframe + Systems (Remove Multi Function Structures) 3		2020 Adv Airframe (Remove Novel Protective Skin) 4	
	%	Value	%	Value
FACT (SFC Factor)	0.00%	1.0000	0.00%	1.000
XNAC (Engine Length)	0.00%	6.000	0.00%	6.000
DNAC (Engine Diameter)	0.00%	2.9375	0.00%	2.9375
XL (Fuselage Length)	0.00%	48.00	0.00%	48.00
SWETF (Fuselage Wetted Area)	0.00%	962.00	0.00%	962.00
WENG (Engine Weight)	0.00%	1045	0.00%	1045
EEXP (Engine Wt. Expon. Factor)	n/a	n/a	n/a	n/a
FRFU (Fuselage Wt. Factor)	0.00%	0.5750	9.20%	0.6333
FRWI (Wing Wt. Factor)	0.00%	0.7240	9.20%	0.7974
FRHT (Horizontal Tail Wt. Factor)	0.00%	0.4450	14.00%	0.5174
FRVT (Vertical Tail Wt. Factor)	0.00%	0.5450	14.00%	0.6337
FRNA (Nacelle Wt. Factor)	0.00%	1.2000	0.00%	1.2000
FRLGN (Nose Lndg Gear Wt. Factor)	0.00%	0.7390	0.00%	0.7390
FRLGM (Main Lndg Gear Wt. Factor)	0.00%	0.7390	0.00%	0.7390
FRSC (Control Surface Wt. Factor)	0.00%	0.8650	0.00%	0.8650
WHYD (Hydraulics Wt. Factor)	0.00%	0.0000	0.00%	0.0000
WELEC (Electrical Wt. Factor)	0.00%	0.3600	0.00%	0.3600
WAVONC (Avionics Wt. Factor)	0.00%	0.2300	0.00%	0.2300
WFURN (Furnishing Wt. Factor)	0.00%	0.4700	26.09%	0.6359
WAC (AC Wt. Factor)	23.64%	1.0870	23.64%	1.0870
WPAINT (Paint Wt. Factor)	0.00%	0.0000	100.00%	0.0670
FCDO (Drag Reduction Factor)	0.00%	1.1861	0.00%	1.1861
TRUW (%NLF Upper Surf. Wing)	0.00%	24.0	0.00%	24.0
TRLW (%NLF Lower Surf. Wing)	0.00%	24.0	0.00%	24.0
TRUH (%NLF Upper Surf. HT)	0.00%	59.0	0.00%	59.0
TRLH (%NLF Lower Surf. HT)	0.00%	59.0	0.00%	59.0
TRUV (%NLF Upper Surf. VT)	0.00%	41.0	0.00%	41.0
TRLV (%NLF Lower Surf. VT)	0.00%	41.0	0.00%	41.0
TRUB (%NLF Upper Surf. Fusel.)	0.00%	48.5	0.00%	48.5
TRLB (%NLF Lower Surf. Fusel.)	0.00%	48.5	0.00%	48.5
TRUN (%NLF Upper Surf. Nacelle)	0.00%	0.0	0.00%	0.0
TRLN (%NLF Lower Surf. Nacelle)	0.00%	0.0	0.00%	0.0
Engine Deck	GE4200ATP		GE4200ATP	

Table 116. Airframe Aerodynamics Technology Modeling Inputs

Modeling Factors / Configuration No.	Airframe Aerodynamics 5		Modeling Factors / Configuration No.	Airframe Aerodynamics 5	
	%	Value		%	Value
FACT (SFC Factor)	0.00%	1.000	WAVONC (Avionics Wt. Factor)	0.00%	0.2300
XNAC (Engine Length)	0.00%	6.000	WFURN (Furnishing Wt. Factor)	0.00%	0.4700
DNAC (Engine Diameter)	0.00%	2.9375	WAC (AC Wt. Factor)	0.00%	0.8300
XL (Fuselage Length)	0.00%	48.00	WPAINT (Paint Wt. Factor)	0.00%	0.0000
SWETF (Fuselage Wetted Area)	0.00%	962.00	FCDO (Drag Reduction Factor)	0.00%	1.1861
WENG (Engine Weight)	0.00%	1045	TRUW (%NLF Upper Surf. Wing)	24.00%	0.00
EEXP (Engine Wt. Expon. Factor)	n/a	n/a	TRLW (%NLF Lower Surf. Wing)	24.00%	0.00
FRFU (Fuselage Wt. Factor)	0.00%	0.5750	TRUH (%NLF Upper Surf. HT)	59.00%	0.00
FRWI (Wing Wt. Factor)	0.00%	0.7240	TRLH (%NLF Lower Surf. HT)	59.00%	0.00
FRHT (Horizontal Tail Wt. Factor)	0.00%	0.4450	TRUV (%NLF Upper Surf. VT)	41.00%	0.00
FRVT (Vertical Tail Wt. Factor)	0.00%	0.5450	TRLV (%NLF Lower Surf. VT)	41.00%	0.00
FRNA (Nacelle Wt. Factor)	0.00%	1.2000	TRUB (%NLF Upper Surf. Fusel.)	48.50%	0.00
FRLGN (Nose Lndg Gear Wt. Factor)	0.00%	0.7390	TRLB (%NLF Lower Surf. Fusel.)	48.50%	0.00
FRLGM (Main Lndg Gear Wt. Factor)	0.00%	0.7390	TRUN (%NLF Upper Surf. Nacelle)	0.00%	0.0
FRSC (Control Surface Wt. Factor)	0.00%	0.8650	TRLN (%NLF Lower Surf. Nacelle)	0.00%	0.0
WHYD (Hydraulics Wt. Factor)	0.00%	0.0000	Engine Deck	GE4200ATP	
WELEC (Electrical Wt. Factor)	0.00%	0.3600			

Table 117. Propulsion Advanced Mechanical Systems and Advanced Component Aerodynamics Technology Modeling Inputs

Modeling Factors / Configuration No.	Adv. Propulsion Mechanical Syst. 9		Adv. Propulsion Aero 10	
	%	Value	%	Value
FACT (SFC Factor)	6.90%	1.0690	15.20%	1.1520
XNAC (Engine Length)	0.00%	6.0000	0.00%	6.0000
DNAC (Engine Diameter)	0.00%	2.9375	0.00%	2.9375
XL (Fuselage Length)	0.00%	48.00	0.00%	48.00
SWETF (Fuselage Wetted Area)	0.00%	962.00	0.00%	962.00
WENG (Engine Weight)	2.50%	1071.125	2.90%	1075.305
EEXP (Engine Wt. Expon. Factor)	n/a	n/a	n/a	n/a
FRFU (Fuselage Wt. Factor)	0.00%	0.575	0.00%	0.575
FRWI (Wing Wt. Factor)	0.00%	0.724	0.00%	0.724
FRHT (Horizontal Tail Wt. Factor)	0.00%	0.445	0.00%	0.445
FRVT (Vertical Tail Wt. Factor)	0.00%	0.545	0.00%	0.545
FRNA (Nacelle Wt. Factor)	0.00%	1.200	0.00%	1.200
FRLGN (Nose Lndg Gear Wt. Factor)	0.00%	0.739	0.00%	0.739
FRLGM (Main Lndg Gear Wt. Factor)	0.00%	0.739	0.00%	0.739
FRSC (Control Surface Wt. Factor)	0.00%	0.865	0.00%	0.865
WHYD (Hydraulics Wt. Factor)	0.00%	0.000	0.00%	0.000
WELEC (Electrical Wt. Factor)	0.00%	0.360	0.00%	0.360
WAVONC (Avionics Wt. Factor)	0.00%	0.230	0.00%	0.230
WFURN (Furnishing Wt. Factor)	0.00%	0.470	0.00%	0.470
WAC (AC Wt. Factor)	0.00%	0.830	0.00%	0.830
WPAINT (Paint Wt. Factor)	0.00%	0	0.00%	0
FCDO (Drag Reduction Factor)	0.00%	1.1861	0.00%	1.1861
TRUW (%NLF Upper Surf. Wing)	0.00%	24	0.00%	24
TRLW (%NLF Lower Surf. Wing)	0.00%	24	0.00%	24
TRUH (%NLF Upper Surf. HT)	0.00%	59	0.00%	59
TRLH (%NLF Lower Surf. HT)	0.00%	59	0.00%	59
TRUV (%NLF Upper Surf. VT)	0.00%	41	0.00%	41
TRLV (%NLF Lower Surf. VT)	0.00%	41	0.00%	41
TRUB (%NLF Upper Surf. Fusel.)	0.00%	48.5	0.00%	48.5
TRLB (%NLF Lower Surf. Fusel.)	0.00%	48.5	0.00%	48.5
TRUN (%NLF Upper Surf. Nacelle)	0.00%	0	0.00%	0
TRLN (%NLF Lower Surf. Nacelle)	0.00%	0	0.00%	0
Engine Deck	GE4200ATP		GE4200ATP	

Table 118. Propulsion Advanced Materials and Manufacturing Technology Modeling Inputs

Modeling Factors / Configuration No.	Adv. Propulsion Mat'l / Manuf. 11		Modeling Factors / Configuration No.	Adv. Propulsion Mat'l / Manuf. 11	
	%	Value		%	Value
FACT (SFC Factor)	11.80%	1.1180	WAVONC (Avionics Wt. Factor)	0.00%	0.230
XNAC (Engine Length)	0.00%	6.0000	WFURN (Furnishing Wt. Factor)	0.00%	0.470
DNAC (Engine Diameter)	0.00%	2.9375	WAC (AC Wt. Factor)	0.00%	0.830
XL (Fuselage Length)	0.00%	48.00	WPAINT (Paint Wt. Factor)	0.00%	0
SWETF (Fuselage Wetted Area)	0.00%	962.00	FCDO (Drag Reduction Factor)	0.00%	1.1861
WENG (Engine Weight)	18.60%	1239.370	TRUW (%NLF Upper Surf. Wing)	0.00%	24
EEXP (Engine Wt. Expon. Factor)	n/a	n/a	TRLW (%NLF Lower Surf. Wing)	0.00%	24
FRFU (Fuselage Wt. Factor)	0.00%	0.575	TRUH (%NLF Upper Surf. HT)	0.00%	59
FRWI (Wing Wt. Factor)	0.00%	0.724	TRLH (%NLF Lower Surf. HT)	0.00%	59
FRHT (Horizontal Tail Wt. Factor)	0.00%	0.445	TRUV (%NLF Upper Surf. VT)	0.00%	41
FRVT (Vertical Tail Wt. Factor)	0.00%	0.545	TRLV (%NLF Lower Surf. VT)	0.00%	41
FRNA (Nacelle Wt. Factor)	0.00%	1.200	TRUB (%NLF Upper Surf. Fusel.)	0.00%	48.5
FRLGN (Nose Lndg Gear Wt. Factor)	0.00%	0.739	TRLB (%NLF Lower Surf. Fusel.)	0.00%	48.5
FRLGM (Main Lndg Gear Wt. Factor)	0.00%	0.739	TRUN (%NLF Upper Surf. Nacelle)	0.00%	0
FRSC (Control Surface Wt. Factor)	0.00%	0.865	TRLN (%NLF Lower Surf. Nacelle)	0.00%	0
WHYD (Hydraulics Wt. Factor)	0.00%	0.000	Engine Deck	GE4200ATP	
WELEC (Electrical Wt. Factor)	0.00%	0.360			

In addition to the technology sensitivity relative to the 2035 turboprop puller configuration, the sensitivity of using the advanced turboprop engine on the baseline B20 configuration is analyzed. Also, the technology sensitivity of the airframe technologies is analyzed by putting the baseline turbofan (GE4600Bscaled) on the 2035 turbroprop puller vehicle. The modeling inputs to simulate these two cases are summarized in

Table 119. Modeling Inputs for B20 with Advanced Turboprop Engine and 2035 Selected Aircraft with Baseline Turbofan

Modeling Factors	B20 + Adv. Turboprop		A20ATP + BL TF	
Configuration No.	7		8	
	%	Value	%	Value
FACT (SFC Factor)	n/a	0.9	0.00%	1.0000
XNAC (Engine Length)	n/a	9.263	0.00%	6.0000
DNAC (Engine Diameter)	n/a	3.5	0.00%	2.9375
XL (Fuselage Length)	n/a	48.00	0.00%	48.00
SWETF (Fuselage Wetted Area)	n/a	962.00	0.00%	962.00
WENG (Engine Weight)	n/a	1072.5	0.00%	1045
EEXP (Engine Wt. Expon. Factor)	n/a	0.59	n/a	n/a
FRFU (Fuselage Wt. Factor)	n/a	0.918	0.00%	0.5750
FRWI (Wing Wt. Factor)	n/a	1.002	0.00%	0.7240
FRHT (Horizontal Tail Wt. Factor)	n/a	0.865	0.00%	0.4450
FRVT (Vertical Tail Wt. Factor)	n/a	0.860	0.00%	0.5450
FRNA (Nacelle Wt. Factor)	n/a	1.18	0.00%	1.2000
FRLGN (Nose Lndg Gear Wt. Factor)	n/a	0.797	0.00%	0.7390
FRLGM (Main Lndg Gear Wt. Factor)	n/a	0.797	0.00%	0.7390
FRSC (Control Surface Wt. Factor)	n/a	0.92	0.00%	0.8650
WHYD (Hydraulics Wt. Factor)	n/a	0.59	0.00%	0.0000
WELEC (Electrical Wt. Factor)	n/a	0.699	0.00%	0.3600
WAVONC (Avionics Wt. Factor)	n/a	0.815	0.00%	0.2300
WFURN (Furnishing Wt. Factor)	n/a	0.718	0.00%	0.4700
WAC (AC Wt. Factor)	n/a	1.435	0.00%	0.8300
WPAINT (Paint Wt. Factor)	n/a	0.067	0.00%	0.0000
FCDO (Drag Reduction Factor)	n/a	1.1861	0.00%	1.1861
TRUW (%NLF Upper Surf. Wing)	n/a	0.00	0.00%	24.0000
TRLW (%NLF Lower Surf. Wing)	n/a	0.00	0.00%	24.0000
TRUH (%NLF Upper Surf. HT)	n/a	0.00	0.00%	59.0000
TRLH (%NLF Lower Surf. HT)	n/a	0.00	0.00%	59.0000
TRUV (%NLF Upper Surf. VT)	n/a	0.00	0.00%	41.0000
TRLV (%NLF Lower Surf. VT)	n/a	0.00	0.00%	41.0000
TRUB (%NLF Upper Surf. Fusel.)	n/a	0.00	0.00%	48.5000
TRLB (%NLF Lower Surf. Fusel.)	n/a	0.00	0.00%	48.5000
TRUN (%NLF Upper Surf. Nacelle)	n/a	0.00	0.00%	0.0000
TRLN (%NLF Lower Surf. Nacelle)	n/a	0.00	0.00%	0.0000
Engine Deck	GE4200ATP		GE4600Bscaled	

Finally, a 2030 advanced reference turbofan configuration is also analyzed, and the modeling inputs to simulate this configuration are summarized in Table 120.

Table 120. Modeling Inputs for 2030 Advanced Reference Turbofan Configuration

Modeling Factors Configuration No.	2030 Adv. Reference AC 6 %	Value	Modeling Factors Configuration No.	2030 Adv. Reference AC 6 %	Value
FACT (SFC Factor)	0.00%	1.0000	WAVONC (Avionics Wt. Factor)	60.0%	0.5750
XNAC (Engine Length)	0.00%	6.0000	WFURN (Furnishing Wt. Factor)	26.1%	0.6359
DNAC (Engine Diameter)	0.00%	2.9375	WAC (AC Wt. Factor)	23.6%	1.0870
XL (Fuselage Length)	0.00%	48.00	WPAINT (Paint Wt. Factor)	100.0%	0.067
SWETF (Fuselage Wetted Area)	0.00%	962.00	FCDO (Drag Reduction Factor)	0.00%	1.1861
WENG (Engine Weight)	0.00%	1045.0	TRUW (%NLF Upper Surf. Wing)	24.00%	0.00
EEXP (Engine Wt. Expon. Factor)	n/a	n/a	TRLW (%NLF Lower Surf. Wing)	24.00%	0.00
FRFU (Fuselage Wt. Factor)	9.2%	0.6333	TRUH (%NLF Upper Surf. HT)	59.00%	0.00
FRWI (Wing Wt. Factor)	9.2%	0.7974	TRLH (%NLF Lower Surf. HT)	59.00%	0.00
FRHT (Horizontal Tail Wt. Factor)	14.0%	0.5174	TRUV (%NLF Upper Surf. VT)	41.00%	0.00
FRVT (Vertical Tail Wt. Factor)	14.0%	0.6337	TRLV (%NLF Lower Surf. VT)	41.00%	0.00
FRNA (Nacelle Wt. Factor)	0.0%	1.2000	TRUB (%NLF Upper Surf. Fusel.)	48.50%	0.00
FRLGN (Nose Lndg Gear Wt. Factor)	15.0%	0.8694	TRLB (%NLF Lower Surf. Fusel.)	48.50%	0.00
FRLGM (Main Lndg Gear Wt. Factor)	15.0%	0.8694	TRUN (%NLF Upper Surf. Nacelle)	0.00%	0.00
FRSC (Control Surface Wt. Factor)	15.0%	1.0176	TRLN (%NLF Lower Surf. Nacelle)	0.00%	0.00
WHYD (Hydraulics Wt. Factor)	100.0%	0.590	Engine Deck	GE3800AR	
WELEC (Electrical Wt. Factor)	15.0%	0.4235			

Fuel Cell Technology Modeling

In addition to the technologies considered in the previous section, fuel cell technologies are also considered and analyzed with the 2035 selected configuration, advanced turboprop puller. An iterative method was established to account for the scaling effects that result when the propulsion system weight and volume change on the advanced turboprop puller reference aircraft. The numbers shown in Table 59 represent the estimated impacts of various fuel cell technologies on this reference configuration. These numbers were obtained by sizing the fuel cell propulsive system using the 2035 selected aircraft dimensions and weight. However, due to the nature of vehicle sizing and synthesis, it is necessary to resize the vehicle until a closed solution is found. When the additional propulsive system weights and wetted areas resulting from the fuselage length increases shown in Table 59 are applied to the vehicle it will scale up in size. The fuel flow factor that represents the effect of using hydrogen as a fuel will have the opposite effect, and in isolation would cause the vehicle to scale down. Furthermore, as the vehicle scales, the propulsive system weights and volumes will also change.

Table 121. Fuel Cell Impacts

	Fuel Factor	Propulsion System Weight	Power Plant Volume	Fuel Volume	Fuselage Length Increase
LH2 PEM Fuel Cell	0.3	3458 lbm	42 cu ft	67 cu ft	7.7 ft
LHS SOFC/GT Hybrid	0.25	3774 lbm	81 cu ft	55 cu ft	9.6 ft
Jet A SOFC/GT Hybrid	0.55	3774 (+3857 for reformer) lbm	(81 PP + 97 reformer) cu ft	0	12.7 ft

In order to assess the impacts of scaling the vehicle the baseline values in Table 59 were used to create a ModelCenter fuel cell sizing environment, shown in Figure 224. Identical environments were created for the PEM and SOFC technologies. A short description of each of the analysis modules follows:

- ***PreConverger*** – Used to adjust FLOPS initial GW estimate in response to increases fuselage length and propulsion system weight.

- ***Flops_DesignSpace_Run –*** Runs FLOPS to size the vehicle with the given fuselage length and propulsion system weight.

- ***PEM_Sizing –*** Uses the values contained in Table 59 along with newly sized vehicle to estimate the fuel volume, power plant volume, and the power plant weight. Power plant weight is estimated by applying the engine scale factor from the sized vehicle to the corresponding base Propulsion system weight in Table 59. The power plant volume is determined in the same manner. The fuel volume is calculated by multiplying the appropriate baseline fuel volume in Table 59 by the ratio of fuel usage between the baseline vehicle and the sized vehicle containing a fuel cell technology.

- ***Propulsion Weight –*** This module takes the weight estimated by the PEM_Sizing module and determines the additional weight that must be added to the sized vehicle in order to arrive at a closed solution.

- ***Fuel_Volume_Calcs –*** This module uses the power plant and fuel volume calculations from the PEM_Sizing module to estimate the increase in fuselage length that is needed to accommodate the fuel cell power plant and fuel.

- ***Fuel_Volume_Converger and Propulsion_Weight_Converger –*** These feedback the estimated propulsion system weights and corresponding volumes into the FLOPS analysis and resize the vehicle until they arrive at a closed solution. The result is a vehicle with a consistent fuselage length to accommodate the power plants and fuel that has also been sized large enough to accommodate the additional weight associated with the fuel cells.

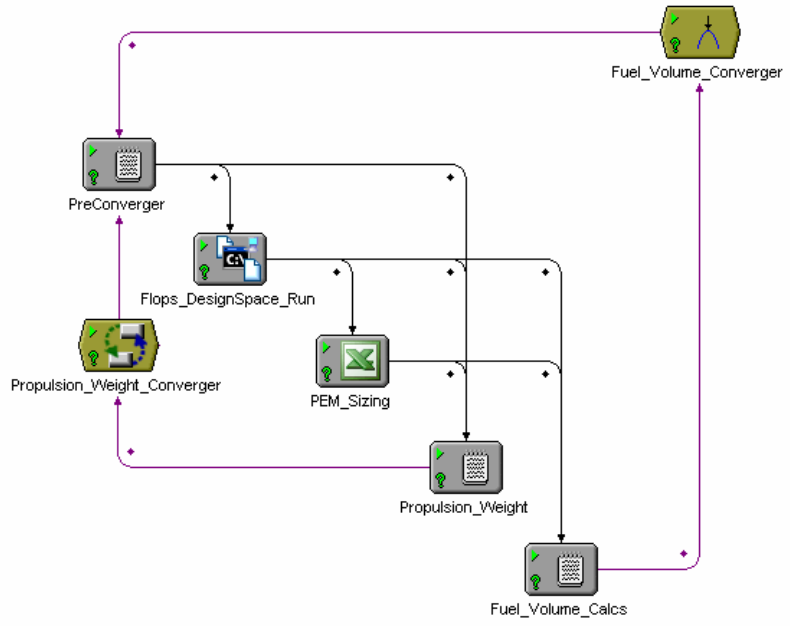

Figure 224. Fuel Cell Sizing Environment

Appendix J: Acronyms

Appendix J: Acronyms

AC	Advisory Circulars
ACES	Airspace Concepts Evaluation System
AEDT	Aviation Environmental Design Tool
AGATE	Advanced General Aviation Transport Experiments
AGB	Accessory Gearbox
AIAA	American Institute of Aeronautics and Astronautics
AIR	Aerospace Information Report
ALCCA	Airline Life Cycle Cost Analysis
ALN	Airline
ALTRAN	Range to alternate airport
ANN	Artificial Neural Net
ANOPP	Aircraft Noise Prediction Program
APPRTM	Approach Time
APU	Auxiliary Power Unit
AR	Aspect Ratio
ARHT	Aspect Ratio of the Horizontal Tail
ARVT	Aspect Ratio of the Vertical Tail
ATIO	Aviation Technology, Integration and Operations
ATS	American Travel Survey
AUTO	Automobile
B-20	Baseline Airliner
BADA	Base of Aircraft Data
BEA	Bureau of Economic Analysis
BERNJ	Bergen County, NJ
BFL	Balanced Field Length
BOW	Basic Operating Weight
BPP	Weight of Baggage per Passenger
BPR	Bypass Ratio
BTS	Bureau of Transportation Statistics
CAA	Computational Aero-Acoustic
CAEP	Committee on Aviation Environmental Protection
CAEP/6	6^{th} Meeting of Committee on Aviation Environmental Protection
CARGOF	Cargo (other than passenger baggage) carried in Fuselage
CATIA	Computer-Aided Three-Dimensional Interactive Application
CD_0	Cruise Drag
CDC	Compressibility Drag Comparison
CDi	Induced Drag Coefficient
CH	Maximum Cruise Altitude
CHD	Chord length
CLDCD	Drag Coefficient Increment Applied to Climb
CMC	Ceramic Matrix Composite
CONUS	Continental United States
CRALT	Cruise Altitude
CRMACH	Cruise Mach Number
DB1B	Airline Origin and Destination Survey
DEAMIN	Minimum Altitude for Descent

DEDCD	Drag Coefficient Increment Applied to Descent
DEMMIN	Minimum Descent Mach Number
DESRNG	Design Range
DF	Fuselage Depth
DIH	Wing Dihedral
DM	Decision Matrix
DNAC	Average Diameter of Baseline Engine Nacelles
DNL	Day Night Level
DoE	Design of Experiments
DOT	Department of Transportation
DSE	Design Space Exploration
EBC	Environmental Barrier Coating
EBF	Externally Blown Flaps
ECS	Environmental Control System
EDET	Empirical Drag Estimation Technique
EDMS	Environmental Data Management System
EIFILE	Name of Engine Deck External File
EMI	Electromagnetic Interference
EPNdB	Effective Perceived Noise in Decibels
EPNL	Effective Perceived Noise Level
ETA	Estimated Time of Arrival
ETAE	Engine locations, fraction of semispan or distance from fuselage centerline
ETAW	Wing station location
ETOPS	Extended-range Twin-engine Operational Performance Standards
FAA	Federal Aviation Administration
FACT	Fuel Flow Factor
FAERT	Decimal amount of aeroelastic tailoring used in design of wing
FAR	Federal Aviation Regulations
FC	Fuel Cell
FCDI	Factor on Induced Drag Coefficient
FCDO	Factor on Profile Drag Coefficient
FCDSUB	Factor on Subsonic Drag
FCM	Fuzzy C-Means
FIPS	Federal Information Processing Standard (county code)
FLAPR	Flap Ratio
FLOPS	Flight Optimization System
FN	Net Thrust
FOIA	Freedom of Information Act
FPR	Fan Pressure Ratio
FRFU	Weight Factor on Fuselage Weight
FRHT	Weight Factor on Horizontal Tail Weight
FRLGN/M	Weight Factor on Noise Landing Gear/ Main Landing Gear Weight
FRNA	Weight Factor on Nacelle Weight
FRSC	Weight Factor on Control Surfaces
FRVT	Weight Factor on Vertical Tail Weight
FRWI	Weight Factor on Wing Weight
FSDRAG	Cessna Proprietary Aerodynamic Prediction Code

FWF	Climb Profile Optimization
GA	General Aviation or Genetic Algorithm
GAMA	General Aviation Manufacturers Association
GDP	Gross Domestic Product
GT	Gas Turbine
GW	Ramp weight
HHT	Decimal fraction of vertical tail span where horizontal tail is mounted
IATA	International Air Transport Association
ICAO	International Civil Aviation Organization
IFR	Instrument Flight Rules
IGENEN	Flag for Indicating Source of Engine Deck
INM	Integrated Noise Model
I-O	Input-Output
IOC	Cruise Option Switch
IRMA	Interactive, Re-configurable Matrix of Alternatives
IRS	Reserve fuel calculation switch
IRW	Flag for Ramp Weight Calculations
ISA	International Standard Atmosphere
IVS	Descent Option Switch (Descent at Optimum Lift-to-Drag Ratio)
JCYNJ	Jefferson City, NJ
JPDO	Joint Planning and Development Office
LAS	Las Vegas McCarran International Airport
LDN	Day Night Level
LEAF	Light Eco-friendly Aircraft Framework
LED	Light Emitting Diode
LH2	Liquid Hydrogen
LP	Low Pressure
LTO	Landing Take-Off
MADM	Multi-Attribute Decision-Making
MAGENTA	Model for Assessing Global Exposure to the Noise of Transport Aircraft
MAPS	Cessna Proprietary Mission Analysis Program
MAXCR	Maximum Power Setting at Cruise
MCO	Orlando International Airport
MFE	Model Fit Error
MLDWT	Design Landing Weight Calculation
MNL	Multinomial Logit
MRE	Model Representation Error
MSA	Metropolitan Statistical Area
MTOGW	Maximum Take-Off Gross Weight
NAS	National Airspace System
NBAA	National Business Aircraft Association
NCAMP	National Center for Advanced Materials Performance
NETAW	Number of Input Wing Stations
NFIN	Number of Fins
nm	Nautical Mile
nmi	Nautical Mile
NOx	Nitrous Oxide
NPCODE	Number of Power Codes

NPD	Noise Power Distance
NPF	Number of First Class Passengers
NPIAS	National Plan of Integrated Airport Systems
NPT	Number of Tourist (Coach) Passengers
NVERT	Number of vertical tails
O-D	Origin-Destination
OEM	Original Equipment Manufacturer
OEP	Operational Evolution Plan
OGV	Outlet Guide Vane
OPR	Overall Pressure Ratio
OPR	Overall Pressure Ratio
PACE	Produced Attracted Connecting Enplanements
PAX	Passenger
PDC	Pulse Detonation Combustion
PEM	Proton Exchange Membrane
PP	Powerplant
RCIN	Instantaneous Rate of Climb for Ceiling Calculation
RDLIM	Limiting or Constant Rate of Descent
RESRFU	Fixed Reserve Fuel
RESTRP	Reserve Fuel as a Fraction of Total Trip Fuel Weight
RH	Relative Humidity
RIMS II	Regional Input-Output Modeling System
ROC	Rate of Climb
RPM	Revolutions per Minute
RQL	Rich Quench Lean
SAE	Society of Automotive Engineers
SAGE	System for Assessing Aviation's Global Emissions
SATS	Small Aircraft Transportation Systems
SFC	Specific Fuel Consumption
SHT	Horizontal tail area
SLS	Sea Level Standard
SOFC	Solid Oxide Fuel Cells
SQL	Structured Query Language
STAR-C^2	Smoothing, Thermal, Absorbing, Reflective, Conductive, Cosmetic
SVT	Vertical tail area
SWEEP	Wing ¼ chord sweep angle
SWPHT	Horizontal tail ¼ chord sweep angle
SWPVT	Vertical tail ¼ chord sweep angle
T/W	Thrust to Weight
TAKOTM	Takeoff Time
TAPS	Twin Annular PreSwirl
TAXITM	Taxi In Time
TAXOTM	Taxi Out Time
TCA	Wing thickness to chord ratio (weighted average)
TCHT	Thickness to chord ratio of horizontal tail
TCVT	Thickness to chord ratio of the vertical tail
TERESA	TEchnology Roadmap for Environmentally Sustainable Aviation
TIES	Identification, Evaluation, and Selection of Technologies

TIMMAP	Missed approach time
TOC	Top of Climb
TOFL	Take-Off Field Length
TOPSIS	Technique for Order Preference by Similarity to Ideal Solution
TR	Wing taper ratio
TRHT	Taper ratio of the horizontal tail
TRL	Technology Readiness Level
TRVT	Taper ratio of the vertical tail
TWR	Thrust to Weight Ratio
ULF	Ultimate load factor
UQETP	Ultra Quiet and Efficient Turboprop
VAC	Volts Alternating Current
VDC	Volts Direct Current
VMMO	Maximum operating Mach number
W/S	Wing Loading
WAC	Weight Factor on Air Conditioning Weight
WAI	Weight Factor on Air Induction System Weight
WAPU	Weight Factor on Auxiliary Power Unit Weight
WATE	Weight Approximation for Turbine Engines
WAVONC	Weight Factor on Avionics Weight
WELEC	Weight Factor on Electrical Weight
WENG	Engine Weight
WF	Fuselage total width
WFLCRB	Total weight of flight crew and baggage
WFSYS	Weight Factor on Fuel System
WFURN	Weight Factor on Furnishings Weight
WHYD	Weigh Factor on Hydraulics Weight
WPMSC	Engine Weight Technology Factor
WPPASS	Weight per passenger
WRATIO	Ratio of Maximum Landing Weight to Maximum Takeoff Weight
WSR	Wing Loading
WSTUAB	Total weight of flight attendants and baggage
XL	Fuselage total length
XLP	Length of passenger compartment
XMLG	Extended main landing gear oleo length
XNAC	Average length of baseline engine nacelles
XNLG	Extended nose landing gear oleo length
YoY	Year over Year

REPORT DOCUMENTATION PAGE

Form Approved
OMB No. 0704-0188

1. REPORT DATE *(DD-MM-YYYY)*	2. REPORT TYPE	3. DATES COVERED *(From - To)*
01- 05 - 2010	Contractor Report	Sept. 2008 - April 2010

4. TITLE AND SUBTITLE
N+3 Small Commercial Efficient and Quiet Transportation for Year 2030-2035

5a. CONTRACT NUMBER
NNC08CA85C

5b. GRANT NUMBER

5c. PROGRAM ELEMENT NUMBER

6. AUTHOR(S)
D'Angelo, Martin M.; Gallman, John; Johnson, Vicki; Garcia, Elena; Tai, Jimmy; Young, Russell

5d. PROJECT NUMBER

5e. TASK NUMBER

5f. WORK UNIT NUMBER
561581.02.08.07.13.03

7. PERFORMING ORGANIZATION NAME(S) AND ADDRESS(ES)
General Electric Aircraft Engines
One Neumann Way
Cincinnati, OH 45215

8. PERFORMING ORGANIZATION REPORT NUMBER

9. SPONSORING/MONITORING AGENCY NAME(S) AND ADDRESS(ES)
National Aeronautics and Space Administration
Washington, DC 20546-0001

10. SPONSOR/MONITOR'S ACRONYM(S)
NASA

11. SPONSOR/MONITOR'S REPORT NUMBER(S)
NASA/CR-2010-216691

12. DISTRIBUTION/AVAILABILITY STATEMENT
Unclassified - Unlimited
Subject Category 01
Availability: NASA CASI (443) 757-5802

13. SUPPLEMENTARY NOTES
This final report was prepared under Glenn Research Center contract NNC08AC85C and monitored by Mark D. Moore of Langley Research Center. The work was funded by the Subsonic Fixed Wing (SFW) project of the Fundamental Aeronautics Program.

14. ABSTRACT

This study develops a future scenario that enables convenient point-to-point commercial air travel via a large network of community airports and a new class of small airliners. A network demand and capacity study identifies current and future air travel demands and the capacity of this new network to satisfy these demands. A current technology small commercial airliner is defined to meet the needs of the new network, as a baseline for evaluating the improvement brought about by advanced technologies. Impact of this new mode of travel on the infrastructure and surrounding communities of the small airports in this new N+3 network are also evaluated. Year 2030-2035 small commercial airliner technologies are identified and a trade study conducted to evaluate and select those with the greatest potential for enhancing future air travel and the study metrics. The selected advanced air vehicle concept is assessed against the baseline aircraft, and an advanced, but conventional aircraft, and the study metrics. The key technologies of the selected advanced air vehicle are identified, their impact quantified, and risk assessments and roadmaps defined.

15. SUBJECT TERMS
Air transportation; Community airports; Transport aircraft; Point-to-point air travel; N+3 goals

16. SECURITY CLASSIFICATION OF:			17. LIMITATION OF ABSTRACT	18. NUMBER OF PAGES	19a. NAME OF RESPONSIBLE PERSON
a. REPORT	b. ABSTRACT	c. THIS PAGE			STI Help Desk (email: help@sti.nasa.gov)
					19b. TELEPHONE NUMBER *(Include area code)*
U	U	U	UU	422	(443) 757-5802